AD-A261 376

DOT/FAA/SD-92/1.1
DOT-VNTSC-FAA-92-7.1

Department
Transportation

...dings of the
...RAFT
...VORTICES

DTIC
ELECTE
FEB 2 5 1993
S C D

93-03948

You may notice a slight asymmetry in this KC-135. Capt. Gilbert will tell you more about it

REPORT DOCUMENTATION PAGE

Public reporting burden for this collection of information is estimated to average 1 hour per response, including the time for reviewing instructions, searching existing data sources, gathering and maintaining the data needed, and completing and reviewing the collection of information. Send comments regarding this burden estimate or any other aspect of this collection of information, including suggestions for reducing this burden, to Washington Headquarters Services, Directorate for Information Operations and Reports, 1215 Jefferson Davis Highway, Suite 1204, Arlington, VA 22202-4302, and to the Office of Management and Budget, Paperwork Reduction Project (0704-0188), Washington, DC 20503.

1. AGENCY USE ONLY (Leave blank)	2. REPORT DATE June 1992	3. REPORT TYPE AND DATES COVERED Final Report

4. TITLE AND SUBTITLE

Proceedings of the Aircraft Wake Vortex Conference
Volume I, Papers 1-29

5. FUNDING NUMBERS

A2070/FA227

6. AUTHOR(S)

J.N. Hallock, Ed.

7. PERFORMING ORGANIZATION NAME(S) AND ADDRESS(ES)

U.S. Department of Transportation
John A. Volpe National Transportation Systems Center
Kendall Square
Cambridge, MA 02142

8. PERFORMING ORGANIZATION REPORT NUMBER

DOT-VNTSC-FAA-92-7.1

9. SPONSORING/MONITORING AGENCY NAME(S) AND ADDRESS(ES)

U.S. Department of Transportation
Federal Aviation Administration
Office of Engineering and Development
Washington, DC 20591

10. SPONSORING/MONITORING AGENCY REPORT NUMBER

DOT/FAA/SD/92-1.1

11. SUPPLEMENTARY NOTES

12a. DISTRIBUTION/AVAILABILITY STATEMENT

This document is available to the public through the National Technical Information Service, Springfield, VA 22161

12b. DISTRIBUTION CODE

13. ABSTRACT (Maximum 200 words)

This volume contains the proceedings of the international conference of Aircraft Wake Vortices held at the Quality Hotel Capitol Hill, Washington, DC, on October 29-31, 1991. The contributed papers discuss technological advances in the knowledge of the phenomenon, its effect on aircraft and airport capacity, detection techniques, and vortex avoidance schemes.

14. SUBJECT TERMS

Aircraft Wake Vortex, Vortices, Vortex hazards, Wake Behavior

15. NUMBER OF PAGES

1138

16. PRICE CODE

17. SECURITY CLASSIFICATION OF REPORT	18. SECURITY CLASSIFICATION OF THIS PAGE	19. SECURITY CLASSIFICATION OF ABSTRACT	20. LIMITATION OF ABSTRACT
Unclassified	Unclassified	Unclassified	Unclassified

TABLE OF CONTENTS

VOLUME I

PAGE

OPERATIONAL CONSIDERATIONS

TRACK A—VORTEX PHYSICS I

VOLUME II

TRACK A—VORTEX PHYSICS II

TRACK B—VORTEX DETECTION

HAZARDS AND STANDARDS

FOREWORD

This international conference on aircraft wake vortices was sponsored by the Federal Aviation Administration (FAA) and cosponsored by Air Line Pilots Association (ALPA), Airports Association Council International (AACI, formerly AOCI), Aircraft Owners and Pilots Association - Air Safety Foundation (AOPA-ASF), Air Transport Association (ATA), Air Traffic Control Association (ATCA), Flight Safety Foundation (FSF), National Aeronautics and Space Administration (NASA), National Center for Atmospheric Research (NCAR), National Oceanic and Atmospheric Administration (NOAA), and National Transportation Safety Board (NTSB). The sessions were held in the Quality Hotel Capitol Hill, Washington, DC, on October 29-31, 1991. The purpose of the conference was to discuss wake vortex phenomena and to exchange information which will guide future research and international cooperation in addressing the wake vortex problem.

The papers were presented in 9 sessions. The titles of the sessions and the respective session chairmen were:

      o   Opening - Dr. Robert E. Machol
      o   National Initiatives - Dr. Robert E. Machol
      o   Operational Considerations I - Louis J. Williams
*   o   Vortex Physics I - Dr. Steven Crow
      o   Operational Considerations II - Hon. J. Lynn Helms
*   o   Vortex Physics II - Dr. James N. Hallock
      o   Vortex Detection - Edward A. Spitzer
      o   Field Measurements - Richard D. Page
      o   Hazards and Standards - Siegbert Poritzky

  * simultaneous sessions

Editing this compendium consisted of chasing down the authors to get the papers, checking the spelling and punctuation, fixing a few verbs, correcting typographical errors, establishing a standard for the format of the papers (e.g., references), fixing a few misquoted equations, etc. As much as I wanted to rewrite or even change some of the text, I resisted; thus, the papers represent the opinions of the authors.

The diligence of Dr. Robert Machol, the Conference Chairman, was apparent to all in attendance. It has been my pleasure to work with him and to present this written archive of the conference.

                                            James N. Hallock
                                          Editor

OPENING REMARKS

Robert Machol
Chief Scientist and Conference Chairman
Federal Aviation Administration

I call this meeting to order. Since I am the first speaker, I have to introduce myself. I am Robert Machol, General Chairman of the Symposium. I used to be a school teacher and now I work for the Federal Aviation Administration.

My first duty and one of my most pleasant is to introduce my boss, Admiral James B. Busey, IV, the Administrator of the FAA.

[Remarks by James B. Busey, Administrator, Federal Aviation Administration]

It's a pleasure to be here today and to welcome all of you to the first international meeting on the wake vortex problem in 14 years. I'm impressed by the fact that so many of you have chosen to attend this symposium. With the high level of expertise we have in this room today, I'm confident that this meeting will be a success. The papers you will present and the discussions you will conduct will surely lead to a greater understanding of the problem.

In addition, this conference presents us with an unparalleled opportunity to open new lines of communication and to establish new personal and professional relationships that can serve as the foundation for future progress on this difficult problem. So it is indeed heartening to see so many people from around the world here today.

It has become a cliche to say that air transportation has changed the world. But it's true. Today, it's almost impossible to imagine a successful business, anywhere in the world, that does not depend on air transportation. And it is equally difficult to imagine a human being, anywhere in the world, who has not benefitted from air transportation in one way or another. Air transportation -- fast, efficient, safe air transportation -- is essential to modern life.

The world's air traffic, which has increased steadily for years, will continue to increase, bringing many benefits -- as well as major challenges. Too many airports are already strained to capacity. We have too much congestion and delay. And the continuing increase in air traffic means that the pressure on system capacity will only become more severe. So we are challenged to increase capacity -- and, at the same time, maintain a high level of safety.

I believe that most of the actions we take to meet these challenges must be international in scope. After all, aviation is increasingly an international activity. That means we must act internationally if we are to build the capacity we need and increase efficiency and safety.

New technology must be applied on a worldwide basis. And we are doing that. In addition, the leading aviation nations must harmonize their aviation rules, regulations, systems, and operating procedures. And we are doing that, too.

Most importantly, we must work together to solve the remaining technical problems that can affect efficiency and safety. One of these, of course, is the problem of wake vortices.

One of the most common phrases that pilots hear from controllers is "caution, wake turbulence." Those words indicate potential danger. They say, in effect, slow down, look out, be cautious.

Wake vortices can kill, as we know from bitter experience. And by forcing us to delay takeoffs and to use longer separation standards for departure and landing operations, they reduce efficiency and restrict airport capacity. No doubt, as traffic volumes increase and as aircraft get larger, the effects of wake vortices on efficiency and capacity will become even greater. But that is a price we can't afford to pay in this age of increasing air traffic that is already straining system capacity.

So we are confronted by a truly difficult challenge -- one of the most difficult in the history of aviation. We must try to find answers to many difficult questions:

*   Can we safely reduce spacing requirements for arriving and departing aircraft?

*   How can we reduce the spacing standards for simultaneou· dependent and independent arrivals to parallel runways?

*   What more can we learn about the special requirements for aircraft that are operating on intersecting runways?

It won't be easy to answer questions such as these. But we must try. And the best way to do that will be to share our knowledge and expertise. The Federal Aviation Administration can't do it alone. We need people like all of you to work with us in solving this problem.

The effort must include everyone who can make a contribution to finding the answers we need -- and that's why I'm so glad that all of you have responded to the call and are willing to come together in a joint effort to see what we can do together.

So let me extend to all of you my personal thanks for being here. With this kind of support, we will surely move forward. Thank you.

[Robert Machol]

Thank you very much Admiral Busey.

<div align="center">

FAA International
Wake Vortex Symposium

</div>

Now let me make some general remarks about the symposium.

<div align="center">

FAA International
Wake Vortex Symposium

</div>

First, note that it is the Federal Aviation Administration's symposium. We are the sponsor and have taken responsibility for arranging the program, for soliciting and choosing the speakers, and for all the financial and logistical arrangements as well as the marketing.

We do have 10 cosponsors, each of whom has helped us with the publicity for the symposium and each of whom has an official representative here. I thank them now for their support, and at an appropriate time I shall introduce these representatives.

<div align="center">

FAA **International**
Wake Vortex Symposium

</div>

Next, note that it is international. In our next session, after the coffee break, we will hear from 6 different representatives of 6 different countries outlining briefly their research programs on this topic. We have in the audience representatives from many other countries: two people have flown in from Tokyo, one from Beijing, one from Johannesburg, and a couple of dozen from Europe!

<div align="center">

FAA International
Wake Vortex Symposium

</div>

Note next that the subject of the symposium is wake vortices. We have almost restricted it to vortices from aircraft --although there will indeed be one paper on wake vortices from submarines -- but we have eliminated other types of vortices. In particular, I have rejected a number of papers on atmospheric vortices, although we welcome here at least one representative from NOAA whose primary interest is in atmospheric vortices.

<div align="center">

FAA International
Wake Vortex **Symposium**

</div>

And finally, let us examine the word "symposium." I am sure you all think you know what the word symposium means, but in fact most of you are incorrect.

<div align="center">

1-3

</div>

sym-po-sium\sim-pō-zē-am   also   -zhe(ē)am\   n,   pl.-sia\-zē-
a,-zh(ē)a\   or   -siums   [L,   fr.   Gk   symposion,   fr.   sypinein
to   drink   together.   fr.   syn-   +   pinein   to   drink—   more   at
POTABLE]   (1603)   1a.   a   convivial   party   (as   after   a   banquet
in   ancient   Greece)   with   music   and   conversation   b.   a
social   gathering   at   which   there   is   free   interchange   of
ideas.

I show here the definition from the Merriam-Webster dictionary. The word comes from 2 Greek words: "sym" meaning together; and "posium," which is cognate with our word puable, and means drinking. The symposium is a drinking party. In ancient Greece, people used to get together in the evening to discuss philosophy, and while they were at it they drank a lot of wine. In our case, the symposium proper will take place this evening. I thank the Boeing Commercial Airplane Group who have contributed a considerable sum of money to buy for us all a number of goodies on which we can munch while we are doing our drinking and meeting one another to talk about philosophy and possibly also about wake vortices. Anyone wearing a symposium badge will be very welcome at this reception.

I doubt that anyone in this audience needs to be reminded that wake vortices are powerful -- literally horizontal tornadoes. But just in case....
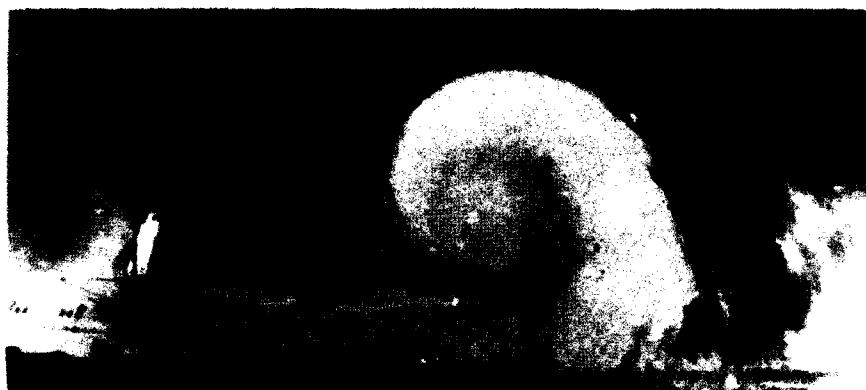
This is a tiny one-person agricultural plane -- note the spraying pipe behind the wing. It is about to land, and since it is still generating lift, it is still generating vortices. This is a smoke generator on the periphery of the vortex; the smoke is picked up and swung around to make this picture. The core is a tiny thing in the center here, and is invisible. I need hardly add that a 747 would generate an even more vigorous vortex. I think most of you have seen this picture.
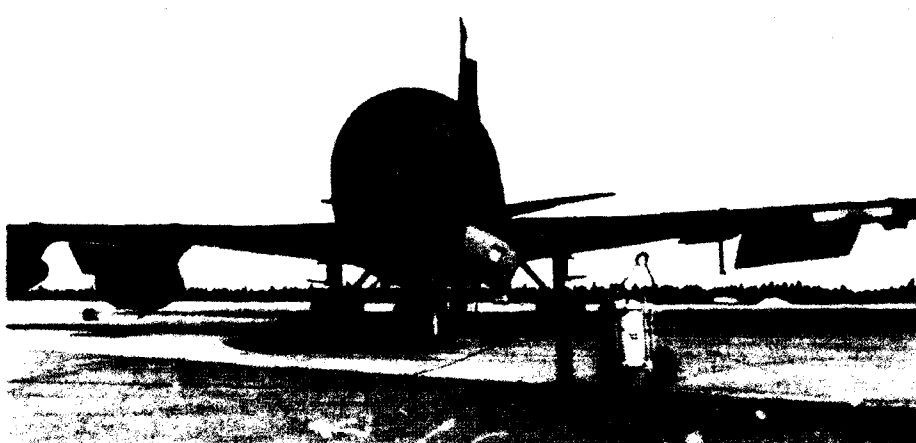
You may notice a slight asymmetry in this KC-135. Capt. Gilbert will tell you more about it this afternoon. It hit a vortex from another 135 at 20,000 feet and shook off a couple of engines.

You will note that we started this meeting on time, and I intend to keep it on time by means of a slight modification of a technique which I learned from Lynn Helms. Each session chairman has been instructed to pass each speaker a little note 2 minutes before the end of his allotted time; two minutes later he passes a second note; and 2 minutes after that he gets out the old Kalashnikov and wastes him.

We are particularly anxious to have audience participation and therefore we have arranged to have 5 minutes at the end of every presentation for questions and discussion.
You have probably noticed that at most meetings the coffee breaks run longer than scheduled and therefore the meeting gets behind. To avoid this, and to make up any time lost in discussions, we have allotted the exceptionally long time of 30 minutes for each break. We do expect that you will be back in your seats before the end of that period; we will start each session on time.

You will be happy to note that we have not arranged any luncheon or dinner meetings. Washington has lots of marvelous restaurants and Myriad Travel who runs our reception desk will be happy to guide you to some of them. For lunch we have allowed 90 minutes each day, and there are ample restaurants within a very few minutes' walk where you can obtain your midday repast.

One of the unusual aspects of this meeting is that different papers have been allotted different periods of time. There are a lot of reasons for this. For example, in the "National Initiatives" section later this morning, Mr. Critchley of the U.K., Dr. Belotserkovsky of the U.S.S.R., and M. Le Roux of France have been allotted only 15 minutes (including the 5-minute question-discussion time) because there are several speakers from each of these countries (including Mr. Critchley and Dr. Belotserkovsky themselves) who will present papers later on in the symposium. On the other hand, Mr. van Woortman of The Netherlands has been given 30 minutes because there is no other paper from that country. Again, you will note that Ms. Amanda Johnson has been given only 15 minutes because that is all she requested, whereas the people from the FAA Tech Center have been given 40 minutes because they submitted several papers which I forced them to combine into one. There were several other reasons for adjusting the time for various papers.

You will note that there have been a few changes from the program that you all saw in this orange brochure; the printed program that was handed out to you, along with abstracts of all the papers, is the official one. These changes were the unfortunate results of exigencies of peoples' schedules. To anticipate further exigencies I have accepted a fascinating, though late-submitted, paper by Dr. Lezius which is at the end of the program. You will note that each abstract is on a single page, and opposite to it is a blank page on which you can take notes.

Each speaker has prepared a written version of his paper under the threat of "no paper; no podium;" that is, if they didn't supply us with a written version to go into the Proceedings, they wouldn't be permitted to speak. Dr. James Hallock will be editing these Proceedings. Jim, will

you please stand up? I have asked each speaker to give his paper to Dr. Hallock. Each attendee will automatically be sent a copy of the Proceedings when they are printed a few months hence. If any of you wish to obtain additional copies of the Proceedings, please go to the registration desk during the break and give the Myriad Travel people $20.00 for each additional copy you wish to purchase. If you want a copy of a paper now, you will have to get it from the speaker. We will also be selling audio tapes, $25 for any one session, $175 for all eight, handling and domestic postage included; again, give your money to Myriad.

As I think most of you already know, we do have a spouse's program. If you have brought a spouse or friend with you, I urge you to register that person at the registration desk. Registered "spouses" will have a badge which will, among other things, get them into this evening's symposium. There is a room for spouses. It is the Board Room on the second floor. Continental breakfasts will be served there to registered spouses each morning, as well as coffee, and Myriad Travel has arranged some tours and other programs and activities for accompanying persons. The color code for badges is; White for most of you, including speakers; Blue for Session Chairs and 2 or 3 others of us; Red for spouses; and Green for Press.

Let me emphasize again that we're anxious to have audience participation. There are microphones here and there. If you wish to ask a question, please go to a microphone. Please give your name and affiliation before your question. If you prefer to be anonymous, cards have been distributed on which you can write questions which will then be collected by Ms. LaBatte—there—and handed up to the session chair.

As I am sure you have noted, we will have parallel simultaneous sessions all day tomorrow. We have asked that each of you indicate when you registered which session you plan to attend. You are, of course, free to change your mind, but it will give us an opportunity to decide which session should go into the larger room. I will make an announcement later today as to exactly which room will have Track A ("Vortex Physics") and which room will have Track B ("Operational Considerations II" and "Vortex Detection"). All of the plenary sessions (which means today and Thursday) will be held here.

I suspect the sessions on Vortex Physics may be the most interesting in this meeting, but I must warn you that some of the papers in those sessions will be technical and might use some fairly hairy mathematics. On the other hand, all of the speakers in all of the other sessions have taken an oath not to use mathematics, although they will feel free to be technical about aviation. If you need to ask what "VFR" means, you may be in the wrong meeting.

It is next my great privilege and pleasure to introduce the keynote speaker, who is my friend, my former boss, and a man whom I admire greatly. He and I have both been in the Navy and have retired with somewhat similar rank, in that each of us wore on our sleeve 2 stripes one-half inch thick, and one stripe of different width. Actually, my third stripe was a quarter-inch and I was a Lieutenant Commander; his third stripe was 2 inches and he was a Vice-Admiral. After having many important positions in the Navy, he was appointed by President Reagan to membership on the National Transportation Safety Board and subsequently to be Administrator of the FAA. He now heads the Air Safety Foundation of the Aircraft Owners and Pilots Association -- Admiral Donald D. Engen.

[*Keynote Address by Donald D. Engen, Air Safety Foundation, Aircraft Owners and Pilots Association*]

Wake vortices can be generated in many ways. Propellers, jet engines, fuselages and wings all produce currents and eddies in the air through which they pass. The vortex that seems the least understood has been the wingtip vortex and this is the principal subject of this symposium.

Wingtip vortices are inevitably generated whenever lift is created and particularly so when the wing is producing a high coefficient of lift. These vortices are left behind an airplane to sink and to drift right or left depending on the wind. Their size and amount of energy are directly related to weight, shape and span of the wing, vertical acceleration, to atmospheric stability and turbulence, and to the distance behind the generating aircraft. The transport airplane can leave an invisible signature which can become a killer. I should hasten to add that the rotary wing of the helicopter also creates vortices, and these will be addressed as well during the Symposium.

These unseen wingtip vortices provide a sense of the unknown and suspense to the pilot that can be heightened by the nearness and size of the airplane ahead. The pilot of the airplane generating the vortex is not necessarily concerned. It is the pilot behind who must address the problem. However, if an airplane could be developed which produced less dangerous vortices, many airlines might be interested because of their abiding interest in enhancing capacity of our airspace, especially at our Air Traffic Hubs.

Prop wash and jet wash are long lasting forms of wake turbulence, which when encountered by a following airplane can significantly challenge the pilot's ability to control the airplane. Some of you may have seen high powered WW II single-engine airplanes roll and in the extreme never regain control when following too closely behind another airplane in its approach to landing? Today the wingtip vortex from heavy airplanes can be far more severe than the thrust generated vortices. Depending on separation, attitude, and speed of both airplanes, that vortex can kill. How can we improve safety and also improve air traffic separation thus increasing airport capacity? This is why we are here.

I have lost two friends to wingtip vortices in different accidents. Each accident happened in a different portion of the flight but each carries a message and typifies the issues that we hope to address at this symposium.

In the mid-1960's during a group photo opportunity above the Mojave Desert, Al White was piloting the XB-70. Grouped around him were four other tactical military aircraft and a photo airplane each flown by friends of mine. One of these was Joe Walker, a NASA Dryden test pilot in an F-104 flying on Al's right wing. Walker was highly experienced and soon was to fly the B-70 as well. The group was flying at about twenty thousand feet and in a slow cruise configuration, thus putting the XB-70 at a moderately high angle of attack. As Joe slid in to a close wing position, behind Al's right wing tip, his F-104 unexpectedly encountered the vortex which was being generated by the wash of the XB-70 right wingtip.

Before anyone could react, the vortex enveloped the close-coupled span of the F-104 and picked up the 104 like a leaf, rolled it left and up. The F-104 then was slammed down inverted on the

tail of the XB-70. Joe was killed instantly, and the F-104 with most of the tail of the B-70 fell away toward the floor of the Mojave Desert below.

The B-70's tail gone, it began to act like all tailed airplanes act without a tail. White escaped after solving some hair raising problems with his individual escape-capsule ejection system. His copilot did not. Two people and two very expensive airplanes were lost; the United States lost an airplane that could have led us technically into supersonic transport, and we pilots woke up to the fact that there was an invisible killer loose in our skies, about which we knew very little.

Twenty-five years later, I was to lose another friend and experienced fellow test pilot, again to wake turbulence. It might appear that he should have known better, because of what had been learned in the intervening years, but still it happened.

It was December, 1989, and a warm, sunny, and clear afternoon in Palm Springs, California. A Piper Archer, with four people -- my friend and three passengers -- approached Palm Springs airport to land. He was on a tight downwind pattern. He was advised by the tower to take his landing spacing on a B-727 still on a straight-in approach to the active runway. My friend turned in close behind the B-727, and as he was about to roll out of his turn to align with the runway, the tower notified him that the B-727 was still on the runway and that he should take his airplane around for another landing attempt. At that instant the Archer began to "wingrock" divergently until the Archer was in a 90 degree right bank. The right wingtip caught the sand adjacent to the right side of the runway, the airplane cartwheeled, and all on board were killed. The precrash movements of the small airplane were classically those of an airplane experiencing wake turbulence.

There were some extenuating circumstances. My friend had his Archer fully loaded, thus shading his performance capabilities. But he was within the weight and balance limits of the airplane. It was his option that he made his approach close to the B-727. Why he did that we will never know. But the crux of the matter was that high energy wingtip vortices from the B-727 had reached out and snatched a very experienced pilot and his three passengers. All were victims of a phenomenon still not fully understood.

I tell of these two separate, but related, events to set an imperative tone for this conference. It is difficult to deal with something that you cannot see. But we must better understand what it is that we are facing.

I have hit wake turbulence in flight while maneuvering airplanes from as low as near ground level to as high as 50,000 feet. In maneuvering flight, the magnitude of the turbulence generated is a function of the "g" load of the airplane crossing ahead. In large measure the severity of the turbulence and length of exposure experienced by the second airplane is determined by its flight path and speed relative to the first airplane.

Today, wake turbulence and separation standards are addressed in the FAA Air Traffic Control Manual for air traffic controllers, in the Airmans Information Manual for pilots, and in FAA Advisory Circular 90-23. The latter two have recently been revised through the efforts of Dr. Bob Machol. The separation standards seem explicit. Wake turbulence is defined and the hazard, as related to following airplanes, is postulated. We understand the effects of span,

speed, and attitude while flying in wake turbulence. We are still not sure how to deal with the problem other than to stay away from it. We still cannot see those vortices and, to the uninitiated, a vortex must seem like witchcraft. It is clear, though, in this busy sky in which we live and work, that separation standards create safety and delay.

How can we reduce that delay, safely? How costly will the monetary or aerodynamic penalty be? How important is it to reduce that delay?

There have been tests to determine optimum airplane spacing. There have been tests to determine how vortices are displaced in a crosswind. There is still much to be learned concerning the effect of meteorological conditions on the generation of the vortex. We will hear about this.

We will hear papers presented that will discuss the operational aspects of encountering and not encountering vortices. Commercial airplane accidents due to such encounters are fewer in the U.S. than in the rest of the world. This in itself is surprising in light of the volume of air traffic in the U.S.

The most recent vortex accident, involving commercial airplanes, occurred in Tashkent in 1988, where a YAK 40 corporate airplane took off and encountered the vortices of an IL 76. The YAK 40 crashed and all on board were killed. We will hear from the British about a number of incidents on approach to Heathrow. A great concern to me is that, while accidents have been few, encounters with vortices are occurring in larger numbers. Increased encounters lower the odds on the next vortex accident. We need to know more.

Many vortex encounters occur because of air traffic controller or pilot lack of knowledge and effective interpretation of the visible parameters. We need to determine what interpretation flexibility should be provided. What constitutes excessive delay? We usually know right away when the interval is too close. What are the permissible tolerances?

Clearly, vortex knowledge and avoidance procedures should be used to provide safety. We cannot afford to have haphazard or less-than-safe procedures. But, the need for improved capacity must not be overlooked. We will hear about operational considerations.

We will hear papers on detection and monitoring. We will hear about major advances in detection by Radar, Lidar Passive IR and inertial devices. Most currently projected Advisory Systems are based upon "not likely to occur" logic. There is need to know where the vortices are. Is one on the projected flight path of the next airplane to land or takeoff?

We will hear papers on the nature of vortices, their generation and their dissipation. Some of these papers are quite technical and use advanced mathematics, but all of these are in the sessions on Vortex Physics tomorrow and those of us who are not mathematicians should be able to follow easily all the other papers. We will hear about microwave and infrared types of sensors for ground and for airborne detection. We will hear about cost/benefit analyses and the increments of capacity enhancement gained through interval between airplanes.

We will hear about the differences between helicopters and airplanes in the generation and encounter of vortices. We will hear about vortex litigation; about databases; about special problems in air to air refueling; and in take-offs spaced seconds apart. We will hear of startling research indicating that certain rare meteorological conditions may lead to exceptionally long-lasting and therefore dangerous vortices. There is much more.

At the very end of the Symposium, we will hear, from a panel of session chairmen, brief summaries of what we heard in their session. This will be followed by a general discussion of what we can conclude and what recommendations we can make. As you listen to the papers, please make notes to help you in the wrap-up discussions.

I am enthused that we could bring together so many diverse interests to focus on such a vexing safety issue as wake vortices. Your presence makes a successful symposium possible. I look forward to hearing your presentations and the discussions that follow, because these will lead to improved knowledge and increased aviation safety.

[Robert Machol]

Thank you very much Don for a most inspiring and relevant keynote address, which I believe gets our symposium off on exactly the right note. I would now like to introduce the first of our technical speakers.

There exists a small group of people whom those of us involved in the vortex program around the FAA refer to as "the wise men." Each of them has been involved in wake vortex research for many years. Each of them is familiar with the mathematics of fluid dynamics and other aspects of wake-vortex theory which I find forbiddingly difficult. Each of them is intimately familiar with research which has been performed on the actual wake-vortex phenomenon. They are: George C. Greene and R. Earl Dunham, Jr., of NASA's Langley Research Center; David C. Burnham, now retired from the Transportation Systems Center and an independent consultant; James N. Hallock who still works for the Transportation Systems Center; and Vernon J. Rossow of NASA's Ames Research Center. By an extraordinary coincidence, these 5 people are the co-authors of the next paper, which will be presented by George Greene. It is entitled "Lessons Learned" and I believe it is supposed to be a summary of what we know and what we have learned, especially in the 14 1/2 years since the last symposium on wake vortices.

WAKE VORTEX RESEARCH
LESSONS LEARNED

George C. Greene and R. Earl Dunham, Jr.
NASA Langley Research Center
Hampton, VA 23665

David C. Burnham
Scientific and Engineering Solutions, Inc.
Orleans, MA 02653

James N. Hallock
John A. Volpe National Transportation Systems Center
Cambridge, MA 02142

Vernon J. Rossow
NASA Ames Research Center
Moffett Field, CA 94035-1000

ABSTRACT

During the 1970's and the early 1980's, the FAA and NASA conducted extensive wake vortex research programs with the goal of safely increasing airport capacity. The FAA program focused on developing an extensive data base and the technology for predicting and/or detecting the presence of a vortex and advising controllers when aircraft separations could be safely reduced. The NASA program emphasized reducing the wake hazard through changes to the aerodynamic characteristics of the aircraft. Both programs made significant technical progress even though neither program resulted in an implementable solution.

Current research has the same goal and many of the same challenges as the earlier research. This paper discusses the most important lessons learned from prior research by both the FAA and NASA and, in particular, how prior research has shaped the issues, requirements, and constraints which will affect any proposed solution.

INTRODUCTION

Airport capacity is a critical factor affecting the growth and efficiency of air transportation. There are many factors which influence capacity; however, ultimately either the number of available runways must be increased or the average spacing between aircraft using existing

runways must be reduced. The current IFR in-trail spacing standards are shown in Table 1 for aircraft categories designated as Heavy, Large, and Small based on their maximum certificated gross takeoff weights. The spacings range from 3 to 6 nautical miles depending on the weight categories of the lead and following aircraft. The 3-nautical-mile spacings were originally due to radar limitations but now may be reduced at some airports to 2.5 nautical miles for some aircraft pairs when other factors, such as runway occupancy times, do not impose minimum limits. The spacings greater than 3 nautical miles are due to wake vortex considerations.

In the 1970's, the FAA, with the assistance of the John A. Volpe National Transportation Systems Center (VNTSC), and NASA substantially increased research efforts directed at finding ways to safely reduce the spacing between aircraft in the terminal area which are imposed by wake vortex constraints. When the research programs began, many aspects of the wake hazard problem were not well defined and the difficulty in finding a satisfactory solution was not fully appreciated. Some felt that the problem did not have a solution and others felt that a variety of solutions were readily available and only required experimental verification. A great deal of information was gathered and an improved understanding of the problem was gained; however, a satisfactory solution to the wake vortex problem was not found.

Although there were and still are a number of difficult technical issues, the most important ones now appear to be solvable. However, the most difficult issues discovered in early research were non-technical ones associated with implementing any solution in a large and complex system environment. Current research has the same general goals as the earlier wake vortex research and will be subject to many of the same constraints. The purpose of this paper is to review some of the early research and highlight the constraints and lessons learned that may apply to any future research program. These comments are based primarily on experience in the U.S. research program; however, the basic problems and issues are similar throughout the world.

SUMMARY OF WAKE VORTEX RESEARCH
LESSONS LEARNED

Wake vortex research has been conducted in the U.S. for over thirty years by a diverse group including participation by the FAA, VNTSC, NASA, the Air Force, the Army, the Navy, aircraft manufacturers, airlines, airport operators, and many university groups. Of this research, the most visible has been the joint research programs sponsored during the 1970's by the FAA and NASA. The NASA program focused on reducing the wake hazard at the source through aerodynamic changes to the aircraft while the FAA program focused on developing measurement techniques and an extensive data base which could be used to develop an operational system for advising air traffic controllers when conditions were appropriate for reducing aircraft spacings.

The research in both areas is extensive and will not be reviewed in detail in this paper. The following sections provide a brief summary of the research in three areas which have provided significant lessons and have a potential impact on current research. The thrust of these comments is that many of the enabling technical problems either have been solved or appear to be solvable. The primary challenges which remain are those which would apply to developing solutions for any large, complex system controlled by a diverse group of people. The comments

emphasize those areas where better communication between the groups developing the technology and the groups charged with implementing solutions or establishing requirements is needed. The research is broken down into three broad areas: 1) the Vortex Advisory System or VAS, 2) wake modification or alleviation at the source, and 3) vortex hazard definition and simulation. The research summaries are followed by suggestions for future research.

For those readers desiring more detail than provided in the summaries, there is an extensive history of published research. For a listing of the abstracts of research articles on aircraft wake vortices from 1923-1990, readers are referred to a bibliography by Hallock.[1] For a more detailed summary of wake-vortex research accomplishments during the late 1960's and the 1970's, readers are referred to the proceedings of four meetings[2-5] and two overviews of the aerodynamic aspects of wake vortices based on information available in 1972 and 1975.[6,7] Surveys[8,9] of the requirements for wake-vortex alleviation and results of ground-based simulations provide guidance as to the level of hazard acceptable to pilots when a vortex wake is encountered. The current status of wake modification research is discussed by Rossow.[10] A review of the requirements of a system for wake vortex avoidance and a method for estimating safe aircraft spacing requirements using airport wake data has been presented by Burnham.[11,12] Descriptions of flight test results[13-20] have been presented and an assessment of vortex research state-of-the-art is given by Hallock.[21]

VORTEX ADVISORY SYSTEM

In 1970 the wake vortex problem was one of safety. Flight tests, conducted by NASA and the FAA, found significant vortex-imposed rolling motions 10 nautical miles behind Heavy jets at altitude. It was not known how long the vortex hazard would persist when aircraft were near the ground during approach, landing, and departure operations. Most of the vortex-caused accidents occurred to Small aircraft on final approach; therefore, the early efforts were primarily concerned with vortex phenomena during landing operations and with reducing the hazard to Small aircraft.

In early 1973 the FAA Air Traffic Service requested that the separation standards be reviewed because the British had promulgated standards which included a 10-nautical-mile separation for a Small category aircraft behind a Heavy. By late 1973 enough data had been collected to demonstrate that the standards for landing commercial aircraft were adequate for preventing hazardous vortex encounters. In 1975, at the instigation of the FAA Systems Engineering and Development Service, the landing separation standards for Small aircraft were revised by adding an extra nautical-mile separation at the runway threshold. At about this time, the emphasis of the wake vortex program shifted from safety to increasing capacity without reducing safety.

The pre-1970 theories describing wake vortex characteristics were very simplistic. It was generally understood that 1) the vortex strength depended on the size, weight, and speed of the generating aircraft, 2) the vortices generally descended and separated when they approached the ground, and 3) the vortex motion was strongly influenced by the ambient wind. However, the lack of field measurements prior to 1970, particularly of vortices near the ground, precluded an in-depth understanding of vortex behavior, particularly decay.

The initial efforts of the wake vortex program at the VNTSC focused on the development of sensor systems for detecting and tracking vortices near the ground. Various sensing techniques were investigated including acoustic, electromagnetic, passive ground wind measurements, pressure, and laser Doppler. Large scale data collection activities began with the installation of several sensor systems at the John F. Kennedy International Airport (JFK) in June 1973 to measure vortices from landing aircraft. Other data collection sites were established at Stapleton International Airport, Heathrow International Airport, and O'Hare International Airport. Data on vortex behavior between the middle marker and runway threshold were obtained on a combined total of over 70,000 landings.

Extensive analysis of the landing data led to the concept of the Vortex Advisory System (VAS). The basic concept of VAS is to adjust aircraft separations for IFR landings on a single runway according to wind measured near the middle marker. Measurements showed that, when the wind vector was outside an ellipse with the minor axis (crosswind) of 5.5 knots and major axis (headwind) of 12.5 knots, no wake vortices remained on the runway more than 80 seconds and it was safe to reduce separations to 3 nautical miles. The VAS was installed at Chicago's O'Hare International Airport in 1977 for a field demonstration. Meteorological towers were installed around the airport to measure the ambient wind near the middle markers of all landing runways. The wind data were fed to a microprocessor which drove a display giving controllers either a red or green light for reducing separations to a uniform 3 nautical miles.

During the field demonstration of VAS, a number of problems and constraints were encountered which had not been anticipated. These have been discussed by Hallock[21] and include 1) the fact that VAS was based on data recorded in the middle-marker-to- threshold region and provided no guidance for reduced spacing near the outer marker or beyond, 2) increased complexity for missed approach procedures for a following aircraft when the lead aircraft is a Heavy, 3) the requirement for use of VAS in VFR as well as IFR conditions with a possible loss of capacity in VFR conditions, and 4) the fact that VAS is a predictive system with no real time ground truth measurements. Perhaps the greatest prejudice against VAS resulted from two vortex encounters experienced by an FAA aircraft which was intentionally flown close behind Heavy aircraft during the VAS demonstration. Even though the FAA aircraft was not obeying VAS guidelines when the encounters occurred, the severity of the encounters were a strong warning of the potential hazards which could exist with VAS when occasional operational errors occur.

Even though VAS was termed a failure as an operational system, it was clearly a success in other ways. The data collection program supporting the development of VAS and supporting theoretical work has provided most of our understanding of wake vortex motion and decay under realistic airport conditions. The data have revised our thinking about vortex decay by showing that vortex pairs decay from the outside while maintaining high velocities near the core, just the reverse of conventional single vortex theory. The data also showed that atmospheric stability, turbulence, ground effects and winds are as important as aircraft category for determining how long a wake hazard lasts. The data base and understanding which were developed are vital to any future programs which attempt to modify separation standards or revise the weight limits for aircraft wake vortex categories.

The VAS was an ambitious undertaking when it was proposed that its goal was to reduce spacings to a uniform 3 nautical miles for all aircraft pairs. This is especially difficult for the

2-4

Small category aircraft following a Heavy which normally has a 6-nautical-mile spacing. Reducing this spacing may not be worth the risk since this aircraft pairing could be avoided or minimized easily by approach procedures and therefore should have a small impact on airport capacity compared to other aircraft pairs. If the goal of VAS had been less ambitious, for example, reducing spacing for like-size or larger following aircraft, it might have received greater support. In addition, there is now the potential for greatly improved vortex detection, both ground and airborne, which might increase the confidence in VAS. In any event, the development of any future VAS-type system should be coordinated with other terminal area automation research and should involve, from an early stage through completion, those who have to implement and use the system. This is important not only to insure that the system is operationally sound but also for the users to develop confidence and a sense of ownership of the technology.

AIRCRAFT WAKE MODIFICATION

Wake modification or alleviation has been a controversial topic from the beginning. Many researchers felt that, since wake vortices resulted directly from the generation of lift, it would not be possible to accomplish any significant wake modification. Other researchers felt that solutions were readily achievable and could be easily developed and incorporated in the current aircraft fleet.

Since the greatest hazard and largest separation distances are required for a Small category aircraft following a Heavy, most of the research was focused on reducing the hazard to an acceptable level for this combination. The difficulty in achieving such a goal was emphasized by flight test results which showed that, at 3-nautical-mile separation, the wake vortices trailing from a B-747 induce, on a Lear Jet following aircraft, a rolling moment equal to about twice its roll control authority. Even though the problem is difficult, researchers in this area have been persistent and have produced a steady stream of ingenious concepts for evaluation with varying degrees of success.

For any alleviation concept to be viable, it must work under all weather conditions, in and out of ground effect, and for all possible aircraft loadings (i.e., fore or aft center of gravity). For retrofit to existing aircraft, it is also required that either the modification costs and performance penalties imposed on the wake-generating aircraft be negligible or that the costs of implementation be recovered quickly through savings generated by higher airport capacities. To date, no alleviation proposals have met these criteria.

The primary problem with retrofit alleviation is not the technical one of inventing an aircraft modification (although that problem is certainly difficult). The real problem is recovering the savings which might be realized through spacing reductions. In order for spacings to be reduced in the current system, an aircraft must essentially be placed in a different weight category (perhaps as both a leader and a follower) or be placed in a "special" category. This would certainly require some type of certification since any reduction in spacing would have a potential impact on safety. There is currently no requirement for wake hazard certification. Even if there were, developing the technical capability and procedures for implementation would be a long and tedious process. It is entirely possible that the cure is worse than the illness in this case.

These comments should not be interpreted as suggesting that wake modification research is not important. The main point is that this research is long term in application and may be accomplished most effectively during the aircraft design phase. Currently, wake hazard is not a significant consideration in aircraft design. It may become more of a consideration due to the greatly expanded use of the airport hub concept. In the past, the benefits of reduced wake hazard for a following aircraft might accrue only to competitors unless all airlines modified their aircraft. Airlines which dominate a hub city now have a direct economic incentive to consider wake characteristics at the time of new aircraft purchase. Since many alleviation concepts have been based on increasing aircraft drag or using devices such as the wing spoilers to increase flow separation and turbulence in the wake, the current trend of designing more efficient high-lift systems for new aircraft may result in even more hazardous wakes unless wake considerations are made part of the design tradeoff. This will require better communication between wake modification researchers and aircraft manufacturers to insure that a balanced approach is taken.

HAZARD DEFINITION AND SIMULATION

One of the first objectives of the flight tests conducted during the early part of the wake-vortex program of the 1970's was the determination of a minimum distance for aircraft of various sizes at which it is safe to enter the wakes of other aircraft. It soon became apparent that lift and yawing and pitching moments induced by a vortex wake are not perceived as hazardous, even though they may at times be objectionable. The vortex-induced characteristic that is perceived as being most hazardous is the rolling moment that is imposed by the coherent rotary motion of the vortex. For this reason, the research program of the 1970's concentrated its efforts on this feature.

In the early flight test programs, the criterion used for controlability was the roll control ratio, the ratio of roll acceleration due to the vortex-induced rolling moment to the roll acceleration possible with maximum aileron deflection. When the roll control ratio is equal to one, the probe aircraft is able to just hold its own against the vortex-induced rolling moment if the controls are applied and changed instantaneously as needed. How much under one the ratio should be to allow for the reaction time of the pilot and flight path corrections is not obvious. Since the trajectory of the aircraft does not usually line up with the vortex axis for large distances, and since the aircraft is often thrown out of the vortex wake by the vortices, the forces and moments are usually temporary or intermittent, thereby causing scatter in the flight test data. Control inputs by the pilot also add scatter to the data as those inputs may alleviate or augment the vortex-induced motions of the aircraft.

Flight test results for various combinations of aircraft sizes were used along with other available information to determine initial separation guidelines at airports. At the time of the initial tests, it was felt that it was adequate to simply have the vortex-induced rolling moment less than the roll control available on any size following aircraft. It was recognized, however, that although the roll excursions experienced at altitude are perceived to be non-hazardous, they would probably be unacceptable near the ground during the last part of a landing or during takeoff.

In order to obtain a better estimate of the magnitude of vortex-induced motions that would be acceptable to pilots, tests were conducted with piloted ground-based simulators[22][23] to obtain repeatable data on excursions caused by wake-vortex encounters and to get a large data base on the hazard perceived by pilots during an encounter. The tests included not only the vortex encounters but also atmospheric turbulence and the usual piloting duties associated with the airport environment. The pilots were given no indication as to whether a vortex was present in the flight corridor or how or when it would be encountered. The piloting task was to fly a 3° glide slope toward a landing with an abort capability if desired. The pilots that had flight experience with wake-vortex encounters before experiencing those on the simulator reported that the simulations were quite realistic.

After a number of simulated encounters had been flown under both visual flight conditions (VFR) and instrument flight conditions (IFR), the separation of occurrences into hazardous and non-hazardous categories was found to correlate best with maximum roll or bank angle. It was concluded from the simulations that under IFR conditions, a maximum roll angle of more than 7 degrees is perceived as hazardous at altitudes of 200 feet or less. The primary reason given by the pilots for rating an encounter as hazardous was proximity of the ground and subsequent altitude loss caused by the encounter. A similarly well-defined boundary between hazardous and non-hazardous conditions was not found for either roll rate or roll acceleration.

The finding that a vortex encounter is considered non-hazardous if the maximum roll excursion is below a certain value prompted studies of the feasibility and effectiveness of an automatic control system on maximum roll angle. It was observed that since the simulator experiments were designed to make the vortex encounter unexpected, the pilot response during a typical encounter first consisted of a time delay of about 0.4 sec. It was then reasoned that a considerable reduction in roll excursion could be achieved if an automatic system were used to command immediate action. The numerical analysis then carried out by Tinling[26] showed that when the full amount of roll control is used with an automatic system and when the roll control ratio is less than one, the angle of roll can be kept within acceptable limits.

The simulator research provided guidance on what a pilot would view as a hazardous encounter. There is no similar consensus on the level of vortex strength which would result in a safe encounter. Therefore, the current spacing standards were intended to be conservative. With the current emphasis on increasing capacity, it is appropriate to ask how conservative the spacing standards really are and if any can be safely reduced. This is especially pertinent since, in VFR operations, pilots routinely reduce spacings to levels below the IFR standards which are themselves well below those which would be predicted to be safe based on the early flight tests at altitude. The primary difficulty is, of course, that it is not possible to conduct definitive full-scale tests near the ground due to safety considerations.

Determining the boundaries of a safe vortex encounter is an important research objective. This is particularly true for Large and Heavy following aircraft since most of the research has concentrated on Small aircraft which are more prone to hazardous encounters. The primary difficulty in studying this problem in a simulator is in specifying the decaying vortex flow field and the aerodynamic interaction between the vortex and the aircraft. Validation of the simulations of this problem to date has consisted primarily of pilot assessments that the encounter feels about right but quantitative evaluations are rare. In addition, Holbrook[27] has

2-7

suggested that aircraft with large roll inertia may have a destructive effect on the vortex during the encounter which might significantly reduce the hazard, particularly to aircraft in the Heavy category.

Burnham[12] has discussed methodology for determining safe aircraft spacings. This methodology is unique in that it uses measured vortex decay data for estimating the wake hazard duration. The hazard model used can be related to an equilibrium or steady-state roll control ratio. It is felt to be accurate to within a factor of about two. This model has proven to be conservative and is used primarily to determine the relative hazard of different aircraft combinations. One reason for the model's conservatism may be that it cannot account for the dynamic aspects of a short duration vortex encounter. Estimating the magnitude of these dynamic effects is currently an active research area.

Table 2 shows results from a simple dynamic analysis presented by Stuever and Stewart.[28] The intent of their study was to perform an initial screening of current aircraft categories, assuming uniform spacing to eliminate the need to model vortex decay, to determine if the relative hazard levels were roughly consistent with the assigned spacing standards. A hazard level of 1.0 was assigned to a pair of 100,000 lb. aircraft (both lead and following) which corresponds roughly to the DC-9 or B-737 size of aircraft. The range of relative hazard for each pair shown in the table results from the range of aircraft weights in each category. Two points concerning the table are especially interesting. First, the Heavy/Heavy relative hazard is about the same as the nominal hazard for the pair of 100,000 lb. aircraft. This suggests that this pair might be considered for reduced spacing, at least based on vortex considerations. Second, the range of relative hazard for the Large/Large group is nearly two orders of magnitude. This shows as expected that the smaller aircraft are at relatively greater risk. It suggests, if correct, that spacings for the larger Large aircraft are conservative if the spacings for the smaller Larges are safe. It also provides a rationale for considering a 4-weight-category system which would be more consistent with international standards.

FUTURE RESEARCH DIRECTIONS

Future research may be broken down into three broad time scales depending on how difficult the technology might be to implement. Wake modification involves changes to large and complex aircraft systems and thus might be designated long term. This does not imply that it is not important since it may be required to keep spacings for future aircraft at the current values. There is an extensive research history even though relatively little research is being carried out at the present time.

In the medium term, variable vortex spacings may be achieved through implementation of a variety of automated terminal area air traffic control technologies.[29] A much improved VAS-type system might be developed since there is an existing experience base (even if unfavorable) for the use of this level of technology. Research in this area might benefit from the improvements in sensor technology which have potential application for both ground and airborne vortex detection.

In the short term, capacity improvements might result from changes to procedures, separation standards, aircraft categories, or other "paper changes" which require minimal hardware development. Since there is a large spread in the weight range for Large aircraft, it may be possible to increase both safety and capacity at the same time. Due to safety limitations, it will not be possible to conduct flight research on spacing criteria near the ground. Therefore, there must be a greater emphasis on the development, validation, and use of simulation for determining minimum safe spacings.

CONCLUDING REMARKS

The FAA "owns" the wake vortex problem and therefore must implement any solutions or initiate any changes to separation standards or aircraft categories. There is a vast wake vortex experience base within the air traffic control network, pilot groups, airport operators, and research groups inside and outside the FAA. If steady progress is to be made, the FAA must provide stable leadership and integrate the experience and technical knowledge of all parties. This task should not be minimized as these groups are rarely required to communicate with each other and may speak different "languages" and certainly have greatly different perspectives on the problem and possible solutions. Strong leadership is required to clearly define the most important issues to be resolved, develop a common understanding of what the term minimum safe vortex spacing means, and forge a better agreement on how separation standards might be changed. The research must be coordinated internationally to maximize the results achievable with current resources. It is especially important that those who are charged with implementing solutions be involved early and continuously in the process to insure that solutions are operationally sound and to develop confidence and a sense of ownership in the solutions.

Table 1. IFR Separation Standards, Nautical Miles

Following Aircraft	Leading Aircraft		
	Heavy	Large	Small
Heavy	4	3	3
Large	5	3	3
Small	6	4	3

Table 2. Relative Wake Hazard

Following Aircraft	Leading Aircraft	
	Heavy	Large
Heavy	0.6-1.1	0.1-0.9
Large	0.9-12	0.15-10

Relative level = 1.0 corresponds to leading and following aircraft each weighing 100,000 lb.

REFERENCES

1. Hallock, J. N., "Aircraft Wake Vortices: An Annotated Bibliography (1923-1990)," Report. No. DOT-FAA-RD-90-30, U. S. Dept. of Transportation, Jan. 1991.

2. Olsen, J. H., Goldburg, A., and Rogers, M., eds., Aircraft Wake Turbulence and its Detection, Plenum Press, 1971.

3. NASA Symposium on Wake Vortex Minimization, NASA SP-409, 1976.

4. Hallock, J. N., ed., Proceedings of the Aircraft Wake Vortices Conference, Report No. FAA-RD-77-68, U. S. Dept. of Transportation, March 15-17, 1977.

5. Wood, William D., ed., FAA/NASA Proceedings Workshop on Wake Vortex Alleviation and Avoidance, Report No. FAA-RD-79-105, U. S. Dept. of Transportation, Nov. 28-29, 1978.

6. El-Ramly, Z., "Aircraft Trailing Vortices--A Survey of the Problem," Technical Report. No. ME/A72-1, Carlton University, Ottawa, Canada, Nov. 1972.

7. Donaldson, C. duP., and Bilanin, A. J., "Vortex Wakes of Conventional Aircraft," AGARDograph No. 204, May 1975.

8. Burnham, David C., "Wake Vortex Alleviation System Requirements," Report No. DOT-TSC-FA427-PM-84-19, U. S. Dept. of Transportation, May 1984.

9. Rossow, V. J., and Tinling, B. E., "Research on Aircraft/Vortex-Wake Interactions to Determine Acceptable Level of Wake Intensity," AIAA Journal of Aircraft, Vol. 25, No. 4, June 1988, pp. 481-492.

10. Rossow, Vernon J., "Prospects for Alleviation of Hazard Posed by Lift-Generated Wakes," proceedings of the FAA International Wake Vortex Symposium, October 1991.

11. Burnham, David C., "Wake Vortex Avoidance Systems: Requirements Analysis," Report No. DOT-TSC-FA527-PM-84-46, U. S. Dept. of Transportation, Nov. 1984.

12. Burnham, David C., "How To Use Vortex Measurements To Set Separation Standards," proceedings of the FAA International Wake Vortex Symposium, October 1991.

13. McGowan, William A., "Calculated Normal Load Factors on Light Airplanes Traversing the Trailing Vortices of Heavy Transport Airplanes," NASA TN D-829, May 1961.

14. Garodz, L. J., "Federal Aviation Administration Full-Scale Aircraft Vortex Wake Turbulence Flight Test Investigations: Past, Present, Future," AIAA Paper 71-97, New York, 1971.

15. Andrews, William H., Robinson, Glenn H., and Larson, Richard H., "Exploratory Flight Investigation of Aircraft Response to the Wing Vortex Wake Generated by Jet Transport Aircraft," NASA TN D-6655, March 1972.

16. Garodz, Leo J., Lawrence, David, and Miller, Nelson, "The Measurement of the Boeing 727 Trailing Vortex System Using the Tower Fly-By Technique," Rept. FAA-RD-74-90, U. S. Dept. of Transportation, Aug. 1974.

17. Smith, Harriet J., "A Flight Test Investigation of the Rolling Moments Induced on a T-37B Airplane in the Wake of a B-747 Airplane," NASA TM-56031, April 1975.

18. Jacobsen, Robert A., and Short, Barbara J., "A Flight Investigation of the Wake Turbulence Alleviation Resulting from a Flap Configuration Change on a B-747 Aircraft," NASA TM-73,263, July 1977.

19. Barber, Marvin R., and Tymczyszyn, Joseph J., "Wake Vortex Attenuation Flight Tests: A Status Report," NASA CP-2170, 1980, pp. 387-408.

20. Burnham, D. C., "B-747 Vortex Alleviation Flight Tests: Ground-Based Sensor Measurements," Report No. DOT-FAA-RD-81-99, U. S. Dept. of Transportation, Feb. 1982.

21. Hallock, J. N., "Aircraft Wake Vortices: An Assessment of the Current Situation," DOT-FAA-RD90-29, U.S. Department of Transportation, Jan. 1991.

22. Sammonds, Robert I., and Stinnett, Glen W., Jr., "Hazard Criteria for Wake Vortex Encounters," NASA TM X-62,473, Aug. 1975.

23. Sammonds, Robert I., Stinnett, Glen W., Jr., and Larsen, William E., "Wake Vortex Encounter Hazard Criteria for Two Aircraft Classes," NASA TM X-73,113, June 1976. (Also FAA-RD-75-206.)

24. Tinling, Bruce E., "Estimation of Vortex-Induced Roll Excursions Based on Flight and Simulation Results," Proceedings of the Aircraft Wake Vortices Conference, FAA-RD-77-68.

25. Hastings, Earl C., and Keyser, Gerald L., Jr., "Simulated Vortex Encounters by a Twin-Engine Commercial Transport During Final Approach," NASA TM 81782, May 1980.

26. Tinling, Bruce E., "Estimates of the Effectiveness of Automatic Control in Alleviating Wake Vortex Induced Roll Excursions," NASA TM 73,267, Aug. 1977.

27. Holbrook, G. T., "Vortex Wake Hazard Analysis Including the Effect of the Encountering Wing on the Vortex," Master's Thesis, The George Washington University, Aug. 1985.

28. Stuever, Robert A. and Stewart, Eric C., "The Role of Simulation in Determining Safe Aircraft Landing Separation Criteria," proceedings of the FAA International Wake Vortex Symposium, October 1991.

29. Evans, James E., and Welch, Jerry D., "Role of FAA/NWS Terminal Weather Sensors and Terminal Air Traffic Automation in Providing a Vortex Advisory Service," proceedings of the FAA International Wake Vortex Symposium, October 1991.

RESEARCH AND DEVELOPMENT PROGRAM FOR A WAKE VORTEX WARNING SYSTEM IN GERMANY

Heinz Winter
Institute for Flight Guidance
DLR, Braunschweig, Germany.

INTRODUCTION

The necessity to use Wake Vortex (WV) separations for aircraft on their final approach to an airport significantly reduces the available runway landing capacity. In 1984 the German Bundesministerium für Verkehr (BMV) initiated a research program to investigate the possibilities for a reduction of the required WV separations at the airport of Frankfurt. Theoretical studies and measurements taken at the Frankfurt airport have led to the definition of a WV Warning System (WVWS) for this airport.

Since 1989 DLR is working on a project to study the potential for capacity improvement at the Frankfurt airport. Amongst several improvements for capacity enhancement, the WVWS was considered and analysed for capacity benefits. These considerations have led to the definition of a project for the implementation of a WVWS at the Frankfurt airport.

In the capacity enhancement study it was found that automation of approach, taxi and departure control is an important precondition for the improvement of the overall capacity situation of an airport like Frankfurt.

CAPACITY ENHANCEMENT PLAN FOR THE FRANKFURT AIRPORT

The runway configuration of the Frankfurt airport is shown in Figure 1. The closely spaced parallel runways (25R/25L or 07R/07L) are used for approaches and departures with dependent parallel operations, whereas the runway (18) can be used for departures only. In the DLR study for capacity enhancement -- among other things -- the following improvements are considered:

- Improvement of approach capacity
    * COMPAS
    * WV Warning System (WVWS)
    * Reduced minimum separation for staggered approaches
    * 4D trajectory control

- Improvement of departure capacity
    *   additional SIDs

- Improvement of ground capacity
    *   Project TARMAC.

For the discussion of the WVWS a brief consideration of two other improvements is important: COMPAS and TARMAC.

COMPAS (Computer Oriented Metering, Planning and Advisory System) is a planning system implemented at the Frankfurt airport in 1989 (Figure 2). It assists the controllers in the management of the arrival traffic by the provision of an optimized plan for the incoming traffic. The planning is done with a time horizon of about 30 minutes. Through a carefully selected set of function keys the controllers can interact with the planning process. The system has been very successfully used by the Frankfurt controllers since its implementation. It will be used for the WVWS to adjust the traffic flow to the available runway capacity and to give the controllers advice for the runways to be used for landings.

TARMAC (Taxi And Ramp Management And Control) is a project of the German Bundesanstalt für Flugsicherung (BFS) and DLR for the development of a system (similar to COMPAS) for ground movement control (Figure 3). This project was started in 1988 and is now in the development phase for an experimental system. For the WVWS, TARMAC can be considered as an extension of the COMPAS functions into the taxi phase and to the departure management.

OVERVIEW OF THE GERMAN PROGRAM

During two extended measurement campaigns (1984-1987 and 1989-1991) WV measurements at the Frankfurt airport have been conducted, the results of which will be discussed in a separate paper by G. Tetzlaff and J. Franke "Vortex Propagation in the Boundary Layer" later in this conference. These measurements were made using an array of propeller anemometers and a LIDAR. The results of the LIDAR measurements will be discussed in another paper by F. Köpp "Investigation of Vortex Structure Using Laser Doppler Anemometer."

With the results of these measurement campaigns, the movement and decay of vortices generated by more than 1000 medium and heavy aircraft have been studied in great detail. It was found that the initial strength of the vortex and the cross wind are the dominant factors for the vortex transport, although the turbulent state of the atmosphere has to be considered as well. Subsequently, a prognosis model for the cross wind component was developed and tested against long-term weather records of the Frankfurt airport.

These results -- together with findings from the capacity study -- have led to the development of three operational procedures for a WVWS. These three potential operational procedures, namely

    *   flow adjustment to predicted wind conditions permitting the reduction of WV separations ("wind prognosis"),

* runway usage strategy with permanent reduced separations dependent on the actual wind ("actual wind"), and

* displacement of the threshold of the left runway of the dual system, so that reduced separations are possible ("displaced threshold")

have been investigated in extensive real-time simulations with controllers from Frankfurt and with pilots from Lufthansa. The results of these simulations will be discussed in a third paper by J. Reichmuth "Alleviation of Wake Vortex Separation Problems at the Frankfurt Airport."

These results have led to the definition of a project for the implementation of a WV warning system at the Frankfurt airport which now will be described in more detail.

CONCEPTUAL STRUCTURE OF THE WV WARNING SYSTEM

From Figure 1 it can be seen that for landings at the Frankfurt airport only the dual system of closely spaced runways is used (dependent parallel operations). At present this system can be operated with a minimum separation of 2.5 nm in a staggered mode, using WV separations.

In the real-time simulations the procedure "displaced threshold" did not find the acceptance of the controllers and the pilots. The two procedures "wind prognosis" and "actual wind," however, have found acceptance, although some improvements were suggested for both procedures by the controllers, which are discussed in J. Reichmuth's paper. These results have led to the conclusion that a combination of the two procedures has to be used as the operational concept for the WVWS at the Frankfurt airport. The fine definition of this combined operational procedure is just under way. A real time simulation is foreseen in the project to validate this procedure with the help of Frankfurt controllers and Lufthansa pilots.

The COMPAS system will play an important role in this concept. One of the features of COMPAS is that the actual "flow" (minimum separations) can be set by the approach controllers using the function keyboard. At the moment this system is only using WV separations for the spacing of the incoming aircraft. In the course of the WVWS project additional separation matrices will be programmed into the system, which can be selected by the controllers in case of changing wind conditions. This is particularly important in the implementation phase of the WVWS at the Frankfurt airport, which will begin by the end of 1992. In this phase a stepwise transition from the present operational procedure, which uses WV separations, to the future system, neglecting the WV separations and using only one standard separation -- of 3 nm -- is planned within a period of 2 years. The COMPAS system will be used in this phase to plan the arrival sequences with the appropriate separations and with a time horizon of about 20 minutes. In addition, COMPAS will also give advice for the runways to be used by the individual aircraft.

It has already been mentioned that in 1992 real-time simulations of the operational concept will be conducted. Subsequently, during the implementation phase at Frankfurt an extensive collection of data will be made and evaluated, to ensure a safe and smooth transition from the present to the future procedures. These data collections will contain -- among other things -- a real-time flow and delay monitoring system, a WV monitoring system, and questionnaires for

controllers and pilots. Similar to the procedure used during the COMPAS implementation at the Frankfurt airport in 1989, the results of these data collections will be evaluated immediately to fine-tune and improve the WVWS during this implementation and transition phase.

CAPACITY GAIN

Capacity investigations have been made at DLR using statistical models and simulation programs. For the capacity improvement project the FAA programs ADSIM and SIMMOD are used, together with the real-time simulation facility ATMOS (Air Traffic Management and Operations Simulator) of DLR. Calculations with statistical models and the real-time simulations mentioned above have shown that considerable approach capacity can be gained from the avoidance of WV separations. The figures calculated with statistical models range from 3 to 8 additional landings/hour and from the realtime simulations from 3 to 5 additional landings/hours. At an airport with a traffic volume like Frankfurt one additional landing/hour brings cost savings of about 10M DM/year due to avoided delays when traffic increases. The final calculations of the expected capacity gain by the WVWS with the SIMMOD and ADSIM programs will be finished by the end of 1991. From initial simulations it has already been seen that such an increase of approach capacity requires a similar increase in ground movement capacity, especially in IFR conditions. The TARMAC project which was mentioned above is supposed to provide this capacity together with the controller support tools to handle the ground traffic.

CONCLUSIONS

In this paper it is described how the transition from basic research to the implementation of a WVWS is conducted in Germany. Extensive measurements, studies, and simulations have led to an implementation project for the Frankfurt airport. From the results of real-time simulations of the WVWS it was concluded that automation tools like COMPAS are required to support controllers in the precise planning of traffic with a time horizon up to 20 min. The implementation of the WVWS at Frankfurt is conducted stepwise and accompanied by careful data recording and evaluation, ensuring a safe and smooth transition. Simulations at DLR will be used to improve the system lay-out even during the field evaluation of the system. A similar implementation philosophy was used for the successful introduction of COMPAS at the Frankfurt airport in 1989.
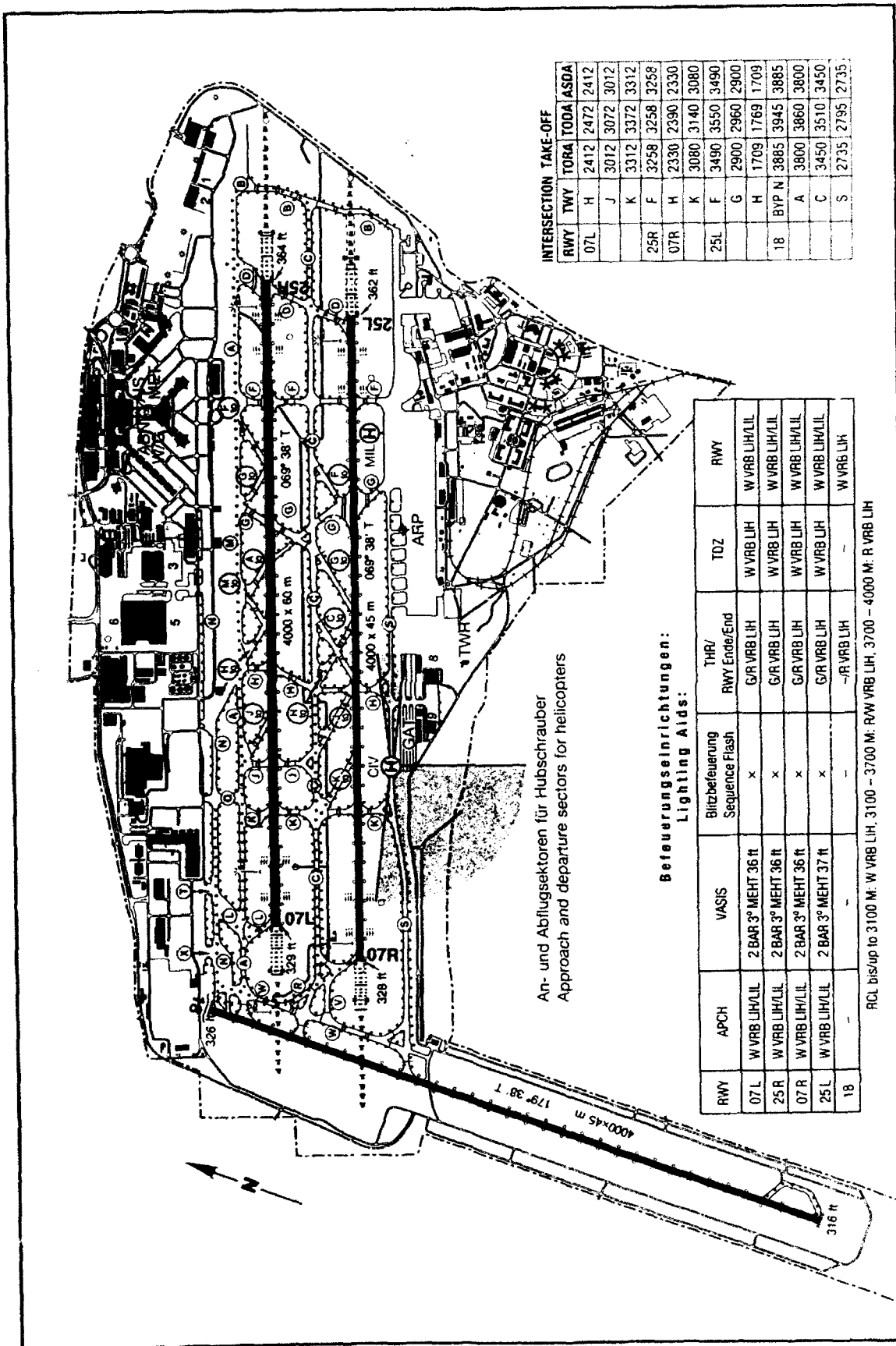
Figure 1. Frankfurt Airport runway configuration.

INTERSECTION TAKE-OFF

RWY	TWY	TORA	TODA	ASDA
07L	H	2412	2472	2412
	J	3012	3072	3012
	K	3312	3372	3312
	F	3258	3258	3258
25R	H	2330	2390	2330
07R	K	3080	3140	3080
25L	F	3490	3550	3490
	G	2900	2960	2900
	H	1709	1769	1709
18	BYP N	3885	3945	3885
	A	3800	3860	3800
	C	3450	3510	3450
	S	2735	2795	2735

Befeuerungseinrichtungen: Lighting Aids:

RWY	APCH	VASIS	Blitzbefeuerung Sequence Flash	THR/ RWY Ende/End	TDZ	RWY
07L	W VRB LIH/LIL	2 BAR 3° MEHT 36 ft	x	G/R VRB LIH	W VRB LIH	W VRB LIH/LIL
25R	W VRB LIH/LIL	2 BAR 3° MEHT 36 ft	x	G/R VRB LIH	W VRB LIH	W VRB LIH/LIL
07R	W VRB LIH/LIL	2 BAR 3° MEHT 36 ft	x	G/R VRB LIH	W VRB LIH	W VRB LIH/LIL
25L	W VRB LIH/LIL	2 BAR 3° MEHT 37 ft	x	–/R VRB LIH	W VRB LIH	W VRB LIH
18	–	–	–	–/R VRB LIH	–	W VRB LIH

RCL bis/up to 3100 M: W VRB LIH, 3100 – 3700 M: R/W VRB LIH, 3700 – 4000 M: R VRB LIH

An- und Abflugsektoren für Hubschrauber
Approach and departure sectors for helicopters

Computer Assisted Arrival Planning
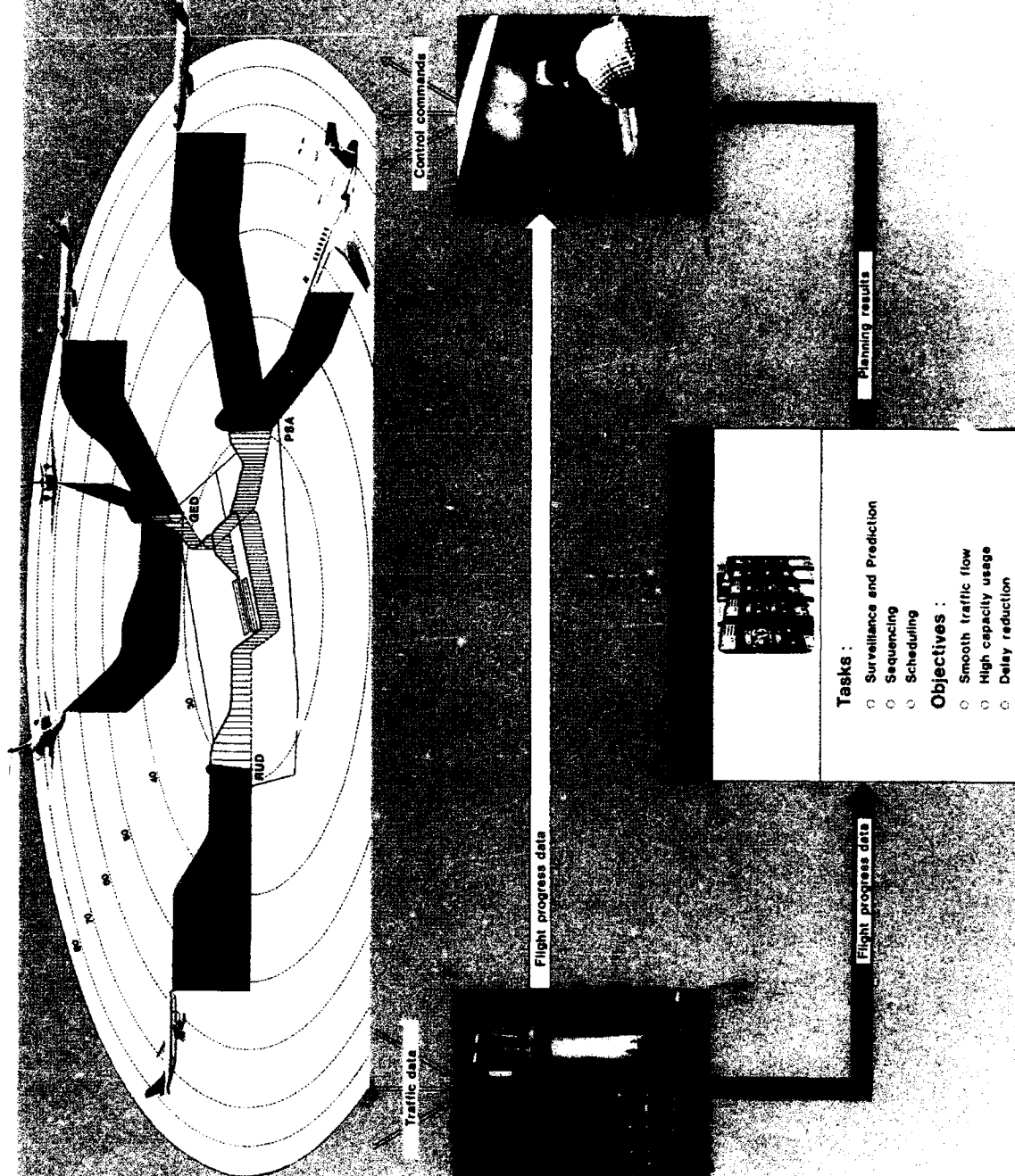
Figure 2. The arrival planning system COMPAS.

TARMAC

Taxi and Ramp Management and Control

Knowledge Base

Ground Operations Planning System
- Optimal Start-up, Push-Back Sequence and Schedule Advisories
- Optimal, Conflictfree Taxi Route Advisories
- Taxi Route Monitoring and Deviation Alert
- Runway Incursion Monitoring

Departure Planning

Airline Operations Management

Weather

Arrival Planning

Airport Operations Management

Surveillance and Identification

Guidance Information

Data Link

Voice

Guidance Signals

Vehicles

Aircraft

Figure 3. The ground movement control system TARMAC.

INCREASED AIRPORT CAPACITY THROUGH REDUCTION OF SEPARATIONS DUE TO WAKE VORTICES

C. Le Roux
DGAC/STNA, Paris

Rèsumè: La rèduction des espacements règlementaires appliquès actuellement, en raison du danger potentiel que repèsente la turbulence de sillage des avions, dans les phases d'atterrissages/dècollages, permettra sans doute de rèduire, du moins partiellement, la saturation de certains aèroports.

L'objectif prèliminaire de la DGAC est de dèfinir un système capable de dètector la turbulence de sillage et de fournir une alarme à l'ATC en temps rèel.

Abstract: The reduction of separation standards due to day to wake vortices during approach and take off phases, will allow without any doubt, an increased airport capacity.

The DGAC first goal is to define a system linked to the ATC allowing a wake vortex detection and alarm display in real time.

SUMMARY

I) FAA LONG TERM STUDY PLAN

II) OPERATIONAL MEANS

III) OPTIMAL VORTEX DETECTION AND ALARM SYSTEM

  *OPERATIONAL NEEDS DEFINITION

  *OPTIMAL REAL TIME VORTEX SENSOR DEFINITION
    -simulation
    -airport tests

  *OPTIMAL REAL TIME VORTEX ALARM SYSTEM
DEFINITION

IV) CONCLUSION

I) FAA LONG TERM STUDY PLAN

DATA COLLECTION

CREATION OF DB1   CREATION OF DB2

AIRCRAFT/SPACING NEW CLASSIFICATION

DEFINITION OF OPERATIONAL MEANS ALLOWING THE
APPLICATION OF THE NEW SEPARATION
STANDARDS
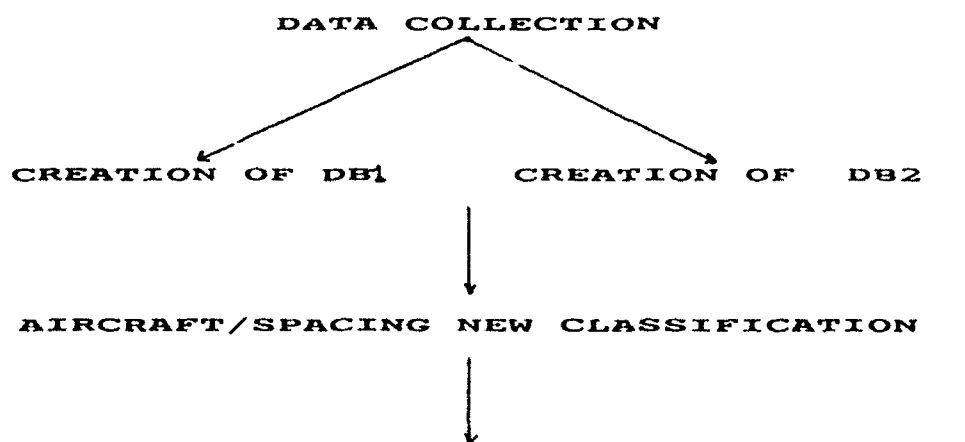
DB1 ="VORTICES MAGNITUDE AND MOVEMENT DATA BASE"

DB2="FOLLOWING AIRCRAFT ALLOWED VORTICES DB"

II) OPERATIONAL MEANS

SEPARATION STANDARDS RELIABLE REDUCTION

↓

POTENTIAL HAZARD KNOWLEDGE

↓

ENVIRONMENTAL MEASUREMENT
(VARIABLE SPACING ALLOCATION)

+

REAL TIME VORTEX DETECTION AND ALARM
(AVOIDANCE PROCEDURE)

↑

DGAC GOAL

III) OPTIMAL VORTEX DETECTION AND ALARM SYSTEM

OPERATIONAL NEEDS   DEFINITION

SENSOR DEFINITION

SIMULATION

AIRPORT TESTS

VORTEX ALARM SYSTEM DEFINITION

OPERATIONAL NEEDS   DEFINITION

GOAL ---> CHARACTERIZE ACCURATELY THE
SURVEILLANCE VOLUME

FIRST PROBLEM APPROACH

MAIN VORTEX CHARACTERISTIC - WIND ROTATION

SENSOR   TILT   PERPENDICULAR TO THE GLIDE

VORTEX HAZARD BETWEEN RUNWAY THRESHOLD AND
MIDDLE MARKER

SURVEILLANCE AREA MUST INCLUDE THE VERTICAL PLAN PERPENDICULAR TO THE RUNWAY AXIS AT MIDDLE MARKER LEVEL

SENSOR DEFINITION

3 POSSIBILITIES ---> LIDAR/SODAR/RADAR

PROBLEMS TO BE SOLVED

GROUND CLUTTER

CUMBERNESS

SPACE AND TIME RESOLUTION
COMPATIBLE WITH GOOD SIGNATURE

COST

SENSOR   PARAMETERS OPTIMISATION THROUGH SIMULATION AND   AIRPORT TESTS

SIMULATION

VORTEX MODEL Vref

SENSOR RESPONSE SIMULATION

ESTIMATED VORTEX CALCULATION Vest
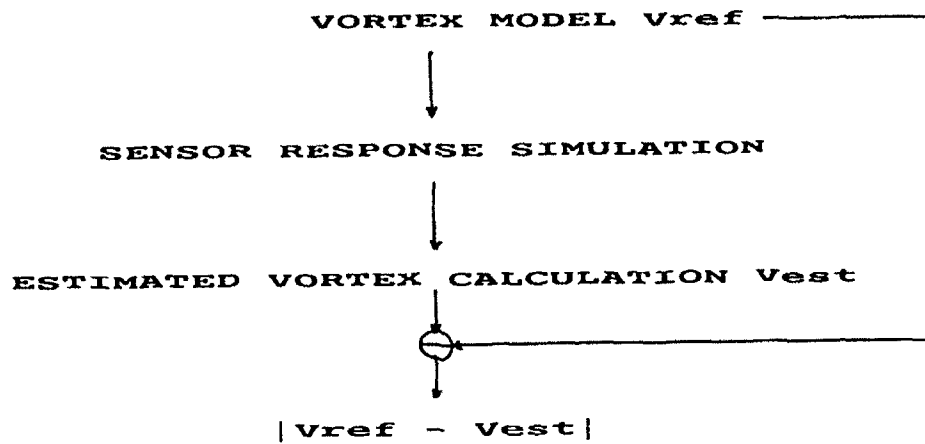
|Vref - Vest|

GOAL----> MINIMIZE |Vref - Vest| BY OPTIMIZING
SENSOR PARAMETERS AND TAKING IN ACCOUNT
CUMBERNESS AND ENVIRONMENTAL CONSTRAINTS

AIRPORT TESTS

VORTICES + SMOKE

OPTIMIZED SENSOR

CAMERA

Vest

Vref

CHECK |Vest - Vref| SMALL
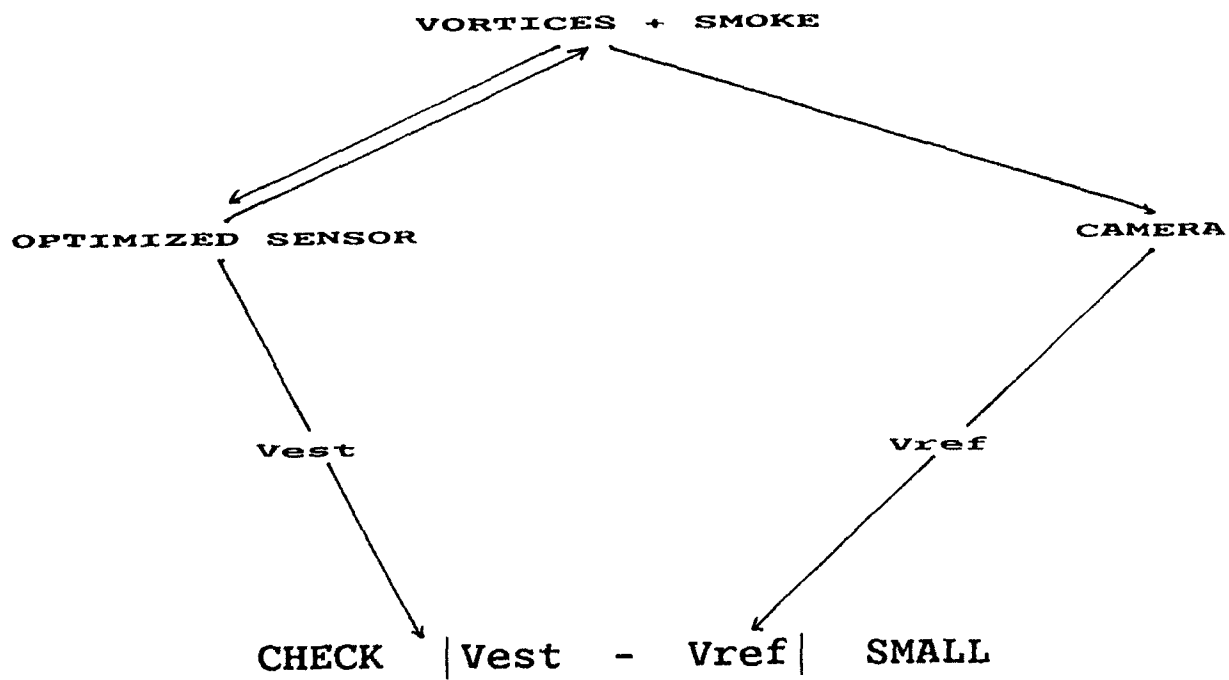
VORTEX ALARM SYSTEM DEFINITION

**REAL TIME VORTEX DATA
ENVIRONMENTAL MEASUREMENTS**

OPTIMAL REAL TIME VORTEX ALARM SYSTEM

IV) CONCLUSION

COOPERATION WITH OTHER COUNTRIES

VORTEX MODEL DEFINITION
INFORMATION EXCHANGES ABOUT   SENSORS DEFINITION

A VORTEX ADVISORY SYSTEM AT SCHIPHOL/AMSTERDAM AIRPORT: FEASIBLE AND MEANINGFUL?

H.J. Berghuis van Woortman
F.R. Polak
National Aerospace Laboratory, NLR
P.O. Box 90502, 1006 BM AMSTERDAM,

The results are given of an aircraft wake vortex measurement program. A wind criterion for a future Vortex Advisory System has been established.

Actual wind data for Schiphol Airport, the Netherlands, concerning 11 months in 1980/81 have been analysed with respect to the feasibility of a VAS-ellipse criterion (semi-axii 7 x 13 kts). The results are based on the peak hours for inbound traffic for runway 06.

On average the windvector lies within the ellipse criterion during more than half the total time a runway can be used. In case the windvector lies within the ellipse, it takes generally not long in succession: in 70% it takes less than 4 minutes. Although a low number of ellipse transitions per hour prevails, transitions of higher frequency ($\geq$ 5 per hour) do occur often enough (30% of total time) to cause problems for the controller to determine whether separations have to be changed or not.

The effect of the above mentioned frequent ellipse transitions can be reduced by the use of a bufferzone. By using a 3 kts-bufferzone around the ellipse criterion and keeping the "red light" on if this zone is not exceeded, about 60% of the highly frequent transitions will be eliminated. These are the transitions which exceed the ellipse boundary with less than 3 kts. The "attention time" are generally very short ($\leq$ 5 min. in 90% of the cases). The "warning times" are even shorter.

It is a general feeling that the present results indicate that the operational benefit of a VAS for Schiphol Airport will be very limited. The main reason for this opinion is that, although the ellipse criterion as such is reliable, due to the rapid and almost unpredictable wind variations which do often occur at Schiphol, the operationally acceptable bufferzone or time lag will probably be so large that, effectively the controller will have to apply large separations almost all the time.

INTRODUCTION

In 1980 and 1981 an aircraft wake vortex measurement has been carried out near runway 06 at Schiphol Airport (References 1,2) by the National Aerospace Laboratory (NLR) on behalf of the Netherlands Department of Civil Aviation (RLD). The main purpose of this measurement program was to develop a suitable criterion to be used in a possible future Vortex Advisory System (VAS) at Schiphol Airport. Such a system must enable Air Traffic Control to determine in real time whether or not the large separations during the approach of smaller aircraft behind heavy aircraft have to be applied. During measurements in the USA it was found that the large separations (up to 6 NM) are necessary only if the wind vector is inside an ellipse (semi-axii 5.5 x 12 kts, major axis in runway direction), because only in that case the conditions are favourable for wake vortices to remain for a long time in the approach zone. If the wind vector is outside this ellipse, separations can be safely reduced to the current minimum of 3 NM. As a result of the 1980/81 measurements at Schiphol, other ellipse dimensions were established for the Schiphol situation, being 7 x 13 kts (semi-axii), provided that the windvector is measured with the meteotower of the Meteo Office near the runway 06 touchdown zone. The reason is that cup anemometers like the one used in this meteotower give systematically higher windspeed readouts during rapid changing wind conditions than the propeller anemometers used in the experimental vortex detection equipment. See also Reference 3.

The purpose of the reported study was to execute an investigation based on recorded actual wind data into the feasibility of the wind ellipse criterion for operational use. A Vortex Advisory System in its simplest form will show the air traffic controller, by means of a red/green indicator, whether the wind vector is inside the ellipse (red light) or outside the ellipse (green light).

The main problem of such a simple system is that often highly frequent red/green/red transitions can be expected. These transitions are treated in "Relation of the Ellipse Criterion to Prevailing Wind Conditions", together with the average time the windvector lies within the ellipse.

Highly frequent transitions form an unworkable situation for the controller. They can be reduced by introducing a bufferzone around the ellipse. For various sizes of this bufferzone a number of characteristic time parameters are analyzed and also the number of bufferzone transitions. To determine the actual effect of the bufferzone on the reduction of highly frequent red/green or green/red transitions a practical method of using the bufferzone has to be defined previously. In this study one example of such a method is investigated. In this example the light remains red if the wind vector moves outwards of the ellipse but lies still in the bufferzone. If the wind vector moves into the bufferzone from the outside, the light stays green until also the ellipse boundary is passed. The properties of the bufferzone are treated in "Effect of Bufferzones".

Because a Vortex Advisory System, which is primarily a system to reduce separations safely during the approach, will offer its greatest (capacity) benefit during hours of traffic peaks, the calculations are made primarily for the peak hours of inbound aircraft at Schiphol Airport.

METHODOLOGY

General

The calculations in this study have been made using a large database of actual measurements at Schiphol Airport. As already mentioned in the Introduction, the ellipse criterion used has semi-axii of 7 and 13 kts. The dimensions of the bufferzone have been varied between 1 and 3 kts width (see Figure 1).

Database

The database consists of 11 tapes, covering 11 months, on which wind measurements at Schiphol Airport are registered. Each minute a registration of wind parameters is given. Each registration consists of an average windspeed and average wind direction (moving averages over 2 minutes), and peak values of the wind speed over the previous 10 minutes. The 1980/1981 vortex measurements which produced the ellipse were based on a part of the same database (References 1 and 2).

Calculated Parameters

The operational feasibility of a Vortex Advisory System, which uses a wind ellipse criterion, depends among others on the total time that the wind vector is inside the wind ellipse and consequently large separations have to be applied. Therefore, the time during which the wind vector is inside the ellipse is calculated as a percentage of the total observation time.

Furthermore, a frequency distribution of the time spans during which the wind vector is continuously inside the ellipse is calculated. This gives information on how long periods of large separations will generally last. Another factor which influences the feasibility of a VAS is how often wind conditions exist during which the wind vector is near the ellipse boundary, causing a high green/red fluctuation rate. Therefore, the number of ellipse passings per hour is calculated, as well as a frequency distribution of it.

To prevent frequent "red/green" transitions, a bufferzone around the ellipse is introduced. Several aspects of such a bufferzone are analyzed. Firstly, the frequency distribution of the time needed for the wind vector to cross the bufferzone, while moving into the ellipse, is calculated. This is called the "warning time" (TW). This is an indication for the time available to the air traffic controller to anticipate a new situation of applying large separations, once a VAS indicated that the wind vector has entered the bufferzone. Secondly, a frequency distribution of a "relaxation time" (TR), being the time needed for an outward moving wind vector to cross the bufferzone, is calculated. This relaxation time is an indication of the delay due to the bufferzone in the transition from a red to a green condition. Thirdly, a parameter called "attention time" (TA) is calculated. This is the time span between the moment that a wind vector moves out of the ellipse, and, having remained within the bufferzone, the moment of a subsequent movement into the ellipse again. In Figure 1 these parameters TW, TR, and TA are illustrated. It must be noted explicitly that

these time parameters are defined and investigated for the present study only and cannot be shown to the air traffic controller in an operational VAS.

RESULTS

Relation of the Ellipse Criterion to Prevailing Wind Conditions

A.   Total time the time vector lies within the ellipse

Assuming that the use of a particular runway is dictated by wind conditions only (no noise preference, a maximum crosswind component of 15 kts and a maximum tailwind component of 5 kts), it is found from the prevailing wind conditions at Schiphol that during the average percentages of the total time the runways can be used (Table 1), the wind conditions are within the relevant ellipses.

From these results its follows that:

-    During peak hours (when short separations are often important), the wind vector lies on average during more than half of the total time within the ellipse criterion boundary.

     This does not imply that only during this time span large separations have to be used, because the frequency of ellipse boundary transitions and the mean time that the wind vector lies in succession within the ellipse are also important (as will be dealt with later);

-    If, instead of only the peak periods, the longer period of the day 5 - 21 h GMT is considered, the average percentage of time that the wind vector lies within the ellipse is greater, due to on average lower wind speeds in the early morning and evening;

-    The percentage for runway 27 is lower than for the other 2 runways, because the strong westerly winds at Schiphol prevail.

     This fact can also be observed from Table 2, which gives the average windrose data from Schiphol as they followed from the measurements.

B.   Frequency distributions of the time that the wind is within the ellipse and the number of transitions of the ellipse boundary.

In Figure 2a the frequency distribution is given of the times during which the windvector is within the ellipse for runway 06, during the peak periods (7 h 30 - 11 h 30, 14 h - 16 h and 17h - 19 h GMT). The distribution is presented in intervals of 4 minutes. From this figure and the detailed numerical results used to produce it, it can be concluded that:

-    In 70% of the cases that the wind vector lies within the ellipse, it takes less than 4 minutes at a stretch, and in 90% of the cases less than 12 minutes. Long periods during which the wind vector lies within the ellipse occur rather seldom.

-    The short periods (< 12 minutes), however, amount together only to about 25% of the total time that the wind vector lies within the ellipse boundaries. Although the tail of the frequency distribution is very "low," it is very extensive, so that the long and the very long periods do contribute considerably to the total time that the wind vector lies within the ellipse.

The mean period length amounts to about 9.5 minutes.

Thus, short periods during which the wind vector is inside the ellipse occur most frequently and they are short when compared to the time needed to change separations in an already established approach sequence. On final approach and base leg, changes are virtually impossible (only overshoots); on the stretches between stacks and base leg, the possibility to change separations depends on the actual traffic situation and is subject to discussion. In many cases the possibility to change separations on short term will be very limited.

The results for the longer period of the day (5 - 21 hrs GMT) for runway 06 and for the peak hours for runway 19R and 27 showed the same characteristics as described above for the peak periods for runway 06.

In Figure 2b, the frequency distribution is given of the number of ellipse passing per hour for the peak periods for runway 06. It shows that 57% of the total time consisted of hours with no transitions and that generally low frequent transitions (< 5 per hour) are prevalent (70% of total time). Nevertheless, ellipse transitions with higher frequencies (≥ 5 per hour) do occur often enough (30% of the time) to cause problems for the controller. The effect of these highly frequent transitions can be dampened by introducing a bufferzone around the ellipse as will be treated in "Effect of Bufferzones."

It is evident from Figure 2b that even numbers of transitions per hour occur far more often than odd numbers. This effect can be explained as follows. Most periods of time that the windvector lies uninterrupted within the ellipse are short compared to an hour. Each period of "wind in ellipse" produces 2 transitions (inwards and outwards). The chance that a short period "wind in ellipse" coincides with a transition from one hour to another is rather small, while only in that case an odd number of ellipse passings per hour can be counted. This means that for low numbers of passings per hour the chance for odd numbers is very small. In case of high numbers of passings per hour the chance for odd numbers rises and equals more or less the chance for even numbers, as can be seen in Figure 2b.

The results for the period 5-21 hrs GMT and for the peak hours for runway 19R and 27 all showed the same tendencies as presented in Figure 2b for the peak hours of runway 06.

Effect of Bufferzones

As explained before, the purposes of a bufferzone around the ellipse criterion is to dampen the effect of highly frequent ellipse boundary transitions. The definition of the "warning time" (TW), the "relaxation time" (TR) and the "attention time" (TA) are already given in

"Calculated Parameters." The numerical values of these parameters have been calculated from the data base for 3 values of the size of the bufferzone, viz. 1, 2, and 3 kts.

In Figures 3, 4, and 5 the frequency distributions in time intervals of 1 minute of TW, TR, and TA are presented for the peak hours of runway 06 for the above mentioned 3 sizes of the bufferzone. It is evident that in the vast majority of the cases the warning, relaxation and attention times are very short (Table 3). In 90% of the cases these times are less than 5 minutes. Especially the warning time TW is generally too short for the controller to be able to change established separations if entry of the bufferzone from the outside should be displayed to him.

The influence of the bufferzone on the frequency of "red/green/red" transitions is dependent on the number of ellipse transitions which do not exceed the bufferzone and how the red or green condition will be defined. If, for example, the VAS-indicator remains red as long as a wind vector which has just moved to the outside of the ellipse, stays within the bufferzone, the percentage Δ of red/green transitions that has been eliminated by introducing the bufferzone, can be represented by:

$$\Delta = \frac{\text{number of ellipse transitions producing a TA}}{\text{total number of ellipse transitions}} = \frac{2 * n_{T_A}}{n_{T_W} + n_{T_R} + 2 * n_{T_A}}$$

In Figure 6 this percentage is given as a function of the dimension of the bufferzone. It shows, e.g., that a 3 kts bufferzone eliminates about 60% of the ellipse transitions, while a 1 kt zone eliminates about 30%.

The relaxation time TR for a 3 kts bufferzone is generally less than 3 minutes, which introduces a 3 kts bufferzone which does not unnecessarily produce long times with a red condition.

The frequency distributions of TW, TR, and TA for the period 5-21 hours GMT for runway 06 and the peak hours for runway 19 and 27 showed only minor differences with those described above.

CONCLUSIONS AND SUMMARY

Actual wind data for Schiphol concerning 11 months in 1980/81 have been analyzed with respect to the feasibility of a VAS-ellipse criterion (semi-axii 7 x 13 kts). The results presented are based on the peak hours for inbound traffic for runway 06, as the differences in the actual wind conditions between the various runways produced no significant differences in the analyzed parameters. Also, the off-peak hours did not change this picture.

This study resulted in the following observations and conclusions.

A.   Ellipse

1.   On average during the peak hours the wind vector lies within the ellipse criterion during more than half the total time a runway can be used (assuming a maximum crosswind component of 15 kts and a maximum tailwind component of 5 kts). This does not imply that only during this timespan large separations always have to be used. The wind variations are of equal importance. Moreover, if the actual use of a particular runway should be determined by vortex dependent criteria, the picture can change considerably.

2.   In case the wind vector lies within the ellipse, it is generally only for a short time in succession: in 70% of the cases the wind vector lies within the ellipse less than 4 minutes.

      Although a low number of ellipse transitions per hour prevails, transitions of higher frequency ($\geq$ 5 per hour) do occur often enough (30% of total time) to cause problems for the controller using the ellipse criterion to determine whether separations have to be changed or not. The frequent changes of the "vortex conditions" using the ellipse criterion as such are not acceptable to the controller in an operational system.

B.   Bufferzone

1.   The effect of the above mentioned frequent ellipse transitions can be reduced by the use of a bufferzone. By using a 3 kts bufferzone around the ellipse criterion and keeping the "red light" on if this zone is not exceeded, about 60% of the frequent transitions will be eliminated. These are the transitions which exceed the ellipse boundary with less than 3 kts. The "attention times" are generally very short ($\leq$ 5 min. in 90% of the cases). The "warning times" are even shorter. This means that, in spite of the bufferzone, the controller often has not enough time to change separations in an established sequence.

C.   Operational aspects

      Various algorithms for using the bufferzone operationally can be designed, e.g., prolonged red light or a yellow light if the wind is within the bufferzone, while previously it was within the ellipse. Also, an extra large bufferzone could be used or an extra long time lag before switching to green.

Nevertheless, it can be expressed as a general feeling that the obtained results indicate that the operational benefit of a VAS will be very limited for Schiphol Airport. The main reason is that, although the ellipse criterion as such is reliable, due to the rapid and almost unpredictable wind variations which do occur often at Schiphol, the operationally acceptable bufferzone or time lag will probably be so large, that effectively the controller will have to apply large separations almost all the time.

Table 1.

Runway	Period	Percentage of time
06	peak periods	57
06	5-21 hrs GMT	62
19	peak periods	54
27	peak periods	50

(Peak periods for inbound traffic mean here:
7 h 30 - 11 h 30, 14 h - 16 h and 17 h - 19 h GMT)

Table 2. Windrose Data For Schiphol

Winddirection	Percentage of observations	Average windspeed (kts)
0° - 30°	6.3	6
30° - 60°	5.5	8
60° - 90°	6.5	9
90° - 120°	5.4	8
120° - 150°	5.3	7
150° - 180°	6.2	7
180° - 210°	9.0	8
210° - 240°	11.3	8
240° - 270°	12.1	10
270° - 300°	10.2	9
300° - 330°	11.9	9
330° - 360°	10.3	9

Total number of observations: 1249392

Table 3.

| Bufferzone →	1 kts	2 kts	3 kts
TW	1 min.	2 min.	3 min.
TR	1 min.	2 min.	3 min.
TA	2 min.	3 min.	5 min.
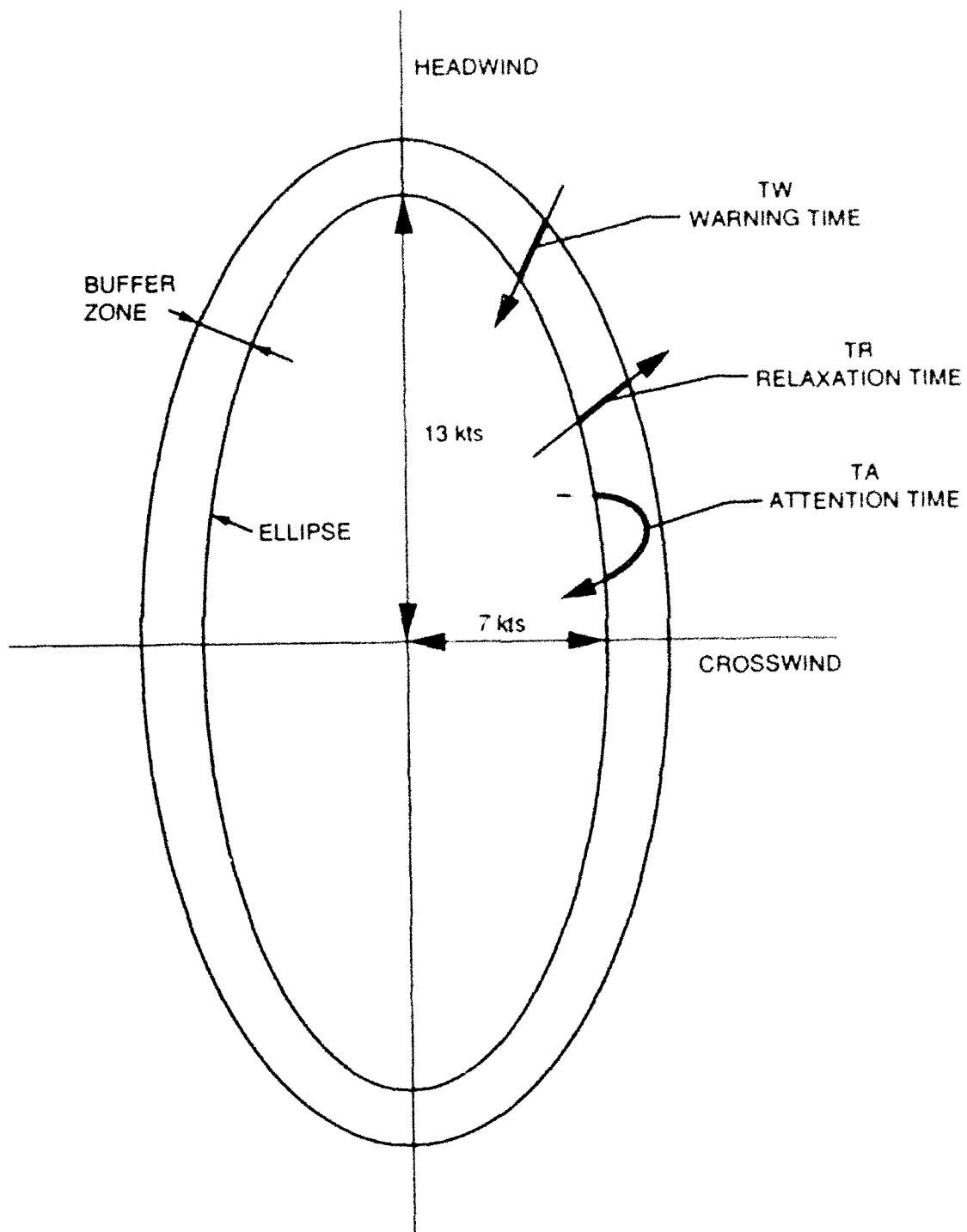
**Figure 1. Ellipse criterion and buffer zone parameters.**
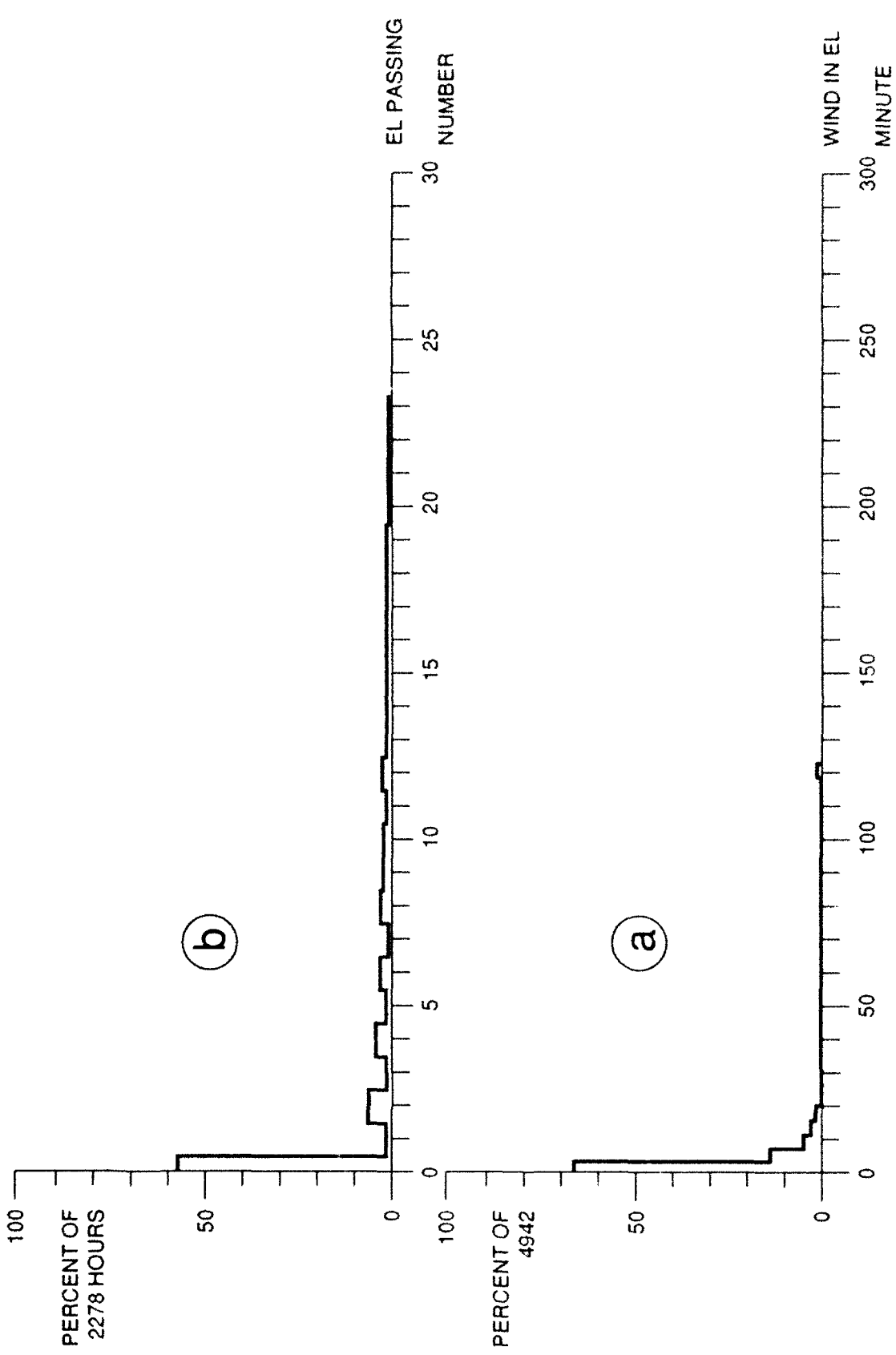
Figure 2. Frequency distribution of the time during which the wind is within the ellipse (a) and the number of ellipse passings per hour (b); peak hours, runway 06.
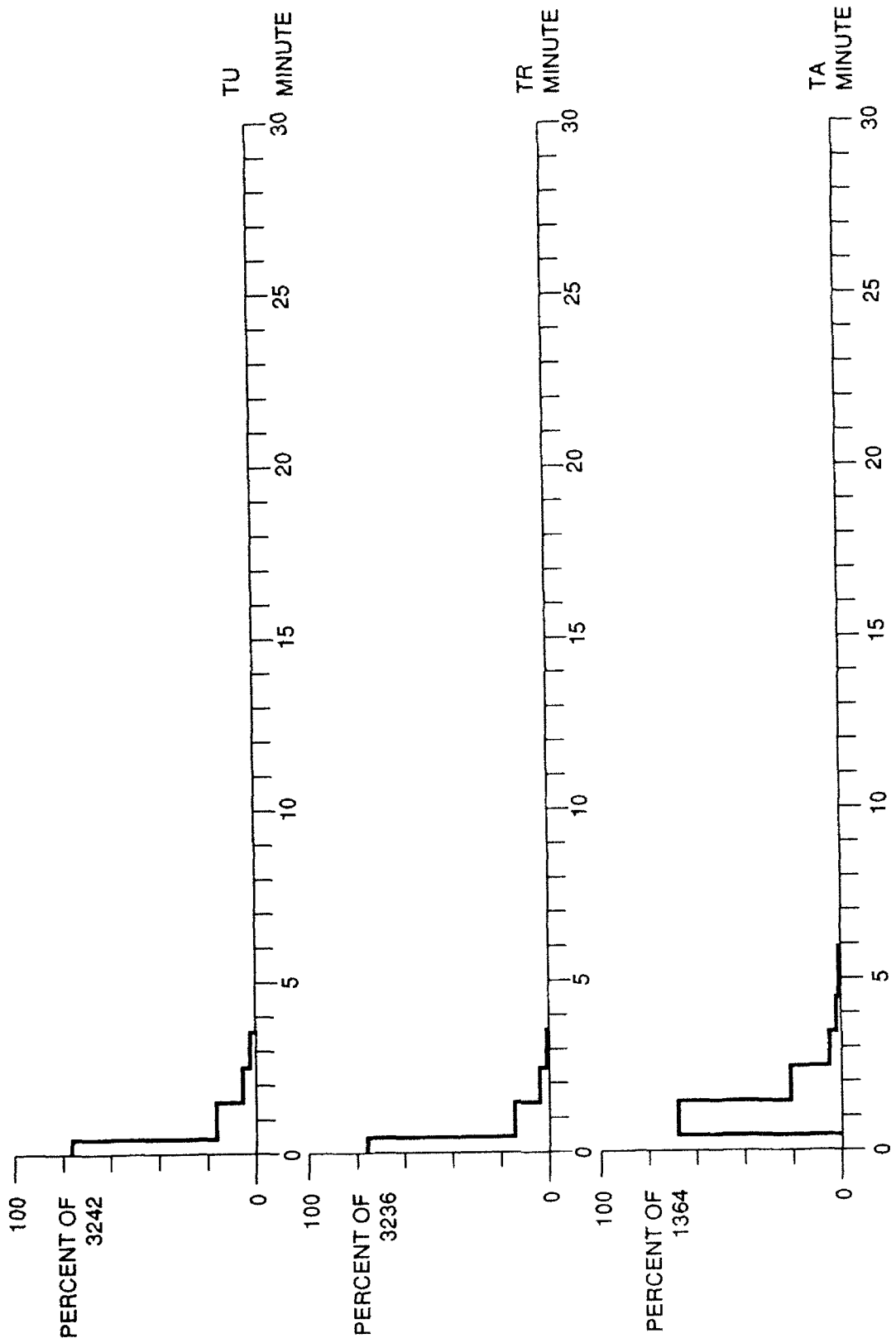
Figure 3. Frequency distribution of the warning time TW, the relaxation time TN and the attention time TA; bufferzone width 1 kt; peak hours, runway 06.
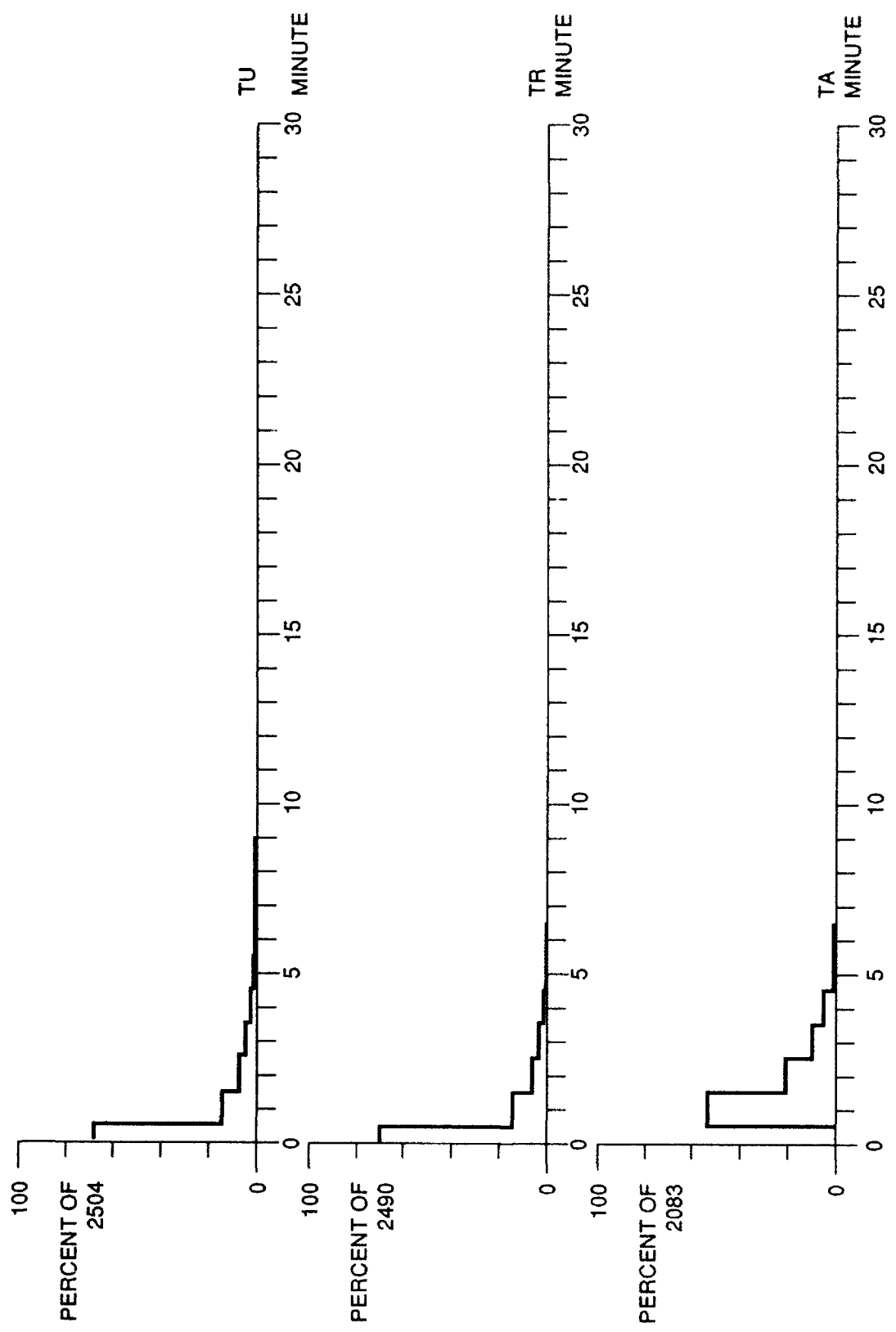
Figure 4. Frequency distribution of the warning time TW, the relaxation time TN and the attention time TA; bufferzone width 2 kts; peak hours, runway 06.
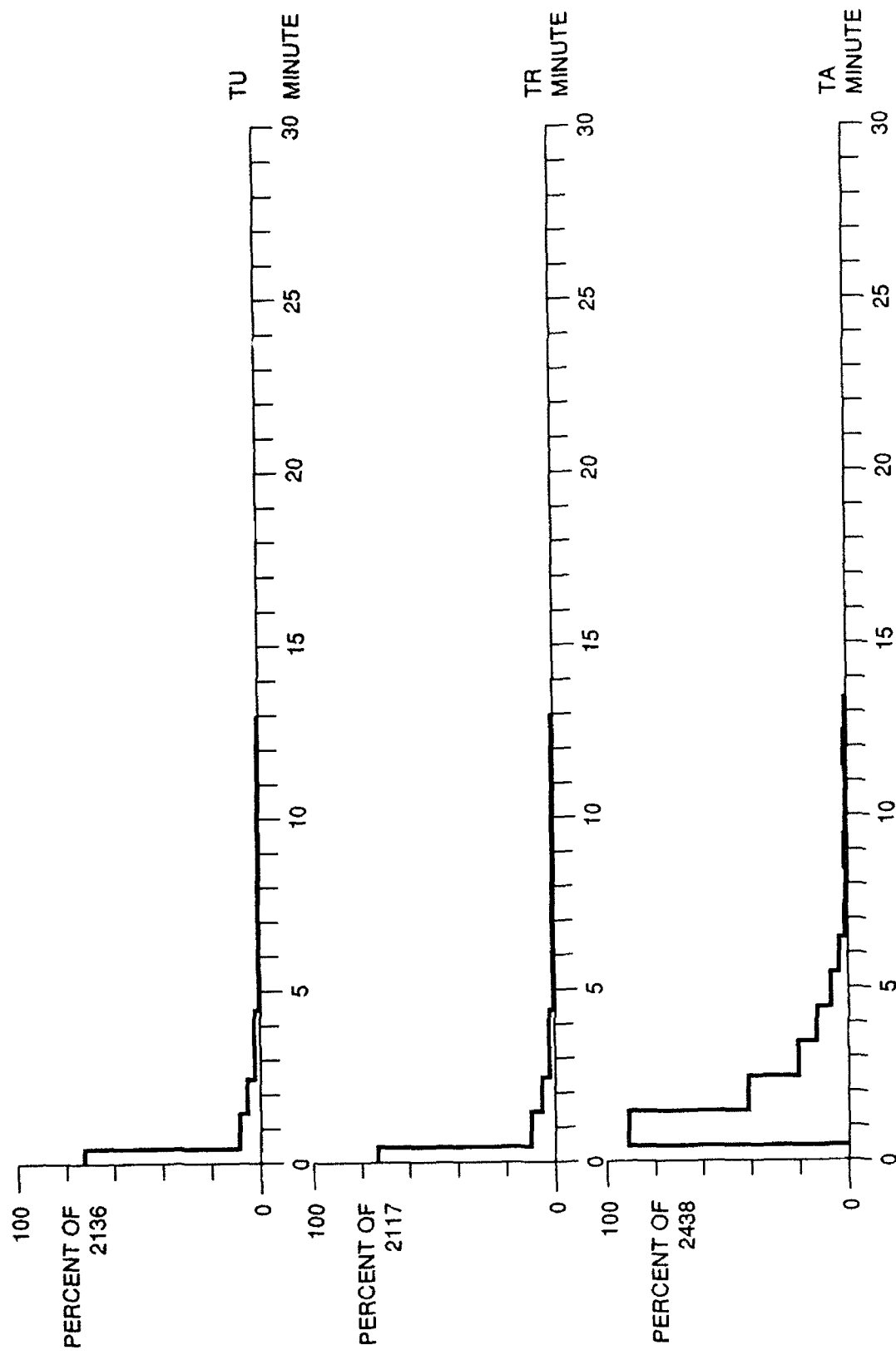
Figure 5. Frequency distribution of the warning time TW, the relaxation time TN and the attention time TA; bufferzone width 3 kts; peak hours, runway 06.
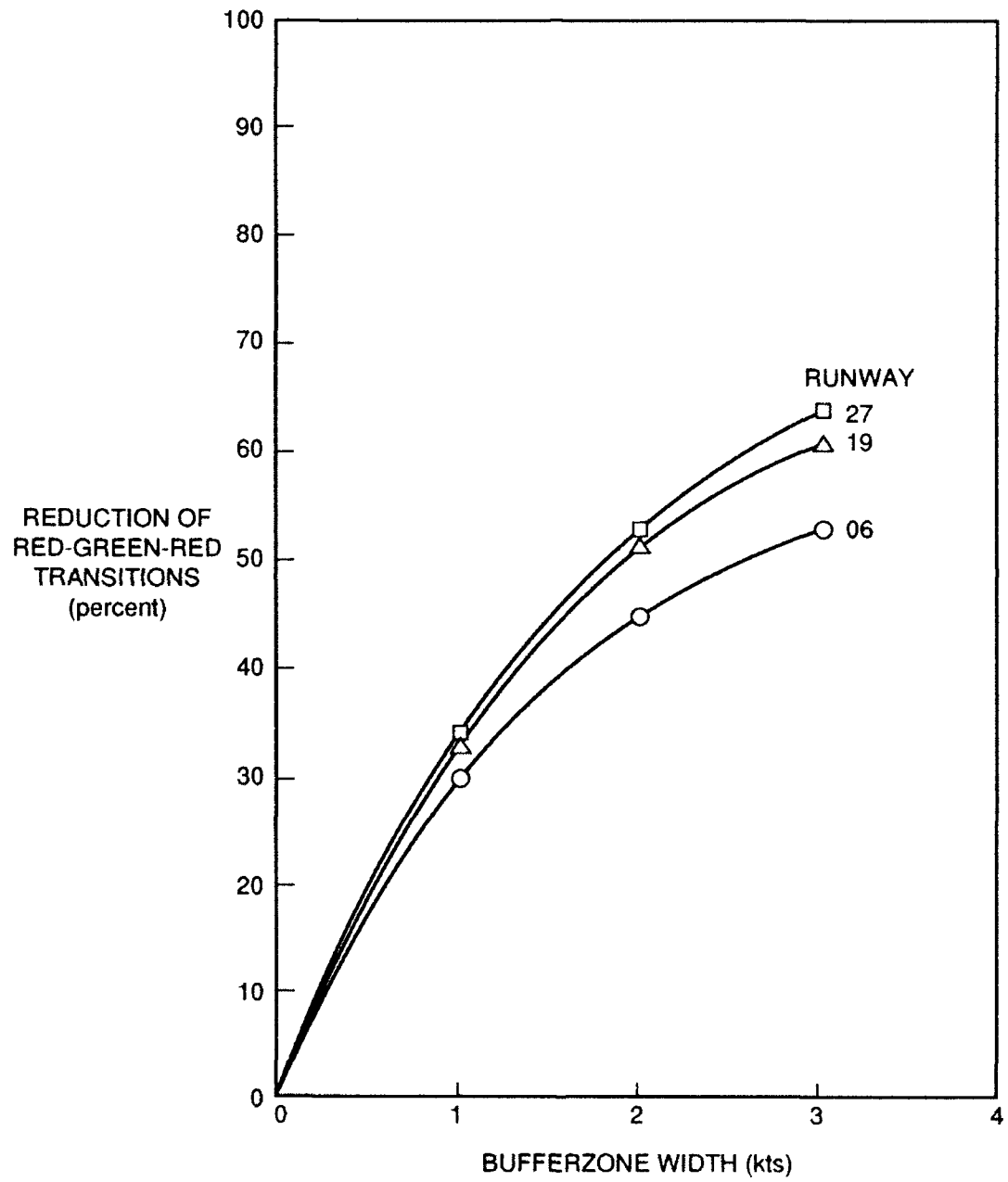
Figure 6. Reduction of red-green-red transitions by introducing
a bufferzone as a function of bufferzone width.

REFERENCES

1.   Laan, J.M. van der, et al., Results from the RLD/NLR Aircraft Wake Vortex Measurement Program, (data collection period April-October 1980), NLR TR 81067 L, June 1981.

2.   Laan, J.M. van der, Results from the RLD/NLR Aircraft Wake Vortex Measurement Program, (data collection period July-October 1981), NLR TR 82058 L, May 1982.

3.   Laan, J.M. van der, Comparison of wind data obtained from a cup anemometer and a set of propeller anemometers. NLR Memorandum VG-83-007 L, April 1983.

WAKE VORTEX: THE PROGRAMME IN THE UNITED KINGDOM

J.B. Critchley
Chief Scientist's Division
UK Civil Aviation Authority
45-59 Kingsway
London
WC2B 6TE

INTRODUCTION

1. Wake vortices have a crucial effect on the UK aviation industry. Heathrow may be more seriously affected than any other airport in the world by the need to apply wake vortex separation minima between successive landing and departing aircraft.

2. Figure 1 shows the Heathrow layout. Operations at Heathrow predominantly use the East-West parallel runways with arrivals and departures segregated. The runway use is alternated between arrivals and departures with the changeover during the afternoon to equalize noise exposure. The constraints on airport capacity, particularly on approach, arise from the nature of the traffic and the segregated mode of operation, which involves streams of closely spaced aircraft; under these circumstances, wake vortices are much more likely to be encountered than with mixed mode operations. Heathrow also has a very 'adverse' mix of aircraft, with both wide-bodied types and small executive jets and props.

3. Figure 2 shows the actual and predicted demand for Heathrow from 1975 to 2005. As can be seen, it is forecast that the demand for Heathrow slots will remain high. It is therefore anticipated that there is a continuing need to make best use of the available capacity, so that the UK must continue to review the wake vortex constraints to maximise - safely - the system capacity.

4. The problems in the UK are not necessarily confined to Heathrow. Recent estimates of UK air traffic for the year 2005 have prompted the UK government to investigate the provision of a further runway to serve the South-East of England. Options being considered include a second runway at Gatwick, Stansted, or Luton. In addition, a second runway is being proposed for Manchester Airport in the North-West of England. Any of these developments could, because of restrictions on land usage, lead to the adoption of segregated modes of operation, which in turn could result in wake vortex separation becoming the principal constraint on traffic growth at other UK airports.

5. The importance of vortex wakes can be seen in the context of main objectives of the UK Civil Aviation Authority, which are set out in Figure 3. Safety is an overriding concern. The objectives stress the requirement to make the best use of the available airspace and airport capacity.

6. Since 1971 the UK has applied Wake Vortex separation criteria between aircraft on approach. Figure 4 shows the development of the rules in the UK. The four group scheme introduced in 1982 was devised as a result of incident data gathered in earlier years, and was designed to provide extra protection for some types of aircraft found to suffer particularly severe disturbance behind heavy group aircraft.

7. The UK 4 leader x 4 follower wake vortex separation categories are compared with the current ICAO separation categories in Figure 5. Figure 6 shows the UK separation criteria.

8. Both the existing sets of criteria, UK or ICAO, are, in the main, empirically based, i.e., on measurements of vortex strength or from analysis of incidents caused by vortex wakes. In view of the limitations with this approach, the changing nature of air traffic demand and the need to make best and yet safe use of the airspace, the UK sees it as essential that there be a focused programme of Research and Development on wake vortex matters.

THE UK RESEARCH AND DEVELOPMENT PROGRAMME

9. The UK programme of work can be divided into three broad subject areas, shown in Figure 7. The first area is the monitoring of the existing criteria. This has been done, and will continue to be done, through the UK wake vortex incident reporting scheme and the associated database and by analysis of the Mandatory Occurrence Reports (MORs) or controller reports under the UK APHAZ scheme. The Wake Vortex incident reporting and analysis scheme is the only one of its type in the world; it is covered in detail in my papers (Refs 1 and 2) on the analysis of incidents reported between 1982 and 1990.

10. The second subject area is termed 'Potential Short Term Expedients'. This title is meant to cover techniques or devices which would make use of the existing basic theoretical and practical understanding of wake vortex behaviour and parameters. The first item in the programme recognises that the existing criteria have been drawn up on cautious assumptions - in particular, conditions of still air, leading to long persistence of wake vortices. It has been shown by the FAA (in Ref 3 for instance), DFVLR (Ref 4) and from the UK database (Ref 1), that the presence of cross winds promotes the drifting or break up of vortices. At many airports, however, wind velocity is particularly variable and, as a consequence, it is difficult to specify regulations or guidance notices which would exploit forecast wind to relax - with safety - wake vortex criteria. As an alternative approach to using predicted wind, the UK is investigating the feasibility of detecting and tracking vortices in order to provide the controller with information to help him decide whether criteria can and cannot be relaxed. Techniques under investigation

include the use of lasers and of radar. These areas of work are described in Trevor Gilpin's paper (Ref 5).

11. The second item refers to the concept that the controllers in the UK have to remember a 4 x 4 matrix of separations. Clearly more wake vortex aircraft groups could facilitate the increase of runway throughput rates, but a constraint on the use of more groups is controller ability to remember large matrices. The issue of computer assistance will continue to be examined but in the short term the UK is considering whether the current categorisations can be safely modified to produce a more easily remembered scheme. A suggestion based on constant increments of spacing is covered in Steve Sherratt's paper (Ref 6).

12. The third area is Longer Term Objectives. If better use of the airspace is to be made, then several things would need to be considered. First, the number of categories of aircraft may have to be increased - the ultimate ideal would be to determine the minimum acceptable separation for each possible pairing of leader/follower aircraft in the meteorological conditions which pertain. Second, the grouping would need to be included as part of any computer assistance provided to future controllers.

13. In order to achieve these goals the prime need is to establish reliable mechanisms for evaluating proposed wake vortex schemes, in terms of both safety and efficiency.

14. The UK proposes to do this by building on the methodology used to determine other separation standards, such as those applied to North Atlantic traffic, which are determined through the use of Target Levels of Safety (TLS) and computer modelling to establish risk levels. For wake vortex risks the TLS could be developed from the Joint Airworthiness Requirement (JAR) 25.1309. This requires that no one factor should contribute a frequency of greater than 10^{-9} to the risk of an accident per flight hour. Based on the average flight length for aircraft in UK airspace, this translates to one accident in 10^9 landings. However, in this context it should be noted that the global risk factor for Instrument Landing Systems set in the ICAO SARP (Ref 7) is 1 accident in 10^7 landings. This global risk factor is defined as 'the average rate of a fatal accident during landing, due to failures or shortcomings in the whole system, comprising the ground equipment, the aircraft and the pilot'.

15. Since the objective of vortex criteria is to avoid accidents, which must therefore be very infrequent events, it is seen as more fruitful to work in terms of a TLS for serious incidents, which would (say) be a factor of 100 higher than that for accidents. It is clear that a serious incident will need to be defined in precise terms; such a definition would have regard to the height of the incident and would consider the induced roll angle in the follower aircraft and any height loss. This leads to a diagrammatic representation of the possible classification, using the JAR terminology, similar to Figure 8.

16. There are two points to note: first, the shapes of the boundaries are not yet known; it will be necessary to determine their shape with the help of airworthiness experts. Second, this approach provides a means of comparing the various different criteria schemes.

17.	As indicated earlier, the UK has recognised that future ATC systems are likely to include considerable computer assistance to controllers; a multiple wake vortex system is almost certain to require computer assistance. Aids to the approach controller have already been under development, both in the UK, through our research programme at DRA Malvern, and in other countries. Steve Sherratt's paper (Ref 6) discusses how the system might be used to support different wake vortex categorisation schemes.

INTERNATIONAL COOPERATION

18.	This paper has considered the UK situation, but wake vortex is a problem faced by many nations. In recognition of this, the UK has formed international agreements to co-operate, and share tasks and information, with the FAA and France on Wake Vortex research. In addition, the UK co-operates informally with the German Authorities.

19.	These agreements are seen as essential to the UK programmes, as they expand the knowledge base, spread costs and promote the implementation of solutions. The UK will, of course, seek to play its full part in the agreements.

CONCLUSIONS

20.	The CAA has an overriding concern to ensure safety of aircraft operations in the UK; it is also tasked with ensuring that the best use is made of UK airspace. These objectives mean that Wake Vortex problems are of serious and continuing concern, particularly in respect of operations at Heathrow. Traffic forecasts and other proposed airport developments indicate that Wake Vortex separation will continue to be an important issue for UK operations.

21.	The UK is developing an extensive programme of research and analysis activity which will address monitoring of the existing criteria, and short and longer term development objectives.

22.	Wake Vortex matters are international and the UK has established a number of bilateral agreements designed to foster co-operation on R&D activities. These will be actively supported.
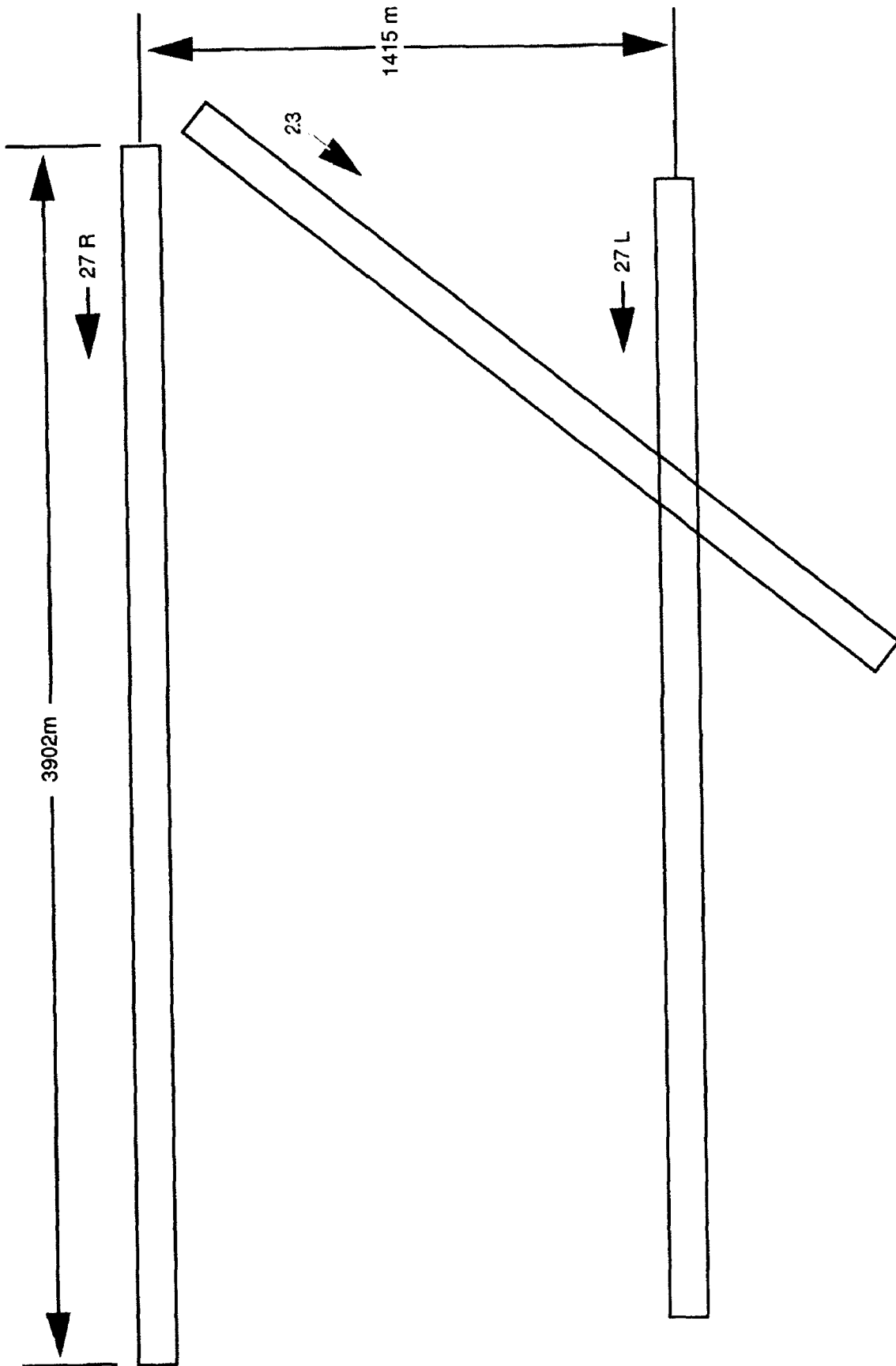
Figure 1. Heathrow runways.

27 R

27 L

23

1415 m

3902m
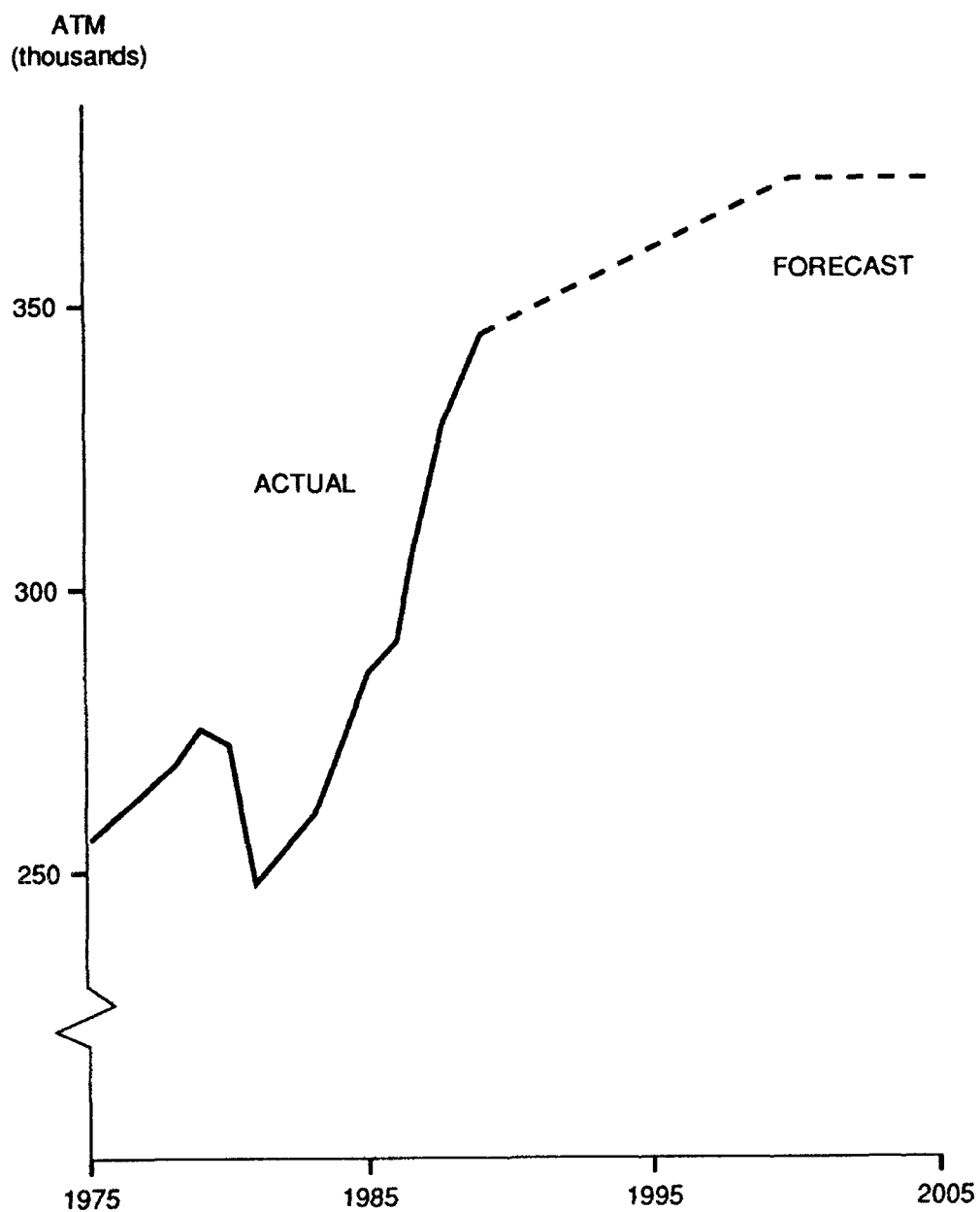
Figure 2. Heathrow Airport: air transport movements.

From CAP 570: Traffic distribution policy and airport and airspace capacity, the next 15 years. CAA July 1990.

6-6

-       Maintain, and where possible increase, existing safety standards.

-       Increase air traffic service capacity in anticipation of increased demand.

-       Increase the flexibility of service to users and optimise the efficiency of their operations.

-       Take advantage of new technology, both in the air and on the ground.

-       Modernise existing systems to increase reliability and efficiency.

Figure 3. UK CAA objectives.

Pre-1972	3 N miles behind Heavy Aircraft
1972	5 N miles/2 minute (separation between large leaders and smaller followers)
1972	UK introduce Wake Vortex Incident Reporting Scheme
1978	ICAO 3 x 3 Matrix Scheme
1982	UK 4 x 4 Matrix Scheme
1983	Wake Vortex Incident Database commissioned

Figure 4. Development of UK wake vortex rules.

CLASSIFICATION

Category	ICAO and Flight Plan (Kg)	UK (Kg)
Heavy (H)	$\geq 136,000$	$\geq 136,000$
Medium (M)	$< 136,000$ $> 7,000$	$< 136,000$ $> 40,000$
Small (S) (UK only)	——	$\leq 40,000$ $> 17,000$
Light (L)	$\leq 7,000$	$\leq 17,000$

Figure 5. Summary of differences between ICAO and UK wake vortex criteria.

Leader Follower	Heavy	Medium	Small	Light
Heavy	4	*	*	*
Medium	5	3	3	*
Small	6	4	3	*
Light	8	6	4	*

+ A corresponding table may be constructed with time equivalents.

* Separation for vortex reasons alone unnecessary.

Figure 6. UK minimum separation for final approach (N miles).+

Monitoring Existing Criteria

- To establish leader/follower combinations noticeably affected by the criteria
- To provide data for Development activity

Potential Short Term Expedients

- Use of Meteorological Factors
- Difference - based Categorisation Schemes

Longer Term Objectives

- Tools for the evaluation of the 'safety' of separation criteria
- Multiple Grouping Schemes
- Computer Assistance to the Controller

Figure 7. UK research and development programme.

MINOR

HEIGHT OF
OCCURRENCE

MAJOR

HAZARDOUS

CATASTROPHIC

ROLL ANGLE
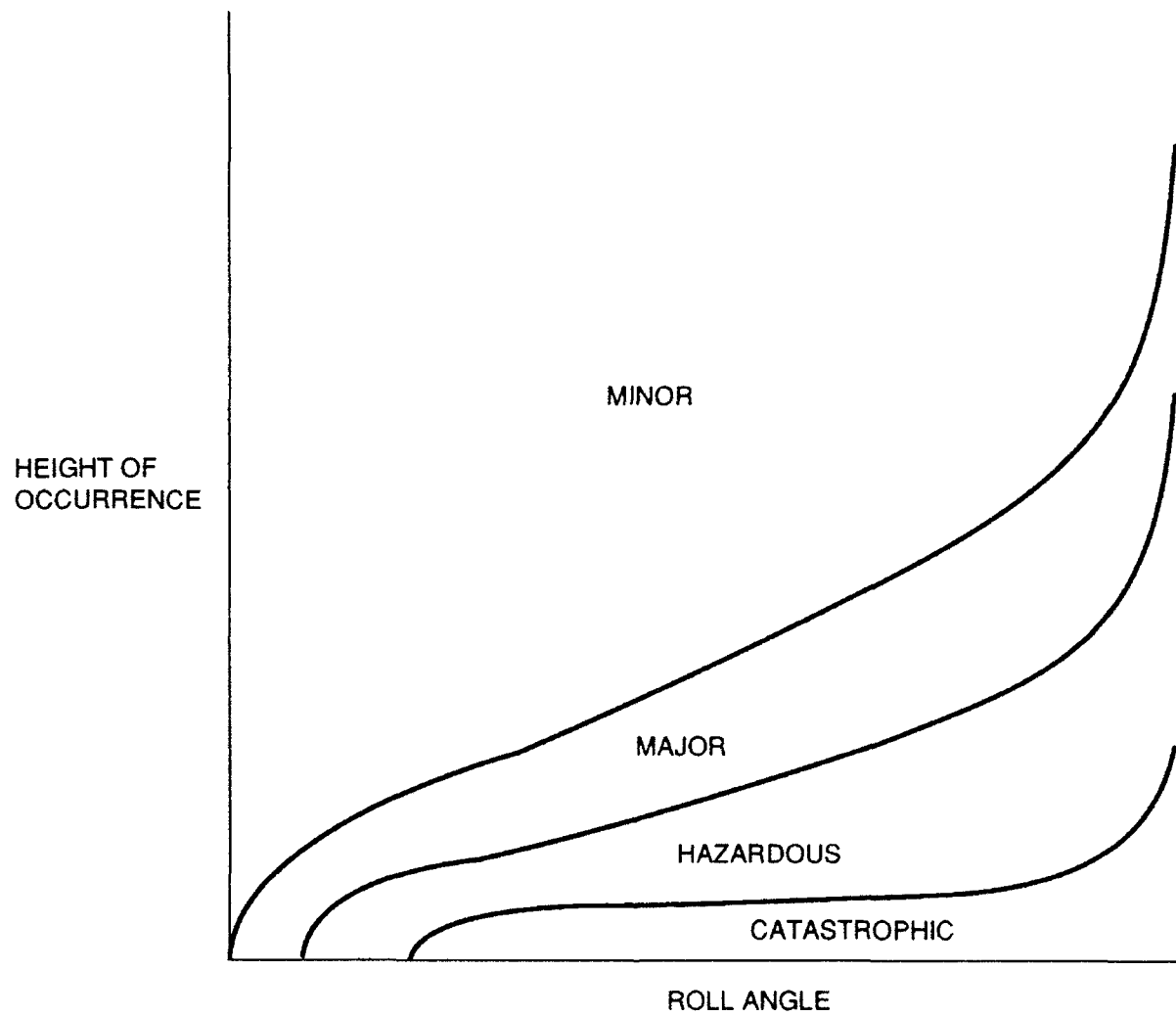
Figure 8. Possible wake vortex JAR 24.1309 categorization
(for illustration only).

REFERENCES

1.   J.B. Critchley, P.B. Foot. CAA Paper 91015: United Kingdom Civil Aviation Authority Wake Vortex Database: Analysis of Incidents reported between 1982 and 1990: August 1991.

2.   J.B. Critchley and P.B. Foot. United Kingdom Civil Aviation Authority Wake Vortex Data base. Analysis of incidents reported between 1982 and 1990. International Wake Vortex Symposium, Washington DC, October 1991.

3.   J.N. Hallock, ed. FAA Report FAA-RD-770-60: Proceeding of the Aircraft Wake Vortices Conference (March 5-7, 1977): 1977.

4.   R. Ulken. DFVLR Communication Note: Investigation into Aircraft Wake Vortex of Landing Aircraft at Frankfurt Airport: May 1988.

5.   T.J. Gilpin: A UK Assessment of Appropriate Technologies for detecting and tracking Wake Vortices in the Approach Area. International Wake Vortex Symposium, Washington DC, October 1991.

6.   S.R. Sherratt: Reclassification of Wake Vortex Groups International Wake Vortex Symposium, Washington DC, October 1991.

7.   Annex 10 to the convention on International Civil Aviation: ICAO SARPS vol 1 page 197: April 1985.

WAKE RESEARCH PROGRAM IN USSR

Professor Sergei M. Belotserkovskii
Central Aerohydrodynamics Institute (TsAGI)
Moscow, USSR

INTRODUCTION

The basic research in this field is conducted in the Central Aerohydrodynamical Institute (TsAGI) and Flight Research Institute (LII) jointly with some other organizations.

This problem is of interest in connection with flight safety maintenance and making a better use of all the possibilities of aviation. The purposes are as follows:

- justification of allowed time intervals at take-off and landing;

- flight in dense echelons;

- refueling in flight;

- load dropping and scattering of small particles;

- safety maintenance of helicopters near obstacles;

- flight accident investigation.

In this connection it is required that the following problems be solved:

- determination of the wake position and the velocity field in the wake;

- the study of the aerodynamical effect of these fields;

- the analysis of the dynamics of disturbed airplane motion;

- the analysis of the load motion and the scattering of small particles;

- helicopter motion near obstacles.

The problem solving is based on the synthesis of three approaches:

(1)   numerical modeling;

(2)   laboratory experiments;

(3)   flight tests.

Two reports are dedicated to the peculiarities of flight tests in USSR. A method of study of wakes behind airplanes is considered in the report presented by Yu. A. Zavershnev and V.K. Kushnerev (Figure 1). Some results of wake tests are given in the report presented by A.N. Zamyatin (Figure 2).

RESEARCH METHODOLOGY

The basic peculiarity of our methodology is as follows. Computer-aided mathematical modeling becomes the main source of information for us. That allows us to answer a large number of questions in a short time, the expenditures being small. Such an approach is especially important when analyzing dangerous situations, for instance, airplane or helicopter flight near the ground or water.

Laboratory experiments and flight tests will always be of great importance for our work. Simplified schemes and models are designed using their results. The semi-empirical taking into account vortex diffusion in the far wake may serve as an example.

The second important role of the experiments is the verification of the main results and deductions made from the calculations. To verify them, it is unnecessary to model the dangerous situation fully. For instance, it is enough to verify the results of modeling the flight at high angles of attack at a sufficient height and not near the ground.

The aerodynamical problems are solved using the method of discrete vortices (MDV). The clarity of the physical images and the constructivity of approach are united with the mathematical validity of the method and its conveniency for computer realization. That maintained a high reliability and economy of our programs (Figure 3).

We have been developing this method since 1950.

VORTEX AEROHYDRODYNAMICS, A NEW BRANCH
OF FLUID AND GAS MECHANICS

At the present time it may be said that the forming of a new original branch of fluid and gas mechanics, vortex aerohydrodynamics, is being finished. It unites various branches of aerodynamics and hydrodynamics where the influence of wakes and vortex boundaries is determinant.

MDV serves as an adequate mathematical description of the considered phenomena. It should be noted that MDV is a natural, convenient and a very efficient combination of the three following aspects of the problem:

- physics,

- mathematics,

- computer calculations.

The problems solved by vortex aerodynamics are as follows:

- separated flow around bodies;

- aerodynamics of airfoils (wings, propellers) when a wake (a stationary or non-stationary one) is formed behind them;

- outflowing of jets into a flooded space and/or a sweeping flow;

- interaction of bodies with free boundaries (a blow of a floating body on the water, entering the water, planing);

- turbulent flows in jets and wakes;

- acoustical characteristics (fields) for the above-mentioned problems.

Possible fields of application are: aviation, including parachute design, ship building, industrial aerodynamics, etc.

Transition from isolated programs to designing a fundamental program set has become a new stage in that field (Figure 4). Some programs from this set may be adapted for personal computers.

SOLVING CLASSICAL PROBLEMS OF AERODYNAMICS

The calculations of near wakes requires solving non-linear problems concerning the flow around an airplane or a helicopter. Wakes are determined in the process of calculations.

The first stage of the method formation was solving classical problems of aerodynamics. Two schemes of the medium have been developed:

(1)   the ideal fluid scheme;

(2)   the scheme "ideal fluid and boundary layer".

Examples of modeling important aerodynamical phenomena are given in Figures 5 to 8.

The approaches developed allowed to describe many known effects without introducing additional hypotheses, namely:

- separated flow around a plate with the formation of Karman's wake (Figures 5-6);

- separated flow around a cylinder (Figure 7);

- rolling up of the vortex sheet at the wing into plaits;

- forming of vortex plaits on the sharp leading edges of wings of various planforms;

- the drop of the thrust and the flutter of a helicopter propeller when a helicopter descends and gets into its own wake (Figure 8).

FAR WAKE

The determination of the far wake is connected with the necessity to take into account vortex diffusion. An approximate method based on the exact solution of an isolated vortex diffusion equation and flight test data concerning real wake decay is developed.

Measurements made in wind tunnels behind airplane models show that the characteristics of the near wakes agree very well with our calculations (Figure 9). But at great distances (more than 1 km) vortex diffusion influence becomes noticeable.

In Figure 10 the development of the wake behind an IL-76 airplane is shown.

SOME APPLICATIONS

The near wake is of major interest for helicopters. It exerts a strong influence on helicopter aerodynamics, especially when we consider flight near the flow boundaries. The influence of the ground on the wake behind a helicopter propeller is shown in Figures 11 and 12.

Helicopters often work near the flow boundaries (mountain slopes, the walls, floor, ceiling of a construction, etc.). Thereby the propeller thrust changes and a rolling moment appears.

The descent and the landing of a helicopter are crucial flight regimes. The correlation of vertical and horizontal velocities must be chosen so that no vortex ring state should occur. Mathematical modeling methods allow curtailing these dangerous and labor-consuming tests considerably.

The maneuvers of fighters and attackers are being performed at high angles of attack. The wing wake acts on the fin-rudder unit. If the airplane has one rudder fin, there occurs a loss of stability and stalling into spin (Figure 13).

During group flights of maneuverable airplanes or flight in dense echelons it is dangerous to get into intensive wakes. Such wakes calculated at high angles of attack (Alpha=25, 45, 90 deg.) are shown in Figures 14, 15, 16.

EXAMPLES OF CATASTROPHY ANALYSES

Methods of mathematical modeling help to establish the causes of aviation crashes in most complicated situations. Two examples of such analyses are given below.

1. In the beginning of 1987 a Yak-40 crashed in Tashkent. It took off after an IL-76. The Yak-40 took off 65 seconds later than the IL-76, so that the requirements of the flight manual were met. All the flight parameters had been deciphered, but the cause of the abrupt roll of the Yak-40 remained unknown. Mathematical modeling gave the solution of the problem: the cross wind (it was known) swept one of the vortices formed by the IL-76 onto the middle of the runway (Figures 17, 18, 19).

    All calculated data agreed with the records of the flight data recorder system of the Yak-40.

2. Mathematical modeling allowed establishing the most probable circumstances of the cosmonaut Yuri Gagarin's death. He died together with an experienced pilot Seryogin in a crash during a training flight in a MiG-15 on the 27th of March, 1968. There was no flight data recorder system in the plane. Nevertheless, all the flight parameters before flying into the ground were determined during thorough investigations. Besides, the airplane position and the flight regime one minute before the crash were known.

    The analysis of the known flight data and modeling of the last minute of flight led us to the following conclusions. The most probable cause of the crash was getting into the wake of another airplane and stalling into spin (Figure 20). The situation was also aggravated by bad weather and shortcomings in the organization of air traffic.

CONCLUSION

To push the problem economically and effectively is to make a wide use of computer simulation methods combined with laboratory and flight experiments.

Most operative and specific results are expected to be achieved in this field.

In the near future it will be very useful to compute admissible areas and time intervals for take off and landing of the main types of aircraft under conditions of various levels of cross wind. Such data makes it possible to increase effectiveness of airfields and make flights safer.

Modern gains of computer vortex aerodynamics also permit to increase effectiveness of:

- air accidents investigation

- helicopter flights close to obstacles

- aircraft and helicopters flight tests

- cargo air-open transportation and air-drop.
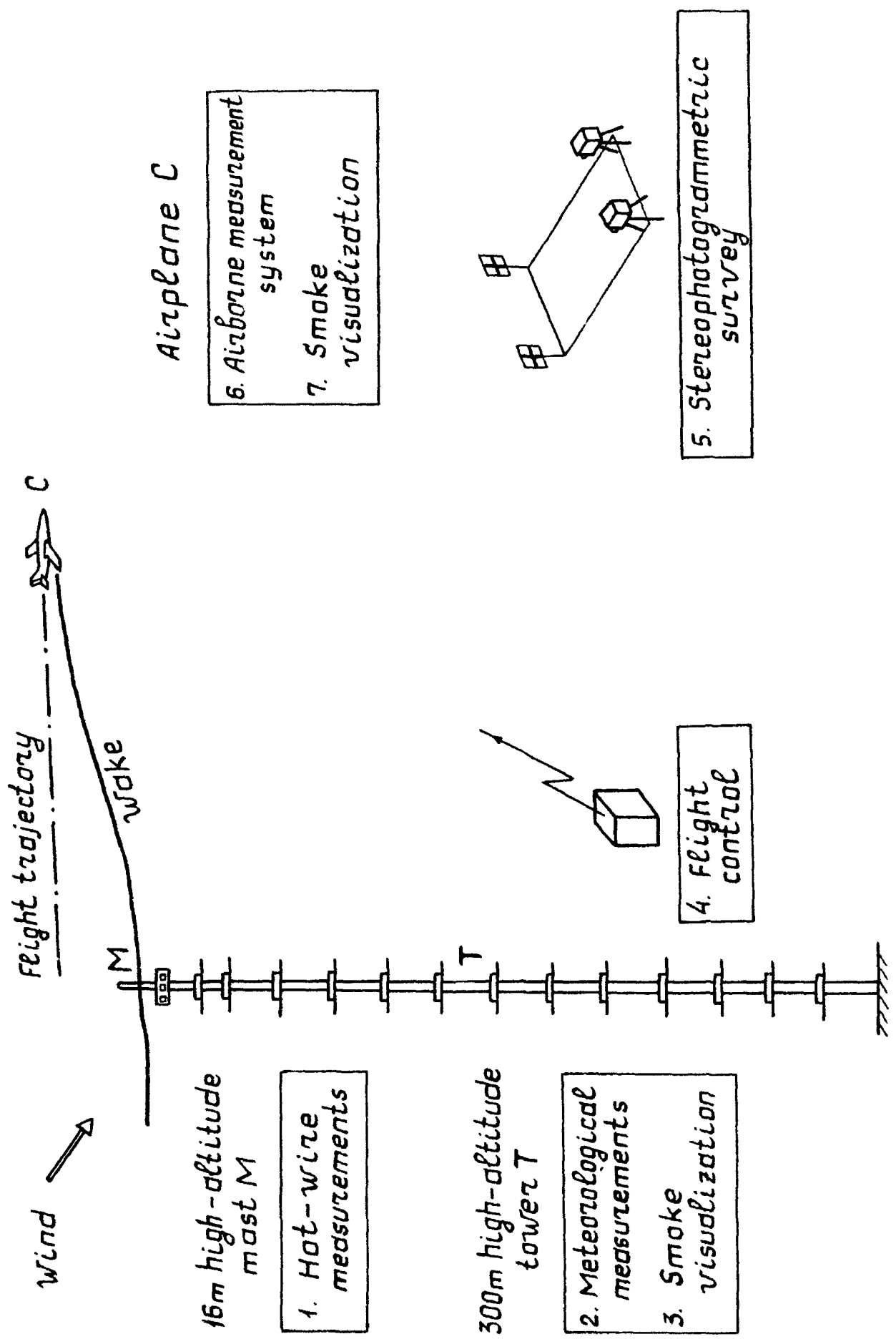
Figure 1. Scheme of the experiment.

Wind

Flight trajectory

wake

C

M

T

16m high-altitude mast M

1. Hot-wire measurements

300m high-altitude tower T

2. Meteorological measurements

3. Smoke visualization

4. Flight control

Airplane C

6. Airborne measurement system

7. Smoke visualization

5. Stereophotogrammetric survey
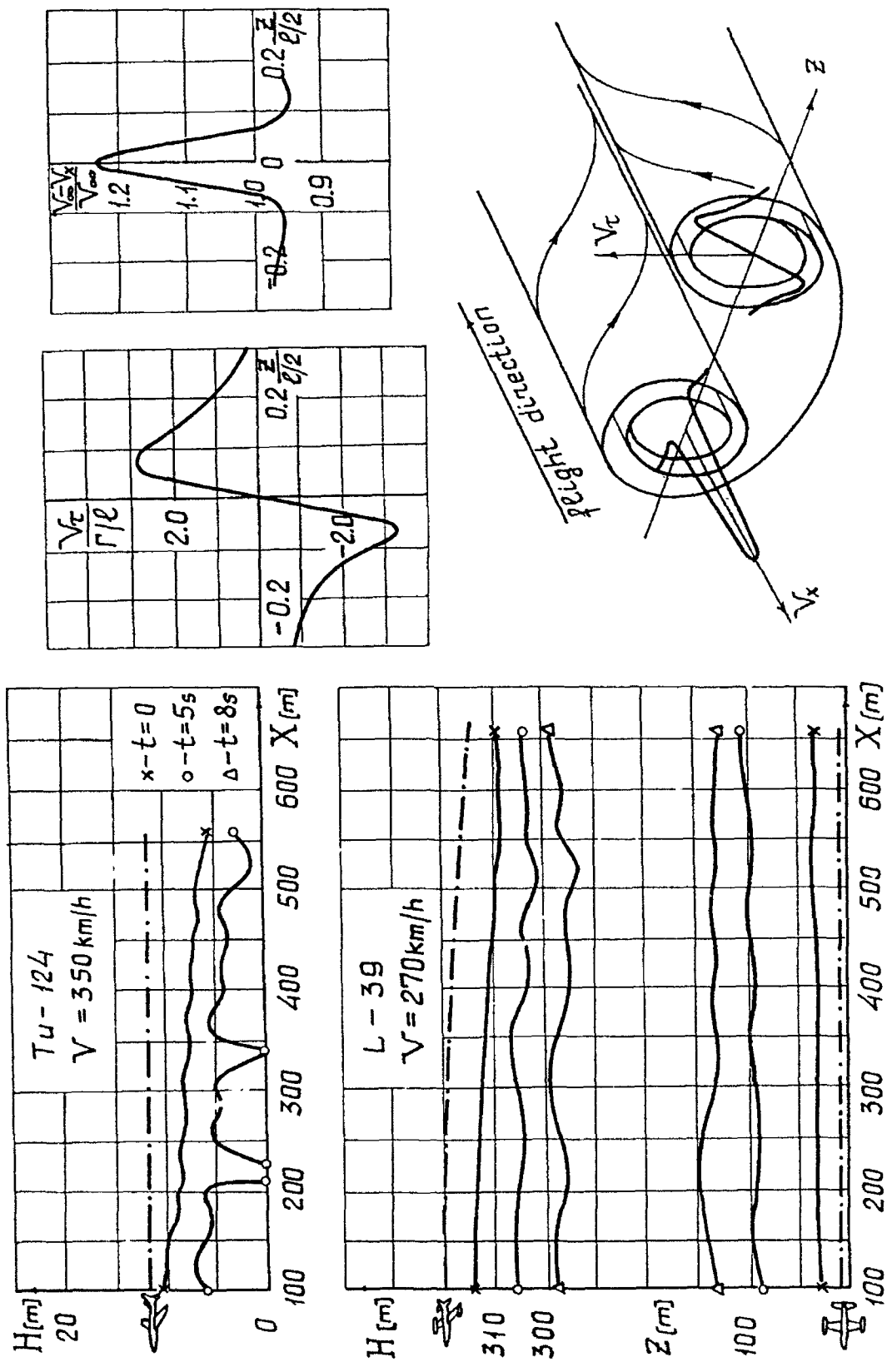
Figure 2. Stereophotogrammetry method; hot-wire method.
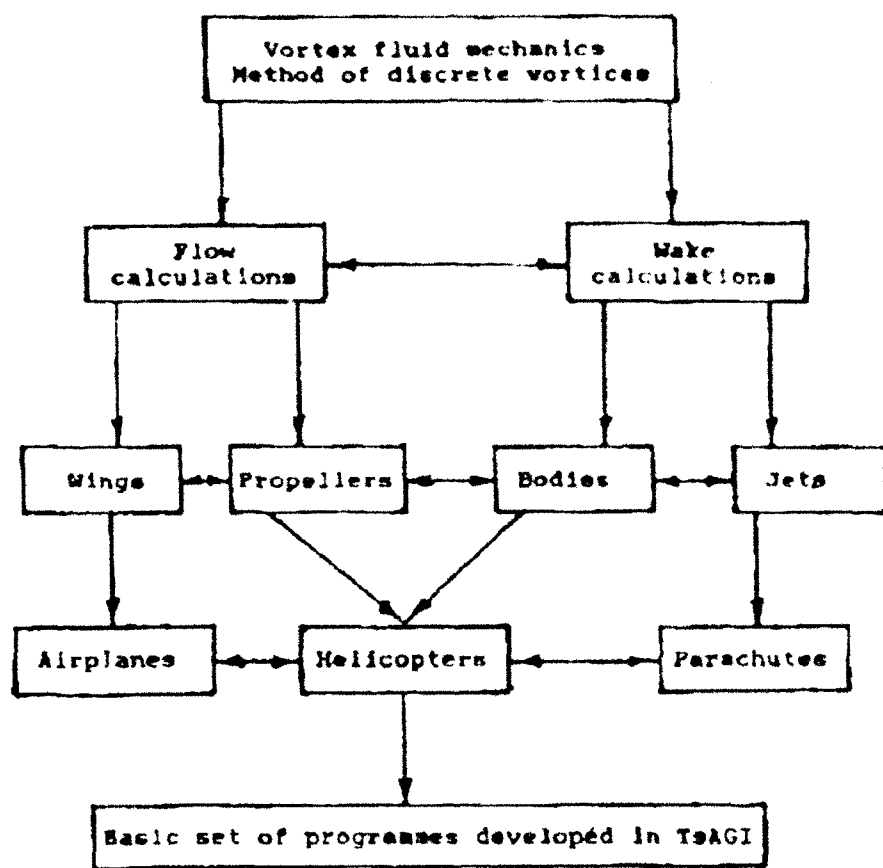
Figure 3. Method of discrete vortices.
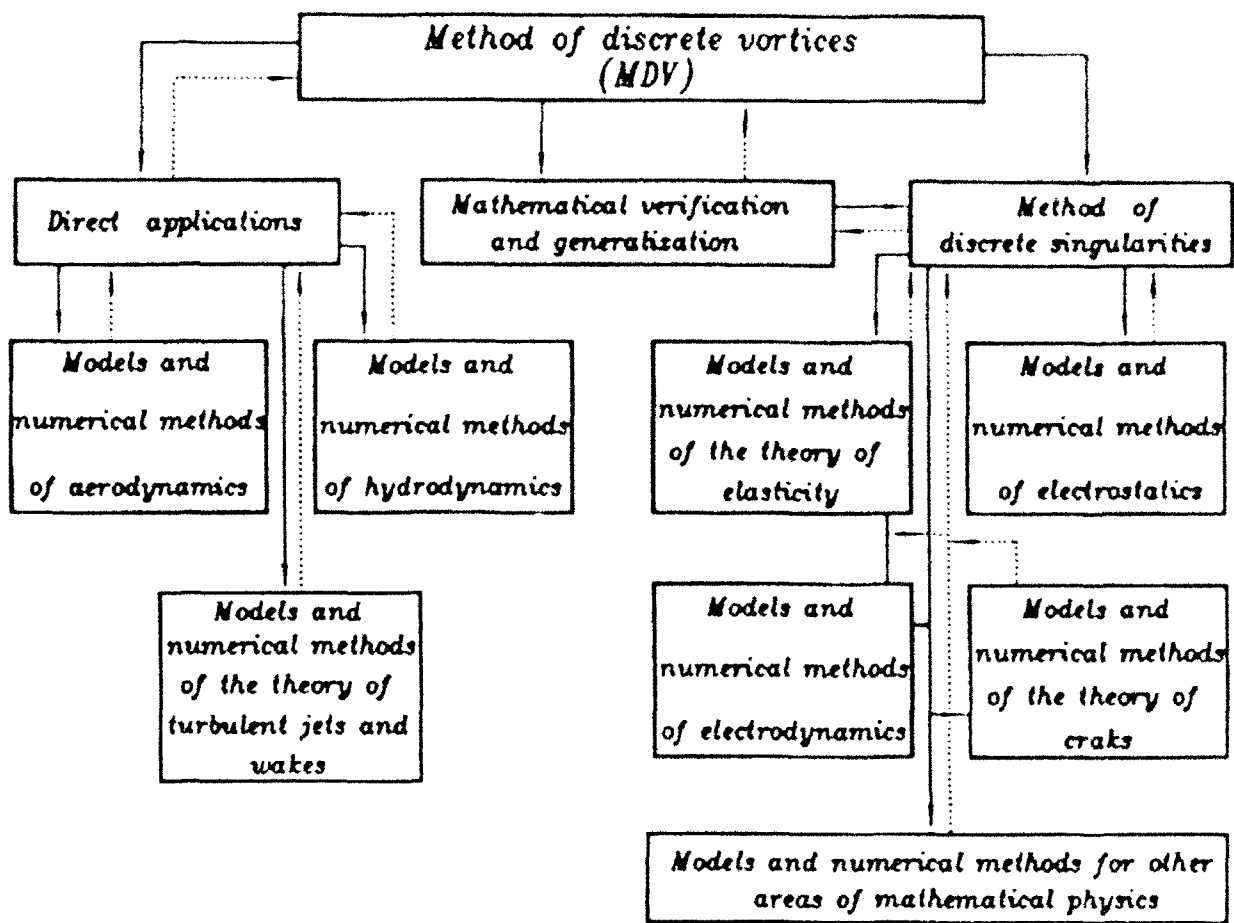
Figure 4. Transition from isolated programs to a fundamental program set.

Figure 5. Asymmetric separated flow past a flat plate for $= \infty$, $\alpha = 90°$:
(a) towing tank tests, (b) calculated.
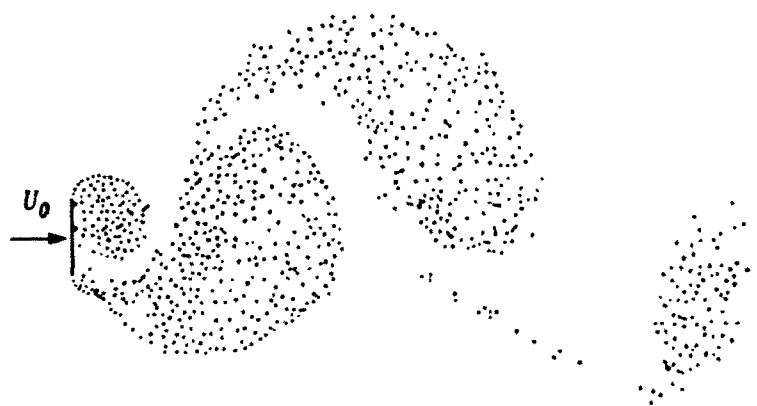
Figure 6. Calculated vortex wake behind a flat plate in the case of asymmetric
flow (Karman vortex street).

Calculated vortex wake behind a cube: A and B
denote the vortex sheet and the turbulent flow
region respectively.

a)

b)

c)

$R_e = 10^5$

$R_e = 6.7 \cdot 10^5$
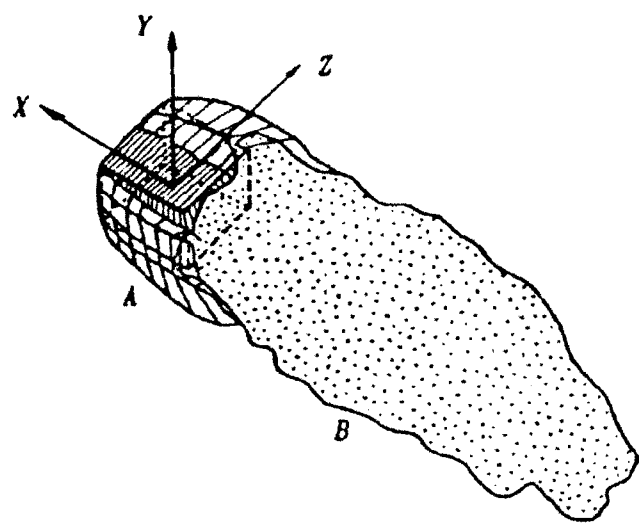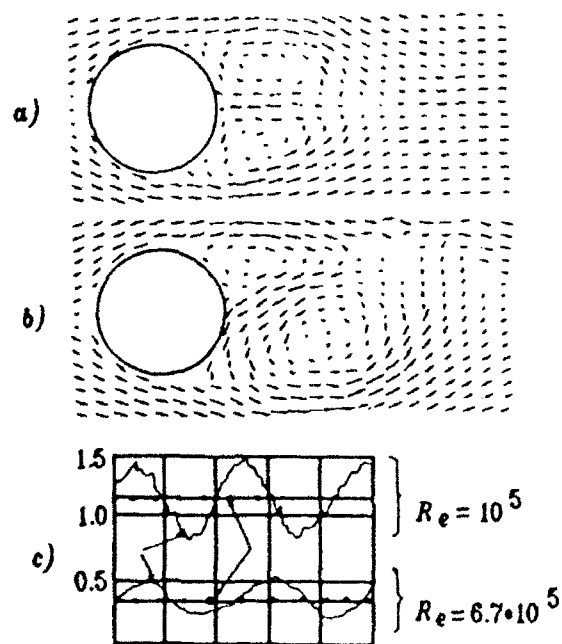
Separated flow past a cylinder: (a) and (b) show
the transformation of a symmetric wake into the
Kármán vortex street, (c) – drag reduction due to
turbulent separation.

Figure 7. Modeling aerodynamical phenomena.
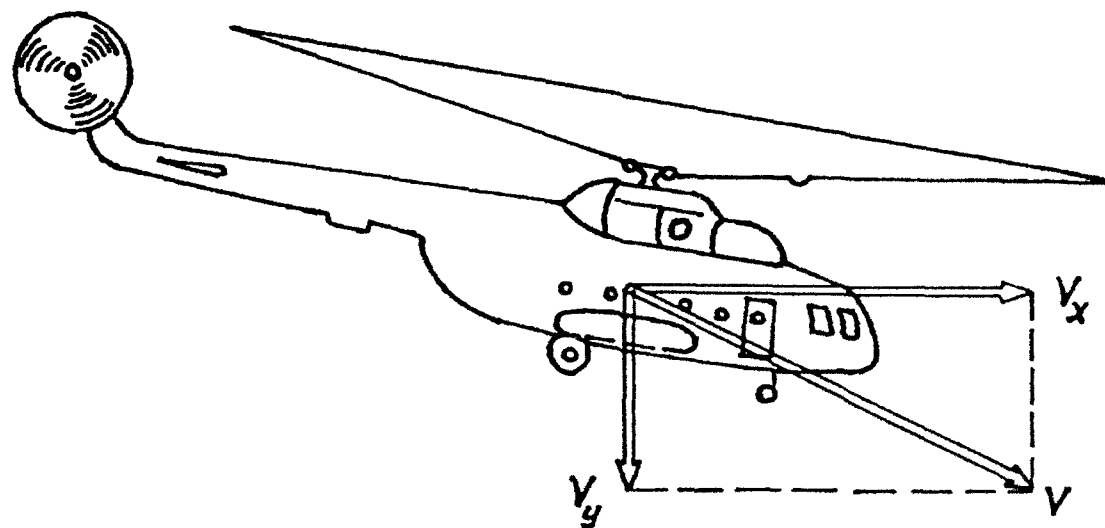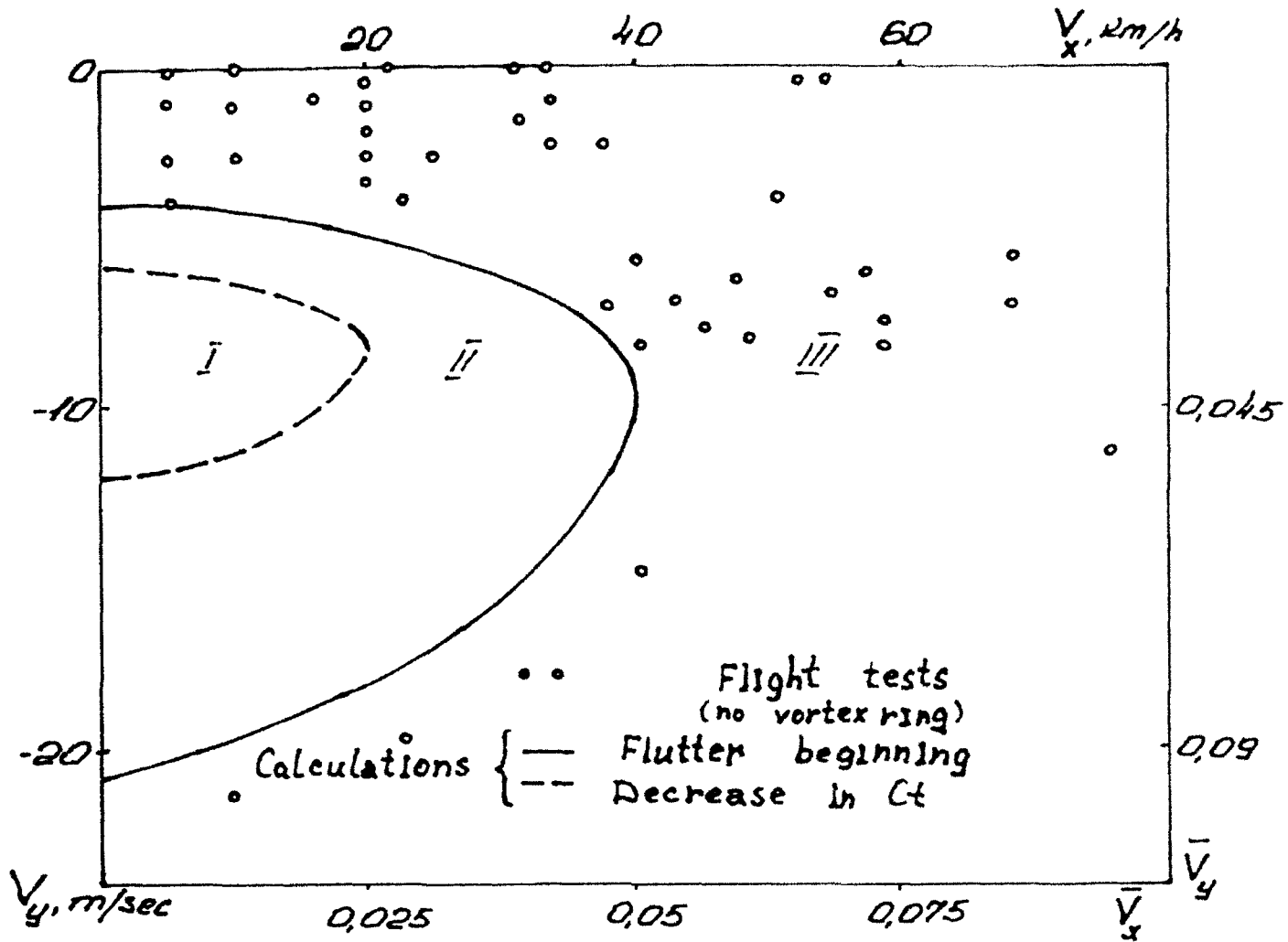
Figure 8. Vortex-ring state for a helicopter Mi-8 and analysis of safe descent regimes for a helicopter.
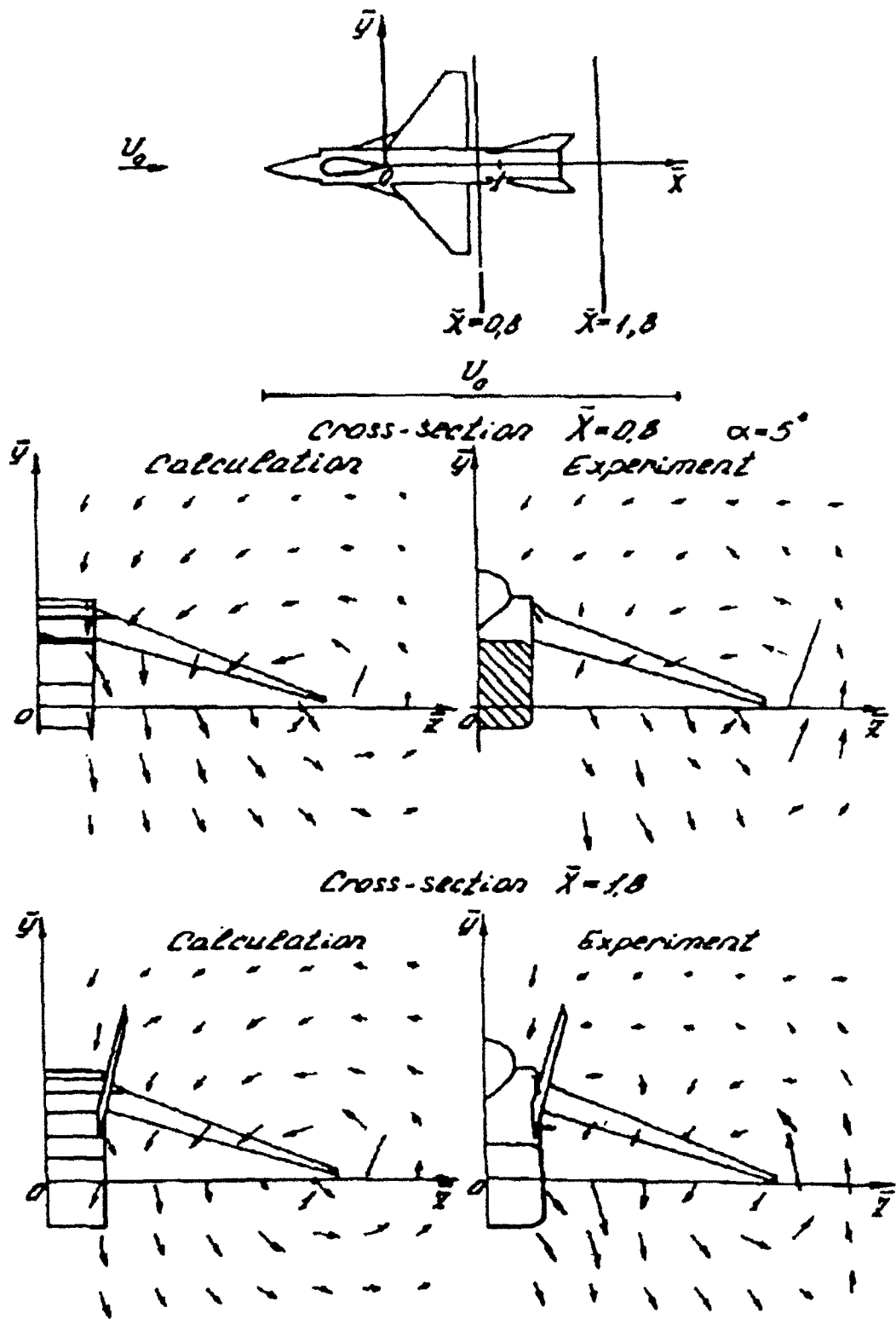
Figure 9. Agreement of calculations and experimental data.
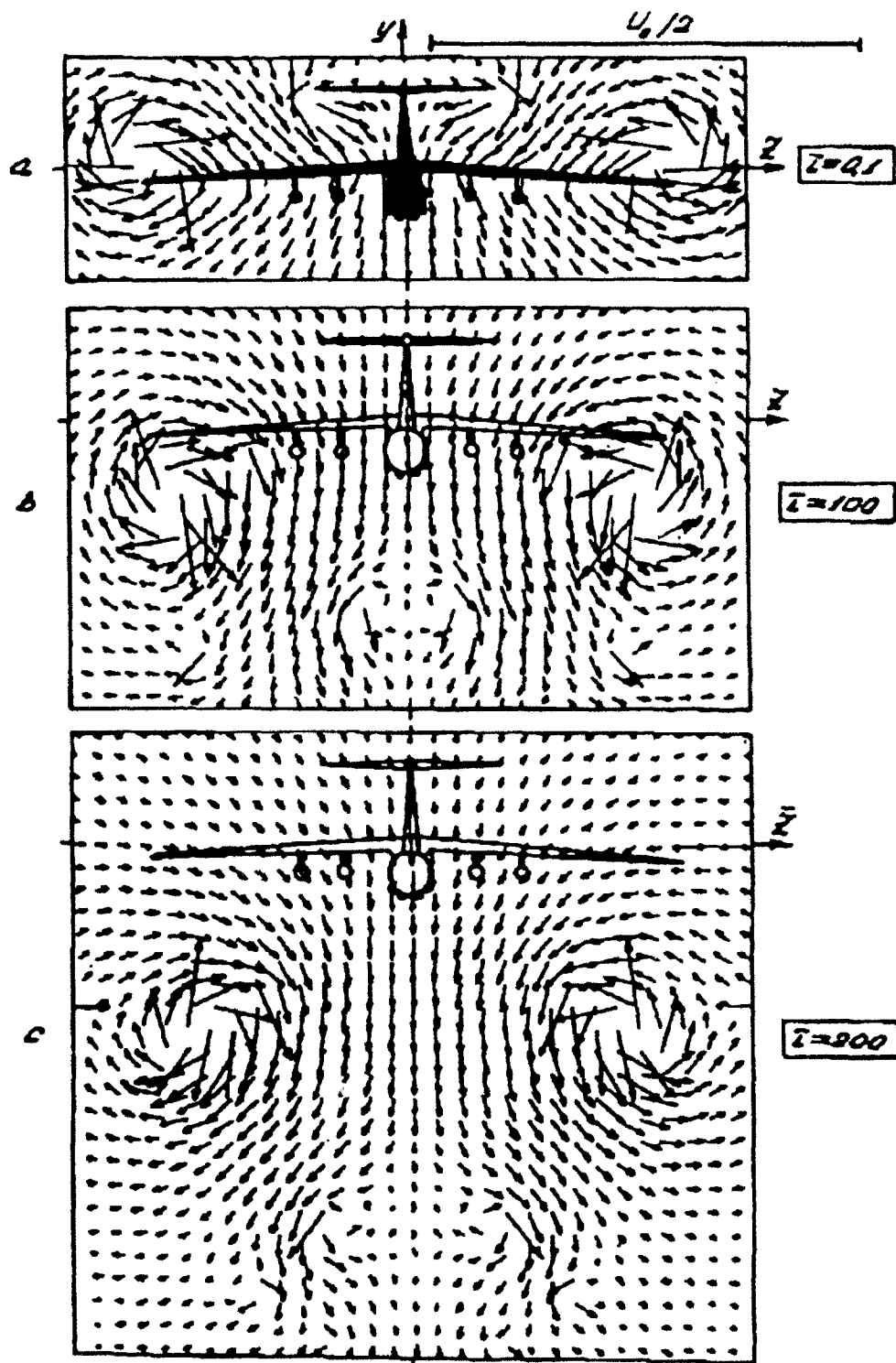
Figure 10. Development of the wake behind the plane IL-76.
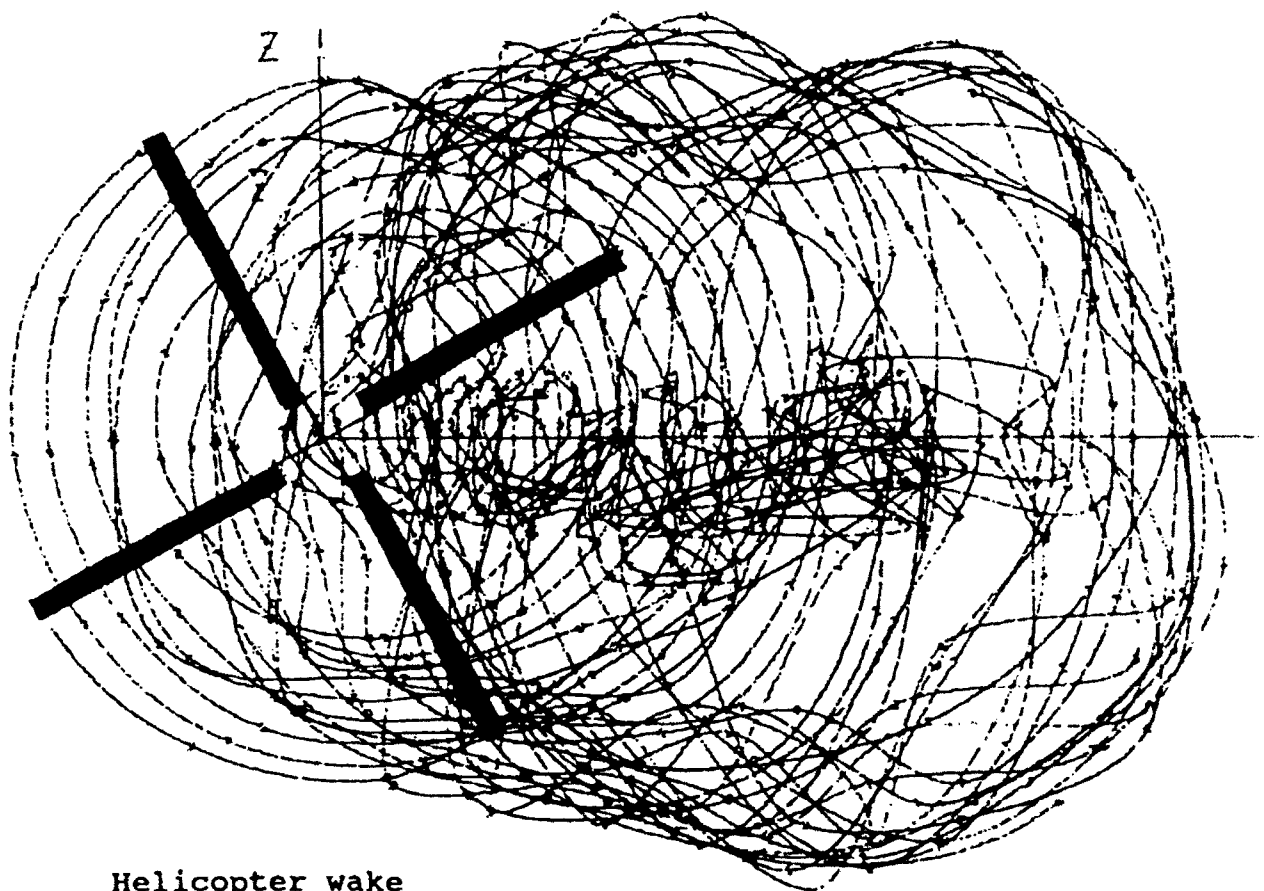
Helicopter wake

Landing

Figure 11. Helicopter wake at landing.

$$\bar{H} = \frac{H}{R}$$
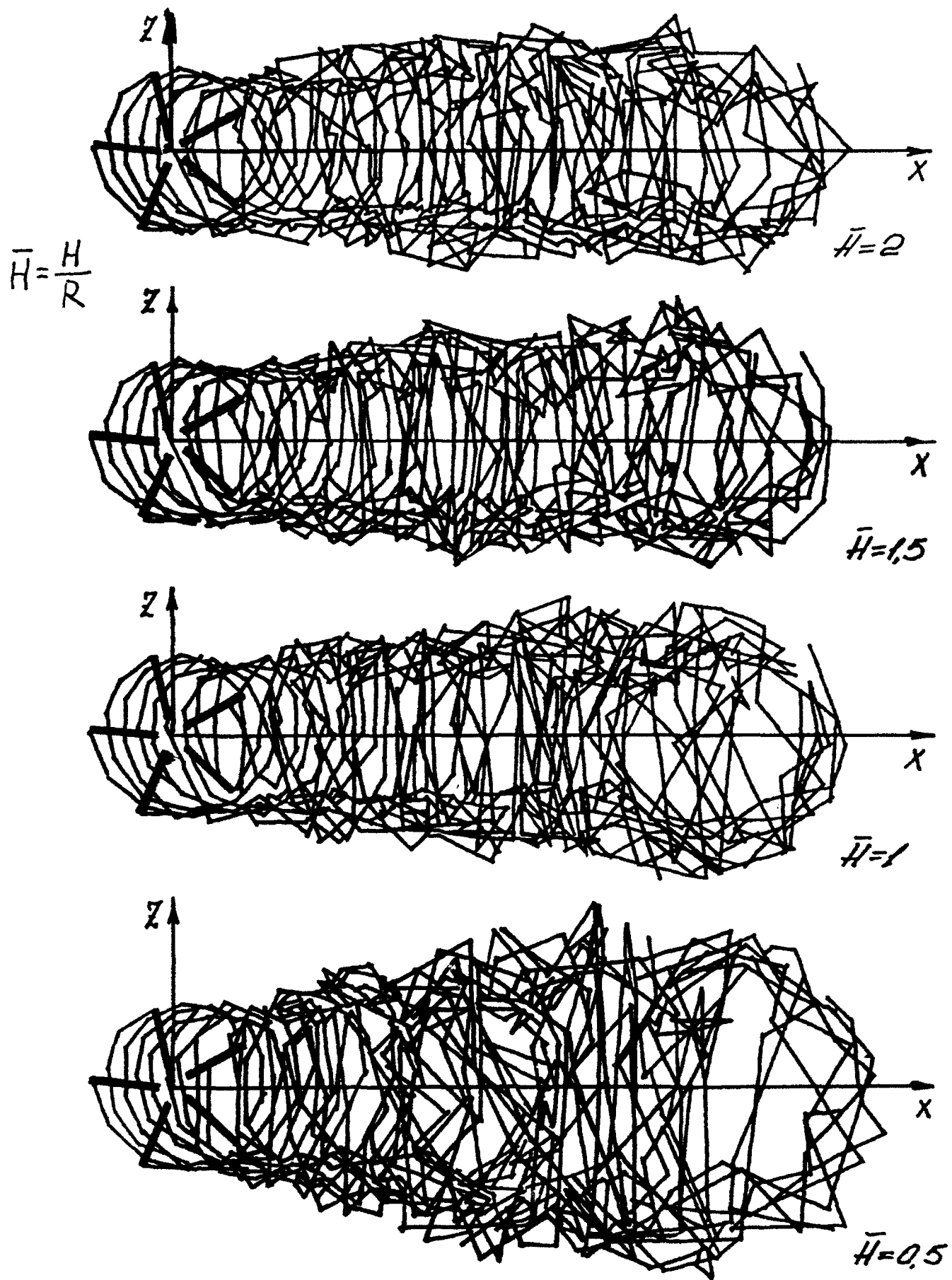
Figure 12. Influence of the ground.
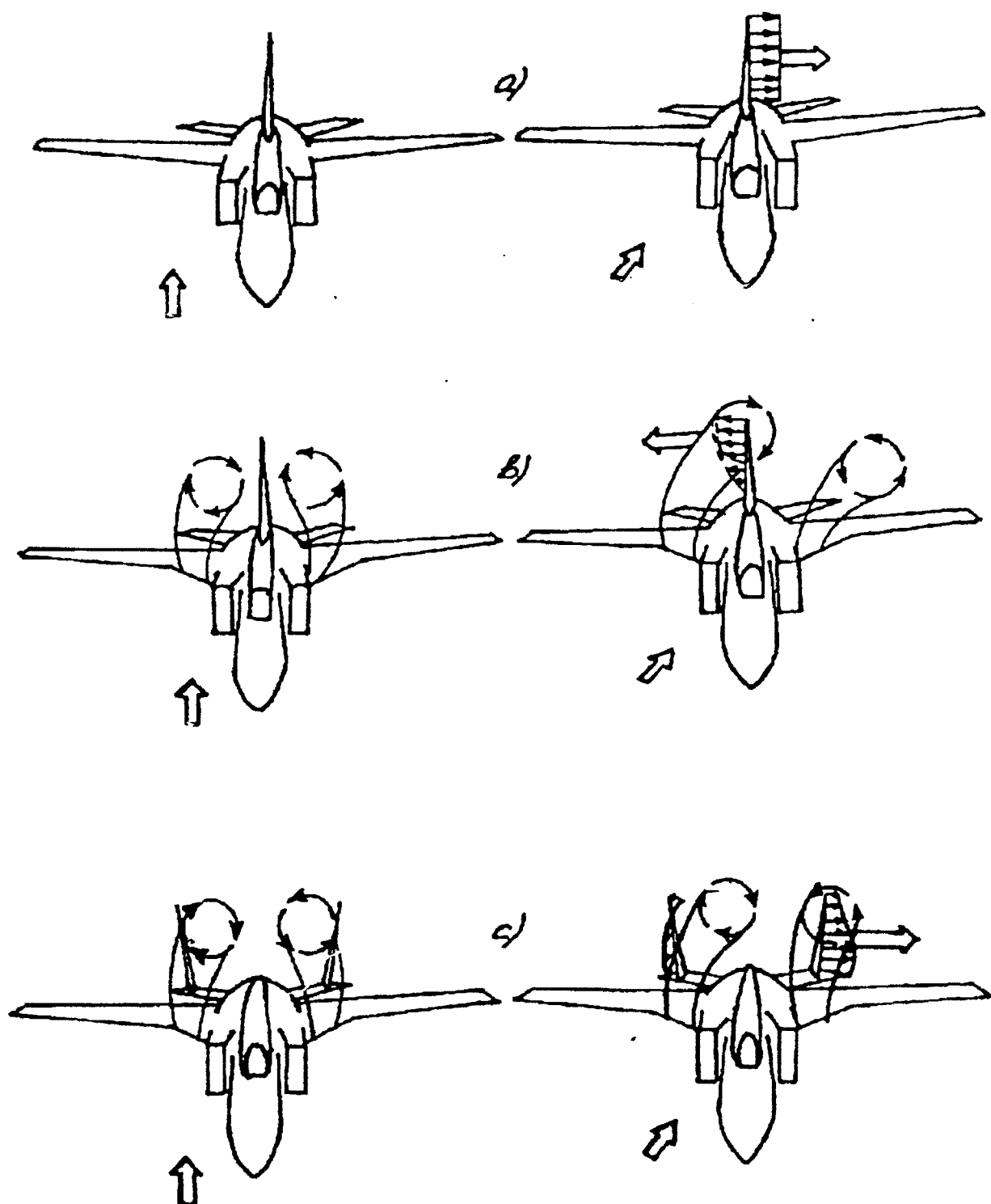
Figure 13. Model of airplane stalling into spin.

$\alpha = 25^o$

$\bar{U}_o$

$\bar{U}_o$
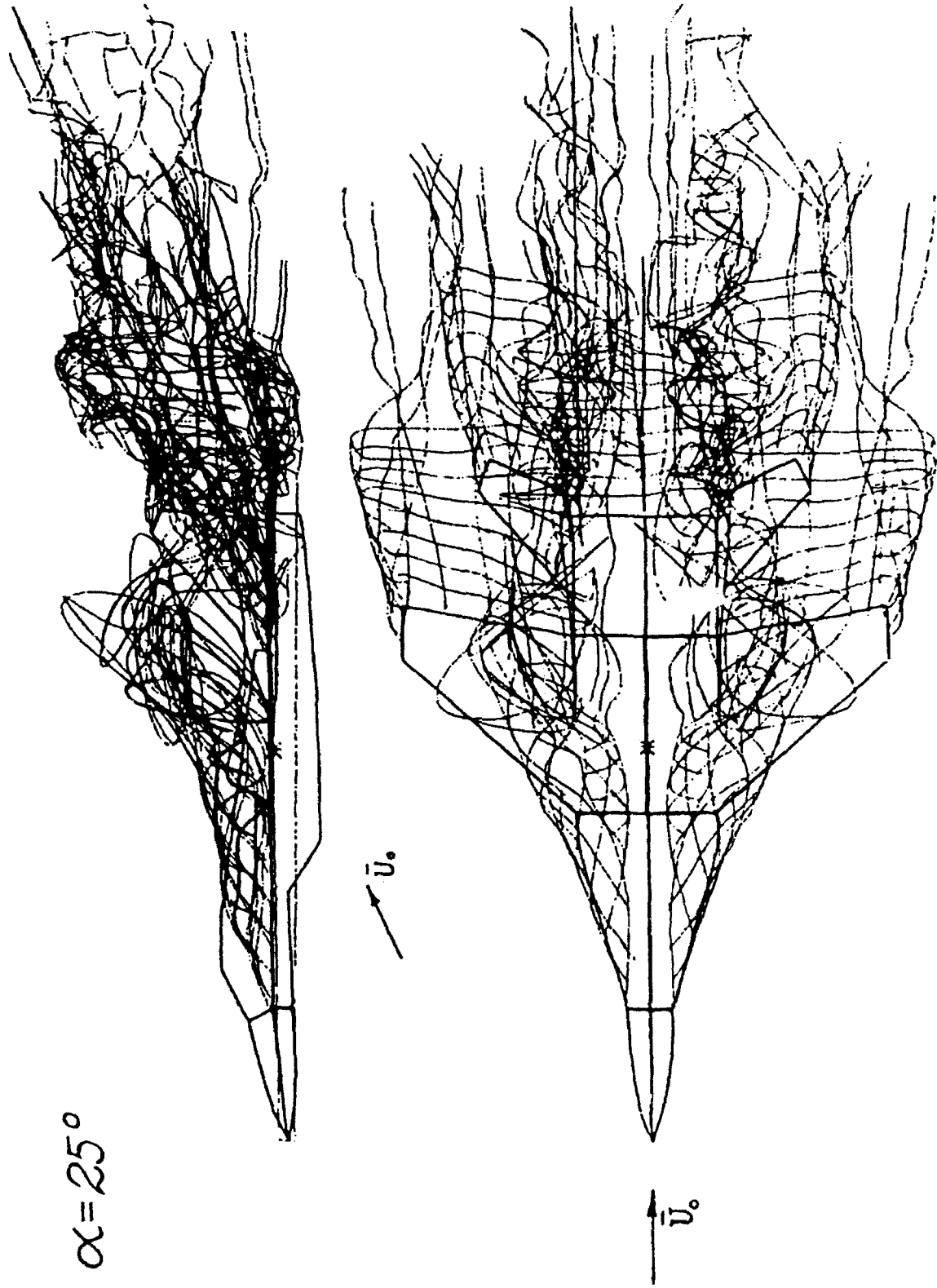
Figure 14. Airplane wake.

$\alpha = 45°$

$\vec{U}_o$

$\vec{U}_o$
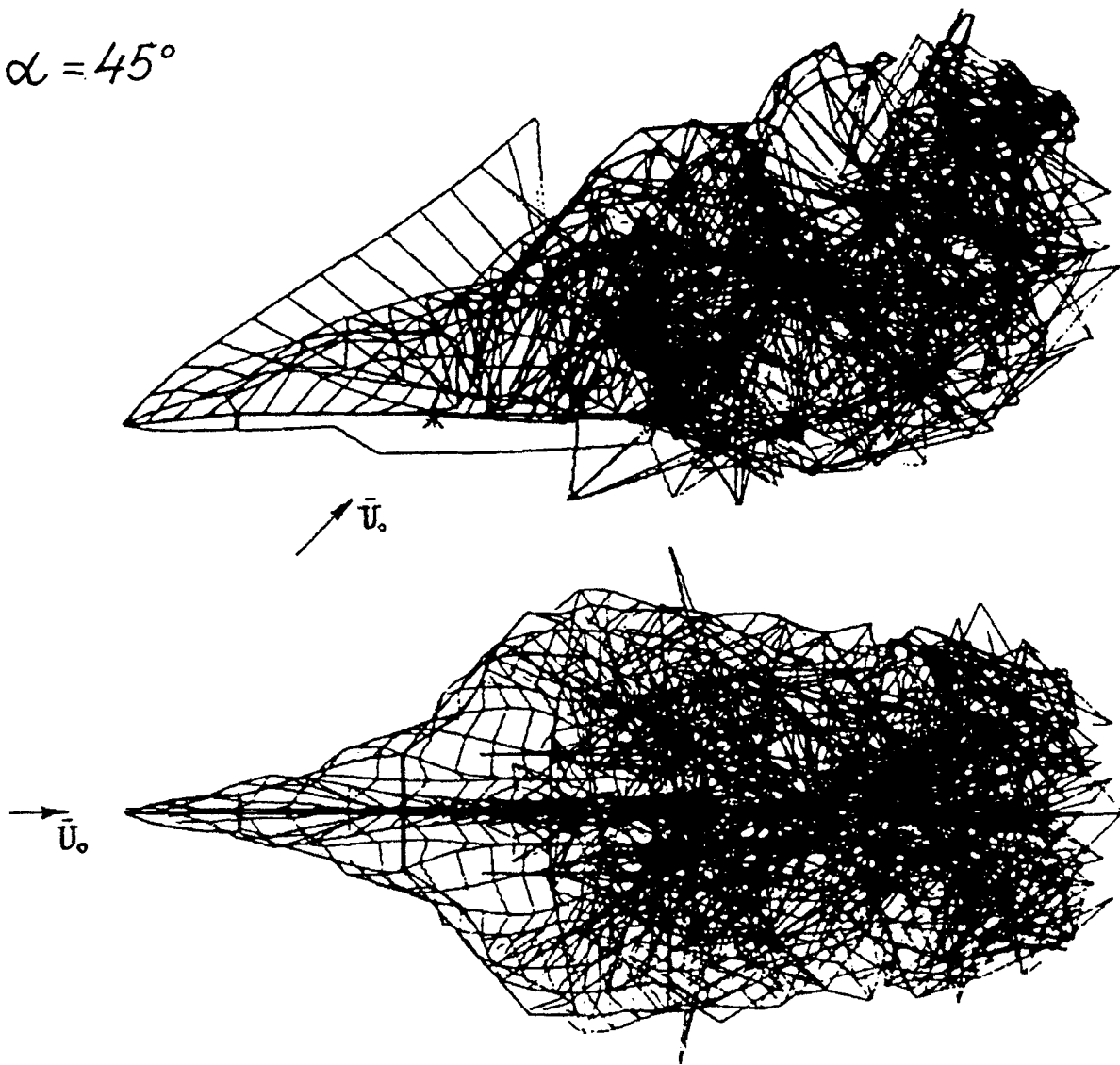
Figure 15. Airplane wake.

$\alpha = 90°$

$\vec{U}_0$

$\vec{U}_0$
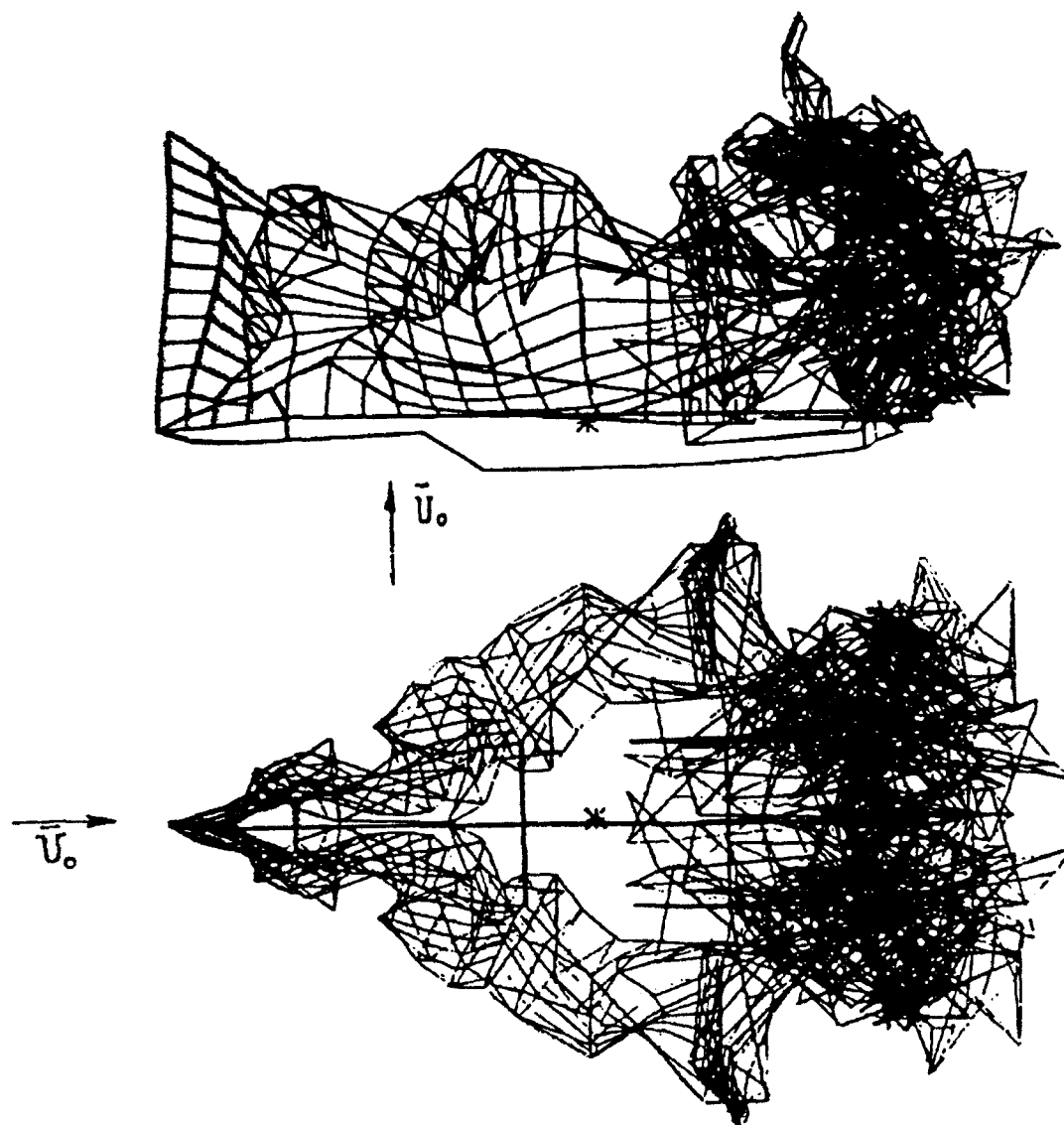
Figure 16. Airplane wake.
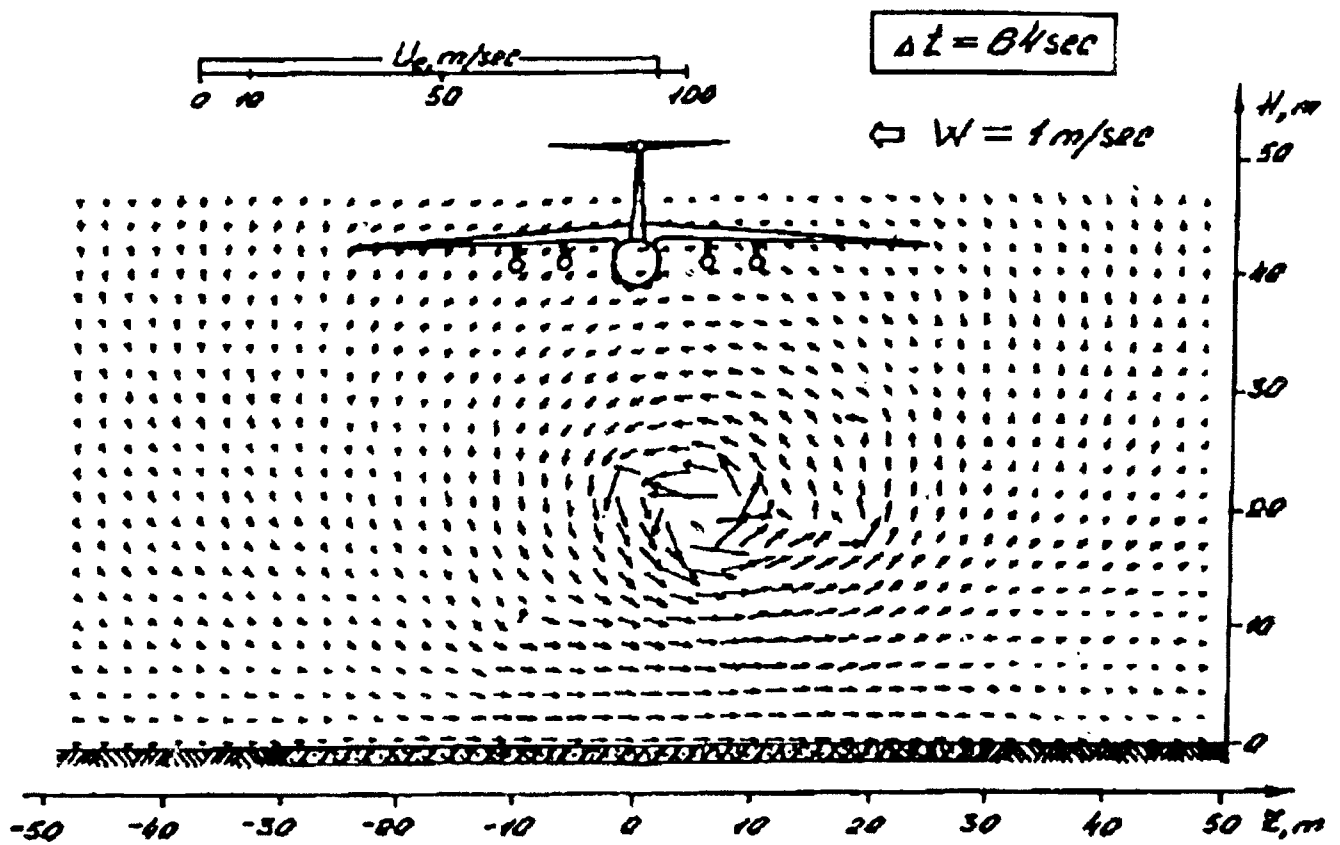
Figure 17. Beginning of Yak-40 taking off.
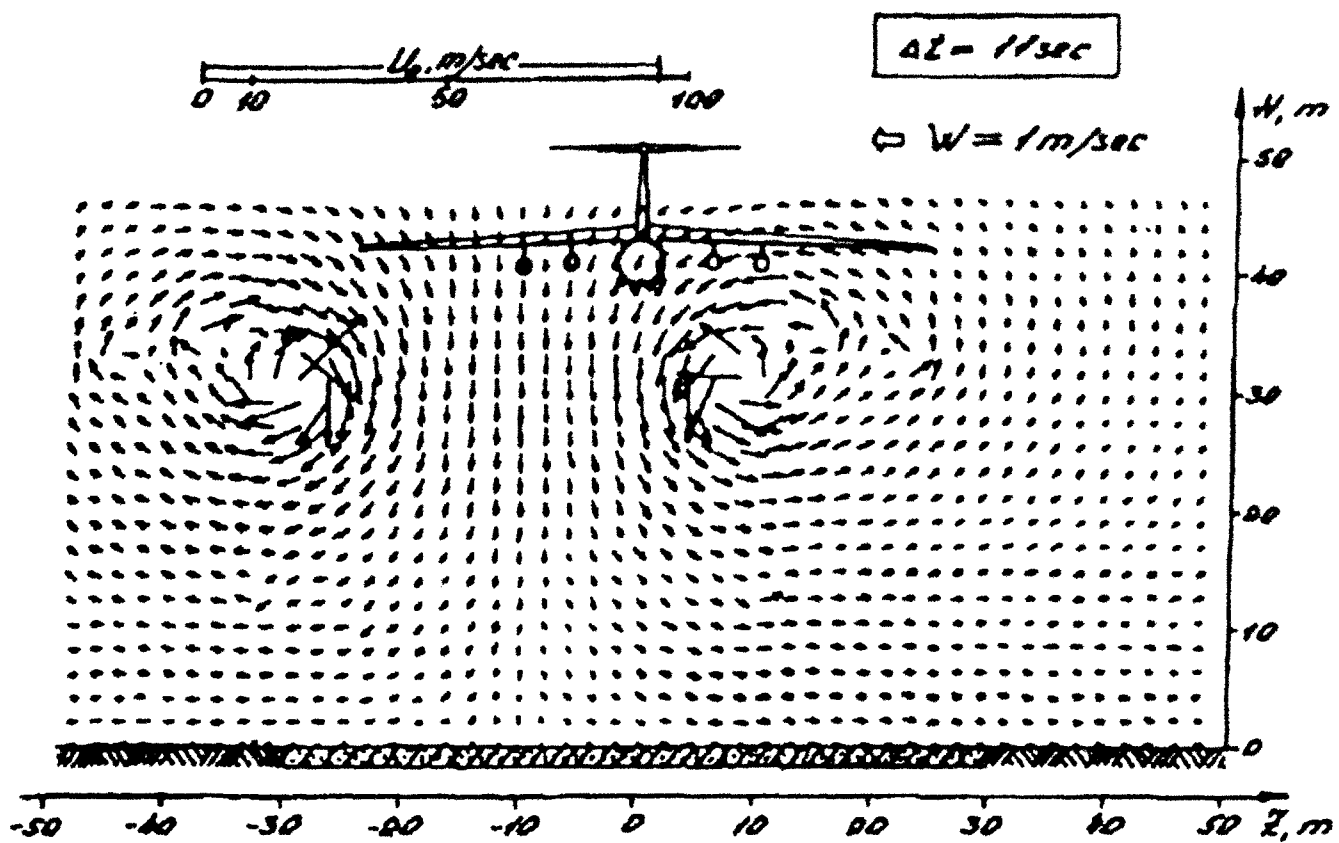
Figure 18. Beginning of IL-76 taking off.
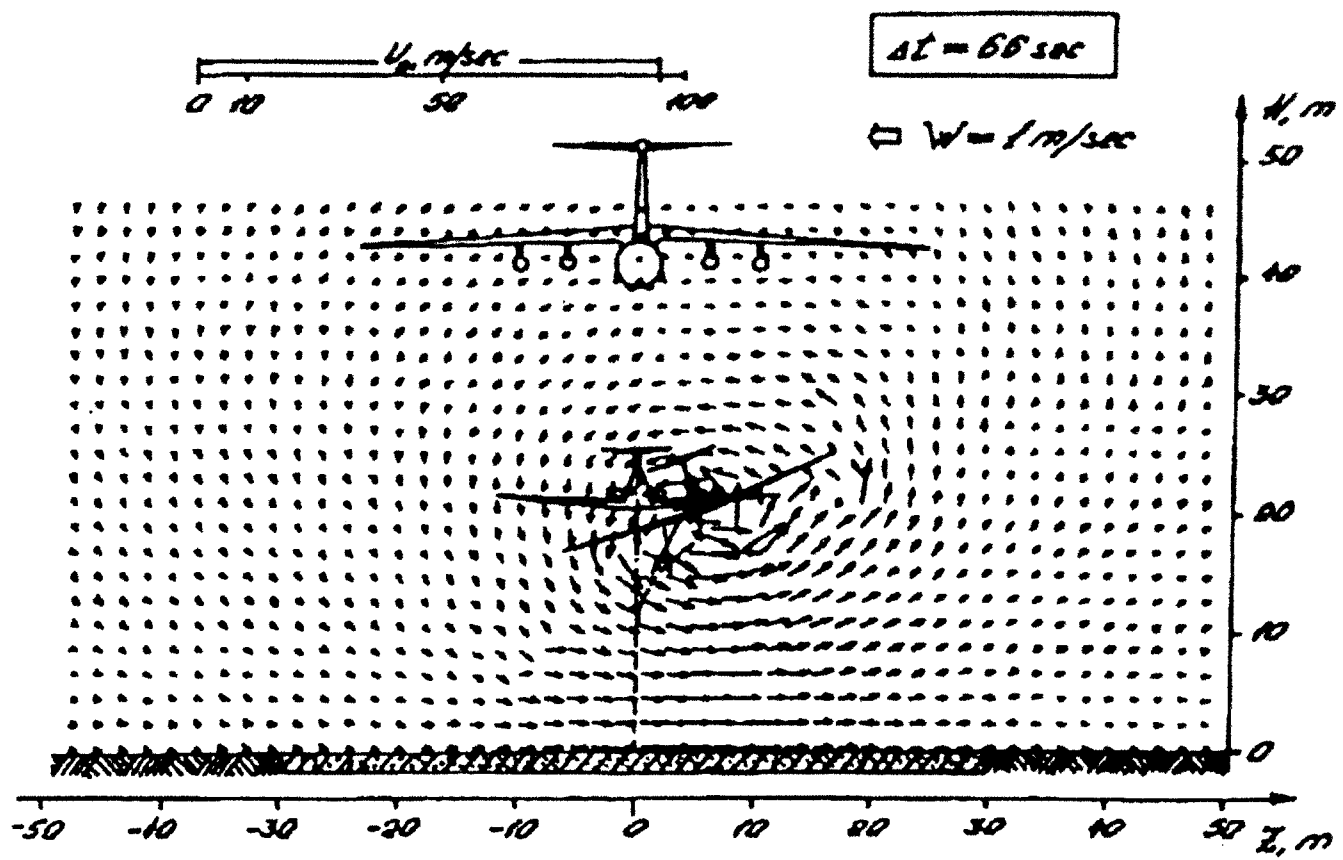
Figure 19. Yak-40 gets into the wake

Last radio reception

4800m ----

Turn from the course
70 deg. to 320 deg.
with descent (15 sec)

Dangerous approach
3500m ---- (getting into the ----
wake); beginning
of the spin (5 sec)

Spin (3 - 5 rotations);
coming out of the spin
(spin stops) (35 sec)

600m ----

Coming out
of a steep dive
(4 sec)
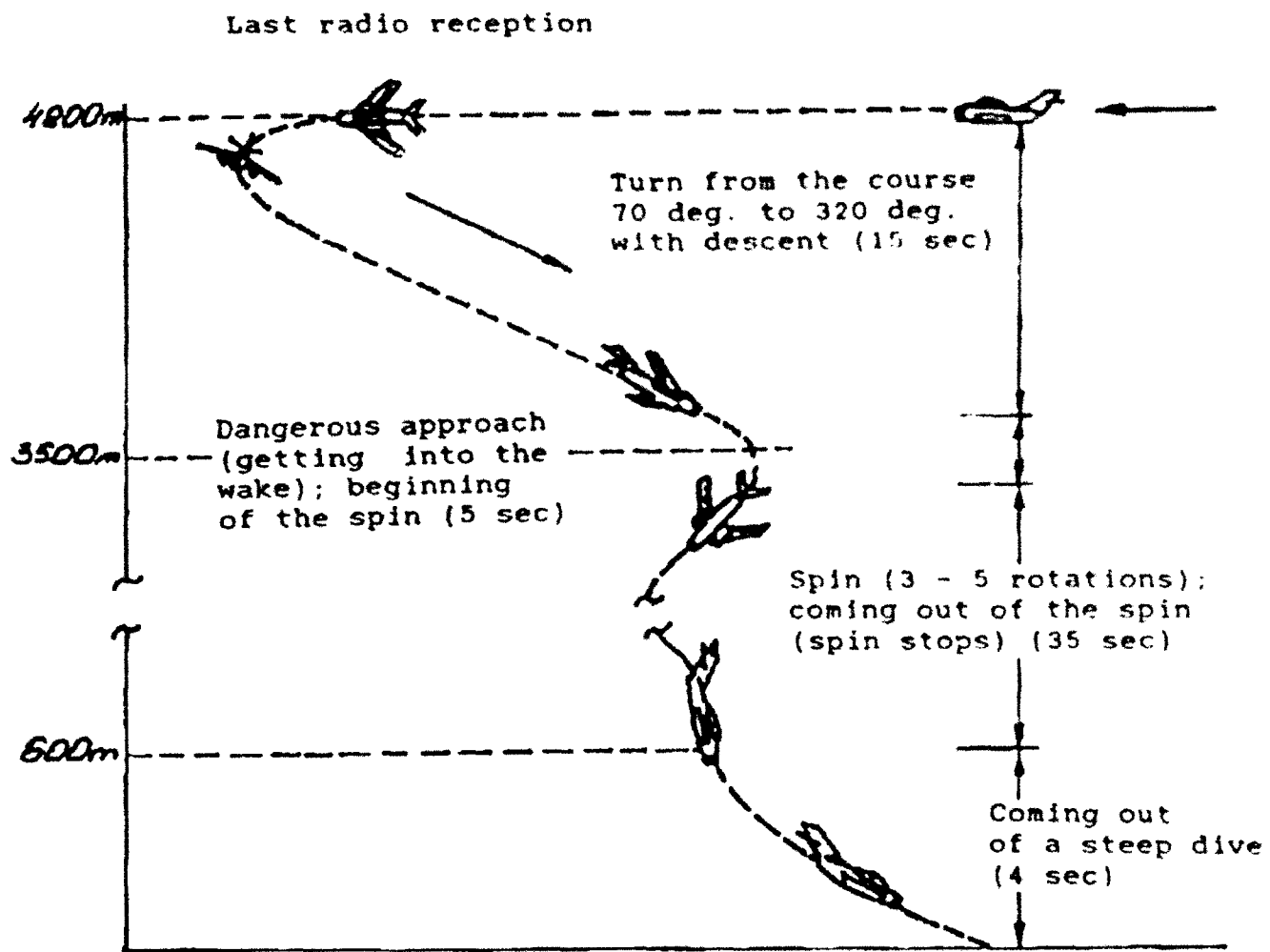
Figure 20. The most probable phases of the last stage of Yu. Gagarin's flight
(time spent for each phase is indicated).

UNITED KINGDOM CIVIL AVIATION AUTHORITY WAKE VORTEX DATABASE: ANALYSIS OF INCIDENTS REPORTED BETWEEN 1972 AND 1990.

J.B. Critchley
P.B. Foot
Chief Scientist's Division
UK Civil Aviation Authority
45-59 Kingsway
London
WC2B 6TE

THE UK WAKE VORTEX DATABASE

The objective of this paper is to report the results of an analysis (Ref 1) of the UK Wake Vortex Incident Database (Ref 2).

The United Kingdom Civil Aviation Authority (CAA) has been operating a scheme since 1972 for the reporting, monitoring and analysis of wake vortex incidents. The data for each incident come from a number of sources: initially from the pilots of the leader and follower aircraft involved in an incident, the UK Meteorological Office, digitally recorded radar data from Air Traffic Control Centres and, in some cases, from the flight data recorders of the aircraft involved. The wake vortex database was computerized in 1983 and the details of each incident were recorded on the database, which is currently maintained by the CAA's ATC Evaluation Unit. The relationship between the data sources is shown in Figure 1.

Since 1982, the UK has used 4 wake vortex weight categories instead of the 3 categories used by ICAO. A matrix of separations for the UK wake vortex categories is shown in Table 1.

Because the wake vortex separation criteria for use in the UK were last changed in 1982, the analysis has been confined to the period 1982 to 1990. In this period there were 515 incidents, 392 of which occurred on the approach to Heathrow. Around 85% of the incidents in the database occurred at Heathrow Airport, the majority of these (90%) involved arrivals. *Consequently, unless specified otherwise, the examination here is solely of Heathrow arrivals.*

Seasonal and Diurnal Variation

In the distribution of incidents with time of day (Fig 2), peaks appear around mid-morning and early evening. Figure 3 shows the distribution of incidents by month; a broad peak during summer and early autumn is apparent. In both cases the peaks coincide with periods of high traffic.

Height of Incidents

Figure 4(a) shows the height distribution of incidents: around 35% of incidents at heights under 4000 feet occur in the band below 500 feet. When this band is examined in more detail (see Figure 4(b)) a peak around 100 to 200 feet is evident. In addition, around 45% of incidents occur in a band between 2,000 and 4,000 feet, with a broader peak at around 3,000 feet.

The strong peak at very low heights can be explained by considering three height bands. Below 50 feet vortices decay rapidly due to interaction with the ground. Above 300 feet or so the vortices usually tend to descend out of the flight path of the following aircraft. However, for the 50 to 300 feet band neither of these processes occur - hence the larger number of occurrences. An explanation for the broad peak between 2,000 feet and 4,000 feet can be constructed from an analysis of the procedures used by aircraft on approach to Heathrow. Aircraft on final approach descend at a roughly constant rate between 3,000 feet and 500 feet, giving rise to a wake vortex incident distribution which is substantially uniform with height. However, during approach to Heathrow, some aircraft are required to fly level at a height of 3,000 feet for up to 5 Nm whilst following the localizer to the runway; so more opportunity exists for these aircraft to encounter trailing vortices generated by preceding aircraft.

Derivation of Incident Rates

In order to use the incident data to give an indication of the magnitude of the risk of an incident occurring under particular conditions, the number of incidents needs to be expressed in terms of 'exposure' to those conditions. Since most vortex incidents occur when aircraft are in a queue to land, the numbers of incidents for each of the various leader-follower aircraft pairs is expressed in terms of the number of these 'queued' arrivals at Heathrow.

Incident Rates for Leader Types

Table 2 shows the number of incidents per estimated 100,000 queued aircraft pairs, which is denoted as the incident 'rate', for various leader aircraft types. Also shown in Table 2 are values for the more severe incidents, i.e., those involving roll angles of 30 degrees or more (Category A incidents).

These values suggest that the B747 and B757 leaders appear to produce significantly higher incident rates than the other aircraft considered, indicating prima facie that they produce stronger or more persistent vortices than the other aircraft in their respective weight categories. This

conclusion applies both to incidents of all severities and to those restricted to Category A incidents only. Professional pilots are not expected to either under report or over report incidents involving higher roll angles, so the fact that the Category A incident rates are also higher for the B747 and B757 suggests that the 'excess' incident rates derived for these aircraft are a true reflection of the situation.

The fact that the B747 is by far the heaviest in the 'Heavy' wake vortex class (maximum take-off weight 371,000 Kg) is a likely explanation for its higher incident rates. However, the cause of the higher B757 incident rates is uncertain.

Incident Rates for Follower Types

Having shown that the B747 and B757 leader aircraft appear to cause relatively large numbers of incidents, it would be useful to establish which follower aircraft seem particularly vulnerable. Table 3(a) and Table 3(b) show the breakdown of the incident rates for specific followers, behind B747 and B757 as leaders. The followers with the highest incident rates are the BAC 1-11, B737 and the DC9. The rates for the Category A incidents are also higher for these aircraft, and the DC9 (which includes derivatives, e.g., MD80 series) has the highest category A rates of all. This could indicate that the DC9 type has certain features which make it susceptible; one possibility is lower roll inertia resulting from the mounting of the engines on the body rather than the wings; but the CAA Study (Ref 1) also recognised that there could be other explanations.

'Acceptability' of Incident Rates

In reviewing the frequency of incidents in the UK database, an attempt is made here to determine whether these rates are 'acceptable'. The judgement of acceptability is based on an assessment of the risk that a wake vortex incident will lead to a fatal accident. Although little quantitative evidence is available in previous work on wake vortices, it was judged in early work (Ref 3) that the likelihood of an accident should be estimated on the nominal basis that it is 1/100 of that of a Category A incident. On this basis, the values in Tables 3(a) and 3(b) for the frequencies of Category A incidents per 100,000 queued arrivals, approximately represent the expected number of accidents per 10^7 landings.

Since the generally accepted target level of safety for the approach phase of flight is one fatal accident in 10^7 flights, the values in Tables 3(a) and 3(b) would on this basis give cause for concern. For example, the risk of an accident per 10^7 landings for a B757 leader and followers such as DC9, BAC 1-11 and B737 is estimated to be 57, 31 and 37 respectively, while for a B747 leader the corresponding risks are 75, 54 and 16. However, since the judgement that the probability of a Category A incident becoming an accident is 1/100 was based on cautious (perhaps over cautious) assumptions, the actual risk of an accident may well be markedly over estimated.

Meteorological Conditions

Wake vortex encounters are believed to be more likely in conditions of low wind and therefore it is very important to identify the relationship in practice between wind conditions and the probability of a wake vortex incident.

To obtain quantities proportional to the *probability* of an incident occurring as a function of parallel or cross wind speed, incident 'rates' are calculated. These rates are expressed in terms of the number of incidents per unit 'exposure' to the parallel or cross wind. Exposure is defined as the fraction of queued landing aircraft per year exposed to the relevant wind values. These rates, which are analogous to the incident rates discussed in section 12, are plotted in Fig 5. As expected, the probability of an incident is higher for low cross wind speeds than for greater cross winds. This can be explained as being the effect of vortices being 'blown sideways' out of the path of the following aircraft.

For the case of the wind speeds parallel to the direction of the aircraft, the corresponding graph is shown in Fig 6. The probability of an incident does not show a strong dependence on parallel wind speed. Parallel winds are not expected to be as 'beneficial' as cross winds in blowing vortices out of the path of following aircraft.

Separation of Aircraft

The separation variable used in this analysis was the separation derived from recorded radar data relating to the time of the incident, if available; otherwise, the separation as estimated by Air Traffic Control was used. Figure 7(a) shows the frequency distribution of the difference between the required minimum separation and the actual separation at the time of the incident. As Fig 7(a) shows there is a strong peak in the distribution centred approximately where the actual separation is equal to the required separation. The decline in incident frequency away from the peak can arise from two effects:

- When actual separations are less than the required minima the frequency of reported incidents decreases. This decrease occurs because large infringements of the separation minima are unlikely, and this factor outweighs the increased risk of an incident at smaller separations.

- Where the actual separations are greater than the required separations (i.e., the difference between required and actual separations is negative) the number of incidents again decreases. This can be explained as being due to the reduced likelihood of an incident at larger aircraft spacings as there is then more time for the vortex to dissipate or to be blown out of the path of the following aircraft; moreover, aircraft are not often given large separations.

The fact that Category A incidents also follow a similar frequency distribution (Fig 7(b)) may suggest that the severity of an incident is not strongly dependent on the separation. This is consistent with the assumption that the main effect of decreasing the separation is to increase the *risk* of an incident rather than its *severity*. (Encounters with vortices while they are actually

8-4

decaying are unlikely as they tend to dissipate rapidly once decay has commenced.) The severity of an incident is governed mainly by the particular portion of a vortex (i.e., the core or extremity) that the follower penetrates.

Incidents between Runway Threshold and Touchdown

It would be expected that the likelihood of an incident becoming an accident should increase with increasing roll angle; and that the accident probability would also increase with decreasing height of the follower.

Table 4 shows those incidents in the database which the follower aircraft was described as being in the 'touch down' phase of flight, that is between the runway threshold and the touchdown itself. It should be noted that in 14 out of the 15 cases in Table 4, the leader was a B757, while in the remaining case a B747 was the leader aircraft. The evidence of a number of incidents occurring in close proximity to the ground must be treated very seriously. The actual and required separations for these incidents show that the separation at the time of the incident was within a nautical mile (either way) of the required separation.

Unresolved Issues

Peaks in the distribution of incidents by time of day and by month of the year are evident. The greatest contribution to these peaks arises simply from the greater traffic at these times, but it is difficult to determine with any statistical confidence whether contributions to these peaks arise from other factors such as a failure of the separation criteria to protect aircraft, whether specific meteorological factors occur at the times of the peaks, or simply that intended separations are not being maintained throughout the approach to touchdown phase.

The risk of a wake vortex incident is seen to depend mainly on the separation between the leading and following aircraft, whilst the severity -- described by the roll induced -- depends on the particular portion of the vortex that is penetrated. This restriction of the definition of severity to roll angle means that no account is taken of height available to make a recovery. No suitable theoretical description of the risk of an incident becoming an accident is yet available: further work is required to enable the more accurate description of risk in terms of aircraft, meteorological and separation variables.

Several approaches to determining the target level of safety have been identified: it may be that the target rate of one accident for 10^7 approaches, itself derived from a target level of entire flights, needs to be reviewed.

CONCLUSIONS

It is not possible to give an adequate theoretical explanation for some of the results obtained from the UK database, but some conclusions may be made.

The analysis of the wake vortex incident database identifies peaks of high incident rate around mid-morning and early evening during summer and early autumn. The peaks generally coincide with periods of high traffic.

The incident 'rate' which is a measure of the probability of an incident, decreases steadily with increasing cross-wind speed. However, there does not appear to be a strong dependence on parallel wind speed.

The greatest frequency of reported incidents occurred to following aircraft in the height band 100ft to 500ft, particularly 100ft to 200ft. Between 2,000ft and 4,000ft a second peak, albeit much smaller, around 3000ft, was noted.

It has been suggested that in the absence of any other measure, it is appropriate to estimate the probability of an accident arising from wake vortex penetration as $^1/_{100}$ that of a serious incident. On that basis, the estimated accident rates for a number of aircraft types exceed the accepted target value of 1 in 10^7 landings for civil aircraft operations. This conclusion needs to be considered carefully: it may be that there is no assurance from incident data that an acceptable degree of safety is being achieved; however it may also be the case that the methods of determining the target value from the incident rate is overly stringent.

Analysis of the incident rates show that the most likely types of leader aircraft to be involved in wake vortex incidents are the B747 and B757. For follower aircraft the analysis has shown that the most susceptible aircraft to incidents of all severities, and also to Category A incident are the BAC 1-11, B737 and DC9. There are indications that the DC9 may be more vulnerable to Category A incidents than the other two aircraft types.

For safety management objectives it is important that monitoring through incident reporting should be continued and given the appropriate publicity.

Table 1. UK Minimum Separation for Final Approach (N Miles) +

Leader Follower	Heavy	Medium	Small	Light
Heavy	4	*	*	*
Medium	5	3	3	*
Small	6	4	3	*
Light	8	6	4	*

\+   A corresponding table may be constructed with time equivalents.

*   Separation for vortex reasons alone unnecessary.

LEADERS

Table 2.

Estimated wake vortex rates and frequencies (per 100000 queued arrivals)

Leader Type		B747	A300/A310	L101	Other Heavy	B757	B737	Other Medium	Small	Light
All incidents	Rate	127	35	56	27	139	6	14	3	0
	Frequency	123	24	22	5	151	13	46	2	0
Category A	Rate	19	6	8	0	21	0.4	3	0	0
Incidents	Frequency	18	4	3	0	23	1	9	0	0

Table 3.

Estimated wake vortex rates and frequencies (per 100000 queued arrivals)

B747 Leaders

Follower Type		B757	B737	DC9	BA11	B727	Other Medium	Others
All incidents	Rate	73	191	224	324	67	180	72
	Frequency	6	35	21	12	3	13	33
Category A	Rate	0	16	75	54	0	14	11
Incidents	Frequency	0	3	7	2	0	1	5

3(a)

B757 Leaders

Follower Type		B757	B737	DC9	BA11	B727	Other Medium	Others
All incidents	Rate	78	291	188	248	58	91	34
	Frequency	11	79	23	16	4	6	12
Category A	Rate	7	37	57	31	0	0	8
Incidents	Frequency	1	10	7	2	0	0	3

3(b)

Table 4. Incidents During 'Touch Down' Phase*

Roll Angle	Actual [Required] Separation (Nm)	Leader	Follower
20	3.[3]	B757	B737
10	3.5 [3]	B757	EA32
0	? [N/A]	B757	B767
20	? [3]	B757	B737
15	4 [3]	B757	BA11
3	3 [3]	B757	B757
5	4.2 [5]	B747	B737
15	2.9 [3]	B757	B737
10	3.3 [3]	B757	HS21
10	2.6 [3]	B757	DC9
5	3 [3]	B757	B737
20	4.3 [3]	B757	DC9
10	2.2 [3]	B757	B737
15	2.4 [3]	B757	B757
20	3 [3]	B757	DC9

*threshold to touch down

8-10

AIRCRAFT AFFECTED
BY VORTICES

REPORT OF
INCIDENT

PILOT
REPORT
FORM

MET OFFICE

TELEX

MET REPORT
FORM

ATC

FAX

ATCEU

DATABASE

TELEX

RADAR
DATA

LONDON
AIR TRAFFIC CONTROL
CENTRE

AIRCRAFT PRECEDING
AFFECTED AIRCRAFT

REQUEST TO
COMPLETE PILOT
REPORT FORM

PILOT
REPORT
FORM
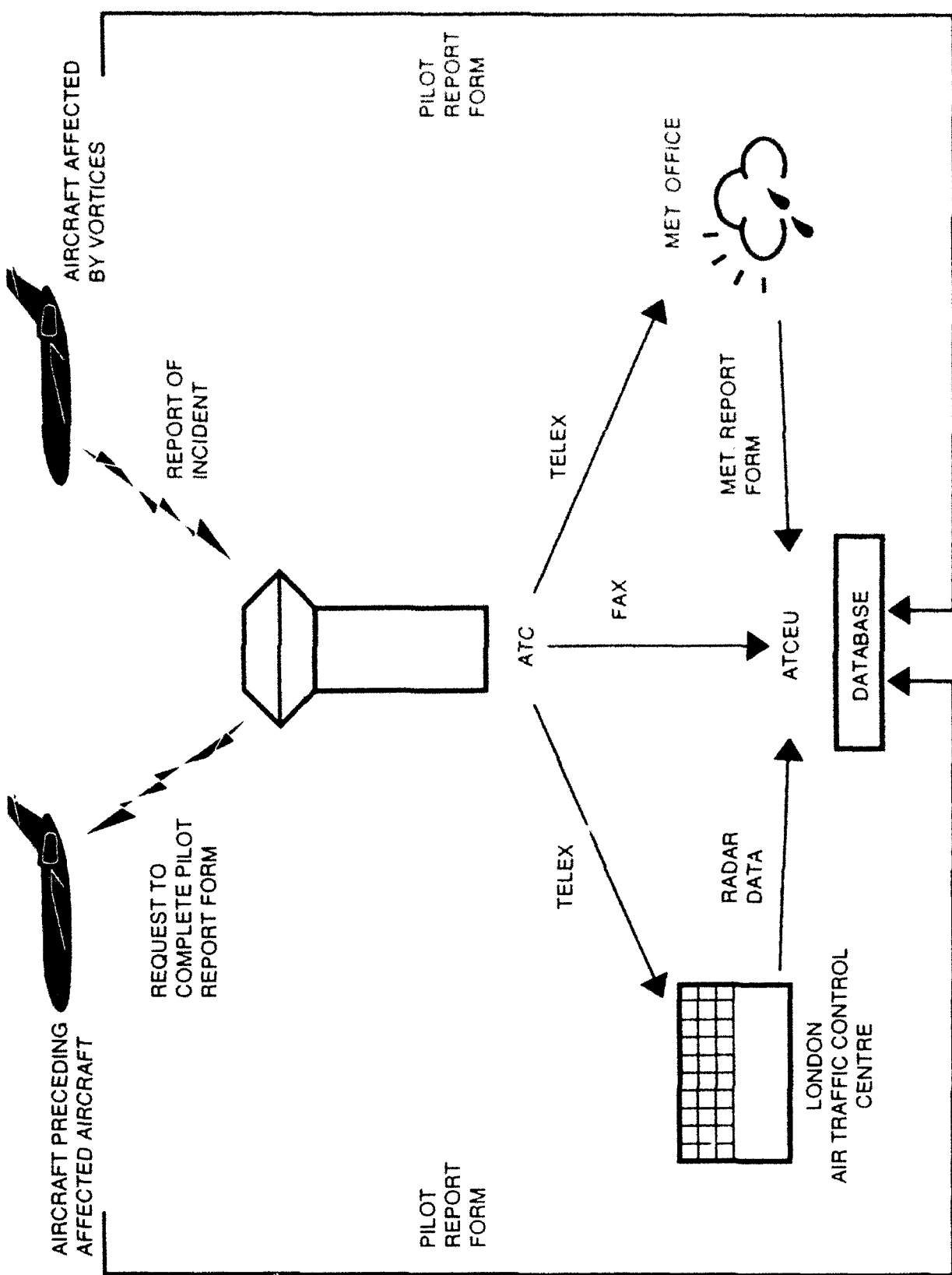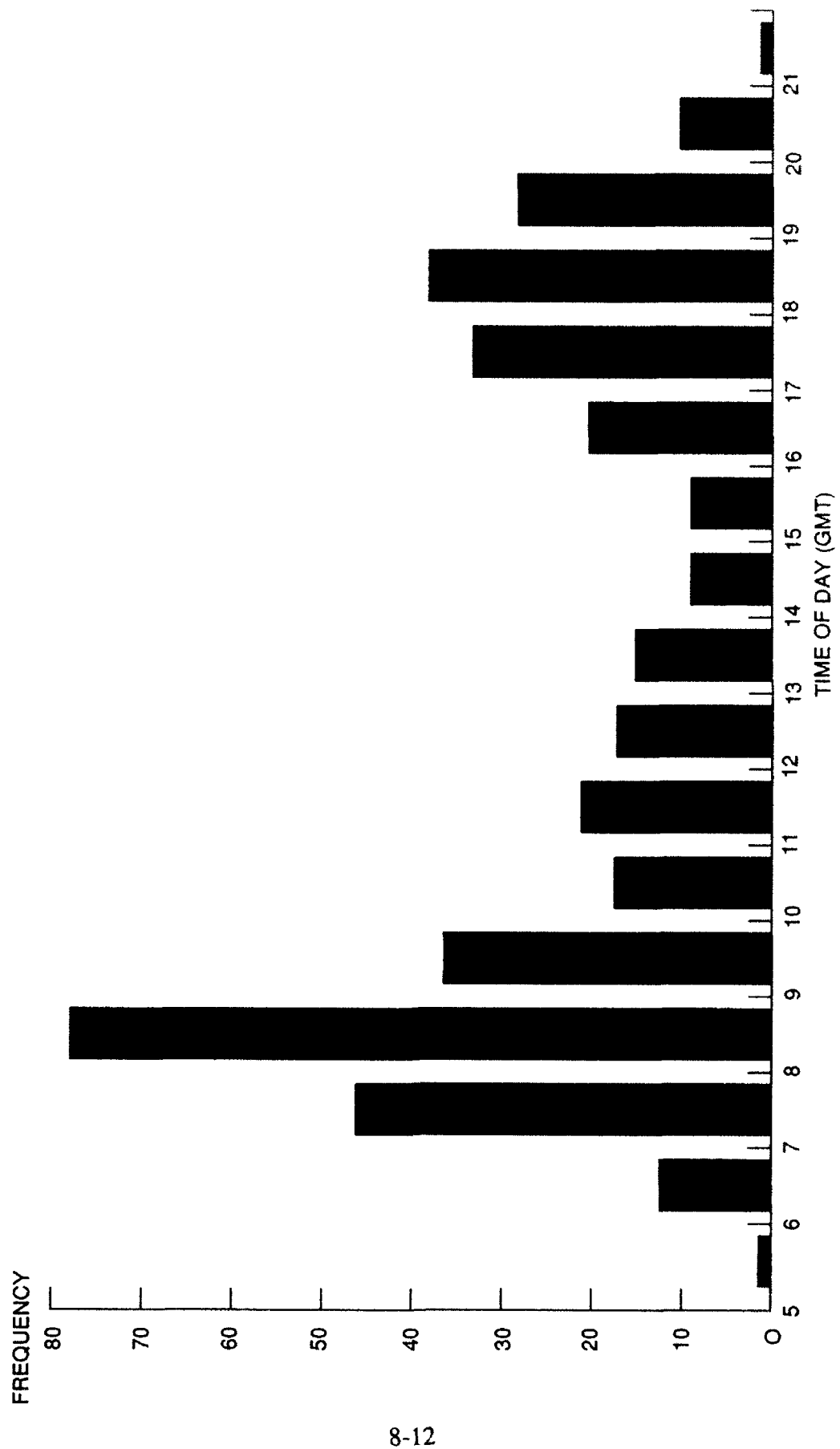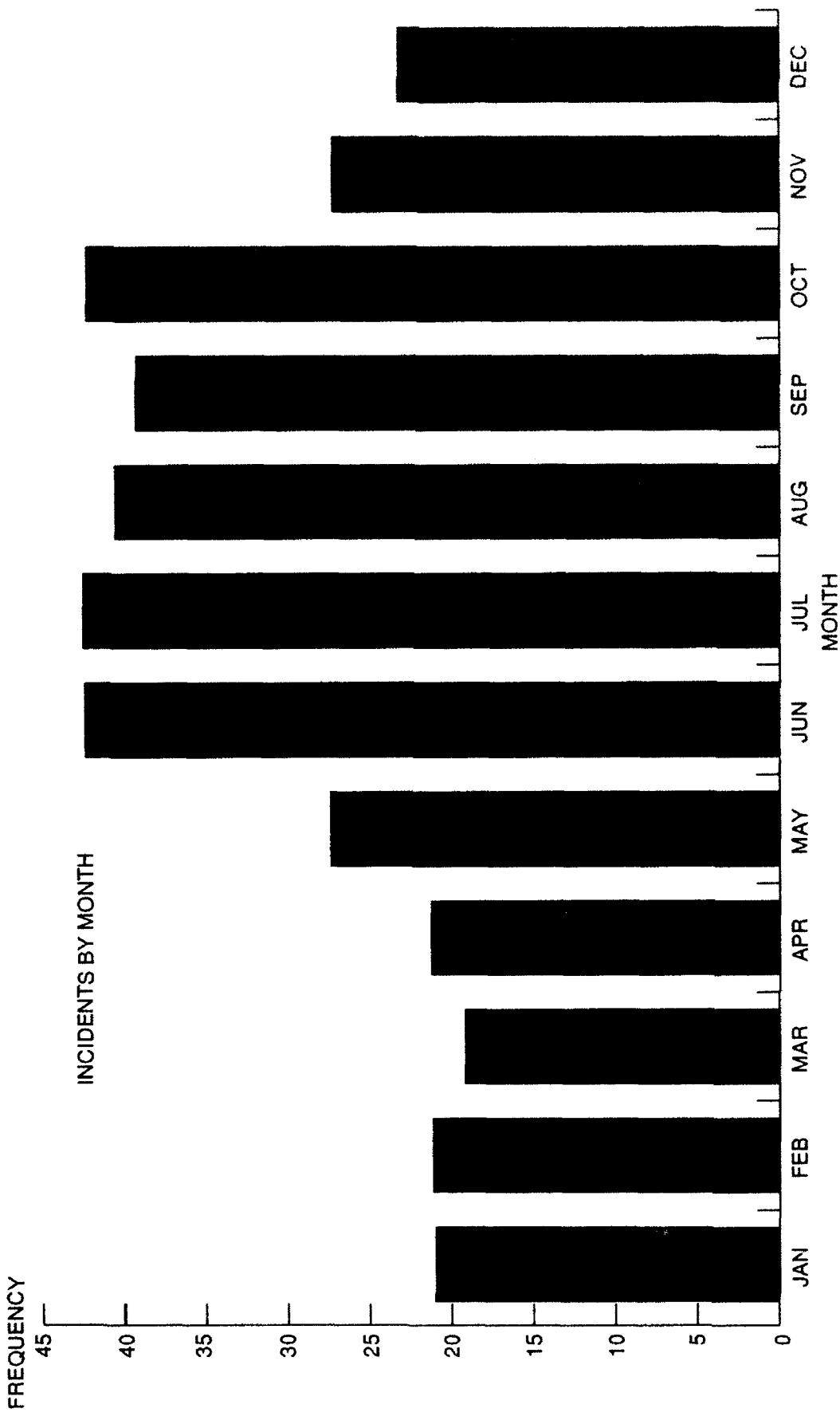
Figure 1.

Figure 2.

Figure 3.

Figure 4A.

Figure 4B.

8-14

CROSS WINDS

Figure 5.

Figure 6.

FREQUENCY

REQUIRED MINIMUM - ACTUAL SEPARATION (Nm)

Figure 7A.

FREQUENCY

CATEGORY A ONLY
(roll angle >30°)

REQUIRED MINIMA - ACTUAL SEPARATION (Nm)
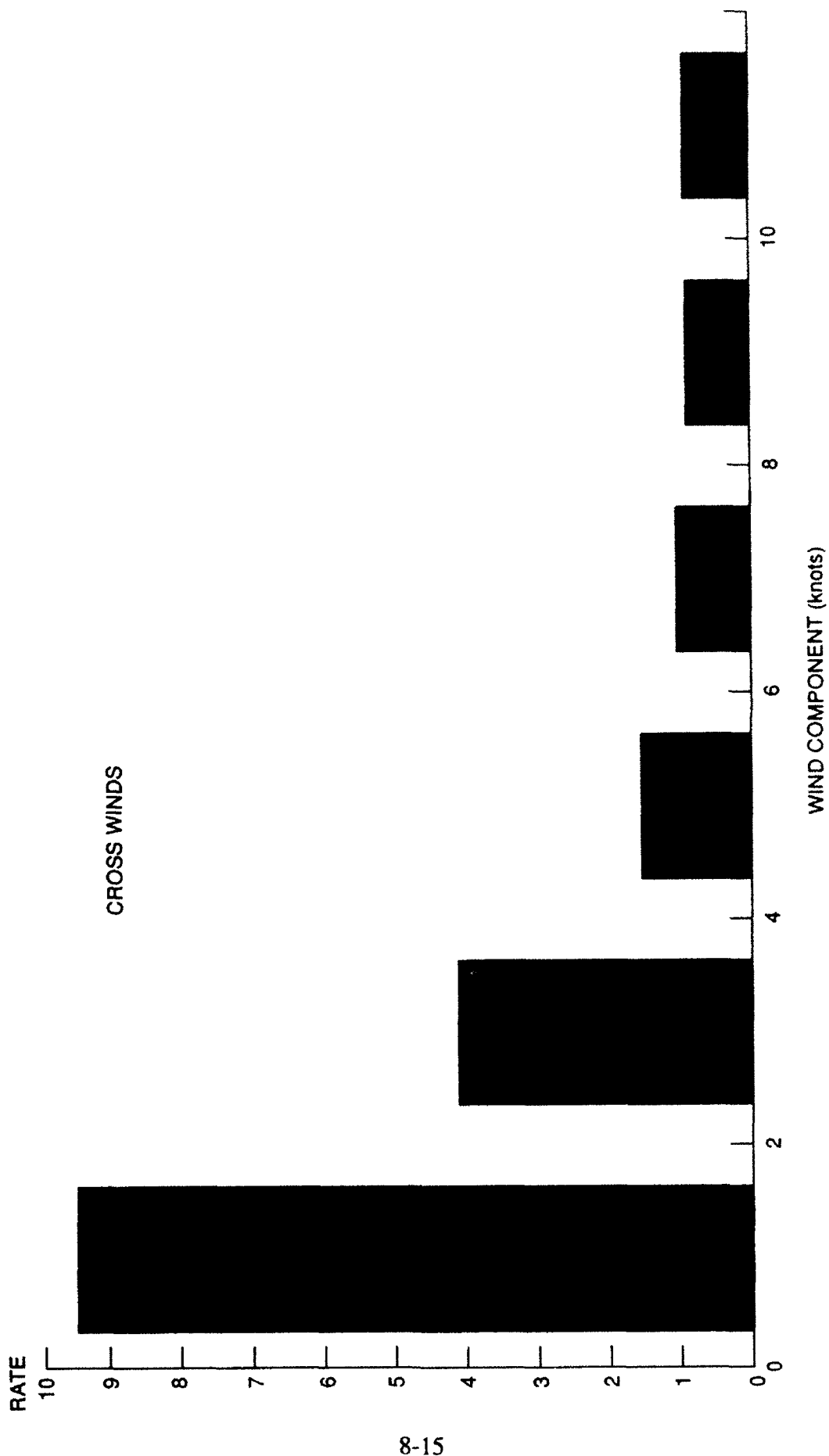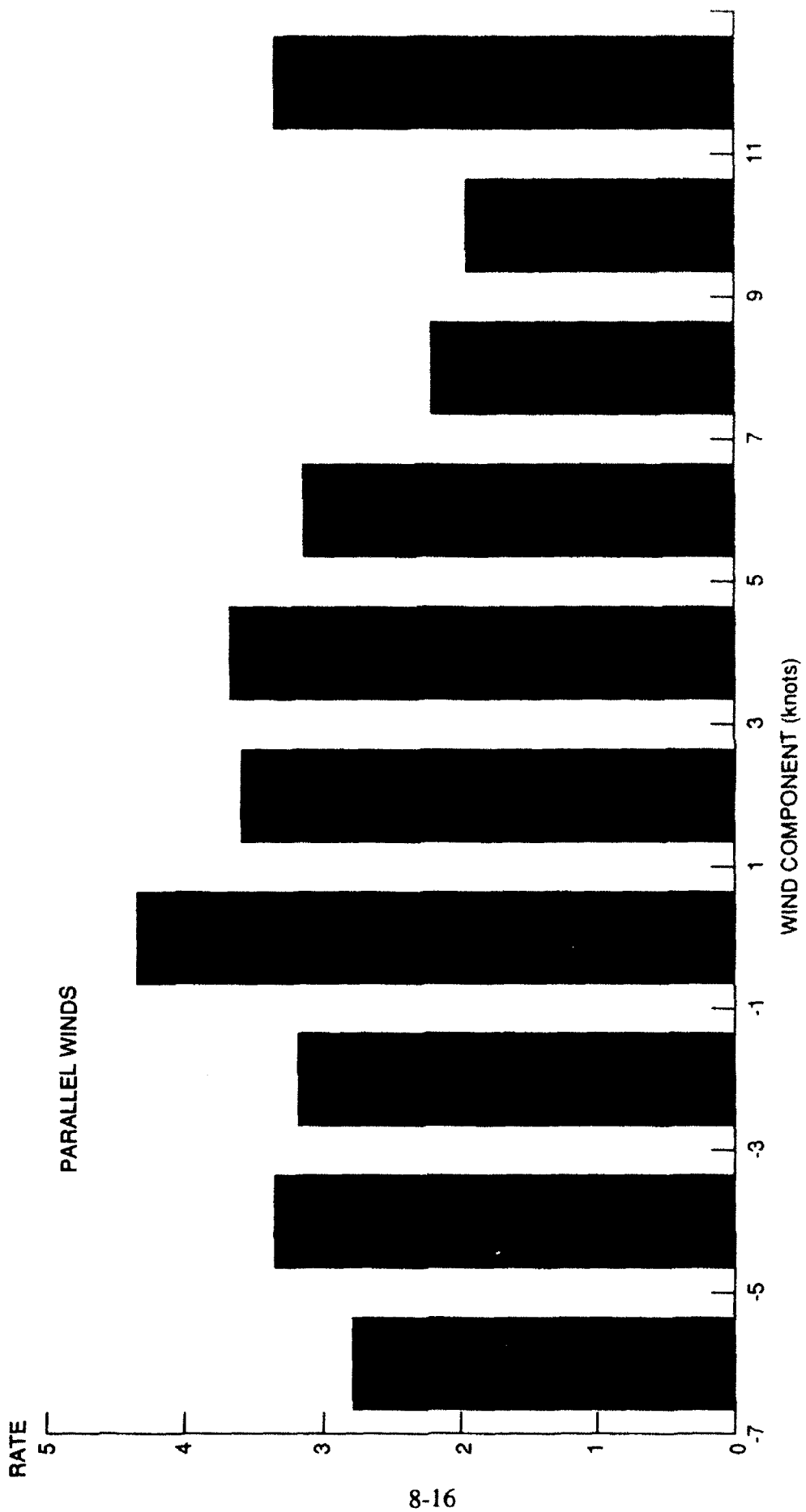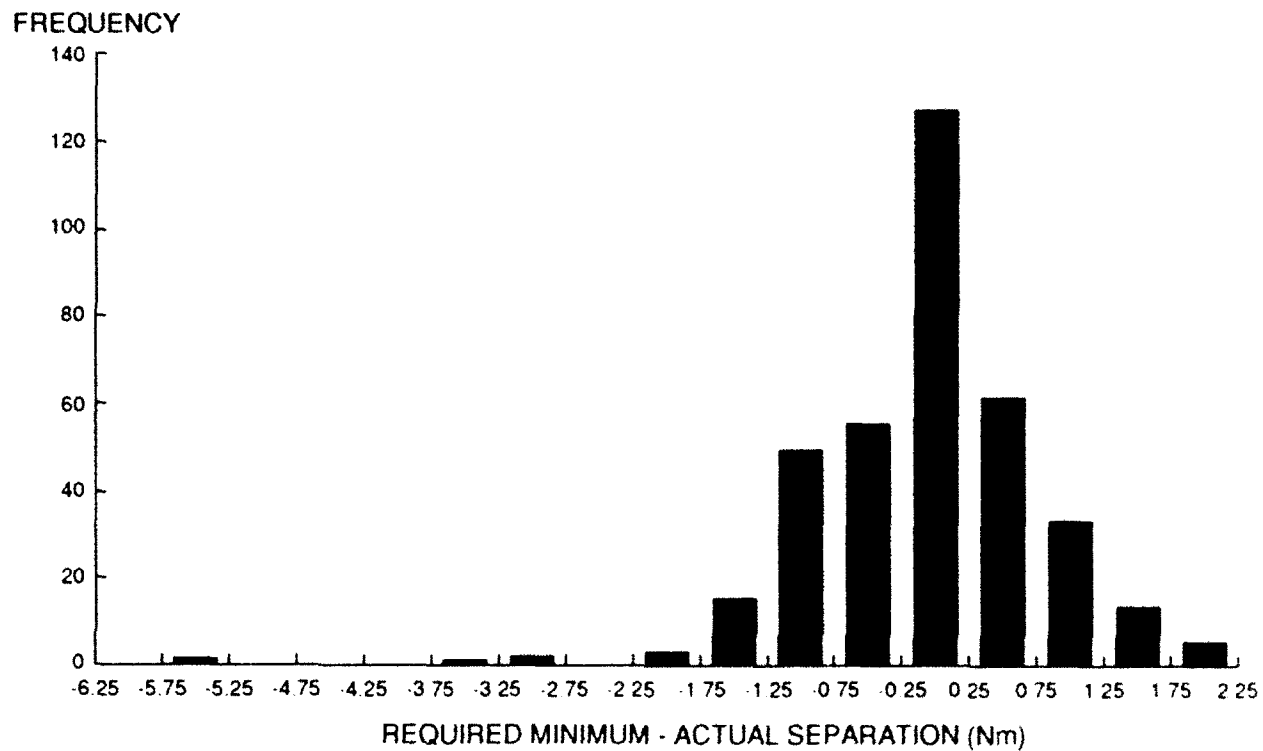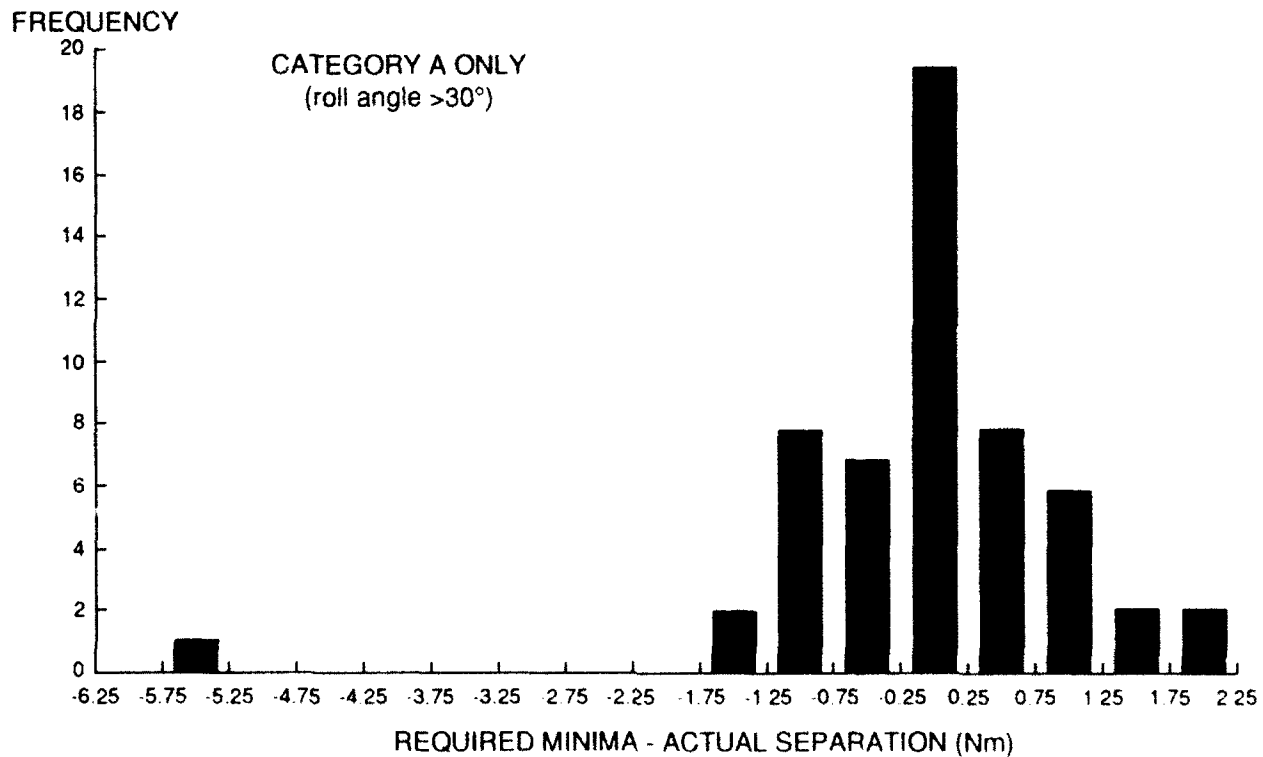
Figure 7B.

REFERENCES

1. Critchley, J.B., Foot, P.B., CAA Paper 91015: United Kingdom Civil Aviation Authority Wake Vortex Database: Analysis of Incidents reported between 1982 and 1990: August 1991.

2. Baggs, C., ATCEU Memorandum 177: The Wake Vortex Reporting Programme: July 1991.

3. Piggott, B.A.M., Pask, J.A., CAA Paper 77012: Wake Vortex Incidents reported in the UK: 1972-1976: June 1977.

TRENDS IN WAKE VORTEX INCIDENTS

Amanda Johnson
Brunswick High School
Brunswick, ME

under the direction of
Dr. Robert E. Machol
Federal Aviation Administration
Washington, D.C.

ABSTRACT

TRENDS IN WAKE VORTEX TURBULENCE INCIDENTS. An analysis of 140 incidents involving wake vortex turbulence over the past 7 years was undertaken to detect trends in these reports. After processing the files, patterns appeared. It was found that a majority of wake vortex incidents occur when a plane of the "large" weight class is preceded by a plane of the "heavy" class. Moreover, a large fraction of the incidents with the heavy/large and the large/large combination had the required spacing required by federal regulations, and most of the incidents happened in the landing/approach phase of the plane's flight, below 1000'.

INTRODUCTION

Wake vortex is a phenomenon created whenever lift is generated. To produce lift, the pressure on the upper surface of the wing must be less than that on the lower side so that the wing rises. But at the same time that the wing is rising to fill in the pressure gap, the air below the wing also flows around the wing-tip in an attempt to equalize the pressure. It is this wing-tip turbulence that creates the "horizontal tornadoes" called wake vortices. In the course of its flight a plane sheds a continuous trail of pairs of vortices that tend to sink until their strength dissipates by viscous decay, which is a gradual but accelerating loss of kinetic energy, or by other immediate ways (Reference 1). But often before the vortex decays, another aircraft encounters the turbulence, and it is in this manner that the vortices become a hazard. When a following plane encounters the wake of its predecessor, it will experience bumping or rolling, and if the strength of the vortex is great enough, the follower may completely lose control of the plane, with catastrophic results.

Atmosphere affects the strength and lifetime of a vortex. Crosswinds, while also changing its path, tend to decrease a vortex's longevity, as does any type of external turbulence (Reference

2). At the other extreme, in a completely still atmosphere where the cooler air is situated beneath the warmer air, vortices also dissipate faster, for their tendency to sink as a natural part of their cycle is inhibited due to the immobility of the atmosphere and they thus lose kinetic energy faster over time. However, in an atmosphere labelled neutrally stable, that is, when the temperature is rising slowly enough at a rate to match the vortices' rate of temperature change, vortices tend to remain, posing obvious danger to a following aircraft (Reference 3). In this situation, where the rates are said to be adiabatic, vortices become a great problem, for they can remain for a longer period of time than current federal separation standards for distance between aircraft necessarily provide for.

Before 1970 the wake vortex problem was little-known. a pilot was required to maintain only a three nautical mile (3 nm) separation from the plane in front of it (Reference 4), and this spacing had nothing to do with the wake turbulence problem. In order to protect passengers and crew from the hazards os wake vortex encounters, however, the federal government implemented a series of new separation standards in 1970 and a revision thereof in 1975 that divided aircraft into three weight categories, Small, Large, and Heavy, with respective weight ranges of less that or equal to 12,500 lbs, between 12,500 and 300,000 lbs, and greater than or equal to 300,000 lbs. Using these classes the FAA developed new separation guidelines. Instead of being a uniform 3 nm, the spacing depended on the weight of the plane and therefore on the strength of vortices it was likely to create. These standards have helped the wake vortex situation in some cases by decreasing the likelihood of a following plane penetrating another's vortices, but they have been found to be too conservative in some cases and not strict enough in others (Reference 5). Therefore more information must be gathered to improve spacing regulations in a cost-efficient but safe manner.

The purpose of this study was to detect trends in a series of wake vortex accidents and incidents. It is necessary that research be done into the spacing and altitudes at which these incidents occur so that any needed changes can be brought to the attention of the federal government. In this manner increased safety in the air can be acquired while at the same time unnecessary restrictions can be eliminated.

METHOD

To discover the areas in which federal regulations must be modified it was necessary to have a sample of vortex-related accidents and incidents. The accidents were research through the National Transportation Safety Board (NTSB), and a total of 31 accidents caused by wake vortex turbulence were found from 1983-1990. Incidents, cases when a crew-member noticed the rolling or itching characteristic of a vortex encounter without an actual accident occurring, were found through a sorting of the voluntarily reported cases of the Aviation Safety Reporting System (ASRS), a program under NASA that offers anonymity to those who report safety hazards or violations. With these two resources there was a total of 140 probable wake vortex problems. These were arranged on a data-base and then sifted through by computer and by hand in an attempt to find definite patterns. Trends were searched for in the areas of altitude, size of leading and following planes, month in which the accidents took place, and time of day at which the accidents occurred.

DATA

The 140 cases provided as data were reorganized several times with respect to different criteria.

The weight combinations and their tendencies with respect to wake vortex accidents and incidents were grouped, and from this grouping several patterns were found. In the cases that reported maintaining legal separation, 15 out of the total 130 cases, it was found that 11 of the cases had a heavy class plane as a leading plane creating the vortices (see Table 1), and 13 had a large as a following plane. (see Table 2) Ten of these cases involved a large plane behind a heavy (Table 3). Out of the system of all reports of incidents, 40% involved a heavy leader and 52.6% had a large leader (Table 4). The least frequent of leaders was the small plane in front, with only 7.4% of all incidents. 51.6% of all incidents involved a large plane following, and 35.8% involved a small as a follower, the least common follower being of the heavy type. (see Table 4) The most frequent combination of leading/following planes was the large/large set, with 25.3% of all incidents being cause by this pair, and 29.2% of these had legal separation. Next were the heavy leading large and the large in front of the small, both with 22.1%. (Table 4)

The months of the year were also taken into account in this study. for both the accidents and incidents combined the months with the most wake vortex encounters appeared to be February and August, each with 12.9% of all problems. Over a three month spread the time-period with the most was June to August with 32.9% occurring during these three months. Over a greater spread, 67.1% of all incidents happened from February to August. (Table 5)

The time of day information was only available on the NTSB reports, so the sampling was only 31 accidents total. But out of these accidents 61.3% occurred from 10 am to 6 pm, and the single time with the most was 1 pm with 16.1%.

The phases of flight of the planes was given in each case studied. By far the greatest number of accidents and incidents happened upon the landing or approach to landing, with 69 out of the 140 incidents occurring at these phases. The cruising phase of flights was the next most frequent (31), followed by take-off with 18 incidents/accidents, climbing, with 13, and descent, having 9 incidents. (Table 6) Also studied were the combinations of flight phases, such as whether the vortices were from a plane behind which the follower landed, or whether the planes took off successively, etc. Mote than 1/3 or all 140 cases occurred because a plane was on approach to landing behind another that was landing. Taking off behind another, sometimes separated from the leader by only a minute, was quite common, with 13 cases involving this situation. The rest of the occurrences happened with both planes cruising or with a plane taking off after another's landing, or vice versa. (Table 7)

Altitudes are an important factor in wake vortex encounters, because the atmosphere has such an effect on vortices. In the ASRS and the NTSB cases combined, there turned out to be 106 instances where the altitude was given. More than half of these (58) occurred below 1000', including situations at landing and a take-off. The number of cases at each altitude continues to decrease fairly steadily as altitude increases, with the exception that there are two incidents at 14,000'. (Table 8) Of the 34 non-landing or take-off incidents/accidents below 1000', 20 were on approach to landing and 5 were directly after take-off. (Table 9)

9-3

DISCUSSION

The data from this research agrees with some of the major trends found in past works, yet with others it differs. In part this has to do with the resources available with which to do this study. The NTSB accidents were helpful because they provided all the necessary information, but there weren't enough to do as thorough a study as is needed for it to be extremely useful. On the other hand, there were many ASRS incidents available to use, but because of the anonymity of the system, much relevant information was omitted by the reporter or deleted in the deidentification process. Therefore many areas that needed study were not examined because the needed data were not there.

Hallock states that "aircraft weighing less than 12,500 lbs have been the primary victims of the vortex problem "(Reference 4), and the results of this experiment uphold this. Aircraft of the small class were shown here to be the most common followers, feeling vortex effects in 51.6% of all accidents. (Table 4) This is expected, since the small type planes are more easily tossed and disturbed by turbulence. The weight class of follower that causes the next greater percentage in incidents is the large class, with 38.9%. (Table 4) This also is explainable, for this class covers a large range of weights, and the lighter end of the heavy class is not much heavier than the small class. In sheer numbers, also, the large class has the most, and the probability of a plane being in this class is relatively high.

The months in which the accidents and incidents occurred with the most frequency were June through August, and this trend fits in with the summer rush in air traffic. These are also the warmer months, and according to Greene and others, when the atmosphere is in the situation of warming (see Introduction), vortices are more likely to have an effect (Reference 3). The air is more likely to be heating in this manner in these summer months than in the winter, so this data is what was expected. The time of day was also predictable because they coincided with normal rush hours; the time period with the most accidents (the ASRS could not be used because this information was not available) was from 10 am to 6 am, 61.3% of the accidents happening at this time.

The flight phase of the planes was another factor that was taken into consideration to a great extent, for it is finding in which phases of flight a majority of the incidents occur that the federal government will be able to remedy the situation. Nearly one half of all accidents happened during the approach to landing and the actual landing. (Table 6) This was expected first of all because of the over-crowing hat airports are experiencing, since air traffic controllers try to squeeze in as many planes as they can, and in doing so they increase the possibility of a vortex encounter, but also the vortex is most likely to linger at the ground level, not being able to sink, and this is the place where another will be most likely to encounter it. On top of this, the most common combination for the follower/leader pair is landing behind landing. (Table 7) Even for the incidents with legal separation this trend holds true, for exactly half of supposedly "safely" separated landings behind other landings has some sort of wake vortex encounter.

The altitude at which the pane was flying is an important factor in dealing with wake vortex incidents. When the ASRS and NTSB data was combined, there were 106 cases with known altitudes (this was one area in which the ASRS reports did not require their reporters to give information, so whether or not to give information, so whether or not to give this information

was entirely the choice of the reporter). More than half of the encounters with wake vortices occurred below 1000', either in the direct vicinity of the runway or at a cruising phase of flight. (Table 8) As the altitudes increased, the number of accidents and incidents decreased nearly steadily. Of the problems reported to be below 1000' bun not actually during take-off or landing, the largest percentage happened as the plane was on approach to landing. (Table 9) Again, this was expected, for it is upon landing that airports are the most crowded, and vortices tend to linger near ground level.

CONCLUSIONS

In some ways this study was inconclusive because of the limitations of the data provided. However, the past research of others has in part been validated to the extent possible by these resources. The state of our air traffic system needs attention, because of the numbers of accidents and even incidents that occur due to wake turbulence. It is also apparent that the classification of the weight categories need to be changed, especially in the case of the large class. Factors such as the state of the atmosphere need to be taken into account along with the time of day and the size of the planes involved.

ACKNOWLEDGEMENTS

Table 1. Weights of Leaders

NUMBER OF INCIDENTS

WEIGHT OF LEADER

☐ HEAVY   ☐ LARGE
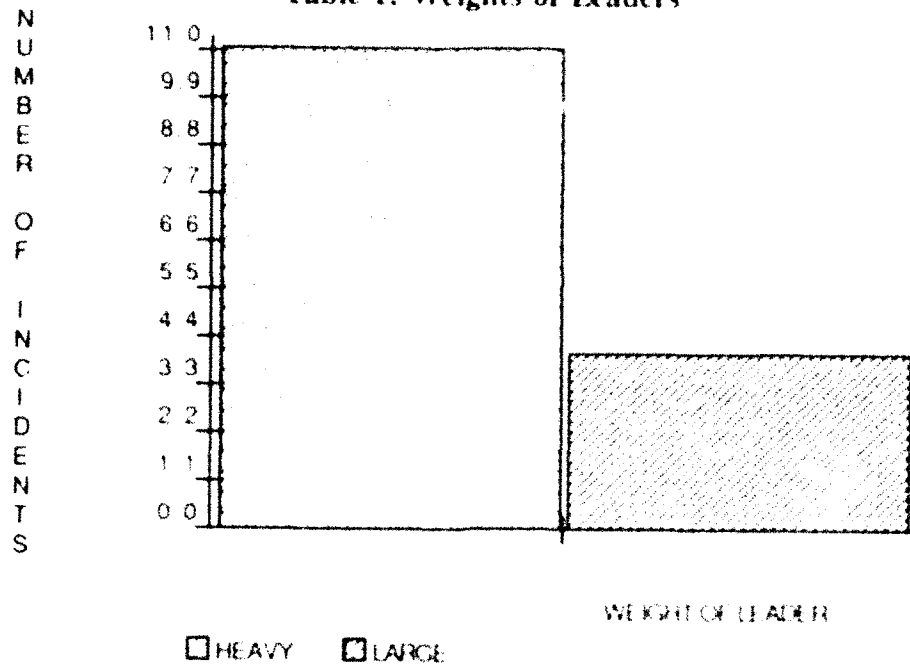
Table 2. Follower's Weight

NUMBER OF INCIDENTS

WEIGHT OF FOLLOWER
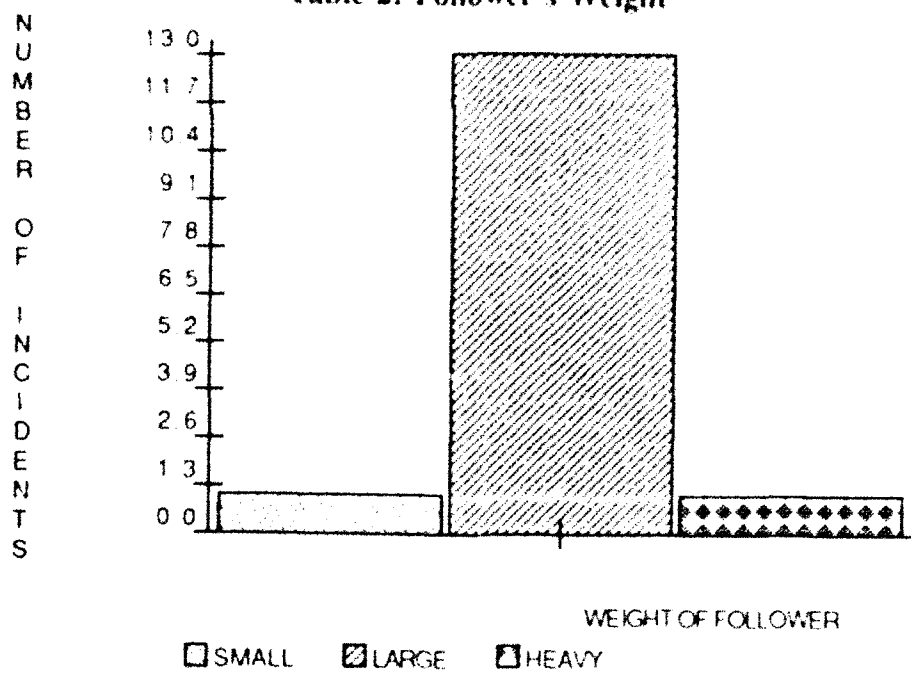
☐ SMALL   ☒ LARGE   ☐ HEAVY

Table 3. Weight Combinations (Incidents with Legal Separation)

LEADING PLANE	FOLLOWING PLANE		
	SMALL	LARGE	HEAVY
SMALL	0	0	0
LARGE	1	3	0
HEAVY	0	10	1

Table 4. Weight Combinations (All Incidents)

LEADING PLANE	FOLLOWING PLANE		
	SMALL	LARGE	HEAVY
SMALL	3	4	0
LARGE	21	24	5
HEAVY	10	21	7

Table 5. Months of Accidents/Incidents
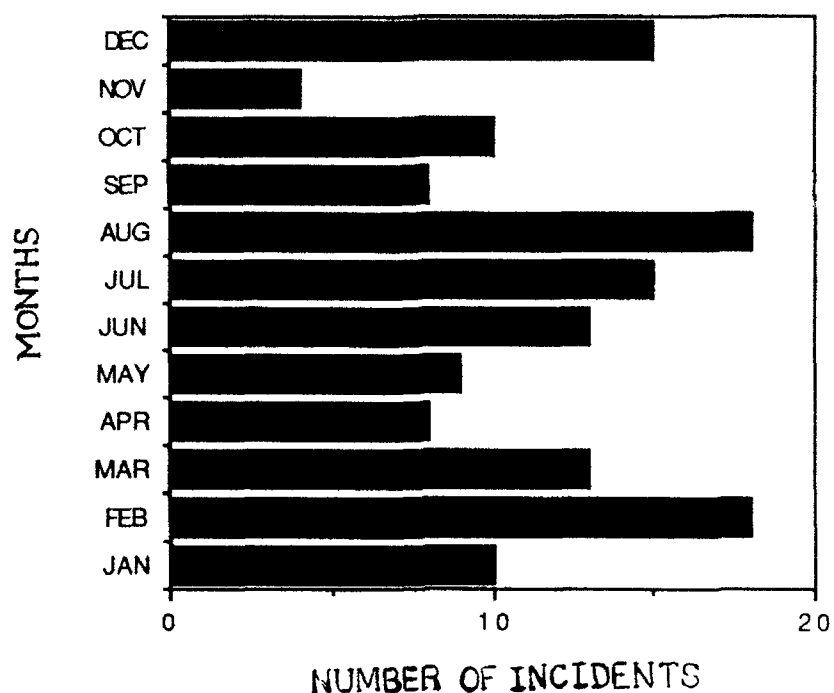
Table 6. Flight Phases of Following Planes

	TAKE-OFF	11.0%
	CLIMBING	10.1%
	CRUISING	21.1%
	DESCENT	8.3%
	APPROACH	34.9%
	LANDING	14.7%
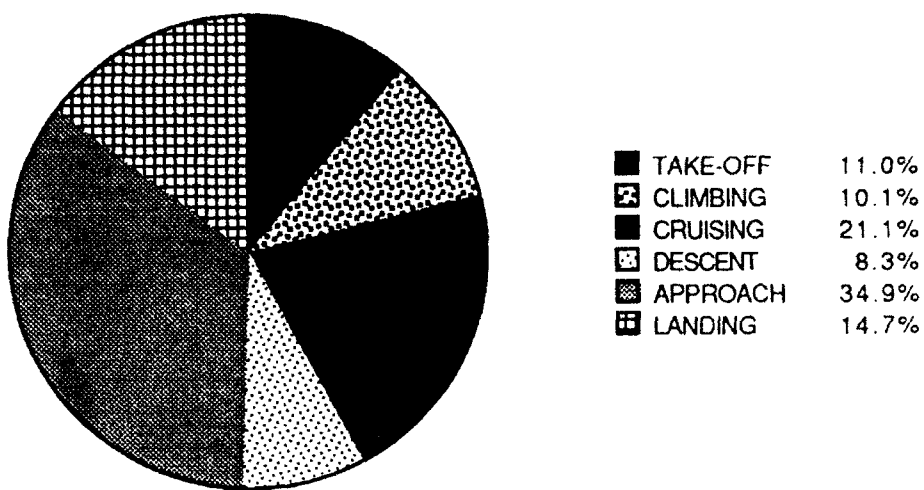
Table 7. Flight Phase Combinations

FLIGHT PHASE OF FOLLOWER/LEADER

LNDNG/LNDNG   T-OFF/LNDNG   LNDNG/T-OFF   T-OFF/T-OFF
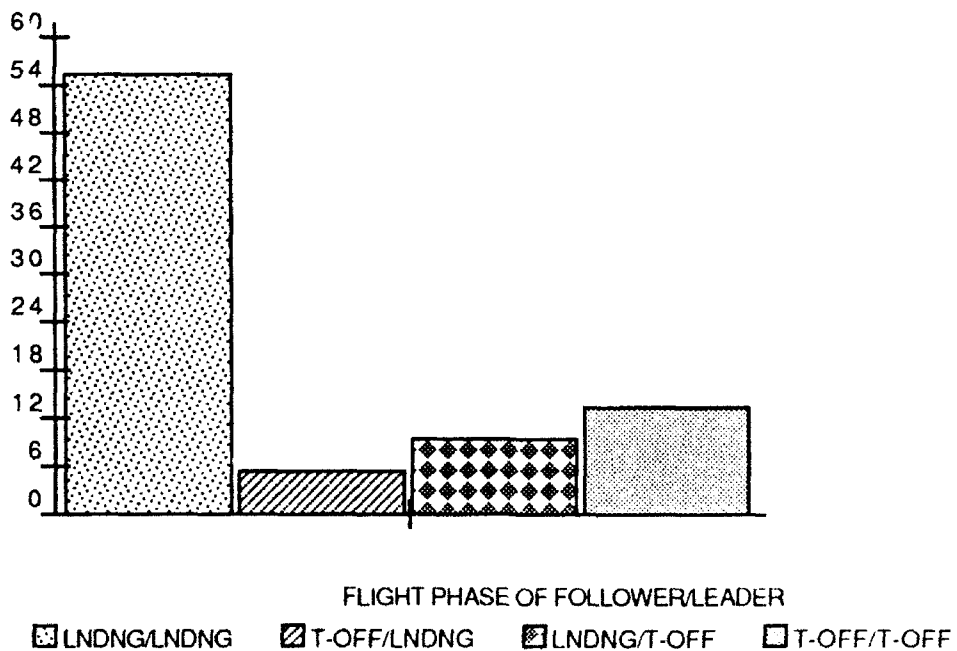
Table 8. Altitudes at Which Accident/Incident Took Place

#OF ACCIDENTS/INCIDENTS AT EACH ALTITUDE
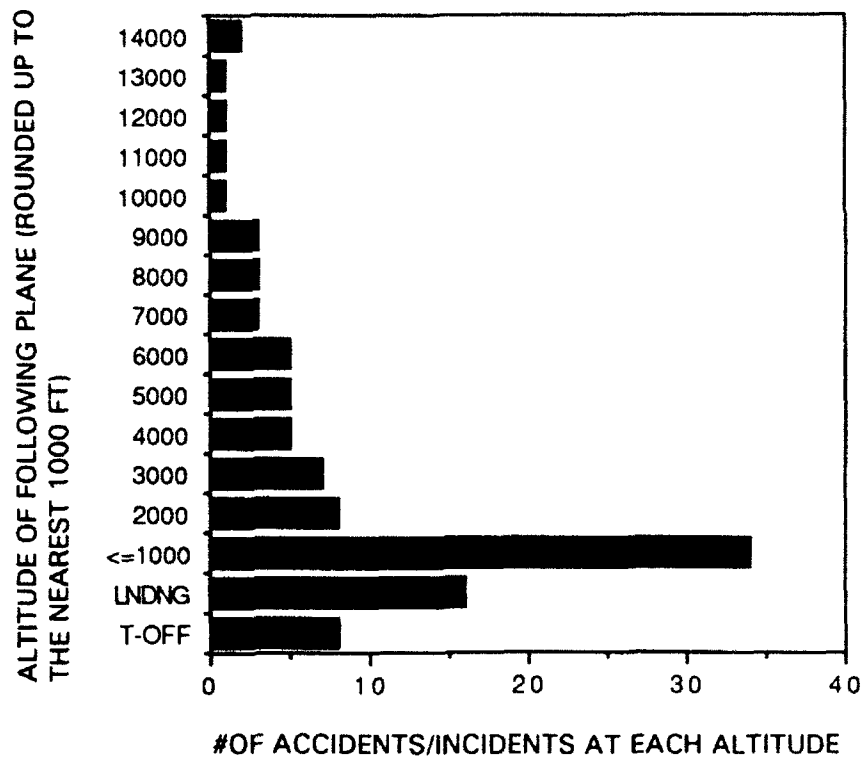
Table 9. Phase of Flight for Incidents

PHASE OF FLIGHT

□ LNDNG   ▨ T-OFF   ▧ OTHER
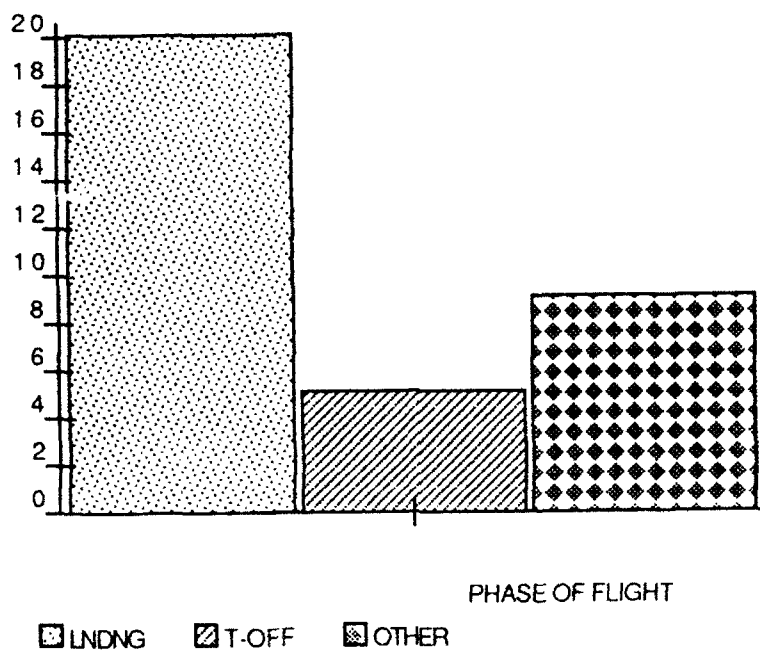
REFERENCES

1. Eberle, W.R., *Update of "Aircraft Wake Vortices: A State-of-the Art Review of the United States R&D Program."* DOT transportation Systems Center: Cambridge, MA, June 1985.

2. Greene, George C., "An Approximate Model of Vortex Decay in the Atmosphere." *Journal of Aircraft.* Vol. 23, No. 7, July 1986. pp 566-573.

3. Satran, D.R. et al., *Vortex Research facility Improvements and Preliminary Density Stratification Effects of Vortex Wakes.* American Institute of Aeronautics and Astronautics: Reno, Nevada, January 14-17, 1985.

4. Hallock, J.N., *Vortex Advisory System Safety Analysis, Vol 1: Analytical Model.* U.S. Department of Transportation: Cambridge, MA, June 1990.

5. Page, Richard D. et al., *Program Plan Wake Vortex.* U.S. Department of Transportation: Atlantic City, May 1990.

6. Hallock, J.N., *Aircraft Wake Vortices: An Assessment of the Current Situation.* U.S. Department of Transportation Cambridge, MA, June 1990.

ICAO WAKE TURBULENCE PROVISIONS

by

GIORA NAGID
Technical Officer, Rules of the Air, Air
Traffic Services and Search and Rescue (RAC/SAR Section)
Air Navigation Bureau
International Civil Aviation Organization (ICAO)
1000 Sherbrooke Street West, Suite 400
Montreal, Quebec
CANADA H3A 2R2

INTRODUCTION

In 1976, the ICAO Ninth Air Navigation Conference recognized the hazards associated with wake turbulence* and, in particular, the safety consequences to the following lighter aircraft which inadvertently penetrates the core of the wake generated by a preceding heavy jet. The Conference noted that action had already been taken by ICAO in 1967 requiring aerodrome controllers, whenever practicable, to advise aircraft of the expected occurrence of hazards caused by a turbulent wake. However, serious concern was expressed by the Conference regarding the slow progress in acquiring knowledge in this field. The Conference developed guidance material on the subject to be introduced by ICAO for world-wide application, and recommended that the guidance material be elevated to the status of Procedures for Air Navigation Services (PANS) once sufficient experience has been gained with its application by States. The guidance material included increased wake turbulence separation minima, to be applied either in radar control (distance separation) or non-radar control (time separation), based on wake turbulence aircraft categories. These separation minima were intended to greatly reduce the potential hazard of wake turbulence.

The ICAO Air Navigation Commission in 1978 agreed that the guidance material developed by the Ninth Air Navigation Conference be included in the relevant ICAO document. The Commission also noted that as a result of the increased wake turbulence separation behind heavy jets, additional delays and capacity constraints at major airports would be inevitable, and that further research was being carried out by several States to reduce this effect.

In ICAO, the term "wake turbulence" is used to describe the effect of the rotating air masses generated behind the wing tips of large jet aircraft, in preference to the term "wake vortex" and "wake vortices" which describe the nature of the air masses.

During the 1980s, the ICAO Secretariat analyzed studies carried out by several States exploring the practicability of reducing the wake turbulence separation minima in order to regain some of the runway capacity lost. These studies have focused on the concept of measuring and averaging wind speeds and directions near the approach end of a runway, comparing them with wind-rose criterion used to determine whether the wake turbulence could be expected to be removed from the runway faster with cross-wind than with a head or tail wind, and displaying the results to the air traffic controllers by means of lights - a red light indicating a need for increased separation and a green light indicating that separation could be reduced. The studies showed correlation between wake turbulence residence times and ambient wind conditions, and indicated that there are certain wind conditions which cause the wake turbulence to drift from the vicinity of the flight path. The results of these studies were encouraging from the technical standpoint. However, practical implementation was not possible due to serious operational problems. It has been found that the incidence of transition through red/green warning lights does not provide sufficient time for the controller to change the separation applied between various types of aircraft in an already established approach sequence. Therefore, further research in this respect was suspended.

Based on the results of ICAO study and following consultation with States, the Air Navigation Commission recommended to the Council of ICAO for approval a proposal to amend the Procedures for Air Navigation Services, Rules of the Air and Air Traffic Services (PANS-RAC, Doc 4444) wake turbulence guidance material and to upgrade it to the status of PANS. The amendment was approved by Council and is envisaged for applicability on 14 November 1991 (for convenience this amendment which was included in the ICAO PANS-RAC, Part V, paragraph 16, and Part X, paragraph 2.8.4, is reproduced in the Attachment to this paper).

DISCUSSION

The strength of the vortices is governed by the mass, speed and shape of the wing of the wake-generating aircraft, but mass is considered to be the primary factor. Accordingly, three aircraft categories, with the maximum take-off mass being the determining factor, were classified by ICAO: Heavy (H) - 136 000 kg or more; Medium (M) - less than 136 000 kg but more than 7 000 kg; and Light (L) - 7 000 kg or less. The optimum number of mass categories of aircraft was discussed in depth by ICAO, but it was considered that it would be difficult enough for the air traffic controllers to provide separation between three categories of aircraft and that to handle more than three would be impracticable.

With the objective of reducing the in-flight hazards associated with the trailing wake turbulence encounters, increased wake turbulence separation minima were developed by ICAO, to be applied either in radar or non-radar control (time separation). The radar separation minima extend from 3 to 6 NM while the time separation varies between two and three minutes, depending on the wake turbulence aircraft categories of the leading and the following aircraft and the phase of flight. It should be noted at this point that wake turbulence accidents (which had occurred primarily to light aircraft behind a heavy or medium aircraft) signified the need to give similar protection to a light category aircraft following a medium category aircraft as was afforded to a light or medium aircraft behind a

heavy category aircraft. It was noted that various types of medium category aircraft with maximum certificated take-off mass (maximum mass) less than 136 000 kg can generate wake turbulence with velocities similar to those generated by the heavy category aircraft. Accordingly, the Commission agreed that a radar separation minimum of 5 NM be introduced, instead of 4 NM, when a light category aircraft is following a medium category aircraft.

The ICAO wake turbulence separation minima are based on a grouping of aircraft types into three categories according to the maximum certificated take-off mass. It was recognized that helicopters also produce vortices when in flight and there is some evidence that per kilogramme of gross mass, their vortices are more intense than those of fixed-wing aircraft. Therefore, helicopters should be kept well clear of light aircraft when hovering or while air taxiing.

At present, the majority of ICAO Contracting States apply the ICAO wake turbulence procedures, particularly those concerning separation behind a "heavy" or "medium" leading aircraft and no implementation difficulties have been reported to ICAO. It should be noted, however, that some modifications were implemented by several States, notably the United States and the United Kingdom, which render their procedures slightly differently from the ICAO procedures.

The United States uses "Heavy", "Large" and "Small" in lieu of the ICAO categories H, M and L as currently contained in the ICAO PANS-RAC. The US informed ICAO that their terms were chosen in order to maintain standardization with existing terms/definitions contained within several US air regulations and that they have been used for many years for reasons other than the wake turbulence aspect. The US breakpoint between the "Large" and "Small" take-off mass is at 12 500 lb, as opposed to ICAO's 7 000 kg (15 500 lb). The US value was based on the Federal Aviation Administration's (FAA) technical analysis of the wake turbulence problem.

The United Kingdom uses "Heavy," "Medium," "Small" and "Light," where the "Medium" is less than 136 000 and more than 40 000 kg take-off mass, the "Small" is at 40 000 or less and more than 17 000 kg and the "Light" at 17 000 kg or less. The UK separation minima when a "Small" aircraft is behind a "Heavy" is at 6 NM, and when a "Light" aircraft is behind a "Heavy" is at 8 NM; "Small" behind "Medium" 4 NM and "Light" behind "Medium" 6 NM. Although somewhat different from the ICAO provisions, the UK indicated that the safety of operations at their aerodromes necessitated these modifications.

CONCLUSION

At present, the ICAO wake turbulence provisions have been implemented by the vast majority of Contracting States. Considerable efforts have been made by ICAO to standardize these provisions world-wide. Nevertheless, some States, including the United States and the United Kingdom, still have provisions which are different from those of ICAO in terms of designation and number of wake turbulence aircraft categories.

The wake turbulence phenomenon and the increased separation minima associated with it are factors limiting airport and airspace capacity. Additional research and development programmes, to detect and track wake vortices with a view to determining their dynamics and decay mechanism, are essential to determine the feasibility of reduced separation between aircraft, which would alleviate congestion and reduce delays at major airports.

ATTACHMENT
ICAO WAKE TURBULENCE PROVISIONS

1.   Wake turbulence categorization of aircraft and increased longitudinal separation
        minima

1.1   Wake turbulence categorization of aircraft

1.1.1   Wake turbulence separation minima shall be based on a grouping of aircraft types
        into three categories according to the maximum certificated take-off mass as follows:

        a)   HEAVY (H) - all aircraft types of 136 000 kg or more;

        b)   MEDIUM (M) - aircraft types less than 136 000 kg but more than 7 000
              kg; and

        c)   LIGHT (L) - aircraft types of 7 000 kg or less.

1.1.2   Helicopters should be kept well clear of light aircraft when hovering or while air
        taxiing. *Note- Helicopters produce vortices when in flight and there is some
        evidence that, per kilogramme of gross mass, their vortices are more intense than
        those of fixed-wing aircraft.*

1.2   Wake turbulence separation minima

1.2.1   The following non-radar separation minima shall be applied:

1.2.2   Arriving aircraft

1.2.2.1   For timed approaches, the following minima shall be applied to aircraft
              landing behind a HEAVY or a MEDIUM aircraft:

              a)   MEDIUM aircraft behind HEAVY aircraft - 2 minutes;

              b)   LIGHT aircraft behind a HEAVY or MEDIUM aircraft - 3 minutes.

1.2.3   Departing aircraft

1.2.3.1   Except as set forth in 1.2.3.2 a minimum of 2 minutes shall be applied
              between a LIGHT or MEDIUM aircraft taking off behind a HEAVY aircraft
              or a LIGHT aircraft taking off behind a MEDIUM aircraft when the aircraft
              are using:

              a)   the same runway;

b) parallel runways separated by less than 760 m;
   Note- See Figure I.

c) crossing runways if the projected flight path of the second aircraft will cross the projected flight path of the first aircraft at the same altitude or less than 300 m (1 000 ft) below;

d) parallel runways separated by 760 m or more, if the projected flight path of the second aircraft will cross the projected flight path of the first aircraft at the same altitude or less than 300 m (1 000 ft) below.

Note- See Figure II.

1.2.3.2   A separation minimum of 3 minutes shall be applied between a LIGHT or MEDIUM aircraft when taking off behind a HEAVY aircraft or a LIGHT aircraft when taking off behind a MEDIUM aircraft from:

a) an intermediate part of the same runway; or

b) an intermediate part of a parallel runway separated by less than 760 m.
   Note- See Figure III.

1.2.4   Displaced landing threshold

1.2.4.1   A separation minimum of 2 minutes shall be applied between a LIGHT or MEDIUM aircraft and a HEAVY aircraft and between a light aircraft and a MEDIUM aircraft when operating on a runway with a displaced landing threshold when:

a) a departing LIGHT or MEDIUM aircraft follows a HEAVY aircraft arrival and a departing LIGHT aircraft follows a MEDIUM aircraft arrival; or

b) an arriving LIGHT or MEDIUM aircraft follows a HEAVY aircraft departure and an arriving LIGHT aircraft follows a MEDIUM aircraft departure if the projected flight paths are expected to cross.

1.2.5   Opposite direction

1.2.5.1   A separation minimum of 2 minutes shall be applied between a LIGHT or MEDIUM aircraft and a HEAVY aircraft and between a LIGHT aircraft and a MEDIUM aircraft when the heavier aircraft is making a low or missed approach and the lighter aircraft is:

a) utilizing an opposite-direction runway for take-off; or
   Note- See Figure IV.

10-6

b) landing on the same runway in the opposite direction, or on a parallel opposite-direction runway separated by less than 760 m.

Note- See Figure V.

WAKE TURBULENCE SEPARATION MINIMA FOR
CROSSING AND FOLLOWING AIRCRAFT
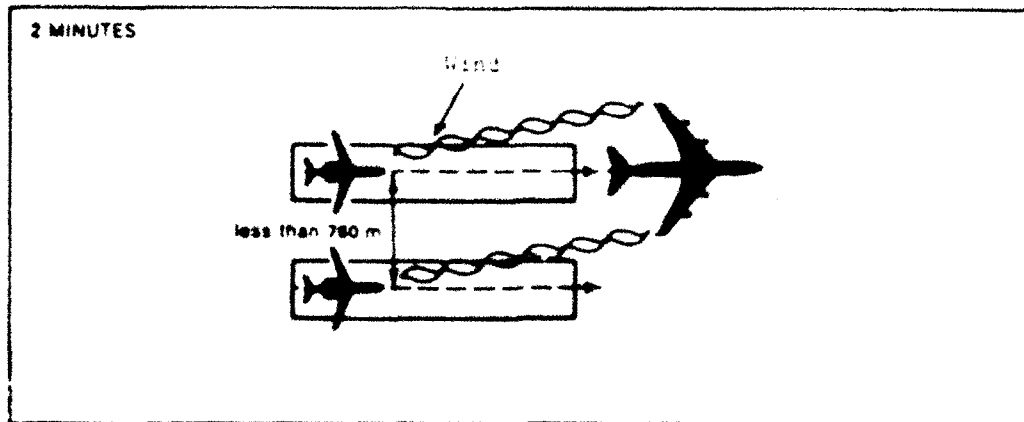
Figure I (see 1.2.3.1 b))

Figure II (see 1.2.3.1 c) and d))

3 MINUTES

less than 760 m
rotation point
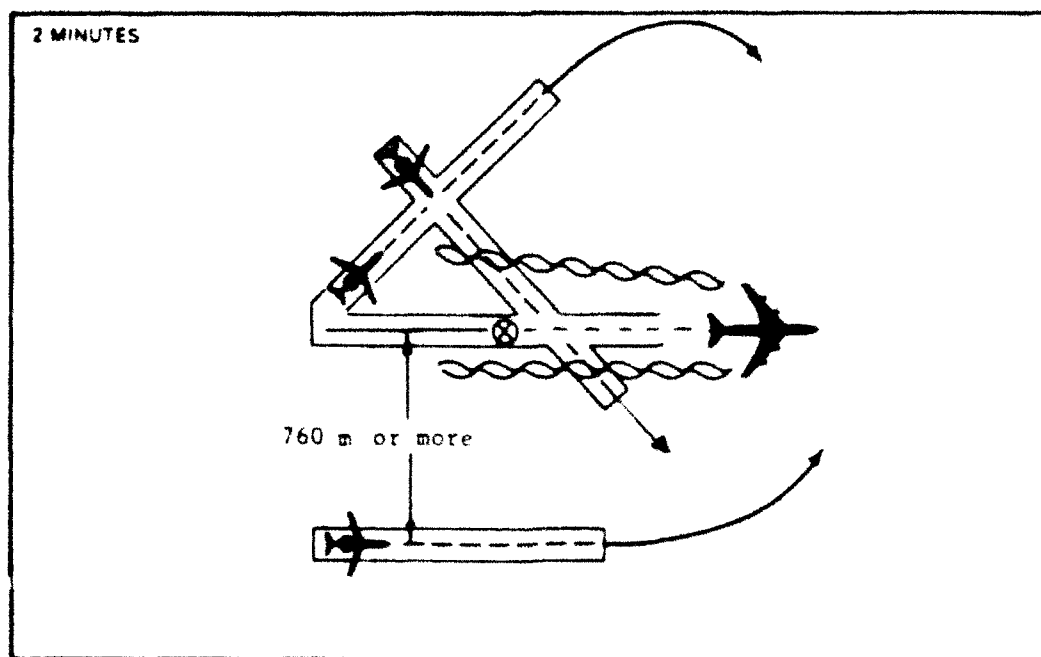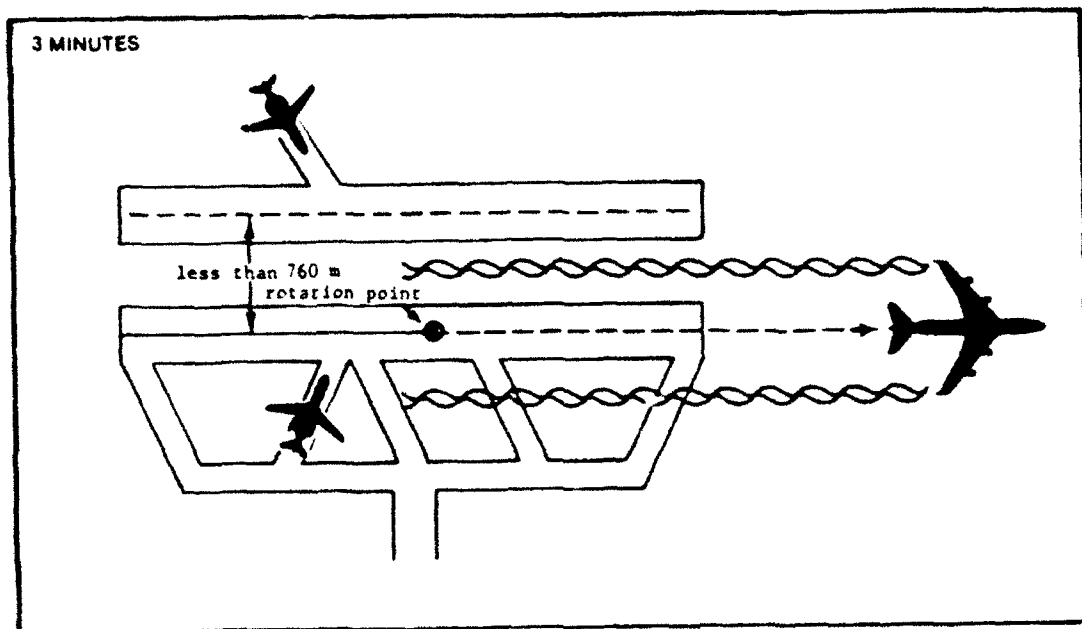
Figure III (see 1.2.3.2 a) and b))

2 MINUTES

2 minutes

Figure IV (see 1.2.5.1 a))

2 MINUTES

less than 760 m

2 minutes

2 minutes
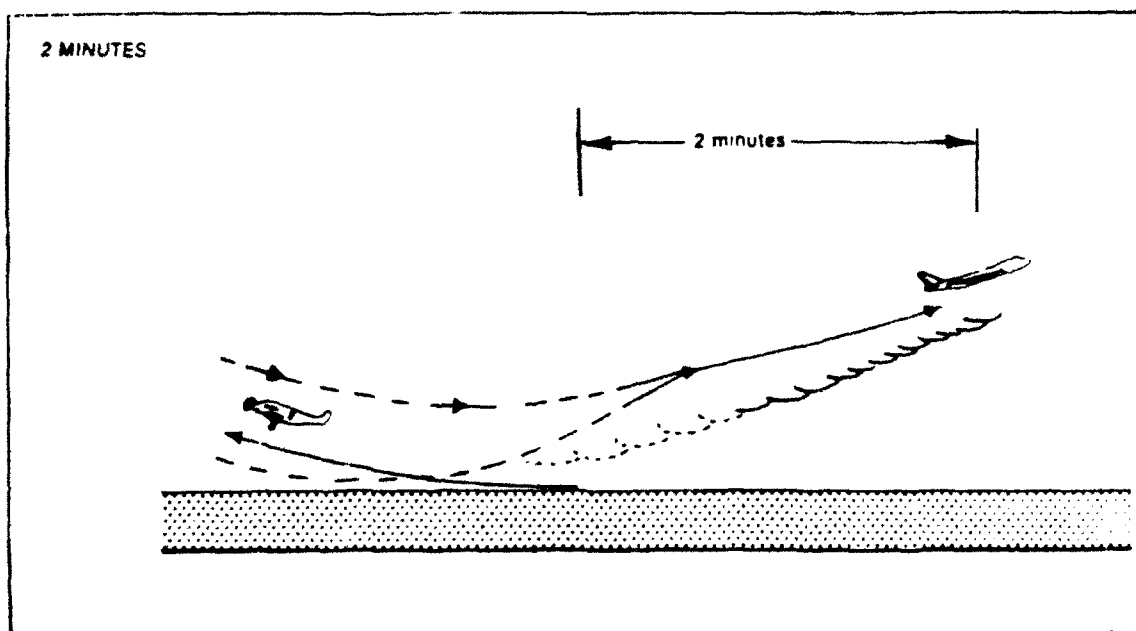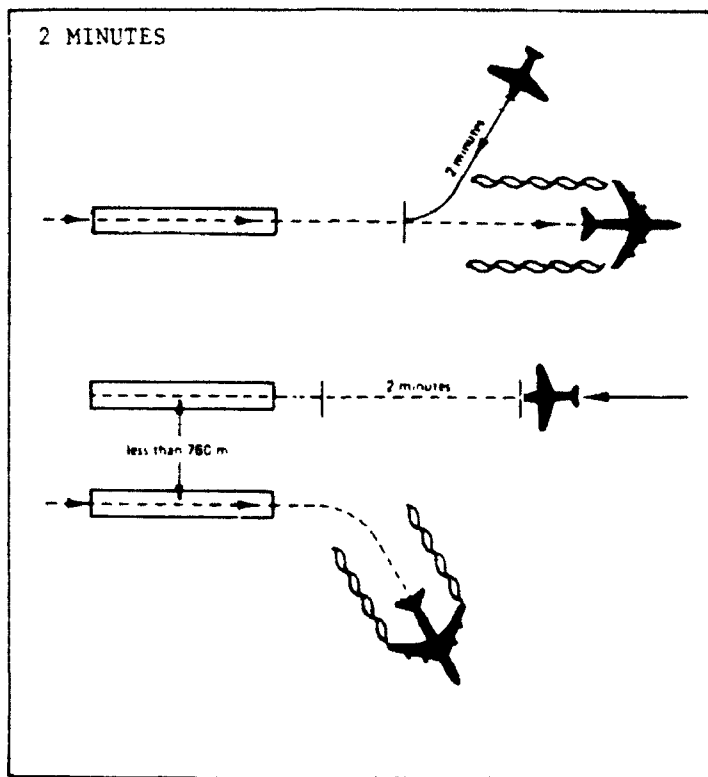
Figure V (see 1.2.5.1 b))

1.3   Radar separation minima

1.3.1   The following ICAO wake turbulence radar separation minima shall be applied to aircraft in the approach and departure phases of flight in the circumstances given in 1.3.2.

Aircraft categories		
Leading aircraft	Following aircraft	Separation minima
HEAVY	HEAVY	7.4 km (4.0 NM)
	MEDIUM	9.3 km (5.0 NM)
	LIGHT	11.1 km (6.0 NM)
MEDIUM	HEAVY	5.6 km (3.0 NM)
	MEDIUM	5.6 km (3.0 NM)
	LIGHT	9.3 km (5.0 NM)
LIGHT	HEAVY	5.6 km (3.0 NM)
	MEDIUM	5.6 km (3.0 NM)
	LIGHT	5.6 km (3.0 NM)

1.3.2   The minima set out in 1.3.1 shall be applied when:

a)   an aircraft is operating directly behind another aircraft at the same altitude or less than 300 m (1 000 ft) below; or

b)   both aircraft are using the same runway, or parallel runways separated by less than 760 m; or

c)   an aircraft is crossing behind another aircraft, at the same altitude or less than 300 m (1 000 ft) below.

Note- See Figure VI.

```
7.4 km (4.0 NM) - HEAVY behind a HEAVY
9.3 km (5.0 NM) - MEDIUM behind a HEAVY

11.1 km (6.0 NM) - LIGHT behind a HEAVY
9.3 km (5.0 NM) - LIGHT behind a MEDIUM
```

7.4/9.3/11.1/9.3 km
(4.0/5.0/6.0/ 5.0 NM)
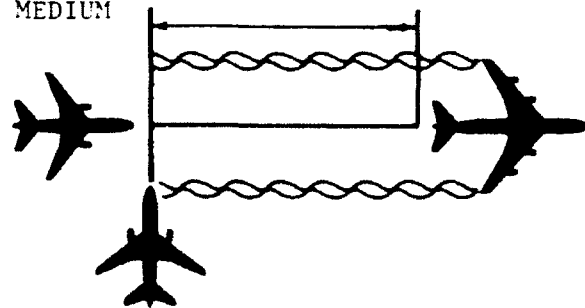
Figure VI (see 1.3.1 and Table)

LOOK AT INCIDENTS AND ACCIDENTS RECORDS AND LEARN TO IMPROVE PILOTS TRAINING

Claude Stouff
Direction Générale de l'Aviation Civile (DGAC)
Paris, France

INTRODUCTION

While many people are doing some research on the wake vortex phenomenon in order to reduce the spacing minima because of the congestion now being experienced at major airports, accidents reports in France show that it would also be wise to look more thoroughly at general aviation and try to improve safety for pilots operating small aircraft u..der visual flight rules (VFR).

Though the recent ICAO DOC 4444 which is now applied in France introduced increased spacing minima because of wake vortex, the procedures defined only apply to flights conducted under instrument flight rules (IFR). The situation is not crystal clear for light aircraft flying under VFR. Concerning the subject of wake vortices, the service that should be provided by Air Traffic Control is not clearly defined.

For the past 3 years, 4 accidents and 1 incident caused by wake vortex have been reported to the French Accidents Investigations Office. In all cases, the aircraft was being operated under VFR for private purposes. As far as public transport is concerned, no accident was reported, only a few incidents which led to internal inquiries within the airline concerned. Not many incidents due to wake vortices are reported because, most of the time, the pilot does not identify clearly wake vortex as the cause, but often thinks it is due to some normal turbulence.

This paper provides a comparative analysis of these accidents and incidents which occurred in France to small airplanes, and gives recommendations for improvements in the two fields concerned, Air Traffic Control and Pilots training.

ANALYSIS OF ACCIDENTS AND INCIDENTS WHICH HAPPENED IN FRANCE

The four accidents and the incident which happened in France since 1989, were all caused by wake vortices though the situations noticeably differed. The main common points between these five cases are that the aircraft involved was always small, was following a big aircraft, was flying under VFR, and that it happened during approach.

It is very difficult, for all of us and also for pilots and ATC controllers, to be aware that the combination of the different parameters which can be observed can lead to a dangerous situation. Accidents or incidents which actually happened can help us to understand some main potentially dangerous situations. In that matter, the five cases analysed below can give a kind of overview of what may happen.

Facts

The first accident happened in Istres, where there is only one runway. A Robin DR 400 presented itself in short final for runway 33, about 2 minutes after a Boeing KC 135F had done a Touch and Go.

The situation is represented in Figure 1. The two aeroplanes are flying under VFR and there is a prevailing wind on the ground from 340° of less than 5 kt. At 1500 ft, another pilot reports a wind from 150° of 12 to 15 kt. The pilot also notices in final, at 200 ft, a light North/North-West wind.

The pilot of the DR400 knows the Boeing's presence. After having been informed by the ATC controller of the touch and go of the KC135F, he says he is going to increase his longitudinal separation in order to avoid the wake vortices generated by the KC135F. Therefore, at 500 ft, he extends his downwind and makes two 360 degrees turns before turning on base. For traffic reasons, the pilot is aiming for an impact point at the very beginning of the runway in order to clear the runway quickly.

In short final, at a height of about 150 ft, the DR400 encounters the right (probably) wake vortex of the KC 135F, and the pilot loses control. The aircraft is destroyed.

The second one happened in Bordeaux. The two aeroplanes were landing on the same runway. A Cessna 177 in VFR arrived in final about 1 min 30 s after the landing of a Mercure (DA01) in IFR.

The situation is represented in Figure 2. There is a wind of 4 to 6 kt, prevailing headwind. The pilot knows the Mercure's presence; but, due to the meteorological conditions, he tries to land as soon as possible.

In very short final, the Cessna encounters the wake turbulence of the Mercure, the pilot loses control and the aircraft touches ground really roughly. The right landing gear is greatly damaged.

The third one happened in Toulouse where there are two parallel runways, separated by 300 meters. A TB20 arrived on final for the 33R about 2 minutes after the landing of a Boeing 747 on the 33L (with a threshold 700 m further than the one of the 33R).

The situation is represented in Figure 3. The two aeroplanes are operated under VFR and there is a crosswind of 4 to 6 kt.

On short final, at about 200 ft, 2 min 14 s after the 747 has touched down, the aircraft encounters the right wake vortex of the 747 and the pilot loses control. The aircraft is destroyed.

In that case, it is interesting to note that it occurred during a test to obtain the professional pilot license (for explanation, see in the abbreviations used for Table 1). The pilot was no beginner and on board were his instructor and the examiner, both having about 6000 hours of flying time. The examiner, seated in the back, thought for a moment about wake vortex, but did not want to interfere and left it to the pilot and his instructor. Then, having a lot of things to watch for, he forgot about it. The instructor admitted that he really did not think about it. As far as the pilot is concerned, because of the test environment, he was concentrating on his approach (trying to take the perfect slope, etc...) and did not think about it either.

They knew the 747 was in the circuit but the controller never pointed it out to them, which would have stressed the possible danger of the 747 wake vortices. Therefore, they missed the outside input which could have led them to take the necessary actions.

The last accident happened in Perpignan which is equipped with two diverging runways (33 and 31); the consequence is that the final approach paths of the two runways are intersecting, the circuit for the 31 being left-handed and the circuit for the 33 being right-handed. A Piper PA22 turned on base for the 31, when an A 320 was touching down on runway 33.

The situation is represented in Figure 4. The PA22 is flying VFR and there is a wind, which is both crosswind and tailwind for runway 31, of 3kt.

During the PA22 downwind for the 31, the ATC controller informs the pilot of the PA22 that there is an A 320 at the end of its downwind for the 33. Because of the poor visibility, the pilot of the Piper decides to make a 360° turn before turning into base in order to avoid collision and, therefore, decides to let the A 320 pass in front of him. In final, at a height of about 180/200 ft, the PA22 encounters the right vortex of the A 320 which had passed there about 1 minute and 40 seconds before at a height of 270 ft. The pilot loses control. The aircraft is destroyed and the pilot dies.

The incident took place in Montpellier, where runway 31 was in service. A Cessna 310 turned in base when an Airbus was about to pass the runway threshold.

The situation is represented in Figure 5. The wind on downwind and base (at 1000 ft) is a cross/tailwind of about 8 kt. The wind on final is a cross/tail wind of 4 kt.

During the Cessna downwind, the controller asks the pilot to extend his downwind in order to let an Airbus pass. The airbus turns on base at 1500 ft, 500 ft higher than the Cessna. The pilot of the Cessna extends his downwind to what he estimates is half a nautical mile. As soon as he is established on base, he encounters the wake turbulence of the Airbus. The aircraft is going into a roll. The pilot lets the aircraft make a complete roll, then takes the control back, 300 ft below.

The spacing applied by the Cessna was not sufficient. The Airbus had passed above at 150 m about 2 minutes and 30 seconds before. With a relatively low wind, the vortices normally descended at a rate of 1m/s.

Analysis

Table 1 is a summary of the five cases and provides a comparison of the main factors involved: the leader aircraft, the injured aircraft, the flight rules under which the small aircraft was flying, the wind, the runway configuration of the aerodrome, the information which was given by the ATC controller to the pilot, the separation applied by the pilot, the height at which it happened, the pilot's qualifications and experience, some remarks and the consequences of the accident.

In the table, the following abbreviations were used:

Consequ:	consequences
TG:	Touch and Go
SFinal:	Short Final
Cross/tail wind:	wind which is both crosswind and tailwind
Cross/head wind:	wind which is both crosswind and headwind
// runway:	parallel runway
Basic License:	it is a private license which only gives you the right to fly in France, without any passenger and in a range of 30 km from the aerodrome of departure.
Prof. Pilot:	it is a French license called the "Professional Pilot" which authorises you to fly for work (photography, agricultural tasks...) and which, if combined with the IFR rating, allows you to fly in public transport with certain restrictions.
MTO conditions:	meteorological conditions
Crash Loc:	location of the crash

You can notice that :

1. in all cases, the "injured" aircraft is flying under VFR.

2. in all cases, the wind speed does not exceed 8 kt.

11-4

3. in the two accidents where the two aircraft involved were to land on the same runway, the wind direction was the same as the runway direction (headwind).

4. in the two accidents where the two aircraft were using two different runways, the wind was a crosswind.

5. on the case of the incident, it did not happen during final approach as in all the others, but on base, and the small aircraft was below the big one.

6. in all cases, the pilot knows the presence of the aircraft preceding him.

7. in four cases, the controller had informed the pilot of the presence and the position of the preceding aircraft.

8. in two cases (Istres and Montpellier), the pilot increases his separation to avoid the vortices of the preceding aircraft.

9. in all cases, the separation is equal to or less than 2 min 30 s.

10. in all cases, the pilot is no beginner and should know about the phenomenon.

This study shows that the wake vortex phenomenon is still not fully mastered. Indeed, even if the pilots have a theoretical knowledge of the phenomenon and of its effects, it seems that, in practice, they have trouble taking into account the moving of wake vortices. It seems even more difficult when there is only a light wind. The use of some parallel or intersecting runways or flight paths complicates the situation even more.

RECOMMENDATIONS

Characterization of the different situations

This analysis shows that pilots and ATC controllers are not fully aware of all the different situations which are potentially dangerous because of wake vortex. There are many parameters to take into account. A characterization of the different situations must be determined and explained in detail to ATC controllers and pilots during their training.

This subject is now being worked on by the specialists who are trying to reduce the spacing minima and who therefore need to find a more accurate classification than the existing ICAO one. The studies take into account the aircraft weight (light, heavy), the propulsion system (turbopropeller, jet aircraft), the aircraft shape and size (wing design, small, big), the flight phase (take-off, approach), the airport configuration (parallel, intersecting or converging runways) and the meteorological conditions (wind, temperature as an indicator of stability or unstability to indicate, for example, the presence of windshear). As we have seen in this study, the wind in the range of 0 to 1000 ft (and not only on the ground) is important and would need to be measured for these studies.

Another way to help the pilots and the controllers to visualize the potentially dangerous situations could be a presentation of various accidents.

Pilot training

In addition to a more comprehensive explanation of the different cases, pilot training should include more precise information on how to avoid wake vortices. At the aerodromes where it can happen, there is usually a very long runway available, and pilots must not forget that one solution is to always stay above the wake turbulence and to choose an impact point further down the runway.

ATC information service improvements

The Air Traffic Control System is not entitled to ensure any spacing between VFR/VFR and VFR/IFR. In those cases, it is only entitled to avoid collision on the ground (until the aircraft has reached 50 ft), therefore, the controllers do take into account the wake vortex phenomenon when giving a clearance for take-off, and they will usually point it out to the pilot of a small aircraft taking-off behind a big one. But, controllers are also entitled to provide another service to VFR flights: INFORMATION on the traffic. This is the service which needs to be improved for the approach phase.

Right now, there is no defined procedure for the ATC controllers concerning wake vortex during approach for small aircraft flying VFR. They only (usually but not always) give information on the position of the big aircraft in the circuit, with no other comment, knowing that, at this time of the flight, the pilot of the small aircraft is the only one responsible for his flight.

The problem is that at the same time, the pilot of the small aircraft, knowing that he is arriving on a controlled aerodrome, often believes (wrongly) that his separation with the other aircraft is ensured by the controller who would not give him the clearance for landing if there was any danger.

Therefore, there is some kind of misunderstanding between the two of them. The controller is the one who knows the aerodrome better, so he should be more aware of the conditions in which there is any risk due to wake turbulence. The pilot does not always put together all the pieces of information he has received about wind, the runway configuration, the position of the preceding aircraft compared to his own. Therefore, if the controller could give him more accurate information pointing out the wake turbulence risk, the pilot would receive, from the outside, some kind of confirmation that there is a potential danger, which would help him to put together all the parameters.

Some people could say that this would be an overload for the controllers; but, I would reply that this kind of situation does not happen all the time. In France, small aircraft flying VFR do not land at major aerodromes so often, and there are not so many cases where the small aircraft arrives right after a big one. So, it does not seem unrealistic to think that the controllers could give a more precise and more oriented information in those cases.

Moreover, the research that is now being conducted in the world in that field could probably, in the future, help both pilots and controllers in their task. If we are able to measure the wake turbulence in the approach area, or the signature of all the big aircraft, we could imagine the following systems :

1. if the controller has a terminal with the measurements outputs right on his desk in order to reduce the spacing minima for aircraft flying IFR, why couldn't he use this information to warn a pilot of a small aircraft flying VFR in the circuit?

2. there could also be a system like a VASI, next to the threshold, visible from at least the start of the final approach, warning the pilot that there is a danger of encounter of wake turbulence.

AKNOWLEDGEMENTS

Table 1. Summary of the Cases which Happened in France since 1989

| Location	ISTRES	BORDEAUX	TOULOUSE	PERPIGNAN	MONTPELLIER
Leader A	KC 135F	Mercure	B 747	A 320	Airbus
Injured B in phase	Robin DR400 short final	Cessna 177 short final	Socata TB 20 short final	Piper PA22 final	Cessna 310 base
FRules B	VFR Approach	VFR Approach	VFR Approach	VFR Approach	VFR Approach
Wind	Headwind(on ground) < 5 kt	Headwind 4 < Vw < 6	Crosswind 4 < Vw < 6	Cross/tail 3 kt	Cross/tail (in base) 8 kt
Runway config.	1 runway	runway 29 in service	Parallel L&R dist.L/R:300m threshold:-700	Diverging A -> 33 B -> 31	Runway 31
Info by ATC	Presence of A A is doing TG	Presence of A		Presence of A doing TG	Asked to extend downwind
Separation applied	2*360° in base In SFin., 2 mn after KC's TG	In final, about 1mn30s after A landed	In final, 2 mn after A landed on // runway	1*360° A above crash loc., 1mn40s before accident	Turns in base 1/2 NM further A,2mn30s before 500ft higher
Height	about 150 ft		200 ft	180/200 ft	1000 ft
Pilot exp. B	PPL,instructor 7500 h	Basic license 230 h	PPL, 475 h,in test for Prof. license	PPL, 723 h	Prof. Pilot Instructor 3453 h
Remarks		due to the MTO conditions, lands quickly	+2 Prof Pilots 6288 & 5838 h	low visibility	lo:t 300ft in complete roll
Consequ.	A/C destroyed 1 serious and 2 light injuries	L/G broken	A/C destroyed 3 injuries	A/C destroyed 1 death	INCIDENT

11-8
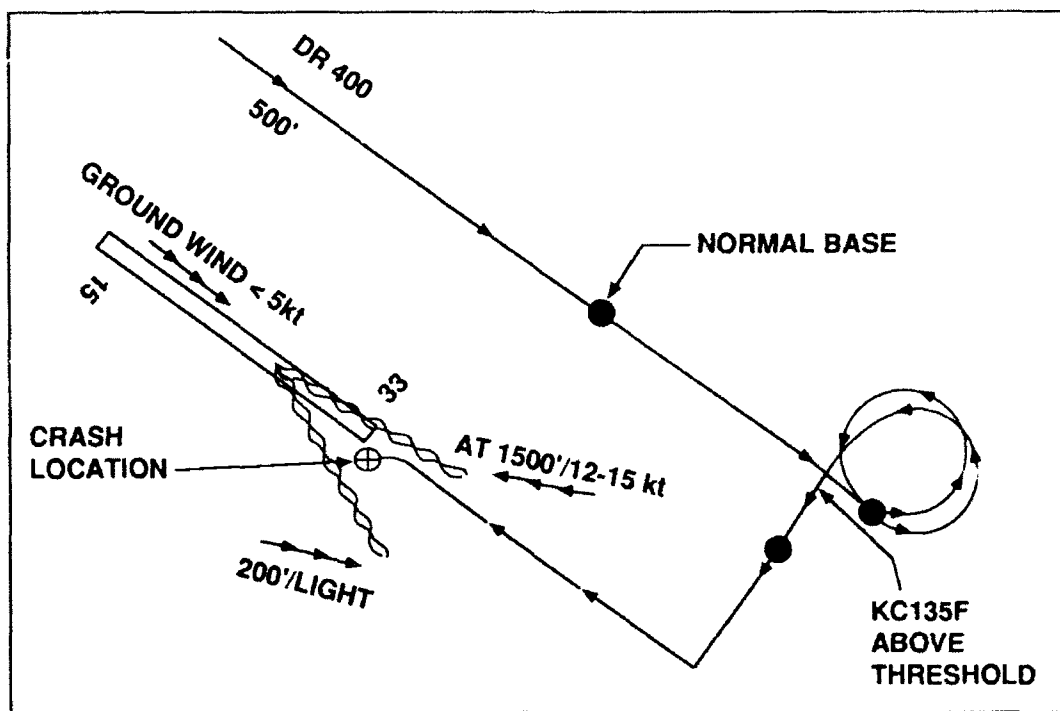
Figure 1. Istres.
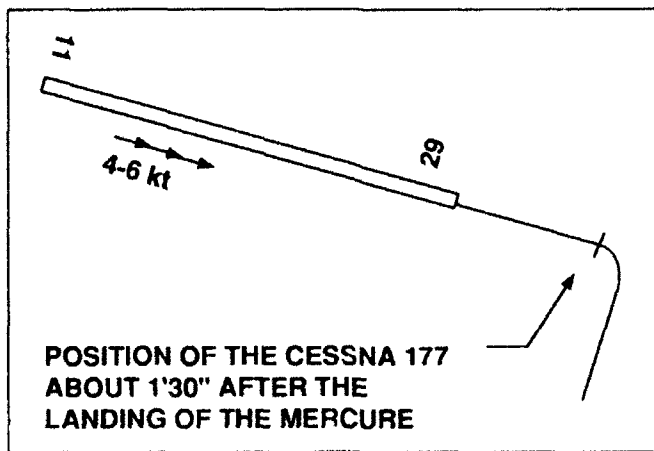

Figure 2. Bordeaux.
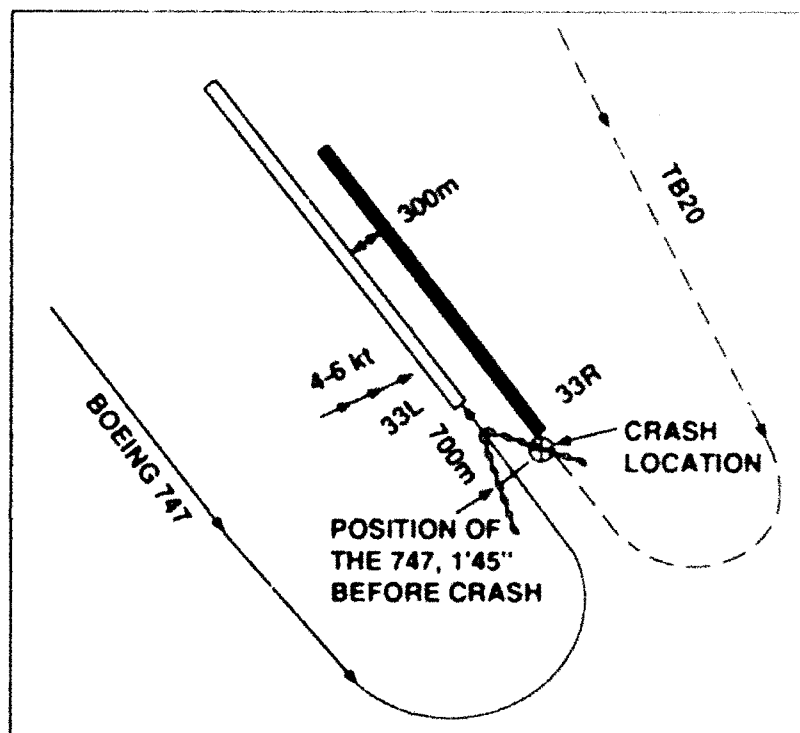
Figure 3. Toulouse.
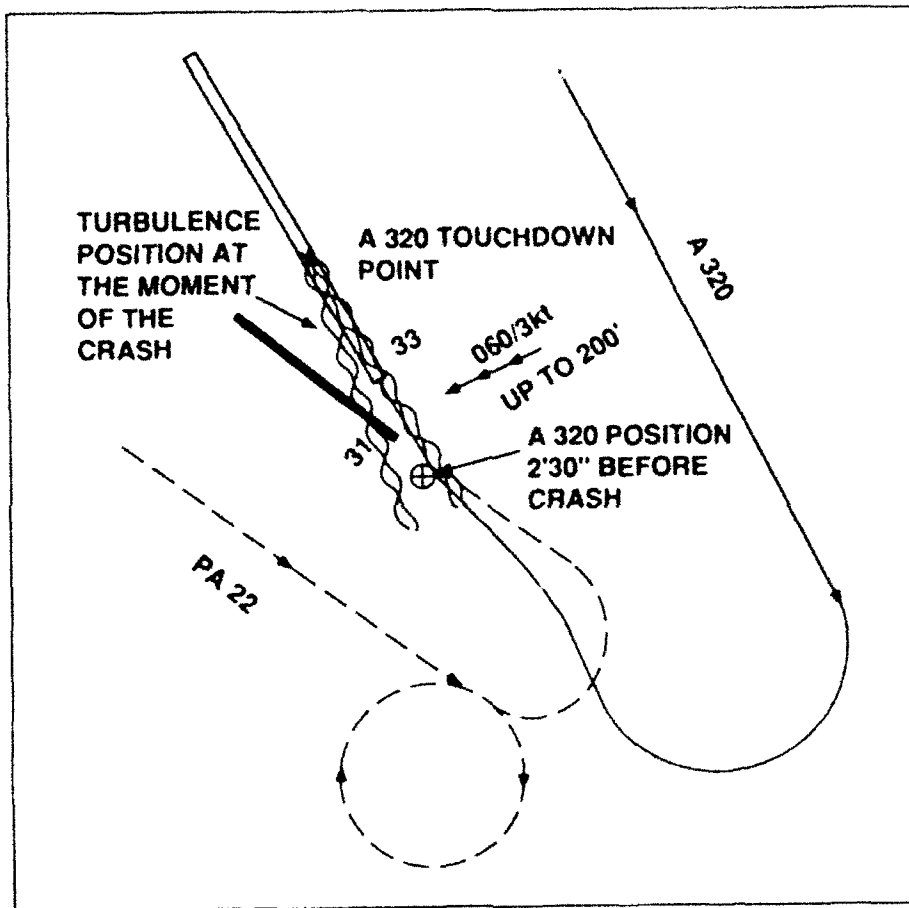
Figure 4. Perpignan.
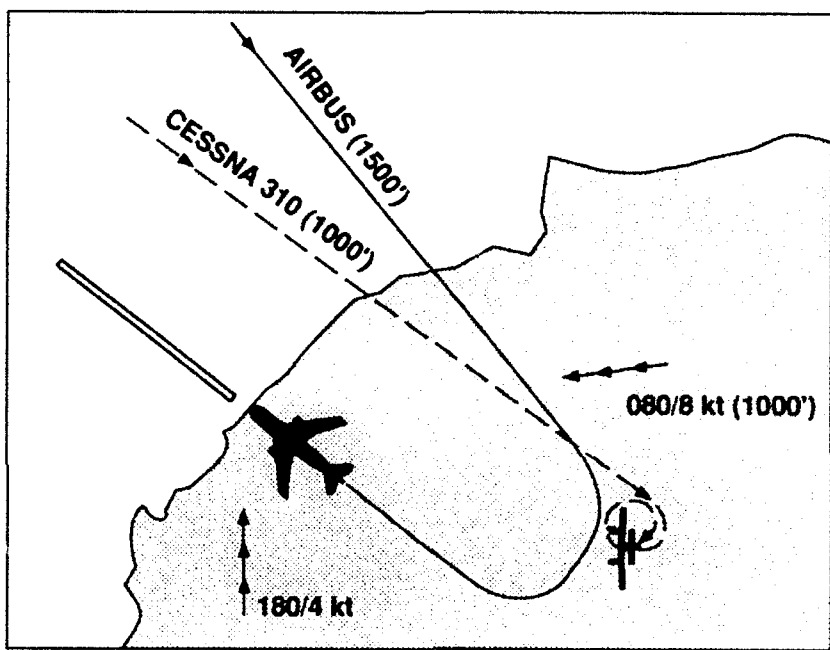
Figure 5. Montpellier.

AERODYNAMIC INFLUENCES
DURING MINIMUM INTERVAL TAKEOFFS
AND AERIAL REFUELING

Tom Gilbert, Captain, USAF
330 CFIS/DOP
Castle AFB, CA 95342-5000

MINIMUM INTERVAL TAKEOFFS

The concept and purpose of the Minimum Interval Takeoff (MITO) is to get a large number of aircraft off the ground safely in a relatively short period of time. The military routinely performs MITOs with as little as 12 seconds between aircraft. This spacing between aircraft can vary, depending upon weather conditions, aircraft configuration (performance factors) as well as type of aircraft. The very things that make MITOs potentially hazardous are the reasons behind the safe separation concept - wing tip vortices.

The effects of a MITO are actually felt during the takeoff roll. Airspeed fluctuations as high as 20 knots can be experienced due to the preceeding aircraft's wake. Slight wing rock can occur but is easily controllable. Due to the preceeding aircraft's climb rate, downwash effects are minimal and not noticeable to the following aircraft once airborne. Wing tip vortices, however, are a large problem and if not properly compensated for, can be disastrous possibly leading to the loss of control of the aircraft.

In theory, if a pilot could keep the aircraft perfectly centered behind the preceeding aircraft, he would experience turbulence but the vortices would tend to "hold" him in position due to their counter rotation. This, however, is never the case and what inevitably happens is that the following aircraft crosses the lead aircraft's flight path entering the vortices on a near parallel heading resulting in a rolling moment. While avoidance is the best answer to the wake vortex problem, the close proximity of the following aircraft makes it impossible to miss these effects entirely.

When the wake turbulence is encountered on a parallel entry a large yawing moment can occur. The natural tendency of the pilot is to introduce rudder to straighten the nose. While this will bring the nose of the aircraft to centerline, it in effect keeps the aircraft in the wake longer. The more prudent procedure is to "ride the wave" keeping the aircraft in a near level attitude with lateral controls and let the vortex spit you out the side. The pilot should never try to climb the aircraft up through the wake as he may already be in a high angle of attack attitude and this could put him into a possible stall condition.

Since avoidance is not likely, the next best alternative is to anticipate wake vortex and minimize the time spent in wing tip vortices. The following techniques are used to accomplish this: 1. The lead aircraft turns downwind once airborne; 2. The following aircraft turn upwind; or, 3. All aircraft use standard fan headings. Using published fan headings is the most widely accepted and practiced technique. With this technique each aircraft is assigned a specific heading to turn to once airborne. The headings are typically in 5 to 10 degree increments off runway heading (see Figure 1). This technique accomplishes several things. First, each aircraft knows exactly where all the preceeding aircraft are going. This assists the pilot in anticipating wing tip vortices. Secondly, it can incorporate wind effect by assigning the leading aircraft downwind headings. If wind is not considered, a crosswind of around 5-10 knots can "push" the vortices of an upwind aircraft directly into the flight path of the following aircraft. Finally from an airspace management viewpoint, the same airspace is always used regardless of wind conditions.

While MITOs have the potential to be dangerous, using one of the above techniques coupled with anticipation and careful planning for wing tip vortices along with proper pilot training, they can be accomplished safely and effectively.

AERIAL REFUELING

During formation flying and inflight refueling, airplanes in close proximity to one another will produce a mutual interference of the flow patterns and alter the aerodynamic characteristics of each aircraft. This is due to the interaction of airflow around the two aircraft. This effect, in general, tends to draw the two aircraft together and the strength of this effect is inversely proportional to the distance. The closer the two aircraft, the stronger the effect. The strength is also directly proportional to the size and weight of the aircraft.

The pilots of both aircraft feel all of these aerodynamic effects as changing control force requirements as the two aircraft maneuver near each other. The leading aircraft at the higher altitude will experience a condition similar to encountering ground effect, although of a larger magnitude (i.e., a reduction in induced drag, a reduction in downwash at the tail and a change in pitching moment nosedown). As the receiver moves from the precontact position (50 feet aft on a 30° angle below the tanker) to the contact position (just under the tail of the tanker), the aircraft encounters a strong changing flow field (see Figure 2).

In the precontact position, the nose of the receiver aircraft is in the area of increased downwash and a nosedown pitching moment must be countered. Moving in closer to the contact position, this downward pitching moment increases until within a few feet of the contact position. At this point (approximately 20 feet), the downwash from the tanker is distributed equally both aft and forward of the receiver's aerodynamic center and the pitching moment subsides to zero. As the aircraft reaches the contact position, there is more downwash aft of the aerodynamic center resulting in a slight noseup pitching moment (see Figure 3).

An area of concern and potential hazard of flying two aircraft in such close proximity stems from low pressure areas created by a receiver flying under the tanker. This can affect the pitot static ports, causing possible erroneous airspeed and altitude indications to both aircraft. The tanker autopilot altitude hold function may sense the low pressure as a climbing indication and

initiate a descent into the lower aircraft. If the relative position of the two aircraft is changing rapidly, the control force requirements will also change rapidly. For this reason one of the basic rules of formation flying is to make all position changes slowly. The direction of the disturbing force is different for every relative position; but generally, forward of the contact position the force is in the direction to bring the two aircraft closer together. Once the receiver is stabilized in the center of the refueling envelope, both aircraft can be flown smoothly throughout a range of changing attitudes and bank angles. If, however, the receiver moves about within the envelope either vertically or laterally or both, the aerodynamic characteristics of the tanker change. This is due to the position of the refueling boom which extends down from the tanker to the receiver. The boom acts in the same manner as a rudder on a boat. If the boom is positioned left of centerline, the tanker will bank left. Conversely if the boom is positioned to the right, the tanker will turn right. If the receiver climbs up in the envelope, the boom essentially becomes streamlined and the tanker will accelerate due to reduced drag. Again the opposite effect is encountered when the receiver is low, increasing drag on the tanker. Potential problems can occur, particularly in elevation deviations when the tanker pilot attempts to compensate for this loss or gain of airspeed. For example, a receiver flies high in the envelope streamlining the boom. The tanker accelerates due to a decrease in drag. This forward movement causes the receiver to fall back in the envelope. The receiver pilot adds thrust to move forward and descends back to the proper elevation. The tanker pilot, at the same time, reduces thrust to slow down back to refueling speed. The result is that the receiver quickly moves forward into a possible underrun condition. If the receiver continues forward past the contact position and underruns the tanker, the receiver's wings will move from a region of downwash into a region of upwash. When the receiver's wings move forward of the tanker's wings into this upwash region, the receiver's lift is suddenly increased and a strong push down by the receiver pilot is required to keep from pitching up into the tanker (see Figure 4). If the receiver were to underrun the tanker to one side so that the wings overlapped on only one side, the pitching tendency would not be quite as strong, but the aerodynamic interaction is such that more lift is generated on the bottom wing. This causes both aircraft to bank in the same direction and the two wings collide since the tanker's wing goes down at the same time the receiver's wing comes up. The flow field behind, below and to the side of the tanker forces the receiving aircraft back toward the centerline in the refueling envelope (see Figure 5).

This is a somewhat desirable condition. When out of position, the receiver will tend to return to centerline as a result of these aerodynamic forces. However, these centering forces are so great that if left unchecked, the aircraft will continue through centerline and stop or slow on the opposite side of the tanker, probably further from centerline. Flight behind the tanker is a constant effort to stay on centerline. If the pilot is out of position on either side of the tanker, the key is not to apply a flight control correction back towards centerline but to release some of the control pressure the pilot is already holding. If the pilot makes control inputs back towards centerline, he will only aggravate a natural tendency for the aerodynamic forces to return the aircraft to the center position. Applying control forces in the direction of the flow field centering forces will overshoot centerline and result in a flight path similar to a "S" pattern behind the tanker (see Figure 6).

How does this look from a receiver pilot's cockpit? Using a B-52 refueling with a KC-135 tanker as an example of large aircraft refueling, the B-52's wingspan exceeds the tanker's by approximately 60 feet. When the B-52 moves well right of centerline, a good part of the right

wing will be in the "clear air" (although it is still affected by the tanker's flow pattern but to a much lesser degree). The result: more lift is being generated from the right wing than the left wing at any given body angle. When this occurs, the lift from side to side is not equal and if no control input is made, the receiver will roll left towards centerline (see Figure 7). The solution is to apply the control forces necessary to hold the receiver in the displaced position (see Figure 8). These forces will naturally oppose the centering forces and result in a stabilized position. Once the aircraft is stabilized, a gradual reduction in control forces will allow the aircraft to return to the center position. The velocity is directly proportional to the momentum. The key to refueling is keeping the movements about all axes slow and controlled so the large momentums can be controlled. Once again as with MITOs, dangers inherent with flying two aircraft at close proximity can be overcome with proper training and an awareness and anticipation of the aerodynamic forces involved.
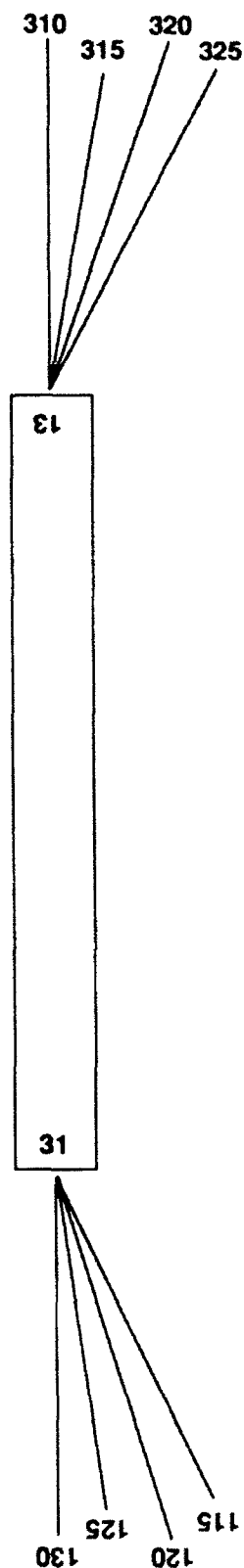
Figure 1. MITO fan headings.
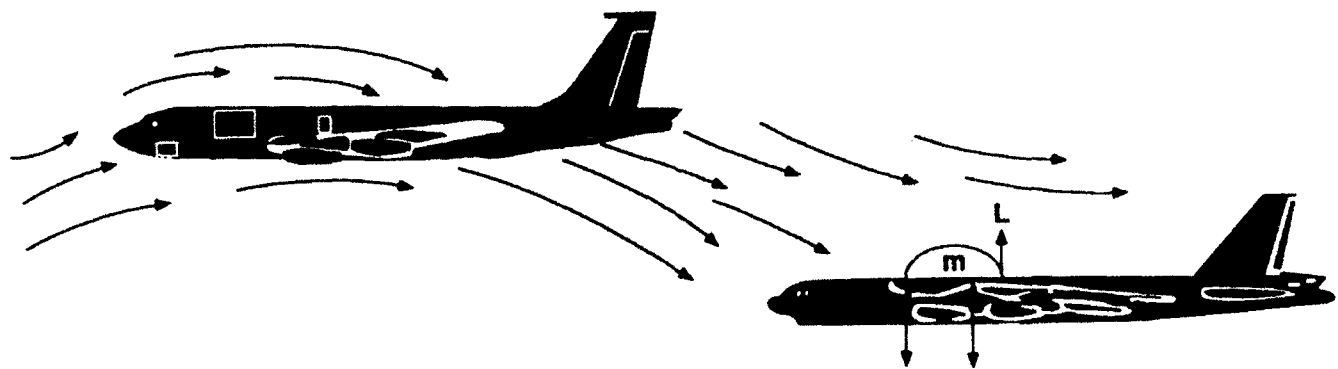
Figure 2. Precontact position (pitch down movement).
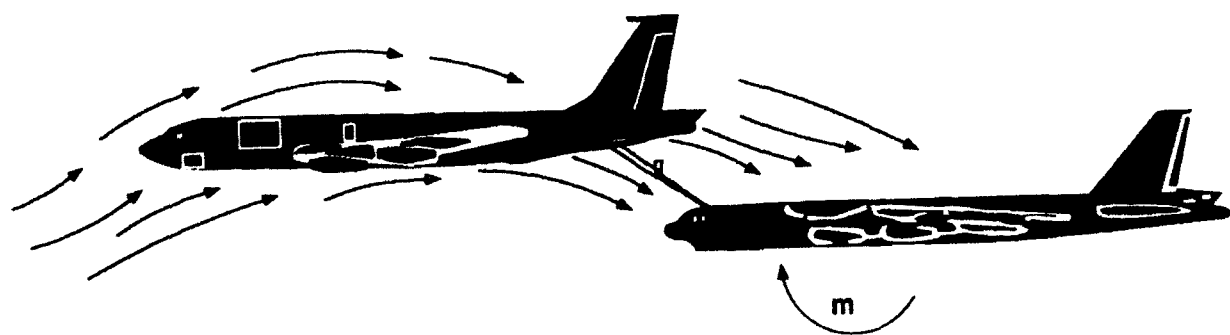
Figure 3. Contact position (slight pitch up movement).
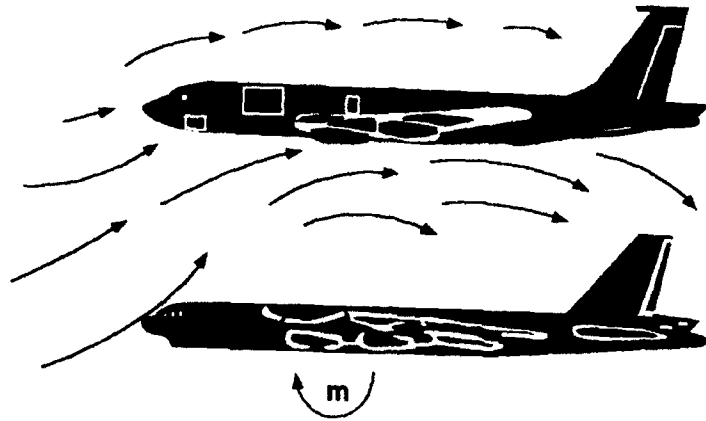
Figure 4. Underrun effects (large pitch up moment).

UPWASH

DOWNWASH
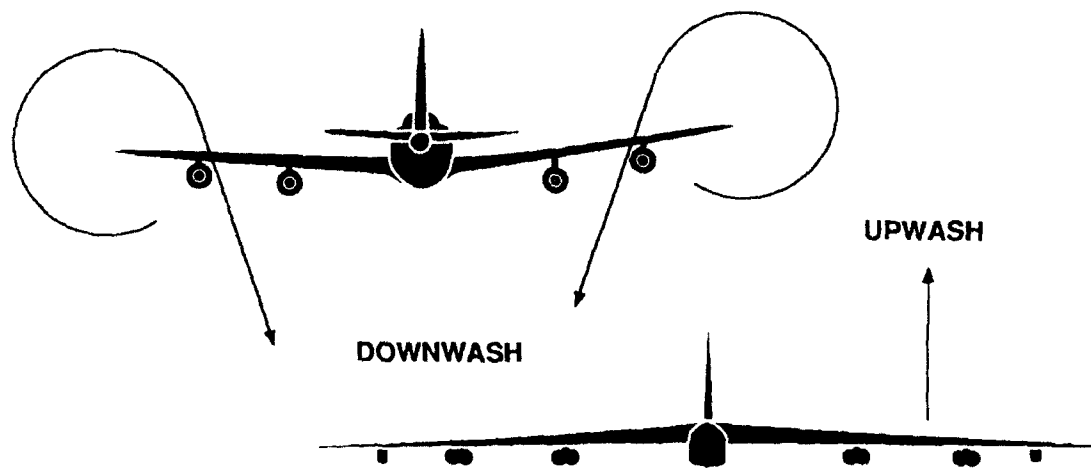
Figure 5. Lateral effects.
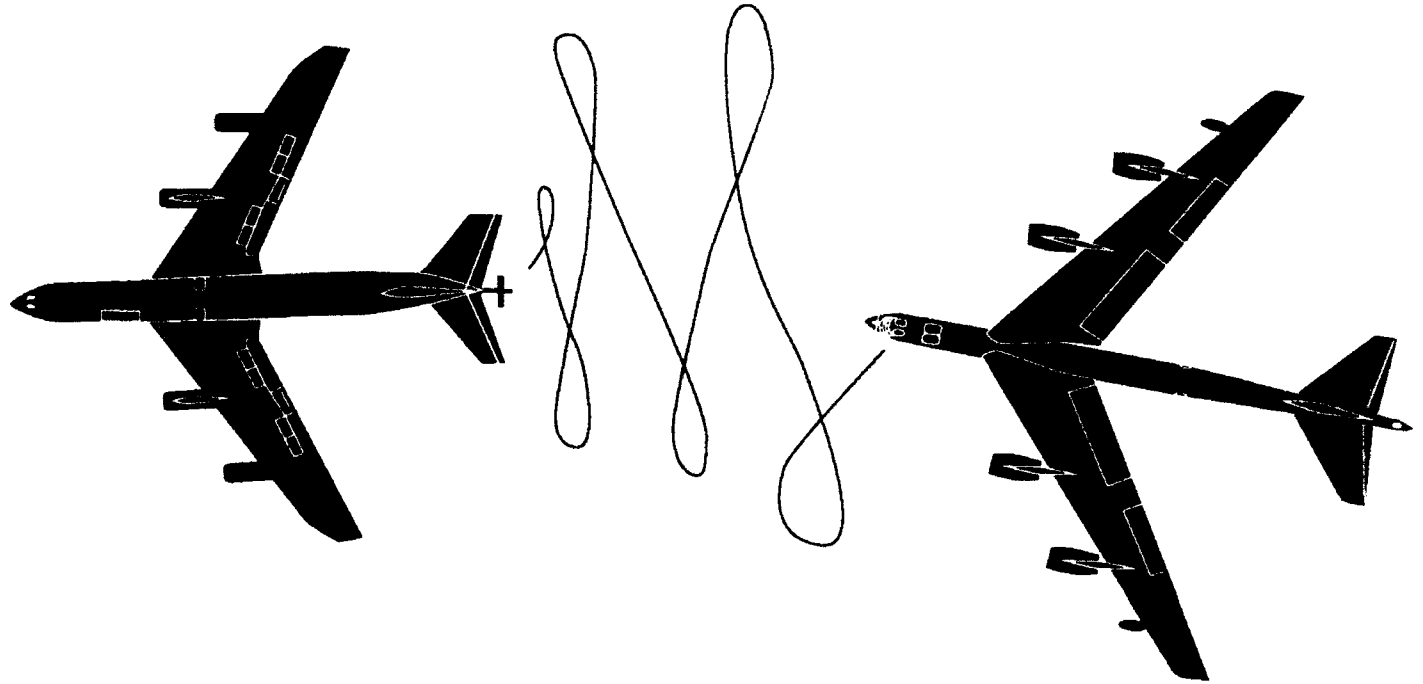
Figure 6. Lateral effects.

HIGHER LIFT ON RIGHT WING

LEFT ROLL
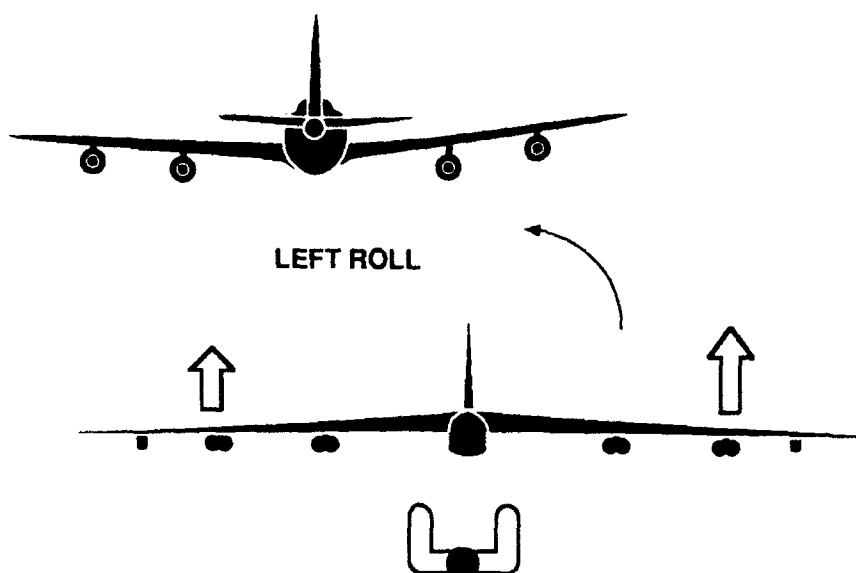
RIGHT OF CENTERLINE - NEUTRAL YOKE

Figure 7. Centerline influences.

EQUAL LIFT ON BOTH WINGS

NO ROLL
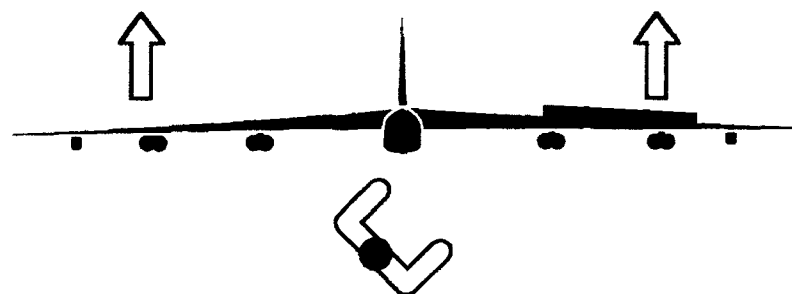
RIGHT OF CENTERLINE - RIGHT YOKE

Figure 8. Centerline influences.

FLIGHT TEST INVESTIGATION
OF THE
WAKE VORTICES GENERATED BY ROTORCRAFT

Joseph J. Tymczyszyn
FAA Retired
Rancho Palos Verdes, California

Keith J. Biehl
FAA Technical Center
Atlantic City Airport, New Jersey

Stephen A. Teager
FAA Technical Center
Atlantic City Airport, New Jersey

INTRODUCTION

Helicopter wake vortices were probed by small airplanes to obtain a direct assessment of vortex hazard as a function of distance behind the generating helicopter. These tests were designed to provide data for establishing Air Traffic Control separation criteria and for comparison with theoretical calculations.

Background

The obvious lack of flight test measurements of helicopter wake turbulence prompted the FAA to undertake a helicopter wake turbulence program in the late 1980's. The result was a flight test program that was a combination of ground based and airborne experimentation, though only the airborne results are presented here. This study is especially timely due to the preponderance of theoretical calculations based on ground tests that preceded these flights. These ground based tests suggest a high wake vortex hazard from rotorcraft and consequently imply large separation distances for safe IFR flight behind rotorcraft.

The tests detailed herein were accomplished despite the limitation of very tight budget contraints. As a result, certain desireable elements of the test, such as instrumentation for the probe airplanes, were not possible. These tests, therefore, relied on kneepad data and prior experience in wake vortex flight experimentation. The tests are considered valid and useful as they represent an accurate duplication and analysis of real world wake vortex hazards of rotorcraft in forward flight.

TEST DESCRIPTION AND PROCEDURES

Generating Helicopters

The probe tests reported in this paper utilized a variety of helicopters. Initial testing used a Bell UH-1H helicopter that belonged to the Pennsylvania Army National Guard and the FAA Technical Center's Sikorsky S-76A. Later tests used a Sikorsky CH-53E assigned to the US Marine Corps, HMX-1, Quantico, Virginia, a US Army Boeing Vertol CH-47D from Fort Eustis, Virginia, and a US Army Sikorsky UH-60 from Fort Monmouth, NJ, in addition to the Technical Center's S-76A. These five helicopters represent a complete range of rotorcraft weight and rotor type.

Each of the generator helicopters was outfitted with a flow visualization system that injected a Corvus oil based smoke into the aircraft wake. For all helicopters but the S-76A, this visualization was accomplished by spraying atomized Corvus oil directly into the helicopter engine exhaust. This system could be operated at all helicopter airspeeds, including hover, and was capable of up to 60 minutes of operation. The S-76A was outfitted with Frank Sanders smoke generators which were mounted to a special truss attached to the aircraft. This system was limited to airspeeds of 40 knots or higher, and had enough fuel for 10 minutes of total operation.

Photographs and relevant weights, dimensions and characteristics of the test helicopters are contained in Appendix A.

Probe Airplanes

The Beechcraft T-34C was tne primary probe airplane. The Bellanca 8KCAB Super Decathlon was used as a secondary probe airplane. Both have the structural and performance characteristics required for helicopter wake vortex probing. They are also similar in size to the small general aviation airplanes most likely to be affected by rotorcraft wake vortices. Two other probe aircraft, the Beechcraft T-34A and the Aero Commander 680E (a twin engine aircraft) were used in preliminary testing during the fall of 1985. Appendix B lists relevant parameters and contain ⁁hotographs of the probe airplanes.

In previous probe tests that studied the wakes from jet transport aircraft, the probe aircraft were instrumented to record their dynamic responses to wake vortex encounters. Unfortunately, funding and time limitations of the helicopter tests precluded outfitting the probe airplanes with the flight test instrumentation required to obtain and record these precise airplane motion and control responses. Although the lack of quantitative response data was an obvious disadvantage, it was largely overcome by using a probe test pilot with considerable experience in probing fixed wing aircraft wake vortices in past FAA/NASA programs.

Probe Test Philosophy and Techniques

Test Philosophy and Hazard Criteria

Probe techniques that were developed during previous FAA/NASA fixed wing vortex test programs were adapted to these tests. These techniques consist of parallel and cross track penetrations, and are described in the sections that follow.

The first separation criteria for HEAVY aircraft were based on the flight tests described in Reference 1, which utilized the Air Force Lockheed C-5A and the Boeing 747 as wake generators. The first results from these tests were based on FAA and NASA pilot qualitative observations. Subsequent analysis of recorded airplane upset data gave almost identical results. Other flight tests (summarized in Figure 25 of Reference 2, which is reproduced in Appendix C) showed consistency between the pilot's hazard assessment and distances where the measured maximum vortex induced rolling moment was equal to the roll control capability of the probe aircraft. Although lacking the rigor that results from thorough aircraft instrumentation, test pilot assessments have proven to be a valid measure of the wake vortex hazard due to the manner in which they were evolved.

It is helpful to recall the procedures and criteria used in prior wake vortex research: The FAA and NASA test pilots involved in the first flights behind the C-5A, 747 and 707 airplanes had previously performed research in approach and landing characteristics and aircraft handling qualities in simulators, instrumented test airplanes and variable stability airplanes.

Prior to flight, the pilots were briefed by the FAA project test pilot on a generalized criteria to be used to determine the limits of upsets (roll, pitch, yaw and any accelerations) which, if encountered during an instrument approach at the published minimums of 200 foot ceiling and 1/2 mile visibility, would permit continuation of the approach rather than a go-around. An additional criteria was to consider the amount of control used, and the most severe airplane excursions which the pilots would tolerate in the most turbulent crosswinds in which they would attempt to land a particular airplane.

For want of a more definitive criterion, a rule of thumb was evolved that suggested that the maximum acceptable bank angle at published minimums would be that obtained by dividing 1200

by the wingspan in feet. Thus, the limits for the Boeing 747 and Beechcraft T-34 (spans 196 feet and 34 feet, respectively) would be, in approximate terms:

1. 1200/200 = 6 degrees of bank for B747

2. 1200/34 = 35 degrees of bank for the Beechcraft T-34 airplane

For the purpose of these tests, the hazardous roll angle limit for evaluating the current probe tests was rounded off to 30 degrees.

Probe Test Pattern

The overall probe test techniques of parallel and cross track penetrations are illustrated in Figure 1.

The probe tests involved three aircraft:

1. A wake generating helicopter equipped with flow visualization system,

2. A probe aircraft, and

3. A safety/photo/chase helicopter that flew near the probe aircraft, generally on the up-sun side.

The three aircraft flew to the test altitude together and then set up the desired test pattern. A common radio frequency was used to coordinate operations and the airspace used for probing was selected so as to be free of conflicting air traffic.

The probe tests were conducted in level flight, and in climbs and descents. All encounters were carried out at altitudes above 3000 feet AGL to allow room for recovery or bailout from severe upsets or structural failure.

Parallel Probing

The parallel probing technique is the most obvious and involves flying into the vortex trail behind and below the helicopter, as visualized by the "smoke trail" that is left behind the generating helicopter by its onboard flow visualization system. On any given run, parallel probing would commence at the maximum distance that the smoke trail was visible to the probe pilots or where some airplane reaction was felt. At helicopter airspeeds above 70 knots, the probe airplane would attempt to probe at constant separation distance until the vortex characteristics were fully evaluated. At slower helicopter airspeeds, the probe airplane could no longer fly the same speed as the helicopter, due to stall considerations. In these cases, the probe airplane would fly its normal approach speed, which was 80 knots for the T-34C and 70 knots for the Decathlon. Under these conditions, probing would occur at decreasing separation until probe airplane control was either completely lost or the pilots became concerned that they were in danger of overrunning the slower moving helicopter.

In conducting the parallel probes, the vortex penetration angle was made as small as possible and entries were made from all directions: above and below, left and right.

The generating, probe, and safety aircraft all flew a long race track pattern. This pattern was usually oriented with its long axis aligned for maximum vortex trail visibility in the probe airplane. Flight along each long side of this pattern would typically last for about four minutes and would constitute one run. On some occasions, notably those which involved slow helicopter airspeeds, individual runs would last for over ten minutes, which allowed ample time for thorough vortex hazard evaluations. Each of the wake generating helicopters, with the exception

13-4

of the S-76A, could produce vortex visualization smoke for about one hour. As a result, approximately 15 typical test runs could be flown for each sortie.

The safety/photo/chase helicopter flew parallel to the probe airplane. Its mission was to document a vortex induced upset when it occurred, to advise on vortex core location, to assist in determining test separation distance, and to order the breaking off of the test run when the separation between helicopter and probe airplane became too small.

Two different piloting techniques were used in these tests. In the first technique, the probe airplane controls were kept neutral. This technique was used to observe the airplane response and is considered the most accurate simulation of an unexpected encounter. In the majority of the test runs, the airplane controls were applied against the upset and the upset angle and amount of control were recorded. This technique allowed for a more rigorous investigation of the wake characteristics; the probe airplane was used as an "airborne torque wrench" to measure the energy that the wake contained.

Parallel penetrations typically resulted in pitch and/or yaw excursions of the probe airplane. Encounters at closer separations often led to control loss.

A high test efficiency was attained during these parallel probe tests. The probe pilots felt confident that they had explored the vortex "hazard volume" very thoroughly for all the test helicopters and that entry into both vortices had been adequately accomplished from almost all conceivable angles.

Cross Track Probing

Cross track probing of the helicopter wake involved maneuvers which would allow the probe airplane to penetrate the vortex trail at angles up to 90 degrees. This type of probing was done primarily in the near field when a parallel probing effort was broken off due to separation concerns. When separation distances became too tight, a right or left 270 degree turn would be flown by the probe airplane to penetrate the vortex trail at acute and perpendicular angles and therefore evaluate the severity of the vortices in angular penetrations. A series of "S turns" would be flown through the vortices, which provided the pilots with an assessment of the energy in the vortex trail as a function of the distance behind the generating helicopter.

Cross track penetrations typically resulted in very short sharp vertical jolts (pitch excursions) rather than excursions in roll or yaw. These vertical impacts were more of a concern from a structural damage standpoint than they were from any loss of control considerations.

The information gained during the cross track penetration tests has direct applicability to any study of the wake vortex hazards to airplanes operating on runways that are perpendicular to helicopter flight paths.

Aircraft Separartion

The distance between the helicopter (vortex generator) and the probe airplane was obtained by the following methods:

T-34A

Air to Air Distance Measuring Equipment (DME) installed in both aircraft.

Decathlon T-34C
Commander

Distances calculated by measuring the distance between the helicopter and the probe airplane to a DME station Aero aligned with the flight path of both aircraft. Distance between the aircraft is the difference in these two distances.

In addition, the safety/photo/chase helicopter would verify the distance between the aircraft and ensure that the probe did not overtake the generating helicopter. This was especially important at very close separation distances and at low helicopter airspeeds. Under these conditions, the smoke density of the generator's flow visualized wake would obscure the probe pilot's vision of the helicopter he was approaching.

Data Recording and Photo-Video Coverage

Data was manually recorded by the non-flying probe pilot and consisted primarily of separation distances, bank angles, estimates of yaw angles, control inputs, vertical accelerations and general comments. In addition, the encounters were video taped and photographed from the safety/chase helicopter, from the ground (where possible) and from a fixed video camera in the probe airplane. The video tape recorder onboard the safety helicopter was also used to record the radio transmissions made by the three aircraft. This gave a running documentary of airspeeds, separation distances, control inputs and responses as well as a visual record of the probe aircraft response to the helicopter wake.

TEST RESULTS

Vortex Upsets

The primary measurement of the probe tests is the observed bank angle of the probe airplane that is generated by a vortex encounter. The two main variables affecting an encounter behind a particular helicopter are the helicopter airspeed and the separation distance. Figures 2 through 5 present composite plots of this bank angle versus separation distance for four helicopters, the UH-1H, UH-60, CH-47D and CH-53E. Unfortunately, despite three test sorties behind the S-76A, not enough upsets were experienced to generate a plot for this helicopter. Roll control data, as detailed below, indicated that the S-76A had less vortex hazard than the UH-1H; however, it should be noted that the most severe upsets behind the UH-1H occurred at airspeeds that were below the minimum speed permitted for the flow visualization system installed on the S-76A.

In general, at small separation distances, upsets are more severe at slower airspeeds than they are at higher airspeeds. At larger separation distances, upsets tend to be more severe at higher airspeeds. This is due to the fact that vortices formed at low airspeeds, though initially stronger than those formed at high airspeeds, have already substantially decayed by the time that the probe airplane reaches them.

Atmospheric turbulence seems to have a negligible effect on vortex encounter severity. Figures 6 and 7 are plots of probe airplane bank angle versus vortex age for the CH-47D and CH-53E helicopters. The data presented in these figures was collected over several days for each helicopter and over the complete range of test airspeeds. As can be seen, these figures show very little difference in encounter severity between morning and afternoon runs, even though the data identified as "morning" was collected very early in the day and should have represented conditions of minimal atmospheric turbulence. These observations suggest that the probe aircraft response behind these two helicopters was only minimally affected by atmospheric turbulence.

Roll Control Power

Criteria to establish separation distances have been greatly refined for instrumented airplanes in previous FAA/NASA flight tests (References 1 and 2). Basically, the definition of these separation distances involves a comparison of the maximum vortex induced rolling moment to the total roll capability of the encountering airplane.

A direct determination of this relationship as it applies to helicopter wakes was made early on the morning of October 8, 1986 under extremely stable weather conditions. In this instance, the probe pilot was able to "balance" the small Decathlon probe airplane in a sideslip condition for several seconds while it was immersed in the wake of the S-76A helicopter. In this manner a direct assessment of the roll and yaw control power required to overcome the vortex induced roll and yaw was possible. These tests were conducted at 4,500 feet AGL, with airspeed for both aircraft decreasing from 110 to 70 knots, and are summarized in Table 1.

Vortex Upset Hazard

The capability of the vortex to cause an unexpected departure of the encountering aircraft from controlled flight depends on the size, weight and speed of the "vortex generator" and on the vortex age. Operationally, the vortex age is reflected in terms of the distance of the encounter behind the vortex generating aircraft. The upset depends upon the type of encounter:

1)   In following flight, the upset is an abrupt roll, yaw or pitch excursion. This type of upset is the primary concern of this report since it determines the longitudinal separation standards.

2)   In crossing flight, the upset is a rapidly varying vertical acceleration.

The following parameters are useful for establishing separation distances for small airplanes behind helicopters:

1) Detectability - The maximum distance at which the influence of the helicopter's wake vortex can be detected by the probe airplane.

2) Hazard Distance - This is a distance, obtained under test conditions, which results in a nominal 30 degree bank upset.

Table 2 lists the measured maximum detectability, measured maximum hazard and suggested minimum IFR separation distances for the helicopters tested during this program. The final suggested IFR separation distance includes allowances for pilot reaction time, more stable atmospheric conditions, the actual IFR environment and other operational factors.

Structural Damage Considerations

Probe tests were continued to less than 0.1 NM behind all helicopters with no evidence of structural damage despite the fact that violent upsets, including loss of control and/or spins, resulted in most cases. Similar exposure behind fixed wing aircraft in the LARGE or HEAVY class would have been far more hazardous from both aircraft response and structural damage standpoints.

On two occasions the probe pilots abandoned a run while flying the light Bellanca Decathlon airplane in the wake of the CH-53E at high speed. During these encounters, an unexpected "shudder," or apparent flapping of the wings, was observed and felt in the probe airplane. This phenomenon was the first ever reported in probe testing and justified immediate abandonment of the runs because of concerns over exciting a catastrophic wing flutter mode. The reaction of the airplane felt as though the vortices of individual helicopter rotor blades were still present in the coalesced wake or that some other rhythmic pattern was at work. That individual blade vortices were still active is not altogether surprising; ground and air observations of the wake flow pattern (as revealed by the flow visualization system) often revealed the presence of individual blade vortices in the overall wake pattern many rotor diameters downstream of the helicopter.

QUALITATIVE OBSERVATIONS

The following qualitative observations are offered; many concern comparisons with the wakes from fixed wing aircraft. It should be noted that the probe tests of fixed wing wakes made use of jet transport aircraft that have significantly larger weights and wingspans.

Visual Characteristics

In forward flight, the port and starboard vortices appear distinctly different, as reflected in the density of the entrained smoke and in the apparent cross sectional areas of each of the vortex

trails. The vortex behind the advancing rotor is consistently smaller, tighter and more coherent, especially as the forward speed increases above 80 knots. In almost every case, a distinct advancing blade vortex core could be seen by the probe pilots or the photo chase pilot. The vortex behind the retreating blade is characterized by a larger diameter, less dense smoke marking and a greater cross sectional area. This visual assessment was also reflected in the vortex effects on the probe airplane; the advancing blade vortex is generally more "solid" and generates more abrupt roll and yaw excursions than the retreating blade vortex. These observations make sense, as the aerodynamic environments on the two sides of the helicopter differ radically as speed increases. On American single rotor helicopters, the starboard vortex is produced by advancing rotor blades and the port vortex by retreating rotor blades. The retreating blades, which operate at a much lower effective airspeed, are at a higher angle of attack in order to produce as much lift as those on the advancing side. This difference is manifested in the different characteristics of the two sides of the wake with increasing airspeed.

The area "contaminated" by the wake turbulence of a helicopter is clearly larger than that of an airplane of comparable size and weight, especially at speeds below 70-80 knots.

Wake Vortex Trajectories

The lateral distances between vortex centers appeared to expand initially and then to contract approximately eight rotor diameters behind the helicopter. Further, vortex core separation was seen to increase in descending flight and to decrease in climbing flight.

The densest smoke observed behind the helicopter first descended and then rose several rotor diameters downstream. This effect is likely due to the location of the smoke generators near the centerline of the helicopter. As the smoke is injected into the flow field, it is first driven down by the rotor downwash and is then swept outward and upward as it becomes entrained in the vortex structure.

Helicopter wakes do not descend in the same predictable manner as do those for fixed wing airplanes; the wakes appear to be more buoyant. A possible explanation resides in the mechanics of rotary wing flight. Helicopters use much more engine power, and hence leave behind much more heat, than an airplane that generates an equivalent amount of lift. It is feasible that the excess hot engine exhaust generated by the helicopter is entrained in the helicopter wake and is therefore responsible in some way for the wake's apparent buoyancy.

Wake Vortex Hazard Volume

The size of the cross sectional area filled with smoke leads the probe pilots to believe that vortex size for rotorcraft decreases with increased airspeed in the same manner as it does for fixed wing airplanes. Further, the apparent vortex size is increased with helicopter size and weight as might be expected. Blade number appears to have an effect on vortex size; an increased number of rotor blades appeared to increase the vortex size. This effect was identified by comparing the wakes from two helicopters of the same weight, but different number of blades; the UH-1H with two blades and the S-76A with four blades. The observation suggests that increasing the number

of blades acts to alleviate the vortex in the same way that flap extension does on fixed wing airplanes. This effect becomes even more evident when the tandem rotor system of the CH-47D is considered. The two rotors appeared to interact in a manner that inhibited the vortex rollup process.

The visual observations of vortex size were correlated with the nature of the probe airplane upsets. At lower airspeeds there was a greater "hazard volume" and the direction of the upsets in roll and yaw was less predictable than it would have been behind fixed wing airplanes. At higher speed encounters, the vortices decayed as separation distances increased. As this occurred, the coherent roll and yaw excursions were replaced by sharp vertical "bumps," which decreased in severity until the smoke trail dissipated or until turbulence was no longer evident.

COMMENTS AND CONCLUSIONS

The probe tests were successful in spite of significant missing information. The lack of probe aircraft instrumentation and meteorological measurements at the test altitudes made interpretation of the test results less precise. Future probe tests should include such capability.

Although the flow visualization was adequate for the probe testing, the tests would have been more efficient if more of the smoke had been injected into the vortex core. This could have been accomplished if the smoke had been injected in an area closer to the rotor blade tips.

The probe tests were accomplished with aircraft that are representative of the smallest members of the general aviation fleet. Therefore the results should be conservative for all airplanes likely to be affected by rotorcraft operations.

Full-scale flight test probing has once again proven to be a safe, accurate and cost effective method of determining both wake vortex strength and hazard, and for determining safe separation distances for following traffic. It should be recognized as a primary tool in this area and should be provided with sufficient priority and funding. Resources should be made available to acquire, instrument and operate a test airplane dedicated to this purpose.

Table 1. Balanced Sideslip Conditions: Decathlon behind S-76A

Airspeed	Separation	Control Input Required
100 kts	0.5 nm	1/2 Aileron & Rudder
80 kts	0.5 nm	3/4 Aileron & Rudder
70 kts	0.4 nm	3/4 - Full Aileron & Rudder

Table 2. Probe Test Separation Distances (N.M.)

HELICOPTER	MAXIMUM DETECTABILITY DISTANCE	MAXIMUM DISTANCE 30 dgr UPSET	RECOMMENDED MINIMUM IFR SEPARATION
UH-1H	1.0	0.7	1.5
S-76A	1.0	0.7	1.5
UH-60	2.4	1.4	2.5
CH-47D	2.7	1.5	2.5
CH-53E	3.1	2.5	4.0

T-34C ILLUSTRATES PARALLEL PROBE TECHNIQUE
DECATHELON ILLUSTRATES CROSS TRACK PROBE TECHNIQUE
(OBVIOUSLY CONDUCTED AT DIFFERENT TIMES BY EITHER AIRPLANE)

UPWASH

INDUCED DOWNWASH

UPWASH

Figure 1. Vortex probing techniques.
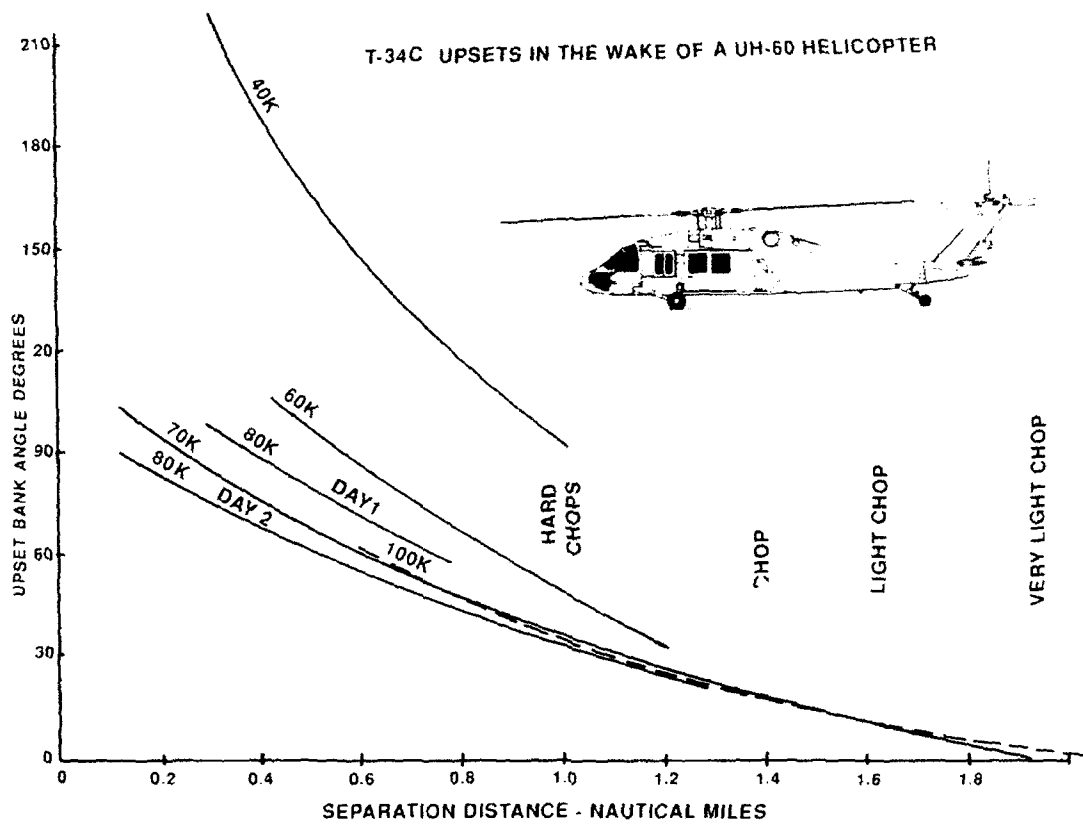
Figure 2. T-34C upsets in the wake of a UH-1H helicopter.

T-34C UPSETS IN THE WAKE OF A UH-1H HELICOPTER
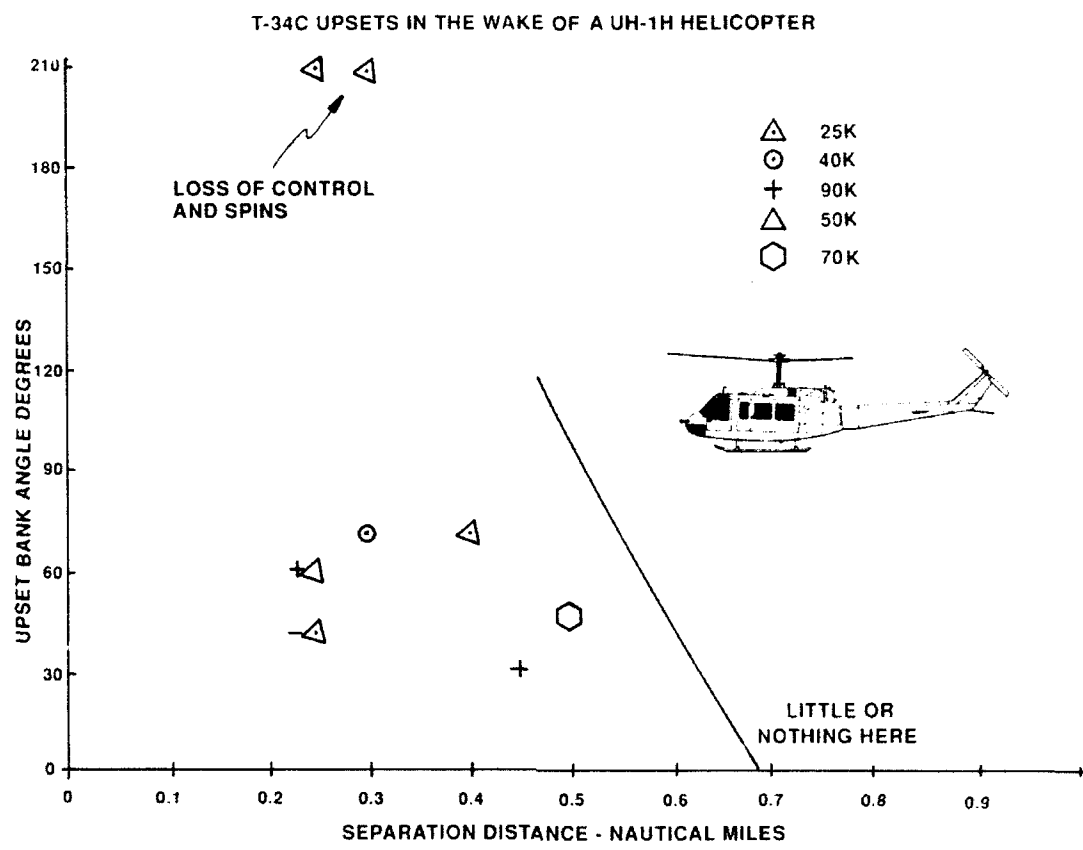
Figure 3. T-34C upsets in the wake of a UH-60 helicopter.
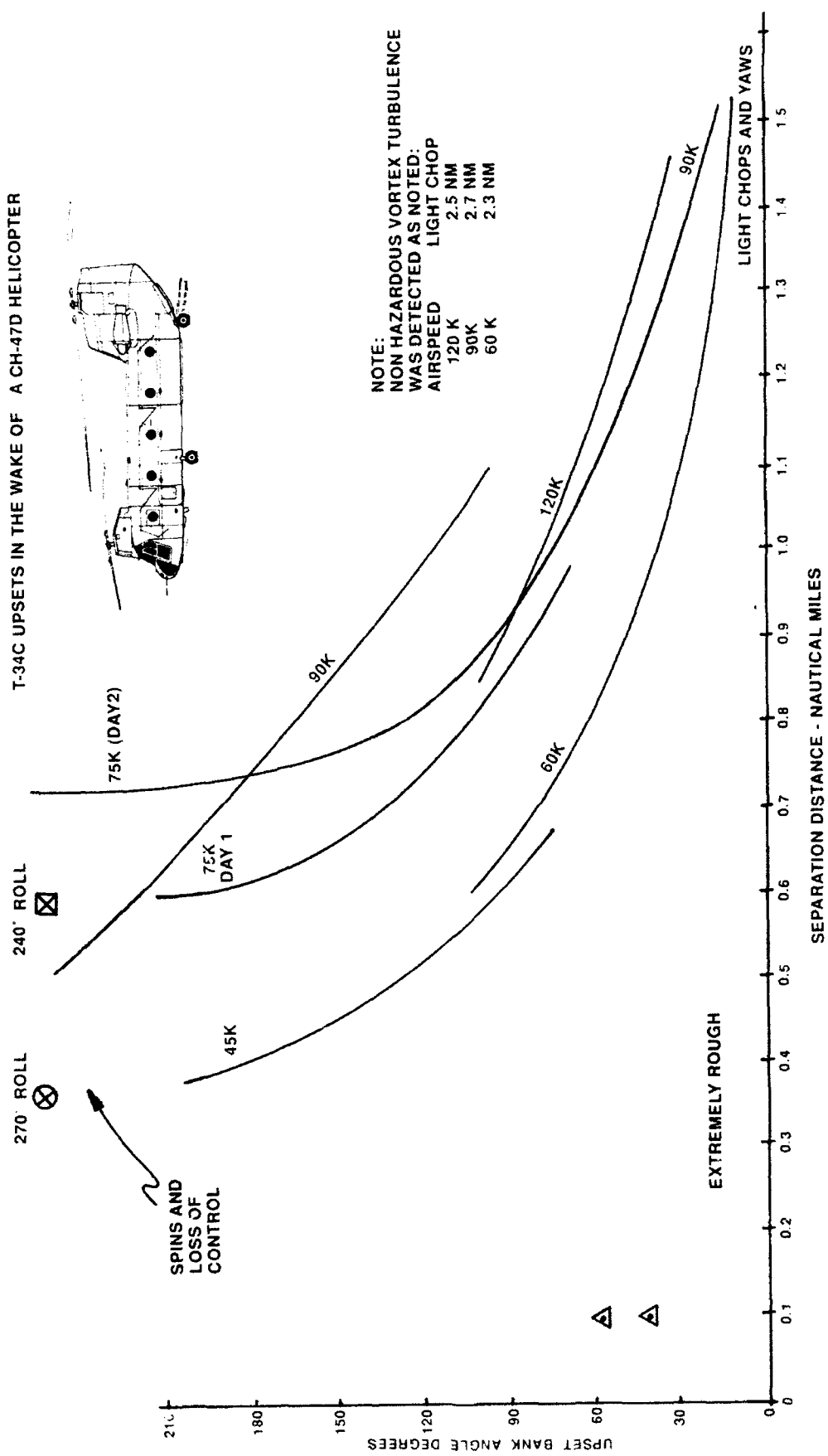
Figure 4. T-34C upsets in the wake of a CH-47D helicopter.
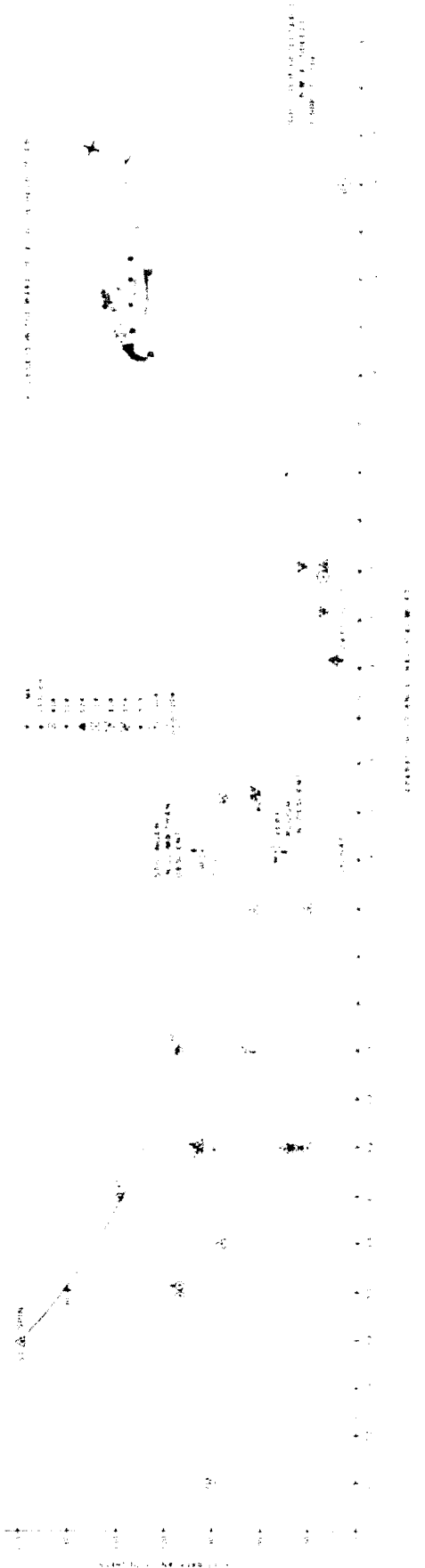
Figure 5. T-34C upsets in the wake of a CH-53E helicopter.

Figure 6. Bank angle versus vortex age for CH-47D.
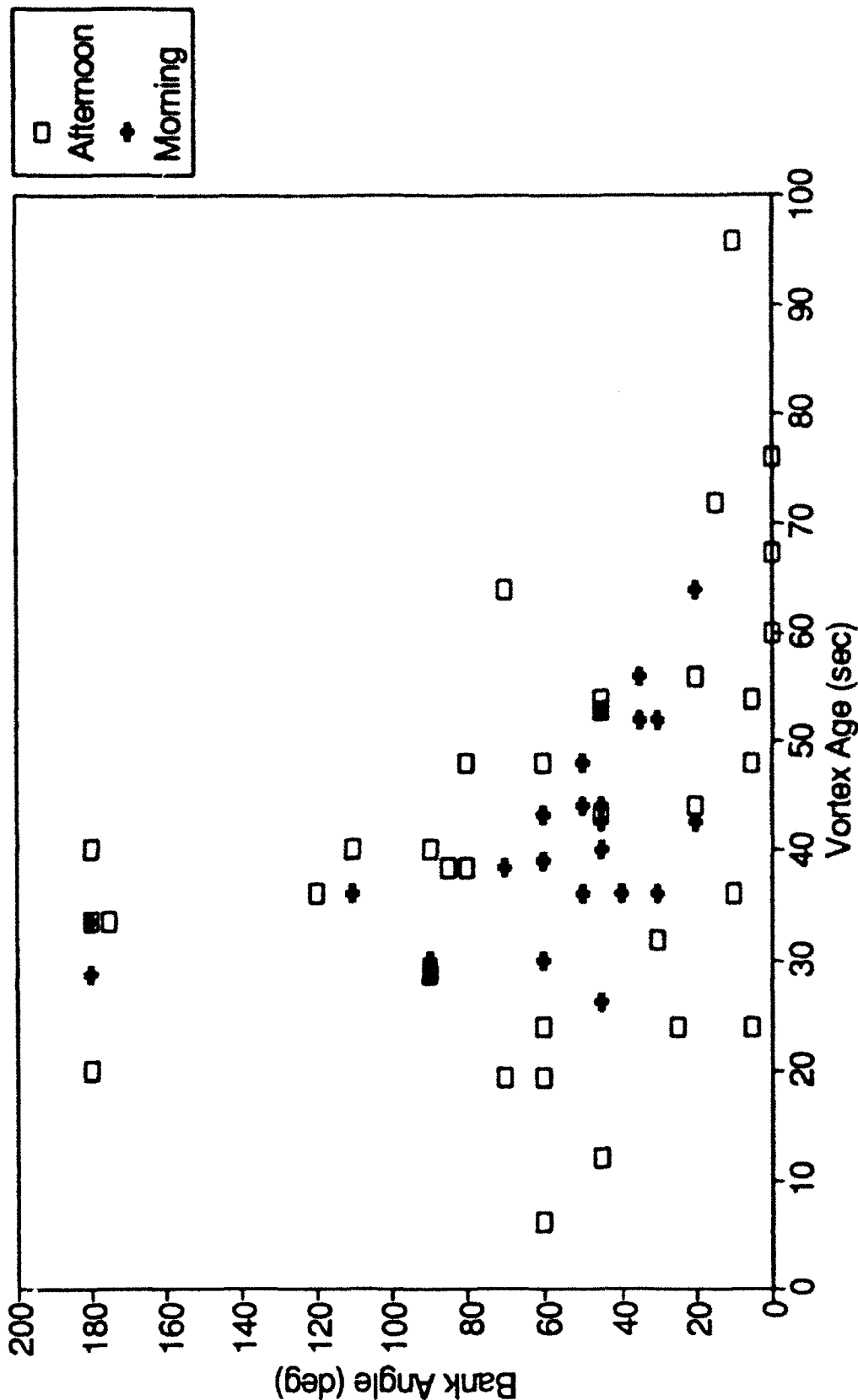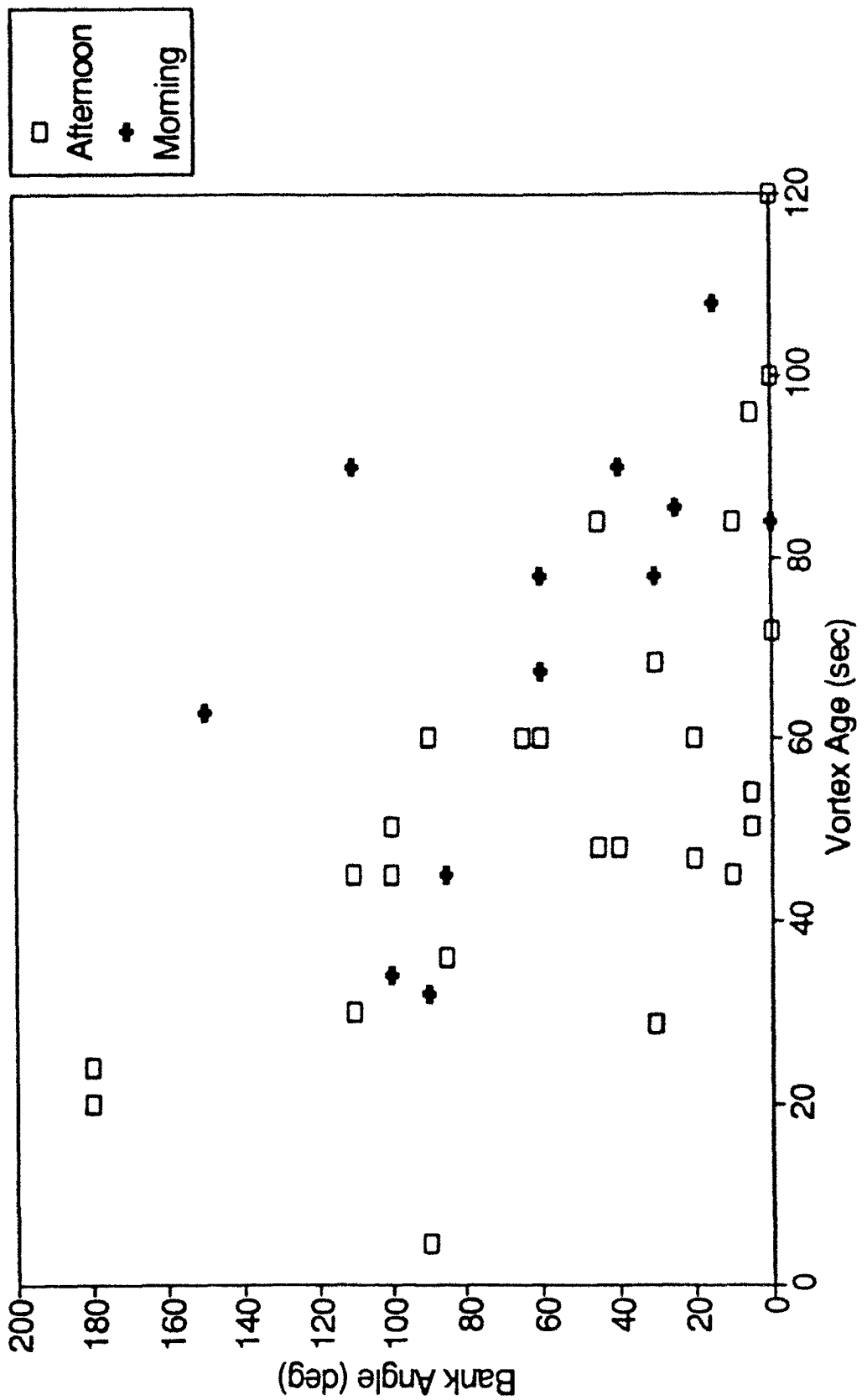
BANK ANGLE VERSUS VORTEX AGE FOR CH-53E

Figure 7. Bank angle versus vortex age for CH-53E.

REFERENCES

1. Tymczyszyn, J.J. and Barber, M.R., "Techniques for Early Demise of Vortices...A Pilot's View," US DOT Conference on Aircraft Wake Vortices, March 15-17, 1977.

2. Kurkowski, R.L., Barber, M.R. and Garodz, L.J., "Characteristics of Wake Vortex Generated by a Boeing 727 Jet Transport during Two-Segment and Normal ILS Approach Flight Paths," NASA TN D-8222, April 1976.

APPENDIX A
TEST HELICOPTERS
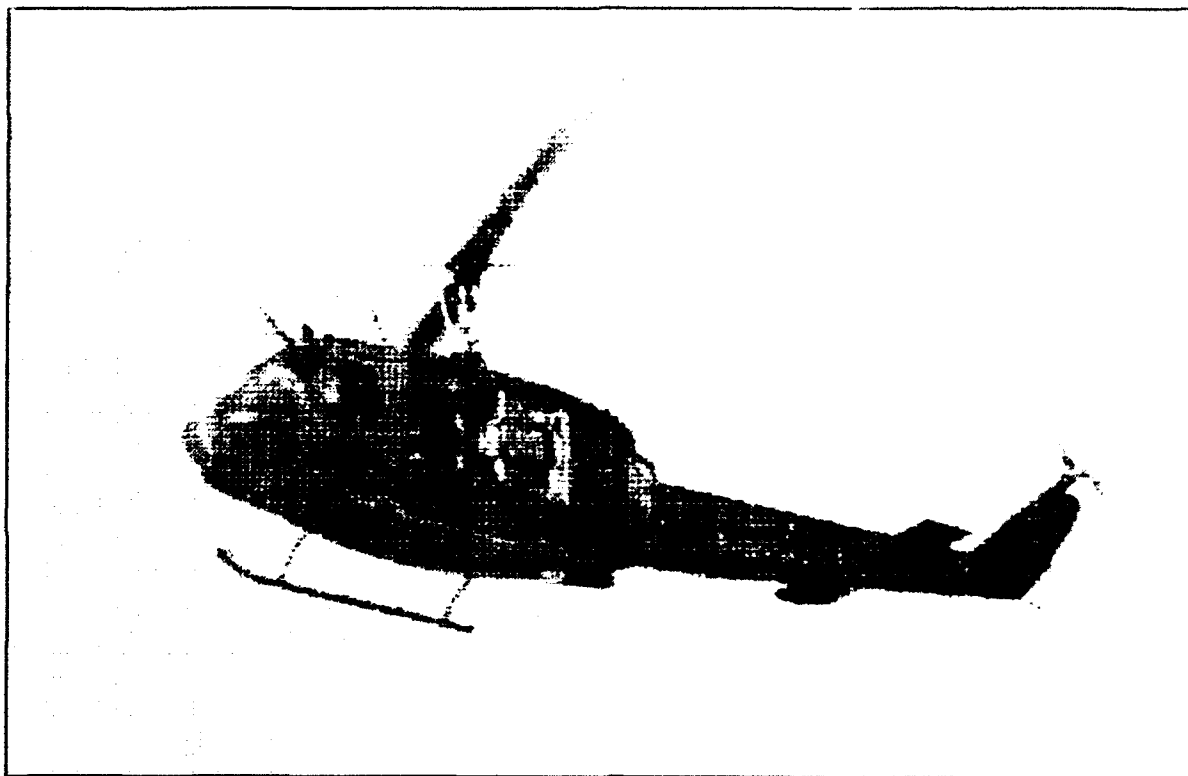
Bell UH-1H "Huey"

Maximum takeoff weight: 9,500 lbs.
Configuration: single rotor, single engine
Rotor type: 2 bladed, teetering hub
Rotor diameter: 44 feet, 0 inches
Rotor chord: 1 foot, 9 inches
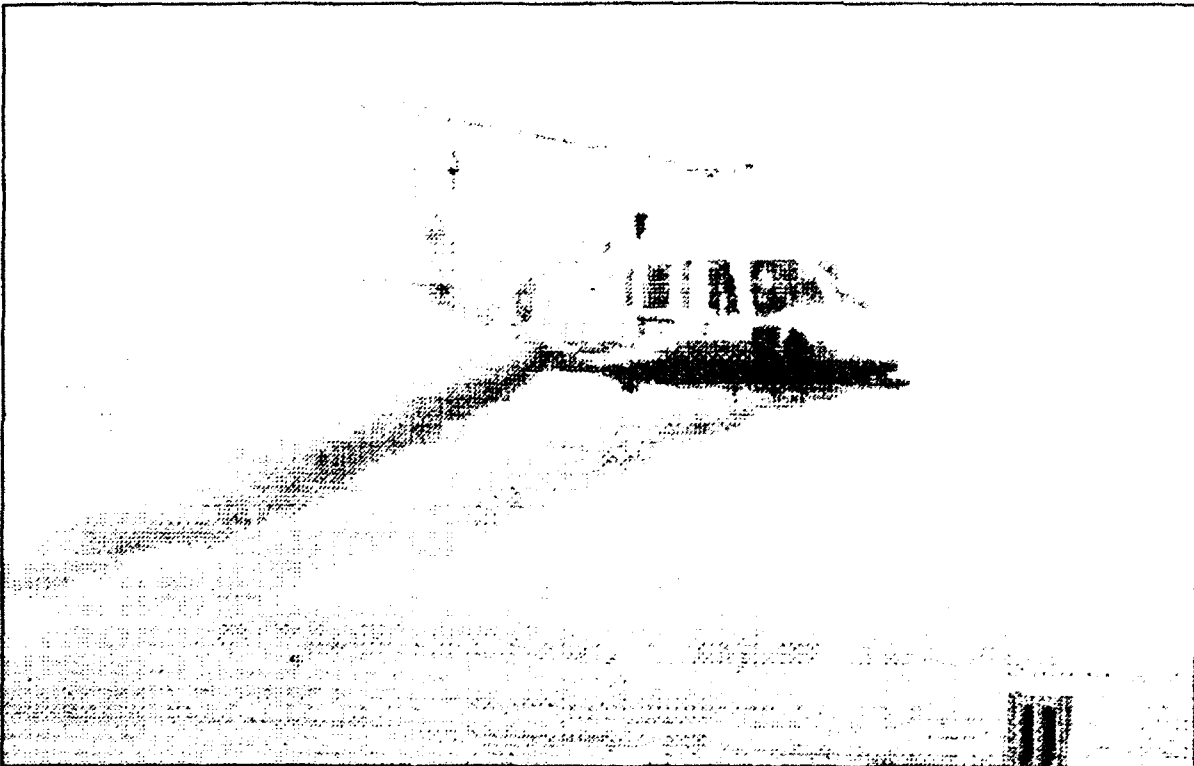
Sikorsky S-76A

Maximum takeoff weight: 10,000 lbs.
Configuration: single rotor, twin engine
Rotor type: 4 bladed, fully articulated
Rotor diameter: 44 feet, 0 inches
Rotor chord: 1 foot, 3 1/2 inches
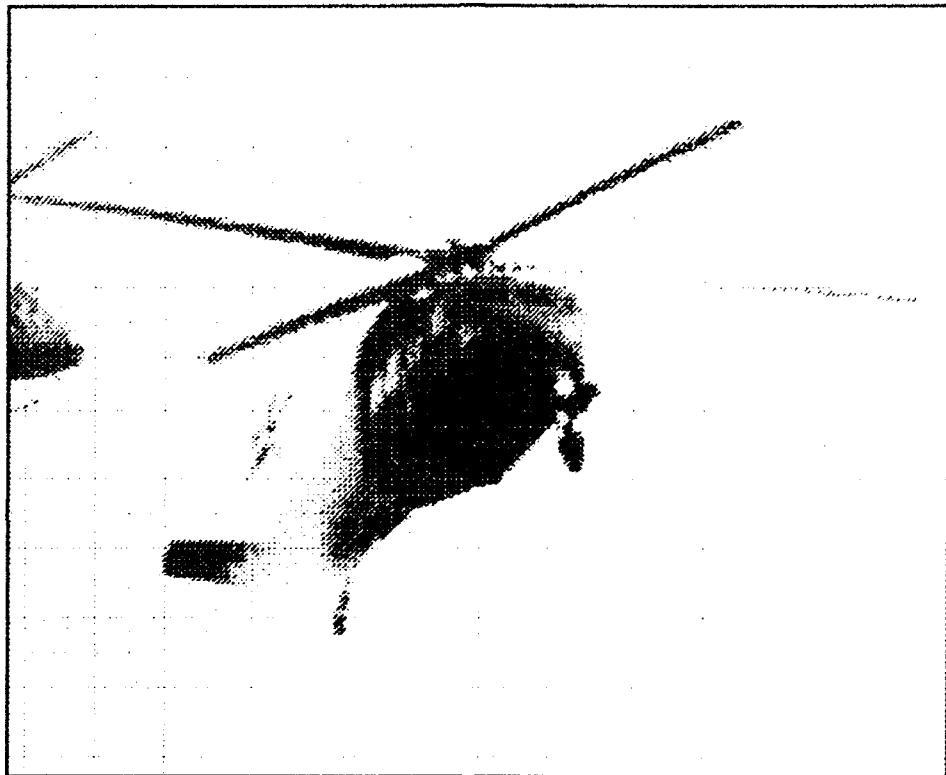
Sikorsky UH-60 "Blackhawk"

Maximum takeoff weight: 20,250 lbs.
Configuration: single rotor, twin engine
Rotor type: 4 bladed, fully articulated
Rotor diameter: 53 feet, 8 inches
Rotor chord: 1 foot, 8 3/4 inches

Boeing Vertol CH-47D "Chinook"

Maximum takeoff weight: 50,000 lbs.
Configuration: tandem rotor, twin engine
Rotor type: two 3 bladed, fully articulated, synchronized
Rotor diameter: 60 feet, 0 inches, both rotors
Rotor chord: 2 feet, 8 inches
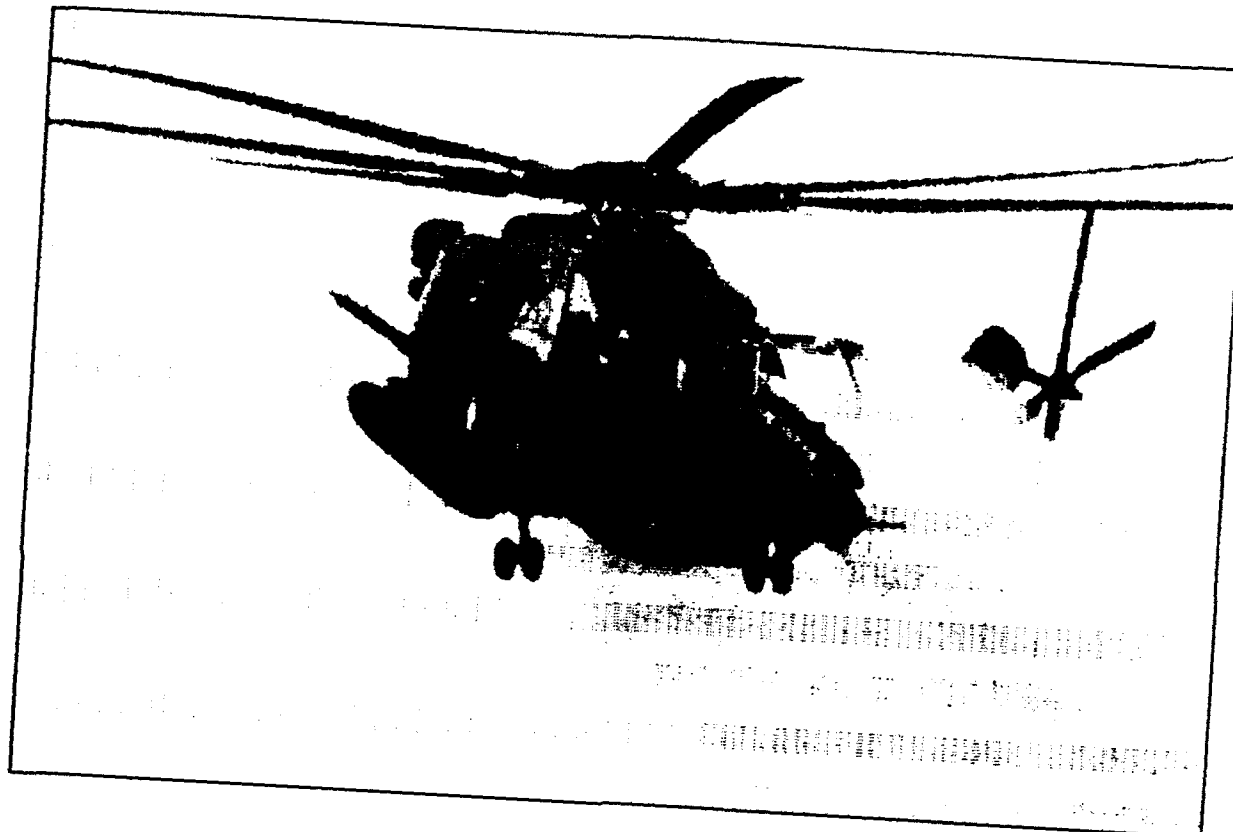
Sikorsky CH-53E "Super Stallion"

Maximum takeoff weight: 69,750 lbs.
Configuration: single rotor, three engine
Rotor type: 7 bladed, fully articulated
Rotor diameter: 79 feet, 0 inches
Rotor chord: 2 feet, 6 inches
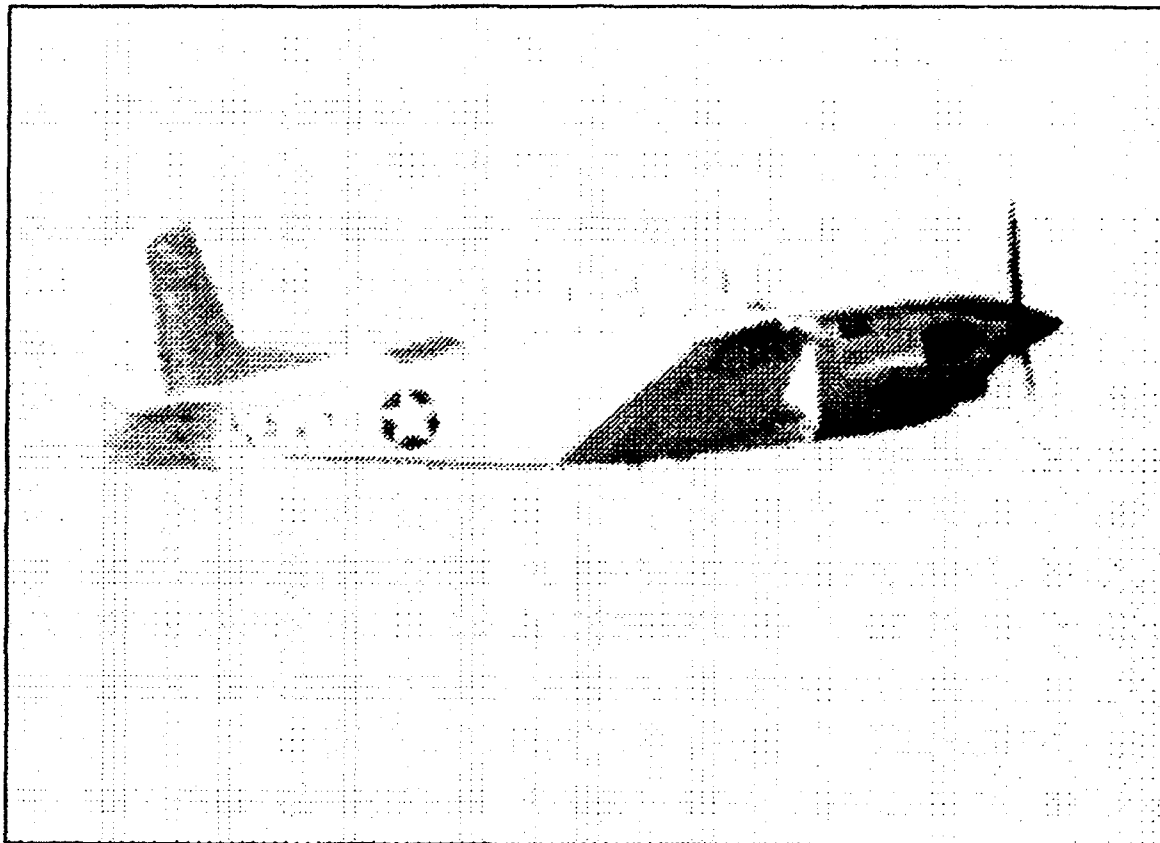
Beechcraft T-34C

Maximum takeoff weight: 4,300 lbs.
Configuration: low wing monoplane
Wingspan: 33 feet, 3 7/8 inches
Wing chord: 8 feet 4 1/2 inches
Wing area: 179.6 square feet
Aileron area: 11.4 square feet
Installed power: 715 shaft horsepower
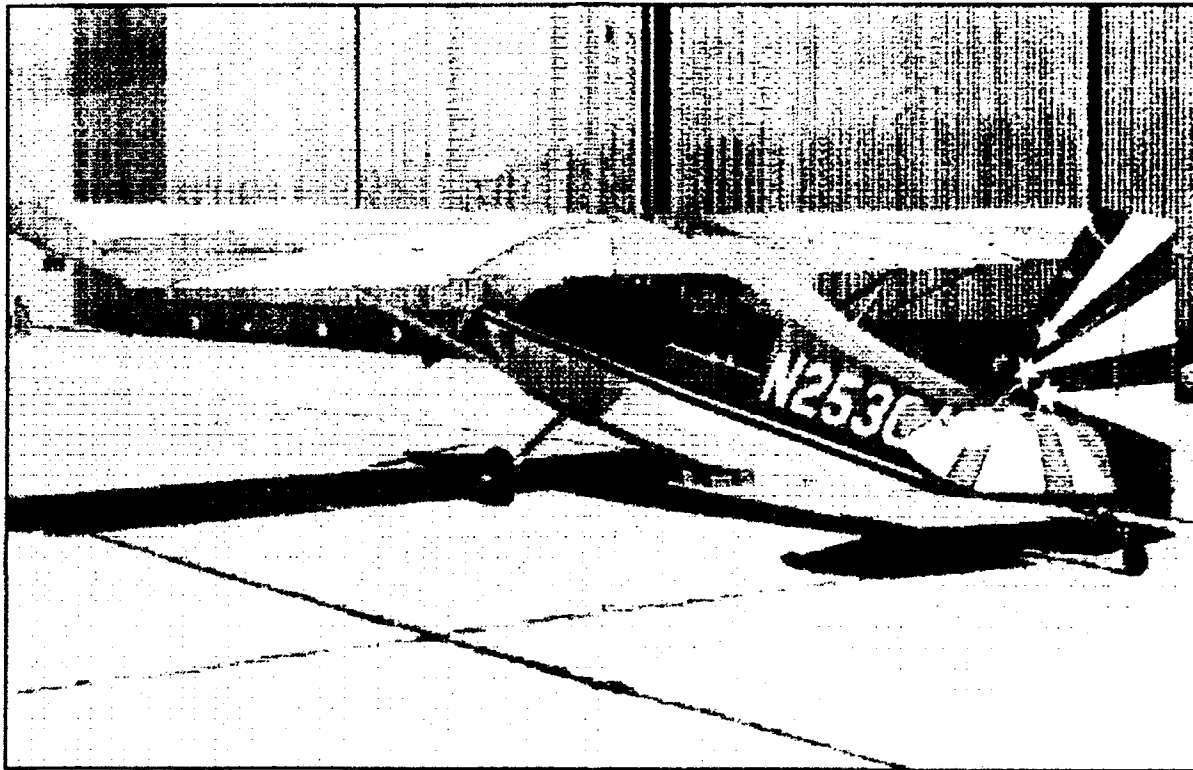
Bellanca 8KCAB Decathlon

Maximum takeoff weight: 1,800 lbs.
Configuration: high wing monoplane
Wingspan: 32 feet, 3 7/8 inches
Wing chord: 5 feet 4 inches (constant)
Wing area: 170 square feet
Aileron area: 20.68 square feet
Installed power: 180 horsepower
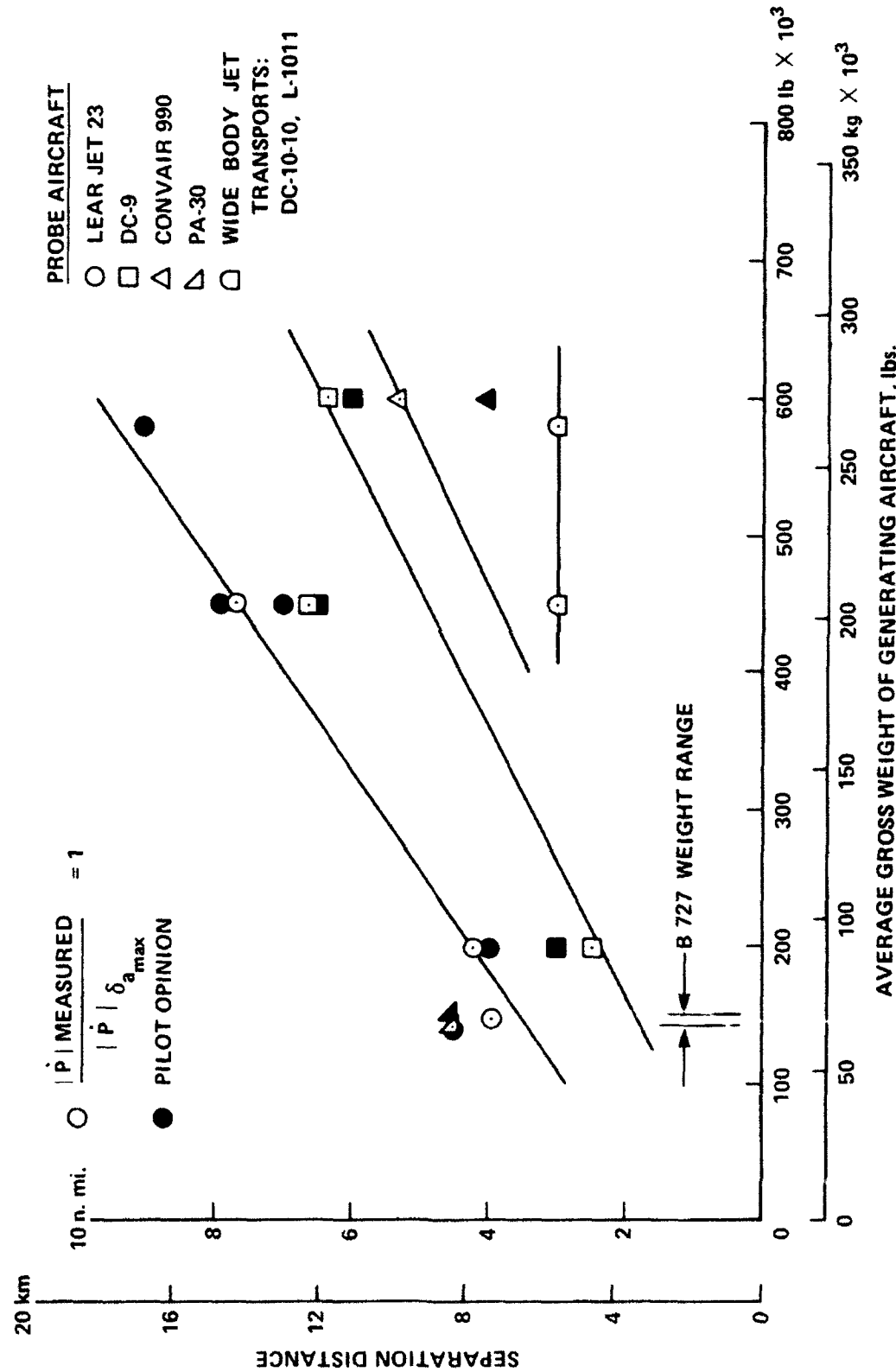
THE RESPONSE OF HELICOPTERS TO FIXED WING AIRCRAFT WAKE ENCOUNTERS

H.C. Curtiss, Jr.
Department of Mechanical and Aerospace Engineering
Princeton University

Zheng-gen Zhou
Design Institute, Harbin Aircraft Factory
Harbin, People's Republic of China

ABSTRACT

Fixed wing aircraft may experience a severe upset if they encounter the trailing vortex of a large jet transport. Limited flight experiments with a teetering rotor helicopter indicate that the response of a helicopter to a trailing vortex encounter is considerably less severe. This paper considers the basic nature of the gust response of helicopters and presents a simplified analytical approach to the problem of predicting the response of a single rotor helicopter to trailing vortex encounter. Consideration is given to the estimation of main rotor flapping as well as the motion of the complete vehicle. The influence of helicopter configuration, main rotor type and helicopter size is discussed and illustrated by calculation of the dynamic response of various helicopters to an encounter with the trailing vortex of a large transport aircraft. Results are compared to flight test. Basic reasons for the difference in severity of the response of fixed wing aircraft compared to helicopters are discussed.

INTRODUCTION

Many investigations of the gust response of helicopters such as found in Reference 1 tend to be concerned with the normal acceleration and structural loading and thus examine the motion over a short time scale of perhaps two or three rotor revolutions. A complex model of the helicopter is employed which includes blade flexibility and non-steady aerodynamics. In order to judge the severity of the upset of a helicopter in an encounter with a fixed wing vortex-wake corresponding to a large amplitude gust, the response over a longer time scale is of interest and it seems reasonable to consider a simpler dynamic model of the vehicle to promote insight into the dominant features of the response. Thus a linearized model is employed and it is assumed that the blade motion can be treated in a quasi-steady fashion since a long time scale is of interest. Some fundamental aspects of the gust response calculation for a helicopter are discussed. The approach presented is applied to the problem of determining the uncontrolled

motion of a single rotor helicopter following an encounter with the tip vortex of a _____e transport aircraft. Full-scale experimental data are used to characterize the velocity distribution of the tip vortex. The gust field is taken to be "frozen," i.e., not changing with time. Two cases are examined. In the first case the helicopter is assumed to encounter the gust field (vortex) by climbing steadily from below, with its velocity vector in the plane of the axis of the vortex (parallel encounter). In the second case, the velocity vector of the helicopter is normal to the vortex axis (normal encounter).

One objective of the study was to examine the sensitivity of the response to different design parameters, since flight test measurements are available only on a teetering rotor helicopter (Reference 2). Consequently the response of three different helicopters are calculated and compared. The three example helicopters are representative of the three rotor types in common use, teetering, articulated with offset and hingeless.

Lateral-directional, longitudinal and fully coupled responses are discussed. For two of the example helicopters, the longitudinal motions are unstable at the trim conditions investigated and consequently these cases are studied using a simple pilot model assuming that the pilot provides a small amount of attitude feedback.

DISCUSSION

Both the magnitude and spatial distribution of the gust velocities are of importance in determining the response of an airplane or helicopter to a gust. However, Reference 2 notes that "the helicopter was found to respond quite differently to a vortex wake than a fixed wing aircraft of similar size." Reference 3 indicates that, while the effect of the mean value of the gust velocity is straightforward and can be directly associated with the dependence of the aerodynamic forces and moments on angle of attack and sideslip, the treatment of the spatial gradients of the gusts is more subtle and depends upon the configuration of the vehicle. That is, while gust gradients can be associated with the angular rate derivatives of the aircraft, the connection between them depends upon the geometry of the aircraft. In many cases in the literature this distinction is not made and the effects of gust gradients incorrectly formulated as for example in Reference 4 where a direct correspondence rotation of the aircraft and the gust field is assumed. As will be shown, especially for a helicopter, the relationships must be treated with care and an approach such as described in Reference 5 associating gust gradients with angular damping derivatives is incorrect. In fact, proper identification of the physical sources of the stability derivatives for helicopters is essential in calculating gust effects. It will be shown that the primary effect responsible for the response of a fixed wing aircraft to a vortex wake, i.e., the association of the roll moment applied to the aircraft with the roll damping acted upon by a roll rate equivalent to the lateral gradient in vertical velocity is not present in the helicopter.

To illustrate the importance of proper identification of the physical effects, consider an airplane encountering a gust with lateral (v) and vertical (w) components which vary both in the lateral (y) and vertical (z) directions shown in Figure 1. If the aircraft were rolling in still air it would experience apparent gradients $\partial w/\partial y$ and $\partial v/\partial z$. However, since the wing is the primary source of rolling moment due to roll rate (roll damping) the effect of these two gradients associated with a gust will be considerably different. The effect of $\partial v/\partial z$ would produce the equivalent of the

contribution of the vertical tail to the roll damping, a small effect, while $\partial w/\partial y$ would produce the wing contribution which is the primary contribution, and thus the equivalent roll rate of the airplane is essentially only due to the gradient $\partial w/\partial y$.

For the helicopter, the interpretation of gust gradients as equivalent aircraft motions is more complex due to the fact that inertial as well as aerodynamic effects come into play in determining the main rotor response to angular motion of the rotor shaft, and the gust gradient effects will be associated only with aerodynamic effects and not inertial effects.

The roll and pitch moments on a helicopter arise primarily from the longitudinal (a_1) and lateral (b_1) flapping, and so the angular accelerations can be approximately written as:

$$\dot{p} = K_x\, b_1 \qquad \dot{q} = K_y\, a_1$$

The angular acceleration produced by a change in flapping depends primarily on the hub configuration. The constant of proportionality will be smallest for a teetering rotor helicopter and largest for a hingeless rotor helicopter, also the roll acceleration induced by an increment in flapping will be a factor of four or so larger than the pitch acceleration due to the large difference in inertias ($K_x > K_y$). The increment in flap angles induced by roll rate can be found from the flapping equation. Consider the equation of motion for the flapping angle of a centrally hinged rotor blade including the effects of an angular roll rate of the shaft, written for simplicity for a hover trim condition,

$$I_b(\ddot{\beta} + \Omega^2\beta) = \frac{pacR^4\Omega}{8}\{-\dot{\beta} + p_A\sin\psi\} - 2I_b\Omega p_1\cos\psi$$

It can be seen that there are two effects of roll rate (p). An harmonic change in angle of attack is produced (p_A) and there is also an inertial or gyroscopic moment produced ($2I_b\Omega p_1$). A lateral gradient in vertical velocity will be equivalent in some way only to the first effect and not the second. Solving for the steady state flapping coefficients for a steady roll rate

$$\beta = -a_1\cos\psi - b_1\sin\psi$$

$$a_1 = \frac{P_A}{\Omega}$$

The longitudinal flapping is due to an aerodynamic effect and the lateral flapping is due to an inertial effect. A lateral gradient in gust velocity will be equivalent only to p_A and thus a parallel encounter will produce pitching motion rather than rolling motion as is the case for a

14-3

$$b_1 = -\frac{16}{\gamma \Omega p_1}$$

fixed wing aircraft. In a cross encounter rolling motion would result. For a hingeless rotor, a small phase shift in flapping occurs such that the gust gradient will produce both rolling and pitching effects but still the response will be very different from a fixed wing aircraft where the gradient can be directly associated with the roll damping derivative. Vertical variations in the gust velocity components have little effect on the rotor flapping as the rotor primarily lies in the horizontal plane. Small effects dependent upon the flapping angle will occur. A detailed analysis of the flapping response is presented in Reference 9.

Gust Field

The flowfield of the tip vortex of a large transport aircraft is the gust disturbance of interest. Its characteristics are based on full scale experimental measurements from Reference 6, shown in Figure 2. The tangential velocity distribution given in Reference 6 is linear for small radii, and equal to,

$$V_T = \frac{V_c(1 + \ln \hat{r})}{\hat{r}} \qquad (\hat{r} > 0.8)$$

where

$$\hat{r} = \frac{r}{r_c}$$

the experimental values of core radius, r_c , and core velocity, V_c, are

$$r_c = 2.51 \text{ m } (8.23 \text{ ft})$$

$$V_c = 16 \text{ mps } (52.5 \text{ fps})$$

These characteristics are for a B-747 vortex wake three miles downstream.

Steady State Flapping Response

First, the steady state flapping response to this gust field with the shaft fixed is considered. As indicated above the magnitude of the flapping induced by the vortex flow field will be indicative of the vortex induced acceleration, as well as possible safety issues associated with flapping limits.

Calculations of the increment in steady state flapping produced by the vortex field are shown in Figures 3 and 4 for two different size helicopter rotors at two advance ratios. Two cases are shown, the rotor hub is located at the center of the vortex $(\hat{Z}_H = 0)$ and at the edge of the core $(\hat{Z}_H = 1.0)$. These calculations indicate the maximum flapping likely to occur. The primary change in flapping occurs in a plane perpendicular to the vertical velocity gradient (longitudinal for a parallel encounter.) The flapping stiffness (p) has little effect on the magnitude of the flapping and primarily produces a small phase shift in the flapping response. The flapping increment (about 6°) is about the same for the large and small rotors because most helicopters have similar tip speeds. There is a trade-off between the weighting factor due to rotor size relative to the vortex core (F_w) (Reference 9) shown in Figure 5 and rotor RPM. In a parallel encounter, longitudinal flapping is induced equal to,

$$\Delta a_1 = \frac{V_c}{\Omega r_c} F_w (\hat{R}_B)$$

V_c and r_c are vortex characteristics. As the rotor radius increases compared to the vortex core radius, the weighting factor decreases (Figure 5), but since the tip speed is constant, the rotor RPM decreases and the ratio of F_w to Ω remains about the same. Thus to the first order, the flapping amplitude is about the same for different size helicopters. It can also be noted by observing that the flapping amplitude for the rotor hub at the edge of the core is about the same as at the vortex center (no lateral velocity) that the lateral velocity component produces only a small increase in flapping. The largest flapping amplitude increase due to a lateral velocity disturbance would occur when the helicopter encountered the vortex while hovering since then the lateral velocity increase would correspond directly to a change in advance ratio. Therefore the effect of the vortex field on the helicopter in a parallel encounter is to produce longitudinal flapping and consequently a pitch acceleration. In a cross encounter, lateral flapping and consequently roll acceleration results. The magnitude of flapping induced while large, tends to indicate that the control power of the helicopter is not exceeded.

Parallel Encounter

In this section, the uncontrolled dynamic response of single rotor helicopters to a parallel vortex encounter is examined and time histories presented for three helicopters representing each of the three rotor types. The helicopter is in a steady state climb with its flight path aligned with the axis of the vortex.

Disturbance

As developed in detail in Reference 9, the equivalent vertical and lateral velocity disturbance velocities produced by the vortex flowfield can be represented as shown in Figure 6. The lateral velocity or sideslip disturbance appears as one cycle of a sawtooth wave and the vertical velocity gradient disturbance is triangular in shape. The disturbance velocities have been faired to zero at ten core radii from the vortex center. Other assumptions regarding the spatial variation of the disturbance velocities at initial encounter had little effect on the response. The time scale of the disturbance is determined by the vertical climb rate of the helicopter.

The maximum equivalent vertical velocity gradient is determined by the effective aerodynamic roll rate calculated by the method presented in Reference 9. The sideslip velocity is taken as the value on the vortex centerline and the averaging discussed in Reference 9 for the main rotor is not used as the effect is not large due to the large size of the vortex. This should give a somewhat conservative result for the magnitude of the lateral velocity response.

The predicted response of a UH-1 for comparison with the flight test data of Reference 2 is also presented. In this case, the generating aircraft was a C-54 and the trailing vortex is considerably smaller. The core radius is estimated from Reference 2 to be 2.4 ft. Averaging of the lateral velocity is employed. The small size of the vortex relative to the helicopter also raises the issue of nonlinear effects due to the motion of the helicopter. Response calculations indicate that there is little lateral translation of the helicopter center of gravity. The tail rotor and vertical tail will therefore encounter a variable velocity field due to yawing of the helicopter and will not on the average experience the maximum lateral velocity on the vortex centerline.

Input to Helicopter

In general, the lateral and longitudinal dynamics of a helicopter are coupled and inputs will appear in all six equations of motion. Considering the six force and moment equations, the following stability derivatives exist related to lateral velocity and roll rate

$$X_v, \ Y_v, \ Z_v, \ L_v, \ M_v, \ N_v$$

$$X_p, \ Y_p, \ Z_p, \ L_p, \ M_p, \ N_p$$

In accordance with the previous discussion to determine which of these derivatives should be included as input terms, the physical source of the derivatives must be identified. In the case of the lateral velocity derivatives, they are all aerodynamic in nature and thus all are included.

The sideslip velocity disturbance to the main rotor can be approximately accounted for by weighting the lateral velocity in the rolling moment equation (9). As this weighting becomes small it indicates that the helicopter is large relative to the vortex and nonlinear effects of movement of the helicopter in the vortex field become more significant. Calculations show that there is little lateral translation of the helicopter in space and thus the primary non-linear effect would be the tail rotor, vertical tail contribution associated with yawing of the helicopter.

14-6

Consequently a weighting of the directional stability which primarily arises from these components is desirable which would depend upon the amplitude of the response. In the calculations that follow no weighting is used for the large vortex encounters $(\hat{R}_a < 3)$ and for the flight test comparison $(\hat{R}_a = 10)$ a weighting of .35 is used on the lateral velocity input.

In general, the large terms tend to be those associated with lateral-directional equations, and the lateral velocity disturbance produces little longitudinal motion. Comparisons between three degree-of-freedom lateral/directional response and the complete six degree-of-freedom response have shown that the response to the lateral velocity disturbance is primarily lateral/directional for the specific helicopters investigated. Some helicopters may have significant values of pitching moment due to lateral velocity (M_v) produced by rotor wake interaction by rotor wake interaction with the horizontal tail which could lead to an increased pitch response (Reference 8), For the vertical velocity gradient, input terms appear as an effective aerodynamic roll rate, consequently, the roll rate derivatives which arise from inertial effects must be identified. As discussed in the previous section, a shaft rolling velocity produces on an articulated rotor longitudinal flapping due to aerodynamic effects and lateral flapping due to inertial effects. For an articulated rotor, the derivatives Y_p and L_p are primarily determined by inertial effects, that is, main rotor lateral flapping due to roll rate and thus these derivatives are set equal to zero for the vertical velocity gradient input. The rolling response is primarily due to M_p. Note that the stability derivative primarily responsible for the response of a fixed wing aircraft to a vortex encounter, L_p, is absent in the disturbance input for a parallel encounter. Consequently, the response of a helicopter to a lateral variation in vertical velocity occurs primarily in the longitudinal axis. Since there is only small roll motion the sideslip disturbance is of considerably more significance.

Vehicle Models

The helicopters are modeled using linearized equations of motion in a conventional Eulerian reference frame. It is important to note that in the time histories presented, the perturbation velocities are with respect to a body axis reference frame. While the calculations indicate large amplitude motions, indicating that nonlinear effects may be present it is considered that the simpler linear model should be reasonably representative of the response and is also better able to promote physical insight into the features of the response. This is shown by comparison with flight test. Three helicopters are examined: a Bell UH-1H (teetering rotor); a Hughes OH-6A (articulated rotor with offset), MBB BO-105 (hingeless rotor). The physical parameters and stability derivatives of the three vehicles are obtained from Reference 5. The UH-1H model includes the feedback provided by the stabilizer bar.

Response Calculations

Time histories of the uncontrolled response of the three helicopters to a vortex encounter are presented and discussed in this section. One problem associated with the uncontrolled response of helicopters is that in many flight conditions they are marginally stable or unstable (without automatic stabilization) and the calculation of the uncontrolled response results in very large amplitude motions which are not of practical interest. This tends to be the situation for both the longitudinal and lateral/directional characteristics near hover and the longitudinal motions in translational flight. The lateral/directional characteristics of the example helicopters at a translational velocity of 60 kts are stable as indicated by the characteristic roots shown in Figure 7. Also shown are the longitudinal characteristics. The hingeless rotor helicopter (BO-105) is unstable and the OH-6 is marginally stable in translational flight while the UH-1H is stable. To gain insight into the lightly damped or unstable cases some results are presented using a simple pilot feedback model.

Figures 8-10 present the lateral/directional response in a parallel encounter for the three helicopters at 60 kts trim speed. Consider the UH-1H response at 60 kts shown in Figure 8. Lateral velocity, roll angle and yaw rate time histories are shown. The lateral gust velocity is also shown and the sideslip of the vehicle is proportional to the difference between these two curves. The lateral velocity response of the vehicle has a shape similar to the input or gust velocity with a time lag due to the inertia and other aerodynamic characteristic of the vehicle. Essentially if the vehicle had no mass, the lateral velocity of the vehicle would tend to be equal to the disturbance velocity. The difference between these two velocities is the sideslip velocity of the vehicle relative to the air, and can be considered as a primary "input" to the rolling and yawing moment equations. That is, if $v = v_v$ there would be little rolling or yawing motion. Figure 8 also shows the relative or sideslip velocity indicating that the roll and yaw motions are primarily produced by this velocity difference.

Figures 9 and 10 show the lateral/directional response to a lateral gust input for the BO-105 and OH-6 at 60 kts. The shapes of the responses are all quite similar to the UH-1H response due to the similarity in dutch roll characteristics of the three helicopters. The peak roll angle of the OH-6A and the BO-105 are 20° and 25° respectively while for the UH-1H it is about 10°. The increase is primarily due to the dihedral effect associated with hinge offset on the OH-6 and the hingeless rotor on the BO-105 (Reference 9). The amplitude increase with rotor type is not directly proportional to dihedral effect due to the fact that the roll damping increases as well tending to counter the gust induced roll motion. The maximum yaw rate experienced is quite similar for the UH-1H and BO-105. The OH-6 exhibits a considerably larger yaw rate response due to its larger directional stability and consequently higher dutch roll frequency. The directional stability characteristics of single rotor helicopters are largely not a function of main rotor type as the primary contributors to the directional stability are the tail rotors, fixed vertical tail surfaces and the fuselage. At 100 kts the responses are quite similar to 60 kts and therefore are not shown. At higher airspeeds than examined in this study, there is a tendency for helicopters to exhibit less dutch roll damping perhaps becoming a more critical case. Note that the yaw disturbance becomes of considerable significance because of the relatively small roll motion.

The longitudinal response of the UH-1H to the vertical velocity gradient is shown in Figure 11 at a trim speed of 60 kts. The amplitude of the response is large although somewhat smoother and perhaps more easily countered by the pilot than the lateral/directional response. This is of course to a large extent due to the nature of the input disturbance shown in Figure 9. Increased airspeed has a strong effect on the pitch response of the UH-1H, the maximum pitch angle reducing by about a factor of two as the airspeed is increased from 60 kts to 100 kts due to the improving longitudinal stability with airspeed.

It may be noted in general from these results that the longitudinal response is quite smooth and probably somewhat easier for the pilot to control then the lateral/directional response which exhibits considerably more of an oscillatory character largely due to the nature of the input as well as the fact that the typical dutch roll motion of a helicopter is relatively light damped and of reasonably high frequency.

Figures 12 and 13 show the effectiveness of pitch attitude feedback in reducing the amplitude of the longitudinal response on the UH-1H and OH-6. A feedback gain of .34 inches of stick per degree of attitude reduces the maximum pitch amplitude by about a factor of four. Similar studies of the lateral/directional axes indicate that roll attitude to lateral control is effective in reducing the roll amplitude but has little influence on the yawing motions as would be expected.

Figure 14 shows a comparison of the calculated six degrees-of-freedom response of the UH-1H to the flight test data of Reference 2. The vortex characteristics employed in this case are V_c = 42 fps and r_c = 2.4 ft. An averaging of .35 was used for the lateral velocity as given by the methods described. The lateral/directional comparison is good indicating the method presented is quite satisfactory for estimating the response. A larger amplitude longitudinal response is predicted; however, there is some indication in Reference 2 that the pilot is using longitudinal stick to counter the pitch disturbance.

Cross Encounter

Since it was noted that the flapping motion induced which produces moments on the helicopter occurs in the plane perpendicular to the gradients an encounter perpendicular to the vortex axis results in a roll response. This section presents a comparison of the roll response of the UH-1H to the BO-105 in a normal encounter at 60 kts. Since the roll response is rapid only a two degree-of-freedom model is used with roll and lateral flapping as degrees of freedom. The input disturbance differs in shape from Figure 6 and is shown in Figure 15. Encounters are shown at translational flight speeds such that the primary disturbance occurs over about 0.5 sec. Approaching the vortex a small counter disturbance would be encountered prior to encountering the main disturbance. This is not included in the calculation but could lead to an improper response by the pilot. (60 kts for the UH-1H and 44 kts for the BO-105). Flap angle, roll rate and roll angle responses are shown in Figures 16, 17, and 18. While the induced flap angles are similar, the roll response is considerably larger for the BO-105 due to the shorter roll time constant and the larger moments induced by flapping. After one second of uncontrolled response, the UH-1H is at 20° roll angle while the BO-105 is at 50° roll angle, a relatively large amplitude, but considerably smaller than would be experienced by a fixed wing aircraft. For the cross encounter, there would also be a vertical acceleration response which would tend to

be relatively small due to the low lift curve slope of a rotor the averaging effect as well as the induced rolling motion. An increment in load factor of somewhat less than one g would be experienced if the helicopter did not roll.

CONCLUSIONS

1. One primary source of the response of a fixed wing aircraft to a vortex flowfield, the roll damping does not appear as an input term for a single rotor helicopter. Helicopter roll rate is not completely equivalent to a vertical velocity gradient.

2. The vortex vertical velocity distribution primarily produces a response of the helicopter in the longitudinal axes for a parallel encounter.

3. The lateral velocity distribution in the vortex primarily produces a lateral/directional response for a parallel encounter.

4. The general character of lateral/directional response of the different types of single rotor helicopter examined was similar. The amplitude of the response was largest for the hingeless and smallest for the teetering rotor. For a normal encounter, rolling is induced by the vortex gradient and the uncontrolled roll motion is considerably larger for a hingeless helicopter compared to a teetering rotor.

5. The approach presented show reasonable agreement with flight test data.

6. For a cross encounter, the motion induced is primarily roll. The amplitude increases as the hinge stiffness increases.

The general nature of the results of this study indicate that it would be highly desirable to conduct studies of the helicopter response using a flight simulator in order to evaluate the ability of a pilot to minimize the response of a helicopter in a vortex encounter. The lightly damped short period dutch roll mode characteristic of a helicopter and the nature of the lateral velocity disturbance may make it difficult for the pilot to reduce the rolling motion induced by the vortex. The nature of the longitudinal response is somewhat smoother and appears more easily controlled.

ACKNOWLEDGEMENT
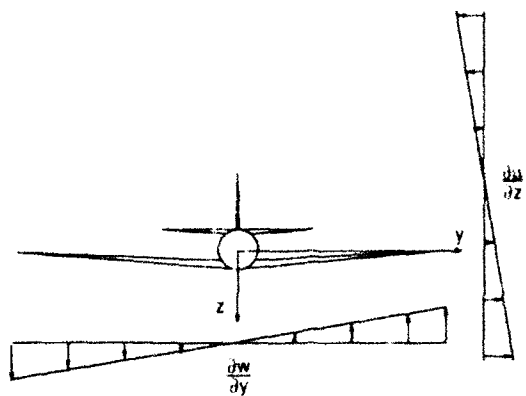
Figure 1. Gust gradients on fixed wing aircraft.
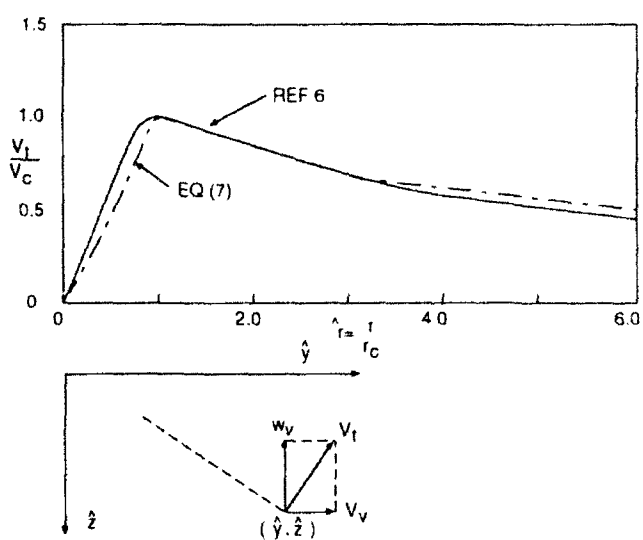
Figure 2. Vortex flow field. Experimental data From Reference 6.
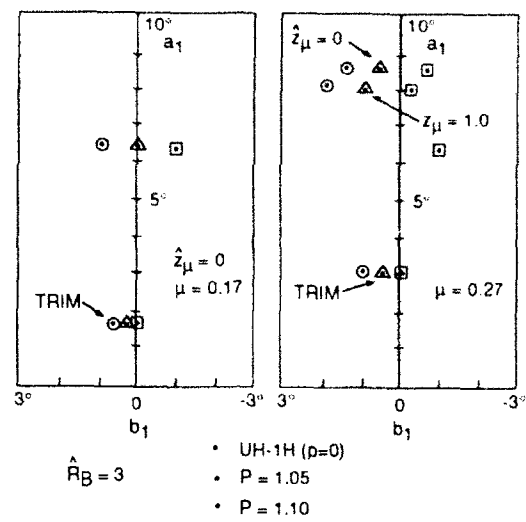
Figure 3. Steady state flapping induced by vortex field ($\hat{R}_B = 3$). Large helicopter (UH-1H).
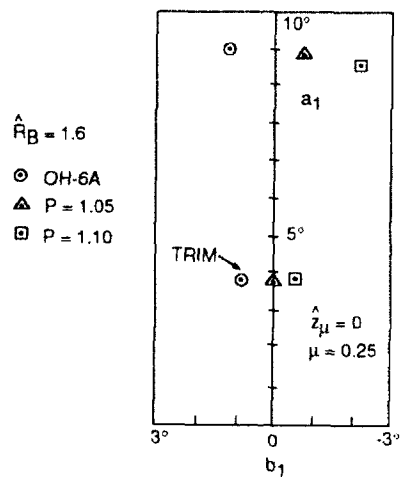
Figure 4. Steady state flapping induced by vortex flow field ($\hat{R}_B = 1.6$). Small helicopter (OH-6A).

14-12
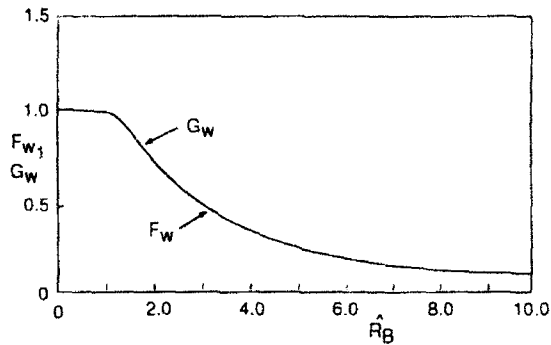
Figure 5. Weighting functions for equivalent aerodynamic roll rate as a function of rotor radius to core radius.
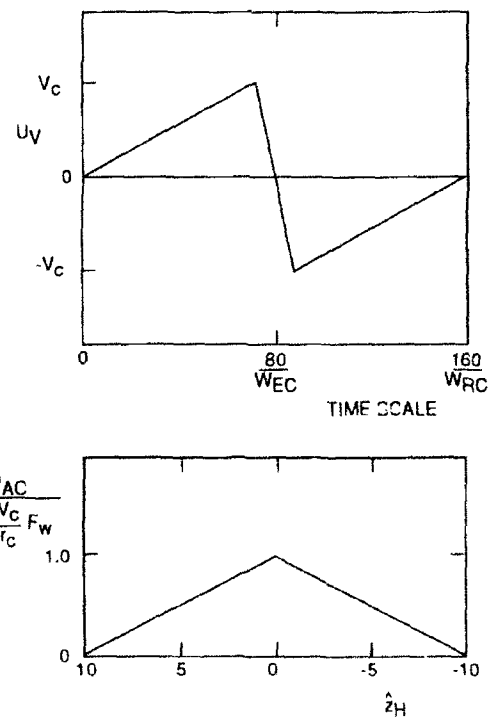
Figure 6. Disturbance inputs for dynamic simulation. Parallel encc_nter.
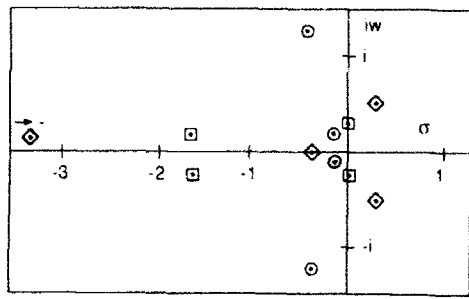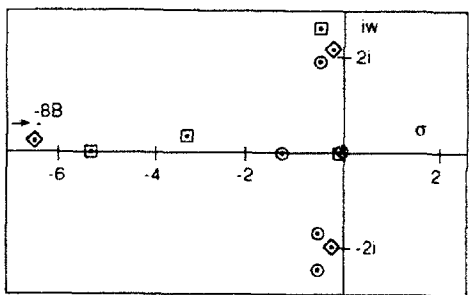
Figure 7. Longitudinal and lateral/directional modes of motion at 60 knots
for helicopters simulated.
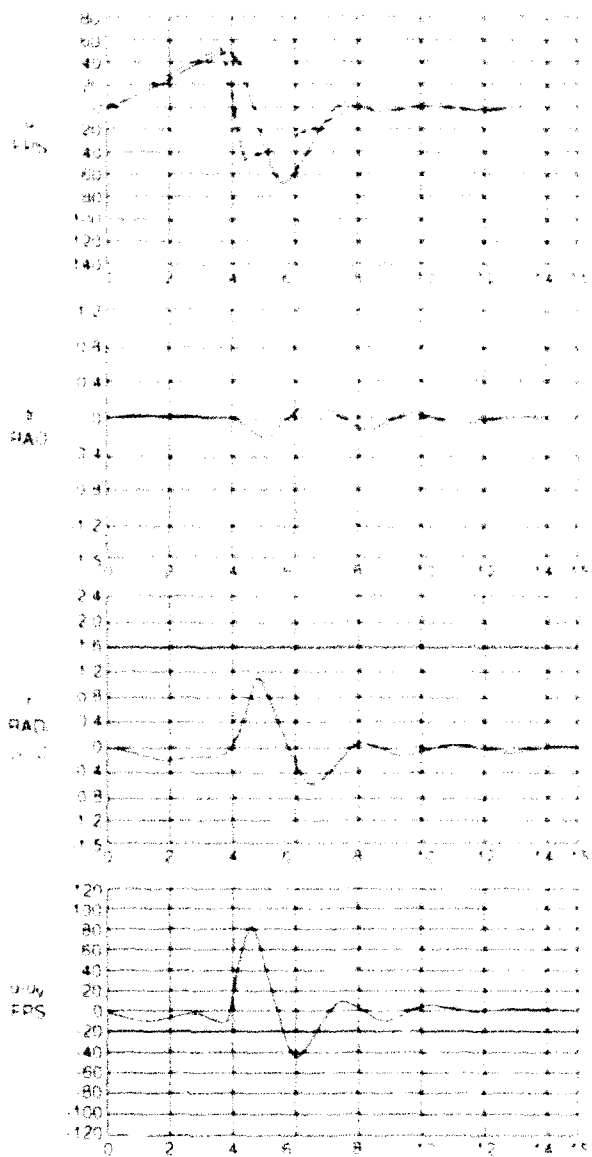
Figure 8. Lateral/directional response to vortex disturbance, UH-1H, 60 kts, 1200 fpm.
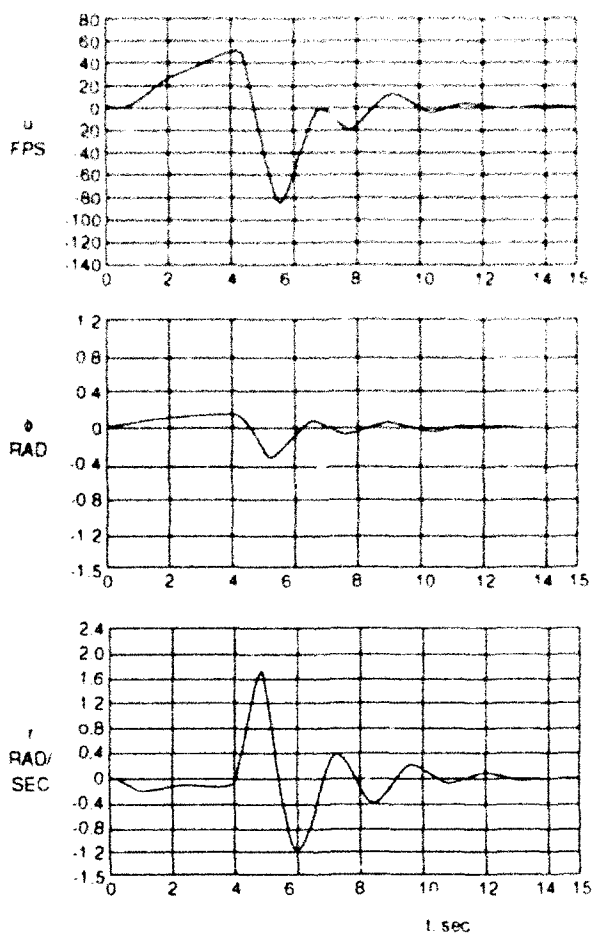
Figure 9. Lateral/directional response to vortex disturbance, OH-6A, 60 kts, 1116 fpm climb velocity.
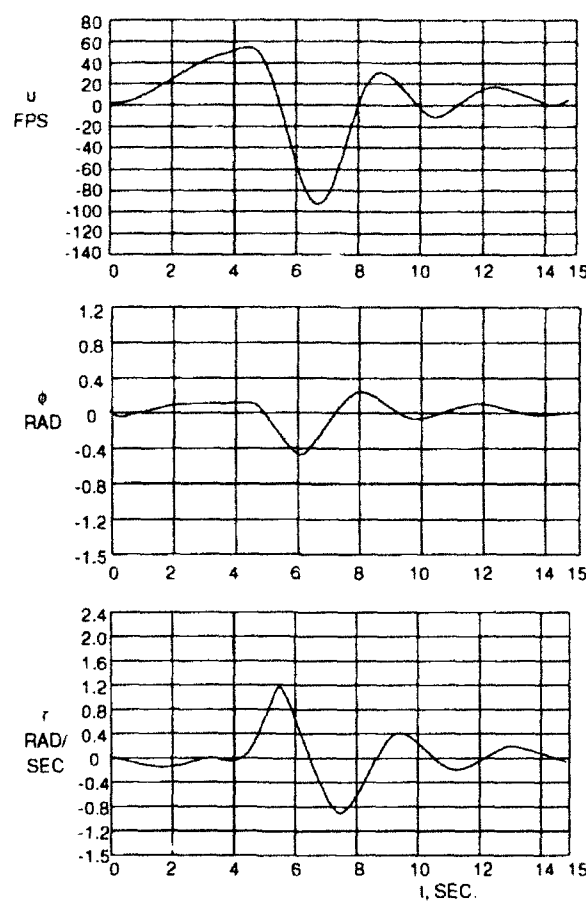
Figure 10. Lateral/directional response to vortex disturbance, BO-105, 60 kts, 1000 fpm climb velocity.
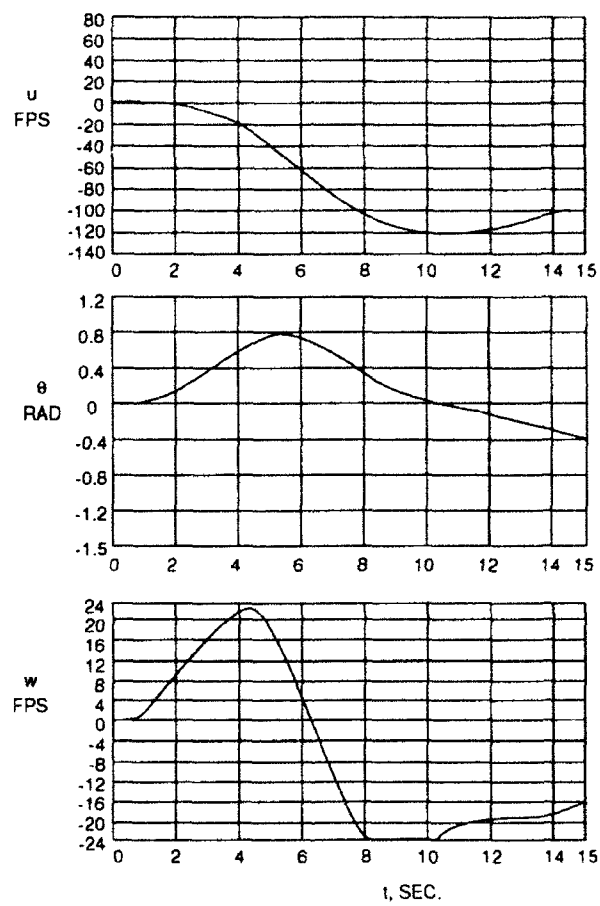
Figure 11. Longitudinal response to vortex disturbance, UH-1H, 60 kts, 1200 fpm climb velocity.
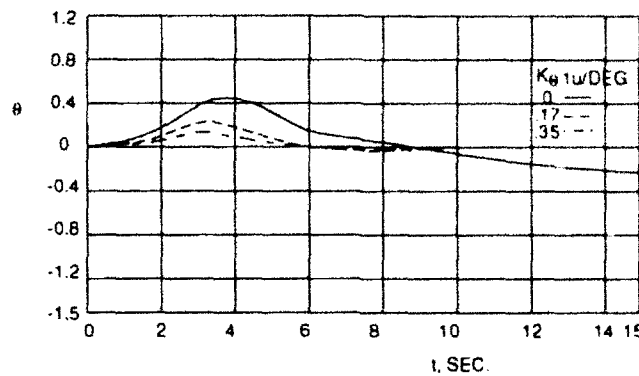
Figure 12. Influence of pitch attitude feedback on pitch response, UH-1H, 100 kts, 1900 fpm climb velocity.
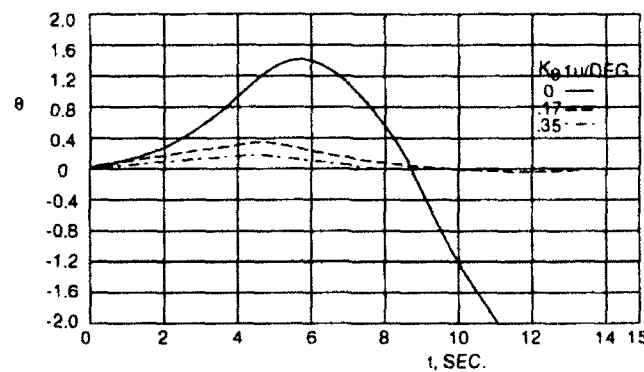
Figure 13. Influence of pitch attitude feedback on pitch response, OH-6A, 60 kts, 1116 fpm climb velocity.

14-19
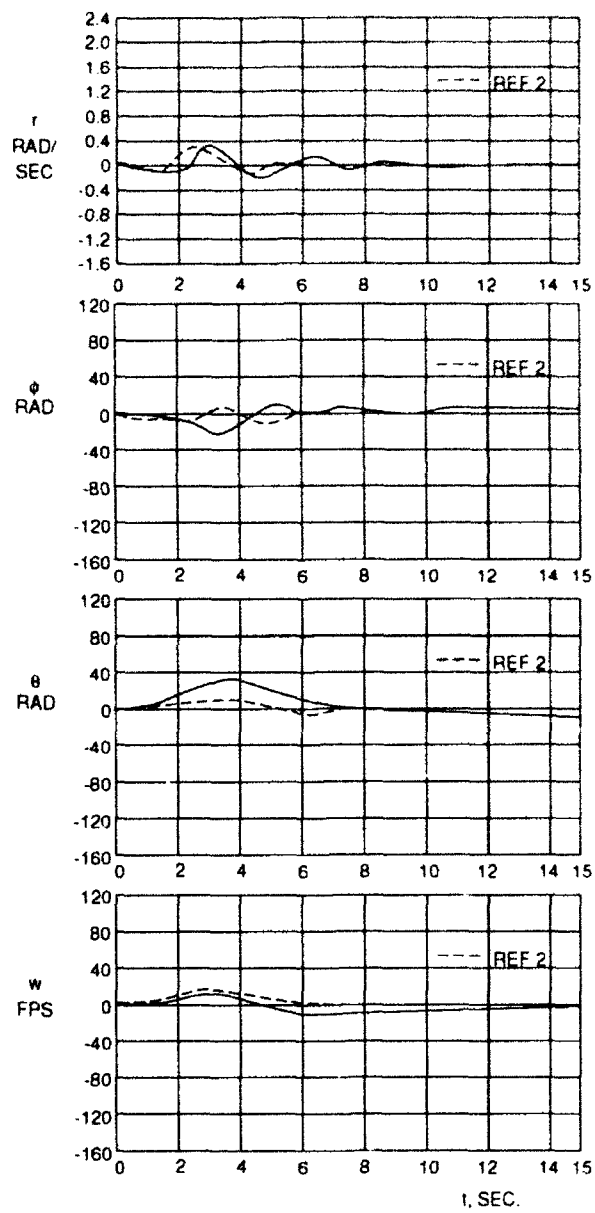
Figure 14. Comparison of predicted response of UH-1H to C-54 trailing votex
with flight test of reference 2, 60 kts.

14-20
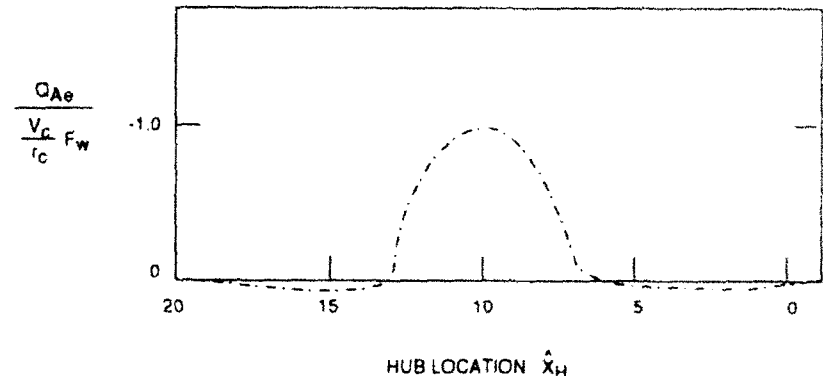
Figure 15. Disturbance for normal encounter.
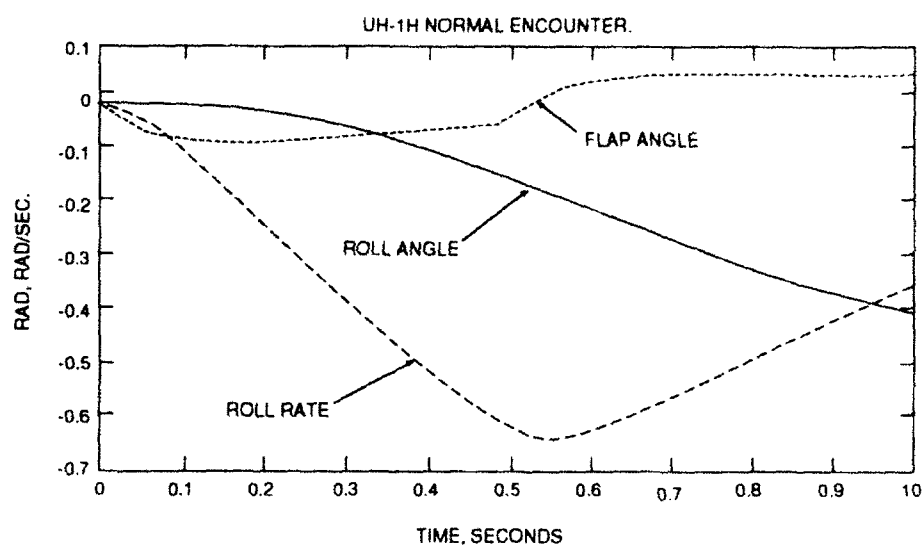
Figure 16. Roll response of UH-1H (60kts) normal encounter.

14-21
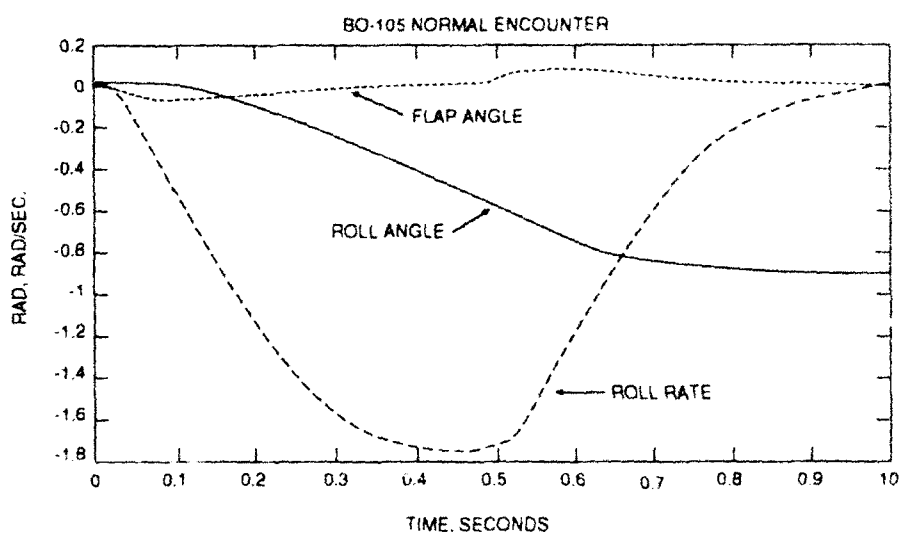
Figure 17. Roll response of BO-105 (44 kts) normal encounter.

REFERENCES

1.   Arcidiacono, P. J., Bergquist, R. R., and Alexander, W. T.: Helicopter Gust Response Characteristics Including Unsteady Aerodynamic Stall Effect, J. American Helicopter Society, Vol. 19, No. 4, October 1974.

2.   Mantay, W. R., Holbrook, G. T. and Campbell, R. L.: Flight Investigation of the Response of a Helicopter to the Trailing Vortex of a Fixed Wing Aircraft, AIAA 3rd Atmospheric Flight Mechanics Conference, Arlington, TX, June 7-9, 1976.

3.   McRuer, P. T., Ashkenas, I., and Graham, D.: *Aircraft Dynamics and Automatic Control*, Princeton University Press, Princeton, NJ.

4.   Frost, W., and Bowles, R. L.: Wind Shear Terms in the Equations of Motion, J. Aircraft, Vol. 21, No. 11, November 1984.

5.   Heffley, R. K., et al: A Compilation and Analysis of Helicopter Handling Qualities Data, NASA CR 3144, August 1979.

6.   Burnham, D. C.: B-747 Vortex Alleviation Flight Tests: Ground-Based Sensor Measurements, DOT-FAA-RD-81-99, February 1982.

7.   Seckel, E. and Curtiss, H. C.: Aerodynamic Characteristics of Helicopter Rotors. Princeton University, Department of Mechanical and Aerospace Engineering Report No. 659, December 1963.

8.   Cooper, D. E.: YUH-60A Stability and Control, AHS Annual Forum, 1977, Preprint 77-33-29-4000.

9.   Curtiss, Jr., H. C. and Zhou, Zheng-gen: The Dynamic Response of Helicopters to Fixed Wing Aircraft Wake Encounters. Paper presented at the Theoretical Basis of Helicopter Technology Conference, Nanjing Aeronautical Institute, Nanjing, People's Republic of China, November 6-8, 1985.

THE ROLE OF SIMULATION IN DETERMINING
SAFE AIRCRAFT LANDING SEPARATION CRITERIA

Robert A. Stuever & Eric C. Stewart
NASA - Langley Research Center
Hampton, VA

ABSTRACT

The role of flight simulation in determining safe aircraft landing separation criteria is reviewed and discussed. A broad conclusion is made that previous vortex-encounter simulations were useful for predicting the general response of an aircraft in the presence of trailing vortices and the type of separation criteria to emphasize. These simulations, however, were generally limited in scope and validation. Broad requirements for an accepted simulation methodology are presented. Key technological issues are addressed, including the addition of high-fidelity vortex models and aircraft/vortex interaction effects in the simulation, and validation of simulations with experimental data. Finally, results from a preliminary one-degree-of-freedom simulation are shown. These indicate that reduced landing spacings may be feasible and that current aircraft categorizations should be reviewed.

NOMENCLATURE

AR	=	aspect ratio	r_g	=	radius of gyration (-)
b	=	wing span (ft)	S	=	wing area (ft^2)
$\bar{c}$	=	mean aerodynamic chord (ft)	V	=	velocity (ft/sec)
C_l	=	rolling moment coefficient	V_{tan}	=	tangential velocity (ft/sec)
$C_{l\alpha}$	=	wing lift-curve slope (rad^{-1})	W	=	weight (lb)
dy	=	incremental span width (ft)	y	=	span station (ft)
h	=	relative hazard indicator	α	=	angle of attack (rad)
I_{xx}	=	roll inertia (slug ft^2)	Γ	=	vortex circulation (ft^2/sec)
L	=	rolling moment (lb ft)	ρ	=	air density (slug/ft^3)
$\bar{q}$	=	dynamic pressure (lb/ft^2)	Φ	=	bank angle (rad or deg)
r	=	radial distance (ft)	$\ddot{\Phi}$	=	roll acceleration (rad/sec^2)
r_c	=	vortex core radius (ft)	ψ	=	horiz. approach angle (deg)

Subscripts:
g   = generator aircraft
f   = follower aircraft
o   = nominal condition
ij   = i-th & j-th configuration

Acronyms:
IFR   = Instrument Flight Rules
VFR   = Visual Flight Rules
DOF   = Degrees of Freedom

INTRODUCTION

Researchers at the National Aeronautics and Space Administration (NASA) recently resumed efforts to study methods for updating current commercial air transport aircraft landing spacing criteria associated with wake-vortex hazards. The goal is to provide a means for safely increasing air-traffic capacity at major airports.

The heart of the program at the Langley Research Center is the development of a validated simulation methodology. The technique will assist in predicting a safe IFR landing separation distance for a given approach scenario. Investigations over the last twenty years revealed the practicality of employing simulation to qualitatively and, to a certain degree, quantitatively study wake-vortex encounters and criteria for avoiding upset conditions. The models used in these studies, however, were generally limited in scope and validity. Implementation of the criteria requires accurate and valid models to determine an envelope of vortex strength, flight parameters, and atmospheric conditions for safe wake-vortex encounters. Langley's projected multi-year, multi-disciplinary program involves a broad mix of theoretical, experimental, and operational studies to implement acceptable models and solidify the validity and practicality of the technique.

The purpose of this paper is to review and discuss the role of flight simulation and its application to the study of wake-vortex hazards. The discussion will begin with a general survey of previous wake-vortex simulation investigations. Modeling techniques and important results will be emphasized. A broad overview of objectives and technical challenges for future simulations is presented. Finally, results from a simple one-degree-of-freedom simulation are shown to point out that changes to current landing spacings and aircraft categorizations should be considered.

PREVIOUS SIMULATION INVESTIGATIONS

As a starting point, consider the following chronological review of previous simulation investigations. Particular attention is paid to modeling schemes, implementation, and limitations which are important to further simulation studies. Pertinent details of each are summarized in Table 1, and a brief review of significant conclusions is presented at the end of this paper.

Early Simulation Investigations

Early simulation investigations followec on the heels of a number of flight test investigations and at least one preliminary simulation study by Hackett and Theisen in 1971.[1] These studies spanned the mid-1970s and were generally an attempt to understand aircraft responses during parallel wake-vortex encounters, define suitable criteria to indicate hazardous conditions, and evaluate schemes for automatically retarding wake-vortex upsets.

Nelson and McCormick

In 1974, Nelson and McCormick[2,3,4] conducted a simulation study to evaluate the general dynamic behavior of aircraft encountering wake-vortices.

In the study, mathematical models of a business aircraft and a DC-9 were used to represent encountering aircraft of two different classes. A pair of linear vortex elements emanating from a Convair 990 were simulated as the hazard. The equations to model the vortex flowfields fit reasonably well with experimental data. Aerodynamic strip theory was employed to calculate the vortex-induced forces and moments across the span of the encountering aircraft. The six-degree-of-freedom (6-DOF) simulation was unpiloted, but not uncontrolled, since analytical transfer functions were used to represent a pilot. The transfer functions had been developed in unrelated studies.

Figure 1 is reproduced to summarize an attempt to validate this simulation. The plot shows a comparison of maximum bank angle of a DC-9 behind a Convair 990 for actual and simulated wake-vortex encounters. The actual encounters were at a variety of in-trail separation distances at altitude and are taken from Andrews[5]. The wake of the Convair 990 was weakly marked by engine smoke. The two lines representing simulated encounters are for the analytical pilot model with only roll control and with both roll and yaw control. Nelson concluded that the addition of yaw control to the roll control was detrimental because it tended to keep the aircraft in the vortex system longer. Inspection of this figure inclines one to conclude that perhaps the simulation methods underpredicted the hazard at small separation distances and greatly overpredicted the hazard at larger distances. Considerable scatter can be seen in the flight test data, however, which was undoubtedly caused by "penetrations" which missed a vortex core or decay of the vortex systems themselves, especially at the larger separation distances. Therefore, any real conclusions which define safe separation standards cannot be based solely on these results.

The investigators generally concluded from their study that penetration angle is significant in the upset magnitude, that reduction in the maximum vortex tangential velocity was not significant, and that a pilot's attempt to control heading may worsen the roll excursion. Interesting cases were discussed in which the encountering aircraft was actually pushed away from the vortex pair for certain combinations of approach conditions.

At about the same time, Johnson, Teper, and Rediess[6] evaluated the effectiveness of an automatic control system for upset alleviation.

A PA-30 and a Convair 880 were modeled and flown in the wake of a Jetstar and a C-5A, respectively. Time-varying vortex models were incorporated into these 6-DOF simulations. Strip theory was used to model incremental aerodynamic effects, and the ensuing models were validated by adjusting strip-theory variables to match known aircraft aerodynamics.

Automatic flight control systems integrated into the two generator/follower aircraft combinations showed that, in fact, they are a feasible option for vortex upset reduction. Significant reductions in maximum bank angle were possible. Results indicated, however, that fairly high feedback gains and control surface deflections were needed to keep the aircraft upright. An interesting tendency for incorporation of heading feedback into the roll control loop was also shown to be detrimental. The aircraft has an initial tendency to yaw in a direction opposite the roll, which negates the roll feedback. Indeed, this phenomenon was observed by Hackett and Theisen in their initial study in 1971.[1]

Sammonds, Stinnett, and Larson

Through the mid-1970s, Sammonds, Stinnett, and Larson[7,8,9] attempted to evaluate the feasibility of simulators for producing realistic wake-vortex encounters and to define criteria for hazardous encounters.

Sammonds' simulation incorporated mathematical models of a Learjet Model 23 and a Boeing 707/720 encountering the wake of a Boeing 727. A time-varying model was used to represent the flowfield and uniform decay of the linear vortex elements. As in Nelson's work, this piloted, 6-DOF, motion-based simulation also employed aerodynamic strip theory to superimpose vortex-induced forces and moments on the nominal aircraft aerodynamics. Development of the simulation is described in Jewell and Stapleford.[10]

Since each of the pilots who flew the simulation had experience in intentional wake-vortex penetrations, their opinions were used to validate it as favorable and realistic. Comparison of simulated wake-vortex encounters with flight tests were also used for validation. The comparison was based on the fact that, for simulated and actual encounters having the same maximum bank angle, the same variables were excited a similar order of magnitude.[7] However, not all responses had the same time-history shape.

The pilots were tasked with flying a 3° glide-slope approach in either VFR or IFR conditions, and were given the option to abort the landing if necessary. The simulation was set up so that the pilot would always intercept a vortex core on an encounter scenario, although not always from the same approach angle. Vortex encounters were rated as either hazardous or nonhazardous by the pilots.

Results of this study revealed that pilot opinion is indeed a valuable asset for defining hazardous-encounter criteria. Specifically, the investigators felt that maximum bank angle, and especially ground proximity, served as the best indicator of a hazardous encounter. Figure 2, reproduced from Sammonds' work, shows representative results from the simulated encounters used to define a hazard criteria. Amidst all the scatter in the data, due partly to variations in approach to the vortex and pilot technique, the investigators were able to draw a line defining a "tentative hazard boundary" for encounter altitude/maximum-bank-angle combinations. Above the line, wake-vortex encounters were acceptable; below it, unacceptable. A similar line could not be drawn for either maximum roll rate or maximum roll acceleration as hazard indicators.

Sammonds and his colleagues also went on to attempt to define hazard boundaries for the two different aircraft, under both VFR and IFR conditions. The results are reproduced in Figure 3. As shown, there is some variation in hazard criteria between the two aircraft for VFR conditions, but IFR conditions yielded almost identical (and more conservative) boundaries. In fact, the figure shows that at the breakout altitude of 200 feet, the maximum roll angle allowed is 7°, about 5° less than for VFR conditions. Perhaps this 5° buffer, while at first appearing small, and visual cues are significant enough in VFR conditions for pilots to "tighten up" their landing separation.

Jenkins and Hackett

Jenkins and Hackett[11] also set out in this period to find reasonable hazard criteria using pilot opinion. Their simulation, a piloted, 6-DOF, fixed-base representation of a C-130 behind a C-5A, incorporated a time-fixed vortex model with an exponential velocity profile outside of the core. Only one vortex was modeled.

The simulation was somewhat unique to the ones reviewed in this paper. The incorporation of vortex-induced forces and moments to the nominal aircraft aerodynamics was not handled with strip theory, but with the more rigorous vortex-lattice technique. The wing, stabilizer, and vertical tail were modeled as a grid of panels. The successful implementation of this method satisfied one of the objectives of the investigation. Although the grid system was fairly simple, this success was also mildly phenomenal and inspiring when the speed of computers in 1975 compared to 1991 is considered.

As in Sammonds' study, the piloting task was to fly a 3° approach in IFR conditions. The position of the vortex and the angle at which it was encountered were random. Validation of the simulation came from favorable comments from the pilots who flew it.

The results of this investigation once again showed that maximum bank angle is a good hazard indicator. Ground proximity was not studied. Jenkins and Hackett were also able to expand upon the simple acceptable/unacceptable standard of Sammonds and implement three vortex-hazard rating scales.

The first scale, dubbed the "Meyer-Hermitage Scale," is shown in Table 2 and was developed in the spirit of the Cooper-Harper rating scale for aircraft handling qualities. The scale assigns a numerical value to each of the vortex-induced aircraft responses perceived by the pilot. Figure

4 shows the use of this scale for defining hazardous encounters. This example represents flight paths which are initially down the center of the vortex, and is based on vortex strength. Deviations to this basic curve were studied for changes in aileron roll-control power, horizontal encounter angle, vertical encounter angle, and vortex core radius. An interesting correlation with the work of Sammonds is shown in Figure 5. Here, the maximum bank angle for all combinations of vortex strength and horizontal approach angle are plotted. The "normal range" which all of the curves converge into represents maximum bank angles which are typically acceptable in all transport flight operations. The investigators comment that this value is approximately 7°, exactly what Sammonds' results indicated. Extension of the curves also indicates that, expectedly, there are combinations of vortex strength and horizontal approach angle which are not acceptable. Encounters with these combinations were rated with a second scale.

This second scale is shown along with a third, similar scale in Table 3. These five- and three-point rating scales represent perceived handling qualities in the roll and yaw axis, respectively. As expected, roll-axis effects were dominant. Figure 6 shows the correlation of maximum bank angle with vortex strength and encounter angle shown in Figure 5, except that a hazard rating has been applied to it. An interesting point is that there is again about 5° or 6° of bank angle that acts as a buffer between a comfortable, acceptable vortex encounter and one that is minimal. Note, however, that the boundary for unacceptable encounters is at 18° of bank, about 5° further than a minimal encounter. This differs from Sammonds' work, and may be due to the fact that encounter altitude was not correlated with maximum bank angle.

Simulation Studies of the 1980s

The second phase of wake-vortex simulations encompassed the 1980s and consisted of at least five noteworthy investigations, one of which is still ongoing. The simulations focused on the effects of parameter variations for parallel encounters, the evaluation of a scheme to avoid wake-vortices altogether, the study of an updated wing/vortex-interaction modeling technique, and the effect of cross-vortex penetrations on operational safety.

Hastings and Keyser

First, Hastings and Keyser[12] completed a study in 1982 of a Boeing 737 encountering the wake of a Boeing 747 in the landing approach. Their study focused on evaluating the effects of variations in horizontal and vertical vortex-encounter position, vortex age, encounter-aircraft airspeed, generator-aircraft lift coefficient, and vortex alleviation on the flight characteristics of the encounter aircraft.

A piloted, 6-DOF, motion-based simulation was employed. The vortex pair was modeled from theoretical and experimental data for conditions both in and out of ground effect. Time variations in the vortex model were represented at four fixed times. These times and the vortex velocity profiles both in and out of ground effect are shown in Figure 7. The purpose of the investigation was to examine the initial response of an aircraft to vortex flowfields. Hence, the vortex models were truncated linearly and were about 250 feet long. In effect, the encountering

aircraft saw a "pulse" from the vortex, which justified fixed vortex models at each of the times. The technique was deemed satisfactory since this was a parametric study. Strip theory was once again used to calculate vortex-induced forces and moments. No mention is made of the validation scheme for assuring correct incorporation of vortex effects, and pilot opinion is assumed.

The results of the study showed that parameter changes which would normally be taken as favorable (e.g., a vertical or horizontal offset from the vortex center, an increase in approach speed, etc.) resulted in reduced vortex-induced roll excursions. Perhaps the most important result is the effect of vortex age on maximum bank angle, reproduced in Figure 8 for approaches both in and out of ground effect. Here, as might be expected — especially after reviewing Figure 7 — decay of the vortex strength reduces the hazard associated with flying through it. The same qualitative effect was seen in this paper for attenuated vortices. In fact, correlation of maximum bank angle with altitude using the criteria proposed by Sammonds and flight-path deviation criteria proposed by a major airline showed that acceptable encounters at 100 feet and 200 feet altitude were possible only for the vortex condition most decayed.

Abbott

In 1984, Abbott[13] reported his evaluation of a scheme for real-time vortex avoidance based on pilot discretion. In his study, a display technique was incorporated to allow multiple glide-path approaches for reducing in-trail separation. Abbott theorized that if the pilot of the following aircraft had some knowledge of the approximate location of the lead aircraft's wake, a glide-path adjustment could be made to avoid it altogether.

The Boeing 737 simulation of Hastings was adjusted to calculate parameters for symbols in the pilot's heads-up display. This included markers representing the lead aircraft's current position, past position (for assuming an approximate location of the wake), and deviation (in time) from a prescribed separation interval. In addition, the vortex pair was allowed to descend at a fixed rate and spread in ground effect. The strip-theory approach of Hastings was retained.

The piloting task was to execute an ILS approach at a major airport. Variations in the lead aircraft's approach were introduced to represent two different approach speeds, failure to exit the runway, and a missed approach. The pilot of the follower aircraft executed a number of approaches for various self-separation intervals.

The most important conclusion from this study was that a pilot could execute a safe ILS approach at separation intervals of 90, 60, and 45 seconds with an acceptable workload. Incorporated with a detection technique or automatic control system, this type of technique could potentially assist a pilot in duplicating a VFR approach (under IFR conditions) and perhaps helping to increase capacity at a given airport.

Although the discussion so far has centered on 6-DOF simulations, Holbrook[14] completed an interesting study about this time using a 1-DOF model. In it, the interaction of a wing with the vortex flowfield, and its effect on the ensuing roll upset, was investigated. The assumption was that the wing altered the vortex flowfield as it passed through it, essentially reducing its strength and the resulting roll upset. It was different from techniques which had been commonly used in which vortex-induced forces and moments were calculated directly from "undisturbed" vortex flowfield velocities.

Conservation of angular momentum was employed to represent wing/vortex coupling. The simplified representation of the following aircraft implemented a rectangular wing planform and strip-theory aerodynamics. The wing was axially centered in a vortex which represented the wake of a wing with either a rectangular, triangular, or alleviated loading. The wing was free to roll for a simulated time of one second. Subsequent maximum bank angle was recorded.

Figure 9 illustrates one of the wing-loading cases examined and is representative of Holbrook's results. In it, maximum bank angle is plotted as a function of generator and encounter aircraft weight. Coupling of the wing and vortex is shown to reduce the maximum bank angle. The data from Figure 9 were then presented in another fashion along with current separation criteria. This is reproduced in Figure 10, and shows contour plots of maximum bank angle for various combinations of leading and following aircraft weight. Holbrook's most important conclusion from these representative figures pointed out that current separation criteria may be overly conservative for some landing scenarios, namely the heavy and large combinations. The idea that the wing and the vortex may also be coupled emphasized this conservatism. He was cautious to point out, though, that implementation of his technique into operational consideration requires experimental validation of the method and consideration of vortex decay.

Konig

The most recent simulations described in the literature involve cross-vortex penetrations and the hazard associated with landing and departing traffic.

Konig[15] examined perpendicular vortex penetrations on takeoff in his study completed in 1989. In it, a Deutsche Lufthansa training simulation of a Boeing 737 was modified to accept the vortex pair of a Boeing 747. His objective was to study the aircraft response and pilot behavior as the vortex was encountered.

The piloted, 6-DOF simulation incorporated an empirical flowfield model of the time-varying, descending vortex pair. The effects of crosswind were included. Differences in vortex-induced effects between the aircraft wing and tail were modeled with a "rotating gust": the aircraft effectively saw the vortex as a change in pitch rate. Validation of the vortex-induced forces and moments came from pilot opinion. Penetrations of one or both of the vortex cores, or above or below them were simulated.

The results of this study showed that even though no critical flight conditions (in terms of altitude loss or stall) were experienced in these encounters, significant g-loads, sometimes exceeding safety limits, were generated on the 737. In fact, McGowan[16] predicted this same effect for light-utility and light-transport aircraft behind larger aircraft in 1961. The pilot could not counteract the buildup of these loads for the short duration that the vortices were encountered.

The simulation used in this study had no aeroelastic or unsteady-aerodynamic effects in it, so an accurate evaluation of the effect of these loads on flight safety could not be made.

Lockheed

Finally, investigators at Lockheed[17] are examining cross-vortex encounters at New York's LaGuardia Airport to determine if reduced-separation standards would pose a hazard. A paper on this study is to be included in these proceedings and the reader is referred to it.

An interim report, however, stated that the initial plans were to incorporate models of a Boeing 727, a DeHavilland DHC-7, and a McDonnell-Douglas A-4 in the wakes of a DC-10 and a Lockheed L-1011 in both piloted and unpiloted, 6-DOF, motion-based simulations. Rankine vortex models (with cores), having strengths derived from experimental data, were added to the aerodynamic data of the following aircraft as incremental lift to the wing.

Validation of the simulation models is expected to come from comparison of flight data and simulator data for the A-4. If the models match, the technique is to be applied to the 727 piloted simulation.

SIMULATION OBJECTIVES AND TECHNICAL ISSUES

With respect to future requirements, a conclusion may be drawn that previous simulation studies were generally limited in scope and validity. While each investigator understandably limited his techniques and models to whatever was necessary to fulfill specific objectives, none of them successfully related generator- and follower-aircraft characteristics, separation distance, and atmospheric (decay) conditions simultaneously. Likewise, even though pilot opinion is certainly valuable and necessary to establish the realism of a simulation, some measure of tolerance is necessary between actual and simulated dynamic response. Therefore, quantitative results from these studies cannot be directly applied to set separation criteria for a given airplane and flight condition.

Limitations from previous studies point out exactly the things that constitute an acceptable methodology. Namely, the incorporation of generator- and follower-aircraft, separation distance, and atmospheric conditions to determine their effect on the perceived hazard. In essence, the idea is to find out exactly which conditions are hazardous to a given aircraft. Successful incorporation of these relationships into a dynamic separation scheme improve the prospects for increased IFR airport capacity and revenue.

Even though NASA is proposing a somewhat new simulation methodology, implementation of it will be based on the lessons learned from previous studies. In other words, previous results pointed out the qualitative nature of a pilot's perception of a hazardous encounter, and about where the quantitative limits of danger lie. The task now is to accurately define the conditions under which hazardous upsets will and will not occur. This involves providing a scheme to predict the strength of a vortex under a given atmospheric condition and time passage, to adequately determine the resulting vortex-induced forces and moments on the aircraft, to accurately predict the ensuing trajectory, and to define acceptable upset limits for each aircraft. (These limits were determined by Sammonds, then Jenkins, for three aircraft on final approach. They are not likely to differ greatly for other aircraft, but there may be changes in them for takeoff, missed approach, etc., flight phases.)

Before this scheme is successfully developed, though, a number of technical issues should be considered.

Validation

First, the most important technical issue leading to an accepted simulation methodology is the validation of models and simulated trajectories with experimental data.

In the past, flight-test measurements of wake-vortex encounters consisted of the interception of the wake along a specified trajectory. Due to the nature of wake turbulence, though, this was necessarily difficult to accomplish precisely. Indeed, Nelson's attempt to validate his simulation showed that firm conclusions could not be drawn because there was so much scatter in the flight-test data.

If three important measurements are made, precise vortex intercepts are not required and validation of the dynamic response is greatly facilitated.

First, the characteristics of the vortex flowfield must be measured to understand the magnitude of the forces and moments on the aircraft (and also facilitate vortex-modeling efforts). The differential aspects of the flow between two wingtips, for instance, can be measured with flow-angle sensors.

The second parameter which must be measured is an inertial vertical and horizontal velocity. The differential flow-angle sensors only measure velocities with respect to the aircraft. Since the aircraft has a natural tendency to return to its initial trim condition, the absolute magnitude of the angle of attack due to the vortex can never be determined with differential measurements alone.

Finally, the position of the aircraft with respect to (at least one of) the vortices must be measured. One has to know an exact position with respect to the vortex core to make an accurate reconstruction and comparison of the trajectory with simulation. This measurement has only been attempted once (Branstetter, Hastings, and Patterson[18]), and is a major technical challenge of NASA's simulation validation scheme.

One conclusion directly related to adequate validation which may be drawn from the work of Sammonds and Figure 3, and also from the Jenkins study, pertains to the 5° maximum bank angle buffer between VFR and IFR conditions. First, the IFR limitation of 7° at the 200 foot breakout altitude is a relatively small bank angle (although perhaps not in an emergency situation at 200 feet!). The buffer of 5° is even smaller. Although the pilots found the vortex-encounter simulation to be quite realistic, there is no other validation to ensure that the mathematical technique used to implement vortex-induced forces and moments on the aircraft was accurate. This certainly does not invalidate the 7° limitation. Instead, since the region of acceptable encounters is so small, and the region between acceptable and unacceptable is even smaller, the effects of the vortex on the nominal aircraft aerodynamic forces and moments must be accurately modeled and validated. Small errors could potentially give significant differences in safe operating conditions.

Agreement on Hazard Definition

Next, the definition of a hazard must be determined and agreed upon by the technical and regulatory communities. Along with that, a decision on whether that requirement (or the magnitude of that requirement) should be the same for all aircraft size/weight/flight categories should be made. As previous investigations have shown, maximum bank angle and altitude are adequate hazard indicators.

Vortex Models

Third, the simulation methodology should include variable, validated vortex models. These models should account for time-dependent and atmospheric-decay factors, such as the Crow instability, temperature inversions, winds, etc. Many of the previous simulation investigations used viscous-decay approximations, but all pertinent atmospheric conditions are important, especially since Greene[19] showed that they may have a significant effect on decay. Indeed, a pure decay alone has been shown to significantly reduce the initial upset due to a wake-vortex upset.[12] Another important consideration is the decay or persistence of the vortex in ground effect, and the manner in which the ground plane modifies the nominal vortex velocity profile (e.g., is it still essentially circular?).

Computational Techniques

An acceptably accurate but computationally quick technique for adding these flowfields to the nominal aerodynamics of the aircraft must be implemented. Most previous investigations used either strip theory or a vortex-lattice technique. This also raises the issue of how any wing/vortex interaction effects proposed by Holbrook should be accounted for. The validation phase of the program will point to the complexity necessary to implement vortex flowfields in real time. One source of confidence is the ever-increasing speed of modern computers and the development of efficient programming languages.

Automatic Control System Issues

Airborne wake-vortex detection research originally started by Branstetter[18] may be included as part of the simulation-validation flight tests envisioned by NASA. One possible application of detection technology is in automatic upset-reduction control systems. Indeed, an interesting conclusion which may be drawn from the work of Johnson[6] and his colleagues is the need to sense the vortex flowfield before the aircraft has a chance to respond to it. If these systems are used to avert wake-vortex hazards, then the location of the sensors on the aircraft becomes important because the same sensors may also be incorporated in an automatic landing system.

Johnson's automatic control system and Nelson's pilot model both point out why the vortex must be sensed. Both were compensatory systems that responded to positions and/or rates which the vortex had induced on the aircraft. These systems required high feedback gains, quick actuators, and control surfaces with great authority to counteract the potentially quick and severe upset capability of a vortex flowfield. If a vortex could be sensed by its flowfield before it has a chance to influence an aircraft's motion, however, an autopilot system should not need as much authority since it will not have to correct an unfavorable condition. This is assuming, of course, that the controls can produce moments large enough to counteract flow-induced moments.

Sensor location for automatic landing control systems normally engaged needs to be assessed. It is quite possible that a vortex encountered on landing approach may be sensed as an increase or decrease in sink rate, thus causing the automatic landing system to adjust with potentially hazardous results. This becomes more significant if reduced separations (into stronger vortices) are proposed for some aircraft classes.

Aeroelastic Effects

Finally, the effects of aeroelastic deflection of the airframe should be considered. Konig's[15] efforts showed that for certain vortex encounters, maximum g-loadings may be exceeded. The effect of airframe deflection on the calculation of vortex-induced aerodynamic forces and moments, and wing/vortex-interaction effects, may be significant.

INITIAL RESULTS FROM CURRENT SIMULATION

This section describes results from a preliminary simulation which was developed to assess the feasibility of changes to the current IFR spacing requirements and/or aircraft categorizations. The calculations were intended to bound the wake-vortex problem for representative aircraft to determine if current spacings provide a uniform level of safety. A simple simulation was used to estimate the roll angle which might result from a vortex encounter. The *relative* hazards of generic aircraft pairs are estimated, and the ensuing results are compared to current separation categories.

The analysis assumes a generic, rectangular wing planform which is placed in the center of a single, straight-line vortex with an assumed tangential velocity distribution

$$V_{tan} = \frac{\Gamma r}{2 \pi r_c^2} \qquad 0 \le r < r_c \qquad (1)$$

$$V_{tan} = \frac{\Gamma}{2 \pi r} \qquad r_c \le r \qquad (2)$$

where

$$\Gamma = \frac{4 W_g}{\pi \rho V_g b_g} \qquad (3)$$

Equation (3) represents the undecayed circulation in the wake of an elliptically-loaded wing. Assume that the wing is free to roll and that all other motions are fixed. Aerodynamic strip theory may be used to approximate the total rolling moment as

$$L = \bar{q} S b C_l = \sum_{i=1}^{n} \bar{q} \bar{c} \, dy \, y_i C_{l_\alpha} \alpha_i, \qquad (4)$$

where α_i represents the incremental angle of attack at each strip due to the vortex flowfield and the wing roll rate.

An indication of the hazard due to a wake-vortex encounter has been shown to be maximum bank angle, found by integrating the roll acceleration

$$\ddot{\Phi} = \frac{L}{I_{xxf}} \qquad (5)$$

twice.

If a nominal leading/following aircraft pair is selected, the relative hazard of any following-aircraft's response to the wake of any other aircraft can be represented by scaling its roll response to the response of the nominal pair. That is,

$$h_{ij} = \frac{\Phi_{ij}}{\Phi_o}. \tag{6}$$

Note that this is simply a comparison of roll responses induced by a vortex. It does not imply anything about whether roll-control powers or pre-determined bank-angle criteria have been exceeded.

For this analysis, representative values of aircraft weight, span, mean-aerodynamic chord, moment of inertia, approach speed, aspect ratio, and lift-curve slope for the aircraft categories shown in Table 4 were selected and are summarized in Table 5. The weight information was taken directly from Table 4. An intermediate weight (in the large category) of 100,000 lb was added to represent a short/medium-range transport common to the current aircraft fleet. The small-aircraft category (less than 12,500 lb) was not included since these aircraft contribute relatively little to the capacity problem at major airports. Typical span and chord values were derived from representative transports featured in *Jane's*.[20] A typical, constant aspect ratio of 7.5 was selected. To ensure uniform dynamic characteristics, the moments of inertia shown in Table 5 were calculated assuming that all the aircraft had the same nondimensional radius of gyration, r_g, as a percentage of the semi-span. An appropriate value for the lift-curve slope was calculated from an expression treated in both McMillan[21] and Rossow[22] (originally attributed to R.T. Jones), and was held constant to keep parameter variations to a minimum. Roll responses were calculated for a simulated time of one second.

The 100,000 lb aircraft behind another 100,000 lb aircraft was selected as the nominal condition. Aircraft in this pair constitute a large portion of the traffic at major airports, and have been observed safely landing in sequence for years. Thus, this pair is a good representative of a roll hazard equal to one.

Figure 11 presents the results of this study. This figure is a logarithmic plot of relative hazard, based on maximum bank angle after one second, as a function of the ratio of follower-weight to generator-weight. The follower-aircraft are represented by four unique symbols, and the generator-aircraft are denoted by a letter next to each data point.

Even though Figure 11 contains a wealth of information, only two points will be discussed here. First, notice that for each equal-size pair (e.g., 300K vs. 300K), the relative hazard is nearly one (at least within a factor of about two). This indicates, as one might expect, that equal-size aircraft are generally safe to land in minimum-spacing sequence. Also notice that the relative hazard decreases for these pairs as the weight increases, which is a conclusion Holbrook[14] reached in his study. Next, note the second point from the left (the "C" circle) and the second point from the right (the "A" triangle). These two points represent the 12,500 lb aircraft behind the 300,000 lb aircraft, and the 300,000 lb aircraft behind the 12,500 lb aircraft, respectively. In other words, these two points bound the relative hazards for the "large" separation category. Note that the difference in relative hazard between these two points is nearly two orders of magnitude. (The difference in relative hazard magnitude between the two outer points is also significant, but these do not reflect aircraft combinations from only one separation category.) Table 6 shows a summary of the data from Figure 11 along with the current IFR separation standards. For the heavy/heavy combinations, the relative hazards are within a factor of two,

with the maximum just over the nominal case. The lower end represents the 500,000 lb aircraft behind the 300,000 lb aircraft, and the other end represents the opposite case. For the heavy aircraft behind the large, the range of magnitudes is fairly large but never gets above one (the 300,000 lb pair). Likewise, for the large aircraft behind the heavy, the hazards start at about one and grow larger. This pair is protected by increased spacing relative to the minimum. The largest range, however, is shown in the block for the large behind large, where there are relative hazard differences of nearly two orders of magnitude. The lower end represents the 300,000 lb aircraft behind the 12,500 lb aircraft, while the upper end is the 12,500 lb aircraft behind the 300,000 lb aircraft.

These results point out that perhaps current categorizations for landing separations are not consistent with the potential hazards involved. The big impact of a 300,000 lb aircraft on a 12,500 lb aircraft (large-large), and the relatively small impact of a 12,500 lb aircraft on a 300,000 lb aircraft support this. If the 12,500 lb aircraft following a 300,000 lb aircraft represents an acceptable level of safety, then one might assume that spacings for larger aircraft in this category have significantly more conservative spacing than required. In that case, a capacity increase might result from splitting this category, with reduced spacing for the larger aircraft.

This analysis gives an estimate of the relative hazard of one aircraft encountering the wake of another. The estimates are naturally first-order since there are obvious limitations in the models. Unfortunately, any *relative* hazard cannot be used to set actual separation distances because an *absolute* hazard criteria (such as maximum allowable bank angle) has not been employed. The absolute hazard may only be found from piloted, 6-DOF simulations in which the limits for a particular aircraft may be examined.

SUMMARY

The role of flight simulation in determining safe aircraft landing separation criteria has been reviewed and discussed. The discussion started with a survey of past simulation studies, and the following relevant observations are offered.

(1)   Vortex encounters may be realistically simulated, and the degree of the hazard associated with the encounter may be measured with pilot opinion.

(2)   The hazard associated with a particular vortex encounter may be correlated to certain flight parameters. In particular, the best indicators are bank angle and altitude.

(3)   The pilot-perceived bank-angle/altitude buffer between a safe and an unsafe IFR approach is fairly small at low altitudes. Errors in simulated vortex-induced forces and moments may therefore be significant in determining separation limitations for a particular configuration.

(4)   Since these errors may lead to small, but relevant, flight-path and bank angle excursions, pilot-opinion is not enough to validate a simulation methodology. The validation should be done with a systematic series of flight tests in which the position of the aircraft with respect to the vortex is measured.

(5)   A decrease in vortex strength provides a subsequent decrease in the maximum bank angle. Similarly, interaction of the vortex with the encountering aircraft may reduce aerodynamic forces and moments and the subsequent upset hazard.

(6)   Automatic control systems and pilot landing aids may allow decreased separation distances currently set by wake-vortex hazards.

(7)   Parameters, such as g-loading, not normally associated with a vortex encounter and whose effects are not accounted for in the simulation models may exceed safe limits.

A further conclusion may be drawn that each study was generally limited in scope and validity. Overcoming these limitations was stressed in a discussion on broad requirements for and technical issues associated with future simulation development.

Results from a preliminary one-degree-of-freedom simulation were shown. These indicate that reduced landing spacings may be feasible for some aircraft pairs and that current aircraft categorizations should be reviewed.

Table 1. Summary of Simulations

YEAR	INVESTIGATOR	ORGANIZATION	VORTEX MODEL	AERO MODEL	DOF	ENCOUNTER DIRECTION	NO. OF A/C GEN / FOL	CONTROLS	VALIDATION
1974	Nelson & McCormick	AFFDL / Penn State	a, g, i	j	6	n, p, q	1/2	Pilot Models	s
1974	Johnson et al	Systems Tech & NASA Dryden	b, g, i	j	6	n, p, q	2/2	Auto Flght Ctrl Sys	t
1975	Sammonds et al	NASA Ames	b, g, i	j	6	n, p, q	1/2	Piloted	r, s
1975	Jenkins & Hackett	Lockheed	c, g, i	k	6	n, o, p, q	1/1	Piloted	r
1982	Hastings & Keyser	NASA Langley	d, g, h, i, e	j	6	n, p, q	1/1	Piloted	r
1984	Abbott	NASA Langley	d, g	j	6	n, p, q	1/1	Piloted	r
1985	Holbrook	GWU / NASA Langley	f	j	1	n	3/1	None	None
1989	Konig	Inst. Fluid Mech Germany	d, e	L	6	o	1/1	Piloted	r
1991		Lockheed	f	m	6	o	2/3	Piloted & Unpiloted	r, s

a: empirical based on experimental data - fixed in time
b: Rankine with core & exponential time decay
c: exponential velocity profile - fixed in time
d: empirical based on experimental data - time-varying
e: includes ground effect estimates
f: Rankine with core
g: axially linear

h: axially truncated
i: fixed in space
j: strip theory
k: vortex-lattice
L: rotating gust
m: incremental wing lift
n: parallel

o: perpendicular
p: vary horizontal approach angle
q: vary vertical approach angle
r: pilot opinion
s: limited data comparison
t: adjustment to known aero

15-17

Table 2. Meyer-Hermitage Vortex-Encounter Rating Scale
(Reproduced from Jenkins and Hackett)[11]

RATING	BROAD DESCRIPTOR	DETAILED DESCRIPTOR
1	Handle with ease	Not recognizable
2		Barely recognizable
3		Recognized – easily controlled
4	Have to work at, but holds fairly good position for turbulent environment	Annoying – but easily compensated for
5		Objectionable – required reasonable pilot compensation
6		Very objectionable –requires best pilot compensation
7	Hard to control, continually "way off" desired position	Controllable, but difficult
8		Controllable with extreme difficulty – landing may be discontinued
9		Marginally controllable –requires maximum pilot skill and effort to avoid crash
10	Uncontrollable	Aircraft lost

Table 3. Controls Evaluation Rating Scheme
(Reproduced from Jenkins and Hackett)[11]

	INADEQUATE			ADEQUATE		
CRASH	NORMALLY WOULD TRY WAVE OFF	NORMALLY WOULD ATTEMPT A LANDING		MEETS MINIMUM	FEELS COMFORTABLE	
R5	R4	R3		R2	R1	ROLL
	Y3			Y2	Y1	YAW
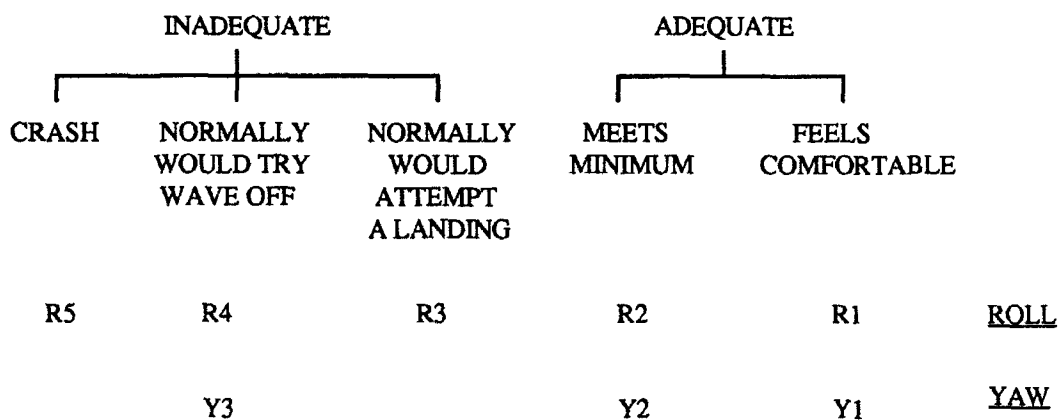
Table 4. Current Commercial-Aircraft Separation Categories

CATEGORY	WEIGHT
Small	< 12,500 lb
Large	12,500 to 300,000 lb
Heavy	> 300,000 lb

Table 5. Representative Aircraft Data for Relative Hazard Study

CATEGORY	W (lb)	b (ft)	c (ft)	Ixx* (slug ft^2)	V (ft / sec)
Large	12,500	50	7	9,700	170
Large	100,000	100	10	311,000	220
Large/Heavy	300,000	150	20	2,100,000	225
Heavy	500,000	200	35	6,200,000	230

* at radius of gyration of 20% semi-span

Note: C_{l_α} = 4.5 per rad

AR = 7.5

Table 6. Results from Relative Hazard Study

Following Aircraft	Current IFR Spacing Standards (nm)		Relative Measure of Wake Hazard	
	Lead Aircraft		Lead Aircraft	
	Heavy	Large	Heavy	Large
Heavy	4	3	0.6 - 1.1	0.1 - 0.9
Large	5	3	0.9 - 12	0.15 - 10

Note: A relative wake hazard of 1.0 corresponds to the lead and following aircraft both at 100,000 lb.

- ● Flight test data (Andrews, et al)
- —— Prediction (roll control)
- - - - Prediction (roll and yaw control)
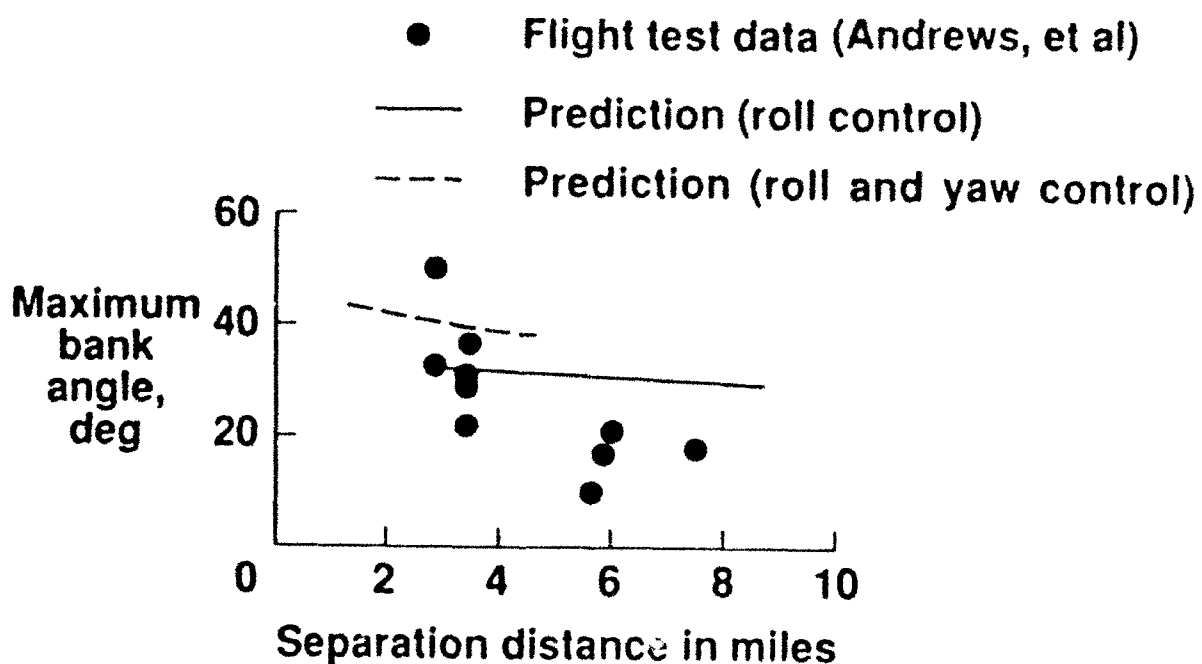
Figure 1. Comparison of predicted and actual maximum bank angle for a DC-9 behind a Convair 990. (Reproduced from Nelson)[4]
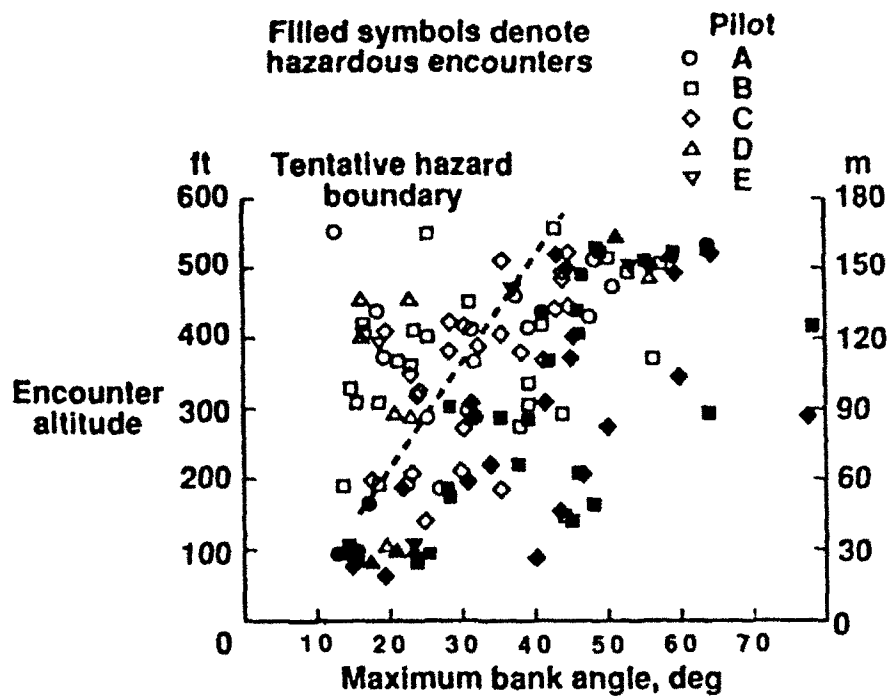
Figure 2. Representative results for vortex encounters under VFR conditions. (Reproduced from Sammonds, et al.)[9]
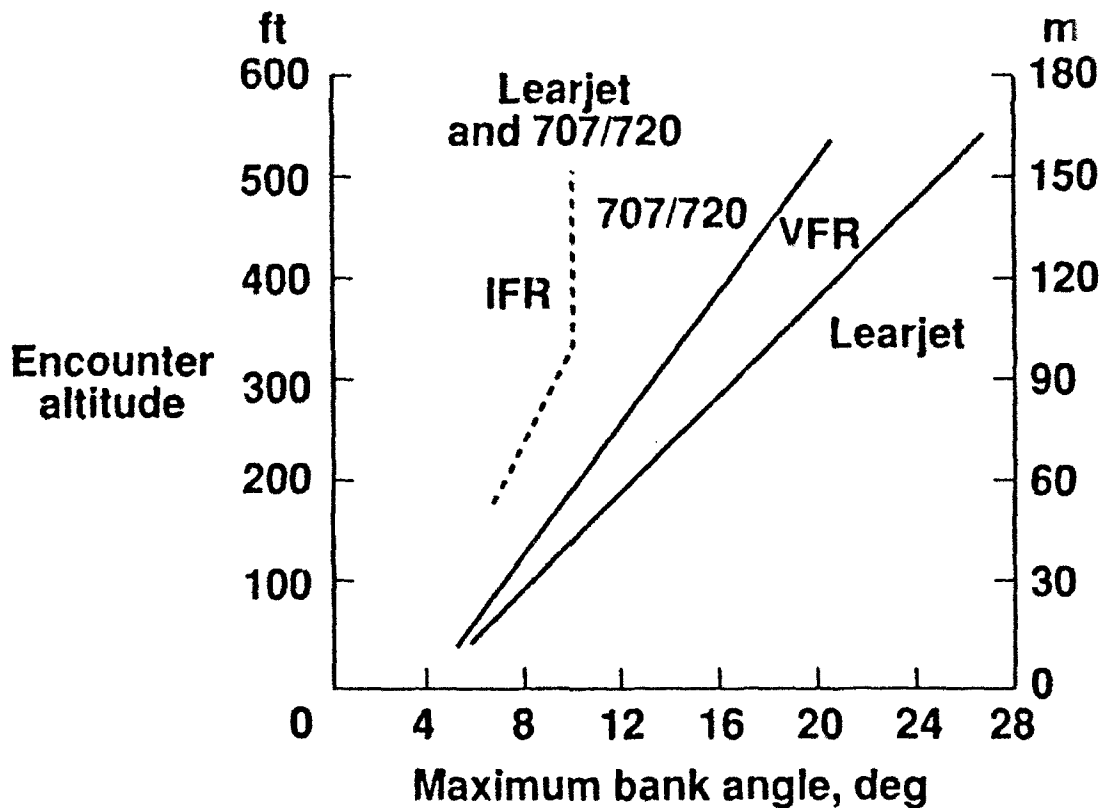
Figure 3. Hazard boundaries for simulated wake-vortex encounters of a Learjet and a Boeing 707/720 behind a Boeing 727.
(Reproduced from Sammonds, et al.)[9]
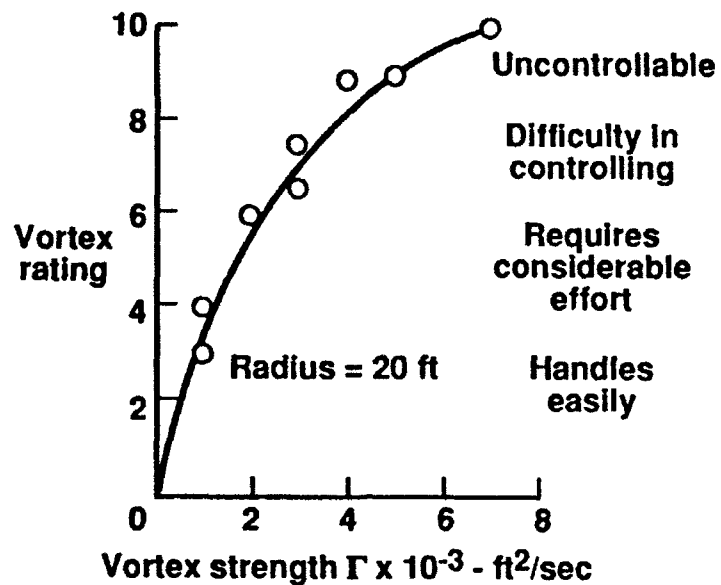
Figure 4. Example of the use of the Meyer-Hermitage Scale to represent pilot-perceived wake-vortex hazard for parallel encounters.
(Reproduced from Jenkins and Hackett)[11]
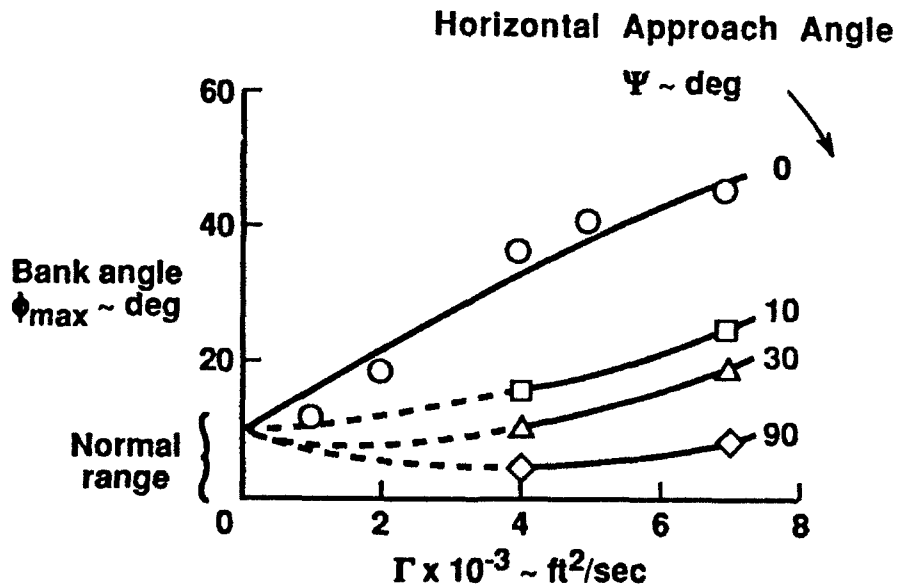
Figure 5. Simulated maximum bank angles as a function of vortex strength and encounter angle. (Reproduced from Jenkins and Hackett)[11]
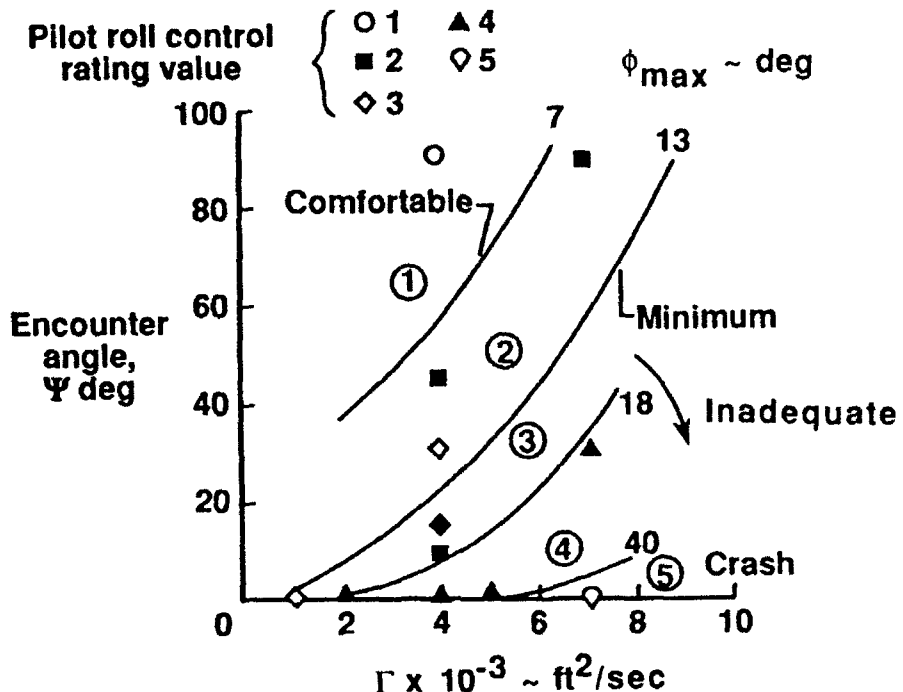
Figure 6. Hazard rating applied to maximum-bank-angle data to define acceptable wake-vortex encounters. (Reproduced from Jenkins and Hackett)[11]
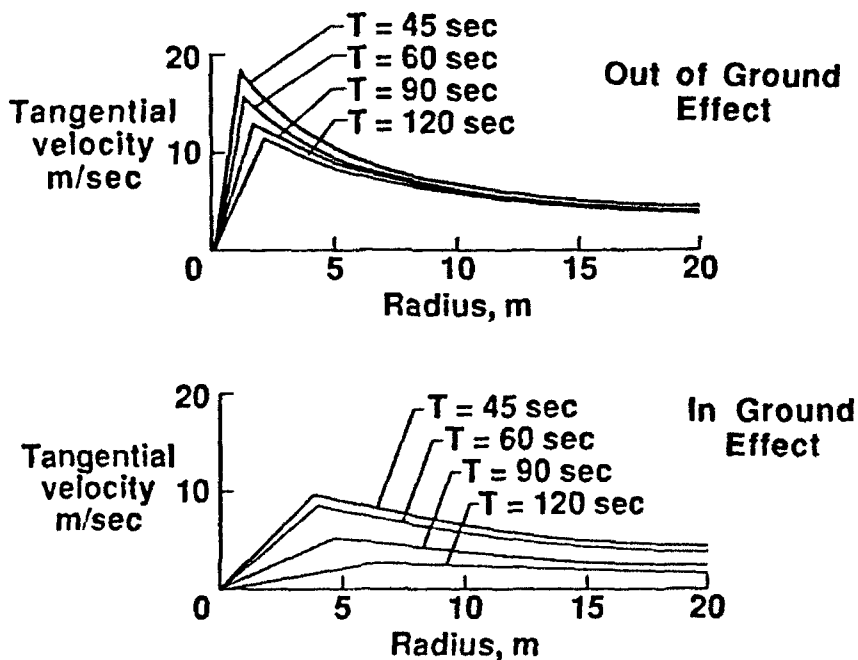
Figure 7. Example of time-dependent vortex models used in a previous simulation study. (Reproduced from Hastings and Keyser)[12]
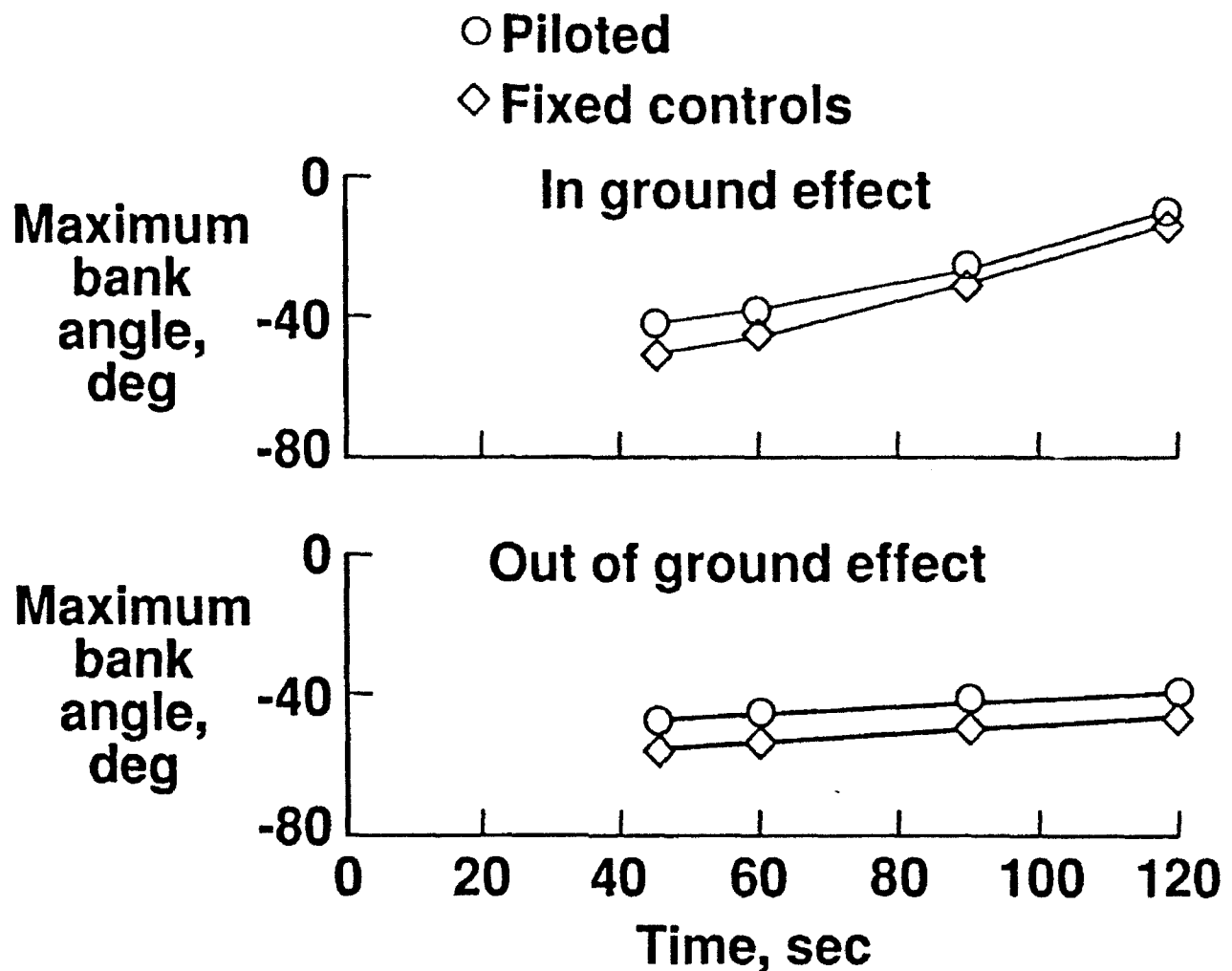
Figure 8. Effect of ground proximity on simulated wake-vortex encounters. (Reproduced from Hastings and Keyser)[12]
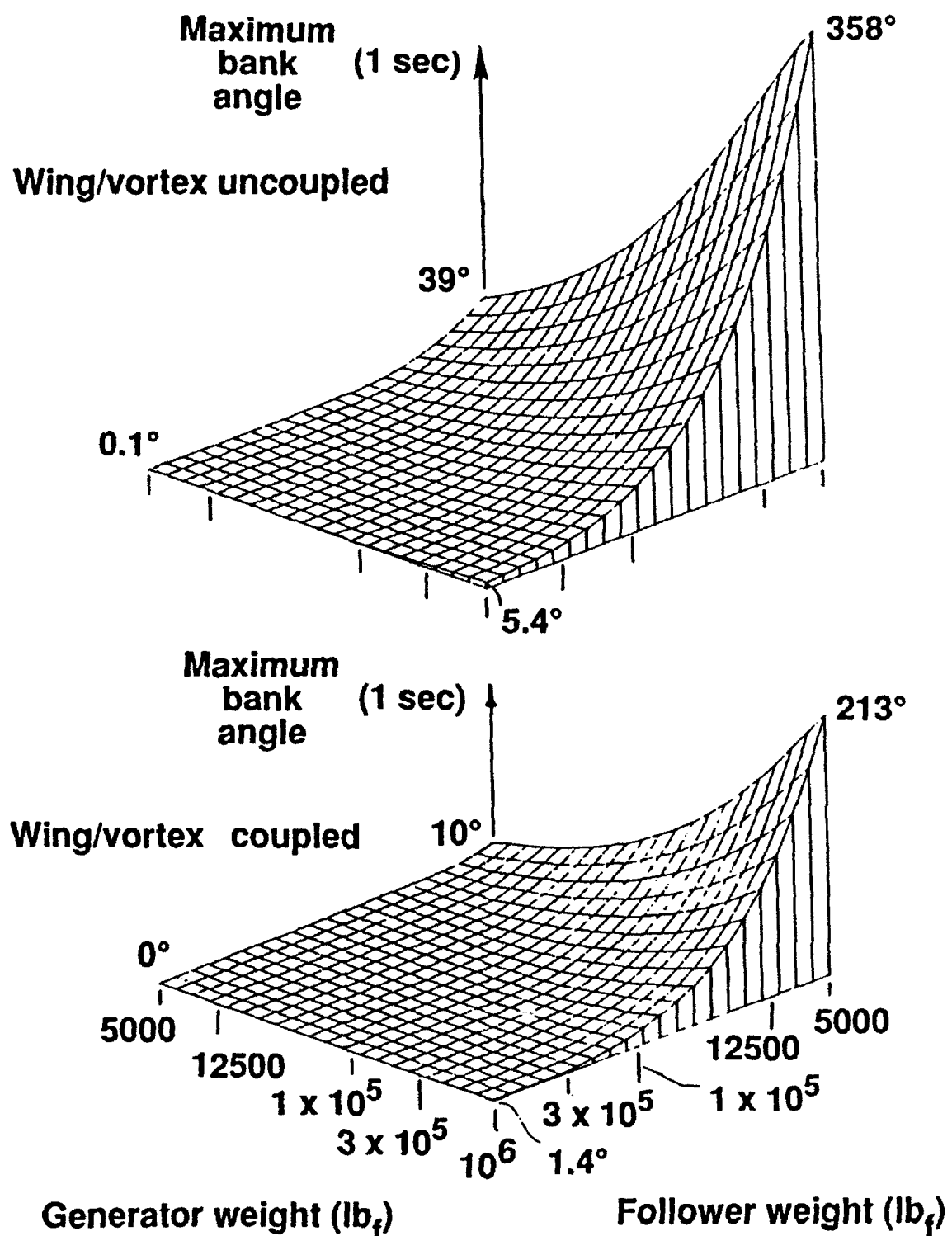
Figure 9. Representative plots of maximum simulated bank angles, as a function of aircraft weight, for both coupled and uncoupled wing/vortex aerodynamics. (Reproduced from Holbrook)[14]
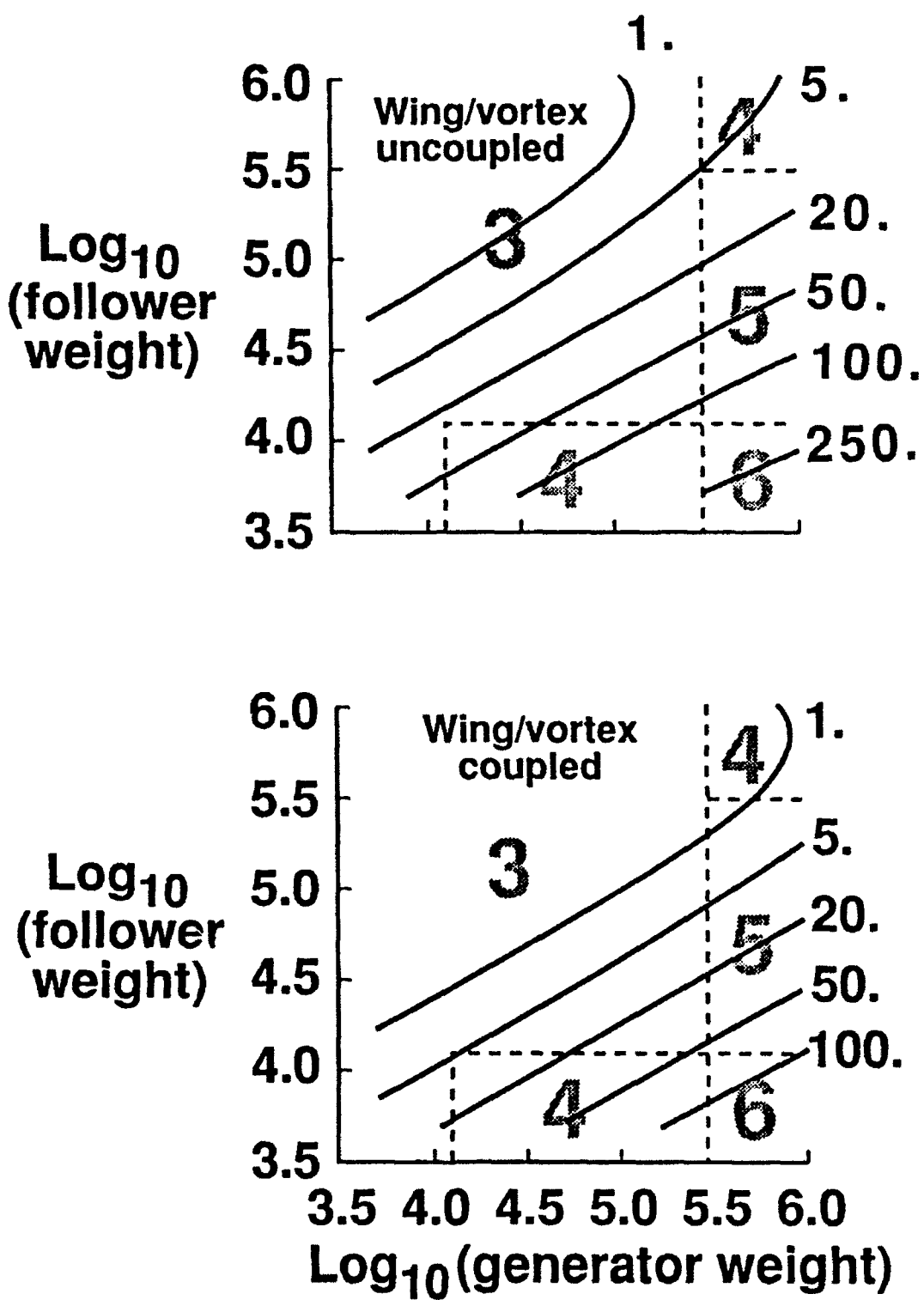
Figure 10. Representative plots of maximum simulated bank angles (solid
lines, in degrees), as a function of aircraft weight, for both
coupled and uncoupled wing/vortex aerodynamics. Current
IFR separation standards are shown along with weight
categorization boundaries (large numerals, dashed lines).
(Reproduced from Holbrook)[14]
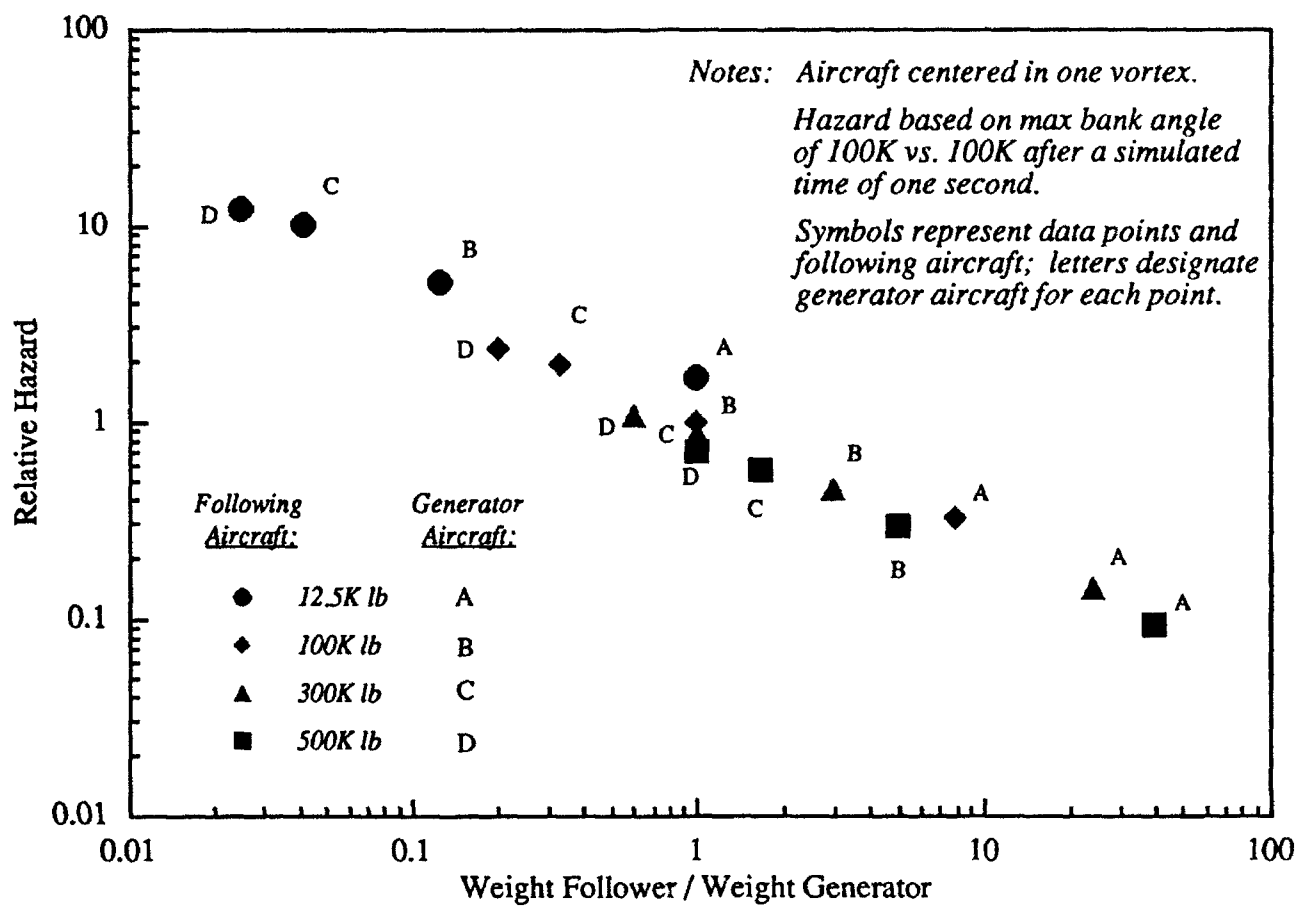
Figure 11. Relative hazards for combinations of four aircraft sizes.

REFERENCES

1. Hackett, J. E., and Theisen, J. G., "Vortex Wake Development and Aircraft Dynamics," *Aircraft Wake Turbulence and Its Detection*, edited by J. Olsen, A. Goldberg, and M. Rogers, Plenum Press, New York, 1971.

2. Nelson, R. C., and McCormick, B. W., "The Dynamic Behavior of an Aircraft Encountering Aircraft Wake Turbulence," AIAA Paper No. 74-774, Anaheim, CA, Aug. 1974.

3. Nelson, R. C., "Dynamic Behavior of an Aircraft Encountering Aircraft Wake Turbulence," *Journal of Aircraft*, Vol. 13, No. 9, Sept. 1976, pp. 704-708.

4. Nelson, R. C., "The Response of Aircraft Encountering Aircraft Wake Turbulence," AFFDL-TR-74-29, Wright-Patterson Air Force Base, OH, June 1974.

5. Andrews, W. H., Robinson, G. H., and Larson, R. R., "Exploratory Flight Investigation of Aircraft Response to the Wing Vortex Wake Generated by Jet Transport Aircraft," NASA TN D-6655, Mar. 1972.

6. Johnson, W. A., Teper, G. L., and Rediess, H. A., "Study of Control System Effectiveness in Alleviating Vortex Wake Upsets," *Journal of Aircraft*, Vol. 11, No. 3, Mar. 1974, pp. 148-154.

7. Sammonds, R. I., Stinnett, G. W., Jr., and Larson, W. E., "Hazard Criteria for Wake Vortex Encounters," NASA TM-X-62473, Aug. 1975.

8. Sammonds, R.I., Stinnett, G. W., Jr., and Larson, W. E., "Wake Vortex Encounter Hazard Criteria for Two Aircraft Classes," NASA TM-X-75113, Jun. 1976.

9. Sammonds, R. I., Stinnett, G. W., Jr., and Larson, W. E., "Criteria Relating Wake Vortex Encounter Hazard to Aircraft Response," *Journal of Aircraft*, Vol. 14, No. 10, Oct. 1977, pp. 981-987.

10. Jewell, W. F., and Stapleford, R. L., "Mathematical Models Used to Simulate Aircraft Encounters with Wake Vortices," Systems Technology, Inc. TR-1035-4, Mountain View, CA, Aug. 1975.

11. Jenkins, M. W. M., and Hackett, J. E., "A Pilot-in-the-Loop, Visual Simulation of Trailing Vortex Encounters at Low Speed," AIAA Paper 75-104, Pasadena, CA, Jan. 1975.

12. Hastings, E. C., and Keyser, G. L., Jr., "Simulator Study of Vortex Encounters by a Twin-Engine, Commercial, Jet Transport Airplane," NASA TP 1966, Feb. 1982.

13. Abbott, T. S., "Simulation of a Cockpit-Display Concept for Executing a Wake-Vortex Avoidance Procedure," NASA TP-2300, Apr. 1984.

14. Holbrook, G. T., "Vortex Wake Hazard Analysis Including the Effect of the Encountering Wing on the Vortex," Master's Thesis, The George Washington University, Aug. 1985.

15. Konig, R., "Aircraft Response and Pilot Behavior During a Wake Vortex Encounter Perpendicular to the Vortex Axis," AGARD-CP-470, Gol, Norway, May 1989, pp. 17.1-17.18.

16. McGowan, W. A., "Calculated Normal Load Factors on Light Airplanes Traversing the Trailing Vortices of Heavy Transport Airplanes," NASA TN D-829, May 1961.

17. Lockheed Missiles & Space Co., Inc., "Flight Simulation and Flight Test of Cross-Vortex Encounters as Experienced at New York's LaGuardia Airport," Contract PA NY/NJ, Huntsville, AL, Sept. 1990.

18. Branstetter, J. R., Hastings, E. C., and Patterson, J. C., Jr., "Flight Test to Determine Feasibility of a Proposed Airborne Wake Vortex Detection Concept," NASA TM 102672 (FAA Report No. DOT/FAA/CT-TN 90/25), April 1991.

19. Greene, G. C., "An Approximate Model of Vortex Decay in the Atmosphere," *Journal of Aircraft*, Vol. 23, No. 7, July 1986, pp. 566-573.

20. *Jane's All the World's Aircraft*, 81st Edition, Jane's Information Group Limited, Surrey, UK, 1990.

21. McMillan, O. J., Schwind, R. G., Nielsen, J. N., and Dillenius, M. F. E., "Rolling Moments in a Trailing Vortex Flowfield," *Journal of Aircraft*, Vol. 15, No. 5, May 1978, pp. 280-286.

22. Rossow, V. J., and Tinling, B. E., "Research on Aircraft/Vortex-Wake Interactions to Determine Acceptable Level of Wake Intensity," *Journal of Aircraft*, Vol. 25, No. 6, June 1988, pp. 481-492.

VORTEX DESTABILIZATION BY A HARMONIC STRAIN-FIELD

M R Dhanak and M P Marshall
Department of Ocean Engineering
Florida Atlantic University, Boca Raton, FL3343 I

ABSTRACT

A mechanism for vortex detabilization is presented. The mechanism is based on the recognition that a pair of vortices, such as in the vortex trail of an aircraft or a vortex in ground effect, impose a weak strain-field upon each other causing the shape of the vortex core to distort from a circle. The presence of a pressure gradient can also induce a strain on a vortex. In general, the strain fields are unsteady and three-dimensional. For plane steady strain-fields, equations of fluid motion suggest that a Rankin-type vortex core of uniform vorticity and elliptical shape can exist[2] in a state in which it (a) is steady and stationary, (b) rotates about its axis or nutates about a fixed axis, or (c) elongates indefinitely smearing the core into a thin layer. In state (a), for sufficiently weak strain fields, a vortex of small enough aspect ratio of the ellipse persists under such a plane strain[1], being robust to small disturbances present in the flow field. It is shown that if, however, a small periodically varying strain-field is superimposed on the basic field, then at certain frequencies and their harmonics, a resonance phenomena takes place which destabilizes the apparently stable stationary vortex in finite time, causing it to flip into states (b) or (c), in which action of instabilities associated with higher, non-elliptical, mode of deformation of the vortex boundary by disturbances in the flow field leads to disintegration of the vortex structure. For a vortex of given strength, the frequencies and amplitude required for destabilization vary with the size of the basic strain-field. The potential of the phenomena for the vortex hazard problem is discussed.

INTRODUCTION

The hazard presented by the vortex trail of a large aircraft such as a B747 during landing is well known. Under normal conditions, such a trail can persist for a few miles downstream of the aircraft and migrate along the ground preventing hazard-free take-offs of other aircrafts. This causes costly delays, especially at airports with a large volume of air traffic. The alleviation of the vortex wake of large aircraft is therefore of considerable importance.

In this paper, a potential mechanism for a systematic disintegration of the structure of the wake vortices is considered. The mechanism exploits the fact that in a vortex interaction problem involving a group of vortices, each vortex experiences a strain-field due to the presence of other vortices. In a model problem, it was shown by Moore and Saffman[1] that a steady, stationary Rankin vortex of elliptical shape with uniform vorticity ω in the core can persist stably in an imposed plane strain provided that the rate of strain is weak enough and the aspect ratio of the ellipse is small enough. This solution is discussed in §2 in relation to a pair of descending vortices or a vortex in ground effect.

Kida[2] showed that beside the steady, stationary solution of Moore and Saffman, other quasi-steady states are possible. Accordingly, depending on the initial conditions, the vortex may rotate, nutate or elongate indefinitely. It is expected that in a state of indefinite elongation or in the other unsteady states with large enough aspect ratio, the vortex would disintegrate through action of instabilities associated with higher, non-elliptical, mode of deformation of the vortex boundary by disturbances present in the flow field. Recently, Moore (private communication) has shown that elongation of the vortex core is associated with loss in energy of the system.

In §3, it is shown that if a vortex in a plane strain is initially in the steady, stationary and stable state described by Moore and Saffman, then the vortex has a natural frequency of oscillation which depends on the aspect ratio of the ellipse. If at time $t = 0$, a small oscillatory component of this natural frequency is added to the basic strain-field, the vortex resonates and flips into one of the other states described by Kida. For small amplitude of the forcing field, the nonlinear system exhibits a limit cycle behavior. However, if this amplitude is sufficiently large, the vortex either attains a large aspect ratio in a state of rotation or nutation or the nonlinear system exhibits chaos and the vortex flips into the state of indefinite elongation. In either case it is expected that the vortex would disintegrate.

In §4, the possible implementation of the mechanism for the case of a vortex pair downstream of an aircraft or for a vortex in ground effect is discussed.

BASIC FLOW FIELD

Consider the pair of vortices, of strength $\pm$ and separated by distance B, shown in Figure 1. The system is equivalent to a motion of a single vortex past a rigid plane midway between the vortices as shown. The pair descends with a steady velocity $\Gamma/2\pi B$ due to the flow induced by one vortex on the other. Suppose we consider the flow field in a frame of reference moving with this velocity and take rectangular axes with the origin at the center 0 of the undisturbed position of the right vortex and 0z along the axis of the vortex. If in this translating frame the right vortex is disturbed so that its axis is no longer along 0z but is displaced by a small amount to $(x\ y$ in the x - y plane, it experiences a velocity, due to the other vortex, approximately given by

$$u = e(y, x, 0) \tag{1}$$

where $e = \tau/2\pi B^2$ the contribution is the leading order term in a Taylor expansion about the origin, 0. Thus the right vortex, to first order, experiences an irrotational plane strain with strain-rate e. Excluding other effects, the motion of the vortex is governed by

$$dx/dt = ey, \quad dy/dt = ex \tag{2}$$

which implies a growing disturbance with growth rate e. Taking proper account of three-dimensional effects, it is evident that for sufficiently small axial wavelengths (Crow[3]) self-induced velocity of the vortex helps to counter this instability. Thus, approximately

$$\frac{dx}{dt} = y(e - \Gamma \frac{k^2}{4\pi} \log(1/\alpha k)), \quad \frac{dy}{dt} = x(e + \Gamma \frac{k^2}{4\pi} \log(1/\alpha k)) \tag{3}$$

where k is the axial wavenumber and a is proportional to vortex core radius and depends on the structure of the vortex. For disturbances of long axial wavelengths, however, the instability will dominate as shown by Crow. The plane strain also affects the vortex structure, distorting its shape. Here, we focus attention on this latter aspect of the problem.

We consider a model problem, one in which a Rankin vortex of uniform vorticity ω is situated in an external irrotational velocity field given by (1) (Figure 2). The fluid is regarded as inviscid and incompressible. Moore and Saffman[1] showed that a steady uniform vortex of elliptical shape can exist in such an imposed strain only if

$$|e/\omega| < 0.15, \tag{4}$$

there being two possible values of the aspect ratio for each value of $|e/\omega| < 0.15$. However, only the one with the smaller aspect ratio is stable and therefore physically likely to occur. Specifically, they showed that for a constant strain-rate $e = e_0$, a steady, uniform vortex of elliptical shape with aspect ratio $\lambda_0 = a/b$, where a and b are respectively the semi-major and semi-minor axes of the ellipse, can exist in the strain field provided that

$$e \equiv e_o = \frac{\omega \lambda_o (\lambda_o - 1)}{(\lambda_o^2 + 1)(\lambda_o + 1)} \tag{5}$$

with the major axis inclined at an angle $\phi = 45°$ to the principal axis of strain. e_o is shown plotted against λ_o in Figure 3. $\lambda_o = \lambda_{oc} \approx 2.89$ corresponds to the maximum value of the strain-rate for which a steady solution exists. For $|e/\omega| > 0.15$, Moore and Saffman showed that a vortex of elliptical shape would disintegrate.

Kida[2] showed that for a given value of $| e/\omega |$, there is in fact a class of steady and unsteady solutions for an elliptical vortex in plane strain with the aspect ratio and orientation of the ellipse, in general, a function of time. If $\lambda(t) = a(t)/b(t)$ now denotes the aspect ratio and $\phi(t)$ the angle between the major axis and the principal axis of the strain at time t (Figure 4) then the rate of change of the aspect ratio and the orientation are governed by

$$d\lambda/dt = 2\lambda\, e \cos 2\phi \quad ; \quad d\phi/dt = -e\frac{\lambda^2 + 1}{\lambda^2 - 1}\sin 2\phi + \frac{\omega\lambda}{(\lambda + 1)^2} \tag{6}$$

Kida showed that for a constant value of the strain-rate e, several states are possible. Depending on initial conditions, the vortex may:

(a) remain in a steady stationary state with e as in (5), in agreement with Moore and Saffman,

(b) nutate about $\phi(t) = 45°$,

(c) perform anti-clockwise rotations, or

(d) elongate indefinitely with $\phi(t) = 0°$.

In (b) - (d), the vortex shape evolves from an ellipse of one aspect ratio and orientation to another of different aspect ratio and orientation whilst the core area remains fixed. Dritschel[4] has shown that a substantial portion of the states in categories (b) and (c) are unstable to higher, non-elliptical, modes of deformation of the vortex boundary by disturbances in the flow field.

PERIODIC STRAIN - FIELD

Suppose that a uniform vortex is in a steady stable stationary state with $e = e_o$. That is, the basic strain-field is weak enough and the aspect ratio $\lambda_o (< \lambda_\infty)$ is small enough for the vortex to be robust to small disturbances in the flow field. Suppose at $t = 0$, a harmonic component is added to the strain-field so that

$$e = e_o (1 + \epsilon \sin \Omega\, t) \tag{7}$$

where ϵ is a small parameter.

Linear Response

For $\epsilon \ll 1$, we consider a perturbation of the aspect ratio and orientation in response to the periodic strain-field,

$$\lambda(t) = \lambda_o + \epsilon \, \lambda_1(t); \quad \phi(t) = \phi_o + \epsilon \, \phi_1(t) \tag{8}$$

On substituting these expressions into (5) and linearizing the equations with respect to ϵ, we obtain

$$d^2\lambda_1/dt^2 + \Omega_0^2\lambda_1 = F_o(e_o, \lambda_o) \sin \Omega t \tag{9}$$

where Ω_o/ω, F_o/ω are functions of λ_o and are shown plotted against λ_o in Figure 4. It may be noted that for the limiting value of $\lambda_o = 1$, which corresponds to a circular core with no strain field, $\Omega_o/\omega = 0.5$ (this case needs to be considered separately since in the basic state, $e_0 = 0$ and the vortex rotates with angular speed $\omega/4$). $\Omega_o^2 > 0$ provided $\lambda_o < \lambda_\alpha$, where λ_α is as in §2. Thus for $\lambda_o < \lambda_\alpha$, the perturbations do not grow exponentially, in agreement with Moore and Saffman1; the pertur'bation (8) corresponds to $m = 2$ in their modal stability analysis. (9) in this case implies that the vortex response corresponds to that of a forced linear oscillator.

For $\Omega \neq \Omega_o$ the solution to (9) is bounded. However, for $\Omega = \Omega_o$, resonance will occur and the aspect ratio will grow linearly in time:

$$\lambda(t) = \lambda_o + \frac{\epsilon \, F_o}{2\Omega_0^2} (\sin \Omega_o t - \Omega_o t \cos \Omega_o t). \tag{10}$$

The maximum value of λ at a fixed time is sketched below for various values of ϵ.

Non-Linear Response

The equations (6) are non-linear so that we need to determine the fate of the linear growth in time at the resonant frequency for large time. One approach, under consideration at present, is to obtain a higher order expansion involving two time scales in order to determine finite amplitude behavior. Here, however, we solve equations (6) numerically using a fourth order Runge-Kutta scheme.

For each value of λ_o the linear growth at the resonant frequency leads to two principal modes of behavior depending on the value of ϵ. If ϵ is small enough, the linear growth in time is curbed but the vortex assumes a new state in which it either rotates or nutates. The non-linear system has a limit cycle solution in this case. If ϵ is large enough, the aspect ratio of the ellipse becomes rather large or the initial linear growth leads to a state of indefinite elongation. Either case suggests a loss in energy of the system and is expected to lead to disintegration of the vortex. The non-linear system of equations exhibits chaos prior to attaining a state of indefinite

elongation. Poincarè plots of $-\sin 2\phi$ against $1/\lambda$ for two values of λ_o and various increasing values of ϵ are shown in Figure 5; a Poincarè plot is a stroboscopic view at each time period, $T = 2\pi/\Omega_o$, of the forcing field in the phase plane as the ellipse evolves in time. In Figure 5(a), the case $\lambda_o = 1.5$ is shown. For $\epsilon < 0.28$ a limit cycle behavior with characteristic islands of points is observed in this case; for $\epsilon \geq 0.28$, the system becomes chaotic with the final point being at $1/\lambda = 0$ and $\sin 2\phi = 0$ which corresponds to an infinitely long ellipse. The corresponding vortex shapes are shown at various times in Figure 6(a). These were checked using the method of contour dynamics for uniform vortices (see for example, Pullin[5]). For $\epsilon \geq 0.28$, the vortex flips to a state of indefinite elongation, implying a loss in energy of the system, and leading to vortex disintegration. Figure 5(b) depicts Poincarè plots in the case $\lambda_o = 1.8$, the corresponding vortex shapes being shown in Figure 6(b); in this case, a limit cycle behavior is observed for $\epsilon < 0.08$, while a chaotic behavior, leading to indefinite elongation is obtained for $\epsilon \geq 0.08$. The minimum value of ϵ required for elongation to occur for a given value of ϵ_o, is shown plotted against in Figure 7; higher values of ϵ are required for weaker basic strain-fields and a more circular-shaped vortex.

It may be noted that even in the state of nutation or rotation with $\lambda_o > \lambda$, a higher, non-elliptical, mode deformation of the core due to the presence of disturbances in the flow field can lead to instability. This is illustrated in Figure 8 for the case $\lambda_o = 1.02$, $\epsilon e_o = 0.037$ where the initial vortex shape is perturbed by a $m = 3$ mode disturbance; m denotes the number of waves on the vortex boundary. The results are obtained from evaluating the motion using contour dynamics. At time $t = 9.25T$, the imposed periodic strain leads to partial clipping of the vortex. Further integration using contour dynamics requires detaching the parts of the contour where distant parts of the boundary come to merge (see Dritschel[6]); it is expected to lead to further disintegration of the vortex.

The vortex can also be destabilized if the frequency of the forcing field is chosen to be a sub or super harmonic of the natural frequency Ω_o of the vortex. In this case, the instability is non-linear and the state of indefinite elongation occurs for values of ϵ greater than in the case of a field with $\Omega = \Omega_o$

DISCUSSION

The effect of periodic straining on the structure of a vortex has been considered. It is shown that a stable, steady vortex in weak steady plane strain has an aspect ratio dependent natural frequency $\Omega_o(\lambda_o)$ of oscillation. If a small harmonic component of this natural frequency is added to the strain field, then resonance occurs, leading to destabilization of the vortex. As a result the vortex flips to a non-steady state of motion. For small values of the amplitude parameter $\mathcal{L}$ of the harmonic component, the vortex flips to a state of nutation or rotation, the non-linear system exhibiting a limit cycle behavior. For sufficiently large value of ϵ, the nonlinear system exhibits chaos and the vortex flips to a state of indefinite elongation.

If the periodic strain is incorporated in (3) we obtain, on assuming that the effect on the logarithinic term is negligible,

$$\frac{d^2x_1}{dt^2} - \left[e^2 - \frac{\Gamma^2 k^4}{16\pi^2} \log^2(1/ak) + \frac{3\dot{e}^2}{4e^2} - \frac{\ddot{e}}{2e}\right] x1 = 0,$$

where $x = ex_1$ and e is given by (7); a similar equation can be obtained for y. The equations suggest that the periodic straining serves to enhance the three-dimensional Crow instability by amplifying shorter wave disturbances and increasing the growth rate of longer wave disturbances.

For a B-47 aircraft travelling at a speed of 720 ft/s, with the ratio of lift coefficient to aspect ratio $C_L/A_S = 0.055$ and separation between its tip vortices B = 90 ft, the steady strain-field corresponds to $e_o/\omega = 0.005$ and $\lambda_o \approx 1.02$ so that in the steady state the vortices are fairly circular; it is expected however that in the vicinity of the fuselage, this aspect ratio will be larger due to the presence of the latter (during approach to landing at a speed of 220 ft/s with $C_L/A_S = 0.18$, the ground effect could increase the strain-rate to e_o/ω 0.02 which implies $\lambda_o \geq 1.08$). For an added minimum oscillatory component of amplitude ϵ $e_o/\omega \approx 0.04$, the vortex flips to unsteady state (b) attaining sufficiently large aspect ratio so as to be susceptible to unstable higher, non-elliptical, mode deformation of the vortex boundary by disturbances in the flow field, as illustrated in Figure 11. The period T of forcing at the natural frequency for this case is approximately 1 s, so that Figure 11 suggests that the process of disintegration is well underway at around 10s for the case shown; these estimates are based on the assumption that the periodic strain is imposed on a pair of vortices in steady motion. For a higher value of e_o/ω or ϵ e_o/ω, this time will be smaller. The periodic strain also enhances the Crow instability as discussed in §3. It may be noted that in the absence of a periodic strain, the time for the vortex pair to touch and pinch-off, following onset of Crow instability is around, 60s.

Implementation of this mechanism involves considering multiple vortices in the wake such that one or more weaker vortices wrap themselves around a tip vortex m the form of helices. The helices propagate down the length of the tip vortex with a characteristic velocity inducing a periodic strain on it. By correct choice of the strength and position of the subsidiary vortices, the frequency of this periodic strain can be set to be the natural frequency of the vortex. The problem is being examined currently together with other issues including consideration of distributed vorticity, external shear and three-dimensional effects. Further to the effect on the Crow instability mentioned above, stretching along the length of a vortex filament induces a change in local distribution of vorticity which will have a bearing on vortex core elongation. Moreover, a vortex experiences three-dimensional strain[7] whose influence on a steady state needs to be determined.

ACKNOWLEDGEMENT
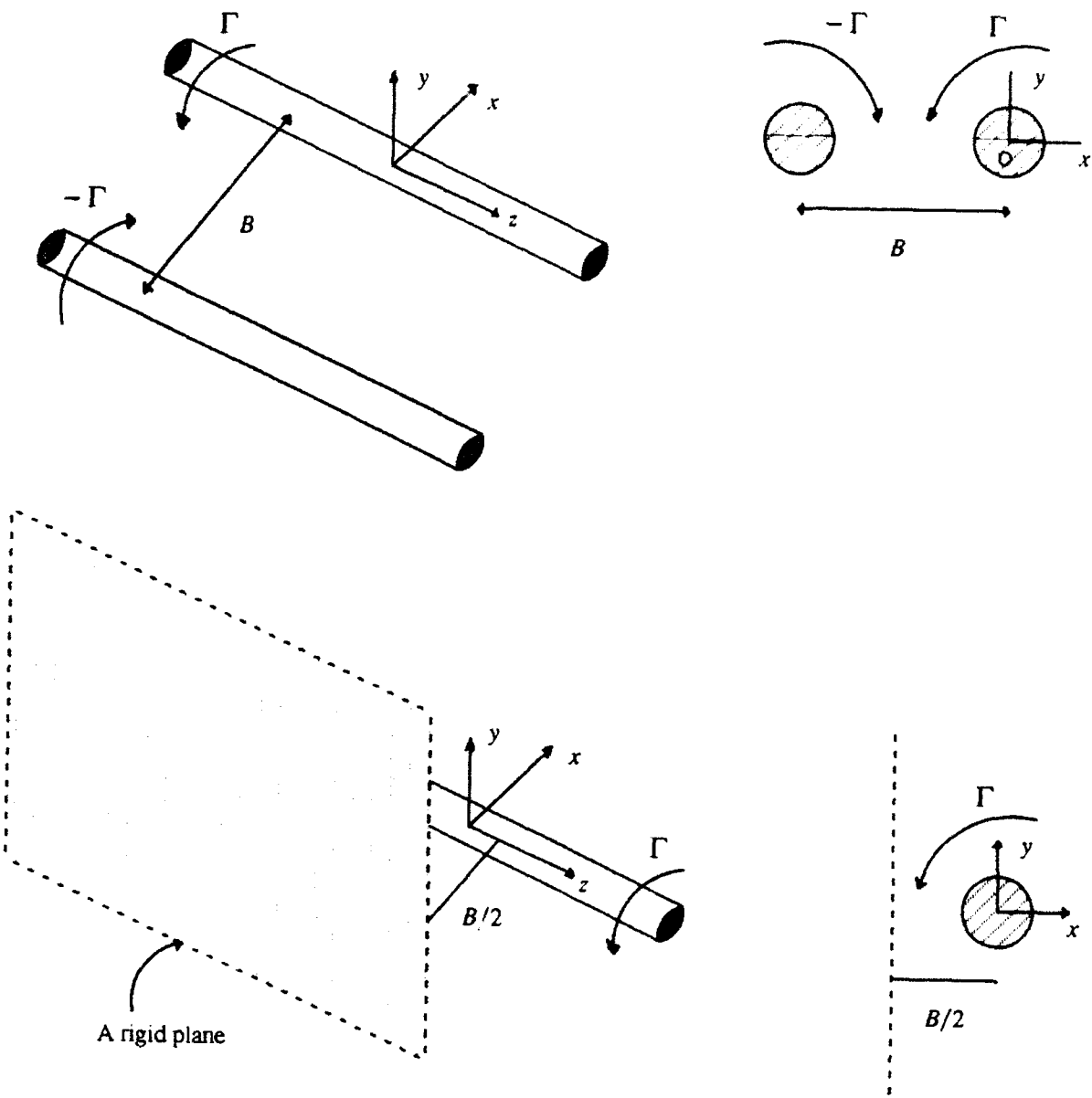
Figure 1. A pair of vortices in steady descent or equivalently the motion of a single vortex past a rigid plane.
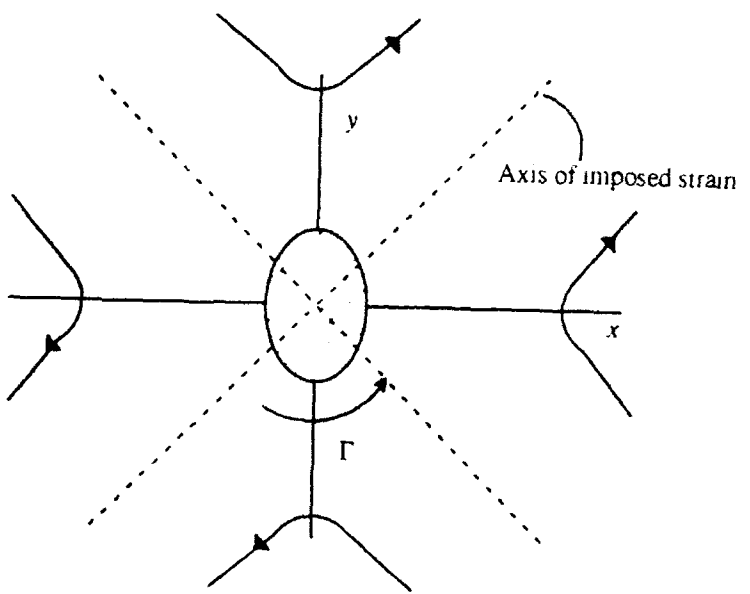
Figure 2. Vortex in steady stationary configuration in imposed strain.
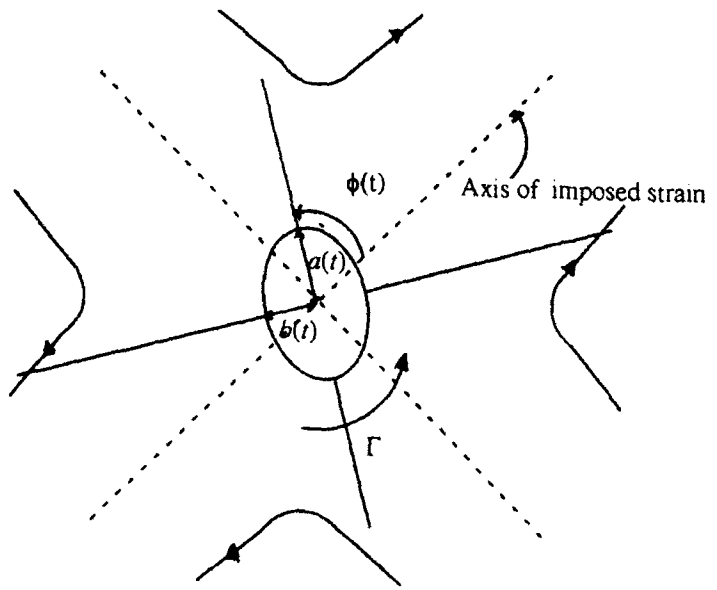
Figure 3. Unsteady solution of vortex in imposed strain. Aspect ratio $\lambda(t) = a(t) / b(t)$.
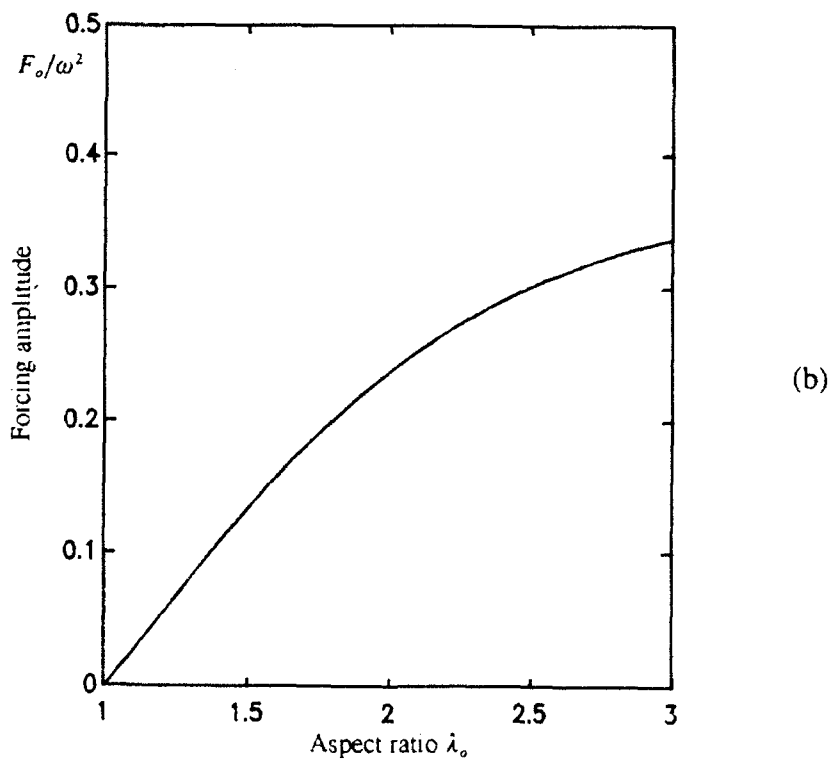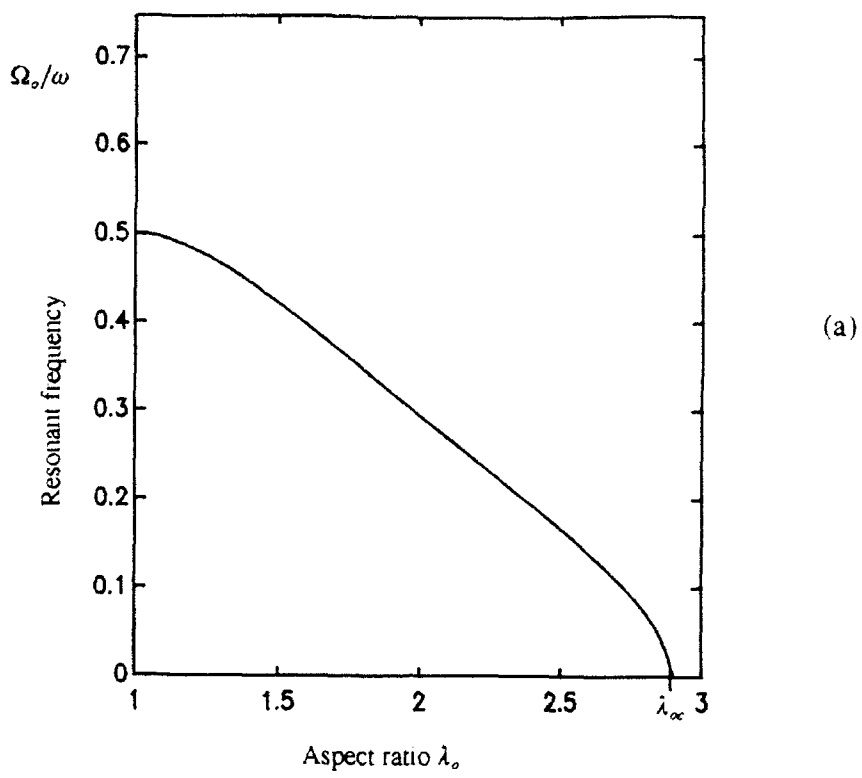
Figure 4. Variation with aspect ratio λ_o of (a) resonant frequency Ω_o / ω and (b) amplitude F_o / ω^2 of the periodic forcing associated with the linear response.
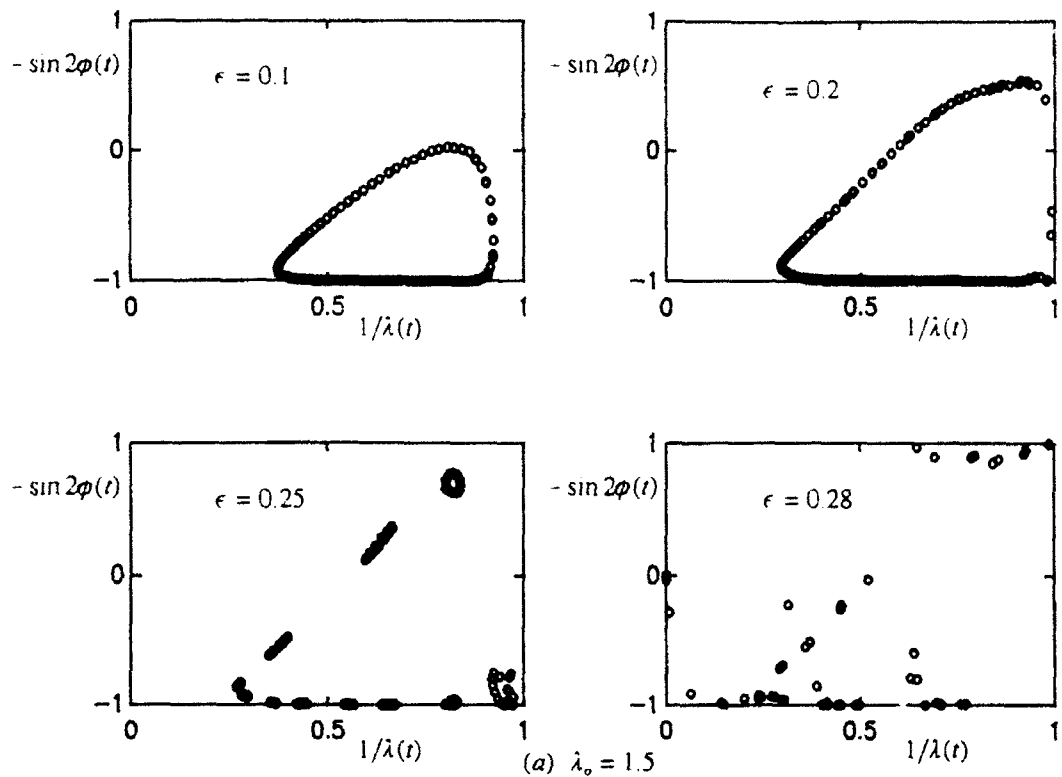
Figure 5. Poincaré plots of the evolution of the vortex for two cases of initial aspect ratio, λ_0; each point represents a stroboscopic view of the evolution at a particular multiple of period T of the periodic strain field. The last inset in each case indicates chaos in the nonlinear system.

Figure 5. **Poincarè plots of the evolution of the vortex for two cases of initial aspect ratio, λ_0; each point represents a stroboscopic view of the evolution at a particular multiple of period T of the periodic strain field. The last inset in each case indicates chaos in the nonlinear system.**

16-11
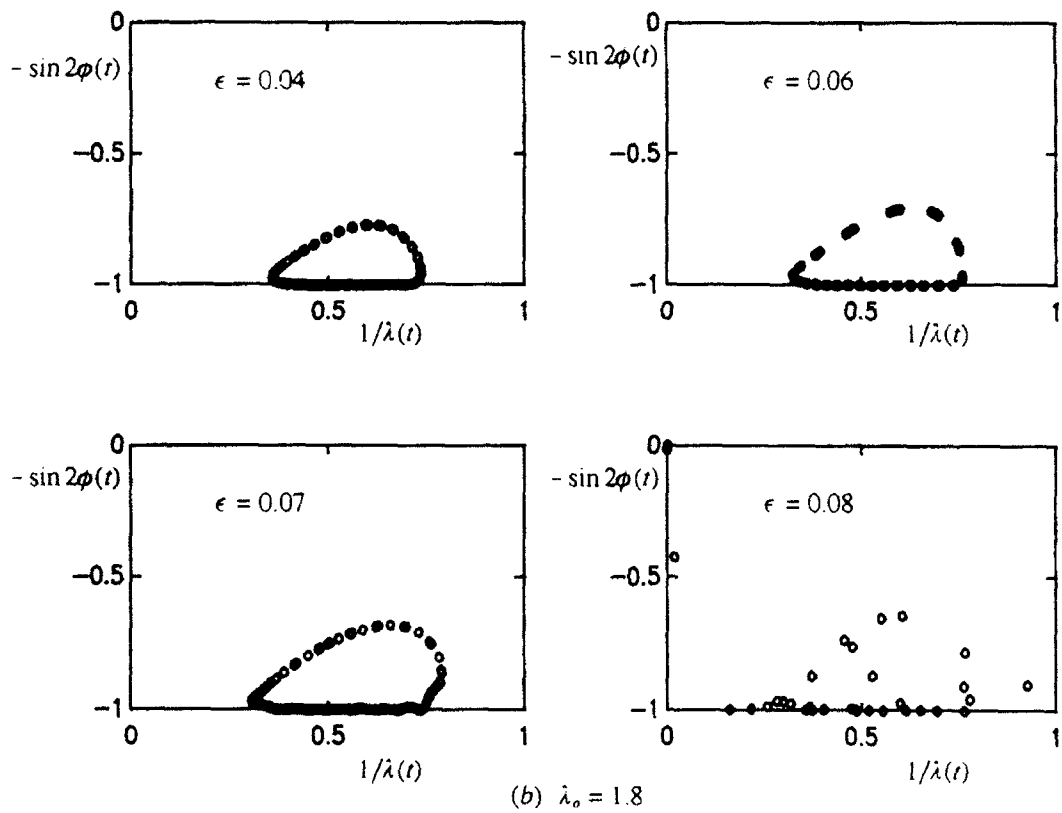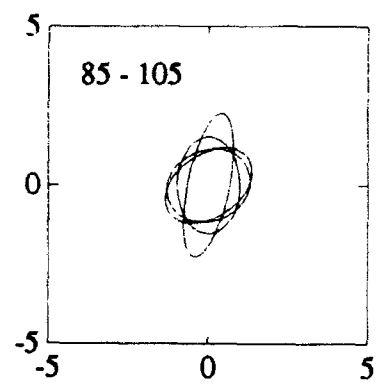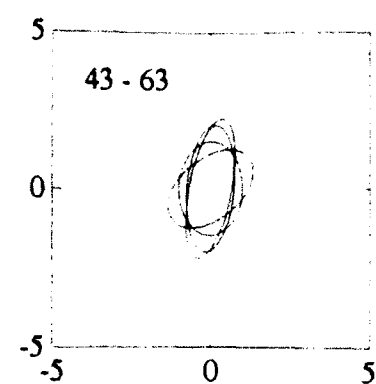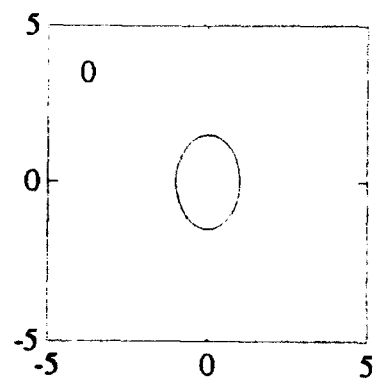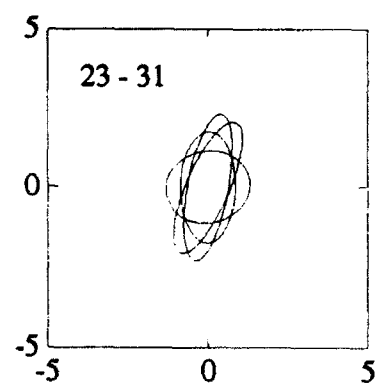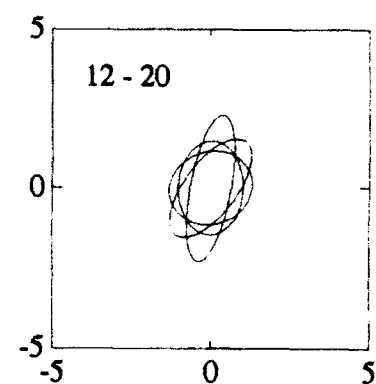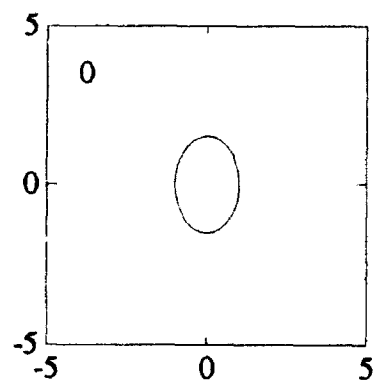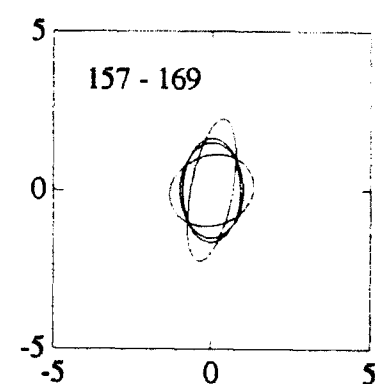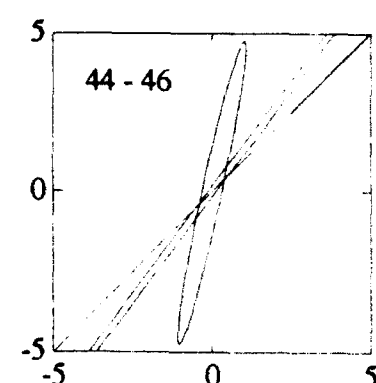
Figure 6(i). Evolution of a vortex core for the case of initial aspect ratio $\lambda_o = 1.5$ with (a) $\epsilon = 0.25$ and (b) $\epsilon = 0.28$. The vortex shape at various multiple of the time period, $T = 2\pi/\Omega_o$, (indicated by the numbers in each sub-plot) of the imposed periodic strain is shown. $\Omega_o/\omega = 0.42$ in the case shown.
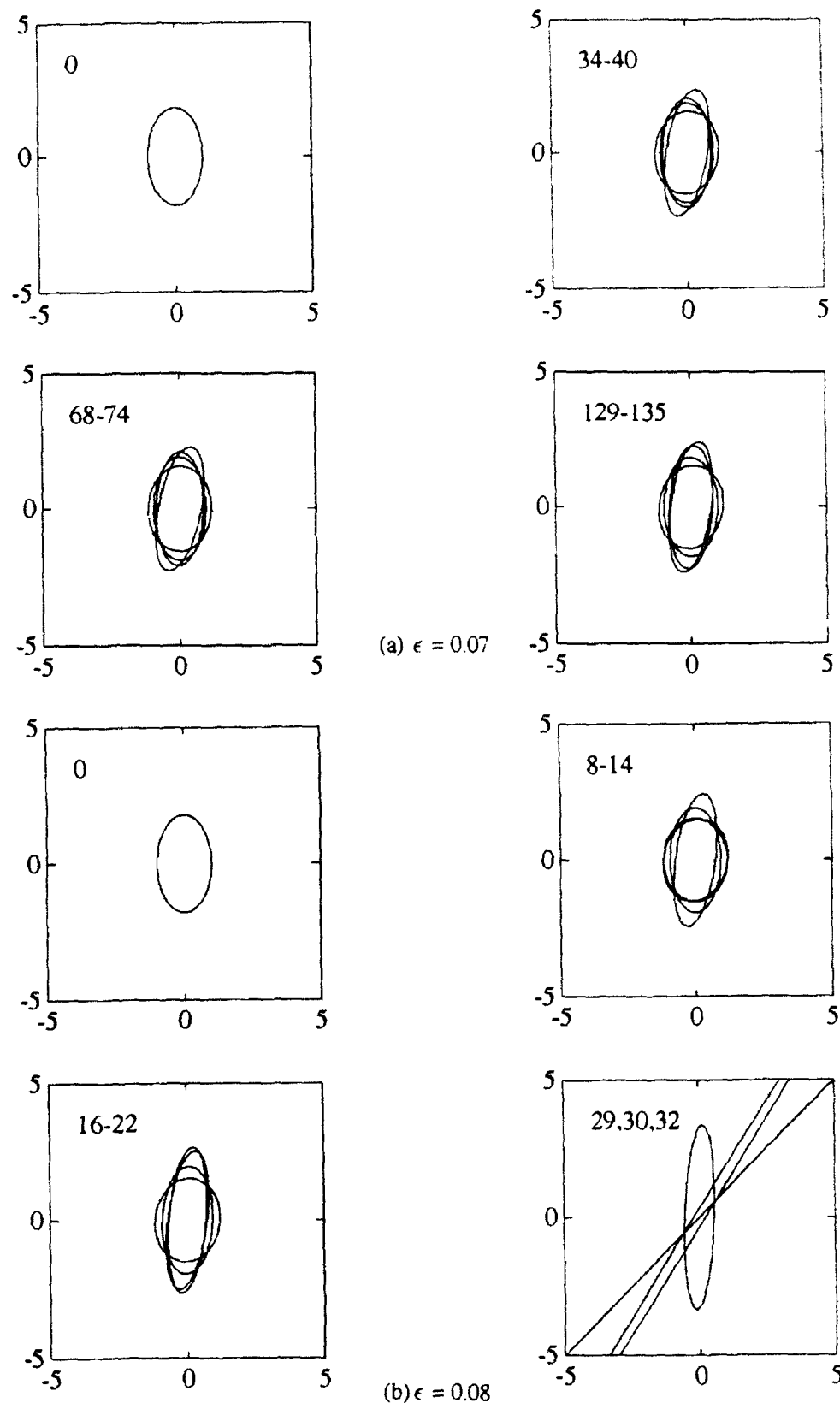
Figure 6(ii). Evolution of a vortex core for the case of initial aspect ratio $\lambda_o = 1.8$ with (a) $\epsilon = 0.07$ and (b) $\epsilon = 0.08$. The vortex shape at various multiple of the time period, $T = 2\pi/\Omega_o$, (indicated by the numbers in each sub-plot) of the imposed periodic strain is shown. $\Omega_o/\omega = 0.35$ in the case shown.
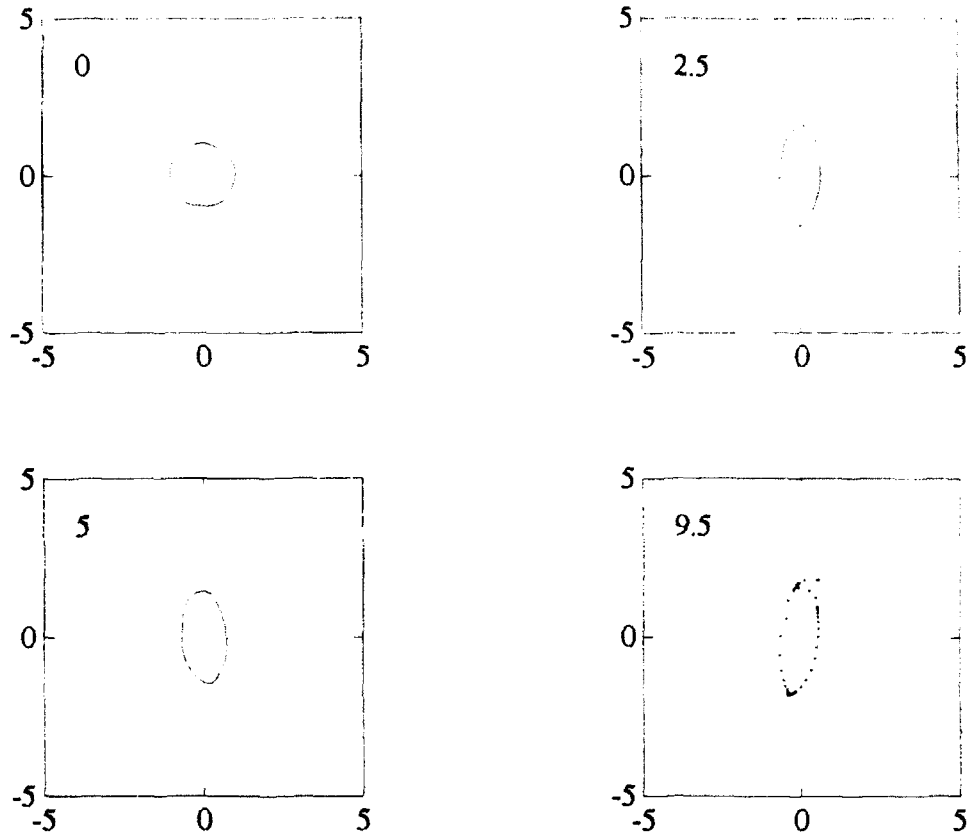
Figure 7. Evolution of a vortex core for the case of initial aspect ratio $\lambda_o = 1.02$ with $\epsilon\, e_o = 0.037$ and a higher (3 wave) mode distortion (of amplitude, 0.5r, where r is the effective core radius) of the boundary. The time in, terms of the period T of the periodic strain, is shown in each subplot. The evolution is followed using contour dynamics. Specific boundary points used are shown in the last subplot to illustrate the deformation explicitly. Further integration requires detaching the 'tails' in the boundary shape.
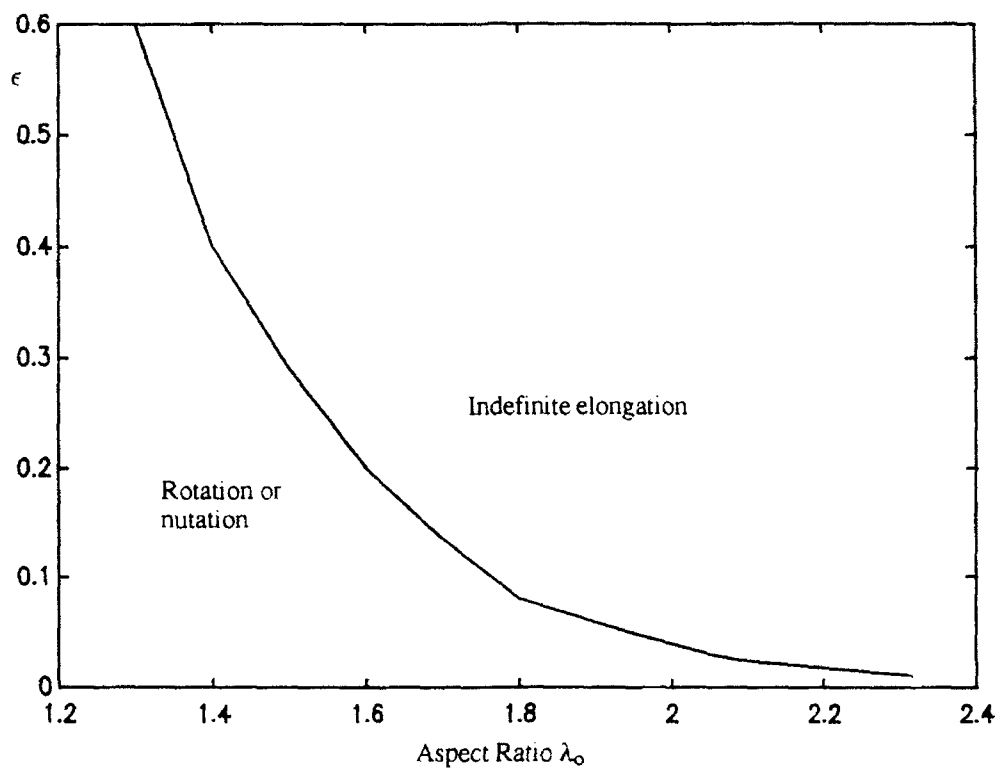
Figure 8. **Minimum value of amplitude ϵ required for the steady vortex core to flip to a state of indefinite elongation.**

REFERENCES

1. Moore, D. W.. and Saffman, P. G., 1971. Structure of a line vortex in an imposed strain. Aircraft wake turbulence and its detection. Ed. Olsen, J. H., and Goldburg, A. Plenum Press. New York.

2. Kida, S., 1981. Motion of an elliptic vortex in a uniform shear flow.). J. Phys. Soc. Japan, 50, 3517.

3. Crow, S. C., 1970. Stability theory for a pair of trailing vortices. AIAA J., 8.

4. Dritschel, D. G., 1990. The stability of elliptical vortices in an external straining flow. J. Fluid Mech., 210,233.

5. Pullin, D. I., 1981. The nonlinear behavior of a constant vorticity layer at a wall. J. Fluid Mech. 108, 401-421.

6. Dritschel, D. G., 1989. Computer Phys. Rep., 10,77.

7. Neu, J. C., 1984. The dynamics of a columnar vortex in an imposed strain. Phys. Fluids., 27., 2397.

PLUME AND WAKE DYNAMICS, MIXING, AND CHEMISTRY
BEHIND AN HSCT AIRCRAFT

R.C. Miake-Lye, M. Martinez-Sanchez, R.C. Brown, and C.E. Kolb
Aerodyne Research, Inc.
Billerica, MA 01821-3976

ABSTRACT

The environmental perturbations caused by the exhaust of a High Speed Civil Transport (HSCT) depend on the deposition altitude and the amount and composition of the emissions. The chemical evolution and the mixing and vortical motion of the exhaust need to be analyzed to track the exhaust and its speciation as the emissions are mixed to atmospheric scales. Elements of an analytic model of the wake dynamical processes are being developed to account for the roll-up of the trailing vorticity, its breakup due to the Crow instability, and the subsequent evolution and motion of the reconnected vorticity. The concentrated vorticity is observed to wrap up the buoyant exhaust and suppress its continued mixing and dilution. The chemical kinetics of the important pollutant species will be followed throughout the plume and wake. Initial plume mixing and chemistry are calculated using an existing plume model (SPF—Standard Plume Flowfield) with additional H/C/O, OH/SO_2, and NO_y chemistry and equilibrium H_2O condensation included. The species tracked include those that could be heterogeneously reactive on the surfaces of the condensed solid water (ice) particles when condensation occurs and those capable of reacting with exhaust soot particle surfaces to form active contrail and/or cloud condensation nuclei (ccn).

INTRODUCTION

The Anglo-French Concorde has shown that commercial supersonic air transportation is feasible. However, since it began commercial operations in the mid-1970s, the Concorde has served a low-volume, premium-fare market with its dozen-plus fleet. Technological advances in the intervening years have created the potential for a large fleet of more economical High Speed Civil Transports (HSCTs) that could serve a large commercial market,[1,2] including trans-Atlantic and Pacific Rim routes in particular. With this possible development, attention has refocused[3] on the environmental impact of a much larger fleet of airplanes operating in a flight regime close to that of the Concorde.

The potential effects of these aircraft on the chemical balance in the stratosphere—and on stratospheric ozone levels in particular—are a primary environmental concern. Atmospheric

modelers[4,5] have already begun to make estimates of the effects of the exhaust effluents of HSCTs on stratospheric chemistry. In doing so, a range of estimated emissions from the as-yet-undeveloped HSCT engines are deposited directly at representative altitudes and latitudes in their models. It is the purpose of the present study to provide initial estimates of chemical and physical changes that may occur between the exhaust leaving the engine and its deposition as a quiescent air mass in the stratosphere.

The exhaust from the large engines propelling a 250+ passenger supersonic airplane will be introduced into the ambient surroundings as a supersonic coflowing jet. Recent studies of supersonic mixing[6,7] indicate that supersonic *convective* Mach numbers suppress mixing in free shear layers, an effect that will need to be accounted for in following the initial exhaust dilution. As this initial dilution is occurring, the vortex sheet shed by the lifting surfaces of the airplane is rolling up and being concentrated in a trailing vortex pair by mutual induction of the distributed vorticity. This vorticity field will begin to affect the diluting exhaust stream and will subject the exhaust to local conditions that are sufficiently different from ambient that significant changes in stratospheric exhaust deposition could result. The vorticity field behind a highly loaded supersonic aircraft configuration can differ dramatically from that of typical subsonic transports.

In the Climatic Impact Assessment Program of the early 1970s, a related study[8] was performed using contrail data collected under that program and then-current understanding of chemistry, condensation physics, and vortex wake development. Just as supersonic flight technology has made great bounds since that time, revolutionary advances have recently been made in atmospheric chemistry. Great strides in the understanding of the stability and development of vortex wakes were being made concurrently with the CIAP program and continued since then and were not fully incorporated into that early study. Thus, while not starting completely anew, the present study represents a significant departure from the CIAP study and will provide a more comprehensive assessment of the chemistry and fluid physics occurring in the vortex wake.

The elements of an analytic model of these processes must include the dynamics of the vortex wake, from roll-up to breakup and dissipation; its interaction with the diluting hot exhaust; the gas-phase exhaust species chemistry; the heterogeneous chemistry occurring on condensed aerosols and soot particles; and the condensation physics governing the creation, or lack thereof, of the condensed aerosols needed for heterogeneous reactions. The stratospheric impact of the net result of all these elements will be felt through their displacement of the exhaust through vortical or buoyant transport[9] or possible sedimentary removal of reactive species, as in polar stratospheric cloud (PSC) denitrification (and dehydration) of the polar stratosphere.[10,11] Any major chemical repartitioning of the exhaust species that is not washed out by subsequent photochemical conversions may significantly affect the composition of the chemical inputs to the global models. An understanding of the structure, motions and persistence of the vortex wake will also be necessary for any attempt to measure the exhaust from an HSCT in flight and for evaluating the wake hazard created for following aircraft.

The analysis reported below represents the development of these several elements of a comprehensive exhaust plume/wake model for supersonic aircraft in cruise conditions. Gas-phase nozzle chemistry and plume chemistry are described in Section 2 and have been applied to understanding the engine exit plane conditions and the subsequent chemical evolution

and condensation physics in the initial exhaust mixing region using extensions of a standard aircraft "plume" code. This chemistry will be applied in the vortex wake regime as well, as a refined model of its dynamics is finalized. The analytical basis for the vortex wake model is presented in Section 3. The integration of these elements and requirements for further development are discussed in Section 4.

PLUME MIXING AND CHEMISTRY

Internal Engine Flow/Finite-Rate Kinetics Model

The internal flow for a hypothetical Mach 2.4 engine design was modeled under realistic engine operating conditions using the ODK PACKAGE code[12] for reacting flows. Emphasis was given to estimating nonequilibrium concentrations of OH and HNO_3 at the nozzle exit plane since emission levels for these species are not currently being measured by propulsion laboratories and they were expected to strongly influence subsequent heterogeneous and homogeneous exhaust plume chemical kinetics. The finite-rate kinetics for the internal engine flow were simulated using the reaction set consisting of 35 reversible reactions given in Table 1. These reactions were selected from kinetic data bases for hydrocarbon and nitrogen combustion chemistry. The hydrocarbon combustion reaction rate parameters were taken from a recent compilation[13] of kinetic rate data for methane combustion. Rate parameters for the reactions describing the nitrogen combustion chemistry were taken from the recent review by Miller and Bowman.[14]

To simulate the internal engine flow, equilibrium calculations were first performed to determine the chemical composition of the flow from the combustor as a function of temperature and pressure. ODK calculations were then performed in three stages to characterize the chemical and physical properties of the flow through the turbine, mixing chamber and nozzle. For each stage, the pressure and temperature at the initial and end axial points were constrained to be consistent with representative GE engine parameters.[15] In addition, when necessary, the mixture was diluted to account for the mixing in of bypass air. Nozzle exit plane species mole fractions obtained by this method compared against equilibrium predictions in Table 2.

Although the one-dimensional exit plume results shown in Table 2 can only approximate the chemistry and flow dynamics of anticipated HSCT engines, they do confirm that significantly non-equilibrium levels of CO, NO, NO_2, HNO_3 and OH can be anticipated at the engine nozzle exit plane. While the engine development community has long accepted the non-equilibrium nature of CO and NO_x emissions, there has been less appreciation of the high (> ppm) levels of OH emitted by gas turbine systems. The predictions presented here are consistent with the optical absorption measurements performed on the YJ93-GE-3 under stratospheric cruise conditions by McGregor et al.[16] during the CIAP program. In that study, mole fractions of exit plane OH exceeded 2×10^{-5} and 4×10^{-5} for cruise power settings equivalent to Mach 2.6 operation at 66 kft and Mach 2.0 at 55 kft.

The standard plume flowfield code, SPF-2,[17] was used to characterize the chemical and physical properties of the combustion exhaust plume associated with an advanced high altitude supersonic aircraft. Model simulations used GE parameters[15] for a hypothetical Mach 2.4 engine to specify initial exhaust emission parameters and 1990 atmospheric models[18] to specify the ambient atmospheric parameters. The SPF code was modified to include an initial estimate of the degree of H_2O condensation based on thermodynamic equilibrium. Initial examination of the plume chemistry focused on the evolution of NO_x, including an evaluation of the impact of ozone oxidation mechanisms and the percentage conversion to HNO_3, as well as SO_x oxidation cycles.

Initial Conditions

The species concentrations and thermodynamic properties used as initial conditions in model simulations of the plume chemistry and mixing are given in Table 3. This includes ambient free stream conditions and the initial conditions for the exhaust at the nozzle exit plane. Exit plane species distributions are based either on reported emission indices (g equiv/kg fuel) or on ODK calculations for the internal engine flow. An exit plane OH mole fraction of 1×10^{-5} representing a rough mean between calculated ODK value shown in Table 2 and the measurements of McGregor et al.[16] was adopted for these plume calculations. For NO_x, an emission index[19] EI NO_2NO_x of 5 was used[20] assuming 10% NO_2 and 90% NO on a molar basis. Ambient free-stream conditions are given for three representative cases. These correspond to the atmospheric conditions appropriate for January 1 and June 1 at a latitude of N47 and June 1 at N85. In all three cases, the altitude was ~18 km. Ambient conditions were obtained from AER's 1990 atmospheric chemistry data base.[18]

Condensation

The SPF-2 code was modified to predict the degree of H_2O condensation during the plume expansion as part of an initial investigation into the potential role of heterogeneous kinetic processes in affecting plume chemistry. Condensation was treated using the standard vapor pressure test for thermodynamic equilibrium. It was assumed that any condensed H_2O particulates that formed would not significantly modify the flow mixing dynamics. A summary of the SPF equilibrium H_2O condensation predictions is given in Table 4 for the three case runs described by the free-stream ambient conditions in Table 3. For comparison, condensation predictions based on Appleman's equilibrium, fully-mixed condensation algorithm[21] are also listed in Table 4. In general, the agreement between these two approaches is good.

Plume Chemistry

The reaction set used to simulate the exhaust plume finite-rate chemical kinetics is listed in Table 5. Rate parameters for these reactions are based on a 1990 NASA evaluation[22] of the chemical kinetics data for use in stratospheric modeling. The reaction set includes reactions to describe NO_x/O_3 reactions and SO_2 oxidation kinetics.

Representative model results are presented in Table 6 which lists the plume mole fractions for nitrogen and sulfur oxides, nitric acid, hydroxyl radical and ozone on the plume axis at axial points 500, 1000 and 2000 feet downstream of the nozzle exit plane. The speciation given in Table 6 is based on model runs using ambient atmospheric conditions appropriate for June 15 at a N47 latitude (case 1 in Table 3). However, similar results were obtained for model runs with ambient conditions corresponding to January 1 at the same latitude (case 2 in Table 3). The only difference was a 1.7 increase in the mole fraction of N_2O_5.

Mole fraction ratios for NO_2/NO, HNO_3/NO_x and SO_3/SO_2 are also given in Table 6 where, in this case, NO_x corresponds to the sum of NO and NO_2 mole fractions. Based on this data, the SPF model calculations indicate that approximately 11% of the initial SO_2 is oxidized to SO_3. NO is oxidized to NO_2 by entrained ambient O_3. NO_2, in turn, is oxidized primarily by exhaust OH. The NO_2/NO ratio is maintained at 0.10-0.11 while approximately 5% of the NO_x is converted to HNO_3. Previous studies by Hoshizaki et al.[8] concluded that about 10-20% of the NO_x emitted is transformed to HNO_3 in the jet plume region, i.e. 1-10 seconds after the exhaust is emitted. Although this represents a significantly larger percentage conversion than predicted in SPF-2 simulations, the discrepancy can be explained in terms of differences in the rate parameters used. The dominant mechanism for formation of HNO_3 is

$$NO_2 + OH + M = HNO_3 + M, \quad k = 2.2 \times (10^{-22}/T^{3.2}).$$
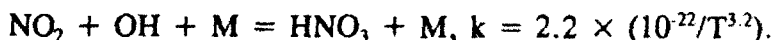
In the early work of Hoshizaki et al.[8] this reaction was treated as a simple bimolecular reaction with a rate constant ($k = 4.8 \times 10^{-12}$) orders of magnitude larger than that adopted in the 1990 NASA evaluation[22] of the best fit to experimental data over the temperature range of interest.

The SO_3 and N_2O_5 created in the exhaust plume will react immediately on contact with contrail droplets or particles to form condensed phase H_2SO_4 and HNO_3, respectively. Exhaust gaseous HNO_3 will also condense onto contrail particles. Each of these species, gaseous SO_3, N_2O_5 and HNO_3 can also be expected to interact with exhaust soot, as can exhaust NO_3[23] and entrained atmospheric O_3,[24] to create oxidized soot surfaces capable of nucleating either exhaust contrails or atmospheric acid/water aerosols after plume mix-out. This soot surface conditioning may be an important plume chemical effect since only 1% of the soot particles formed by burning jet fuel can immediately condense water vapor at typical plume supersaturation ratios without such conditioning.[25] We plan to incorporate these heterogeneous processes in future plume chemistry models.

VORTEX WAKE DYNAMICS

The scales and regimes involved in the dispersion of pollutants from the exhaust of stratospheric aircraft have been discussed by several authors mainly in connection with the CIAP studies in the '70s.[26,27] The early part of the process (the first hour) was described in some detail by Hoshizaki et al.,[28] who called this period "the wake regime". The first few tens of seconds of this period are characterized by the dominant role of the aerodynamic flowfield of the aircraft (first through the momentum of the jet itself, and later through the effect of the aircraft sinking vortex pair). Wake dispersion, after an ill-defined transition, is dominated by environmental effects, such as wind shear.

17-5

Based on the analysis of horizontal and vertical photographs of B-52 contrails, Ref. 28 concluded that in a first phase, called the "jet regime", the engine plumes grow by ordinary turbulent mixing to fill the recirculating vortex pair cell (of dimensions roughly 1.2 × 1.5 times the wing span). The attraction to the wing tip vortex cores was noted, but dismissed as a minor effect. After this time (~ 10 s), the effluent remains horizontally confined by the cell, but detrainment from the top as the cell descends leads to vertical growth. This "vortex" phase ends at about 100 s with the breakup of the vortex pair, following which the wake remnants gradually lose their organized motion and ambient effects dominate. The effect of the aircraft was noticed, however, for as much as one hour, since different aircraft lead to different dispersion rates on that time scale. This conceptual model (along with the models of Holdeman[29] and Nielsen[30] which ignored wake interactions) were later also applied to the analysis of supersonic YF-12 flight data. The interpretation of the growth of this wake is complicated by the visualization method used, as will be discussed below.

As will be discussed more fully in later sections, the depth of the pressure and temperature minima induced by the rolled-up wing-tip vortices scale as the square of the Mach number, and inversely with the square of the wing aspect ratio. Thus, what was found to be a minor effect when examining transonic aircraft may become a very important effect for a low aspect ratio supersonic aircraft. The horizontal densitometer scans of B-52 contrails (Hoshizaki *et al.*, Ref. 28) already show two peaks at the expected vortex core locations, and many other observations (see for instance photographs in Ref. 32) indicate the persistence of these two separate, well-defined and non-growing columns of condensation material up to the time of vortex breakdown.

The extent of plume gas trapping in the low pressure troughs caused by the vortical motion, and the degree to which exhaust gas is able to escape and be detrained from the sinking recirculating vortex pair cell determine the effectiveness of the vortex confinement and mixing suppression. These factors are strongly dependent on the relative spanwise location of the engines and the vortex cores, and also on the "attraction" of these cores, as measured by their pressure trough depth. The trapped and the detrained portions of the exhaust gas follow very different dilution and cooling histories. While the classical Appleman[21] treatment (isobaric mixing of effluent and ambient air) should be applicable to the detrained portion, the portion captured by the vortex cores may undergo significantly lower temperatures during mixing, due to adiabatic expansion into the low pressure of the core. Since, to begin with, stratospheric conditions of interest are typically within ±10°C of the Appleman contrail threshold, these deviations may well initiate ice formation in the cores under conditions for which contrails would not be predicted ordinarily. In addition, the trapped gas dilutes at a much reduced rate, and this may provide ice growth times and/or chemical reaction times much longer than otherwise expected.

Given the stronger confining effect of the vortex cores in a supersonic, as compared to a transonic, aircraft, it is not even clear whether substantial detrainment from the descending vortex pair cell is to be expected in the supersonic case. If vertical detrainment were either absent or strongly reduced, the morphology of the effluent distribution at the end of the vortex wake would be quite different from what has been accepted since the studies in the 1970s. In the YF-12 data of Ref. 31, there was little vertical growth in the wake regime, amounting to as little as 1/4 of that predicted by the "detrainment" model of Ref. 28. Unfortunately, interpretation of these supersonic cruise data is complicated by the fact that the measurement was

based on in-flight fuel dumps from the aircraft centerline. Only those portions of the dump which mixed with the warm buoyant plume would be subject to vortex capture, leaving the rest free to detrain.

An additional difference between conventional and supersonic aircraft wakes must be mentioned here. For most conventional aircraft, the vortex pair becomes unstable and breaks up into irregular vortex rings at about the same time as its vertical motion is arrested by the stable atmospheric stratification. Organized vertical motion would in any case be ended by the latter effect at this point, and the coincidence has led to an identification of "vortex pair breakup" with "vorticity dissipation". In the supersonic case, however, the vortex pair has more vertical momentum, and its vertical motion will continue (in the form of vortex rings) well after the straight vortex system has broken up. This will probably lead to pollutant deposition at lower altitudes (by a few hundred meters) than expected, and also to longer than expected confinement times. The effect may also be significant in terms of wake hazards to other aircraft.

The Turbulent Plume Growth with Buoyancy Effects and A Model for Plume-Vortex Interactions sections and Appendices A and B provide a more detailed discussion of these effects, based on a series of simplified analytical models which are intended to approximately quantify their relative importance and scales.

Analysis

Aircraft and Vortex Parameters

Table 7 summarizes the parameters assumed for our vortex wake analysis. The airplane is a Mach number 2.4 design beginning its cruise at 17.4 km altitude. For estimates of wake properties, an elliptic loading distribution has been adopted, and the vortex
roll-up distance was estimated based on Ref. 33.

The structure of the vortices after roll-up has been calculated based on the Betz-Donaldson model,[33,34] according to which the circulation originally bound to the wing outboard of a spanwise location y_1 will end up rolled into the inner part of the trailing vortex core, within a radius r from its center—which equals the distance from y_1 to the centroid of the circulation distribution outboard of y_1. For the assumed elliptic loading, this model predicts a tangential velocity distribution near each core given by

$$\frac{v_\theta}{v} = 0.25 \, \frac{C_L}{AR} \sqrt{\frac{b}{r}} , \tag{1}$$

where v is the flight speed, C_L the lift coefficient, AR the wing aspect ratio, b the wing span and r the distance to the vortex core. This has been confirmed in tests,[33] and it appears to hold to radii much smaller than the classical core size estimate of Prandtl,[34] with the result that v reaches higher values near the core than expected on the basis of a model with all the vorticity

concentrated in the Prandtl core. The validity of the Betz-Donaldson model has been debated,[35] and no rigorous basis for it seems to exist. We use it here simply as a convenient semi-empirical device.

Using Eq. (1), several quantities of interest can be calculated. The centripetal acceleration v_θ^2/r is, using the parameters in Table 7,

$$g \text{ centripetal } \cong \frac{3500}{r^2} \text{ (in MKS units).} \tag{2}$$

With reference to Figure 1, this gives 26 m/s^2 at the inboard plume location, and 73 m/s^2 at the outboard plume location. This shows that centripetal buoyancy effects will be strong and will compete with (perhaps dominate) those of upwards buoyancy and turbulent detrainment of effluents from the cell's edge. Notice (Eq. (1)) that the peculiar features of the HSCT (small AR, high v) greatly emphasize this effect. For a transonic airplane of the same wing area but with a lift coefficient of 0.5 and an AR of 10, $g_{centripetal}$ would be less by a factor of 17.2 at the same value of b/r. This makes plume/wake interaction a secondary issue for such aircraft, and may account for its dismissal by Hoshizaki et al.[28] and, more generally, for the lack of attention it has elicited so far.

The pressure gradient set up by the vortex follows easily from the hydrostatic radial force balance $\partial p/\partial r = -\rho v_\theta^2/r$. From Eq. (1) and ignoring the relatively small effects of compressibility the local depression, $\Delta p = p_\infty - p$, is seen to vary as $1/r$. Assuming adiabatic expansion, the corresponding temperature depression is found to be

$$\frac{\Delta T}{T_a} = \frac{6(\gamma - 1)}{\pi^4} \frac{M^2 C_L^2}{AR^2} \frac{b}{r}. \tag{3}$$

For the parameters of Table 7, we find $\Delta T(K) \cong -3.5/r(m)$. Once again, for typical transonic aircraft the corresponding ΔT is less by a factor of 83, making it almost unobservable.

The vortex system is known to break up due to growth of the Crow instability (vortex bursting is unlikely at the moderate C_L of cruise). The estimate for breakup time given in Table 7 ($t_B \cong 15\tau$) is consistent with data of Ref. 36 for a quiescent atmosphere, and is 50% longer than the estimate given by Hoshizaki et al.[28] for tropospheric conditions.

Turbulent Plume Growth with Buoyancy Effects

The initial spread of the engine plumes must be controlled by turbulence generated by the plume/ambient velocity shear. However, centripetal buoyancy effects must be felt strongly, as noted, and will eventually dominate the plume dynamics. The overall dynamics is fairly complex, and we will attack it initially by considering simpler model problems. The first

17-8

question is the estimation of the time after which buoyancy dominates over jet growth. To this end, we temporarily ignore the shearing of the plume by the vortex flowfield, and consider a buoyant round engine jet in the co-flowing airstream. The analysis is relegated to Appendix A, and is based on the use of a turbulent diffusivity model which combines those of Prandtl[37] for a coflowing jet and of Morton, Taylor and Turner[38] for a rising linear plume. The resulting jet diameter is found to evolve with distance x as,

$$\frac{D}{D_0} = [1 + \theta \, G \, (\xi)]^{1/3},$$ (4a)

where

$$\xi = \chi/\ell \quad , \quad \ell = \frac{1}{19} \, \frac{\eta_{ov}}{1 - \eta_{ov}} \, \frac{c_p \, T_a}{g_{eff}} \quad ,$$ (4b)

and

$$\theta = 0.061 \, \frac{F \, \ell}{\rho v_\alpha^2 \, D_0^3}$$ (4c)

and

$$G(\xi) = \xi \, \sqrt{1 + \xi^2} + \ln (\xi + \sqrt{1 + \xi^2}) \quad .$$ (4d)

Here, η_{ov} is the overall engine efficiency (fuel heat value to thrust), F is the engine thrust and D_0 is the engine nozzle diameter. The acceleration, g_{eff}, could be either the actual gravitational acceleration, or the centripetal acceleration calculated in Aircraft and Vortex Parameters.

By examination of Eqs. (4a)-(4d) we can see that when $\xi \ll 1$, $D \cong x^{1/3}$ (jet-dominated regime), and when $\xi \gg 1$, $D \cong x^{2/3}$ (buoyant plume regime). The two are nearly equivalent at $\xi = 2$. For the parameters of Table 7, and using the centripetal g for either engine, as in the previous section, we find that $\xi = 2$ is reached when $D/D_0 = 2.17$ (outboard engine) or $D/D_0 = 2.89$ (inboard engine). Thus, by the time centripetal buoyancy becomes the dominant plume growth mechanism, the dilution ratio (proportional to $(D/D_0)^2$) is about 4.7 to 8.3, depending on which engine is considered. For comparison, using "natural" gravity (g =9.8 m/s^2), the crossover occurs when $D/D_0=4.60$ (dilution ratio = 21), by which time the plumes would fill a substantial fraction of the vortex cell.

The analysis above has not accounted for the effects of compressibility on turbulent jet mixing. Ref. 6 shows substantial mixing suppression when the "convective Mach number," M^* exceeds about 0.5. M^* is measured with respect to an intermediate frame in which both pressure and total pressure are equal for both streams. In the case of equal specific heat ratios, this reduces to

$$M * = \frac{v_2 - v_1}{a_2 + a_1} .$$ (5)

where v and a are the respective flow and sonic velocities of the two streams. In our case (Table 7) $M^* \cong 1.01$, and the initial mixing rate should be reduced by a factor f_c between 0.2 and 0.4.[6] The factor f_c will then approach unity as mixing proceeds and the relative Mach number decreases. The effect on the above analysis would be that the average f_c would multiply both θ and ℓ.

A Model for Plume-Vortex Interactions

The fluid mechanics of the turbulent buoyant jet in the flowfield of a concentrated vortex is too complex to be adequately analyzed here, but we will at least account for the salient features in an attempt to estimate the capture time of the engine exhaust into the vortex cores. The following assumptions are made:

a. The plume is convected and sheared by the (un-modified) Betz-Donaldson vortex flow. The shearing spreads the plume around a circle centered at the vortex core, at a rate proportional to the difference $v\theta(r-D/2)-v\theta(r+D/2)$ where r is the distance to the core and D is the transverse plume size (See Figure 2).

b. The plume cross-section grows by entrainment of ambient air, in proportion to its inward radial velocity times its projected area (Morton-Taylor-Turner model[38]). No account is taken of axial flow, except that the model of the previous section is used to estimate a plume diameter as it begins to be affected by the vortex.

c. The radial motion is obtained from a momentum balance, using the centripetal buoyancy described in Aircraft and Vortex Parameters.

Letting A be the plume cross-section at a given time, and $\Delta\rho$ the mean density defect in the plume, mass conservation imposes

$$\frac{d}{dt} = (A\Delta\rho) = 0 .$$ (6)

The entrainment rate assumption gives

$$\frac{dA}{dt} = \alpha \, \Delta s \, v_r \quad , \tag{7}$$

where Δs is the tangential plume spread (Figure 2), v_r is its radial velocity (inwards), and $\alpha \cong 0.94$ is chosen to correspond for the circular cylinder case to the value used in Ref. 28.

Equating the buoyancy force to the rate of momentum increase due to mass accretion gives

$$\alpha p_a v_r^2 \, \Delta s = \frac{v_\theta^2}{r} A \Delta \rho \quad , \tag{8}$$

Finally, the shearing assumption is expressed as

$$\frac{d}{dt}\left[\frac{\Delta s}{r}\right] = D\frac{\partial}{\partial r}\left[\frac{v_\theta}{r}\right]. \tag{9}$$

where D is assumed constant.

Combining Eqs. (6)—(9) with the expression Eq. (1) for $v\theta$ leads to a set of differential equations, for which closed-form solutions can be obtained:

$$\frac{vt}{b} = 0.61\alpha \, \frac{AR}{C_L} \, \frac{(r_0/b)^{5/2}}{(D_0/b)(\Delta\rho/\rho)o} \left[1 + 2.95 \sqrt{\frac{D_0/r_0}{\alpha(\Delta\rho/\rho)_o}} \right.$$
$$\left. \left[1 - \left[\frac{r}{r_0}\right]^{5/2} - \left[\frac{r}{r_0}\right]^{5/2} \left[1 + \frac{5}{2}\ln\frac{r_o}{r} \right] \right] \right] \tag{10}$$

and

$$\frac{A}{A_0} = 1 + \frac{2}{\pi} \left[\frac{r_0}{D_o}\right]^2 \left[\left[\frac{D_0}{r_0} + \frac{\sqrt{D_0/r_o} + 1/2\beta}{\beta}\right] \right.$$

$$- \left[\frac{r}{r_0}\right]^2 \left\{ \left[\sqrt{\frac{D_0}{r_0}} + \frac{\ln(r_o/r)}{\beta}\right]^2 + 1 \right. \qquad (11)$$

$$\left. \left. \frac{1}{\beta}\left[\sqrt{\frac{D_0}{r_0}} + \frac{\ln(r_0/r) + 1/2}{\beta}\right]\right]\right]$$

where

$$\beta = \frac{4}{3}\sqrt{\frac{\pi}{4\alpha}\left[\frac{\Delta\rho}{\rho}\right]_0} \quad , \qquad (12)$$

and also

$$\Delta\theta = \left[\sqrt{\frac{D_o}{r_0}} + \frac{\ln(r_o/r)}{\beta}\right]^2 \quad , \qquad (13)$$

$$\frac{\Delta\rho/\rho}{(\Delta\rho/\rho)_o} = \frac{A_0}{A} \quad . \qquad (14)$$

For application, the initial distance r_0 is 6.9 m for the outboard and 11.5 m for the inboard engine. The initial diameter D_0 and dilution (or density depression $(\Delta\rho/\rho)_0$) can only be approximately selected to account for the turbulent growth rate in the initial jet stage. A rough estimate, based on the arguments of the previous section (ignoring compressibility effects) gives (for an engine jet diameter of 2 m) initial diameters of 4 m and 5 m for the outboard and inboard engine respectively. Correspondingly, the density depressions $(\Delta\rho/\rho)_0$ are 0.122 and 0.0816, since the value at the engine face is 0.51.

Figures 3 and 4 show the subsequent evolution of plume-core distance r, angular spread $\Delta\theta$ of the sheared plume and overall dilution ratio A/A_{jet}. Since the radial pressure gradient intensifies towards the vortex center, the radial velocity of the plume is seen to increase with time, despite the progressive dilution. Thus, although it is not clear what distance r to pick as the end of the "capture" process, one can make a reasonable estimate of the "capture time". For instance, Eq. (10) indicates a finite time for r → 0, and this can also be seen from the downwards turning of the r(t) curves in Figs. 3 and 4. Perhaps a more reasonable capture time can be chosen as that at which r equals the original plume diameter D_0 (after allowing for the initial turbulent spread) or, what is nearly equivalent, that at which the plume has been fully spread into an annulus ($\Delta\theta$ = 360°). This gives for the outboard engine about 90 wing spans, by which time the overall dilution (including initial turbulent growth) is about A/A_{jet} = 28. The process is slower for the inboard engine, and it takes 350 wingspans to capture that plume, with an overall dilution ratio of 56.

The basic wake time scale (Table 7) is $\tau = (2AR/C_L)$ (b/V), in terms of which roll-up takes approximately 1.5τ and break-up takes 15τ (or, for our values of AR and C_L, 56 and 560 wingspans, respectively). We see therefore that a) the time for the plume capture process scales also as the basic time τ (see Eq. (10)), and b) for both engines, the capture time is intermediate between those for roll-up and break-up, as required for validity of the modeling approach.

It is interesting to observe, in connection with point a) above, that, for a given geometry and initial density defect, plume capture occurs at a fixed fraction of wake breakup time, independent of Mach number. Thus, of the two factors which are clearly different between transonic and supersonic aircraft (AR and M), only one, AR, remains to shorten the capture time in relation to wake lifetime. The reason why flight speed does not influence the time ratio is that all processes, including buoyant radial velocity and azimuthal vortex velocity, scale up together as v (see Eqs. (1) and (8)). This fact can be exploited for setting up experimental simulations of these phenomena in water tanks. The Mach number is still important however, in dictating deeper temperature and pressure minima in the supersonic case, and hence strengthening centripetal buoyancy when compared to natural buoyancy. Whether or not these stronger temperature depressions lead to enhanced condensation depends on the degree of dilution ultimately achieved by the captured plume (see Condensation Considerations).

The Last Stages of the Vortex Regime

As noted in Table 7, the wake is expected to survive as an organized cylindrical vortex cell for about 22 s. According to our analysis in A Model for Plume-Vortex Interactions, the vortex cores at breakup time may contain a large fraction of the engine exhaust, at a dilution smaller than would have been expected in the absence of the vortices, and at a few degrees lower temperature. In attempting to extrapolate from this point, several questions arise:

    a.   For how much longer will the confining effects of vorticity prevent or delay plume dispersion?

    b.   Under what conditions will the higher plume vapor concentration and lower temperature lead to contrail formation?

c.   If condensation does occur, will the confinement time be long enough for significant heterogeneous chemical interactions to occur or for particles to grow to precipitation sizes?

Vortex Dynamics After Break-up

Unfortunately, the fluid mechanics of the broken-up vortex system is still poorly understood, and so, only very rough estimates can be made on the important question a). Experimental and analytical stability results[36] indicate that reconnection due to growth of the Crow instability tends to produce irregular elongated ring vortices with aspect ratios of the order of 4:1. Dhanak and DeBernardinis[39] followed numerically the evolution of an elliptical ring vortex of this type and found that, after an oscillation in which the short and long axes interchange positions, the cores touch in the middle and reconnection can be expected, leading to two roughly 2:1 rings. These are then structurally stable, and oscillate as described. The time for subdivision of the original ring is (for our parameters) about 5 s.

If we can ignore temporarily the disturbing effects of wind shear, the smaller rings may continue to descend for some time, as they entrain new air by turbulent diffusion, and consequently grow in size and slow down. Glezer and Coles[40] did careful measurements of the evolution of circular turbulent rings in water, and showed that similarity exists in this motion provided a "virtual origin" is identified. In Appendix B we show that their results can be explained by means of a simple entrainment hypothesis, for which the entrainment parameter is derived from the data. As explained in Appendix B, the linear dimensions of the ring increase as $(1 + t/t_1)^{1/4}$, where $t_1 = \pi a_0/2\beta v_0$ (a_0 = initial core radius, v_0 = initial ring velocity, and $\beta \cong 0.01$). For an estimation, assume in our case an initial ring diameter 1.5 times the linear vortex spacing (i.e., 48 m), and an initial core diameter 0.1 of the ring diameter (a_0 = 2.4 m). Since v_0 must be close to the linear vortex pair velocity of 4.9 m/s, we calculate $t_1 = 76$ s.

The effects of atmospheric stratification must be also considered at this point. As the air mass enclosed within the vortex cell sinks into a stably stratified atmosphere, it will undergo adiabatic warming due to the higher pressures encountered, and will develop buoyancy. The effect of this buoyancy will be to eventually lead to an oscillatory vertical motion at the Brunt-Väisälä frequency,

$$N = \sqrt{\frac{g}{T_\alpha}\left[\frac{dT_\alpha}{dz} - \frac{dT}{dz}\right]} \quad , \tag{15}$$

where $(-dT_\alpha/dz)$ is the atmospheric lapse rate, and

is the warming rate of the descending air (H_p is the pressure scale height of the atmosphere).

$$- \frac{dT}{dz} = \frac{\gamma - 1}{\gamma} \frac{T}{H_p} \tag{16}$$

However, a second effect of the descent-induced buoyancy is of interest to us. This is the production of vorticity opposite in sense to that of the wing vortices. The mechanism is clear from the 2-dimensional vorticity equation:

$$\frac{\partial w/\rho}{\partial t} + \bar{u}.\nabla \left[\frac{w}{\rho} \right] = - \frac{1}{\rho} \nabla \left[\frac{1}{\rho} \right] \times \nabla p \quad . \tag{17}$$

The pressure gradient ∇p points vertically down, while $-\nabla 1/\rho$ is concentrated on the cell's edges, and points outwards from the cell. Thus, baroclinic vorticity is generating along the cell's edges, in the sense contrary to that in the vortex cores. At the time buoyancy stops the cell's descent, the total counter-vorticity created is also sufficient to cancel that of the wing vortex system, although its distribution is different. We can therefore expect the vortex system, whether in the form of the undisturbed cylindrical vortex cell, or of its successor ring vortices, to vanish in the vicinity of the lowest point of the Brunt-Väisälä cycle. This occurs when $Nt \cong \pi/2$, with the vertical descent distance being then $\Delta z = -w_0/N$ (w_0 = initial descent velocity). This behavior can be clearly seen in the water-tank data of Ref. 36, and was also assumed by, for example, Greene[41] in his model of wake decay.

For our parameters, with $dT_a/dz = 0$, $H_p = 6380$ m, we calculate $N = 0.0210$ radians/s, and the stratification-induced vortex destruction can be expected to happen at $t = \pi/2N = 75$ s, after a total descent of $-\Delta z = 232$ m. Notice that this is 2.4 times longer than the time required for Crow instability to occur, so that a substantial period (44 s) can be anticipated during which the ring vortices formed after breakup can retain their individuality and continue to trap the engine effluent. The amount of turbulent entrainment into the rings in this time can now be estimated from our Appendix B results. With $t_1 = 76$ s, the ring linear dimensions will increase by $(1 + 44/76)^{1/4} = 1.12$, with additional dilution by a factor $(1.12)^3 = 1.41$.

Condensation Considerations

A slight modification of the classical Appleman argument[21] concerning contrail formation will help illustrate the potential vortex effects. Assuming that each kg of burnt fuel produces 1.29 kg of water vapor and 43 MJ of heat, of which the fraction $1-\eta_{overall} \cong 0.5$ appears as sensible heat in the plume, and that the plume dilutes continuously by isobarically mixing with air at temperature T_a and moisture w_a (g/kg), its average temperature and moisture will evolve together according to

$$T = T_\alpha + 17.7(w - w_\alpha) \quad . \tag{18}$$

In Figure 5, we have represented in a T—w plot the water and ice vapor saturation lines (for an air density of 0.135 kg/m³). The plume material will, according to Eq. (18) evolve down an inclined straight line of slope 1/17.7 towards the existing atmospheric conditions (T_a, w_a). If this line intersects the water saturation line, droplets will condense on existing condensation nuclei, and immediately freeze to form ice particles. These then persist even as the plume dilutes below the water saturation line, and will re-evaporate only after the ice saturation line is re-crossed.

In the presence of the vortex depression, however, both the ambient air and the plume gas are expanding and adiabatically cooling as they mix. Ignoring differences in the specific heat ratios, Eq. (18) must then be modified to

$$T = \left[T_\alpha + 17.7(w - w_\alpha) \right] \left[\frac{p}{p_\alpha} \right] \frac{\gamma - 1}{\gamma} \tag{19}$$

where $\gamma = 1.4$. Tracing the plume trajectory in the T—w plane now requires knowledge of the relationship between local pressure at the plume location and degree of dilution at that point.

As an example, consider a dry stratosphere at T_a = 215 K which, as Figure 5 shows, is at the threshold for contrail formation for this air density (plume expansion along abc). Using the interaction model in Section 3.1.3 we can calculate at each core-plume distance r the corresponding dilution ratio A/A_0 and temperature depression (Eq. (3)). Starting from an engine-exit value w = 20 g/kg, we can then calculate the new plume trajectory a'b'c (Figure 5), which shows definite contrail formation. The last portion of the a'b'c curve is shown dotted, as it corresponds to the poorly understood process of vortex dissipation and final dilution.

The above results indicate an increase by about 2°C of the minimum atmospheric temperature required to form a contrail. The possible global significance of this is best appreciated by reference to Figure 6, which is the result of straightforward application of Appleman's criterion. The region labelled ALWAYS corresponds to temperatures lower than that at points like c in Figure 5, where contrails form even in dry air. The region labelled NEVER corresponds to temperatures greater than T_b in Figure 5, where contrails would not form even in a saturated atmosphere. By inspection of Figure 6, the cruising altitude range (17-20 km) for a Mach 2.4 aircraft contains a significant proportion of conditions lying no more than a few degrees from the ALWAYS limit. Thus there could be a noticeable impact on the frequency of contrail formation associated with wake-induced cooling. It may be, however, that a more significant effect than this contrail probability increase is the reduced dilution and extra confinement time provided by the wake vortices.

The size to which the contrail ice particles can grow is mainly determined by the concentration of active condensation nuclei (cn) in the plume; kinetic limitations are less important, except perhaps for diameters over 10 μm. Unfortunately, not much is known about cn production by engines, and even less about their activation mechanisms. Knollenberg[42] sampled a Sabreliner contrail in saturated ice conditions and estimated 10^{10}/m^3 active cns at the engine exhaust plane. Rosen and McGregor[43] measured photoelectrically the total carbon particle concentration some 600 m behind an F-104 plane. Their data seem to indicate a total particle concentration of about 2.5×10^{10}/m^3 extrapolated to the engine exhaust. On the other hand, Hoffmann and Rosen[44] encountered an 18 hour old SR-71 contrail which had sheared to a horizontal width of 20-90 km (but with a vertical thickness of only 200 m), and estimated emission of 3×10^{13} to 12×10^{13} m^3 particles greater than 0.01 μm (not necessarily all active). The fraction of all particles emitted which become active cns is also uncertain. Hallett et al.[25] measured a conversion fraction of 1 to 3% for JP-4 fuel, but the 3% level was only achieved after aging for 20 hours.

From the example of Figure 6, it is possible to have about 50% of the original vapor in the form of ice particles when the ambient temperature is near the contrail threshold. Assuming also 1.29 kg of water/kg of fuel and p = 50 mb, T_{exit} = 450 K, and letting n (m^3) be the active nucleus concentration at the engine exhaust, we estimate an eventual mean particle size

$$\bar{R}(\mu m) \cong \left[\frac{10^{11}}{n} \right]^{1.3} \tag{20}$$

which, for the range of estimates of n given above implies $\bar{R}$ values between 2 and 0.06 μm.

A 2 μm radius particle of pure water, falling through dry air at 210K, would evaporate fully in about 10 s and settle no more than about 1 cm. This would indicate the lack of any contrail settling. However two modifying factors may occur in the case of an HSCT contrail. a) Lean-burner combustors, being developed for emissions reduction, will produce much less soot than conventional burners—perhaps by two or more orders of magnitude. Active cn levels may be significantly lower still Hallett et al.[25]. This may lead to cn concentrations approaching background levels and hence (Eq. 20) to much larger particles. b) The extended confinement of exhaust products may lead to the formation of significant surface layers of nitric acid trihydrate (NAT) and other hydrated acid species on the ice particles (see Eqs. 21-28). This would lower their vapor pressure and essentially prevent re-evaporation, with the result of a much larger settling distance for a given particle size.

The acid gas processing of the condensed exhaust water begins with the plume/wake chemical effects described in Plume Mixing and Chemistry. The chemistry modeled there includes the formation of acid gases and their precursors (HNO_3/N_2O_5 and H_2SO_4/SO_3). These gases are formed through the scavenging of exhaust OH radicals and reaction with entrained atmospheric O_3. They are then available for heterogeneous chemistry processes that can change exhaust speciation through processes like:

$$N_2O_5 + H_2O \ (c) \rightarrow HNO_3 \ (c) \ , \tag{21}$$

$$SO_3 + H_2O \ (c) \rightarrow H_2SO_4 \ (c) \ , \tag{22}$$

$$HNO_3 + H_2O \ (c) \rightarrow HNO_3 \ (c) \ , \tag{23}$$

$$H_2SO_4 + H_2O \ (c) \rightarrow H_2SO_4 \ (c) \ , \tag{24}$$

$$HCl + H_2O \ (c) \rightarrow HCl \ (c) \ ; \tag{25}$$
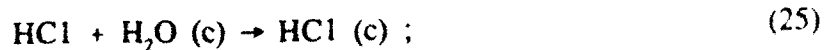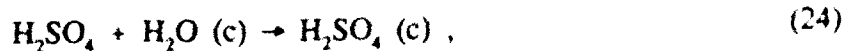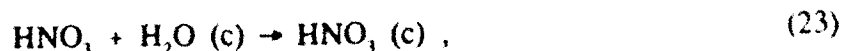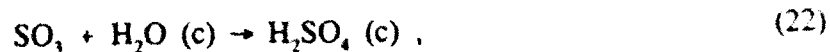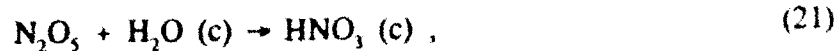
temporarily removing plume and atmospheric acid gases from the gas phase or setting up the liberation of reservoir atmospheric chlorine:

$$ClONO_2 + H_2O \ (c) \rightarrow HOCl \ (c,g) + HNO_3 \ (c) \ , \tag{26}$$

$$ClONO_2 + HCl \ (c) \rightarrow Cl_2 \ (g) + HNO_3 \ (c) \ , \tag{27}$$

$$HCl + HOCl \ (c) \rightarrow Cl_2 \ (g) + H_2O \ (c) \ . \tag{28}$$
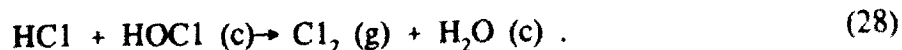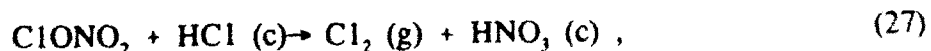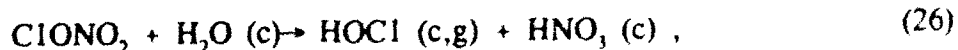
The activation of plume/exhaust soot to ccn will occur on particles through their reaction with acid and oxidizing gases. In future work, we will model both this soot activation process and the kinetic nucleation and growth of contrail particles, a process which depends directly on the degree of plume/wake water vapor supersaturation, determined by the plume/wake temperature

and entrainment/detrainment profiles and the number of active condensation nuclei. Particle formation and growth through the wake dispersal regime depend on more than the simple equilibrium H_2O condensation considered in H_2O Condensation. Clearly, in this heterogeneous chemical environment, the relevant condensation phenomena determine the degree to which gravitational settling can drop the particle and its associated acid gases and exhaust particulates to lower altitudes less conducive to ozone depletion.

SUMMARY AND CONCLUSIONS

The mixing, chemistry and condensation in the exhaust flowfield behind an HSCT were modeled as a first step in following the engine emissions to their eventual deposition in the atmosphere. Finite rate chemistry was simulated internal to an engine for conditions that are representative of engine cycles that would be used in propelling an HSCT. This simulation was used to calculate exhaust emissions at the engine exit plane where super-equilibrium concentrations of CO, NO, NO_2, HNO_3 and OH were estimated to be present.

The exhaust emissions were followed from the engine exit plane using the standard plume flowfield code, SPF-2. The plume code was initialized using estimated emission indices or calculated exit plane concentrations. The chemical kinetics in the plume code were upgraded for these calculations to include the chemistry for atmospherically active species. NO_x in the plume was partially converted to HNO_3 through reaction with the OH radical to leave over 5% of the NO_x as HNO_3 600 m downstream of the exhaust exit. SO_2 was also oxidized (to SO_3) so that in excess of 10% of the SO_x is available for direct conversion to H_2SO_4 upon contact with condensed H_2O.

Equilibrium water condensation was also added to the upgraded plume code to begin to include some of the condensation phenomena needed to incorporate heterogeneous chemical reactivity in the plume. Contrail formation was predicted for several altitude-latitude-season combinations. These predictions based on equilibrium H_2O condensation were consistent with the Appleman algorithm for contrail occurrence.

The SO_3, N_2O_5 and HNO_3 produced in the plume react and/or condense on the aqueous exhaust aerosols to form condensed acid solutions. These species as well as NO_2 and entrained atmospheric O_3 can also oxidize carbonaceous soot particles emitted with the exhaust. The oxidative activation of additional nucleation sites affects the size and quantity of condensed particles available for heterogeneous chemistry. The aerosols formed and activated in the plume are subjected to the vortical flowfield in the wake of the airplane, which transports and processes the particles and gases until the wake disperses.

The vortex wake due to a Mach 2.4 airplane was analyzed to estimate its effects on the transport and mixing of the exhaust emissions. For parameters representative of a low aspect ratio supersonic aircraft, the circulation due to the rolled-up vorticity convects and shears the exhaust plume as it wraps the exhaust gases around the core. Since the emissions are warmer than the ambient, the pressure gradient generated by the vorticity attracts the less dense gas toward the core.

The vorticity has rolled up into a concentrated trailing vortex pair within about 56 wingspans behind the airplane. This vortex wake then propagates in the stratified atmosphere until the mutual interaction between the two vortices of the pair causes reconnection and the formation of elongated elliptical vortex rings at about 560 wingspans. The "capture" of the exhaust plumes by the vortices is dependent on engine placement but, for the case considered, the outboard exhaust is captured at about 90 wingspans while the inboard exhaust takes 350 wingspans. These values depend on the airplane configuration (aspect ratio) but not on its speed (Mach number). However, the speed does affect the intensity of the vortices, their pressure field, and thus the attraction and possibly the confinement of the exhaust.

The same chemistry that occurs in the plume continues as the exhaust is transported and mixed by the vorticity in the wake until wake dispersal, with subsequent atmospheric transport. The kinetics used in calculating the evolution of the plume will be incorporated into the vortex wake model to follow the chemistry from the capture of the exhaust through the dispersal of the wake. The simplified analysis performed in the present study provides insight and estimates of the dominant processes that are occurring throughout the wake and further can be used to generate first order estimates of the flow properties. However it is apparent that the several individual vorticity-induced phenomena are, in fact, strongly coupled and a more detailed, presumably numerical, analysis will be necessary for quantitative estimation of the evolution of the emitted exhaust gases and their transport.

ACKNOWLEDGEMENTS

Table 1. Reaction List for HSCT Internal Engine Flow Model

reaction $\qquad$ rate constant $(\text{cm}^3\text{molecule}^{-1}\text{s}^{-1})$

$$k = A\, e^{(-E/RT)}/T^N$$

reaction	A	N	E/R (K)
$2H + M = H_2 + M$	1.50×10^{-29}	-1.3	0.0
$2O + M = O_2 + M$	5.20×10^{-35}	0.0	-900.0
$H + O + M = OH + M$	1.30×10^{-29}	-1.0	0.0
$OH + H + M = H_2O + M$	6.10×10^{-26}	-2.0	0.0
$CO + O + M = CO_2 + M$	1.70×10^{-33}	0.0	1510.0
$2OH = H_2O + O$	3.50×10^{-16}	1.4	-200.0
$OH + H_2 = H_2O + H$	1.06×10^{-17}	2.0	1490.0
$OH + H = H_2 + O$	8.10×10^{-21}	2.8	1950.0
$OH + O = H + O_2$	7.50×10^{-10}	-0.5	30.0
$OH + CO = CO_2 + H$	2.80×10^{-17}	1.3	-330.0
$H + O_2 + M = HO_2 + M$	1.77×10^{-30}	-1.0	0.0
$H + HO_2 = 2OH$	2.80×10^{-10}	0.0	440.0
$HO_2 + H = H_2 + O_2$	1.00×10^{-10}	0.0	1070.0
$HO_2 + H_2 = H_2O_2 + H$	5.00×10^{-11}	0.0	13100.0
$2OH + M = H_2O_2 + M$	1.60×10^{-33}	-3.0	0.0
$2HO_2 = H_2O_2 + O_2$	3.00×10^{-12}	0.0	0.0
$H_2O_2 + OH = H_2O + HO_2$	2.90×10^{-12}	0.0	160.0
$NO + O = O_2 + N$	6.31×10^{-15}	1.0	20820.0
$O + N_2 = NO + N$	3.02×10^{-10}	0.0	38370.0
$NO + H = OH + N$	4.37×10^{-10}	0.0	25370.0
$NO_2 + H = NO + OH$	5.76×10^{-10}	0.0	740.0
$NO_2 + O = NO + O_2$	1.66×10^{-11}	0.0	300.0
$N_2O + O = 2NO$	1.15×10^{-10}	0.0	13400.0
$N_2O + H = N_2 + OH$	1.26×10^{-10}	0.0	760.0
$NO_2 + M = NO + O + M$	1.82×10^{-08}	0.0	33000.0
$2NO_2 = 2NO + O_2$	3.31×10^{-12}	0.0	13500.0
$HO_2 + OH = H_2O + O_2$	2.40×10^{-08}	-1.0	0.0
$HO_2 + O = OH + O_2$	2.90×10^{-11}	0.0	-200.0
$HO_2 + M = H + O_2 + M$	2.00×10^{-05}	-1.2	24363.0
$CO + O_2 = CO_2 + O$	4.20×10^{-12}	0.0	24000.0
$CO + HO_2 = CO_2 + OH$	2.50×10^{-10}	0.0	11900.0
$H_2O_2 + H = H_2O + OH$	4.00×10^{-11}	0.0	2000.0
$H_2O_2 + O = OH + HO_2$	1.60×10^{-17}	2.0	2000.0
$CO_2 + O = CO + O_2$	2.80×10^{-11}	0.0	26500.0
$NO_2 + OH + M = HNO_3 + M$	2.20×10^{-22}	-3.2	0.0

Table 2. Internal Engine Flow Properties[*]

	combustor equil.	turbine equil.	turbine ODK
p (atm)	13.609	11.3	11.3
T (K)	2050.0	1398.0	1383.0
time (s)	NA	0.0033	0.0033
Mach no.	NA	2.17	2.17
CO	1.20×10^{-4}	1.52×10^{-7}	2.44×10^{-5}
CO_2	6.84×10^{-2}	5.94×10^{-2}	5.93×10^{-2}
H	3.26×10^{-6}	1.21×10^{-9}	1.54×10^{-6}
HNO_3	3.28×10^{-10}	2.09×10^{-11}	6.24×10^{-10}
HO_2	1.61×10^{-6}	1.93×10^{-8}	6.97×10^{-7}
H_2	2.84×10^{-5}	7.91×10^{-8}	7.87×10^{-6}
H_2O	7.61×10^{-2}	6.62×10^{-2}	6.61×10^{-2}
H_2O_2	1.90×10^{-7}	2.61×10^{-9}	1.65×10^{-8}
NO	5.99×10^{-3}	5.54×10^{-4}	5.20×10^{-3}
NO_2	2.17×10^{-5}	3.16×10^{-6}	7.29×10^{-6}
N_2	7.47×10^{-1}	7.54×10^{-1}	7.52×10^{-1}
N_2O	1.08×10^{-6}	3.31×10^{-8}	7.89×10^{-7}
O	7.95×10^{-5}	2.76×10^{-7}	3.23×10^{-5}
OH	9.41×10^{-4}	1.93×10^{-5}	2.09×10^{-4}
O_2	9.23×10^{-2}	1.11×10^{-1}	1.08×10^{-1}

	mixing chamber equil.	mixing chamber ODK	exit plane equil.	exit plane ODK
p (atm)	1.18	1.20	0.042	0.042
T (K)	1046.0	1049.0	430.0	434.0
time (s)	0.006	0.006	0.0009	0.0009
Mach no.	0.26	0.26	2.85	2.84
CO	2.02×10^{-11}	1.07×10^{-5}	5.67×10^{-31}	1.09×10^{-5}
CO_2	3.22×10^{-2}	3.24×10^{-2}	3.22×10^{-2}	3.24×10^{-2}
H	3.52×10^{-14}	1.49×10^{-9}	0.0	6.12×10^{-9}
HNO_3	3.06×10^{-11}	4.46×10^{-9}	4.78×10^{-12}	4.07×10^{-8}
HO_2	3.05×10^{-10}	1.04×10^{-7}	1.03×10^{-20}	9.77×10^{-8}
H_2	2.70×10^{-11}	1.07×10^{-6}	4.17×10^{-28}	1.03×10^{-6}
H_2O	3.57×10^{-2}	3.59×10^{-2}	3.57×10^{-2}	3.59×10^{-2}
H_2O_2	7.23×10^{-11}	2.56×10^{-8}	3.66×10^{-19}	2.44×10^{-8}
NO	4.85×10^{-5}	2.81×10^{-3}	1.66×10^{-11}	2.81×10^{-3}
NO_2	1.76×10^{-6}	8.72×10^{-6}	1.70×10^{-9}	8.73×10^{-6}
N_2	7.66×10^{-1}	7.68×10^{-1}	7.66×10^{-1}	7.68×10^{-1}
N_2O	3.45×10^{-9}	4.30×10^{-7}	8.74×10^{-16}	4.30×10^{-7}
O	2.17×10^{-10}	1.56×10^{-7}	1.22×10^{-27}	1.55×10^{-7}
OH	1.39×10^{-7}	4.21×10^{-6}	8.13×10^{-19}	3.40×10^{-6}
O_2	1.56×10^{-1}	1.56×10^{-1}	1.57×10^{-1}	1.56×10^{-1}

[*] species concentrations are in mole fraction

17-22

Table 3. Initial Conditions for HSCT Plume Flowfield Model[*]

	exhaust	free stream case 1	case 2	case 3
latitude		N47	N47	N85
altitude(km)		18.4	17.85	18.3
date		June 15	January 1	January 1
p(atm)		0.0734	0.0712	0.0573
T (K)	5.61×10^2	2.19×10^2	2.17×10^2	2.05×10^2
v (ft/s)	4.30×10^3	2.34×10^3	2.32×10^3	2.26×10^3
CO	2.37×10^{-5}	1.99×10^{-8}	1.98×10^{-8}	1.69×10^{-8}
CO_2	3.17×10^{-2}	3.50×10^{-4}	3.50×10^{-4}	3.50×10^{-4}
H	1.00×10^{-7}	1.43×10^{-20}	2.81×10^{-21}	0.0
H_2	0.0	5.18×10^{-7}	5.19×10^{-7}	5.20×10^{-7}
H_2O	3.02×10^{-2}	4.20×10^{-6}	4.20×10^{-6}	4.86×10^{-6}
HO_2	0.0	1.02×10^{-12}	3.30×10^{-13}	0.0
H_2O_2	0.0	3.51×10^{-12}	2.11×10^{-12}	0.0
N_2	0.779	0.790	0.790	0.790
NO	4.32×10^{-5}	2.43×10^{-10}	5.87×10^{-11}	0.0
NO_2	4.80×10^{-6}	8.50×10^{-10}	4.29×10^{-10}	0.0
O	0.0	6.06×10^{-13}	3.11×10^{-13}	0.0
OH	1.00×10^{-5}	1.27×10^{-13}	2.76×10^{-14}	0.0
O_2	0.159	0.210	0.210	0.210
O_3	0.0	2.48×10^{-6}	2.46×10^{-6}	3.02×10^{-6}
HNO_3	0.0	3.71×10^{-9}	3.32×10^{-9}	7.39×10^{-9}
NO_3	0.0	1.23×10^{-12}	1.71×10^{-12}	0.0
N_2O_5	0.0	3.57×10^{-10}	6.09×10^{-10}	0.0
SO_2	6.91×10^{-6}	0.0	0.0	0.0

[*] species concentrations are in mole fraction

Table 4. SPF Equilibrium H_2O Condensation Predictions

	case 1	case 2	case 3
latitude	N47	N47	N85
altitude(km)	18 4	17.85	18.3
date	June 15	January 1	January 1
T(K)	219.3	216.7	205 2
p(atm)	0.0734	0.0712	0.0573
SPF Equilibrium H_2O Condensation predictions	no	no	yes
Condensation algorithm predictions (Ref. 21)	never	uncertain	always

Table 5. Reactions List for Plume Chemistry/Mixing Model

reaction — rate constant $(cm^3 molecule^{-1} s^{-1})$

$$k = A\, e^{(-E/RT)}/T^N$$

reaction	A	N	E/R (K)
$H + O_2 + M = HO_2 + M$	5.2×10^{-28}	1.6	0.0
$OH + O = H + O_2$	2.2×10^{-11}	0.0	240.0
$OH + H_2 = H_2O + H$	5.5×10^{-12}	0.0	-4000.0
$OH + OH = H_2O + O$	4.2×10^{-12}	0.0	-480.0
$OH + OH + M = H_2O_2 + M$	6.6×10^{-29}	0.8	0.0
$OH + HO_2 = H_2O + O_2$	4.8×10^{-11}	0.0	500.0
$OH + H_2O_2 = H_2O + HO_2$	2.9×10^{-12}	0.0	-320.0
$HO_2 + O = OH + O_2$	3.0×10^{-11}	0.0	400.0
$HO_2 + H = OH + OH$	4.2×10^{-10}	0.0	1900.0
$HO_2 + H = H_2 + O_2$	4.2×10^{-11}	0.0	-700.0
$HO_2 + HO_2 = H_2O_2 + O_2$	2.3×10^{-13}	0.0	1200.0
$H_2O_2 + O = OH + HO_2$	1.4×10^{-12}	0.0	-4000.0
$N + O_2 = NO + O$	1.5×10^{-11}	0.0	-7200.0
$N + NO = N_2 + O$	3.4×10^{-11}	0.0	0.0
$NO + O + M = NO_2 + M$	4.7×10^{-28}	1.5	0.0
$NO + HO_2 = NO_2 + OH$	3.7×10^{-12}	0.0	480.0
$NO + NO_3 = NO_2 + NO_2$	1.7×10^{-11}	0.0	300.0
$NO_2 + O = NO + O_2$	6.5×10^{-12}	0.0	240.0
$NO_2 + O + M = NO_3 + M$	8.1×10^{-27}	2.0	0.0
$NO_2 + OH + M = HNO_3 + M$	2.2×10^{-22}	3.2	0.0
$NO_2 + NO_3 + M = N_2O_5 + M$	9.9×10^{-20}	4.3	0.0
$NO_3 + O = NO_2 + O_2$	1.0×10^{-11}	0.0	0.0
$O + O_2 + M = O_3 + M$	3.0×10^{-28}	2.3	0.0
$O + O_3 = O_2 + O_2$	8.0×10^{-12}	0.0	-4120.0
$H + O_3 = OH + O_2$	1.4×10^{-10}	0.0	-940.0
$OH + O_3 = HO_2 + O_2$	1.6×10^{-12}	0.0	-1880.0
$NO + O_3 = NO_2 + O_2$	2.0×10^{-12}	0.0	-2800.0
$NO_2 + O_3 = NO_3 + O_2$	1.2×10^{-13}	0.0	-4900.0
$OH + HNO_3 = H_2O + NO_3$	7.2×10^{-15}	0.0	1570.0
$SO + O_2 = SO_2 + O$	1.4×10^{-13}	0.0	-4550.0
$SO + O_3 = SO_2 + O_2$	4.5×10^{-12}	0.0	-2340.0
$SO_2 + OH + M = HSO_3 + M$	7.5×10^{-23}	3.3	0.0
$HSO_3 + O_2 = HO_2 + SO_3$	4.0×10^{-13}	0.0	0.0
$SO + NO_2 = SO_2 + NO$	1.4×10^{-11}	0.0	0.0
$SO + OH = SO_2 + H$	8.6×10^{-11}	0.0	0.0
$SO_2 + O + M = SO_3 + M$	4.0×10^{-32}	0.0	-2000.0

Table 6. Plume Centerline NO_x, SO_x, and Oxidizer Speciation (Mach 2.4; N47; 18.4 km; June 15)

species	mole fractions			
	exit plane	500 ft	1000 ft	2000 ft
OH	1.0×10^{-5}	1.4×10^{-7}	1.4×10^{-8}	1.9×10^{-9}
O_3	0.0	2.1×10^{-6}	2.4×10^{-6}	2.4×10^{-6}
NO	4.3×10^{-5}	6.2×10^{-6}	2.0×10^{-6}	9.4×10^{-7}
NO_2	4.8×10^{-6}	6.2×10^{-7}	2.0×10^{-7}	1.0×10^{-7}
NO_3	0.0	2.1×10^{-11}	4.5×10^{-12}	8.1×10^{-13}
N_2O_5	0.0	2.1×10^{-10}	3.2×10^{-10}	3.4×10^{-10}
HNO_3	0.0	2.4×10^{-7}	1.1×10^{-7}	5.9×10^{-8}
SO_2	6.9×10^{-6}	9.5×10^{-7}	3.0×10^{-7}	1.4×10^{-7}
SO_3	0.0	6.8×10^{-8}	3.2×10^{-8}	1.6×10^{-8}
NO_2/NO	0.11	0.10	0.10	0.11
HNO_3/NO_x	—	0.035	0.05	0.056
SO_3/SO_2	—	0.07	0.11	0.11

Table 7. Assumed Aircraft Data for Wake Dynamics

Wing area: $A_W = 660 \text{ m}^2$ Span: $b = 39$ m

Weight (cruise): $W = 2.76 \times 10^6$ N

Flight altitude: $Z = 17.4$ km   Aspect Ratio: $\dfrac{b^2}{A_W} = 2.30$

Mach No.: $M = 2.4$ Speed: $v = 708$ m/s

Atmosphere: $\rho = 0.135 \text{ kg/m}^3$, $T = 217$ K, $p = 83.8$ mb

Lift coefficient: $C_L = 0.124$

Exhaust temperature: $T_e = 445$ K

Fuel/air ratio: 0.0155

Airflow: $m_a = 97$ Kg/s/engine

Exhaust speed (relative):   1430 m/s

Wake time scale: $\tau = 2\dfrac{AR}{C_L}\dfrac{b}{v} = \dfrac{\rho v b^3}{W} = 2.04$ s

Vorticity roll-up time: $t_{r.u.} \cong 1.5\tau = 3.07$ s

Vorticity roll-up distance: $x_{r.u.} = vt_{r.u.} = 2170$ m (56 b)

Rolled-up vortex spacing: $2\bar{y} = \dfrac{\pi}{4}b = 30.6$ m

Centerline vortex circulation: $\Gamma_0 = \dfrac{4}{\pi}\dfrac{W}{\rho v v} = 943 \text{ m}^2/\text{s}$

Self-induced descent velocity: $w_0 = \dfrac{\Gamma_0}{2\pi(2\bar{y})} = 4.90$ m/s

Vortex break-up time: $t_{v.b.} \cong 15\tau = 30.7$ s

Vortex break-up distance: $x_{v.b.} = vt_{v.b.} = 21.700$ m (556 b)
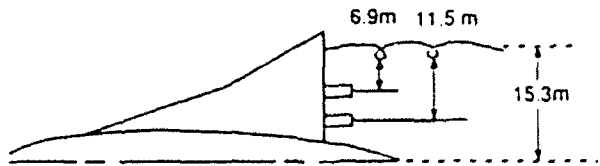
Figure 1. Engine location with respect to rolled-up vortex core. The core is at $(\pi/4)(b/2)$ from centerline.
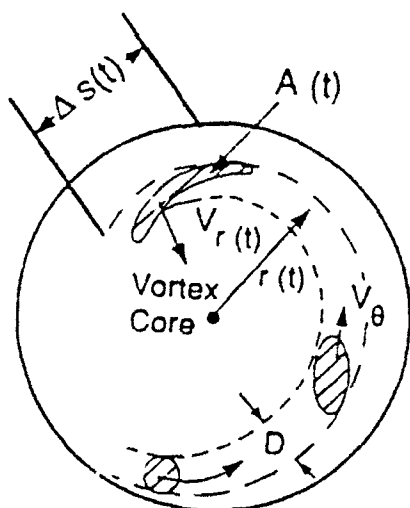

Figure 2. Geometry of plume trapping in a plane transverse to the flight path.
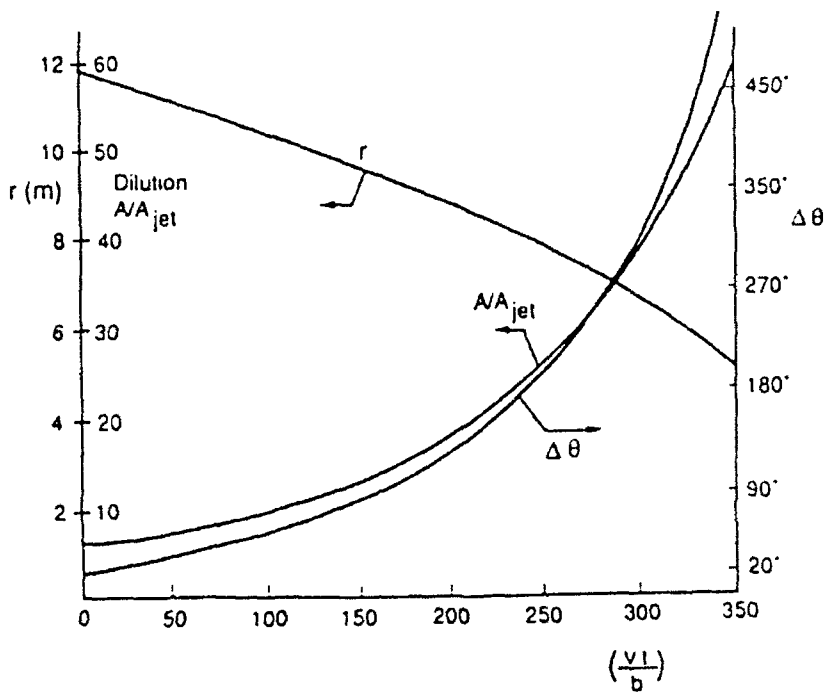
Figure 3. Inner engine jet mixing and displacement. Initial jet diameter, $D_0 = 5$ m, distance from vortex core, $r_0 = 11.5$ m, and density difference, $(\Delta\rho/\rho)_0 = 0.0816$.
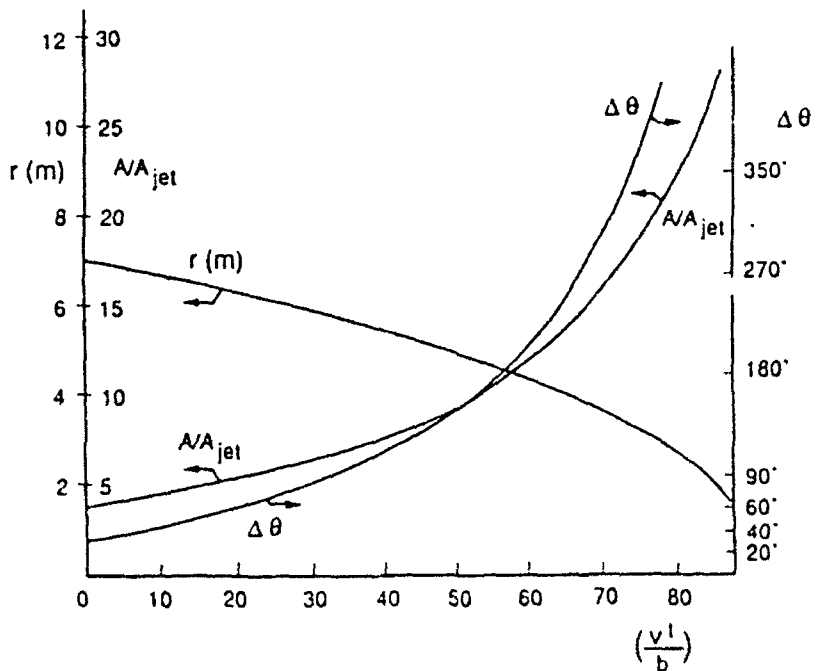

Figure 4. Outer engine jet mixing and displacement. Initial jet diameter, $D_0 = 4$ m, distance from vortex core, $r_0 = 6.9$ m, and density difference, $(\Delta\rho/\rho)_0 = 0.122$.

17-27
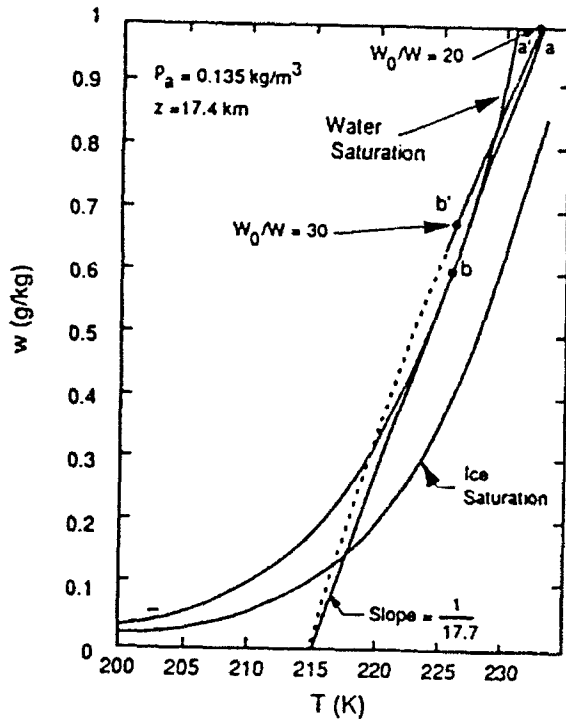
Figure 5. Temperature—Water vapor content (T-w) plane with water and ice saturation curves overlaying exhaust dilution trajectories.
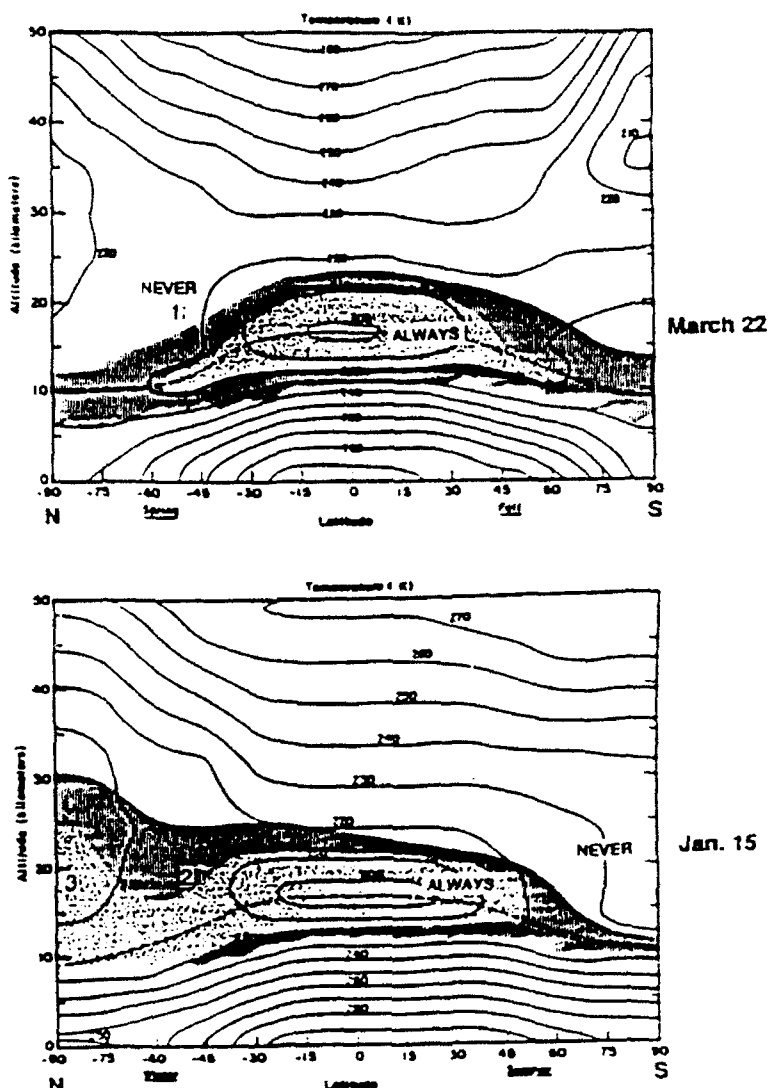
Figure 6. Predictions using equilibrium, fully-mixed condensation algorithm.

REFERENCES

1. Boeing Commercial Airplane Co., "High-speed civil transport study" NAS Contractor Rep. CR-4233, 116 pp., 1989.

2. Douglas Aircraft Co., "Study of high-speed civil transports" NASA Contractor Rep. CR-4235, 168 pp., 1989.

3. Johnston, H.S., Prather, M.J. and Watson, R.T., "The Atmospheric Effects of Stratospheric Aircraft: A Topical Review," NASA Ref. Publ. 1250, January 1991.

4. Douglass, A.R., Carroll, M.A., DeMore, W.B., Holton, J.R., Isakson, I.S.A., Johnston, H.S. and Ko, M.W.K., "The Atmospheric Effects of Stratospheric Aircraft, A Current Consensus," NASA Ref. Publ. 1217, January 1991.

5. Weisenstein, D., Ko, M.K.W., Rodriguez, J.M. and Sze, N.D., "Impact of Heterogeneous Chemistry on Model-Calculated Ozone Changes due to HSCT Aircraft," to be submitted to *Geophys. Res. Letts*.

6. Papamoschou, D., and Roshko, A., "Observations of Supersonic Free Shear Layers," Paper AIAA-86-0162 from AIAA 24th Aerospace Sci. Meeting, Reno, NV, 1986.

7. Gutmark, E., Schadow, K.C. and Wilson, K.J., "Mixing Enhancement in Coaxial Supersonic Jets," Paper AIAA-89-1812 from AIAA 20th Fluid Dynamics, Plasma Dynamics, and Lasers Conference, Buffalo, NY, 1989.

8. Hoshizaki, H., Anderson, L.B., Conti, R.J., Farlow, N, Meyer, J.W., Overcamp, T., Redler, K.O., and Watson, V., "Aircraft Wake Microscale Phenomena," Chapter 2 in CIAP Monograph 3, Department of Transportation Washington, DC, DOT-TST-75-53.

9. Overcamp, T.J. and Fay, J.A., "Dispersion and Subsidence of the Exhaust of a Supersonic Transport in the Stratosphere," *J. Aircraft*, Vol. 10, 1973, pp. 720-728.

10. Wofsy, S.C., Salawitch, R.J., Yatteau, J.H., McElroy, M.B., Gandrud, B.W., Dye, J.E. and Baumgardner, D., "Condensation of HNO_3 on Falling Ice Particles: Mechanism for Denitrification of the Polar Stratosphere," *Geophys. Res. Letts.*, Vol. 17, March Supplement 1990, pp. 449-452.

11. Fahey, D.W., Kelly, K.K., Kawa, S.R., Tuck, A.F., Lowenstein, M., Chan, K.R. and Heidt, L.E., "Observations of Denitrification and Dehydration in the Winter Polar Stratospheres," Nature, Vol. 344, 1990, pp. 321-324.

12. Yousefian, Y., Weinberg, M.H. and Haimes, R., "PACKAGE: A Computer Program for the Calculation of Partial Chemical Equilibrium/Partial Chemical Rate Controlled Composition of Multiphase Mixtures Under One-Dimensional Steady Flow," Aerodyne Research, Inc., Report No. ARI-RR-177, February 1980.

13. Tsang, W. and Hampson, R.F., "Chemical Kinetic Data Base for Combustion Chemistry. Part I. Methane and Related Compounds," *J. Phys. and Chem. Ref. Data*, Vol. 15, 1986, pp. 1087-1279.

14. Miller, J.A. and Bowman, C.T., "Mechanism and Modeling of Nitrogen Chemistry in Combustion," *Prog. Energy Combust. Sci.*, Vol. 15, 1989, p. 287.

15. Matulaitis, J.A. and Krause, F.H., GE Aircraft Engines; Cincinnati, OH; personal communications, 1990.

16. McGregor, W.K., Seiber, B.L. and Few, J.D., "Concentrations of OH and NO in YJ93-GE-3 Engine Exhausts Measured In Situ by Narrow-Line UV Absorption," *Proceedings of the Second Conference on CIAP*, 1972, pp. 214-228. Few, J.D., and Lowry, H.S., III "Reevaluation of Nitric Oxide Concentration in Exhaust of Jet Engines and Combustors," AEDC-TR-80-65, 1981.

17. Dash, S.M., Pergament, H.S. and Thorpe, R.D., "The JANNAF Standard Plume Flowfield Model: Modular Approach, Computational Features and Preliminary Results," *Proceedings of the JANNAF 11th Plume Technology Meeting*, CPIA Pub. 306, 1979, pp. 345-442.

18. 1990 Conditions Atmospheric Chemistry Data, Atmospheric and Environmental Research, personal communication, 1990.

19. The emission index for NO_x is reported as the mass equivalent of NO_2. This notation $(EI(NO_2)NO_x)$ resolves any possible ambiguities associated with NO_x EIs and allows the reporting convention in terms of NO_2 to be explicitly indicated. Clearly, EIs for NO and NO_2 can only be meaningfully summed to NO_x if the preceding subscripts match.

20. An emission number of 5 was chosen as it represents a design goal of the NASA HSRP program and has been used in initial atmospheric impact assessment calculations—see Ref. 2.

21. Appleman, H.S., "The Formation of Exhaust Condensation Trails by Jet Aircraft," *Bull. Amer. Met. Soc.*, Vol. 34, January 1953, pp. 14-20. Also U.S. Air Force Air Weather Service, "Forecasting Aircraft Condensation Trails," Chapter 1 of the Air Weather Service Manual 105-100 (1960), reissued as Report No. AWS/TR-81001, September 1981.

22. DeMore, W.B., Sander, S.D., Golden, D.M., Molina, M.J., Hampson, R.F., Kurylo, M.J., Howard, C.J. and Ravishankara, A.R., "Chemical Kinetics and Photochemical Data for Use in Stratospheric Modeling," JPL Publication 90-1, Jet Propulsion Laboratory, Pasadena, CA, January 1990.

23. Ahkter, M.S., Chughatai, R.A. and Smith, D.M., "Reaction of Hexane Soot with NO_2/N_2O_4," J. Phys. Chem., Vol. 88, 1984, pp. 5334-5342.

24. Smith, D.M., Welch, W.F., Jassim, J.A., Chughatai, A.R. and Stedman, D.N., "Soot-Ozone Reaction Kinetics: Spectroscopic and Gravimetric Studies," *Appl. Spectros.*, Vol. 42, Nov./Dec. 1988, pp. 1473-1482.

25. Hallett, J., Hudson, J.G. and Rogers, C.F., "Characterization of Combustion Aerosols for Haze and Cloud Formation," *Aerosol Sci. Tech.*, Vol 10, 1989, pp. 70-83. Also Hudson, J.G., Hallett, J. and Rogers, C.F., "Field and Laboratory Measurements of Cloud-Forming Properties of Combustion Aerosols," *J. Geophys. Res.*, Vol. 96, June 1991, pp. 10,847-10,859.

26. CIAP, 1975, Monograph 2 "Propulsion Effluents in the Stratosphere," DOT-TST-75-52, 485 pp. NTIS, Springfield, VA.

27. CIAP, 1975, Monograph 3 "The Stratosphere Perturbed by Propulsion Effluents," DOT-TST-75-53, 765 pp. NTIS, Springfield, VA.

28. Hoshizaki, H.L., Anderson, L.B. and Conti, R.J., "High Altitude Aircraft Wake Dynamics," *Proc. 2nd Conf. on CIAP*, DOT-TSC-OST-73-4, 1972, pp. 263-284.

29. Holdeman, J.D., "Dispersion and Dilution of Jet Aircraft Exhaust at High-Altitude Flight Conditions," *J. Aircraft*, Vol. 11, 1974, pp. 483-487.

30. Nielsen, J.N., Stahara, S.S., and Woolley, J.P., "Injection and Dispersion of Engine Exhaust Products by Trailing Vortices for Supersonic Flight in the Stratosphere," Paper AIAA 74-42 from AIAA 12th Aerospace Sci. Meeting, 1974.

31. Farlow, N.H., Watson, V.R., Lowenstein, M., and Chan R.L., "Measurement of Supersonic Jet Aircraft Wakes in the Stratosphere," Second Int. Conf. on Environmental Impact of Aerospace Operations in the High Atmosphere, Am. Meteorology Soc., Boston, 1974, pp. 53-58.

32. Scorer, R.S. and Davenport, L.J., "Contrails and Aircraft Downwash," *J. Fluid Mech.*, Vol. 43, 1970, pp. 451-464.

33. Donaldson, C. DuP. and Bilanin, A., "Vortex Wake of Conventional Aircraft," AGARDOGRAPH 204, 1975.

34. Widnall, S.E., "The Structure and Dynamics of Vortex Filaments," *Annual Rev. Fluid Mech.*, Vol. 7, 1975, pp. 141-165.

35. Bera, R.K., "Do Inviscid Vortex Sheets Roll-up?" Project Document CF 9010, National Aeronautical Laboratory, Bangalore, India, May 1990.

36. Liu, H.T. and Srnsky, R.A., "Laboratory Investigations of Atmospheric Effects on Vortex Wakes," Flow Research, Inc., Flow Tech. Rep. No. 497, February 1990.

37. Schetz, J., **Injection and Mixing in Turbulent Flow**, *Prog. Aero. and Astro.*, Vol. 68, 1980, pp. 52-61.

38. Morton, B.R., Taylor, G.I., and Turner, J.S., "Turbulent Gravitational Convection from Maintained and Instantaneous Sources," *Proc. Royal Soc. London A*, Vol. 234, 1956, pp. 1-23.

39. Dhanak, M.R. and DeBernardinis, B., "The Evolution of an Elliptic Vortex Ring," *J. Fluid Mech.*, Vol. 109, 1981, pp. 189-216.

40. Glezer, A. and Coles, "An Experimental Study of a Turbulent Vortex Ring," *J. Fluid Mech.*, Vol. 211, 1990, pp. 243-283.

41. Greene, G.C., "An Approximate Model of Vortex Decay in the Atmosphere," *J. Aircraft*, Vol. 23, July 1986, pp. 566-573.

42. Knollenberg, R.G., "Measurement of the Growth of the Ice Budget in a Persisting Contrail," *J. Atm. Sci.*, Vol. 29, October 1972, pp. 1367-1374.

43. Rosen, J.M. and McGregor, R., "Jet Engine Soot Emission Measured at Altitude," *J. Aircraft*, Vol. 11, 1974, pp. 243-245.

44. Hoffmann, D.J. and Rosen, J.M., "Balloon Observations of a Particle Layer Injected by a Stratospheric Aircraft at 23 km," *Geophys. Res. Letts.*, Vol. 5, June 1978, pp. 511-514.

APPENDIX A

Buoyant Turbulent Jet in a Co-flow

Consider the jet depicted in Figure A1, issuing with some velocity and temperature excess into a parallel stream. A top-hat model of the distributions will be adopted for simplicity. The fluxes of axial momentum and of enthalpy will be conserved, while the vertical momentum flux increases with distance due to the buoyancy. The convection velocity will be approximated by the external velocity u_e. We then have

$$\rho_e u_e (u - u_e) \frac{\pi D^2}{4} = F = \text{constant} , \qquad (A.1)$$

$$\rho_e u_e c_p (T - T_e) \frac{\pi D^2}{4} = Q = \text{constant} , \qquad (A.2)$$

$$\frac{d}{dx} \left[\rho_e u_e w \frac{\pi D^2}{4} \right] = \rho_e \frac{T - T_e}{T_e} g \frac{\pi D^2}{4} . \qquad (A.3)$$

These equations must be supplemented by one which describes the turbulent diffusion and its effect on jet growth. In general,

$$u_e \frac{dD^2}{dx} = 4D_t \qquad (A.4)$$
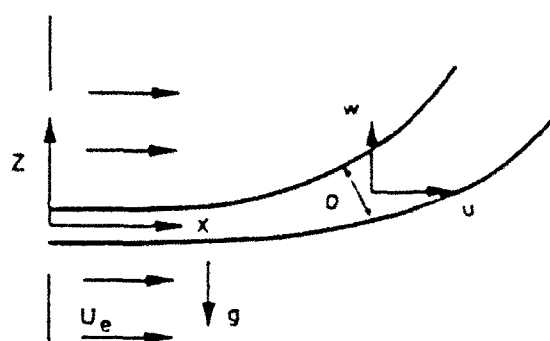
Figure A1. Buoyant jet geometry.

Where D_t is the "turbulent diffusivity". For a non-buoyant jet, a reasonable approximation is[37] $D_t = kD$ $(u-u_e)$, with $k = 0.016$. For a non-flowing cylindrical plume the Morton-Taylor-Turner[38] model gives $Dt = \alpha Dw$ $(\alpha \simeq 0.3)$. These two limiting forms can be interpolated by assuming

$$D_t = K \ D \ \sqrt{a^2 w^2 + (u - u_e)^2} \quad , \qquad\qquad (A.5)$$

where $a = \alpha/K \simeq 19$.

For the case of an engine exhaust in flight $(u_e = v)$, F represents the engine's thrust, and Q its thermal energy output. Hence, if η_{ov} is the overall propulsive efficiency,

$$\frac{Fu_e}{Q} = \frac{\eta_{ov}}{1 - \eta_{ov}} \quad , \qquad\qquad (A.6)$$

To integrate these equations, $u-u_e$ from Eq. (A.1) and w from Eq. (A.3) (after integrating) are substituted into (A.5) to give D_t as a function of D and x. This is then substituted in (A.4), and integration gives the results quoted in Eqs. (4a)-(4d).

APPENDIX B

A Model for Turbulent Vortex Ring Evolution

The similarity results obtained experimentally by Glezer and Coles[40] for the growth and slowing down of a turbulent vortex ring can be understood and extrapolated by a simple model based on an entrainment hypothesis. We assume:

a.   The vortex core cross section increases at a rate proportional to its own radius and to the ring velocity. With reference to Figure B1.,

$$\frac{d(\pi a^2)}{dt} = \beta \ av \quad . \qquad\qquad (B.1)$$

where β is an empirical constant.

b.   Geometrical similarity is preserved, i.e., R and a grow in the same proportion:

$$\frac{\alpha}{\alpha_0} = \frac{R}{R_0} \quad .$$

(B.2)

c. The vertical momentum is preserved. In combination with (B.2), this gives

$$\alpha^3 v = \alpha_0^3 v_0 \quad .$$

(B.3)
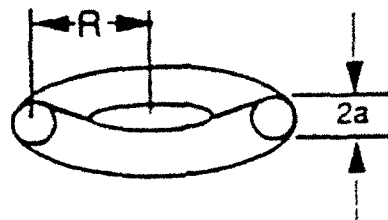
Figure B1. Geometry of descending vortex ring.

Eqs. (B.1), (B.2) and (B.3) can be combined to obtain explicit laws for the time histories of the various quantities, including the distance x travelled by the ring. Ref. 37 introduced the distance x_0 and time t_0 which act as the origin for the measured self-similarity. These quantities are both negative, i.e., the "virtual origin" occurs upstream of the point of creation of the vortex ring. Our analytical results, of the same form as the data trends, are

$$\frac{\alpha}{\alpha_0} = \frac{R}{R_0} = (1 - \frac{t}{t_0})^{1/4} \quad ,$$

(B.4)

$$\frac{v}{v_0} = (1 - \frac{t}{t_0})^{-3/4} \quad ,$$

(B.5)

$$\frac{x}{x_0} = 1 - (1 - \frac{t}{t_0})^{1/4} \quad ,$$

(B.6)

where

$$t_0 = -\frac{\pi \alpha_0}{2\beta v_0} \quad , \tag{B.7}$$

$$x_0 = -\frac{2\pi \alpha_0}{\beta} \quad . \tag{B.8}$$

In Glezer's experiments,[40] $v_0 = 128$ cm/s for the piston producing the rings. For the ring itself, we take $v_0 = 64$ m/s. Also, $R_0 = 0.953$ cm, and $a_0 \simeq 0.2 R_0$, as estimated from the data. The measured virtual origin parameters were

$$t_0 = -0.44 \text{ s}, \quad x_0 = -145 \text{ cm}.$$

Using these results, (B.8) gives $\beta = 0.00825$, while (B.7) gives $\beta = 0.0106$. Thus the model appears to give a reasonable description of the data using

$$\beta \simeq 0.01 \quad . \tag{B.9}$$

CONTROL OF WING-TIP VORTICES

Daniel M. Nosenchuck
William S. Flannery
Garry L. Brown
Department of Mechanical and Aerospace Engineering
Princeton University
Princeton, New Jersey 08544

ABSTRACT

Experiments have been carried out which demonstrate the potential of using a redistribution of vorticity (through small changes in wing geometry) to affect significantly the core size of a wing-tip vortex. Prior to the experiments, the particular change in geometry which produced the increased core area was predicted using a numerical simulation and an optimization procedure.

INTRODUCTION

Increased understanding of the underlying structure in various turbulent flows has opened the way to some level of control. The principal technological goal is the control of flows at high Reynolds number with flows over lifting surfaces being of particular interest. 'Tip-vortex' flows and longitudinal vortical flows resulting from three dimensional separation for both aerodynamic (e.g., wings, rotors, flaps, control surfaces) and hydrodynamic (e.g., submarine sails, bow-planes, stern appendages, propellor) lifting surfaces are possible areas of application. In aviation the formation of strong longitudinal vortices behind heavy aircraft developing large lift coefficients (Ref. 1) accounts for large induced transverse wake velocities that lead to large separation distances and relatively long time intervals (e.g., Federal Aviation Regulation mandated 2-minute separation minimums between subsequent takeoffs and/or landings) to avoid hazardous flight conditions.

Numerous approaches to modify wing-tip and other longitudinal vortices have been proposed and studied (e.g., Refs. 2 and 3)). These approaches include methods which either deal with decreasing the initial strength of the longitudinal vorticity as it forms, or attempt to modify the behavior of the vortex once it forms. Examples of the former approach include altering wing/body designs to reduce transverse pressure gradients and the use of active/passive control surfaces to modify span-loading and minimize control

surface deflections. The latter approach often focuses on the creation of additional vorticity to alter the downstream trajectory of the primary vortex.

Recent work on axisymmetric vortex breakdown (Ref. 4) has drawn attention to the two helices in a swirling flow, namely the velocity and vorticity helix, and the specific role of the ratio of the velocity helix angle to the vorticity helix angle in determining whether or not vortex breakdown is possible. This work led us to explore further the possibility of controlling the longitudinal vorticity shed from a lifting surface by mechanisms that could affect these helix angles. One mechanism that seemed promising was the possibility of affecting the initial stability of the distribution of vorticity shed from a lifting surface. It is well-known from studies of mixing layers, for example, and the forcing of other free shear flows that redistributing in time the magnitude of the shed vorticity can greatly increase the rate of growth of a primary initial instability and subsequently the overall rate due to the interaction and amalgamation of 'vortices' or areas of concentration of vorticity. These were the principal motivations for the present work.

APPROACH

The rollup of a trailing vortex sheet is dependent on the circulation per unit span and corresponding wing loading (and hence geometry). Thus modifications to the planform will alter the spanwise distribution of shed vorticity. It was our intention to seek a re-distribution of the vorticity which, because of a change in the stability of the sheet, would lead to a significantly increased vortex growth rate. In that case there would be an attendant decrease in the velocity helix angle and a corresponding decrease in the maximum azimuthal velocity which would help to mitigate the wake hazard. A computational approach was developed which utilized simple analytical and numerical vortex-based simulation techniques to predict the rollup process as a function of wing geometry and upstream conditions. This method was then used as the core of an automatic optimization procedure where wing-geometry perturbation was primarily driven by the resultant vortex growth. By this procedure it was found that small planform perturbations near the tip led to the desired increase in core growth rates of greater than twice the baseline core diameter in the near wake (at one-half chord downstream of the trailing edge).

The emphasis of the current work is on high Reynolds-number attached flows, at relatively low AOA with the numerical simulation used as a design tool to filter candidate geometries for their potential to promote instabilities leading to rapid growth of the longitudinal vortex in the near wake. Thus, the emphasis was placed on developing a fast approximate simulation procedure which incorporated the essential physical mechanisms and which might be used to estimate vortex locations and radii within five chords downstream of the trailing edge.

Because of the approximations used in the numerical simulation, it was essential to establish a corresponding experiment to confirm whether the predicted geometry indeed produced a vortex instability and if so, whether the larger 'core' area persisted

downstream for a significant distance or reorganized into a tight vortex. Water channel validation experiments were performed at low Reynolds number ($Re_{chord} \approx 2 \times 10^4$) due to facility limitations. Because the simulation is based on a large Reynolds number approximation, it was anticipated that the low-speed experiments could represent a more challenging case, although the first-order effects of turbulent diffusion at high Reynolds number may be similar to laminar diffusion at this much lower Reynolds number.

The experiments were qualitative, with flow visualization being the prime diagnostic. A laser-fluorescing dye was used to mark the flow in the vicinity of the tip. Laser sheets were then used to obtain cross-sections of the tip-vortex in the wake, which were qualitatively compared with the predicted vortex.

VORTEX CONTROL INVESTIGATIONS

Numerical Vortex Simulation

A first-approximation numerical simulation was developed to predict flows with predominantly longitudinal vorticity in the wake of lifting surfaces. The procedure is based on direct vortex-element interactions, and uses an initial distribution of vorticity obtained from analysis, other numerical solutions, or experiment. The initial vortex sheet strength is directly related to the geometry (chord distribution $c(z)$ and local angle-of-attack (AOA) $\alpha_0 + \alpha(z)$ dependent on spanwise camber-line twist), as well as upstream conditions, which may vary with spanwise distance (e.g., $U_\infty(z)$. At present, wake development is based on a point-vortex direct interaction, and simulates quasi-three-dimensional steady flows, with negligible transverse vorticity ($\omega_y + \omega_z \approx 0$). A detailed description of the code, called CWV-10 (Complex-geometry Wake Vortex), will be published elsewhere.

The inputs to the calculation were the chord $c(z)$ and mean-line $mf(x,y)$ distributions of lifting surfaces, the upstream velocity field $U_\infty(z)$ and mean angle-of-attack α_0, and other relevant parameters. The outputs include pseudo 3D vorticity field $\omega_x(x,y,z)$ and 3D particle paths, velocity field $v(x,y,z)$ and $\omega(x,y,z)$, and the tip-vortex centroid location $(y,z)_{r-core(x)}$, a measure of the mean core radius and wake perturbation moments.

To find a wing geometry that would result in increased vortex growth, the radius was used as part of a cost function in a simple optimization procedure. As shown in Figure 1, the code was given a set of computer-generated wing-geometry parameters that were based on the previous simulations. These parameters were constrained to alter geometry only in the tip region (with approximately constant planform area maintained) where the longitudinal vorticity is relatively large, and contributes most to the rollup process. A list of perturbation functions was provided to the optimizer, including sawtooth and sinusoidal trailing-edge planform perturbations and damping functions. Relevant baseline wing parameters, such as local chord and AOA distributions, were also made available to the optimizer as possible modifiers to the perturbation functions.

For optimization purposes, a tip-vortex growth to twice the baseline diameter within one-half of a chord downstream of the trailing edge was specified. Typical runs to simulate and judge a single candidate design varied between approximately 5 minutes and 100 minutes on a VAXstation 3100 based on the number of vortex elements and extent of the streamwise domain.

The CWV-10 code is intended for use as a preliminary design tool used to rapidly screen candidate hydrodynamic slender lifting-surface designs for certain attributes, such as tip-vortex growth rates. Once a particular design has been targeted for further study based on the initial filtering operation, more detailed codes and/or experimental models can be used.

Experiments

Experiments on baseline and modified wings were performed in the Moody Hydrodynamics Laboratory at Princeton University. A water channel with a test section 8.2 m long and 1.5 m wide provided a test environment with large spatial and long temporal scales. Flow management foam, screens, and honeycomb, generate spanwise flow nonuniformities of less than 5 % and a turbulence intensity of less than 0.3% in the test section free stream. The test-section velocity used in all experiments was 14 cm/sec. The walls of the test-section are glass to permit flow visualization.

A baseline model (based on an idealization of a low aspect-ratio submarine sail) was fabricated out of aluminum. The baseline planform geometry consisted of an elliptical leading edge, constant width after-body, and wedge trailing edge. As seen in Figure 2, the model had a root chord of 15.2 cm, with a half span of 15.2 cm. The model was mounted on a ground plane.

The technique of scanning laser-sheet visualization (Ref. 5), was used to provide real-time three-dimensional nonsteady volumetric flow imaging. Disodium fluorescein dye was injected into the leading edge of the model near the tip to mark the tip-vortex flow. A rotating polygonal mirror was used to position the laser sheet in the y,z (transverse) plane at 40 discrete locations, typically between -0.5 < x/c < -3.0. The mirror stepping rate was variable, and could step rather slowly to follow the free stream velocity, or rapidly (at 10,000 steps/sec) to 'freeze' the wake. A 128 x 128 x 8-bit Reticon digital camera recorded the images. The resultant data, consisting of a series of two-dimensional sheets, represented a space-filling three-dimensional volume. The data were digitally compressed and transferred in real-time to a VAX 8200 for subsequent display processing on an SGI IRIS 4D-70GT graphics workstation. The net effect is to record the entire laser-dye field each time the sheet is traversed through the flow. Qualitative results from these data are discussed in the next section.

RESULTS

Numerical Investigation of Tip-Vortex Flows

The baseline model used for numerical and experimental investigations is described in the Vortex Control Investigations – Experiments section. A number of candidate tip perturbations were automatically generated and evaluated. Several are shown in Figure 3. In these examples, the perturbation function is a damped sinusoid, scaled by the local chord $c(z)$. The variations in trailing edge geometries are primarily due to wavenumber k and perturbation amplitude a_0. A constraint to the optimizer was that the integrated wing-loading could vary no more than 2 % from the baseline case.

After investigating nearly 300 candidate designs in the perturbation parameter space with limited success, the optimizer found a functional form with a particular wavenumber, amplitude, and spanwise position that resulted in the growth of the tip vortex to twice the unperturbed radius at $x/c = -0.5$. This initial result from the optimization runs is shown in Figure 4, along with the predicted tip-vortex growth rates for the baseline and modified wings. In this case, the wing is untwisted, and has only trailing-edge planform perturbations.

It is interesting to note that the mere presence of spanwise fluctuations in vortex strength near the tip is not sufficient to induce increased vortex growth. The results of a wing modification which did not result in the required growth compared to the baseline is shown in Figure 5. Case A represents a tip perturbation, similar to that shown in the previous figure, which diffuses the core, while Case B represents a comparable 'inverted' alteration of planform which did not significantly alter the predicted growth of the vortex core.

Tip-vortex cross-sections (Figure 6) and particle paths (Figure 7) are compared in the near-wake ($0 < x/c < -0.5$) for the baseline and modified tips. Multiple cores, whi‍ch appear to be kinematically unstable are evident in the flow field downstream of the modified tip. The computed velocity distribution of the baseline and modified flows are given in Figure 8 which indicate that in the near wake at $x/c = -0.4$, the modified tip vortex produces a peak velocity in the transverse plane that is roughly half that of the baseline case.

Experimental Investigation of Tip-Vortex Flows

A preliminary experiment was performed in the free surface water channel to determine whether the substantial effects predicted by the numerical model were observed. Two wing models (baseline and modified planform for a predicted two times the growth rate) with planforms shown in Figure 4 were tested at ($Re_{chord} \approx 2x10^4$), $\alpha = 8°$. Downstream transverse cross-sectional views of the vortex cores for both cases are illustrated in Figure 9. The laser sheet was slowly stepped through the wake, while the digital camera integrated each image for one second. Due to a small unsteadiness in the core location

and radius, attributed in part to the presence of weak free-surface waves, the image indicates a slightly larger diffusive effect than was instantaneously observed.

To illustrate directly the different vortex wakes, the baseline and modified models were simultaneously tested, side-by-side with 16 cm lateral spacing[1] The laser sheet was set to scan the wake continuously at a rate of ten complete wake traversals per second.

A one-second time-exposure of the planform view (x,z) is compared in Figure 10 with a 1/15 second exposure of the core cross-sections (laser sheet stationary). Since the same dye reservoir supplied the laser dye to both models at the same flow rates, it is apparent that the vortex has grown significantly with respect to the baseline case. Figure 11 compares the modified and baseline cases downstream at $x/c = -5.0$. Again, the increased diffusion of the modified tip vortex is evident in that the laser-dye has nearly diffused below the fluorescence detection threshold.

Summary and Discussion

Numerical and experimental investigations of tip-vortex flows were conducted with the goal of increasing the growth of the core and reducing the azimuthal velocity. The tip region of the wing was modified in an attempt to redistribute the vorticity in a manner that would lead to an initial dynamic instability that would modify the roll-up process. A simple hydrodynamics longitudinal vorticity code (CWV-10) was developed to act as an approximate predictor of the near-wake behavior of trailing wing vortices. Numerical simulations were then performed on a number of candidate wing-tip designs, with the goal of finding a small perturbation to the design that would lead to a rapidly growing tip-vortex. A low-aspect ratio wing, initially motivated by the need to modify and control the flow near submarine sails, was established as the baseline case. Several hundred candidate tip re-designs were automatically investigated in a simple optimization procedure. A class of damped sinusoidal perturbations at the trailing edge, created by the optimization procedure, was found to increase the growth rate of the baseline tip-vortex by roughly a factor of two based on mean core radius.

Experimental investigations were then conducted in a water channel. The Reynolds Number was relatively low for these experiments: $(Re_c = 2 \times 10^4)$. Flow visualization was used to compare the vortex growth between the baseline and modified wings. Preliminary results indicate that the qualitative agreement between the numerically predicted and experimentally observed tip-vortex growth rates is good at moderate angles of attack ($< 10^\circ$) for attached flow.

A detailed comparison of the drag on the baseline and modified wings has not yet been made. However, based on a simple initial observation of the numerically-predicted effect of tip modifications on downwash alone, it appears that there may be a small decrease

---

[1] Interference effects were found to be minimal when the lateral spacing was varied

(e.g., 5% – 20%) in the induced drag. It must be emphasized that this result is preliminary, and does not account for variations in viscous drag.

This work represents a case of CFD being used in a different way from *evolutionary* aerodynamic design. In essence it was based on the use of the simplest numerical models which incorporated the underlying dynamics of the vorticity field. Various preliminary intuitive ideas regarding the use of large trailing-edge modifications and/or, vortex generators to create 'opposite-sign' or destablilizing 'control-vortices' generally led to effects that were either too small to be appreciable, or had a negative impact on other criteria such as drag.

In the present work the numerical approach, based on physical insight and simple Biot-Savart vortex interactions, was used *ab initio* to design models which were subsequently tested. The numerics were not changed or modified as a result of these experiments. Without CWV-10 and automatic optimization, it would have been unlikely that a desirable wing-tip geometry would have been found without much trial and error.

Current work is directed at further control of the tip vortex using other tip perturbations which could be developed to affect the velocity and vorticity helix angles, and is also focusing on the control of longitudinal mid-span and tip-vortices shed from double delta planforms, with attached flow. Early results indicate that particular leading edge perturbations in the vicinity of the mid-span double-delta juncture lead to a rapidly diffusing vortex core.

It is critical to validate that the rapid tip-vortex growth and diffusion persists at large Reynolds numbers. Experiments will likely be performed in a subsonic wind tunnel to determine if the high-Re simulations of the tip-vortex behavior are valid.

ACKNOWLEDGEMENTS
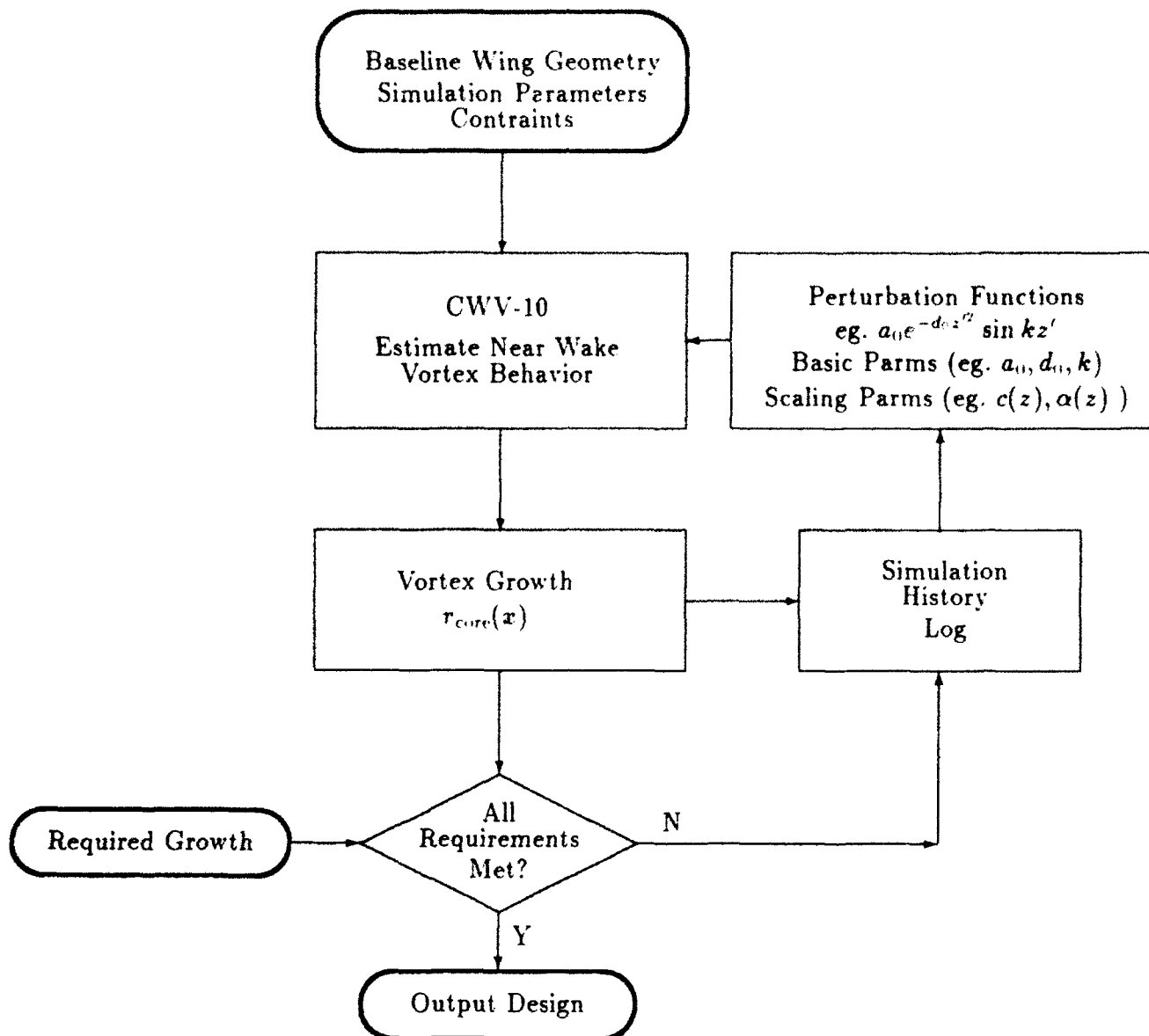
Figure 1. Flow chart of CWV-10 wing optimizer program.

U_∞ ↓   ↑ $+x/c_0$

$b_0 = 15.2\ cm$

$c_0 = 15.2\ cm$

−1.0   −0.64   ∅ $+z/c_0$

Planform View

$+y/c_0$

$+x/c_0$

1.∅   ∅.2   ∅.∅

0.65 cm

4:3 Elliptical
Leading
Edge

Elevation View
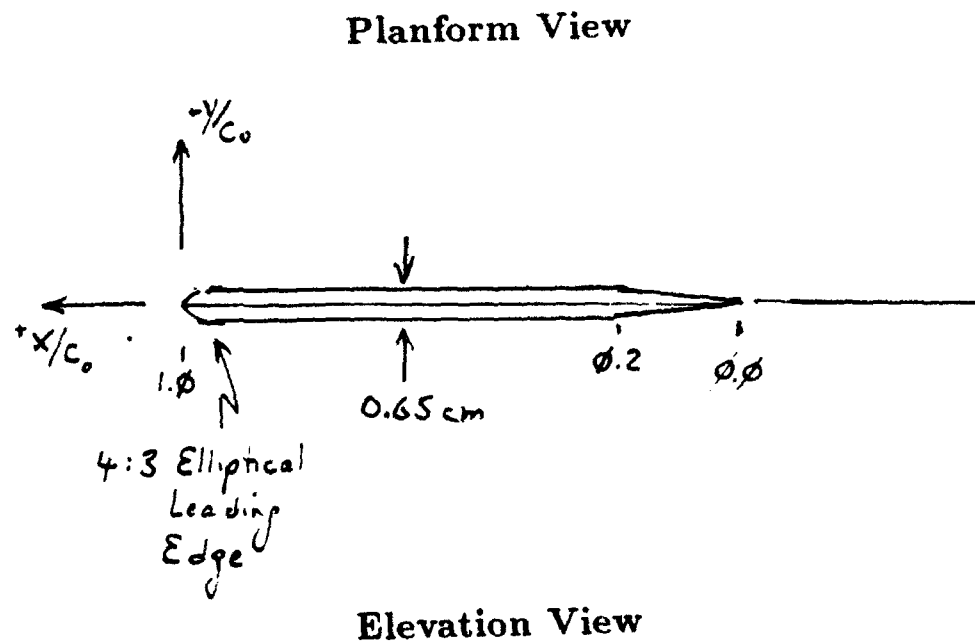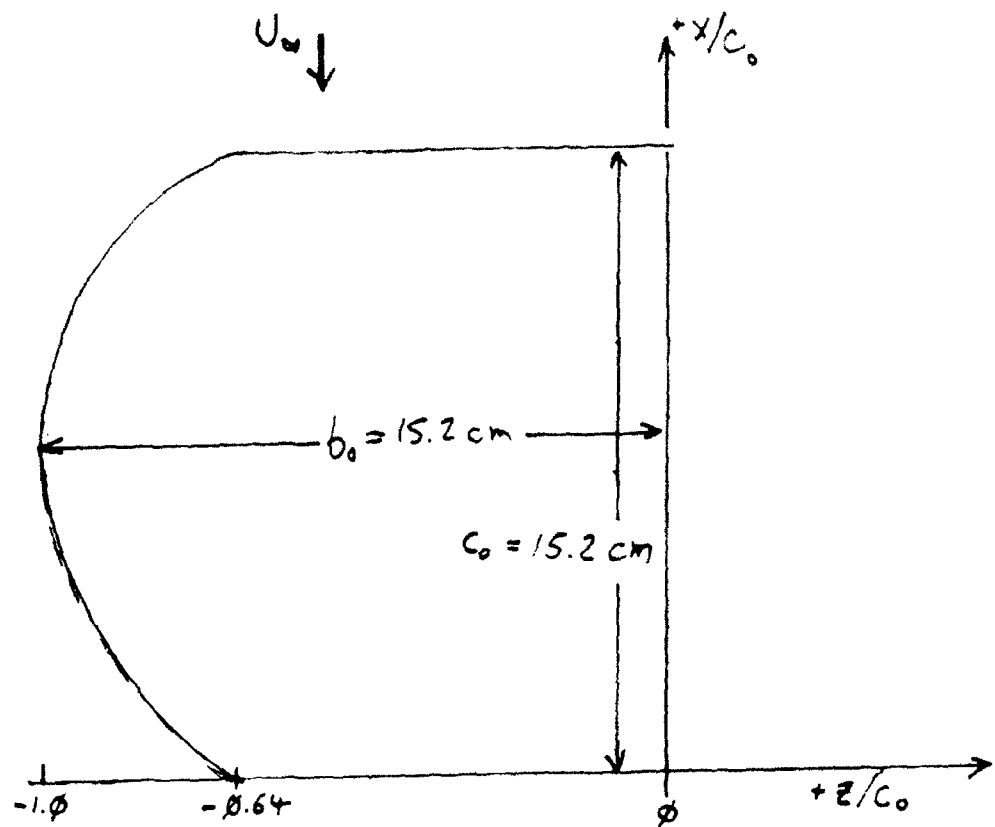
Figure 2. Baseline wing model.
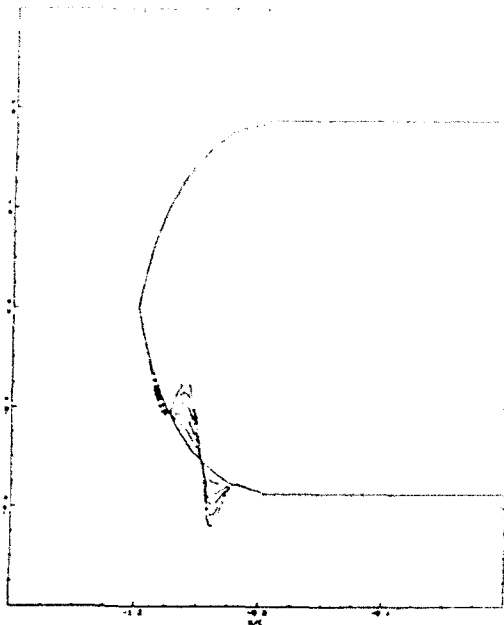
$k = 2;\ a_0 = 0, .1, .2, .3, .4, .5$
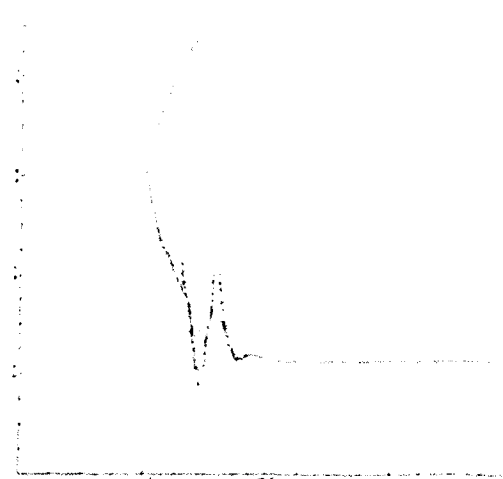
$k = 3;\ a_0 = 0, .1, .2, .3, .4, .5$
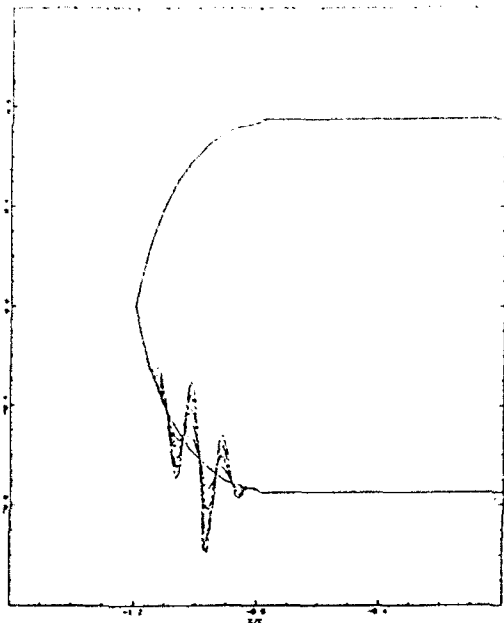
$k = 4;\ a_0 = 0, .1, .2, .3, .4, .5$
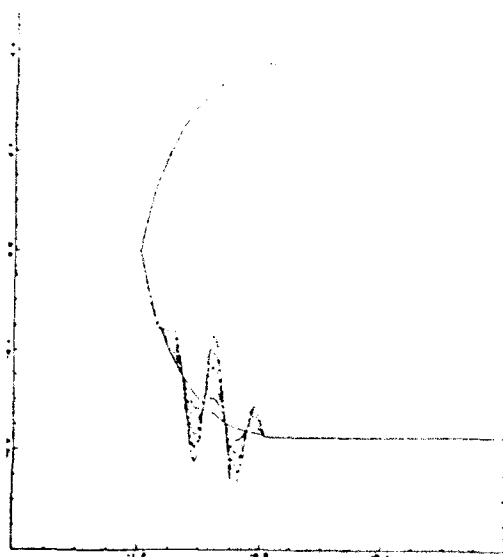
$k = 3;\ a_0 = 0, .1, .2, .3, .4, .5$
(undamped)

**Figure 3. Several numerically-investigated tip modifications.**
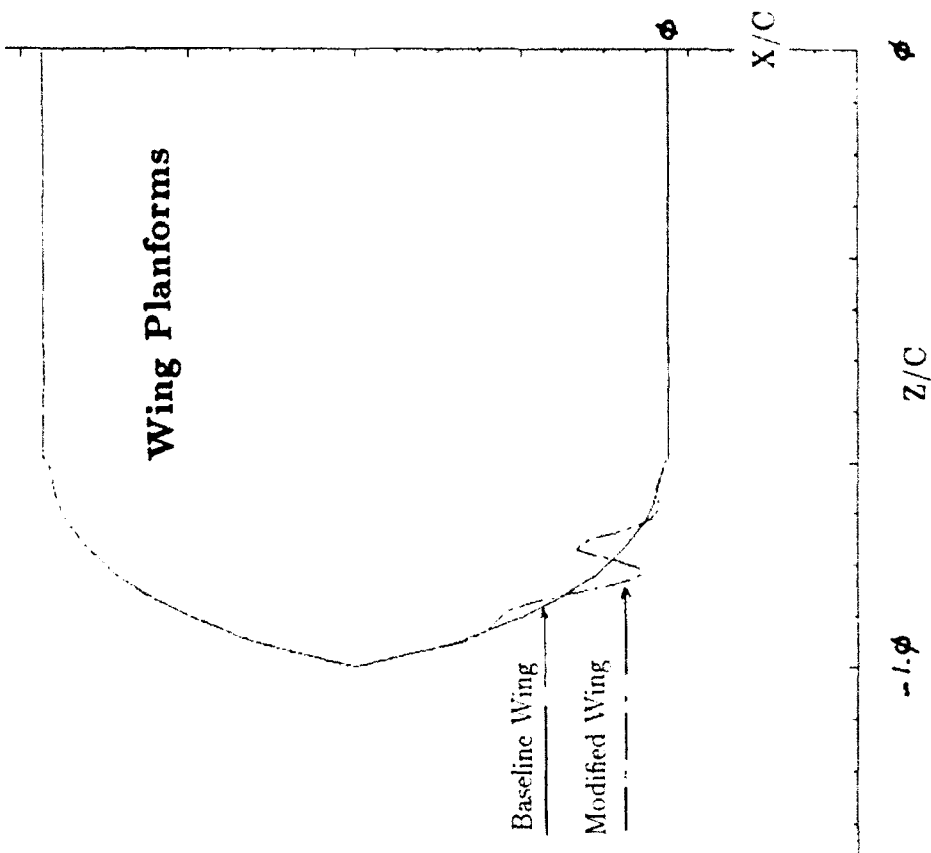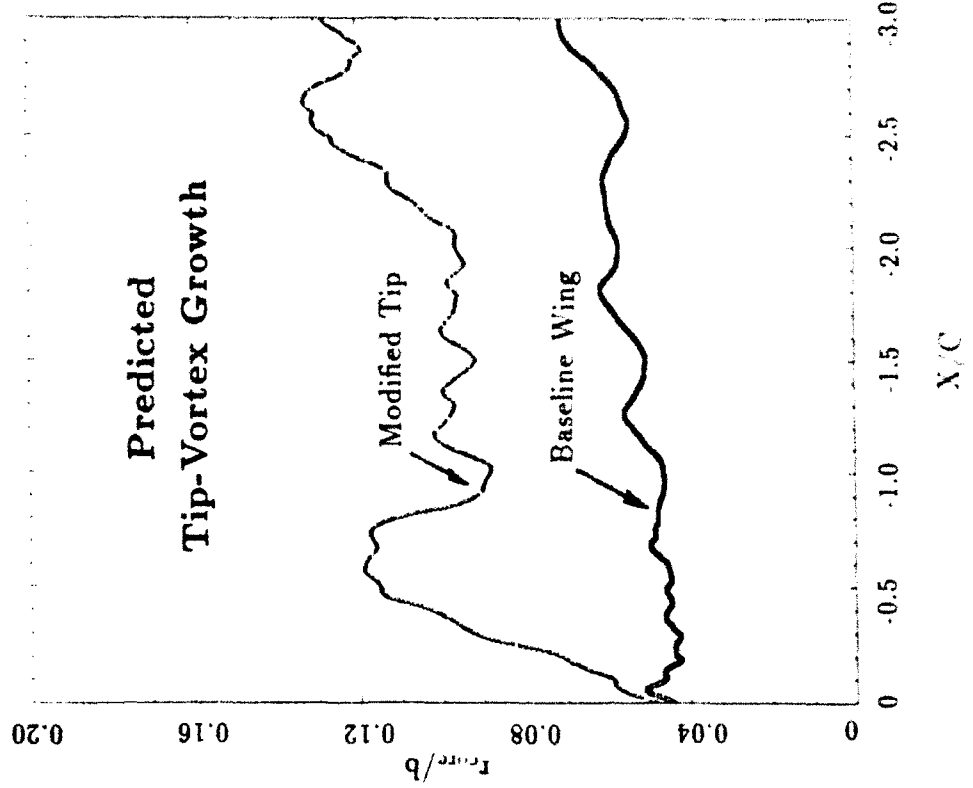
Figure 4. Result of initial wing optimization.
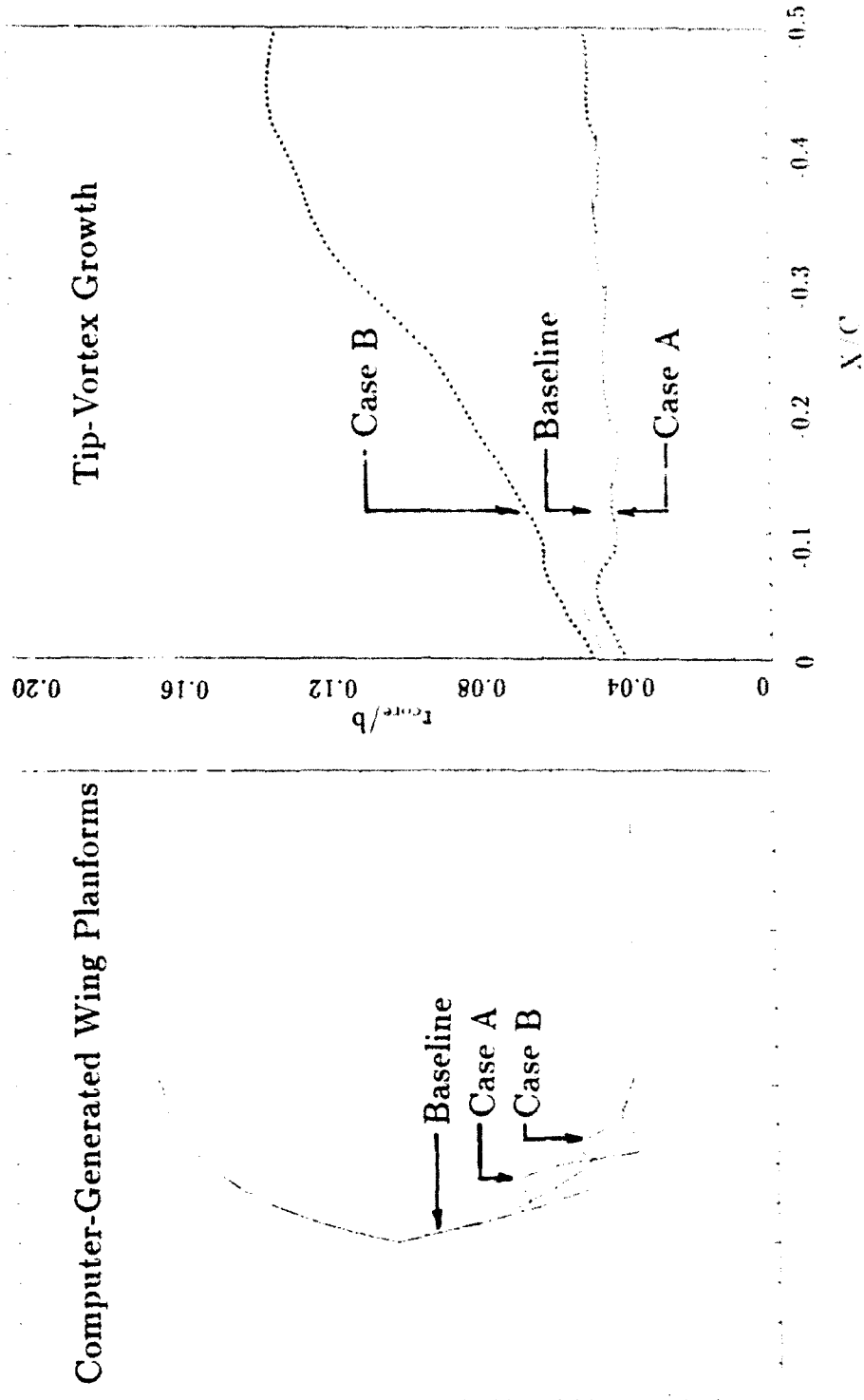
Figure 5. Comparison of different wing modifications.

$x/c = -0.1$

-0.2

-0.3

-0.4

-0.5

z/c z/c
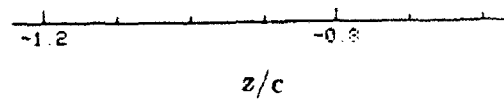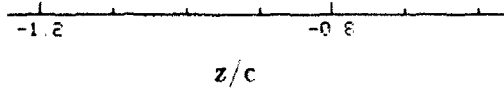
Baseline Wing   Modified Tip

36% Tip ; $\alpha = 7^o$

Figure 6. Numerically-simulated tip vortex cross sections.

Baseline Wing   Modified Tip

Simulation Extends $\frac{1}{2}$ Chord

View: Behind Trailing Edge – Looking Upstream

Figure 7A. Numerically-simulated tip vortex wakes.
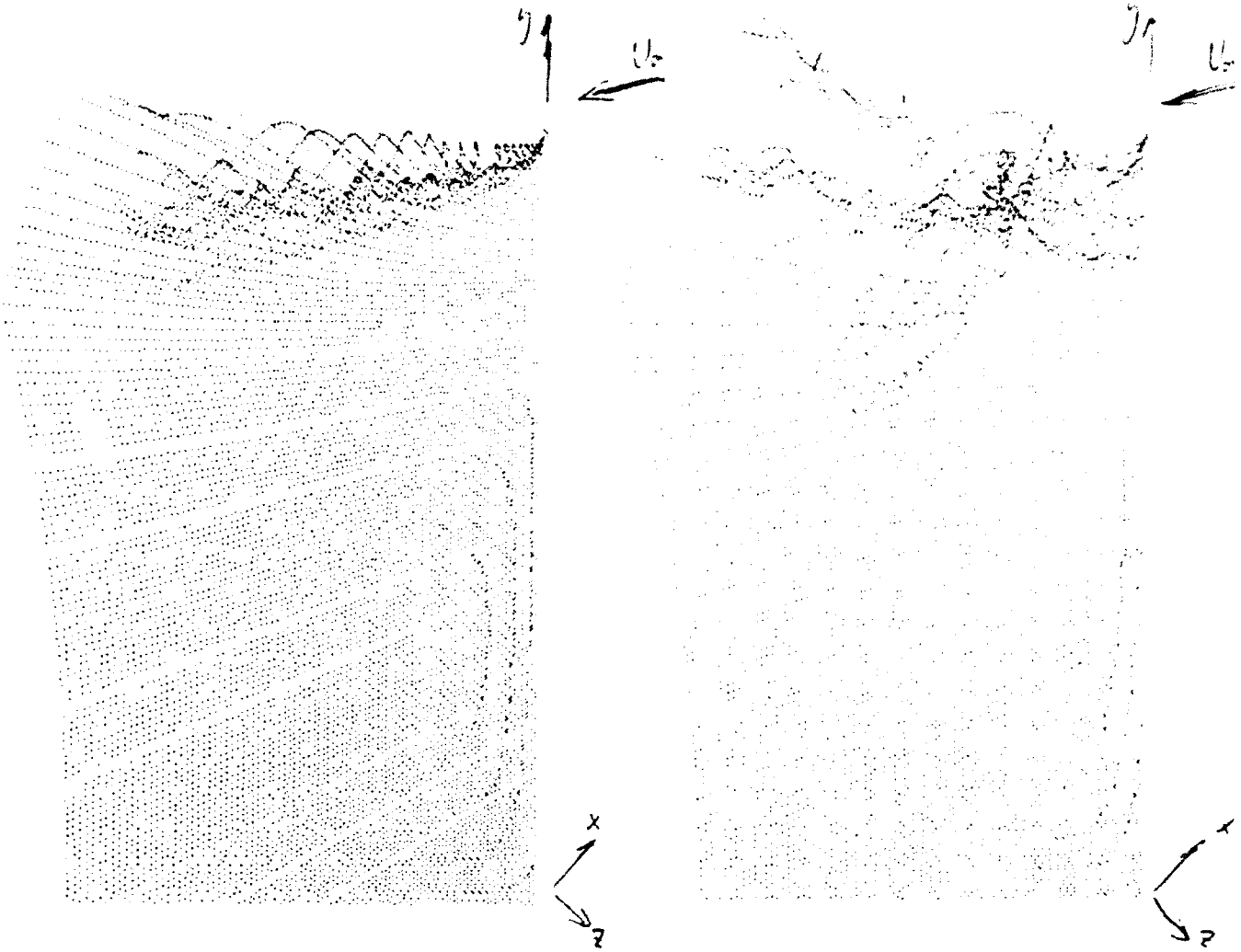
Baseline Wing   Modified Tip

Simulation Extends $\frac{1}{2}$ Chord
View: Behind Trailing Edge – Quartering View Upstream

Figure 7B. Numerically-simulated tip vortex wakes.
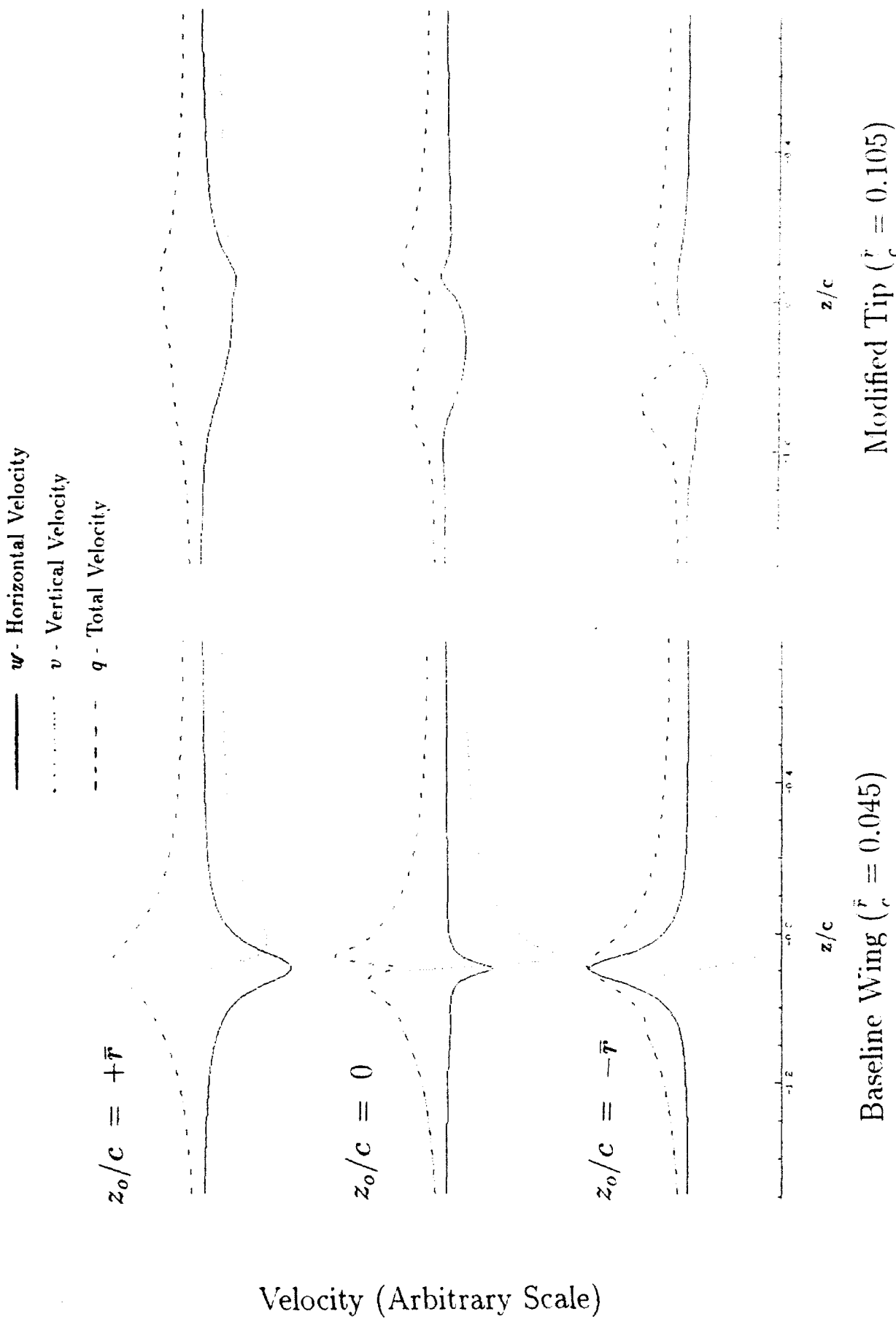
Figure 8. Calculated lateral velocity (v, w) from tip vortex.

Velocity (Arbitrary Scale)
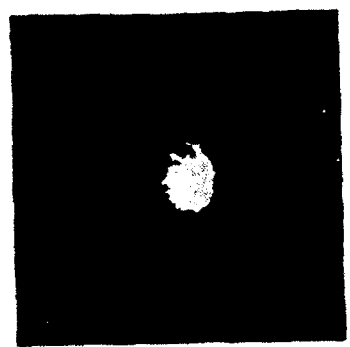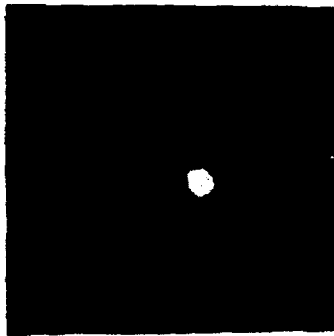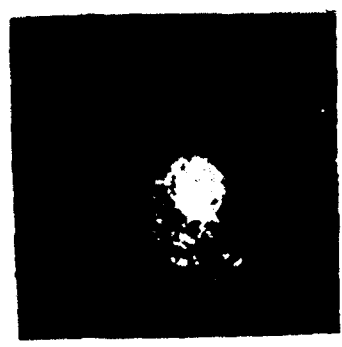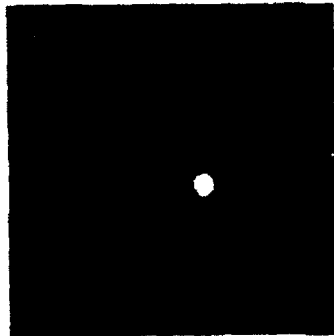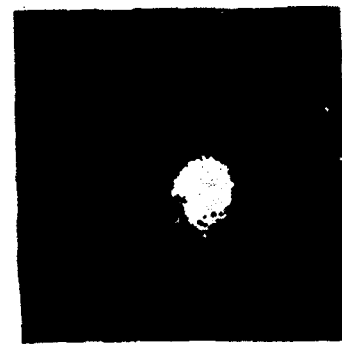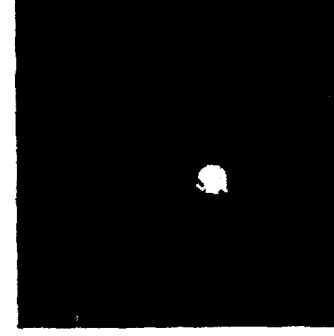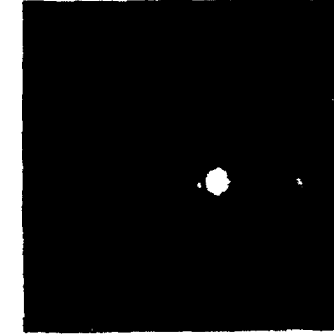
A: Modified Tip   B: Baseline Wing   1 frame/sec

$Re_c = 16,700$ $\alpha_0 = 8^o$

X/C

Figure 9. Experimental laser-sheet cross sections of wing-tip vortex.

18-17

End View
A-A
$r \sim 2.3c_0$

Top View

r/c_0

Baseline Wing

Modified Tip

U_∞
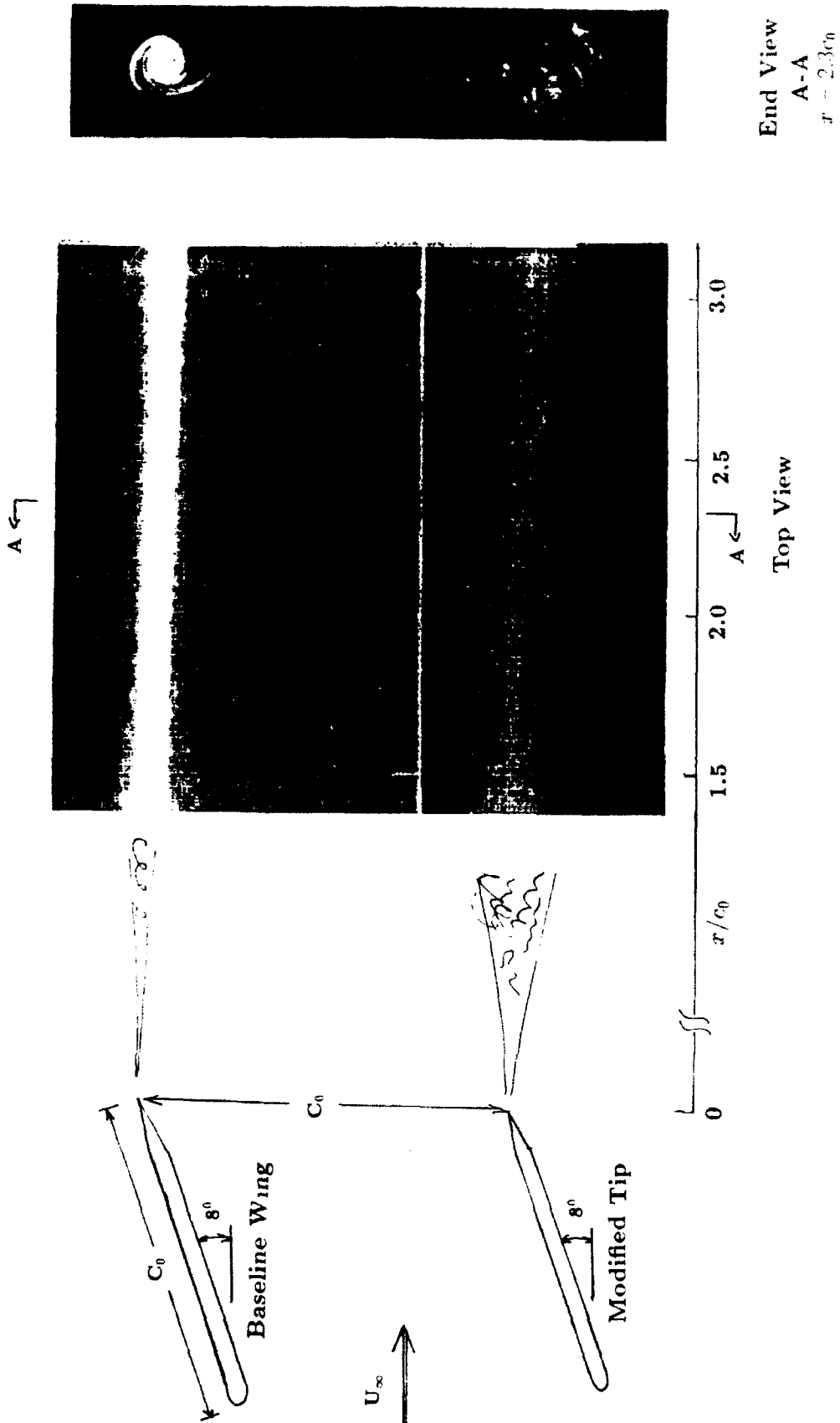
Figure 10. Experimental comparison of wing-tip modifications.

Baseline Wing Geometry
Minimal Core Diffusion

Modified Tip Geometry
Enhanced Core Diffusion

Figure 11. Effect of wing-tip planform modification on tip vortex core diffusion,
experimental transverse laser-sheet visualization.

REFERENCES

1. Donaldson, C.D. and A.J. Bilanin, "Vortex Wakes of Conventional Aircraft," AGARDograph No. 204, 1975

2. "Wake Vortex Minimization," NASA SP-409, Proceedings of a Symposium held in Washington DC, 1976.

3. Bushnell, D.M. and C.D. Donaldson, "Control of Submersible Vortex Flows," NASA Technical Memorandum TM-102693, 1990.

4. Brown, G.L. and J.M. Lopez, "Axisymmetric Vortex Breakdown Part 2 Physical Mechanisms," J. Fluid Mech., Vol. 221, pp. 553-576, 1990.

5. Nosenchuck, D.M. and M.K. Lynch, "Three-Dimensional Flow Visualization Using Laser-Sheet Scanning," Proceedings of the AGARD Conference on Aerodynamic and Related Hydrodynamic Studies Using Water Facilities, AGARD Conference Preprint No. 413, pp 18-1 - 13, 1986.

AMELIORATION OF TRAILING VORTICES VIA INJECTION

Martin Lessen
Yates Memorial Professor of Engineering (Emeritus)
University of Rochester
12 Country Club Drive, Rochester, NY 14618

ABSTRACT

The assumptions underlying the calculation of the turbulent trailing line vortex and the principle of marginal instability are examined. The similarity solution for the turbulent trailing vortex is developed and the power laws derived. The inviscid stability of the vortex is studied and the maximum swirl ratio for instability is obtained analytically.

INTRODUCTION

The wake vortex problem has been with us for a long time. Not only are wake vortices a hazard to following aircraft but they limit air traffic into an airport because of increased airport spacing requirements. In wake vortex dissipation the wake vortex hazard is ameliorated as opposed to wake vortex detection and avoidance.

Most trailing vortices have a high spin ratio; the ratio of the maximum tangential velocity to the axial velocity is large. Such vortices are hydrodynamically stable as opposed to low spin ratio trailing vortices whose minimum critical Reynolds numbers may in some cases be less than that for the axial wake deficit velocity distribution without any swirl at all as in Lessen, Singh and Paillet (ref.1) and Lessen and Paillet (ref.2). According to the rationalle of the principle of marginal instability as in Lessen and Singh (ref.3), Lessen and Paillet (ref.4), and Lessen (ref.5), an inviscidly unstable unbounded, quasi-parallel flow at large Reynolds number behaves like a marginally unstable "laminar" flow at its critical Reynolds number with the level of turbulence supplying the turbulent viscosity to keep the average flow at its critical Reynolds number. The implications of marginal instability will be discussed further along in the paper.

Similarity solutions for jets, wakes, and shearing layers have been known for a long time and have been obtained by the methods of Prandtl (ref.6) using the mixing length hypothesis, Reichardt (ref. 7) and Goertler (ref.8) using an eddy viscosity hypothesis, and others. Townsend (ref. 9, p 107) states that "the assumption of an eddy viscosity, constant within the turbulent fluid, leads to remarkably accurate descriptions of the mean velocity distributions in self preserving flows...". In addition, Townsend (*ibid.*, p 128) and Corrsin (ref. 10) noted that the effective Reynolds number

based on the eddy viscosity is independent of the 'true' Reynolds number (based on the molecular viscosity) for unbounded self preserving flows. Corrsin further observed that the effective Reynolds number for the round jet and plane wake were of the same order of magnitude as the "lower critical numbers of laminar free shear layers" even though at the time of his writing, such a lower critical Reynolds number had not yet been calculated. Townsend estimated that the 'effective' Reynolds numbers for such turbulent flows should lie in the range 14-21.

The distinguishing feature of turbulent jets, wakes and shearing layers is the existence of a point of inflection in the mean velocity profile for the case of plane flows; in the case of swirling flows such as trailing vortices, there exists a point in the axial-swirling average velocity distribution that behaves mathematically like a point of inflection. Such flows are highly unstable and have low minimum critical Reynolds numbers. The interaction of a disturbance with such highly unstable flows will not greatly affect the stability of such flows whereas for bounded flows without a point of inflection, the interaction of a disturbance with the flow might cause the existence of a point of inflection and greatly affect the stability characteristics of the flow. Malkus (ref. 11) postulated an extremum principle for turbulent flows but its application to plane Poiseuille flow did not reproduce observations.

The principle of marginal instability yielded results that compared well with the observed spread of a round jet (Lessen and Singh (ref. 3)) and the break-point of a jet (Lessen and Paillet (ref. 4). The principle also yielded the fixed angle of spread of turbulent shear layers as well as the fixed dominant disturbance dimensionless wave number observed by Brown and Roshko (ref. 12).

All of the foregoing suggests that one way of dealing with trailing vortices consists of rendering them highly unstable by blowing a jet down their axes. The resulting turbulent vortices would then behave as though they were laminar at their minimum critical Reynolds number and the peak vorticities would diffuse rapidly in a radial direction.

ANALYSIS

The Navier-Stokes eq   scribing the flow of an incompressible fluid may be written for a cartesian coordinate syst.... as

$$v_{k,k} = 0$$

$$\rho \left(\frac{\partial v_i}{\partial t} + v_k v_{i,k} \right) = -p_{,i} + \mu v_{i,kk} \qquad (1)$$

where v_i is the velocity vector, $v_{i,k}$ is the velocity gradient tensor, ρ is density, p is the pressure and μ is viscosity.

If the flow considered is 'turbulent' let

$$v_i = V_i(x_k) + u_i(x_k, t)$$

$$p = P(x_k) + \Pi(x_k, t) \qquad (2)$$

such that

$$\overline{u_i} = \overline{\Pi} = 0$$

where $(\overline{})$ denotes an average over a suitable space or time interval.

Substituting eq. (2) into eq. (1), one obtains

$$\rho\left(\frac{\partial u_i}{\partial t} + V_k V_{i,k} + V_k u_{i,k} + u_k V_{i,k} + u_k u_{i,k}\right) = -P_{,i} - \Pi_{,i} + \mu(V_{k,k} + u_{k,k}) \qquad (3)$$

Taking the average of eq. (3) yields

$$\rho V_k V_{i,k} = -P_{,i} + \mu V_{i,kk} - \overline{\rho u_k u_{i,k}} \qquad (4)$$

Since

$$\overline{\rho u_k u_{i,k}} = \overline{(\rho u_k u_i)}_{,k}$$

one can define a stress $\tau_{ki}^{(R)}$ such that $\tau_{ki}^{(R)} = -\rho \overline{u_k u_i}$ and $-\overline{(\rho u_k u_i)}_{,k} = \tau_{ki,k}^{(R)}$

For a quasi-parallel, unbounded, self-preserving (similarity) flow Prandtl, Goertler, Reichardt, and Townsend found that a close description of the average flow V_i could be obtained by hypothesizing that

$$\tau_{ki}^{(R)} = \mu^{(\bullet)}(V_{k,i} + V_{i,k}) \qquad (5)$$

where $\mu^{(\bullet)}$ is the turbulent or eddy viscosity.

Since

$$\tau_{ki}^{(R)} = \mu^{(\bullet)} V_{i,kk} + \mu^{(\bullet)}_{,k}(V_{k,i} + V_{i,k})$$

the averaged Navier-Stokes equations (4) can be written as

$$\rho V_k V_{i,k} = -P_{,i} + (\mu + \mu^{(\bullet)})V_{i,kk} + \mu_{,k}^{(\bullet)}(V_{k,i} + V_{i,k}) \qquad (6)$$

Eq. (6) will later be utilized to obtain the average velocity distribution of a turbulent trailing vortex.

The properties of the disturbance of the average flow will now be investigated. Subtracting eq. (4) from eq. (3) yields the equation for the disturbance.

$$\rho\left(\frac{\partial u_i}{\partial t} + V_k u_{i,k} + u_k V_{i,k}\right) = -\Pi_{,i} + \mu u_{i,kk} - (\rho u_k u_i)_{,k} + \overline{(\rho u_k u_i)}_{,k} \qquad (7)$$

The disturbance equation (7) differs from the usual, linear Orr-Sommerfeld equation by virtue of the last terms - $(\rho u_k u_i)_{,k} + \overline{(\rho u_k u_i)}_{,k}$.

If each spectral line of the disturbance described by eq. (7) is analyzed separately, the energy flow from average flow to the disturbance and between the different Fourier components of the disturbance may be ascertained. As regards the fundamental spectral line of the disturbance, this component is self-excited and the energy input to it comes from the Reynolds stress interacting with the average flow

$$- \frac{1}{2} \overline{(\rho\, u_k\, u_i)} \left(V_{k,i} + V_{i,k} \right)$$

The fundamental of the disturbance loses energy through interaction with the second harmonic and thereby pumps energy into the second harmonic via the term $-(\rho\, u_k\, u_i)_{,k}$.

The energy from the first harmonic is $-\frac{1}{2}(\rho\, u_k\, u_i)(u_{k,i} + u_{i,k})$.

In the foregoing expression, $(\rho\, u_k\, u_i)$ consists of fundamentals and second harmonics interacting to yield a fundamental in part. This fundamental interacting with the fundamental of $\frac{1}{2}(u_{k,i} + u_{i,k})$ yields the scalar energy flux in part that proceeds to the second harmonic.

In a manner analogous to the hypothesis of eq. (5) the wave Reynolds stress is first defined as

$$\tau_{k,i}^{(w)} = -\rho\, u_k\, u_i + \overline{\rho\, u_k\, u_i}$$

and then

$$\tau_{k,i}^{(w)} = \mu^{(e)} \left(u_{k,i} + u_{i,k} \right) \tag{8}$$

where u_i in the last expression consists only of the fundamental.

Substituting eq. (8) into eq. (7) yields

$$\rho \left(\frac{\partial u_i}{\partial t} + V_k\, u_{i,k} + u_k\, V_{i,k} \right) = -\Pi_{,i} + \left(\mu + \mu^{(e)} \right) u_{i,kk} \tag{9}$$

which for the fundamental u_i and Π is the usual Orr-Sommerfeld system. Equation (9) is linear and all non-linear effects have been included through $\mu^{(e)}$.

In the turbulent flow, the amplitude of the fundamental is fixed, therefore the flow is neutrally stable in that sense. $\mu^{(e)}$ therefore takes on such a value as to insure neutral stability. The wave number of the fundamental is such that $\mu^{(e)}$ is maximized for neutral stability, hence the flow is at its minimum critical Reynolds number (based on $\mu + \mu^{(e)}$).

Since $\mu^{(e)}$ is generally much greater than μ in a turbulent flow, it generally suffices to define the effective Reynolds number in terms of $\mu^{(e)}$.

THE TURBULENT TRAILING VORTEX FLOW FIELD

The turbulent trailing vortex flow field can be investigated by considering a boundary layer approximation to the averaged Navier-Stokes equation as in eq. (6).

Consider axially symmetric flow in a cylindrical polar coordinate system x,r,q with velocity components u, v, w where $\frac{\partial}{\partial x} << \frac{\partial}{\partial r}$, $\mu << \mu^{(e)}$, $\mu^{(e)} = \mu^{(e)}(x)$,

$$\frac{\partial u}{\partial x} + \frac{1}{r}\frac{\partial}{\partial r}(rv) = 0$$

$$u\frac{\partial u}{\partial x} + v\frac{\partial u}{\partial r} = -\frac{1}{\rho}\frac{\partial p}{\partial x} + \frac{\mu^{(e)}}{\rho r}\frac{\partial}{\partial r}\left(r\frac{\partial u}{\partial r}\right) \qquad (10)$$

$$u\frac{\partial w}{\partial x} + v\frac{\partial w}{\partial r} + \frac{vw}{r} = \frac{\mu^{(e)}}{\rho}r\frac{\partial}{\partial r}\left(\frac{1}{r}\frac{\partial(rw)}{\partial r}\right)$$

For the far field of a trailing vortex

$$u = U_\infty + h$$

where U_∞ = constant free stream velocity and

$$|h| << |U_\infty|$$

$$|h| = O|w|.$$

If the viscosity induced pressure gradient in the axial direction is neglected due to an overpowering core injection, eq. (10) may then be written to first approximation in u, w, v as

$$\frac{\partial u}{\partial x} + \frac{1}{r}\frac{\partial}{\partial r}(rv) = 0$$

$$U_\infty\frac{\partial u}{\partial x} = \frac{\mu^{(e)}}{\rho r}\frac{\partial}{\partial r}\left(r\frac{\partial u}{\partial r}\right) \qquad (11)$$

$$U_\infty\frac{\partial w}{\partial x} = \frac{\mu^{(e)}}{\rho}r\frac{\partial}{\partial r}\left(\frac{1}{r}\frac{\partial(rw)}{\partial r}\right)$$

The implications of neglecting the axial pressure gradient are that the induced upstream axial flow is neglected. As seen in Batchelor (ref. 13), the velocity distribution of this flow is the same as the injected downstream flow and differs from it only by a scale factor. Therefore the solution of eq. (11) for the axial flow multiplied by a suitable scale factor would reproduce the turbulent analogue to the Batchelor solution. A similarity solution to eq. (11) may be found as follows; let

$$\chi = \int_0^x \frac{\mu^{(\bullet)}}{\rho} dx' \; ; \; \eta = r \chi^m$$

$$\Psi = U_\infty g(\eta) \; ; \; w = \frac{f'(\eta)}{\eta} \chi^{2n}$$

Eq. (11) becomes

$$m U_\infty \frac{1}{\eta} (\eta g')' = \chi^{2m+1} \frac{1}{\eta} \left[\eta \left(\frac{g'}{\eta} \right)' \right]'$$

$$n U_\infty \frac{1}{\eta} (\eta f')' = \chi^{2n+1} \left(\frac{f''}{\eta} \right)' \tag{12}$$

For a similarity solution, it is seen that

$$m = n = -\frac{1}{2}$$

The maximum value of the velocity defect which is the velocity scale U_m may be written as

$$U_m = U_\infty \chi^{2m} = U_\infty \chi^{-1}$$

Also, since $\delta \sim \chi^{1/2}$ and R_δ is constant, $\mu^{(\bullet)} \sim \chi^{-1/2}$. Therefore $x \sim \chi^{3/2}$, $U_m \sim x^{-2/3}$, $\delta \sim x^{1/3}$, and $\mu^{(\bullet)} \sim x^{-1/3}$.

With respect to the azimuthal velocity w, the foregoing arguments apply as well as the same velocity scale. The swirl ratio is therefore fixed over the flow field to this approximation.

THE INVISCID INSTABILITY OF A TRAILING VORTEX

The inviscid instability of a trailing line vortex was investigated in detail in Lessen, Singh, and Paillet (ref. 1) using numerical techniques. Some overall stability characteristics can be obtained however using analysis and this will be briefly reviewed here.

Consider the Navier-Stokes equations without viscous terms in cylindrical polar coordinates where (u, v, w) are the velocity components in the (x, r, θ) directions and

$$u = U(r) + F(r) \exp\left[i\left(\alpha x + n\theta - \alpha ct\right)\right]$$

$$v = 0 + i\frac{\psi(r)}{r} \exp\left[i\left(\alpha x + n\theta - \alpha ct\right)\right]$$

$$w = W(r) + H(r) \exp\left[i\left(\alpha x + n\theta - \alpha ct\right)\right]$$

where $|F| \ll |U|, |H| \ll |W|$ and $\psi = O(F)$.

The resulting equations for the perturbations F, ψ, H can be manipulated into a single equation for ψ

$$\left(\frac{S}{r}\psi'\right)' - \frac{1}{r}\left[1 + \frac{\gamma a(r) + b(r)}{\gamma^2}\right]\psi = 0 \tag{13}$$

where

$$a(r) = r\left[S\left(\frac{\gamma'}{r} + \frac{2nW}{r^3}\right)\right]'$$

$$b(r) = -\frac{2\alpha W S}{r^2}\left[\alpha(rW)' - nU'\right]$$

$$S = \frac{r^2}{n^2 + \alpha^2 r^2}$$

$$\gamma = \alpha(U-c) + \frac{nW}{r}$$

If eq. (13) is multiplied by $\tilde{\psi}$ and integrated term by term from r = 0 to r = ∞ the imaginary part of the resulting relation is

$$\text{Im}\int_0^\infty \frac{1}{r}\left[\frac{ar+b}{\gamma^2}\right]|\psi|^2\, dr = 0$$

yielding the condition that if there exists an $r = r_c$ where

$$\gamma(r_c) = \alpha\left[U(r_c) - c_r\right] + \frac{nW(r_c)}{r_c} = 0$$

then

$$a(r_c)\,\gamma(r_c) + b(r_c) = 0$$

19-7

and

$$[a\,(r_c)\,\gamma\,(r_c) + b\,(r_c)]' = 0 \qquad (14)$$

This condition is the analogue of the Rayleigh (ref. 14) inflection point theorem for plane, parallel flows and gives a necessary condition for instability. $r = r_c$ defines the location of the "critical" layer and it is assumed that the flow studied will have only one such layer.

An additional condition for instability of plane parallel flows developed by Fjortoft (ref. 15) may also be extended to the problem under investigation.

If eq. (13) is multiplied by $\tilde{\psi}$, integrated term by term from $r = 0$ to $r = \infty$, the real part of the resulting equation is

$$-\int \frac{S}{r}|\psi|^2\,dr - \int \frac{|\psi|^2}{r}\,dr - RI \int \frac{1}{r}\frac{(a\gamma+b)\,|\Psi|^2}{\gamma^2}\,dr = 0$$

or

$$RI \int \frac{1}{r}\frac{(a\gamma+b)}{\gamma^2}|\psi|^2 dr < 0$$

which in connection with the conditions of eq. (14) yields

$$[a\,(r_c)\,\gamma(r_c) + b\,(r_c)]'' = 0 \qquad (15)$$

Eq. (15) is the analogue of the Fjortoft condition for plane parallel flows which states that the vorticity must have a maximum in the flow field for inviscid instability.

The criteria eq. (14) and (15) will now be applied to the trailing vortex. Taking the mean velocity profiles from eq. (12) normalized by suitable velocity and length scales U_s and r_s respectively.

$$U\,(r) = e^{-r^2}; \; W\,(r) = q\frac{(1 - e^{-r^2})}{r};$$

and

$$q = \frac{\Gamma_\infty}{2\pi r_s U_s}$$

where q is the swirl parameter or ratio, and Γ_∞ is the circulation of the vortex at large r.

The first extended Rayleigh condition yields (since $\gamma\,(r_c) = 0$)

$$b(r_c) = 0$$

or

$$\alpha (rW)'_c - n U'_c = 0 \; .$$

Since

$$\frac{(rW)'}{U'_c} = \frac{2\,r_c\,q\,e^{-r_c^2}}{-2r_c\,e^{-r_c^2}} = -q$$

then

$$\alpha\, q = -n \tag{16}$$

The second and third conditions are automatically satisfied. Eq. (16) corresponds to the upper branch of the neutral stability curve in α, q space for infinite Reynolds number; the lower branch comes from Lessen, Singh, and Paillet (ref. 3). The two branches, for n = -1, intersect at

$$q = 1.66$$

above which no instability for this mode exists. It is significant that observed trailing vortices do not seem to be unstable at swirl ratios higher than about 1.6.

Significantly, values calculated by numerical integration of the disturbance equations fall precisely on the curve given by eq. (15).

DISCUSSION

In the Analysis section, the equations for the average velocity distribution of a turbulent injected trailing vortex are derived with the substitution of an eddy viscosity for turbulent momentum transport. The equations for the disturbance flow field are then developed with a similar approximation for the turbulent viscosity to that for the average velocity flow field. By characterizing the finite amplitude effects of first harmonic disturbance energy leaking into the second harmonic as eddy viscosity, the disturbance is treated mathematically as a linear instability problem with the disturbance being neutrally stable.

In the Turbulent Trailing Vortex Flow Field section, the turbulent trailing vortex flow field is analyzed in detail using the technique of the Analysis section. It is seen that the resulting similarity solutions are the same as those for the analogous laminar flow and that within the approximations made, the swirl ratio of the flow field is constant over the entire flow field.

In the Inviscid Instability of a Trailing Vortex section, the inviscid instability characteristics of a trailing vortex are investigated analytically and it is found for the fundamental disturbance, that the swirl ratio of the vortex must be below a value of 1.66 for instability and hence turbulent diffusion of the vortex to occur.

In the foregoing analysis, the effect of an axial pressure gradient in the vortex core has been neglected. As Batchelor (1964) has pointed out, this pressure gradient is really not negligible. As the vortex moves downstream from the airfoil, the rigid body rotating vortex core diffuses outward radially and the pressure within the vortex core is given by the tangential velocity of the vortex at the edge of the core. Since this velocity decreases downstream, the pressure rises downstream and an axial pressure gradient therefore causes an upstream flow in the vortex core. It has been assumed that axial injection into the vortex would overpower this tendency, yet the swirl ratio in the actual case would increase in the downstream direction.

For vortex injection to be effective in dissipating trailing vortices, injection to such a degree would be necessary so as to render the vortices hydrodynamically unstable sufficiently far downstream that the vortex wake hazard to an ensuing aircraft would be greatly diminished.

REFERENCES

1. Lessen, M. ; Singh, P. J. & Paillet, F. L. (1974) The stability of a trailing line vortex. Part I inviscid theory, J. *Fluid Mech.* 65, 753.

2. Lessen, M. & Paillet, F. L. (1974) The stability of a trailing line vortex. Part II. Viscous theory, J. *Fluid Mech.* 65, 769.

3. Lessen, M. & Singh, P. J. (1974) Stability of turbulent jets and wakes. *Phys. Fluids* 17, 1329.

4. Lessen, M. & Paillet, F.L. (1976) Marginal instability of turbulent shearing layers and the break point of a jet. *Phys. Fluids* 19, 942.

5. Lessen, M. (1978) On the power laws for turbulent jets, wakes and shearing layers and their relationships to the principle of marginal instability. J. *Fluid Mech.* 88, 535.

6. Prandtl, L. 1925 Über die ausgebildete Turbulenz. Z. *angew. Math. Mech.* 5, 136.

7. Reichardt, H. 1941 Über eine neue Theorie der freien Turbulenz. Z. *angew. Math. Mech.* 21, 257.

8. Goertler, H. (1942) Berechnung von Aufgaben der freien Turbulenz auf Grund eines neuen Naherungsansatzes. Z. *angew. Math. Mech.* 22, 244.

9. Townsend, A.A. 1956 *The Structure of Turbulent Shear Flow.* Cambridge University Press.

10. Corrsin, S. 1957 Some current problems in turbulent shear flows. In *Naval Hydrodynamics.* chap. 15. Nat. Acad. Sci. - Nat. Res. Counc. publ. 515.

11. Malkus, W. V. R. 1956 Outline of a theory of turbulent shear flow. J. *Fluid Mech.* 1, 521.

12. Brown, G.L & Roshko, A. (1974) On density effects and large structure in turbulent mixing layers. J. *Fluid Mech.* 64, 775.

13. Batchelor, G. K. (1964) Axial flow in trailing line vortices. J. *Fluid Mech.* 20, 645

14. Rayleigh, Lord (1880) *On the stability or instability of certain fluid motions.* , Scientific Papers 1, 474-87 ,Cambridge University Press.

15. Fjortoft, R. (1950) Applications of integral theorems in deriving criteria of stability for laminar flows and for the baroclinic circular vortex. *Geophys. Publikasjones,* 17, 5,52.

COMPUTERIZED STUDY OF VORTEX AEROHYDRODYNAMICS OF AIRCRAFT AND HELICOPTERS

Sergei M. Belotserkovskii
Central Aerohydrodynamics Institute (TsAGI)
Moscow, USSR

His "Professional Hobbies":

- the Method of Discrete Vortices (MDV)
- Computational Vortex Fluid Mechanics

The main research in the USSR are conducted by Central Aerohydrodynamics Institute (TsAGI) (calculations, computer simulations, wind-tunnel tests) and by Flight Research Institute (LII) (in-flight experiments) with participation of some other institutions.

The principle objective is to ensure flight safety and to make better use of the potential of aircraft, helicopters and airfields.

To meet these demands it is necessary to study;

- wake vortices behind aircraft and helicopters;
- their effects on other aircraft and bodies;
- dynamics of disturbed motion of the bodies.

The most operative and cheap approach was selected, i.e., systematic computer simulation with selective experimental wind-tunnel and in-flight tests.

For these purposes the following means have been developed:

- The Basic Software Package (for supercomputers) to solve the problems of nonsteady aerodynamics and turbulent wakes;

- applied programs (for personal computers) to solve problems of flight dynamics and aerodynamics.

Series of Monographs in
The Method of Discrete Vortices

Editor-in-Chief
Professor Sergei M. BELOTSERKOVSKII,
Central Aerohydrodynamics Institute (TsAGI), Moscow, USSR

The series of monographs presents systemized results of prolonged research carried out by Prof. Sergei Belotserkovskii and his followers and colleagues in the area of computational fluiddynamics.

Numerical solution of a wide class of problems is based on a concept employing the method of discrete vortices. The approach allows to consider various aspects of vortex fluid mechanics, including:

- separated flows past bodies,

- aerodynamics of lifting surfaces (wings, propellers, rotors) taking into account formation of vortex wakes (both stationary and nonstationary),

- outflow of jets into flooded space/co-current flow,

- interaction of solid bodies with free boundaries (impact of a floating body, water entry, hydroplaning),

- turbulent flows in wakes and jets,

- acoustic characteristics (fields) related to the above problem.

Applications encompass aviation (parachute manufacturing included), shipbuilding, industrial aerodynamics, environmental studies, et cetera.

The monographs are addressed to scientists, engineers, students specializing in computational fluid dynamics and related areas of application.

The series includes the following monographs:

Volume 1 Vortex Fluid Mechanics. Numerical Experiment Based on
the Method of Discrete Vortices
By S. M. Belotserkovskii

Volume 2 Jets and Their Interaction with Wings
By V. I. Babkin, S. M. Belotserkovskii, V. V. Gulyaev, A. V. Dvorak,
and A. A. Kolganov

Volume 3 Nonlinear Theory of Wings in Incompressible Flow
By S. M. Belotserkovskii, A. I. Zhelannikov, A. A. Kolganov, and
M. I. Nisht

Volume 4 Simulation of Turbulent Wakes and Jets
By S. M. Belotserkovskii and A. S. Ginevskii

Volume 5 Propeller/Rotor Aerodynamics
By S. M. Belotserkovskii, B. E. Loktev, S. D. Shepilov

Volume 6 Simulation of Separated Flows Past Bodies of Arbitrary
Configuration
By S. M. Belotserkovskii, V. N. Kotovskii, M. I. Nisht,
and R. M. Fyodorov

Method of discrete vortices (MDV)

- Direct applications
  - Models and numerical methods of aerodynamics
  - Models and numerical methods of hydrodynamics
  - Models and numerical methods of the theory of turbulent jets and wakes
- Mathematical verification and generalization
- Method of discrete singularities
  - Models and numerical methods of the theory of elasticity
  - Models and numerical methods of electrostatics
  - Models and numerical methods of electrodynamics
  - Models and numerical methods of the theory of craks
  - Models and numerical methods for other areas of mathematical physics

THEORY

Wake Vortex Symposium

PRACTICE

Taking into account diffusion in the wake

Airplane

$$Re = \frac{U_e B}{\nu}$$

Wake

$$Re_* = \frac{U_e B}{\nu_*}$$

$$\frac{\nu_*}{\nu} = f(C_y, AR, Re)$$

f – is known from flight experiments

$$\frac{Re_*}{Re} = \frac{\nu_*}{\nu} \ll 1$$

IV. Far wake.

Velocities induced by vortices
(taking into account diffusion)
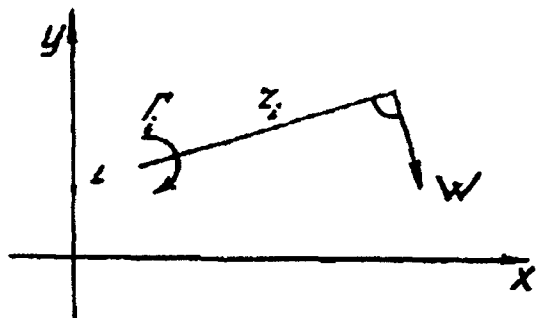
$$\frac{W_{x_i}^*}{W_x} = \frac{W_{y_i}^*}{W_y} = 1 - e^{-\frac{z_i^2 Re_*}{4\tau}}$$
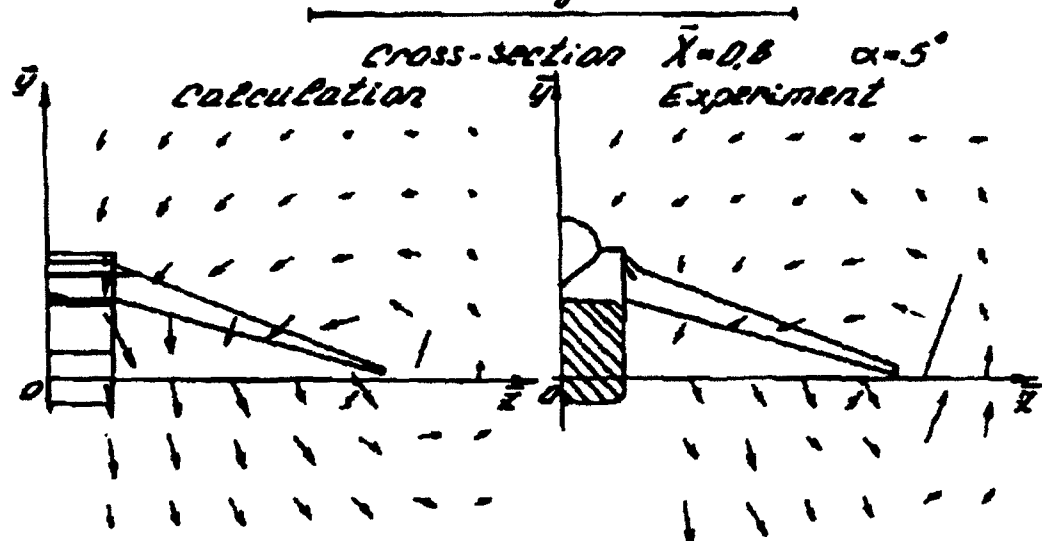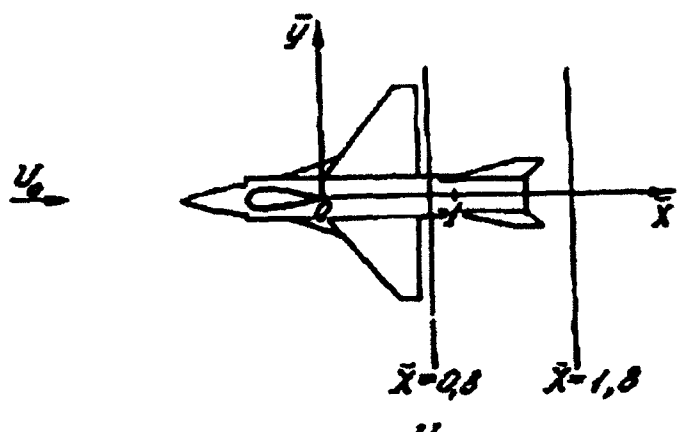
$$\tau = \frac{t U_e}{b}, \quad z_i^2 = (\bar{x}_i - \bar{x})^2 + (\bar{y}_i - \bar{y})^2$$

$\bar{y}$

U_∞

O

$\bar{x}$

$\bar{x}=0,8$ $\bar{x}=1,8$

U_0

Cross-section $\bar{x}=0,8$ $\alpha=5°$

$\bar{y}$ Calculation $\bar{y}$ Experiment

O $\bar{z}$ O $\bar{z}$

Cross-section $\bar{x}=1,8$

$\bar{y}$ Calculation $\bar{y}$ Experiment

O $\bar{z}$ O $\bar{z}$

$$\alpha = 5°, \ \bar{y} = -0.2$$

——— Calculation

• • Experiment

——— Flight test
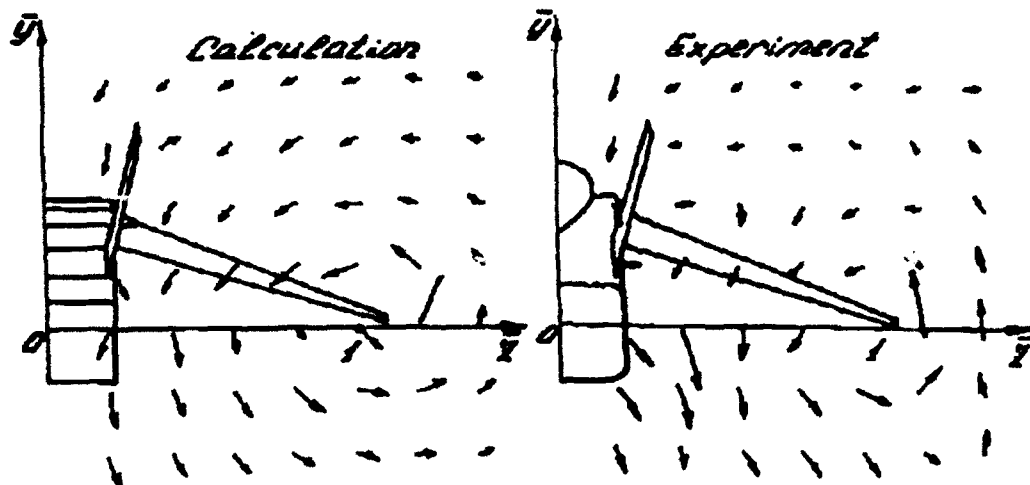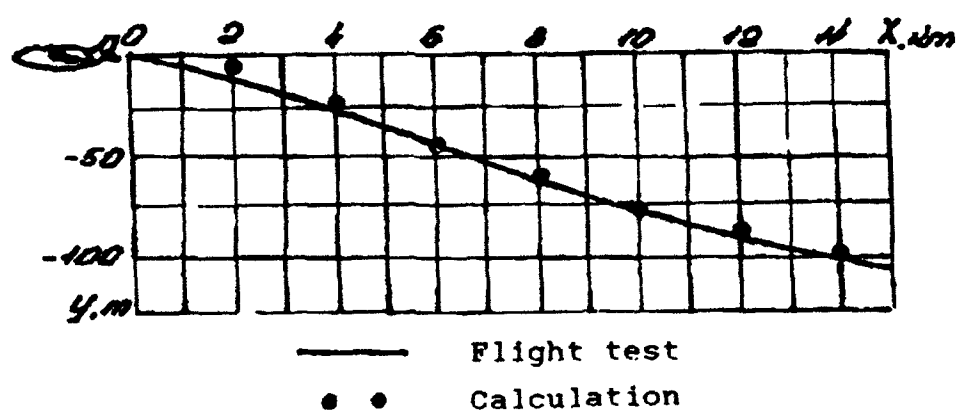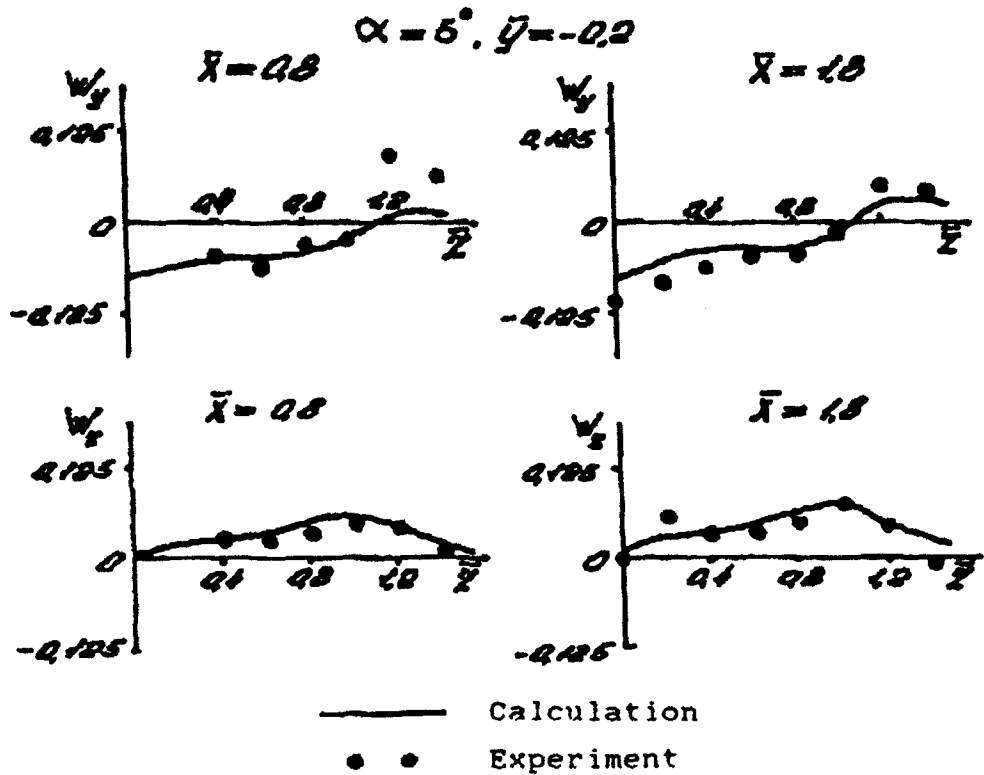
• • Calculation

Asymmetric separated flow past a flat plate for
= ∞, α = 90°: (a) towing tank tests,
(b) calculated.
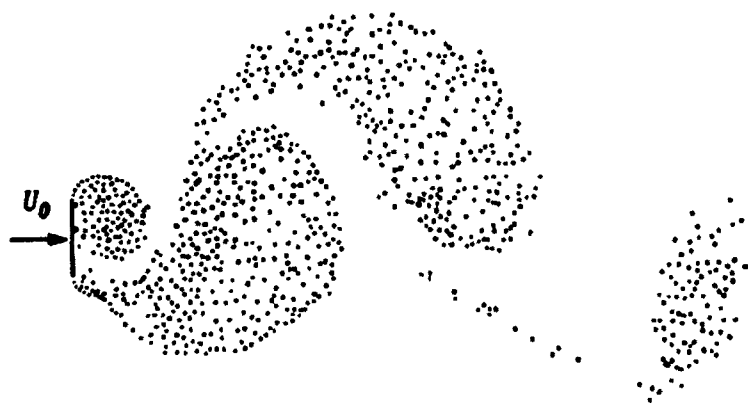
Calculated vortex wake behind a flat plate in the
case of asymmetric flow (Kármán vortex street).
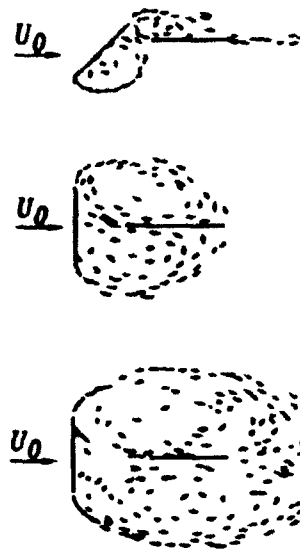
Evolution of asymmetric separated flow past a plate
into a symmetric flow, $= \infty$, $\alpha = 90°$: (a) towing
tank tests, (b) calculated.
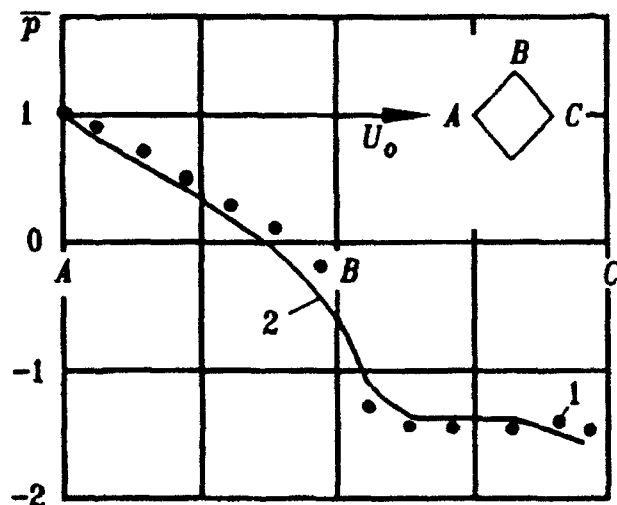
Pressure distribution at the surface of a rhombus
(1 – experimental data, 2 – calculated results).
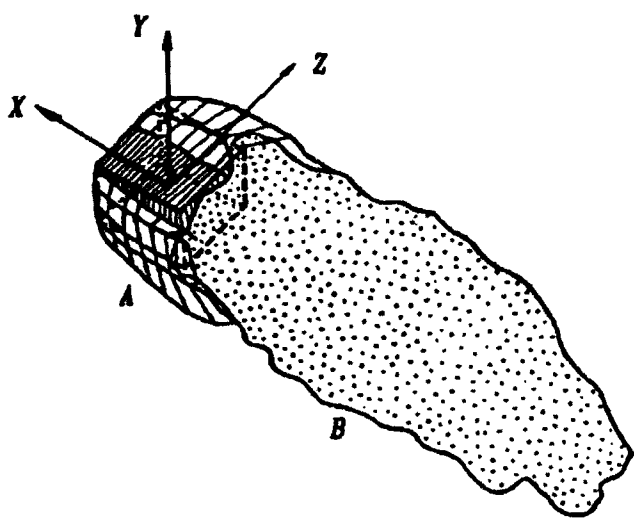
Calculated vortex wake behind a cube: A and B
denote the vortex sheet and the turbulent flow
region respectively.

Separated flow past a cylinder: (a) and (b) show
the transformation of a symmetric wake into the
Kármán vortex street, (c) — drag reduction due to
turbulent separation.

$$\bar{H} = \frac{H}{R}$$

$\bar{H} = 2$

$\bar{H} = 1,5$

$\bar{H} = 1$

$\bar{H} = 0,5$
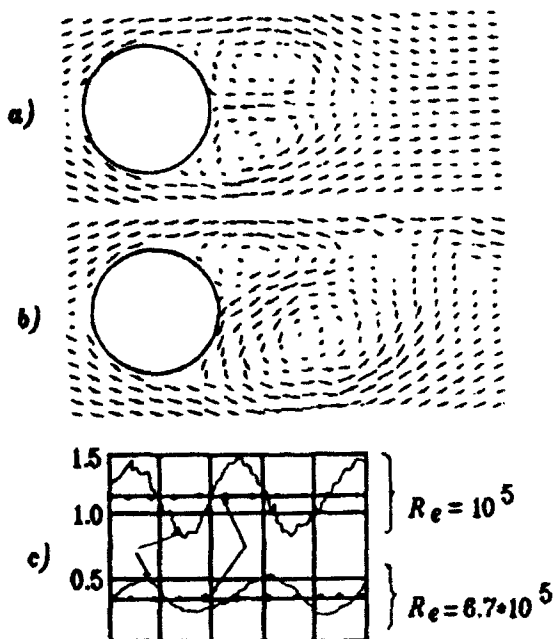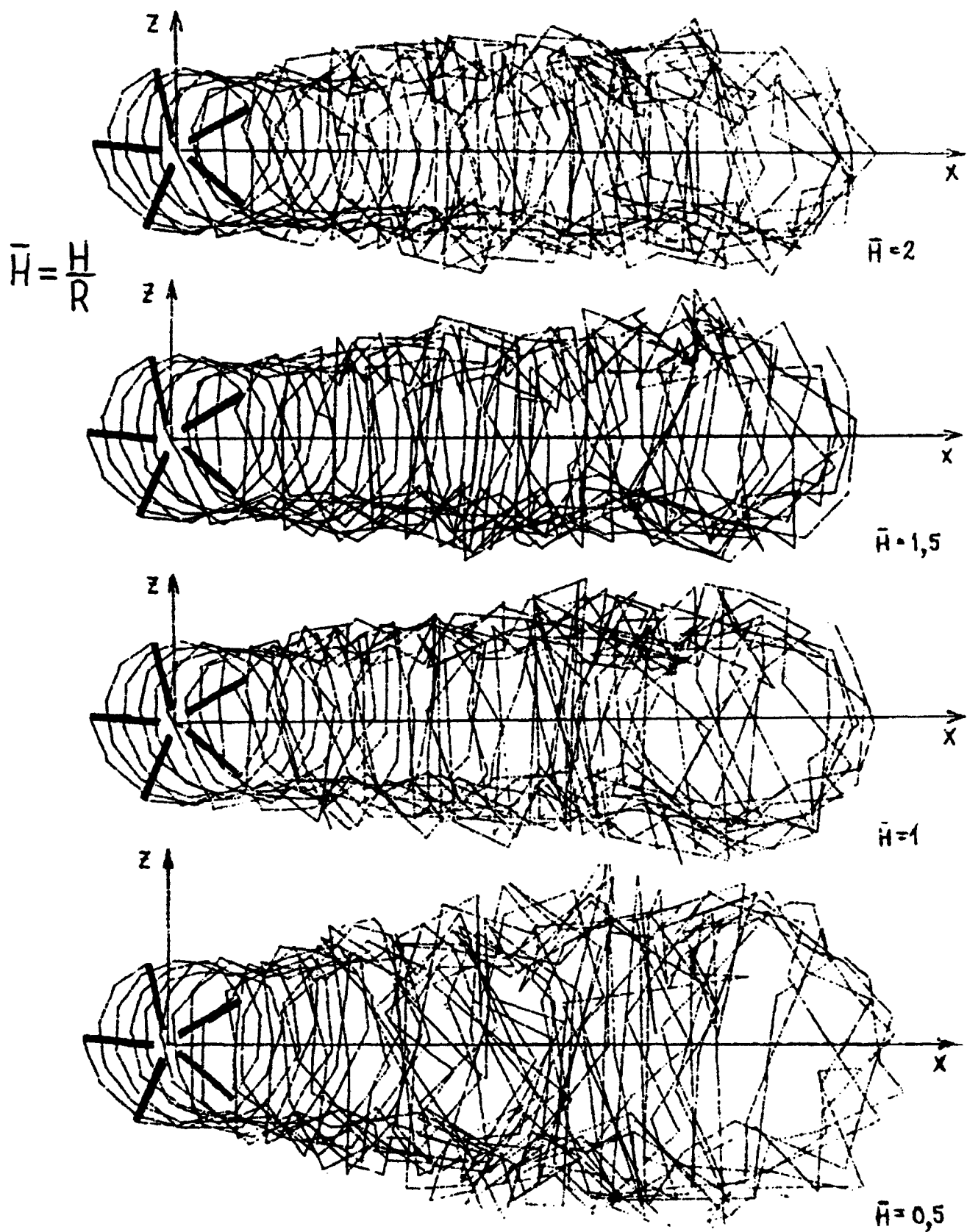
Influence of the ground
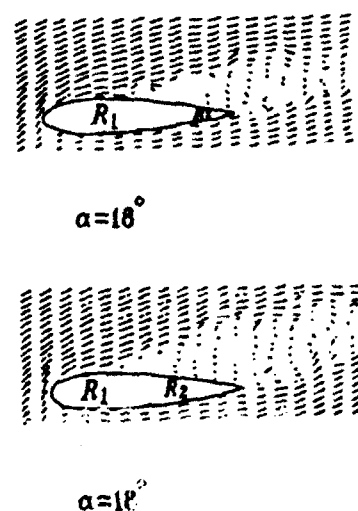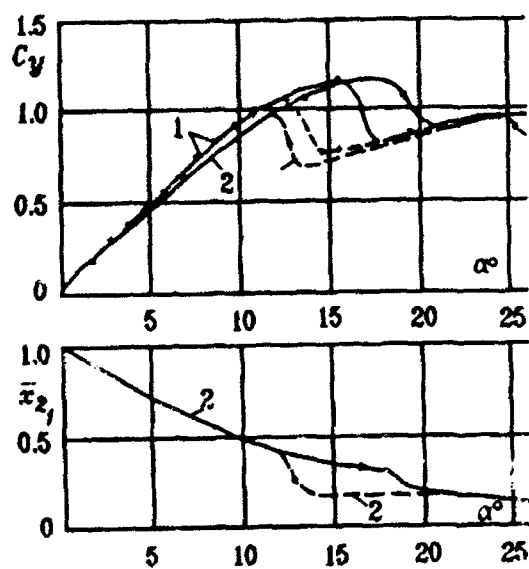
Model of static hysteresis. Different values of lift are obtained, depending on how the angles of attack are changed: from smaller to larger ones (a) or vice versa (b).
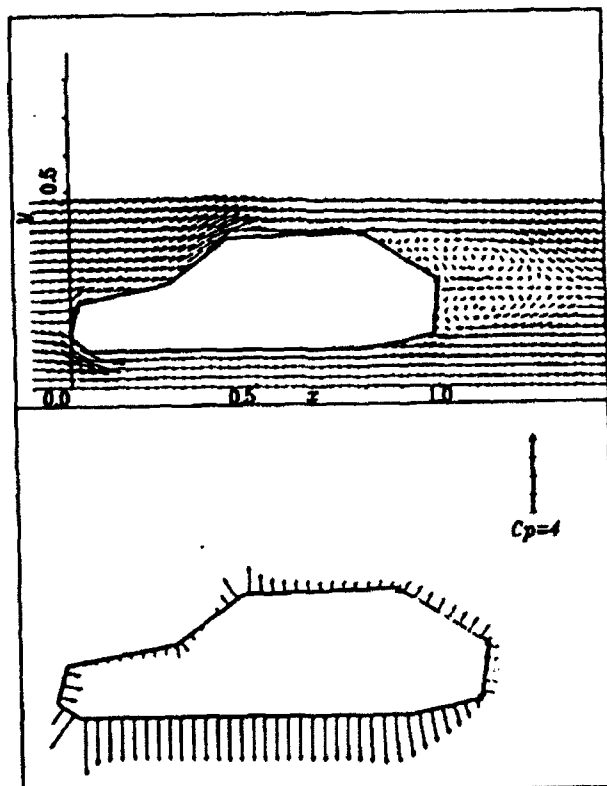
Flow past a car outline near the ground: (a) flow velocity field, (b) aerodinamic loads.

20-13
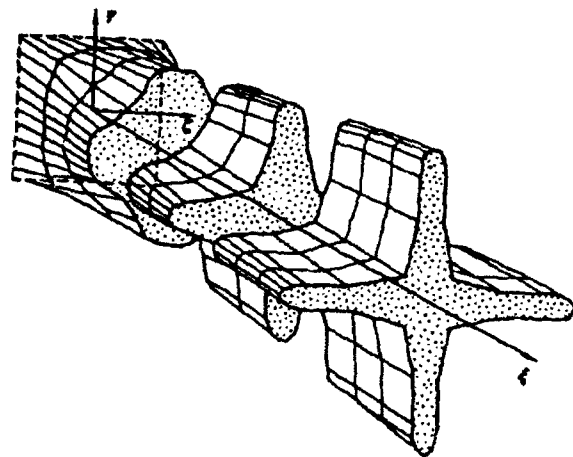
A jet outflowing from a convergent quadrangular
channel behaves in a way similar to the one shown
in the preceding figure: it is star-like too but
has four beams perpendicular to the channel's
walls. The upper portion of the figure shows the
calculated flow, the lower one – experimental
outflow of a water jet into air.
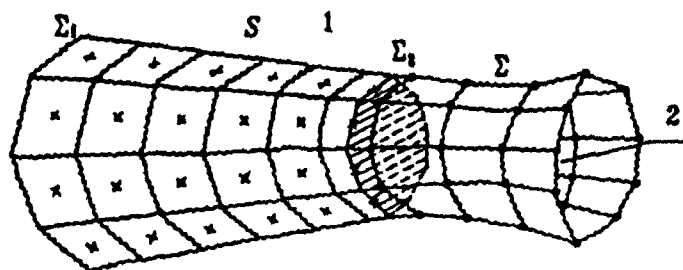
Vortex model of a nozzle (1) and a nonstationary jet (2).
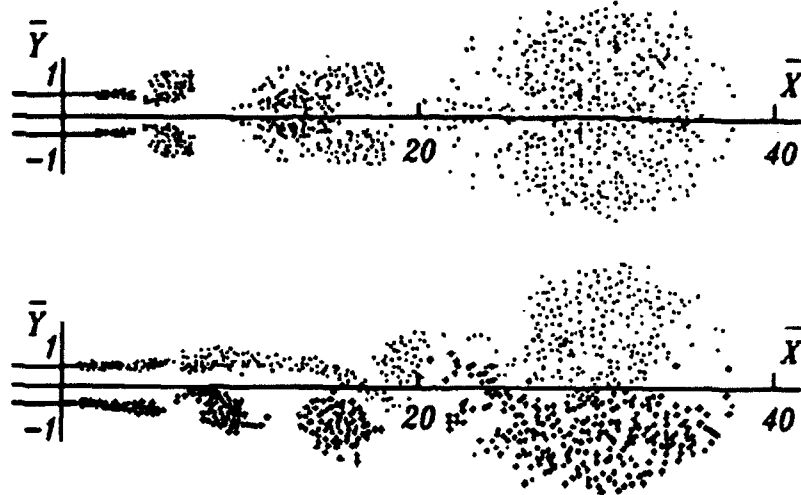
Discrete vortices modeling boundaries of a plane jet.The upper and the lower portions of the figure show, respectively, flows calculated subject to the condition of the flow being symmetric and in the absence of the condition.
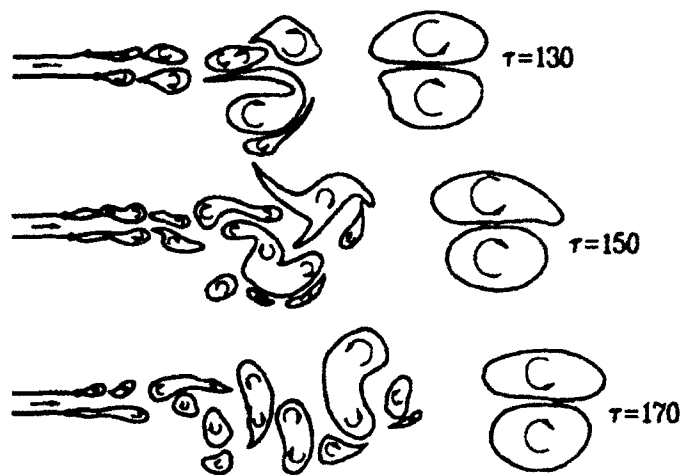
Formation and development of coherent vortex
structures in a plane jet outflowing into a flooded
space.
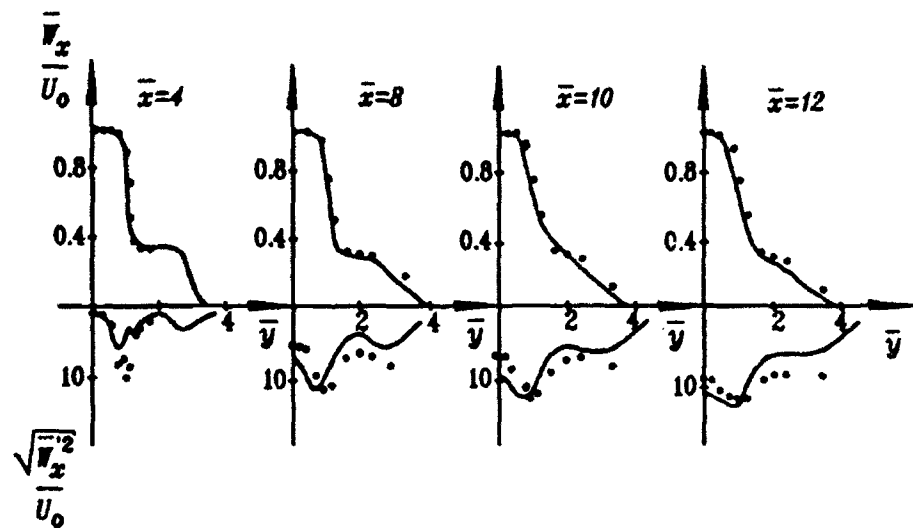
Variation of the 1st and the 2nd order moments
across circular co-axial jets. The lines and the
points show calculated and experimental data
respectively.
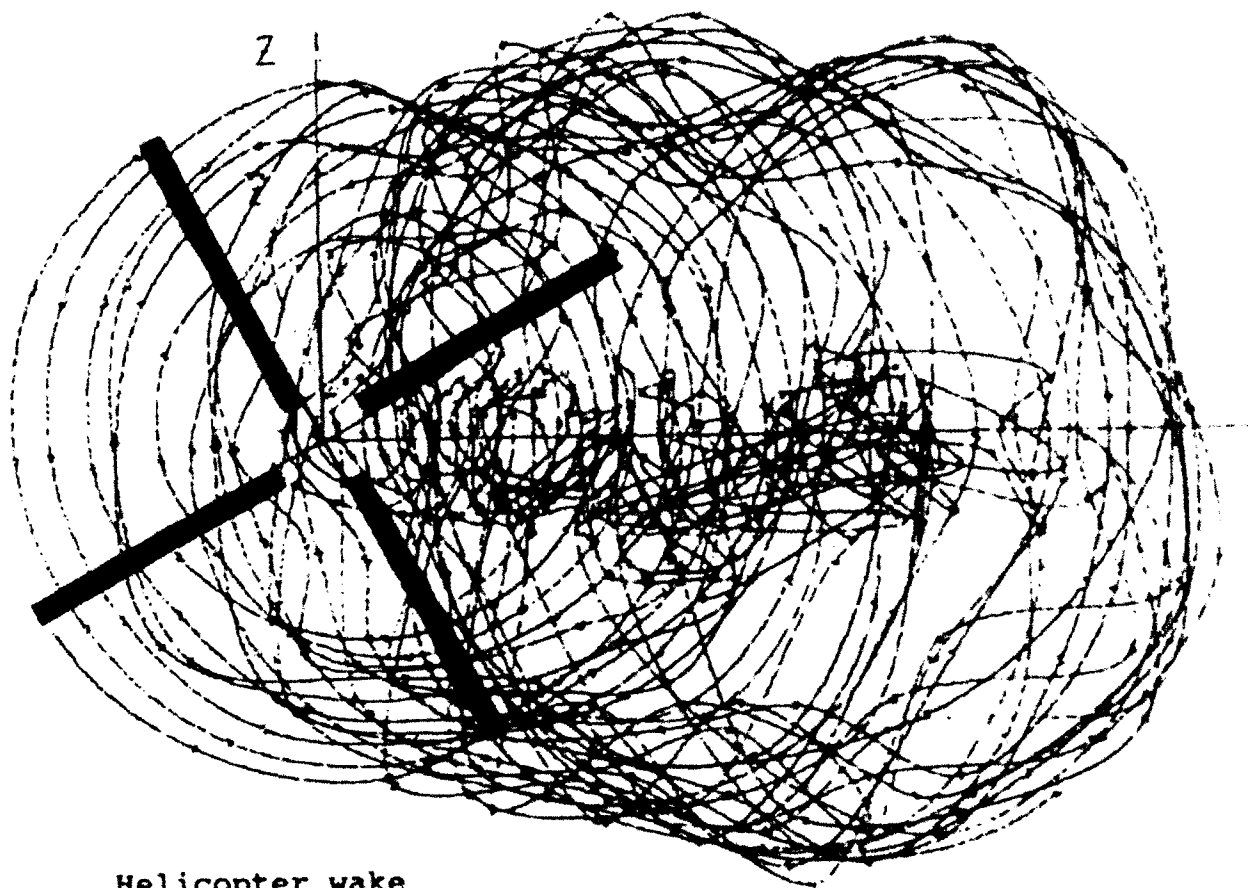
Helicopter wake

Landing
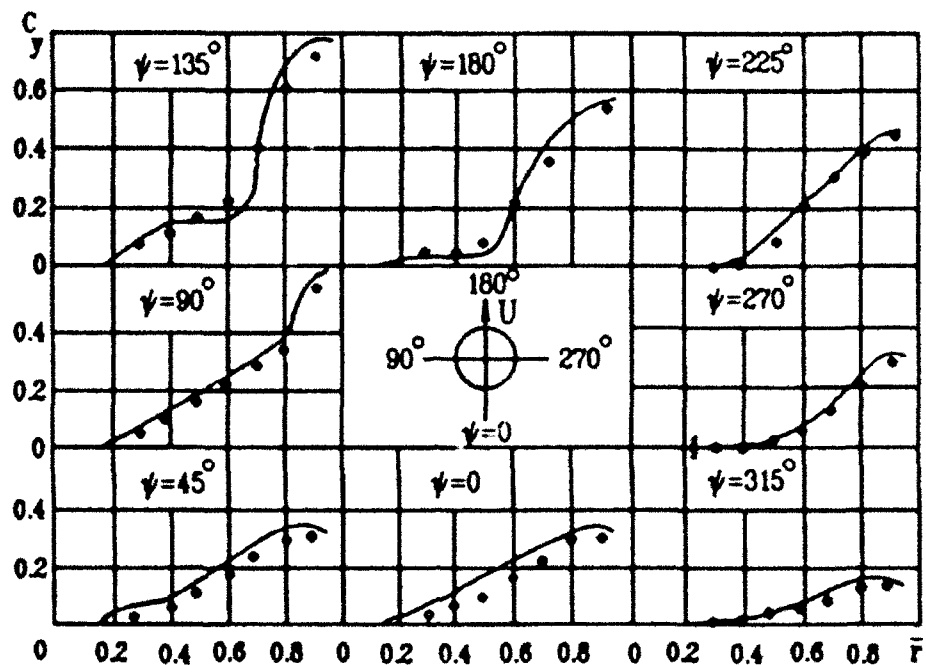
Comparison of calculated results and experimental
data on the normal force coefficient for a blade of
a four-blade rotor. The oblique oncoming flow mode
(u = 0.25) (lines show calculated results, poits –
experimental data).
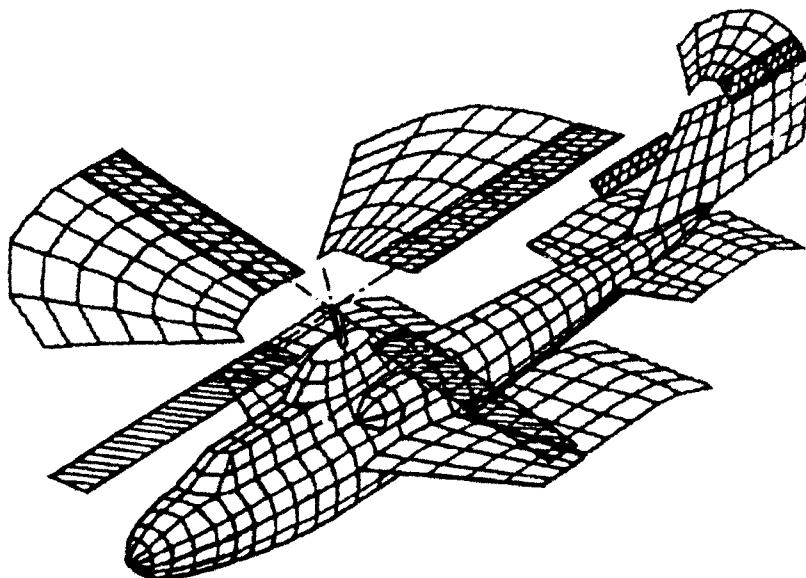
Vortex scheme for calculating a helicopter in the
case of nonstationary motion.
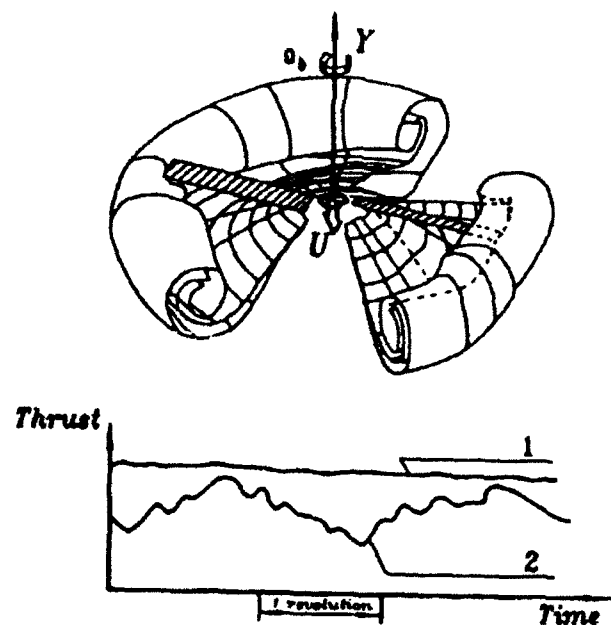
flow past a helicopter rotor in the case of vertical
descent: (a) the normal mode, (b) the "vortex ring"
mode (the rotor operates in its own wake).
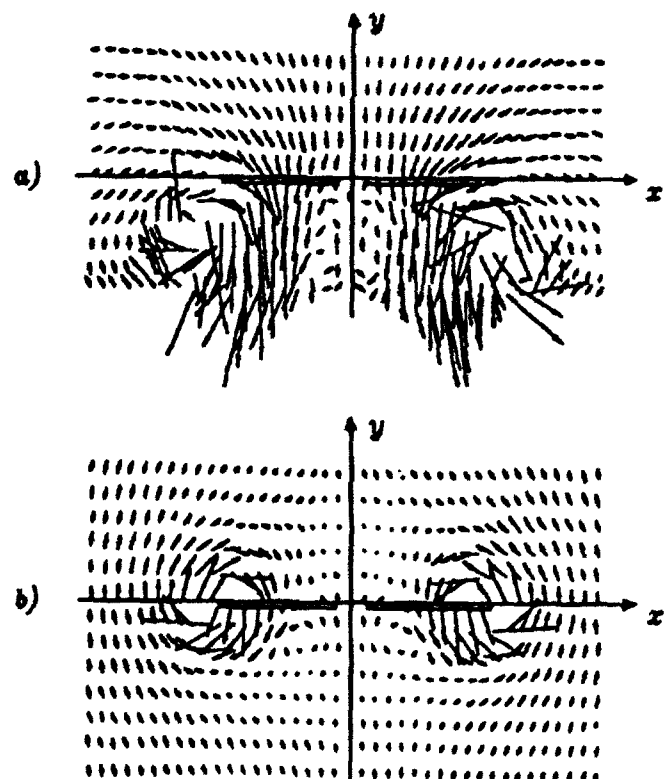
Flow field near a vertically descending rotor :
(a) the normal mode, (b) the "vortex ring" mode.
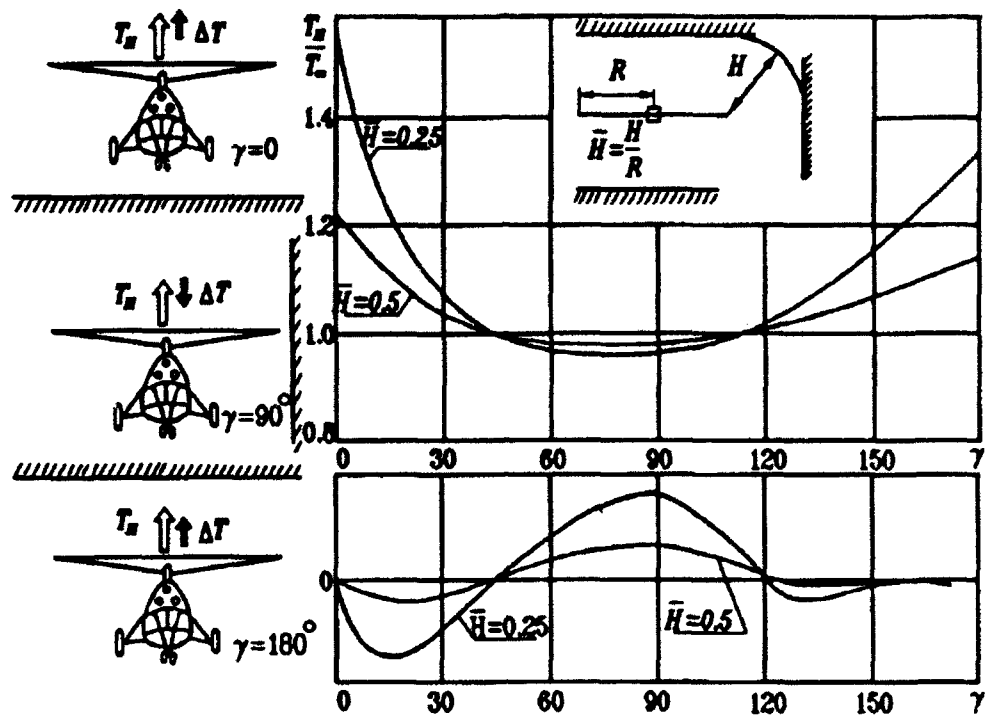
The effect of obstacles on the thrust. T_H and the
roll moment M_X of a Helicopter (H is the distance
from an obstacle, R the rotor radius, the obstacle
inclination angle).
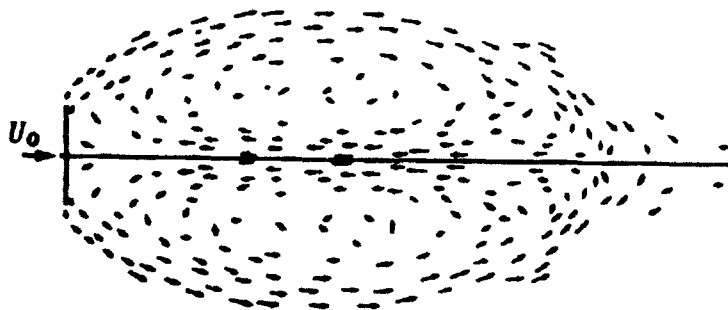
Symmetric separated flow past a flat plate for $= \infty$,
$\alpha = 90°$: (a) towing tank tests, (b) calculated.
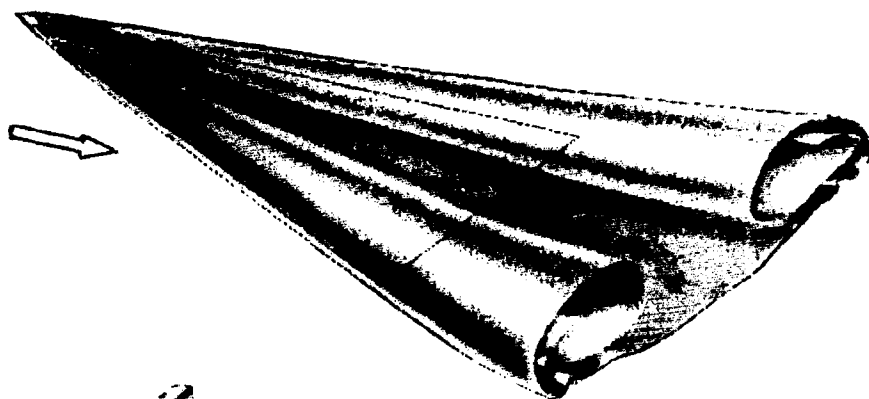
Delta wing
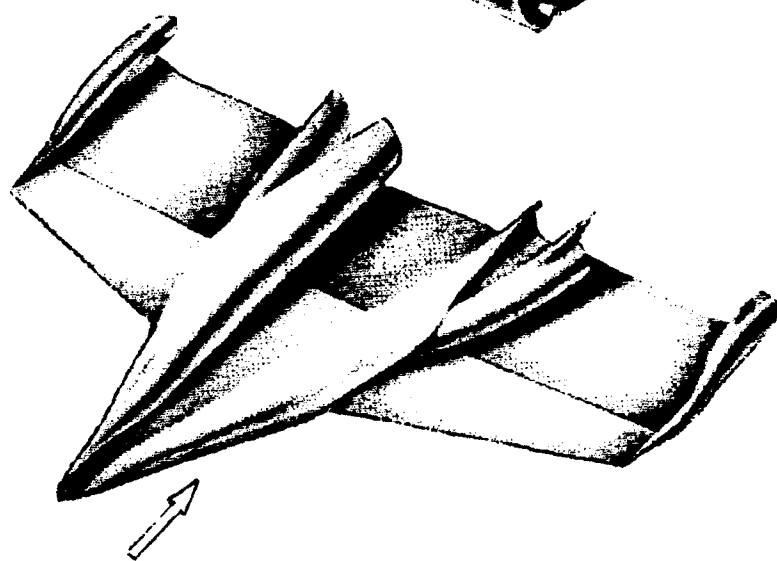
Swept wing
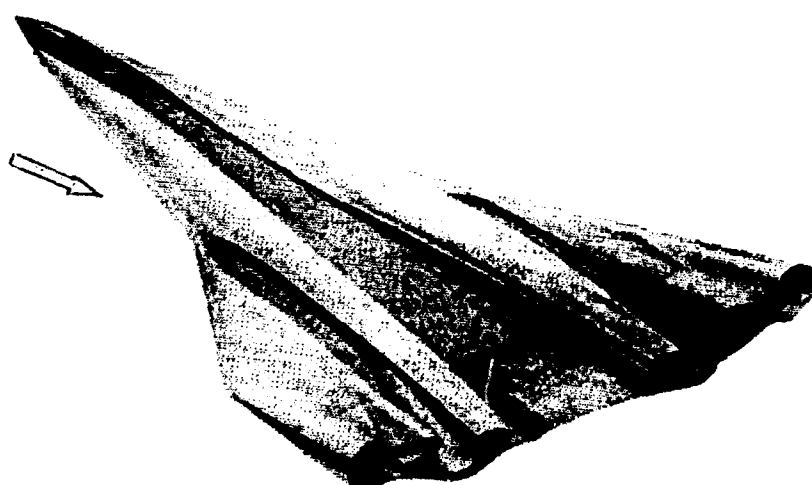
Wing of
slender
ogee
planform
(for instance,
a wing of an
airplane like
"Concord" or
TU-144)

Vortex structures at various airplane wings
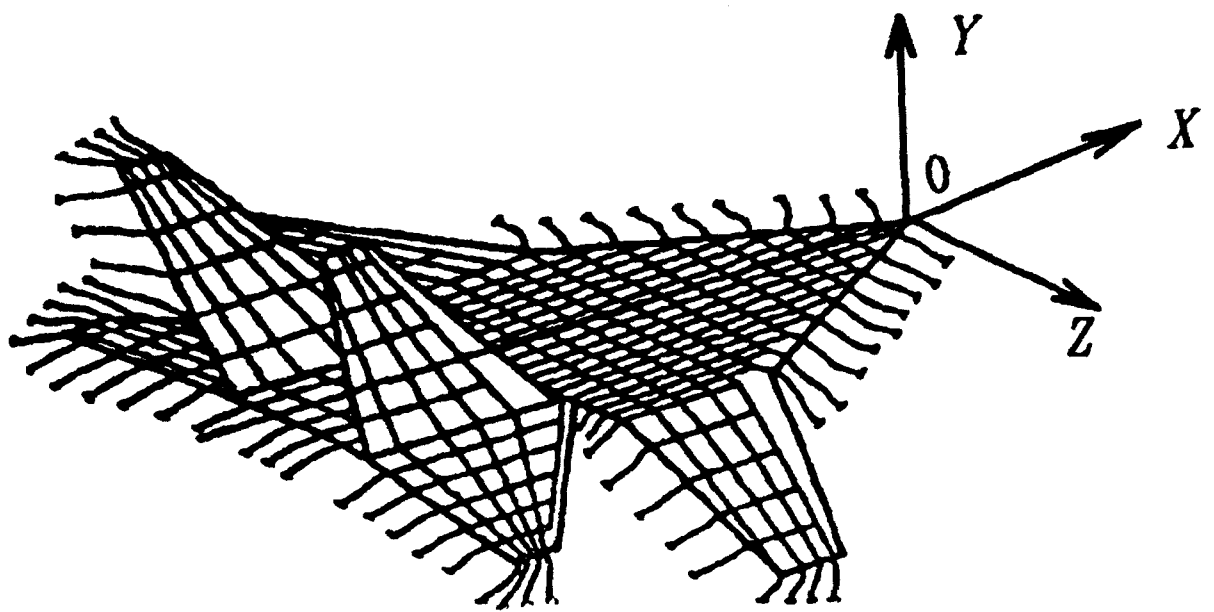
Simplified scheme of an airplane used for solving
nonlinear problems

Airplane wake

$\alpha = 25^{\circ}$

$\bar{U}_{\circ}$

$\bar{U}_{\circ}$

$\alpha = 45°$

$\vec{U}_o$

$\vec{U}_o$

Airplane wake

$\alpha = 90°$

$\vec{U}_o$

$\vec{U}_o$
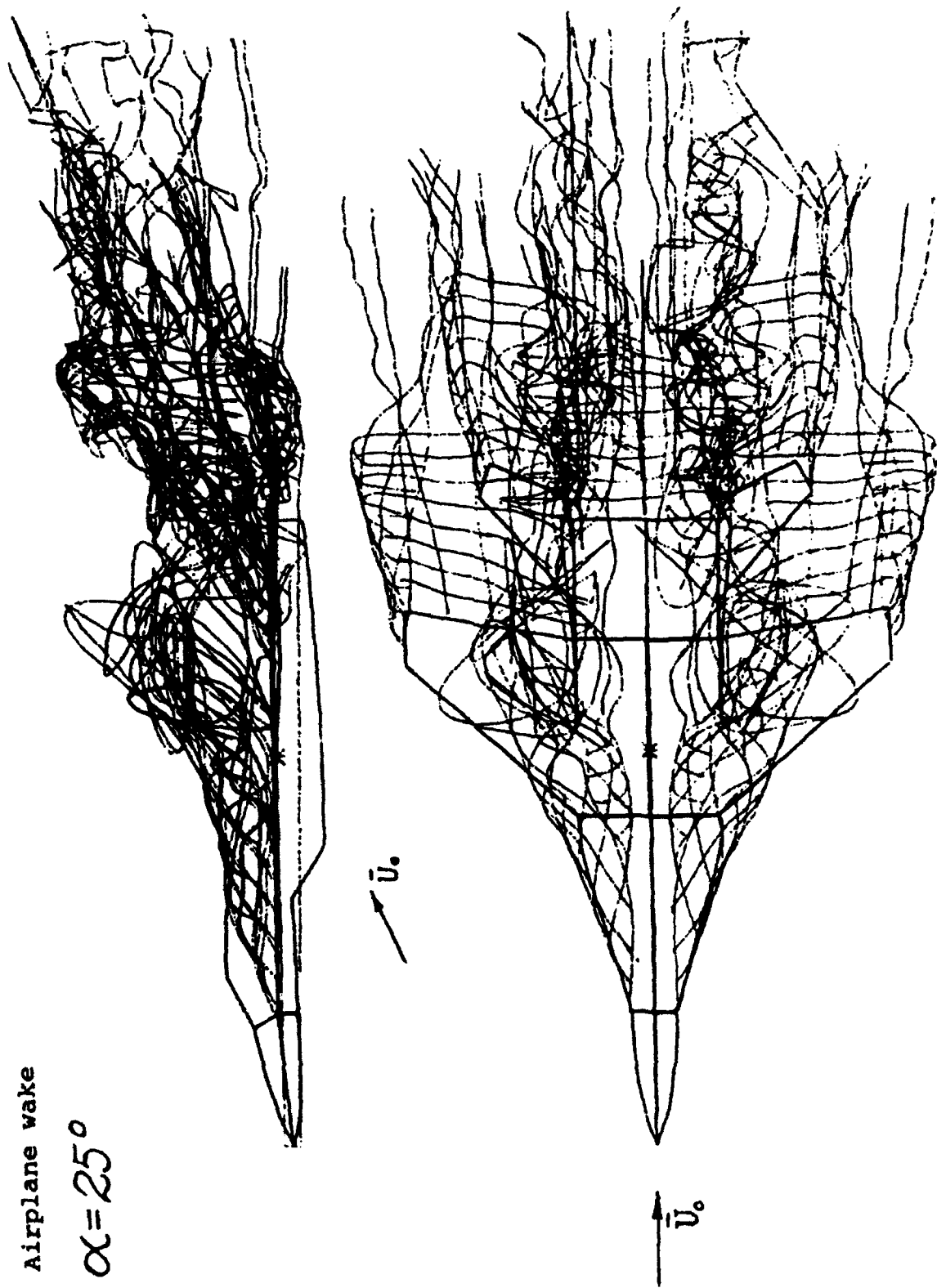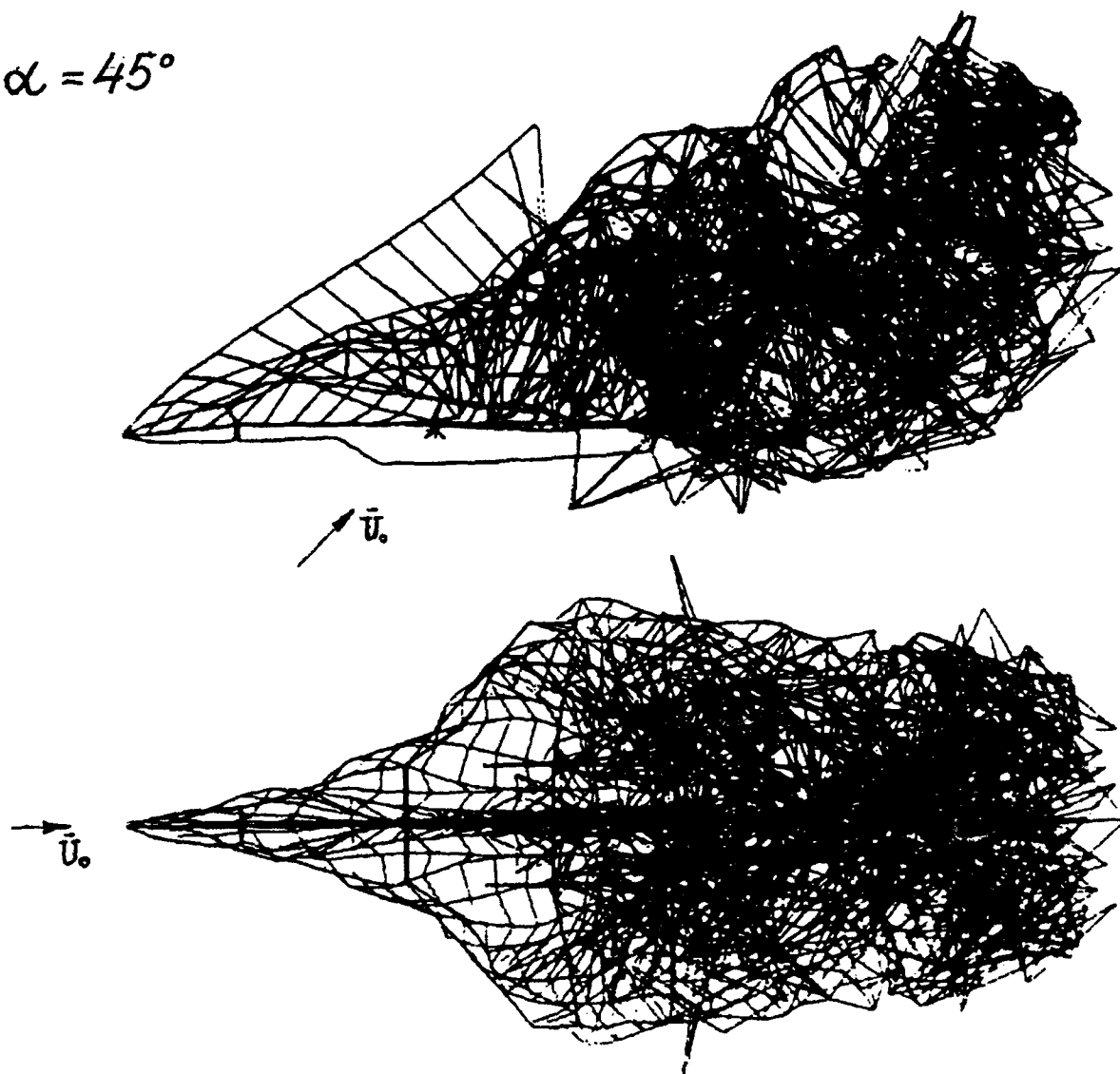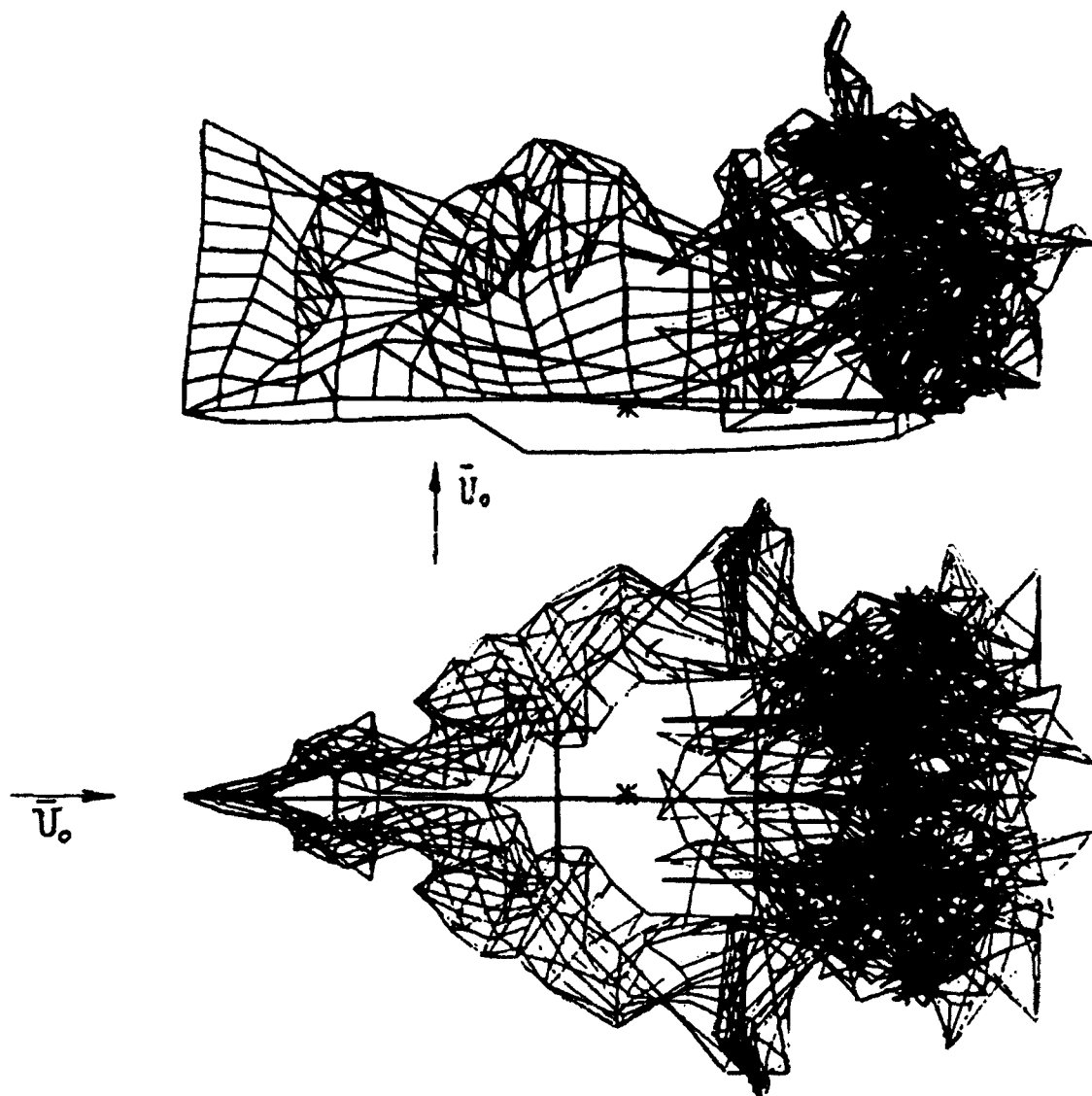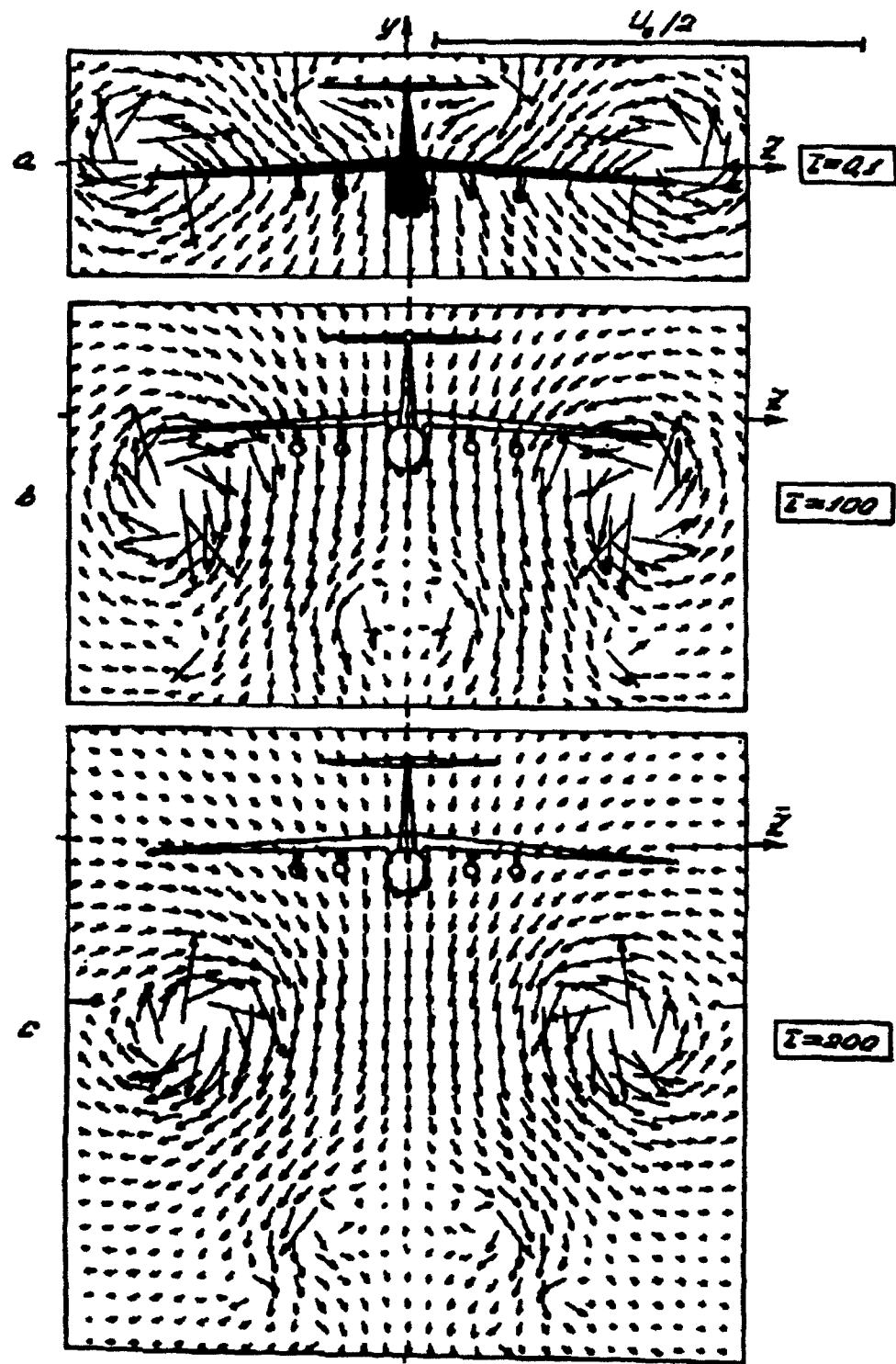
Airplane wake

Development of the wake behind
the plane IL-76
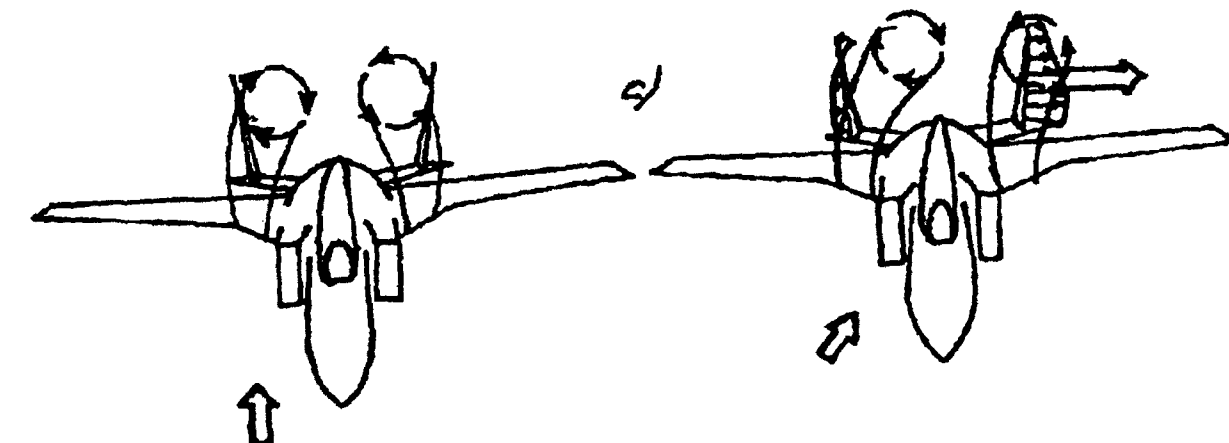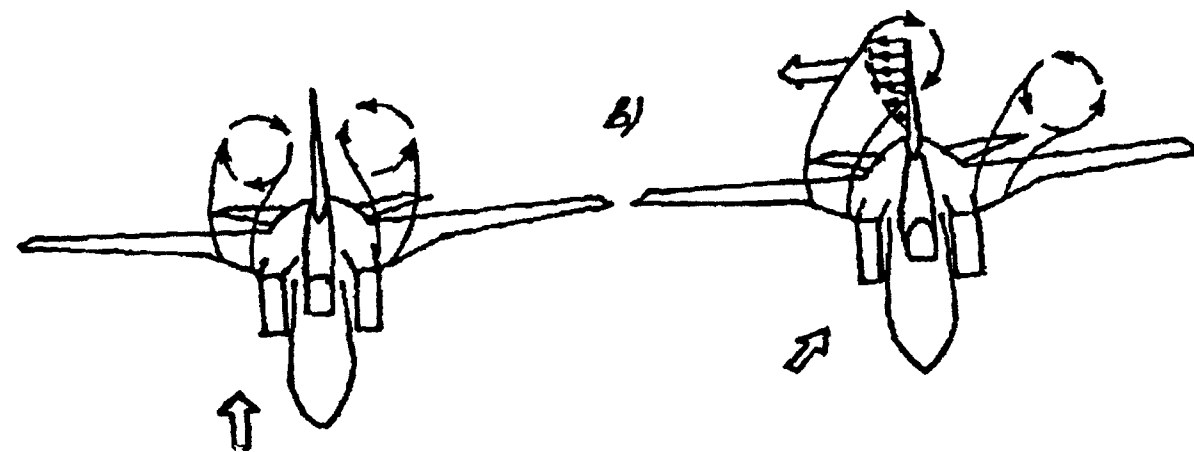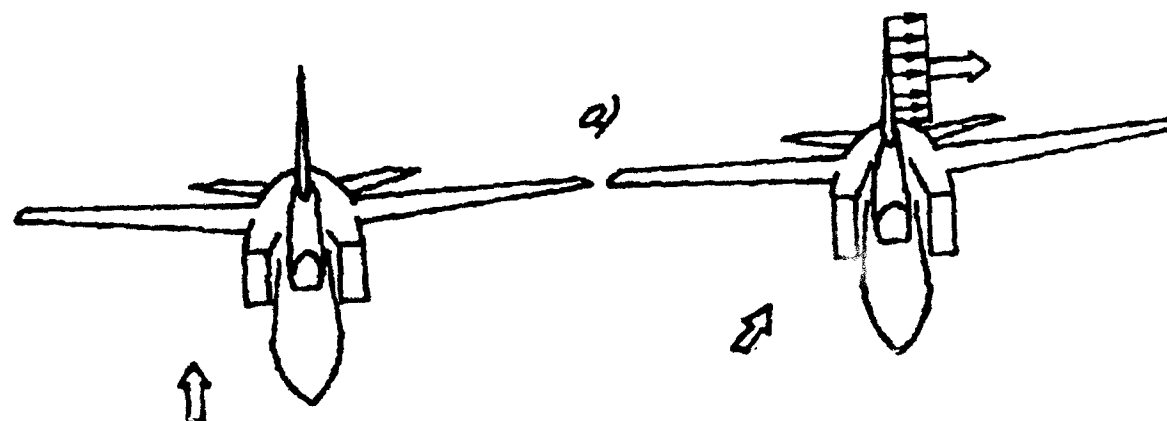
Model of airplane stalling into spin

Vortex-ring state for a helicopter Mi-8
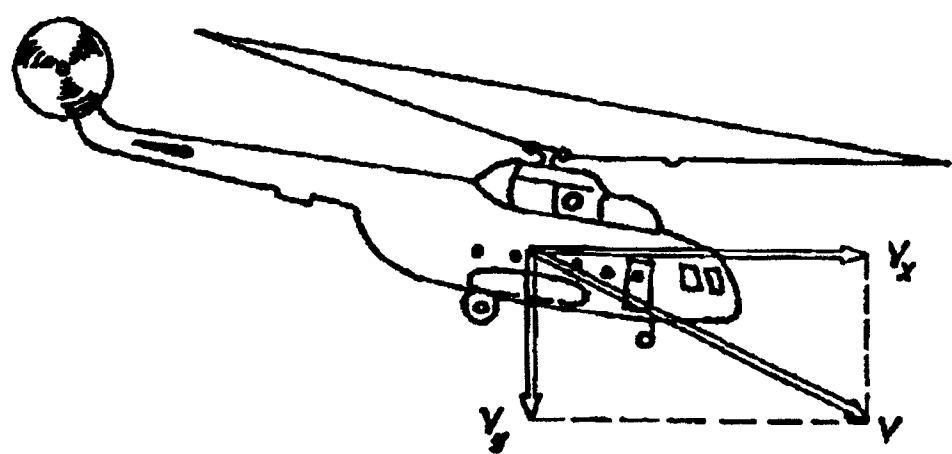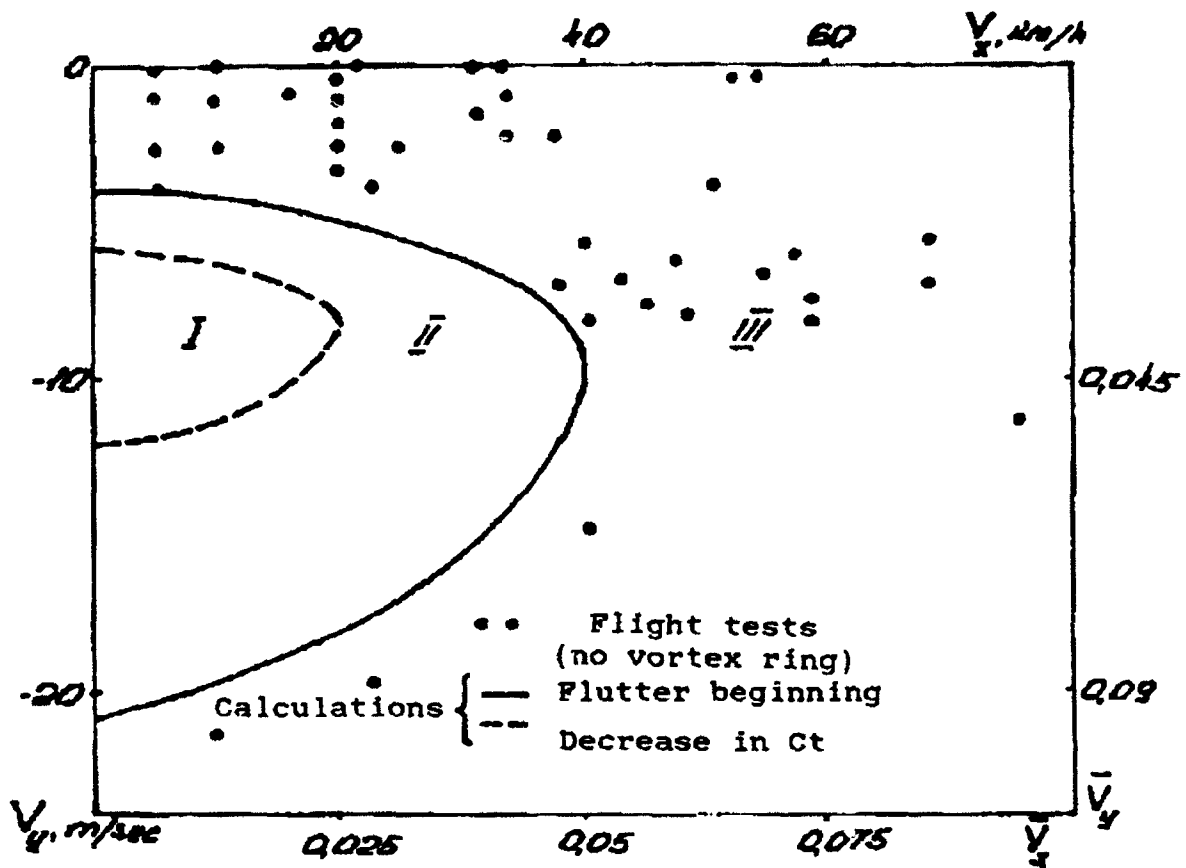
Analysis of safe descent regimes for a helicopter

Beginning of Yak-40 taxiing off

$\Delta t = 84sec$

$U, m/sec$

$\Leftrightarrow W = 1 m/sec$

Beginning of IL-76 taxiing off

$\Delta t = 11 sec$

$U_0, m/sec$

$0 \quad 10 \quad 50 \quad 100$

$\Leftrightarrow W = 1 m/sec$

H, m
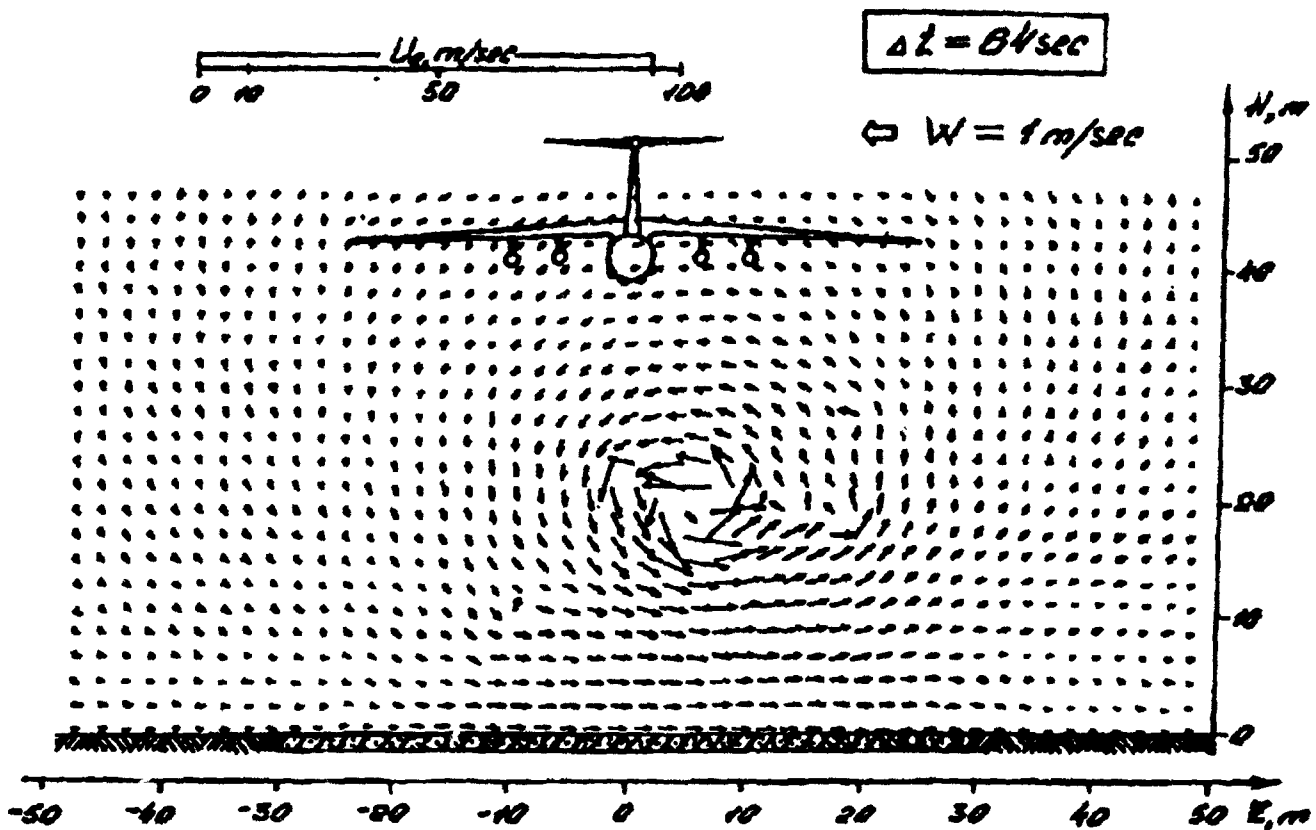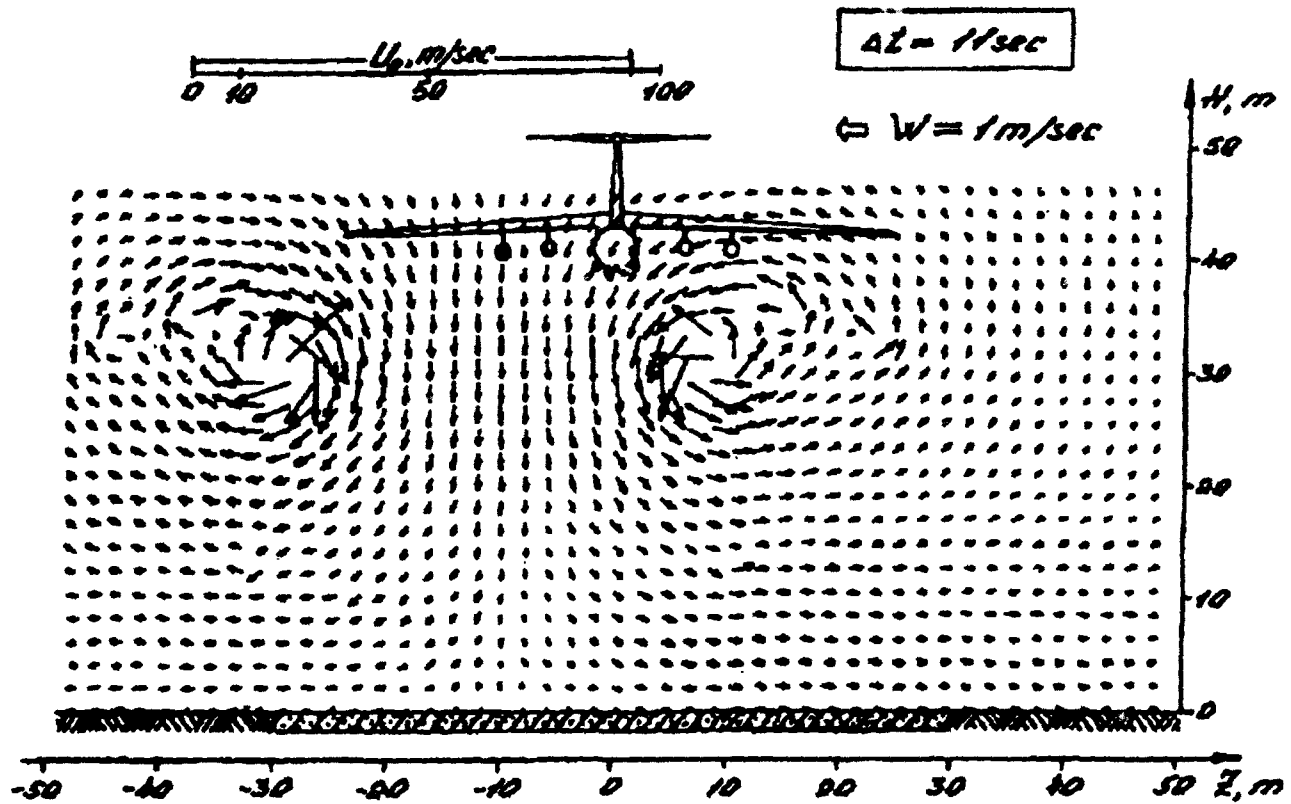
Analysis of the crash when Yak-40 took off after IL-76

Yak-40 gets into the wake
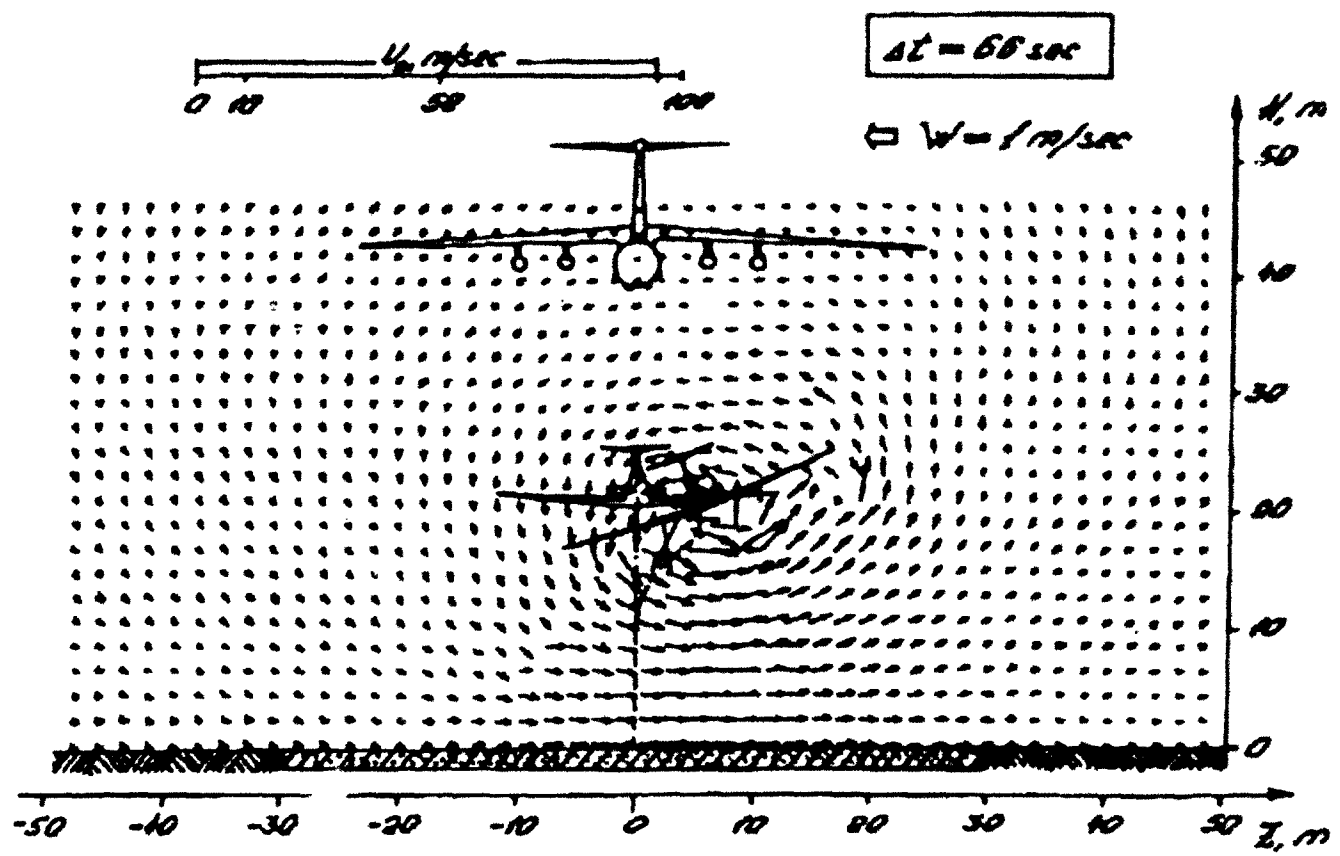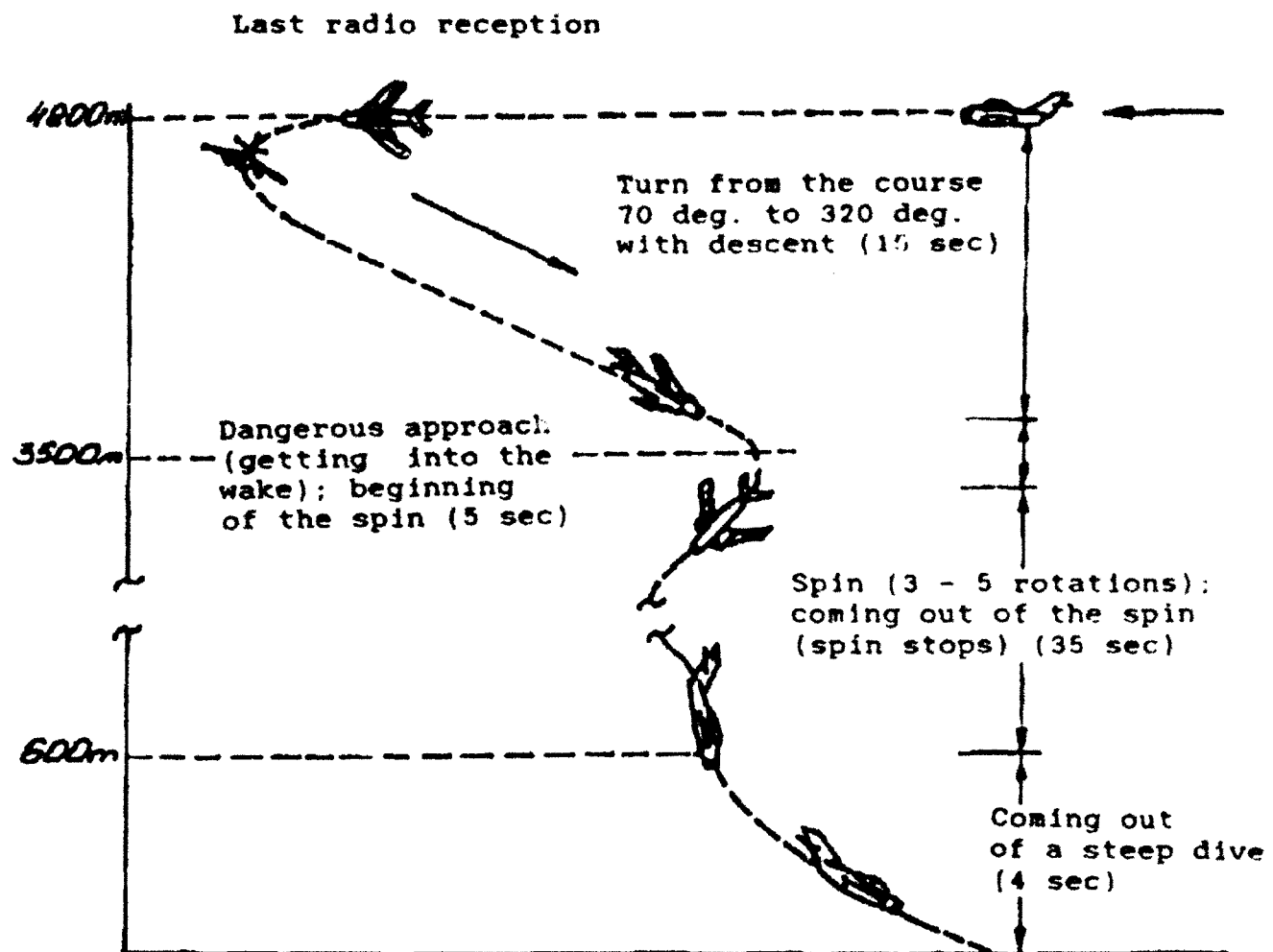
$\Delta t = 66\,sec$

$W = 1\,m/sec$

Last radio reception

4800m

Turn from the course
70 deg. to 320 deg.
with descent (15 sec)

3500m — Dangerous approach
(getting into the
wake); beginning
of the spin (5 sec)

Spin (3 - 5 rotations);
coming out of the spin
(spin stops) (35 sec)

600m

Coming out
of a steep dive
(4 sec)

The most probable phases of the last stage of
Yu. Gagarin's flight (time spent for each phase is
indicated).
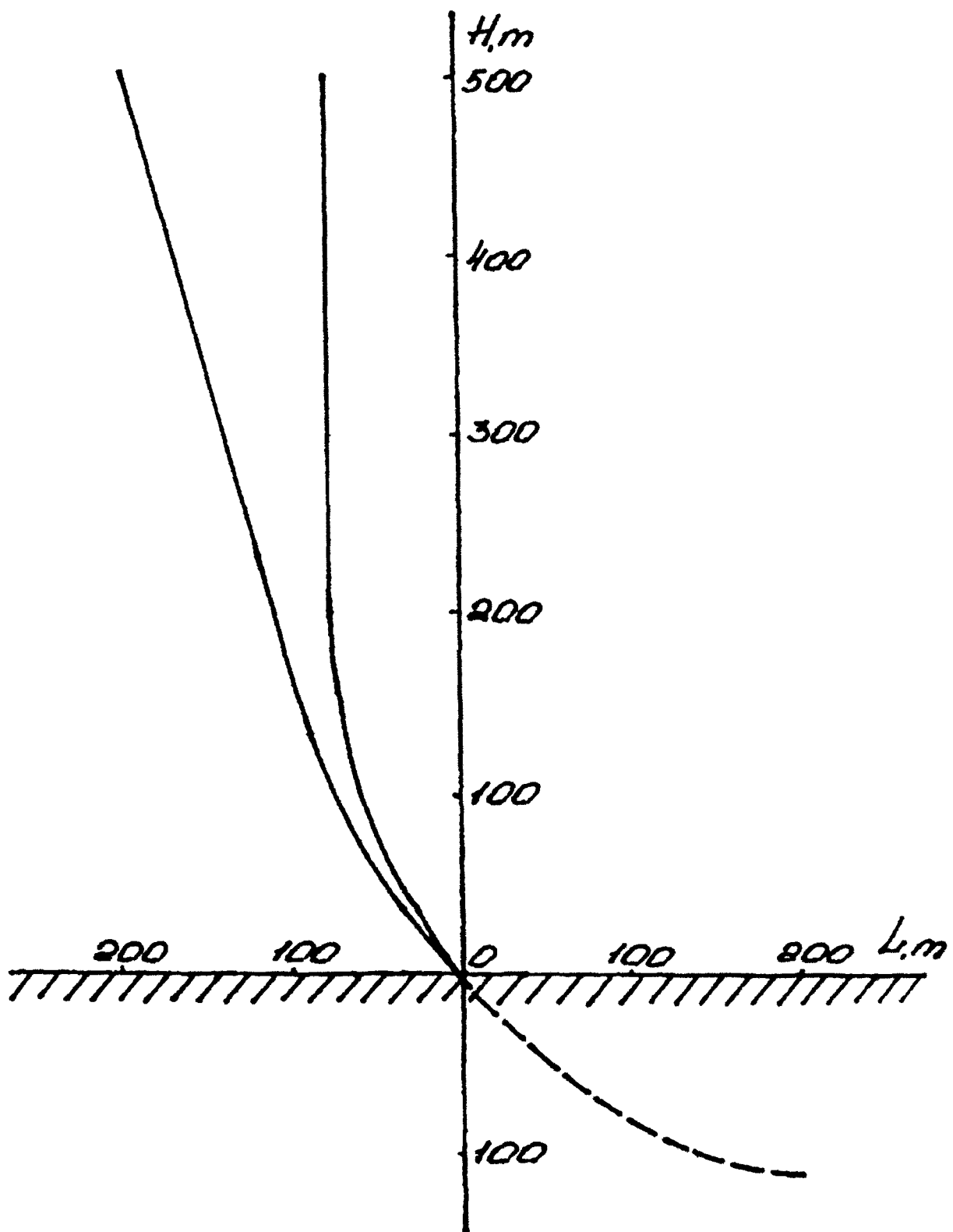
Most probable airplane trajectories for the last phase of flight to the ground (the dashed line indicates the trajectory extension).

METHODS OF STUDYING AN AIRPLANE VORTEX WAKE STRUCTURE IN FLIGHTS AT LOW ALTITUDES

Y.A. Zavershnev
V.K. Kushnerev
A.N. Zamyatin
Flight Research Institute
Moscow, USSR

Vortex wake is a source of hazards for airplanes flying into it, so vortex wake research is urgent. Actual (flight) wake data are the most reliable basis for developing methods to reduce its adverse effects.

For civil aviation, of prime interest is the wake effects in flying at low altitudes:

- just over the runway (0 to 20 m),

- in the takeoff and approach area (0 to 300 m).

Vortex wake is a rather complex physical phenomenon, the research of which requires a special procedure. The procedure must provide for the following three groups of measurements:

- the wake characteristics recording,

- measuring the flight parameters of the airplane generating vortex wakes,

- meteorological data acquisition in the wake development region.

As far as the low altitude range is concerned, a ground method for the research was chosen using a high mast (Figure 1). In fact, two schemes were applied:

- with a mast 16.5 m high when operating over the runway (a telescopic radio mast is used),

- when operating at higher altitudes with a mast 330 m high (the tower of the Institute of Experimental Meteorology is used).

To establish wake characteristics the thermoanemometric method of measurements, smoke visualization and stereophotogrammetric surveying of the visualized vortex cores are used.

In order to estimate the wake flow velocity vector the thermoanemometric method is adopted. The arguments for this method are as follows:

- due to small sizes of the hot-wire probes local measurements can be provided;

- for the velocity range of interest of 1 to 40 m/s, there is no problem with the signal interpretation; King (perpendicular flow) and Bradshaw (oblique airflow) laws fit well enough;

- the necessary frequency band (0 to 15 Hz) is easily implemented with any hot-wire anemometer circuit; a constant-temperature (CTA) circuit is really used with output filtered.

At the same time, the thermoanemometry application faces a number of problems which are solved as follows:

- measuring the three components of the wake flow velocity (V_x, V_y, V_z) is provided with a three-wire probe, therein the wires are placed separately in oriented miniature tubes (Figure 2);

- the relationship between the hot-wire anemometer signal and the flow deflection angle is determined experimentally in the calibration wind tunnel tests; certainly, it is difficult to provide the cosine calibration curve (Fig. 3): in the range of $|\psi| < 20°$ the plateau introduces an error of $\Delta_1 = 7\%$ into the velocity component measurement;

- the tube flow separation at $|\psi| > 20°$ results in signal fluctuations, but these are in the high frequency band and eliminated by filtering;

- zero and probe sensitivity factor instabilities are taken into account with individual calibration and "electrical zero" record following each apparatus switch-on and warm-up; as a whole, the error of the velocity component measurements did not exceed $\Delta = 13\%$;

- the above probes allow measuring only absolute values of the flow velocity components - $|V_x|$, $|V_y|$, $|V_z|$ and do not indicate their signs; this limitation presents difficulties for the data processing and analysis. However, through the measurement redundancy (to be more exact, because of their multiple-point nature) one can usually select a combination of signs which meets all the data available for the flow in the areas where the probes are located.

More complex gages were developed later, which permitted the sign definition for all flow velocity components if the sign of one of them is known. These gages have six sensitive wires each which are openly placed in the flow, thereby comprising two systems of the three

perpendicular wires (Figure 4). King and Bradshaw laws application yields the equation set to determine the flow velocity components which also might be used for automated processing of the measurement results.

The hot-wire gates were located along a mast 16.5 m long, 15 to 17 in number, spaced 0.7 to 1.0 m apart.

To record the vortex core geometry, the wake smoke visualization and the visualized wake stereophotogrammetric survey methods were used. For this purpose, smoke devices were suspended under each airplane outer wing, usually two in number, which can be operated in any combination required. Each smoke device provided stable smoke generation during 5 min; contrasting white and orange smokes were used.

Stereo surveying of the visualized vortex cores was performed with a pair of synchronized cameras intended usually for aerial photography. These cameras have improved distortion and other aberration parameters. The cameras and check marks were aligned on the ground with the standard geodetic procedure; a base of $B=100$ m was used (Figure 5). The stereophotos were handled on a classical Carl Zeiss Jena stereocomparator. As the research practice has shown later, when operating at a distance of 1000 m this method permits reliable recording of the disturbed vortex core geometry (including the wavelength, the distance between the cores, etc.), as well as acquisition of vortex "bursts" photos, arched segments over the runway, etc.

The dynamic vortex flow visualized pattern was also recorded by the cine cameras with the vortices passing through the hot-wire gage locations.

Combined application of the vortex visualization and thermoanemometric measurement results makes it possible to note such wake vortex features as the presence of the inverse (as compared to the flight direction) core axial flows. Continuous data on the velocity components, $V_x(t)$, $V_y(t)$, $V_z(t)$, provide a simple solution of some significant kinematic problems: determination of the vortex flow core position and sizes; recording of the maximum circumferential and axial vortex velocities; estimation of the vortex descent, etc.

The second group of parameters specific to the flight mode of the vortex-generating airplane is measured with usual methods adopted for flight testing.

One specific feature of the above studies is the need for the airplane flight control, so that its vortex wake passes through the placed gages and the phenomena under consideration develop in sight of the mounted photo and cine cameras. This important moment of the experiment was provided by:

- preliminary calculations of the airplane fly by trajectory lateral, ΔL, and vertical, ΔH, deviations relative to the mast with the gages mounted;

- performing a number of test flybys with the evaluation of hits and correction of the ΔL and ΔH value deviations by the flying control officer on the ground;

- check flying with the refined ΔL and ΔH deviations.

With preliminarily estimates of the deviations, it was taken into account that the vortex wake descended at $V_y = -(4V_\infty C_L)/(\pi^3 \lambda)$ and drifted at a wind speed of $V_L = W \cos K$. For convenience and efficient operation, the flying control officer had preliminarily prepared plots of $\Delta L = f(W_L, X, V_\infty)$, $\Delta H = f(X, V_\infty)$ (Figure 6), according to which ΔL and ΔH were set for the first test flyby with account for the actual wind data (W,K), flight speed ($V\infty$) and longitudinal coordinate (X) of the wake section under study.

Usually after 3 or 4 test flybys an exact (precise) wake hit on the measurement mast was possible.

When considering the role of the meteorological factors, the studies were conducted in the mast zone of the Institute of Experimental Meteorology (IEM). To analyze the results, data on the temperature fields, air pressure and wind velocity in the atmospheric ground layer were used. The turbulence level was determined based on the wind speed fluctuations measured with the acoustic anemometer. This part of the work was carried out under a contract with IEM using the equipment and procedures adopted by the Institute (Figure 7).

Overall, the technique presented above allowed a necessary volume of the investigations to be performed and a base of actual motions to be created for the airplane vortex wake in flying at low altitudes. The results of the studies are described in [2], [3].

Wind

Flight trajectory

wake

C

Airplane C

M

T

16m high-altitude mast M

1. Hot-wire measurements

300m high-altitude tower T

2. Meteorological measurements

3. Smoke visualization

4. Flight control

5. Stereophotogrammetric survey

6. Airborne measurement system

7. Smoke visualization
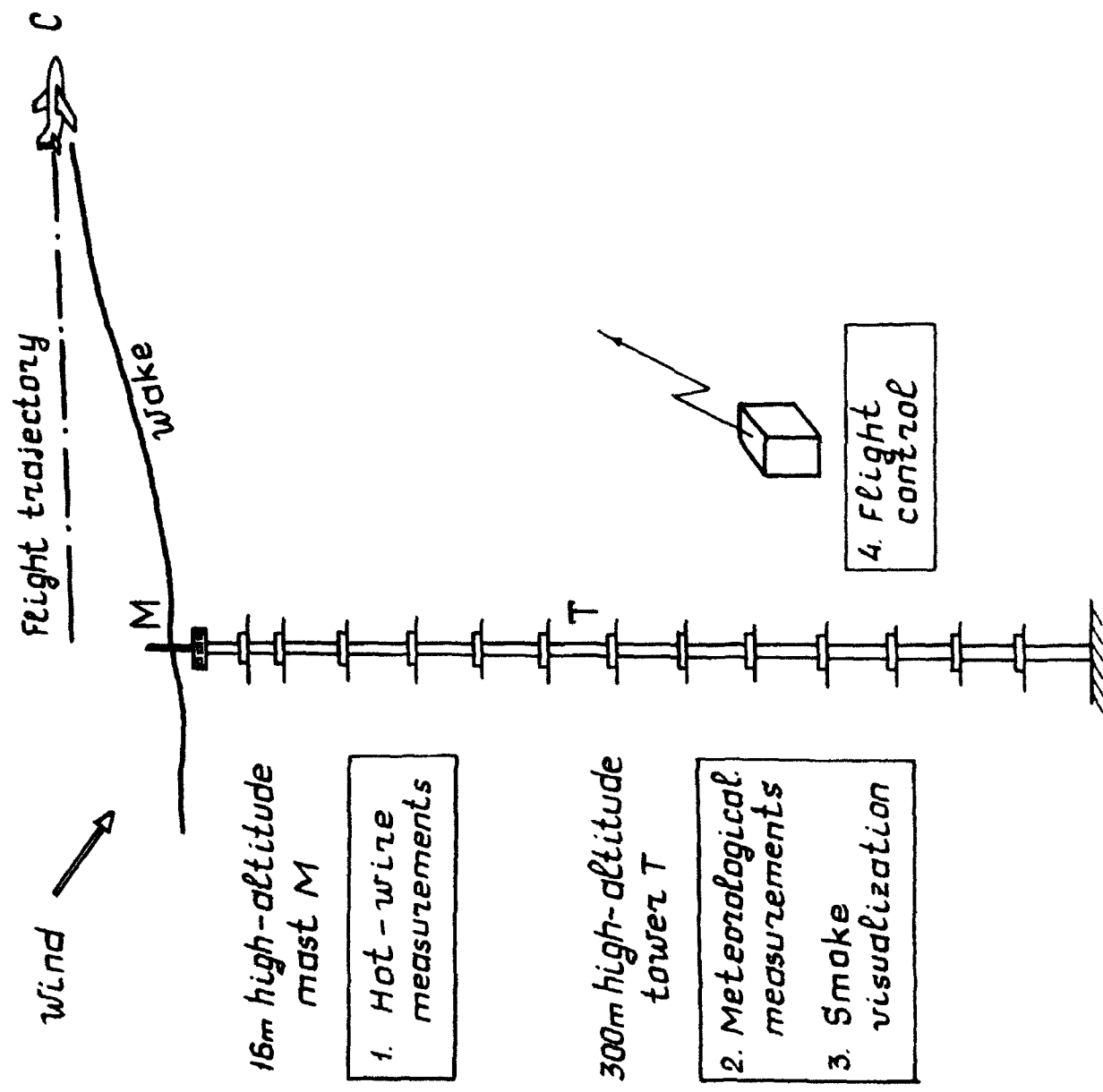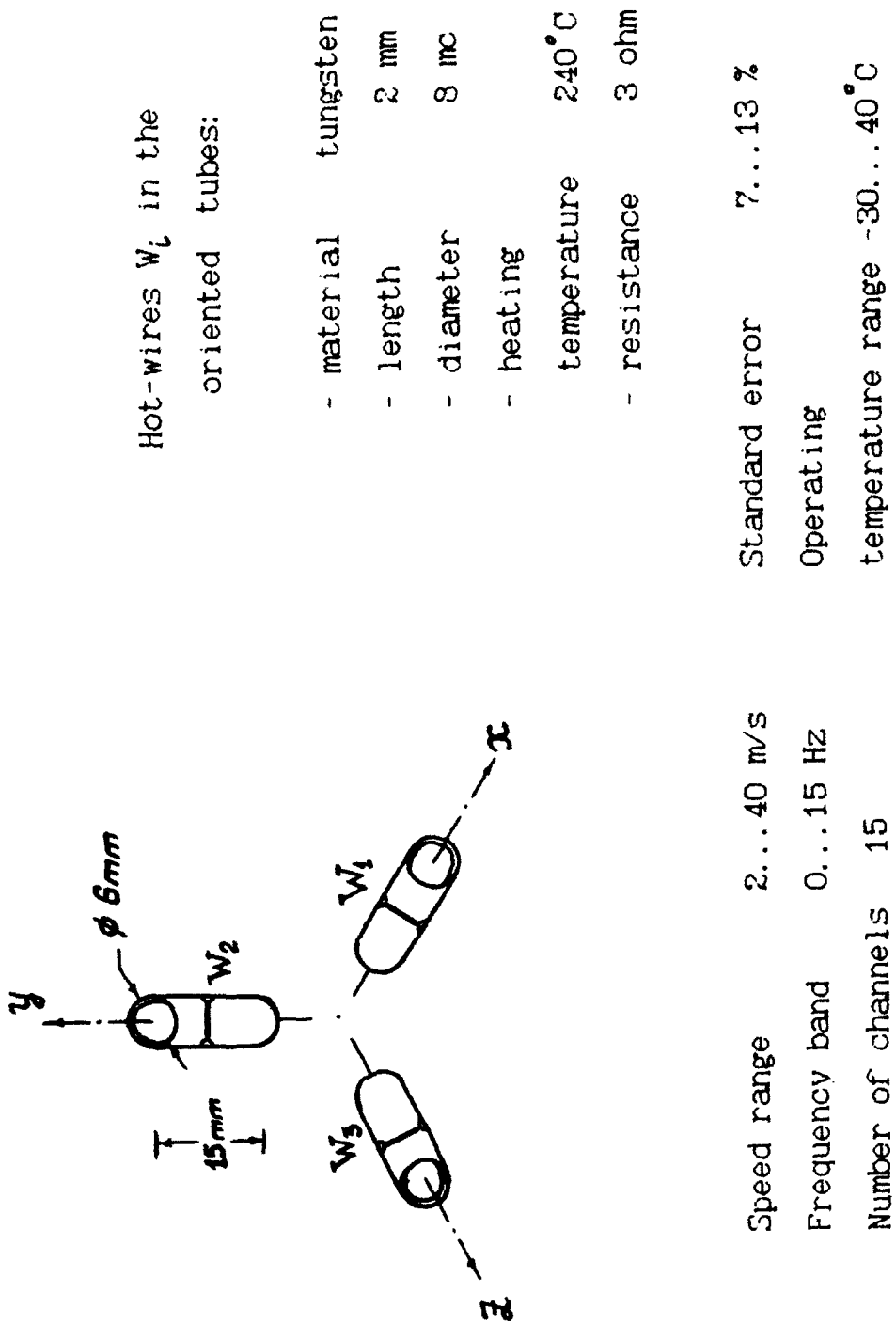
Figure 2. Tree-component hot-wire anemometer.
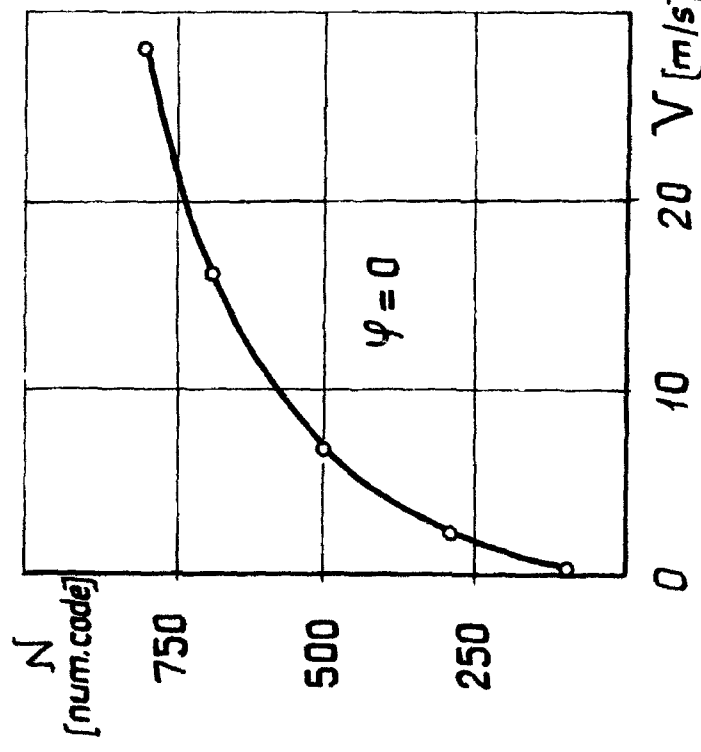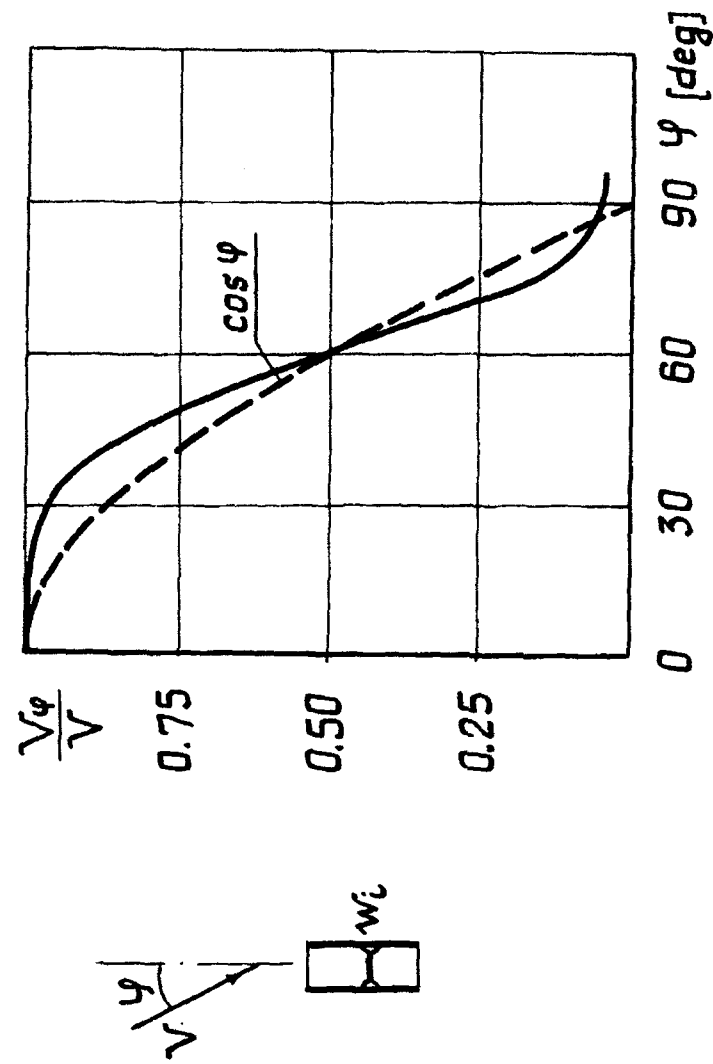
$$J^2 = K(T_e - T)(A_0 + B_0 \sqrt{V})$$

N_i – output signal (w_i)

$$V_i = f(N_i)$$

Figure 3. Hot-wire probe performance.
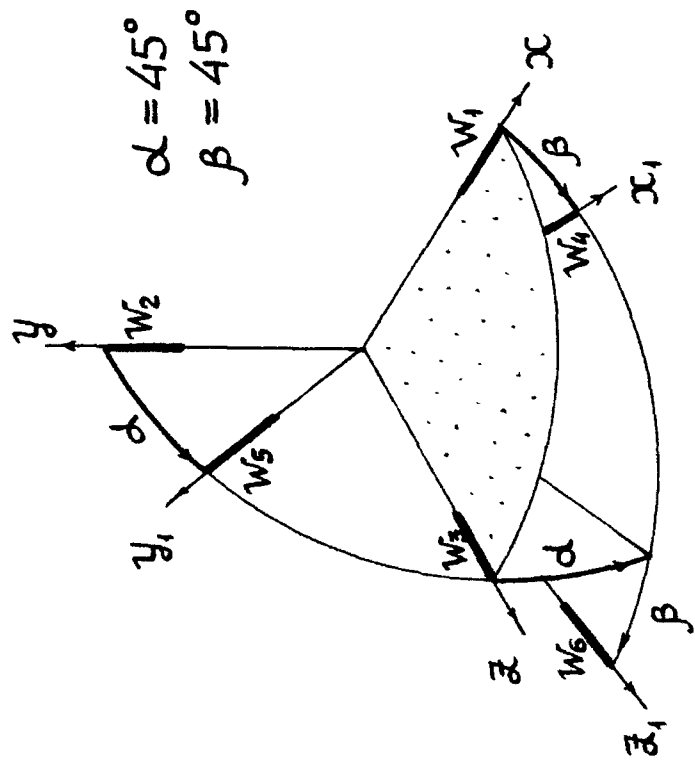
$$\begin{bmatrix} A-1 & 0 & 0 & 1 \\ 0 & A-1 & 0 & 1 \\ 0 & 0 & A-1 & 1 \\ 1 & 1 & 1 & -1 \end{bmatrix} \begin{bmatrix} V_x^2 \\ V_y^2 \\ V_z^2 \\ V^2 \end{bmatrix} = \begin{bmatrix} U_1^2 \\ U_2^2 \\ U_3^2 \\ 0 \end{bmatrix}$$

$$\begin{bmatrix} A-1 & 0 & 0 & 1 \\ 0 & A-1 & 0 & 1 \\ 0 & 0 & A-1 & 1 \\ 1 & 1 & 1 & -1 \end{bmatrix} \begin{bmatrix} V_{x_1}^2 \\ V_{y_1}^2 \\ V_{z_1}^2 \\ V^2 \end{bmatrix} = \begin{bmatrix} U_4^2 \\ U_5^2 \\ U_6^2 \\ 0 \end{bmatrix}$$

$$\begin{bmatrix} \cos\beta & -\sin\alpha\sin\beta & \cos\alpha\sin\beta \\ 0 & \cos\alpha & \sin\alpha \\ -\sin\beta & -\sin\alpha\cos\beta & \cos\alpha\cos\beta \end{bmatrix} \begin{bmatrix} V_x \\ V_y \\ V_z \end{bmatrix} = \begin{bmatrix} V_{x_1} \\ V_{y_1} \\ V_{z_1} \end{bmatrix}$$

$\alpha = 45°$
$\beta = 45°$

W_i - hot-wires

N_i - output signal (W_i)

$U_i = f(N_i)$

$U_i^2 = V^2 \cos^2\varphi_i + A \cdot V^2 \sin^2\varphi_i$

$A = const \quad (A = 0.12)$
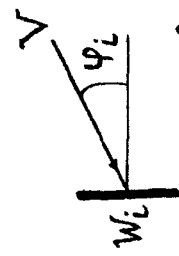
Figure 4.   Scheme of the three-component anemometer with six hot-wires.

$$B = 100\,m$$
$$f = 200\,mm$$
$$2\beta = 48°30'$$
$$\sigma_P = 0.04 \div 0.05\,mm$$
$$X = 1000\,m$$
$$\sigma_x = 2.3\,m$$
$$\sigma_z = 0.5\,m$$
$$\sigma_H = 0.25\,m$$
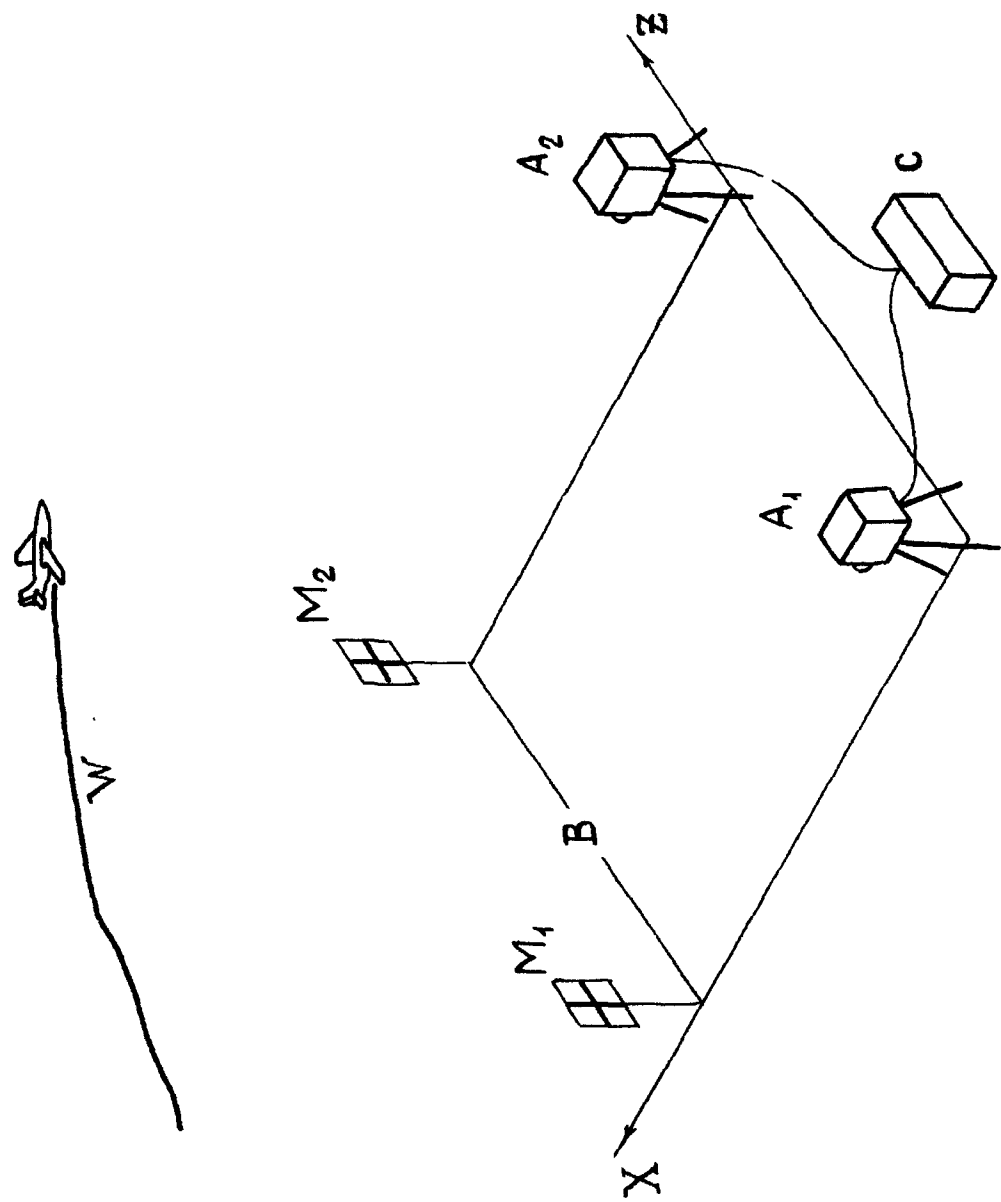
Figure 5. Stereophotogrammetric survey
A_1, A_2 - aerial cameras
M_1, M_2 - reference marks
C - control unit
W - vortex wake

Tu – 124

$G = 35000\ kg$
$S = 120\ m^2$
$\lambda = 5.2$
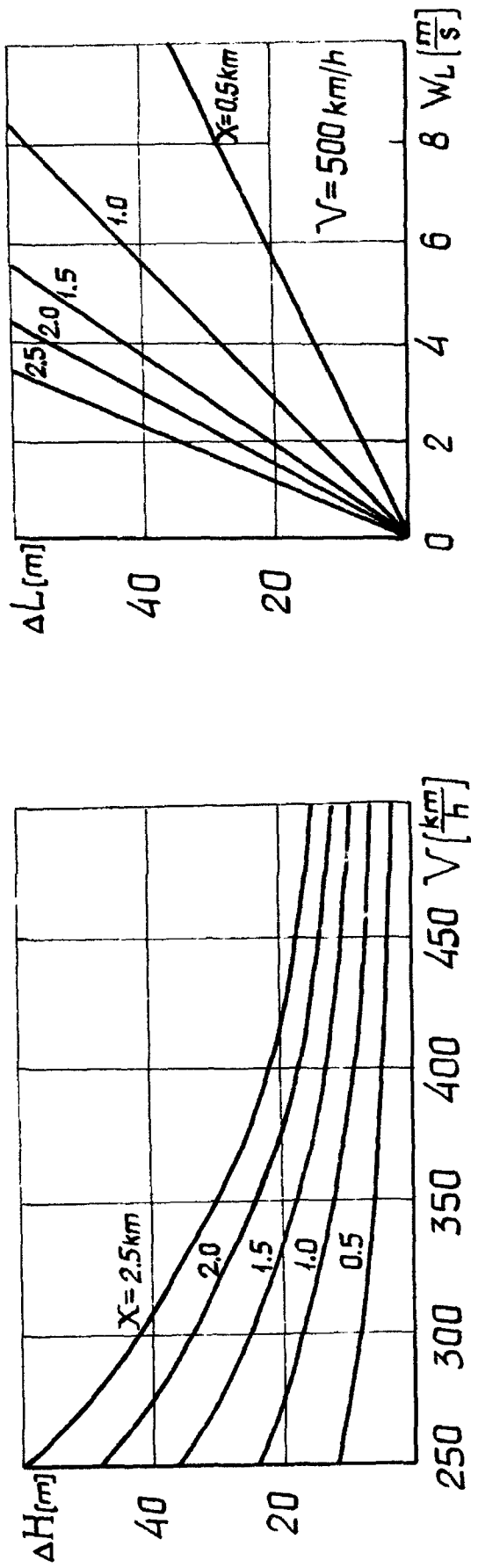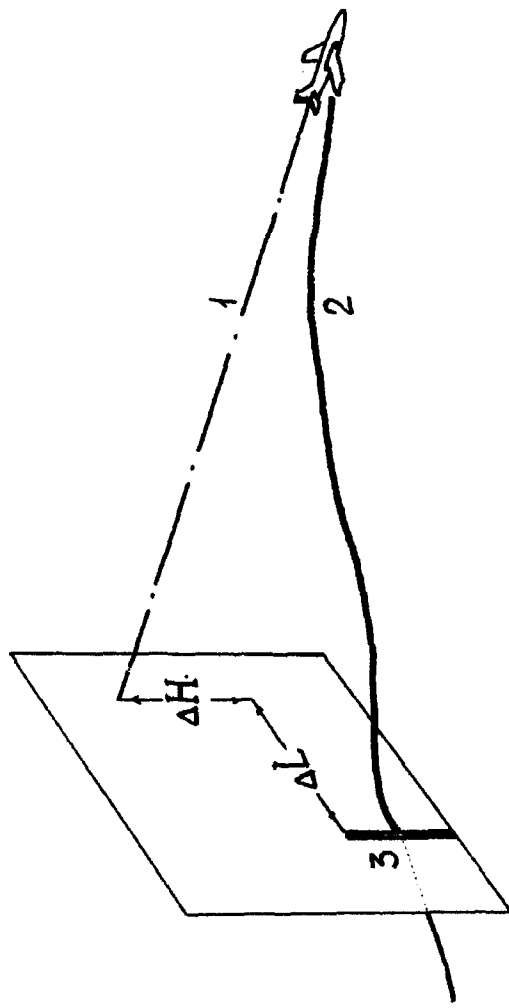
Figure 6. Nomograms for ΔH and ΔL
1 - flight trajectory
2 - vortex wake
3 - testing mast

Variations of temperature ΔT

Thermocouples

Range   -2 ... +2° C

Standard error   0.05°C

Frequency
band   0.0003 .... 0.7 Hz

Variations of wind speed ΔW

Acoustical anemometer

Range   -7 ... +7m/s

Standard error   2 %

Frequency band   0...5 Hz

Base 30sm   Frequensy 30KHz

Temperture T

Resistance thermometers

Range   - 5 ... +45°C

          -45 ... + 5°C

Standard error   0.2°C

Wind W,d

Wind prob 9A-1

Range   W 1.5 ... 50 m/s

          d 0 ... 360°

Stand. error W (0.5+0.005W)

          d   10°

Figure 7. Meteorological measurements.

REFERENCES

1.   Mironov, A.D., Zamyatin, A.N., Korolev, A.A., etc., "Methods of Aerophysical Flight Research," M.: Machinostroenie, 1985.

2.   Zamyatin, A.N., Gratchov, V.S., "Full-Scale Studies of Structure and Development of a Vortex Wake of a Medium Trunk-Route Aircraft in the Atmospheric Boundary Layer". 14th ICAS Proceedings, 1984. Toulouse.

3.   Zamyatin, A.N., "Real Research of Different Class Airplane Vortex Wakes at Low Altitudes." Report at the International Wake Vortex Symposium, 1991, Washington, DC.

PROSPECTS FOR ALLEVIATION OF HAZARD POSED BY LIFT-GENERATED WAKES

Vernon J. Rossow*
NASA Ames Research Center
Moffett Field, CA 94035-1000

ABSTRACT

A review is first made of the successes and failures of previous attempts to bring about a substantial reduction in the rolling-moment hazard posed by the vortices that trail from the wings of subsonic transport aircraft. It is concluded that one of the more promising wake-alleviation schemes uses the span loading on the wing to produce vorticity distributions in the wake that will bring about large self-induced cross-stream velocities. When this characteristic has been established, the vorticity in the wake is convected about so that the coherent rotary velocities are turned into large-scale random motions that decompose quickly into a non-hazardous wake. It appears that a wide range of span-loadings/wake-vortex distributions will produce these large-scale, self-induced motions. It remains however, to find those that bring about the desired wake dynamics with the least addition of drag and complexity to the wake-generating aircraft. A combined theoretical and experimental research program at NASA Ames Research Center is directed at finding design guidelines for implementation of wake-vortex alleviation on subsonic transport aircraft. The experimental part of the program will include tests in the 80- by 120-foot wind tunnel at scale distances up to one and one-half nautical miles.

---

*Senior Scientist, Fixed Wing Aerodynamics Branch.

NOMENCLATURE

b =   wing span

c =   chord

C_L =   lift coefficient $= L/qS$

C_l =   rolling-moment coefficient $= M/qSb$

C_{l_v} =   wake-vortex-induced rolling-moment coefficient

$C_{l\delta}$ =   aileron-induced rolling-moment coefficient

h =   height of wing fins

L =   lift

M =   rolling moment

p =   rolling velocity

$\dot{p}$ =   roll acceleration

$\dot{P}$ =   ratio of roll accelerations $= \dot{p}_v/\dot{p}\delta m = C_{l_v}/C_{l\delta m}$

q =   dynamic pressure $= \rho U^2/2$

r =   radial distance from axis of vortex

S =   wing planform area

t =   time

T = $t\,U_\infty/b_g$

u,v,w =   velocity components in x,y,z directions

U_∞ =   velocity of aircraft

W =   weight

x =   distance in flight direction

X, Y, Z =   x/b, y/b, z/b

y =   distance in spanwise direction

z =   distance in vertical direction

Γ =   circulation in vortex

α =   angle of attack

δ =   aileron deflection

θ =   pitch angle relative to vortex axis

ρ =   air density

ϕ =   roll angle

Subscripts

f =   following or probe aircraft

g =   wake-generating aircraft

m =   maximum

v =   vortex

INTRODUCTION

Figure 1 illustrates the kinds of interaction forces that a lift-generated wake can induce on a penetrating aircraft. Although the lift and yaw forces imposed on the following aircraft by the wake can be disconcerting and sometimes dangerous, the hazard posed by the rotary motion of the air in the vortices is usually perceived as of most concern. As mentioned in previous papers, these rotary motions are not only well organized, coherent flow fields, but they also often persist many span lengths behind aircraft with conventional wings unless some mechanism such as turbulence in the atmosphere is present to disperse the wake more rapidly. For this reason, the wake-vortex alleviation program conducted by NASA has concentrated on finding ways to reduce the rolling moments induced by the rotary velocities of trailing vortices; and, why little or no attention is given to the other wake-vortex induced forces imposed on following aircraft.

An approximate rule[1-3] has been suggested as a guideline for determining when a vortex wake has been adequately alleviated. The guideline states that the rotary flow field of a non-hazardous vortex wake must not impose a rolling moment more than approximately one-half of the aileron-induced rolling-moment capability of the aircraft that encounters the aircraft; that is,

$$\dot{P} = \text{ratio of roll accelerations} = \dot{p}_v / \dot{p}_{\delta m} = C_{l_v} / C_{l \delta m} \leq 0.5 \qquad (1)$$

This condition specifies that sufficient roll control must be available on board the encountering aircraft to not only overcome but also to correct for any vortex-induced rolling motion. Since the roll-control capability of many transport aircraft is around[3], $C_{l \delta m} = 0.06$, eq. (1) indicates that the maximum vortex-induced rolling moment should not exceed $C_{l_v} = 0.03$. The difficulty in achieving such a goal is illustrated by recalling[4,5] that the wake vortices of the B-747 induce a rolling moment on a Learjet or T-37 type of following aircraft around $C_{l_v} = 0.12$ at a scale distance of about one-half nautical mile behind the wake-generating aircraft. Hence, if an alleviation scheme is to be successful, the wake-vortex induced rolling moments must be reduced by a factor of about four if the wing span of the following aircraft is appreciably smaller than that of the generator. (A smaller reduction in rolling moment coefficient is sufficient if the two aircraft are comparable in size.) Any alleviation scheme that is able to bring about such a reduction in wake-induced rolling moment must provide acceptably safe conditions for all aircraft at the 2 nmi separation distance, must work in all weather conditions and for all possible aircraft loadings (i.e., fore or aft center of gravity locations), etc. Furthermore, the same mechanism should be effective for all span ratios in the fleet and not just for selected

aircraft. Any penalties imposed by the alleviation scheme on the wake-generating aircraft must be negligible during cruise and the cost of implementation should be recovered quickly through savings generated by higher airport capacity. This has been the goal of the wake-alleviation program being conducted by various government organizations[6,7]. The objective of the alleviation part of the program is to provide design guidelines that will produce wakes wherein the rotary velocities in the wake are not only small enough that the foregoing rolling-moment criterion is satisfied but that the velocity gradients are also so small that an abrupt entry into or departure from a lift-generated wake will result in neither aircraft excursions nor accelerations that go beyond the limits determined as safe and acceptable. Furthermore, the structure of the vortex wake must be so benign that the magnitude of the loads is nearly independent of the direction of penetration, of the amount of curvature of the wake vortices and of any intermittency or changes in the vortex structure along its axis. That is, the penetrating aircraft must be able to enter, leave, or remain at the most intense part of the vortex wake on a continuous basis without excessive loads being induced on any components of the aircraft.

Consideration is first given to the various mechanisms that disperse lift-generated wakes. The discussion points out some of the attributes and shortcomings of the various alleviation schemes, and considers the prospects of the various mechanisms for reducing the wake-vortex hazard by the substantial factors needed in order to achieve acceptable alleviation. The background and elements of the wake-vortex alleviation program at NASA Ames Research Center are then described.

MECHANISMS FOR DISPERSION OF WAKE VORTICES

The following list presents the various wake-vortex dispersion mechanisms in approximately the chronological order in which they were identified. The details of the listing is somewhat arbitrary and is not intended to include all of the concepts that have been investigated.

1. Viscosity and turbulence.
   a. Natural decay.
   b. Turbulence injection.
   c. Atmospheric turbulence.

2. Small-scale vortex instabilities.
   a. Axial/rotary flow instabilities.
   b. Vortex breakdown.

3. Large-scale vortex instabilities.
   a. Instability after sinusoidal displacement.
   b. Wing loading for certain wake dynamics.
   c. Excitation by roll oscillations.
   d. Vortex Injection.

VISCOSITY AND TURBULENCE

Natural Decay

One of the earliest estimates of vortex decay is presented in Lamb's book[8] as

$$v_\theta = \frac{\Gamma}{2\pi r}\left(1 - e^{\frac{-r^2}{4\nu t}}\right) \tag{2}$$

At time t=0, all of the vorticity is concentrated at the origin in a line vortex of circulation, The equation then expresses the diffusion with time of the concentrated vorticity into the space surrounding the origin, or center of the vortex. Such a closed-form result is convenient and has been used in a variety of studies to model vortex decay as a function of time. It is noted that the variation of the circulation in eq. (2) depends on the parameter, $r^2/\nu t$. The usefulness of eq. (2) is somewhat restricted because laminar flow is assumed and because the radial distribution of vorticity corresponding to eq. (1) does not have the latitude to approximate the vortex structure found in the wide variety of lift-generated vortices.

Measurements made of the maximum circumferential velocity in lift-generated vortices in water tow tanks[9,10] and in flight[11] exhibit a two-stage decay history. Typical data are shown in Figure 2 as a function of distance behind the wake-generating wing, which may also be considered as time after the vortex was generated. When the vortices are influenced by only the naturally occurring viscosity and turbulence generated by shear forces in the vortex structure, the maximum circumferential velocity changes very little for distances of 40 span lengths or more. The velocity then decays roughly as $1/\sqrt{t}$. The slowly-changing region immediately behind the generating aircraft is usually referred to as the plateau region. In that part of the vortex decay history, the variation of the rotary velocity with radius is closely approximated by inviscid rollup theory[12,13,14]. Since a wide variety of wing planforms exhibit the same plateau and decay characteristics, Iversen[15] correlated the data obtained in both ground-based facilities and in flight into a single curve. These results emphasize the fact that naturally occurring vortex decay behind wings of conventional

design will not provide enough reduction in wake-induced rolling moments to influence greatly the separation distances deemed to be safe. In fact, 40 spans behind a B-747 is already about 1.3 nmi before decay begins. A significant change in the wake at 2 nmi is therefore not to be expected unless some sort of radical change is made in the structure of lift-generated wakes to enhance their rate of decay or dispersion.

Turbulence Injection

Since the natural decay of a wake vortex is too slow for a consistent spacing of aircraft at 2 nautical miles, one of the first alleviation mechanisms tried was the injection of turbulence into the wake by use of spoilers, splines, other wingtip devices, and engine exhaust. It was found that these devices are effective in reducing the rotary velocities in wake vortices so that the maximum velocity in the plateau region of decay is reduced. Unfortunately, as exhibited by the curves in Figure 2, a reduction in the initial value of the circumferential velocity leads to an increase in the downstream extent of the plateau region so that the net decay of the vortex far downstream is not greatly influenced. A further disadvantage of turbulence injection is that a reduction in the rotary velocities near the axis of the vortex does not greatly reduce the rolling moment imposed on following aircraft whose wing spans are substantially larger than the diameter of the vortex core. Two examples[16,17] that occurred early in the NASA wake-vortex program of the 1970's are now discussed. The first involved a spoiler mounted on the wingtip of a Convair 990. A wind tunnel study indicated that a relatively small wing-tip spoiler was capable of reducing the maximum rotational velocity in the shed vortex by a factor of about three. When a scaled version of the device was tested in flight on one wingtip of a Convair 990, Figure 3, the pilot of a Learjet that encountered the wake could not distinguish the difference between the vortices shed by the treated and the untreated wingtips. Instruments onboard the Learjet penetrating aircraft did show however, that the roll acceleration imposed on the probe aircraft was lowered from 4.4 to 2.4 rad/sec^2 as it moved from the untreated to the treated trailing vortex. Some of the difference between the two observations behind the two wingtips may have been due a difference in the path of penetration by the probe aircraft. Since roughly the same result occurred on several penetrations, it is more likely that the results of the roll acceleration instrumentation do represent the alleviation achieved. It is believed that the correct explanation lies in the fact that both the alleviated and the non-alleviated vortex roll accelerations experienced by the pilot exceeded the aileron-induced roll capability of the Learjet (1.15 rad/sec^2) by a large amount (i.e., P = 3.8 to 2.1). Under those circumstances, the pilot perceived that he was experiencing overpowering rolling moments from the vortex and the difference indicated by the instrumentation was not apparent to him. This experience again points out the fact that effective alleviation must bring the wake-vortex induced rolling moments down to the point where the parameter $P \leq 0.5$ as mentioned previously.

In the second example of turbulence injection to be discussed here, the size of the device used to inject turbulence into the wake was increased in size relative to the aircraft in order to achieve an acceptable level of alleviation. The configuration consisted of a spline or umbrella-type apparatus that trailed just behind the wingtip of a four-engine propeller-driven transport[17]; Figures 4a and 4b. When the modified and unmodified aircraft were tested in flight, the wake-induced rolling moment on a small propeller-driven aircraft was found to be reduced by about 72% so that $\dot{P}$ ≈ 0.55. As expected, flight in the modified vortex wake by the probe aircraft was found to be a controllable situation at separation distances of less than two nmi   The disadvantage of the spline device was that it increased the landing drag of the C-54 by about a factor of two. It is informative to examine the wake history of the configuration because, as illustrated in Figure 4c, the reduction occurs almost immediately behind the C-54 and, as typical of a plateau region, little or no decay occurs during the next 8 km. At that point, natural decay appears to have reduced the vortex intensity behind the unmodified aircraft to the point where the two wakes have roughly equivalent rolling-moment hazards. This result appears to again support the contention that turbulence injection affects the plateau region of vortex decay but not the far-field decay. Further effort[18-21] was expended in this area because it was likely that spoilers already on board most large transport aircraft might be sufficient as turbulence generators for at least a reduced level of hazard. Hence, the cost of implementation would be quite reasonable. The effect of the thrust of jet engines as turbulence injecting devices was also studied[22]. However, the alleviation achieved with spoilers, engine thrust, and other turbulence injection devices appears to consist primarily of a reduction in the rotary velocities near the core of the vortices and did not seem to accelerate the decay of vortices in the far field enough to provide the needed alleviation. A number of other devices that rely on turbulence injection were also tested experimentally[23].

It was concluded therefore, that one of the configurations tested did produce enough alleviation to satisfy the requirements of a 2 nmi spacing but it had unacceptably high penalties. As far as future prospects are concerned, further improvements in wake-vortex alleviation with turbulence injection are not likely because the size of the mixing eddies needed to significantly reduce the hazard posed by wake vortices at the two nautical mile goal should be on the order of the wing span. In contrast, eddies produced by on-board turbulence devices are of a size that is probably less than one-tenth of the span of the generating aircraft, which is too small to demolish the structure of the vortex wake. Furthermore, injection of turbulence increases the drag of the aircraft and may create unwanted dynamic loads on the aircraft structure.

The atmosphere is the best turbulence injection apparatus currently available. Not only does it provide large-scale turbulence in the lower atmosphere that has a scale and energy level capable of rapidly dispersing vortex wakes[24-26] but it is available at no cost. Unfortunately, this service is intermittent and does not always occur when needed. Since this wake dispersion assistance is very effective, studies have been undertaken on how to best implement reduced aircraft separation distances based on the more rapid dispersal of wakes during windy periods[27], and to use conventional spacings during calm periods. The problem with implementation lies in the difficulty in defining the boundary between adequate and inadequate wind periods, and of coordinating the air traffic with the weather. Although the original concepts had some disadvantages, it is likely that an innovative system involving atmospheric instrumentation, aircraft guidance and monitoring can provide a system for increased airport capacity.

SMALL-SCALE VORTEX INSTABILITIES

Small-scale instability usually implies that the vortex flow field is susceptible to disturbances in the region of the vortex core or center. It is not always clear as to how the vortex structure will change if a disturbance of adequate magnitude does occur. The size of the disturbances considered in the analyses are more on the order of the core diameter than on the order of the wing span. The resulting fluid motion then causes a disruption in the orderliness of the flow field near the vortex axis that produces mixing of the flow within and near the vortex core[28-30]. If the mixing is restricted to the core region, the outer part of the vortex flow field is not greatly disturbed and mixing with regions beyond the wingtips does not occur. In those cases, numerical results generated by Bilanin[31] show that even though large increases in the diameter of the vortex core can be produced, almost no reduction is effected in the rolling moment induced on a wing placed in the vortex flow field. It is reasoned that the numerical results are pointing to the fact that the total angular momentum had been redistributed in the region of the core but no mechanism is present to decrease it. This result shows again that, if vortex wakes are to be alleviated, a mechanism must be introduced into the wake dynamics that has the capability of rapidly distributing angular momentum over distances of at least the wing span of the wake-generating aircraft. Redistribution of the angular momentum over such a large region is required if the vortex-induced rolling moment is to be lowered by the factors of 2 to 4 needed to alleviate the wake by an adequate amount.

Various other attempts were made during the 1970's to alleviate the wake-vortex hazard by placing a diversity of devices on the wing in order to trigger instabilties in the lift-generated

vortices[23]. In almost all cases, the rotary velocities in the vortex core were reduced along with the torque induced on a penetrating wing. However, the wake alleviation achieved was usually insufficient and extrapolation to an adequate level would require devices which carried unacceptable penalties for the wake-generating aircraft.

LARGE-SCALE VORTEX INSTABILITIES

Consideration is given here to vortex mechanisms that bring about mixing in vortex wakes that have a scale on the order of the wing span of the wake-generating aircraft or larger. If mixing occurs on such a scale, vorticity will be rapidly convected not only within the wake and across the centerplane but also into regions beyond the wingtips of the wake-generating aircraft. The downward momentum in the air due to lift on the wing is then spread rapidly over an area much larger than the wingspan of the wake-generating aircraft so that the lift-generated disturbances are tolerable to any following aircraft.

Instability After Sinusoidal Displacement

One of the first mechanisms observed to bring about the disruption and dispersion of a single pair of wake vortices is the sinusoidal self-induced instability identified by Scorer[32] and correctly explained by Crow[33]. If the disturbances to the two vortices in a pair are in phase, the single-pair instability produces regularly spaced waves on the vortices that lead to the linking of the vortices across the span so that the vortex pair is converted from two nearly straight lines into a sequence of irregularly shaped loops of vorticity[32,33]. The loops of vorticity spread the vortical region behind the aircraft and enhance the decay and dispersion of the wake velocities laterally over several spans of the wake-generating aircraft. Although the alleviation process is effective, the time required to accomplish the needed wake spreading and decay of the sinuous vortex filaments is unacceptably long. The process occurs most readily when the generating aircraft is in an aerodynamically clean configuration so that the vortex cores are small and the rotary velocities high[34]. When the vortex cores are large due to the deployment of landing gear and flaps, the process is slow to start and may not occur at all. Therefore, efforts have been made to ensure and to accelerate the onset of the Scorer-Crow instability by manipulating control surfaces[35] (or the entire aircraft) in order to impress waves on the vortex lines as they are generated to reduce the time required to achieve rapid growth in wave amplitude and wake disruption.

Following some flight tests at Dryden with aircraft undergoing roll oscillations[21], a study[36] was made using numerical analysis of the dynamics of vortex filaments that are given an initial displacement of sinusoidal waves that are in-phase (i.e., pitch oscillations)

or out-of-phase (i.e., roll oscillations); Figure 5. When the initial disturbances given to the two vortices in a pair are in-phase, Figure 5a, the results are in agreement with the results of Crow[33]. However, when the initial disturbances given to the two vortices in a pair are out-of-phase, Figure 5b, the plane of the disturbances rotates until they are horizontal and then stops. The two vortex filaments in the pair then form a sinusoidally-shaped track that resembles a path flown if an aircraft were executing lateral oscillations. When that configuration of vortex filaments is reached, it appears to be stable and the waves no longer grow. Only the very slow process of viscous decay then remains to render the wake harmless. This vortex dynamic was not only predicted by numerical analysis[36] but also observed in flight tests conducted with wide-body transport aircraft undergoing sinusoidal roll oscillations[21]; Figure 6. The smoke trail in Figure 6b, that is roughly sinusoidal, persisted almost unchanged until the camera was turned off indicating that the new vortex structure is quite stable and persistent.

If a mixture of disturbances are introduced into a vortex wake that consists of a single pair, it is not always clear whether the loop-forming destructive instability[32,33] will occur or whether the vortices will make the transition to the highly stable sinusoidal trail in the horizontal plane that persists for long periods of time[36]. Therefore, if vortex wakes are to decompose quickly on a consistent basis, something must be added or changed in the vortex wake to make large-scale mixing occur on a regular basis without the possibility of going to an alternate configuration that is stable.

Wing Loading Tailored For Certain Wake Dynamics

In the early part of the NASA wake-alleviation program of the 1970's, it was reasoned that the hazard posed by wake vortices was increased by the rollup process. Therefore, if it were possible to design the vorticity distribution in a wake so that the original configuration was the same as the final one far behind the aircraft, it might be possible to design a wing that sheds a less hazardous wake-vortex system. The method used to design the wakes made use of the well-known point-vortex approximation in the Trefftz plane to analyze the velocity distribution in the vortex wake. Figure 7 illustrates the technique for elliptic span loading. By use of this method[37], two vortex wakes were designed for supposedly constant motion; Figure 8. The first wake was designed so that the vortex wake shed by each side of the wing rotated as a solid sheet. The resulting span loading corresponds to the loading for minimum wing-root bending, which tapers approximately linearly from the center of the wing to the tip. Time-dependent numerical calculations, Figure 9a, and wind tunnel tests[15] both showed that this tailored vortex wake shed by each side of the wing did not stay as a flat sheet that rotated as a unit, but broke up into several vortices. Since the loading on the wing tapered linearly to the tip, the bound circulation at the centerline of the

wing and the total circulation in the vortex are increased above that required for elliptic loading; Figure 9a. As a result, the net torque induced on a penetrating aircraft by the wake is about the same or larger than that from elliptic loading.

A second wake-vortex configuration[37] that was studied assumed that the span loading was such that all of the vorticity shed by the wing into the wake translated downward at the same velocity so that the wake was unchanged with time. At first it seems that the span loading should be elliptic. It is well known, however, that the two outboard vortices shed by an elliptically loaded wing do not translate downward with the main body of the wake, but have a strong upward velocity; Figure 7. If all of the vortices, including the two at the wingtips, are to translate downward at the same velocity, the wake consists of vortices whose strength alternates in sign, and whose magnitude oscillates about elliptic loading; Figure 9b. If a large number of point vortices is used to represent the wake, the oscillations in magnitude are smaller than if a small number of vortices is used. The span loading, therefore, consists of a square-shaped sawtooth superimposed on top of an elliptically shaped loading; Figure 9b. Numerical analysis of the time-dependent motion of the wake shows that the wake translates unchanged as predicted. However, if a small disturbance is given to one or more of the vortices used to represent the wake (as a test for stability), the various vortices in the wake form pairs that make large excursions in the cross-stream direction; Figure 9b. These motions suggest that such a wake would be effective in producing the large-scale mixing desired for rapid dispersion of lift-generated wakes. Therefore, when ground-based tests were started with models of the Boeing 747 in the early 1970's, two of the configurations considered were designed by deflecting either the inboard or the outboard flaps only and leaving the other flap stowed. It was found that deflection of only the outboard flaps (the (0°/30°) configuration) resulted in a more hazardous wake for a given lift coefficient. However, deflection of only the inboard flaps (the (30°/0°) configuration) resulted in a much reduced wake hazard for a given lift[4,5,14]. Subsequent analysis of the corresponding span loadings and the wakes showed that such a result should have been anticipated because of the magnitude and location of the vortices being shed by the two configurations.

When the experimental part of wake-vortex program began in the 40- x 80-foot wind tunnel at NASA Ames, the wake-generating model was mounted right-side up on a strut from the floor so that the strut interfered with the wake of the model; Figure 10. Consistent results for the induced rolling moment in the wake could not be achieved. That is, measurements made in the wake of a B-747 model sometimes showed that the wake was alleviated and other times not. When the model was mounted upside down on a slender strut as shown in a subsequent figure, the interference of the support strut on the vortex wake was reduced to the level where alleviation was consistently indicated for the (30°/0°) configuration. Therefore, when flight tests were begun with the B-747, it was recommended that the first

flights be made with the landing gear retracted to avoid any possible adverse interaction of the wake from the landing gear with the alleviation mechanism.

It is now well known that the wake of the B-747 is greatly alleviated when the landing gear is retracted but only a little when the gear is deployed or the aircraft is slightly yawed[38,39]. The mechanism at work was not realized until an additional smoke generator was mounted on each wing just outboard of the fuselage. When flights were made over Rosamond Dry Lake at low altitude with the inboard smoke generators turned on, the mechanism responsible for the alleviation and the reason for it not working when the landing gear are deployed became apparent[4]; Figure 11. With the gear retracted, the vortices shed by the inboard flaps have small high velocity cores that are essential for the linking and loop-forming instability. When the landing gear are deployed, a large amount of turbulence and low energy fluid are produced that is drawn into the cores of the vortices shed by the inboard end of the inboard flaps. The low energy fluid causes the cores of the inboard vortices to enlarge and slow down enough that the single-pair sinusoidal instability and vortex linking does not occur; Figure 11. When pictures taken of the earlier flight tests at Dryden are examined, it appears that the same type of vortex interaction is taking place but the linking process was not visualized because smoke-generators had not yet been placed on both ends of the inboard flap of the B-747.

Examination of the flow visualization results obtained in the wake shed by a wing designed for sawtooth span loading indicates that the same wave instability and vortex linking occurs there also. The wake dynamics was most apparent in experiments conducted by Orloff and Ciffone[10] in a water tow tank on a generic wing with seven flap segments on each side. In one case, the flaps were deflected alternately up and down across the span in order to generate sawtooth loading[15]. It was found that, shortly behind the wing, the vortices formed pairs that made large cross-stream excursions that finally led to linking and loop formation. When a wing with the same shape was tested in the 40- x 80-foot wind tunnel, it was found that the torque on a following wing was much reduced until the lift on the wing became large enough to dominate all of the sub-vortices in the wake from the deflected flaps[14]. These results indicate that large flap deflections are required for large amounts of alleviation at lift coefficients of interest for landing and takeoff. Hence, such an alleviation scheme becomes unwieldy and inefficient if the landing flaps are not used judiciously to generate the vortices of opposite sign needed to produce large excursions and strong interactions. When the vortex pairs are of comparable strength, they interact to bring about large excursions and loop formation between vortices so that the wake vorticity is quickly dispersed. However, when the angle of attack of the wing is increased to the point where the wing-tip vortex becomes dominant, wake organization is restored so that alleviation is diminished. It remains therefore, to develop guidelines for the design of lifting surfaces that produce highly dispersive multiple vortex wakes. The penalties

associated with these designs can then be evaluated to determine the feasibility of such an alleviation scheme.

Excitation by Roll Oscillations

The foregoing example suggests that turbulence injection is detrimental to the successful function of the linking and loop-forming instability in two vortices of opposite sign. A remarkable experiment that at first appears to be a counter-example is available from the 1970 NASA flight test program. The example occurred near the end of the flight test program at Dryden. As a last-minute check on the resilience of vortices that had been alleviated by means of turbulence injection using spoilers, several flights were made where the wake-generating aircraft executed a series of roll-oscillation maneuvers. The roll oscillations were used to simulate the curving structure of vortices that might occur when a wave off is given to an aircraft during landing. That is, the research was being done to find out if the magnitude of the alleviation obtained with spoilers deployed on the B-747 would be adversely affected by rapid turns that occur during a wave-off. To everyones surprise, the alleviation achieved with spoilers deployed during roll oscillations was far greater than achieved with the spoilers deployed during straight and level flight. The alleviated wake was described by the pilots as one that induced a bumpy ride for the penetrating aircraft but also one that appeared to have little or no coherent rotary motion[21].

When the spoilers were not deployed on the B-747, no alleviation was forthcoming when roll oscillations were executed. Furthermore, when the same rolling motion was given to the L-1011 aircraft, with or without spoilers deployed, no enhancement of the alleviation occurred. In both of these two cases, the wakes formed into a single vortex pair that underwent motions that eventually led to the stable configuration consisting of lateral oscillations in the horizontal plane like those in the out-of-phase examples in Figures. 5b and 6. Subsequent numerical simulation of the two flight experiments with vortex filaments whose strengths are based on computed span loadings[40] showed that the finite displacement of the filaments by the roll oscillations brings about a large amplitude displacement of two inboard pairs of the vortices in the wake of the B-747 ($30^{\circ}/0^{\circ}$) configuration, Figure 12, but not in any of the other aircraft configurations[40]. In the computations, it is assumed that deployment of the outboard spoilers decreased the wing loading there so that the wake approximates the one shed by the ($30^{\circ}, 0^{\circ}$) configuration. An alleviation based on such a mechanism is impractical because the required rapid rolling maneuvers cause passenger comfort to be compromised, and because the dynamic loads imposed on the generating aircraft produce unacceptable structural fatigue. The aerodynamic alleviation achieved with these kinds of large-scale mixing mechanisms by the various configurations suggests that large-scale vortex instabilities are sensitive to

turbulence injection and to initial displacements given to the vortex filaments. Some configurations do not work with turbulence injection and others are insensitive to turbulence but all require a special span loading to drive the large-scale excursions of the vortices. The wake conditions appear to be very non-linear and individual in their response.

Vortex Injection

As already mentioned, several configurations have demonstrated theoretically and experimentally that vortex interactions are an effective means for bringing about the large-scale mixing needed for the substantial amounts of wake alleviation needed to satisfy the requirements imposed by the criterion that $P \leq 0.5$. These results suggest that a more global approach should be taken in the search for an ideal wake-alleviation scheme. The reasoning used indicates that not only should the span loading on the aircraft be used to bring about strong vortex interactions, but a vertical distribution of vorticity should also be used to assist in the development of wake instabilities. A vertical distribution in the wake vorticity is achieved by injecting not turbulence but an extra or auxiliary vortex above or below the vortex wake of the wing. Vortices above or below the wing wake should give the wake an initial spanwise velocity that can be used to bunch vorticity to bring about strong vortex interactions. That is, when the vortex wake is approximately flat, the induced velocities are in the vertical direction so that the wake first moves vertically. As time progresses, vertical displacements or distortions in the wake become large enough that lateral velocities become appreciable and self-induced spanwise motions of the vorticity occur. A vertical distribution of vorticity is achieved by placing vertical lifting surfaces like fins or winglets on top of or below the wing. The wake can then have substantial thickness from its inception and lateral displacement of vorticity begins immediately at the trailing edge of the wing. It was reasoned that the spanwise motion imparted to the vorticity shed by the wing has the capability to bunch or disperse the vorticity shed by the wing to promote early break up of the wake vorticity before rollup has taken place. Another advantage expected is that strong vortex interactions begin immediately behind the wing rather than several spans behind the wing without waiting for the vortices to first roll up. It was proposed therefore that vortices be injected into the wake to generate vortex configurations that interact strongly[41,42]. Two numerically generated examples of the wake dynamics generated by vortex injection, Figure 13, illustrate the kinds of wake action that can be generated.

Since the 40- x 80-foot wind tunnel was readily available for tests of short duration, several wind tunnel entries were made in order to test the vortex injection concept and to find design guidelines experimentally[41,42]. A diagram of the experimental setup is presented in Figure 14 along with a plan view of the model of a B-747 used as the wake-generating

aircraft. As indicated in Figure 14a, the model is placed on a slender, streamlined strut at the entrance of the test section to the wind tunnel. The wake-generating model had its landing gear and leading-edge slats fully extended, the horizontal tail was set at 0° relative to the fuselage or aircraft reference plane (i.e., the horizontal tail is at 0° when the aircraft is at 0°), and the wing was designed so that the flaps could be deployed in their stowed, takeoff, or full-landing position. A representation of the Gates Learjet or the T-37B was used as the following model (b_{fin} = 13.1 in., AR_f = 5.5, b_{fin}/b_g = 0.19). It was placed at the downstream end of the test section on a support strut mounted on a tower which could be raised and lowered and also translated across the airstream. Movement of the following model permits a survey to be made of the vortex wake shed by the wake-generating aircraft so that contours of equal rolling moment can be drawn and the maximum value established. The downstream tower could be located at distances as large as 80 feet (25 m or 13.6 generator spans) behind the wake-generating aircraft. Based on the 70.5 inch span of the B-747 model, the 80-foot station corresponds roughly to a one-half mile scale distance behind a full-scale aircraft. During a typical run, the following model is held fixed at various vertical and lateral positions in the wake for about one minute. The rolling moment at each position fluctuates due to motion or meander of the wake from the wake-generating model. The maximum value measured at each location is then used to map out rolling-moment contours, and to determine the overall maximum rolling moment in the wake for that configuration. In the wind tunnel, a few configurations were tested at α_g= 0°, 4°, 8°, and 12°. Most however, were tested only at 4° (C_{Lg} = 1.2) to expedite the investigation of a wider variety of configurations.

In the wind tunnel tests, the devices used to inject vortices into the wake consisted of vertical surfaces, or fins, mounted on the wing at a large angle of attack to the local airstream; Figure 14b. A variety of fin shapes were tested at spanwise and chordwise locations along the upper and lower surfaces of the wing. This search technique showed that fin locations on top of the wing at about the quarter-chord station were much more effective than those on the bottom. It is believed that the greater effectiveness on top of the wing is attributable to the higher dynamic pressure over the wing as compared with under the wing. The higher velocity over the top of the wing produces a greater lift and therefore a stronger vortex on a fin of the same size. The search technique also showed that the effectiveness of the fins being used to inject the vortices depends strongly on their spanwise location; Figure 15a. That is, the span loading associated with the (30°/30°) configuration of the B-747 is most susceptible to alleviation when a fin is placed about half way from the centerline to the wingtip. Other wing shapes or span loadings will probably have another preferred fin location. When the alleviation achieved with wing fins is compared with that achieved with other alleviation methods, Figure 15b, it is noted that vortex injection can provide enough alleviation to attain a level of wake rolling moment that

satisfies the criterion $P \leq 0.5$, so that a following aircraft with $b_{fin}/b_g = 0.19$ can retain satisfactory control throughout the encounter.

Further results showed that the reduction in rolling moment induced on the following model was approximately linear with angle of attack of the fin, Figure 16, and with fin chord length, Figure 17, but not with fin height, Figure 18. In fact, the results in Figure 18 indicate that fin height is beneficial only for moderate heights. The original idea for increasing alleviation by increasing the depth of the vortex wake has merit then only for a quite limited extent of depth. The concept that more is better is true only for a small range because then fin height becomes detrimental. All of the results indicated that the stronger the vortex shed by the fin, the more alleviation that can be achieved, Figure 19. The effect of two different fin configurations on the lift and drag of the model as measured in the wind tunnel and in a water tow tank is presented in Figure 20. The smaller circular arc fins appear to provide the needed alleviation with less penalties in lift and drag. This result is consistent with the test results that indicate that those fins with circular arc or elliptical planforms yield the strongest vortex for the smallest fins. The best configuration found for the B-747 in the test time available was a combination of two circular arc fins on each wing as shown in the photographs in Figure 21.

NASA AMES WAKE ALLEVIATION PROGRAM

Vortex injection was chosen as the alleviation mechanism to be studied in the present NASA Ames Research Center program because the amount of alleviation achieved is roughly proportional to the strength of the vortex being injected and the alleviation is not an on or off process. That is, the tests to date indicate that vortex injection is an alleviation mechanism found that has the characteristic that the alleviation changes continuously and systematically with the parameters that govern the vortex strength and location. Since the alleviation mechanism and, therefore, the theoretical guidelines for the design of wing fins for maximum alleviation are sketchily known, implementation of vortex injection by means of wing fins or some other device is not straightforward at this time. A research program now in progress at NASA Ames is directed at improving the understanding of the use of various wake-vortex distributions to achieve non-hazardous vortex wakes. The program is an extension of the previous theoretical and experimental work. The theoretical work will be directed at finding analytical and numerical guidelines for the alleviation found experimentally with the wing mounted fins. The experimental program will be patterned after the 1970 NASA program[41,42]. One improvement over the earlier tests in the 40- x 80-foot wind tunnel, is that future tests will be carried out in the 80- x 120-foot wind tunnel ; Figure 22. The larger tunnel and a constant area portion of the circuit downstream of the test section permit data to be taken at downstream distances as large as 300 feet , or 50

spans behind a model of 6-foot span. The strut for the wake-generating model and the translating tower are being redesigned and rebuilt to accommodate the expanded test conditions. Since the previous tests were conducted some time ago in the 40- x 80-Foot Wind Tunnel, tests will first be made on the repeatability of the earlier results. If those tests are satisfactory, the wake of the B-747 model will be probed with generic models of wings of larger transport aircraft to determine the alleviation achieved with wing fins when the span ratio of the following wing is between 0.2 and 1.0. The experimental program will then use a model of the DC-10 as the wake-generating aircraft. Once again a search and correct procedure will be used to find wing-fin combinations and locations that provide the most alleviation with the least penalties. As these tests progress and theoretical models are studied, improved design guidelines should become apparent. In the tests with the B-747 and DC-10 models, other ways for injecting vortices near the wing will also be tried. These two subsonic transport models were chosen for testing because they were available on loan from Langley Research Center and because they were tested extensively in the 1970 program.

If reasonably satisfactory results are achieved in the wind tunnel with the two wake-generating models that are now available, wake alleviation with vortex injection will be tried on other aircraft. If interest exists on the part of airframe manufacturers, an effort will be made to carry out these tests cooperatively. It is to be noted that a critical element in the program is the availability of wake-generating models and the large 80- x 120-foot wind tunnel so that downstream distances of up to one and one-half nautical miles can be studied.

The most successful configurations developed in the wind tunnel must be tested at full scale in flight. Such a decision will no doubt depend on the likelihood of success, the estimated penalties associated with a retrofit, and the alternatives available for relieving airport congestion at the time of the decision. If a flight program is undertaken, it will probably parallel the previous one quite closely. Some changes will be required but the use of smoke generators for flow visualization and the procedures used to conduct the test will probably not be greatly different. Further ground-based tests will then be used to support the flight tests and to extend the knowledge obtained to other aircraft.

CONCLUDING REMARKS

A review is first presented of the different ways in which vortex wakes decay and disperse. Vortex wakes become harmless too slowly when only natural processes govern the decay. Efforts to accelerate the demise of the energetic rotary velocities in the vortices have led to a considerable amount of theoretical, ground-based and flight data. Of the wake alleviations

methods explored, the mechanism of vortex injection with wing fins appears to provide sufficient alleviation that responds in a continuous and systematic fashion to input parameters. The injection of vortices appears to be effective because it disperses a lift-generated vortex wake by setting up a self-induced velocity field that scatters and disorganizes the wake vorticity. It also has the advantage that the redistribution of vorticity begins immediately behind the generating aircraft so that the alleviation process will probably be less susceptible to atmospheric conditions. For these reasons, the research program at NASA Ames will study vortex-injection methods theoretically and experimentally. The objective of the investigation is to find guidelines for the design of wings that shed vortex wakes with rotary velocities so low that following aircraft can safely enter, leave or remain in the wake on a continuous basis. The study will also look for those wake-vortex distributions that are initially highly unstable in a way that causes the vorticity to progressively spread to larger cross-sections of the wake, rather than first rolling up into highly organized vorticies that persist far behind the wake-generating aircraft. The approach in this program will use theoretical models to guide experiments planned for the 80- x 120-foot wind tunnel. Although the test program will concentrate initially on aircraft presently in the subsonic transport fleet, the goal of the theoretical and experimental study of alleviation devices is to find design guidelines that enable aircraft designers to build alleviation features into an aircraft at its inception. In summary, alleviation of lift-generated wakes by aerodynamic means is a difficult task but a review of previous results indicates that the prospects for success are good.
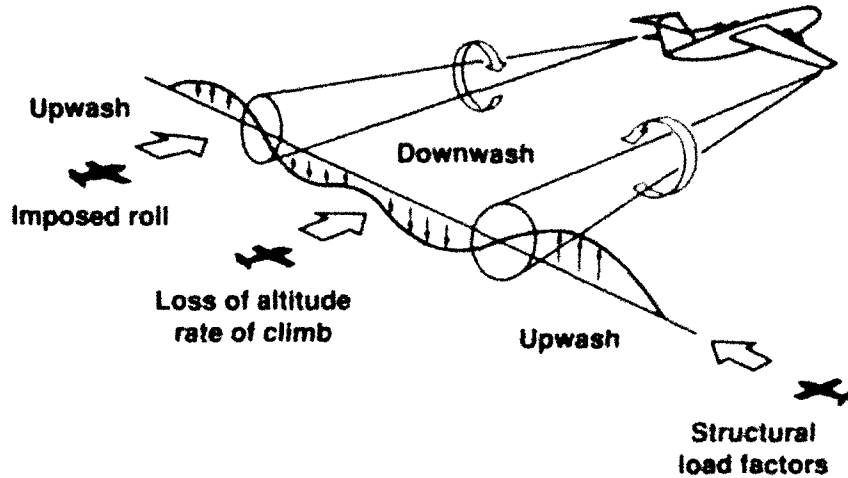
Figure 1. Schematic of possible encounters with a lift-generated wake by a following aircraft.
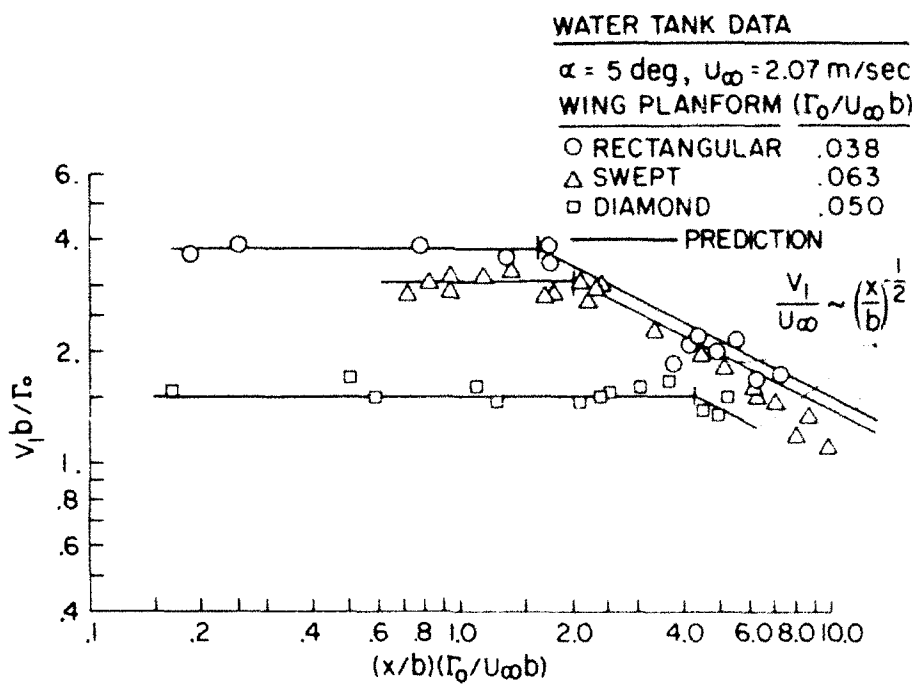
Figure 2. Water tow tank results for the maximum circumferential velocity as a function of downstream distance for several wing planforms; $U_\infty = 2.07$ m/sec, $\alpha_g = 5°$; from Ciffone and Orloff[10].
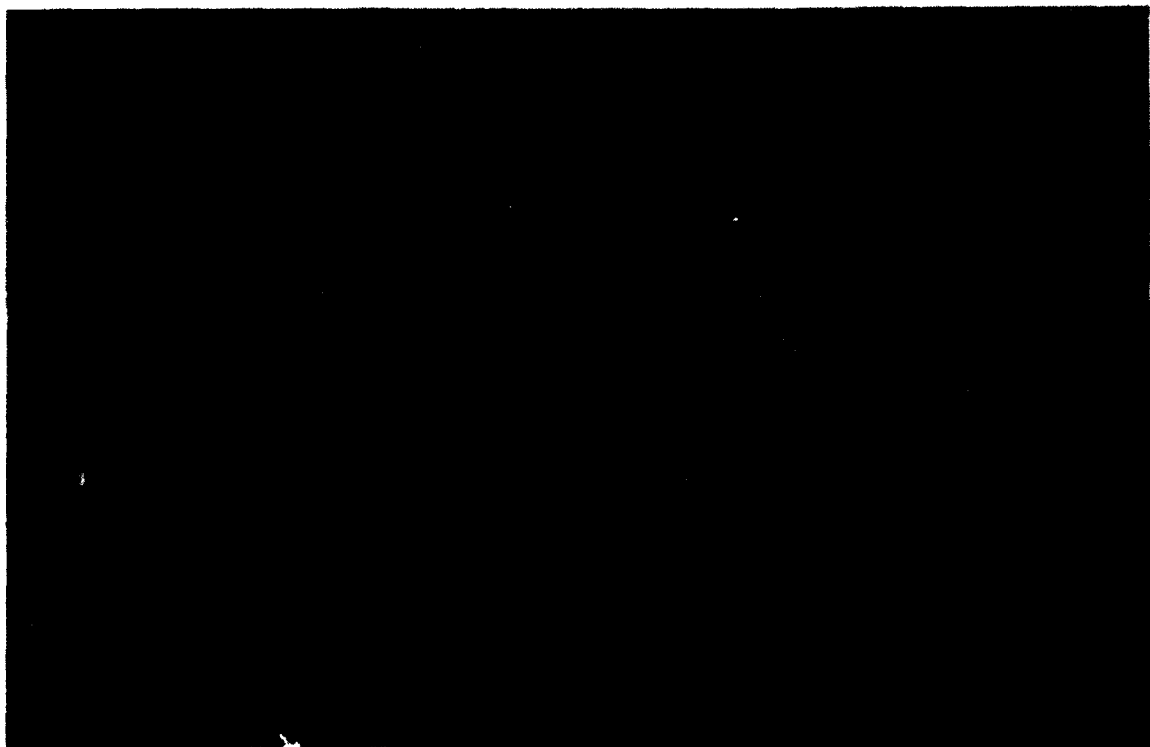
Figure 3. NASA Ames Convair 990 with vortex dissipater installed
on left wingtip; from Corsiglia et al.[17].
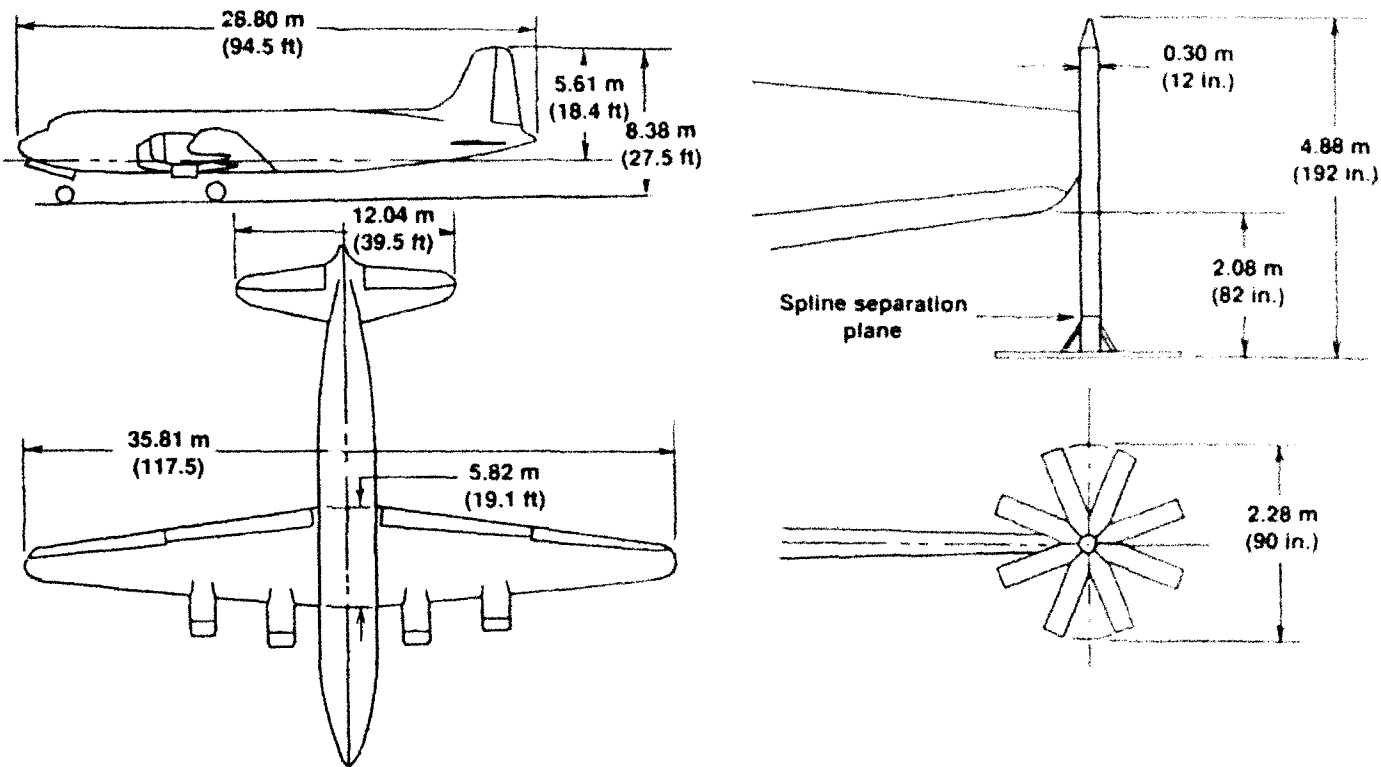
a. **Diagram of unmodified wake-generating aircraft.**

b. **Sketch of spline assembly at wingtip.**
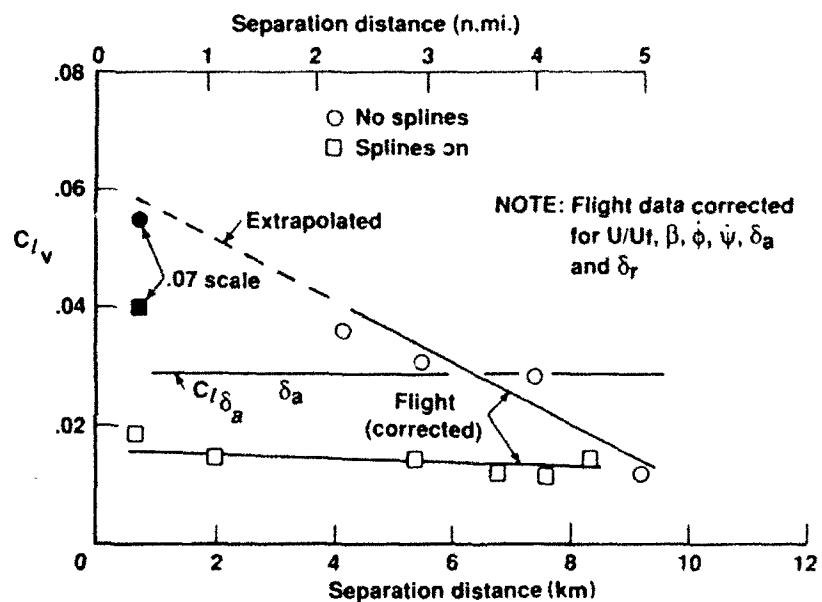
c. **Results for vortex-induced rolling moment on single engine probe aircraft obtained in a ground-based facility and in flight.**

Figure 4. Vortex attentuation on C-54 by use of spline attached to pod on wingt: ·· from Patterson et al.[17].
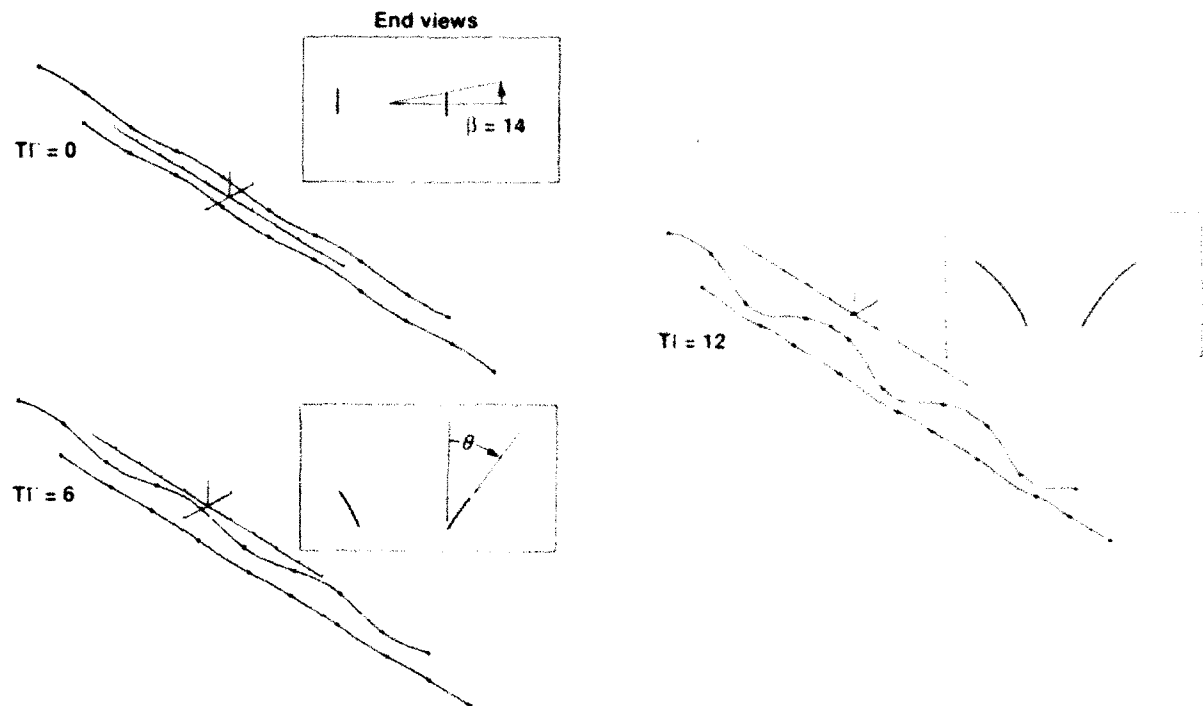
a. Waves in-phase grow indefinitely; simulates pitch oscillations.
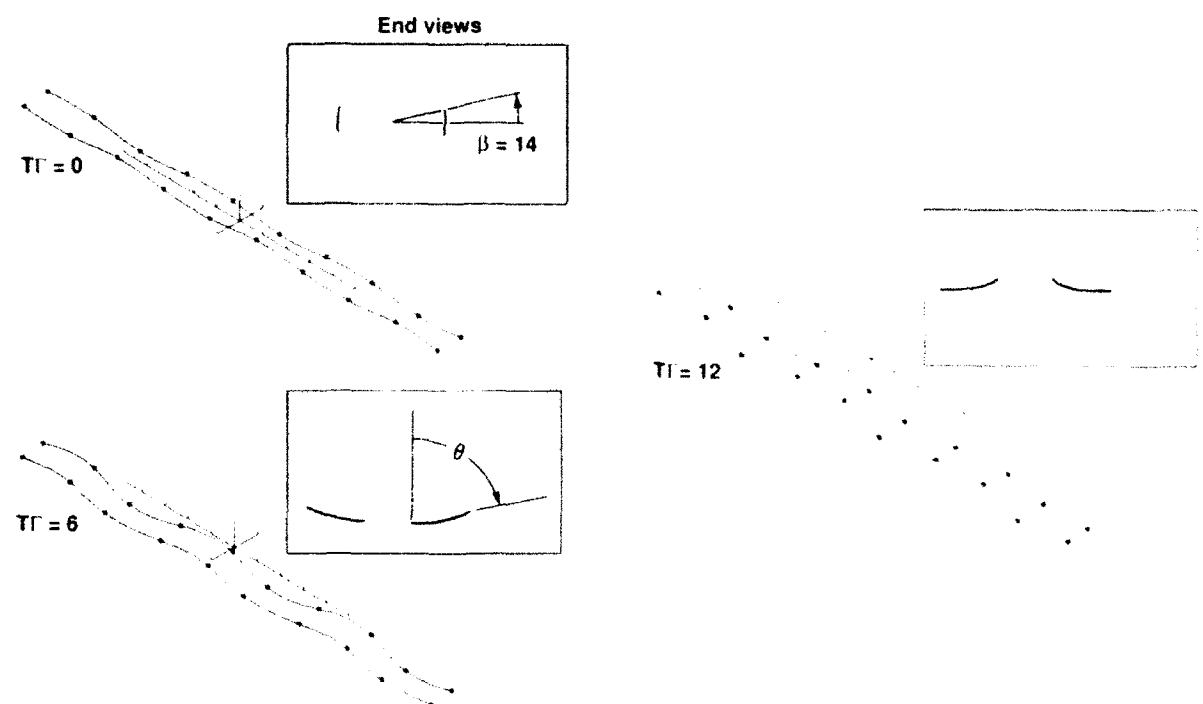
b. Waves out-of-phase go to a stable configuration; simulates roll oscillations.

Figure 5. Oblique and end views of time development of structure of pair of
vortex filaments that has been given an initial displacement of sine waves of
amplitude 0.23 b_g and wavelength 6 b_g; from Rossow[36].
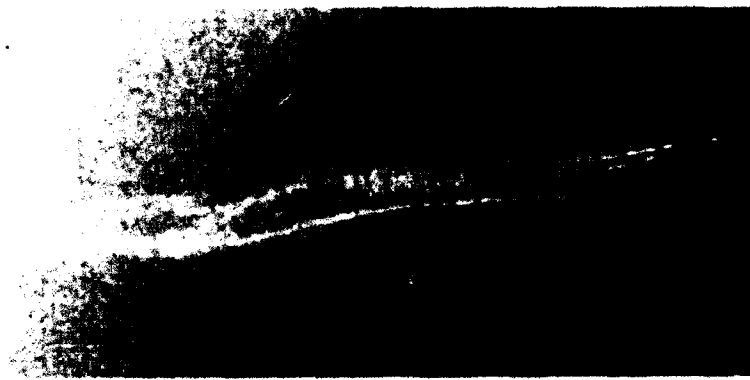
a. Several spanlengths behind aircraft where multiple vortex pairs initially shed by aircraft have merged into a single pair.
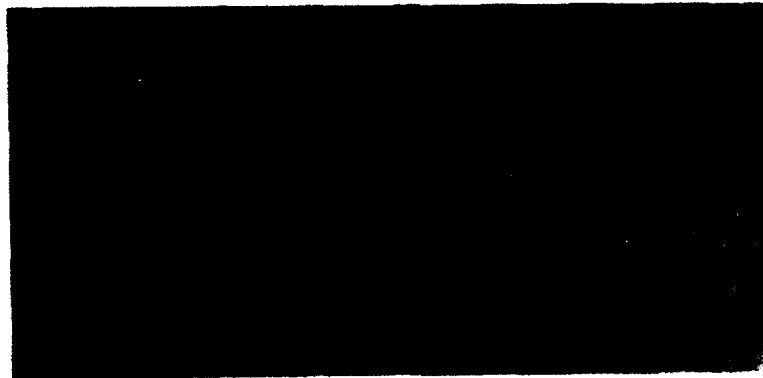
b. About two nautical miles behind aircraft where vortex planes have rotated to horizontal attitude to produce a stable and persistent sinuous shape of vortices with nearly parallel axes.

Figure 6. Photographs of vortex wake of L-1011 following roll-oscillation maneuvers of about 7° amplitude. From flight tests conducted by Barber and Tymczyszyn[21]

Courtesy of M. R. Barber and R. M. Rhine.

Span loading and downwash   Wake structure
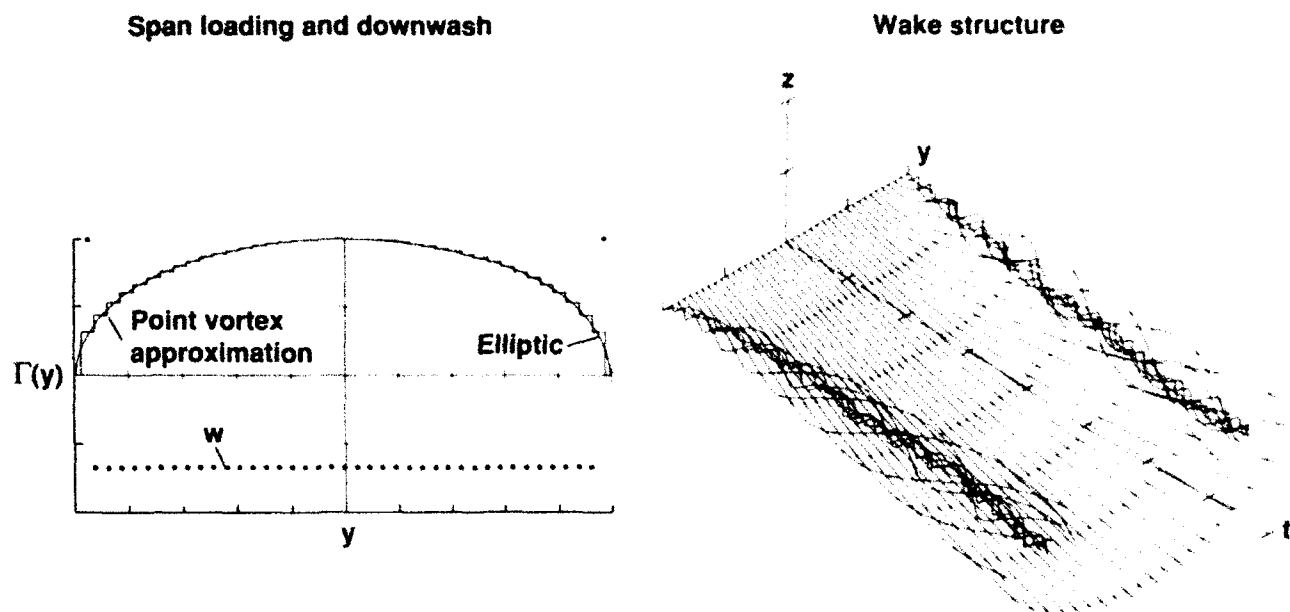
**Figure 7. Point vortex simulation in Trefftz plane of wake
structure shed by elliptically loaded wing[37].**

a. Tailored loading.   b. Sawtooth loading.
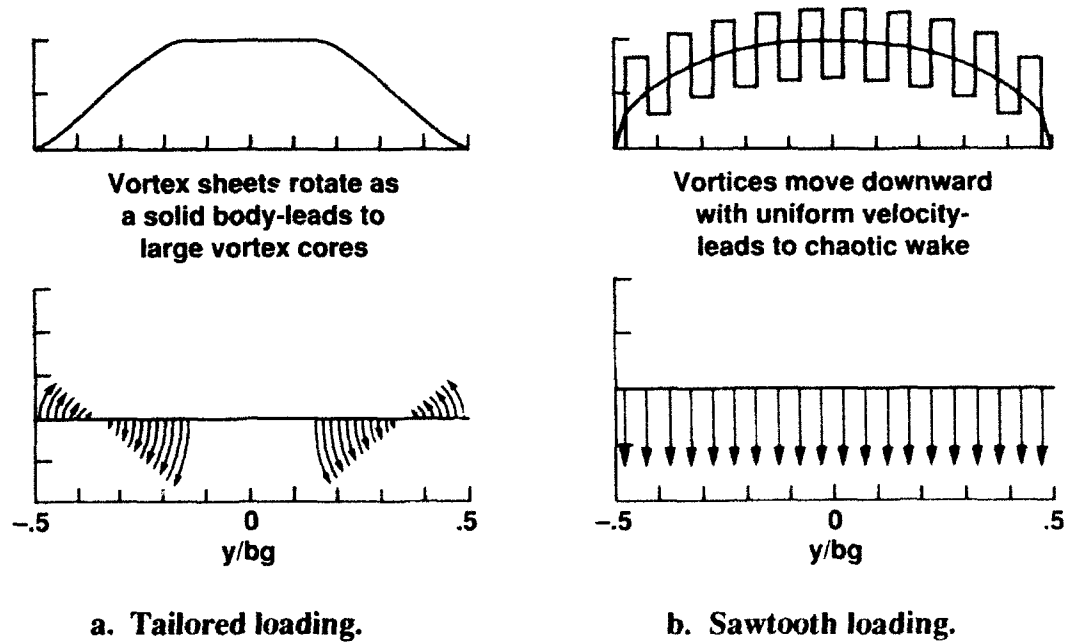
**Figure 8. Two span-load distributions designed so that their vortex
wakes do not roll up in the conventional sense but stay in
approximately the same shape as when shed[37].**

Span loading and downwash

Wake structure
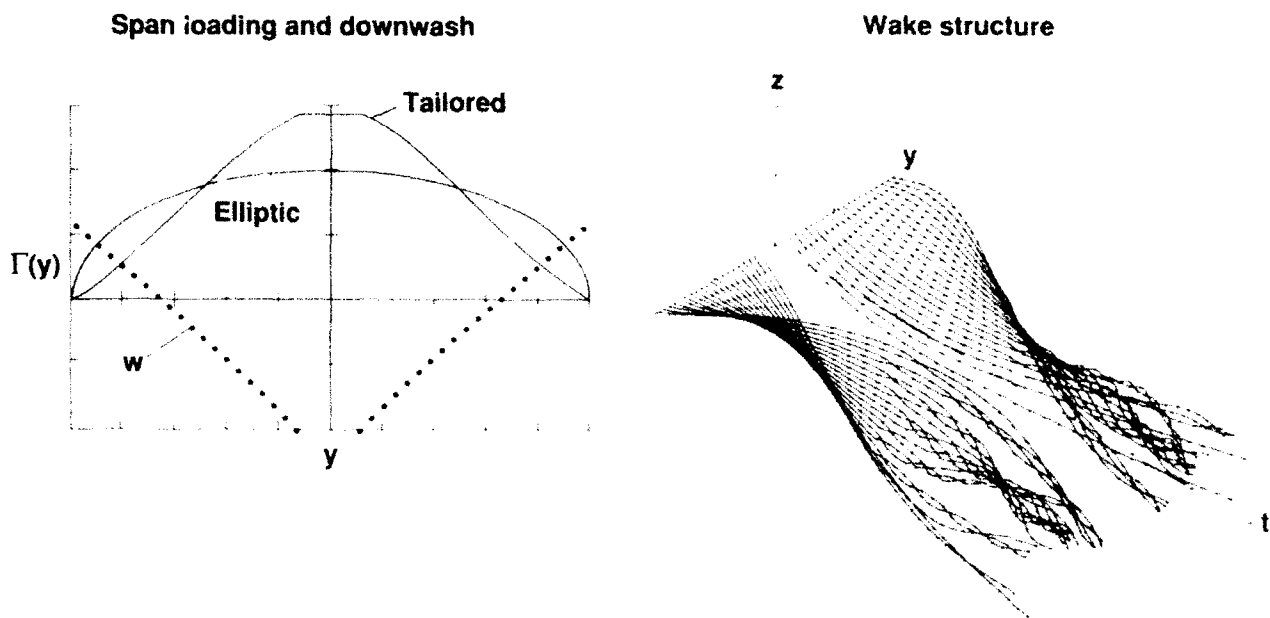
a. Span loading tailored so that vortex wake shed by each wingtip
rotates as a rigid sheet; corresponds to span loading for
minimum wing-root bending moment.

Span loading and downwash
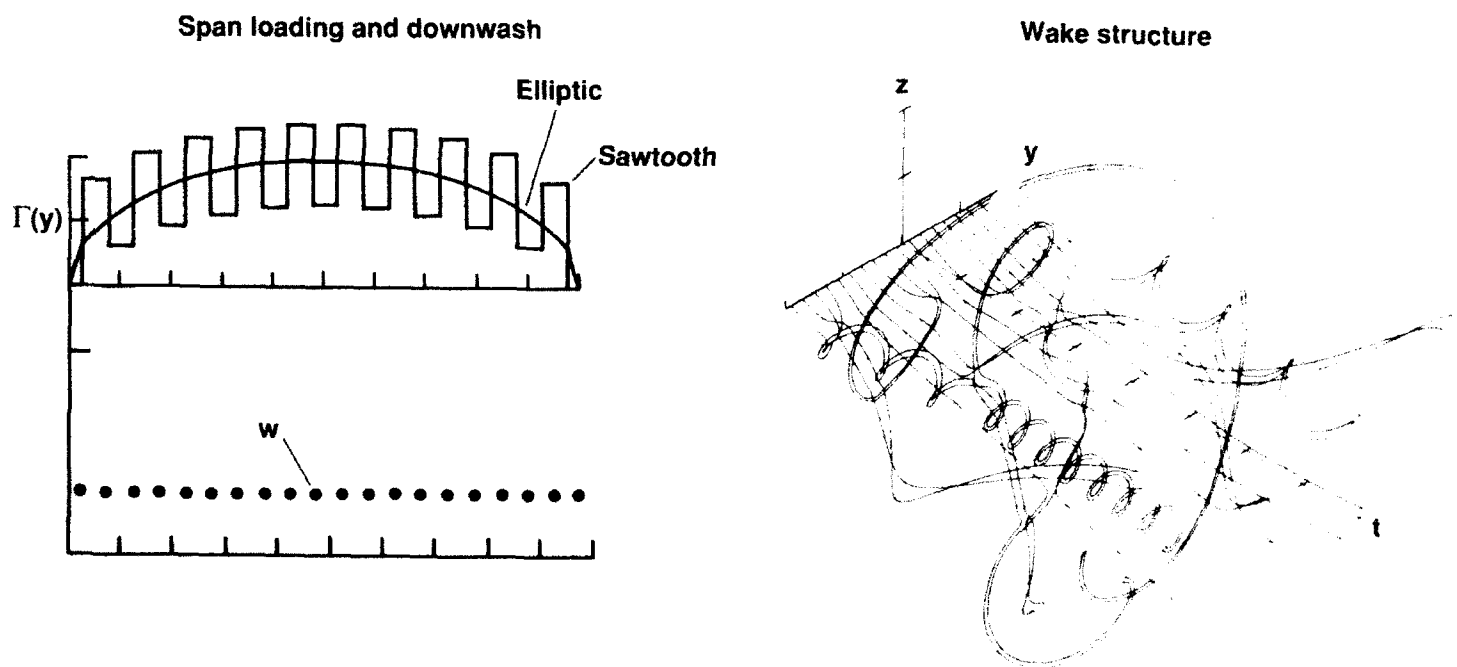
Wake structure

b. Span loading designed so that all vortices in the wake translate
downward at the same velocity.

Figure 9. Point-vortex simulation in Trefftz plane of time-dependent motion of
vorticity in two wake structures that were designed to
not roll up but to move in a specified manner[37].
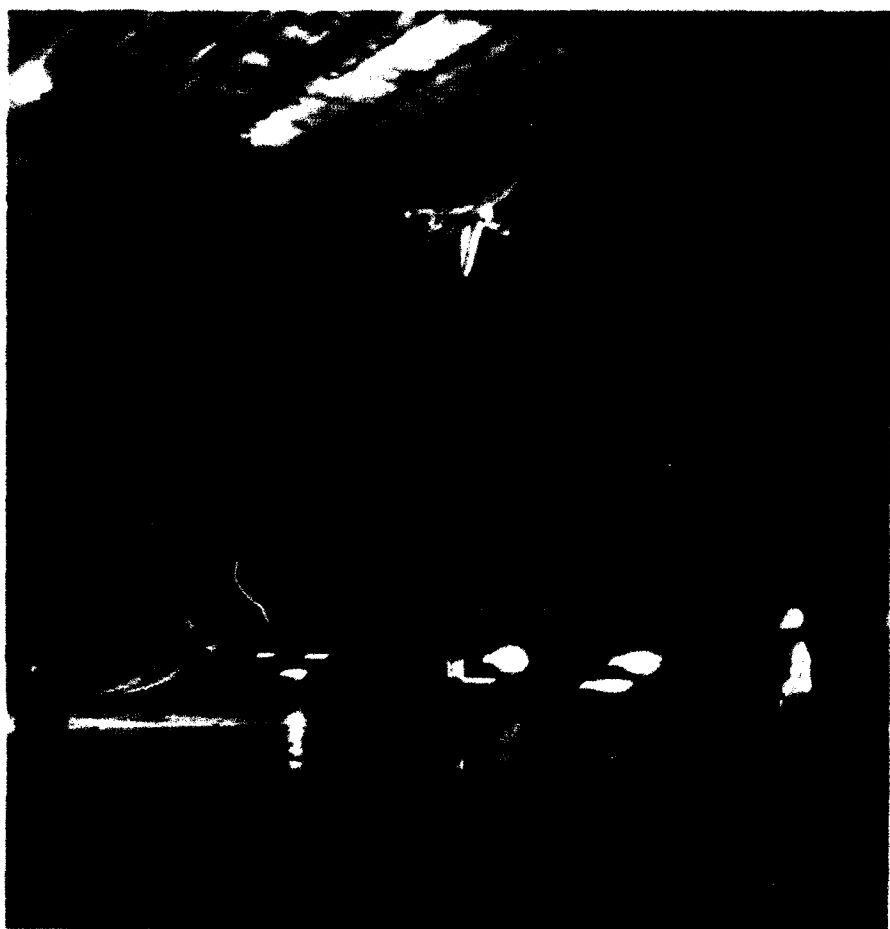
Figure 10. Strut configuration used to support B-747 wake-vortex generating model
during first entry into 40- x 80-foot wind tunnel.
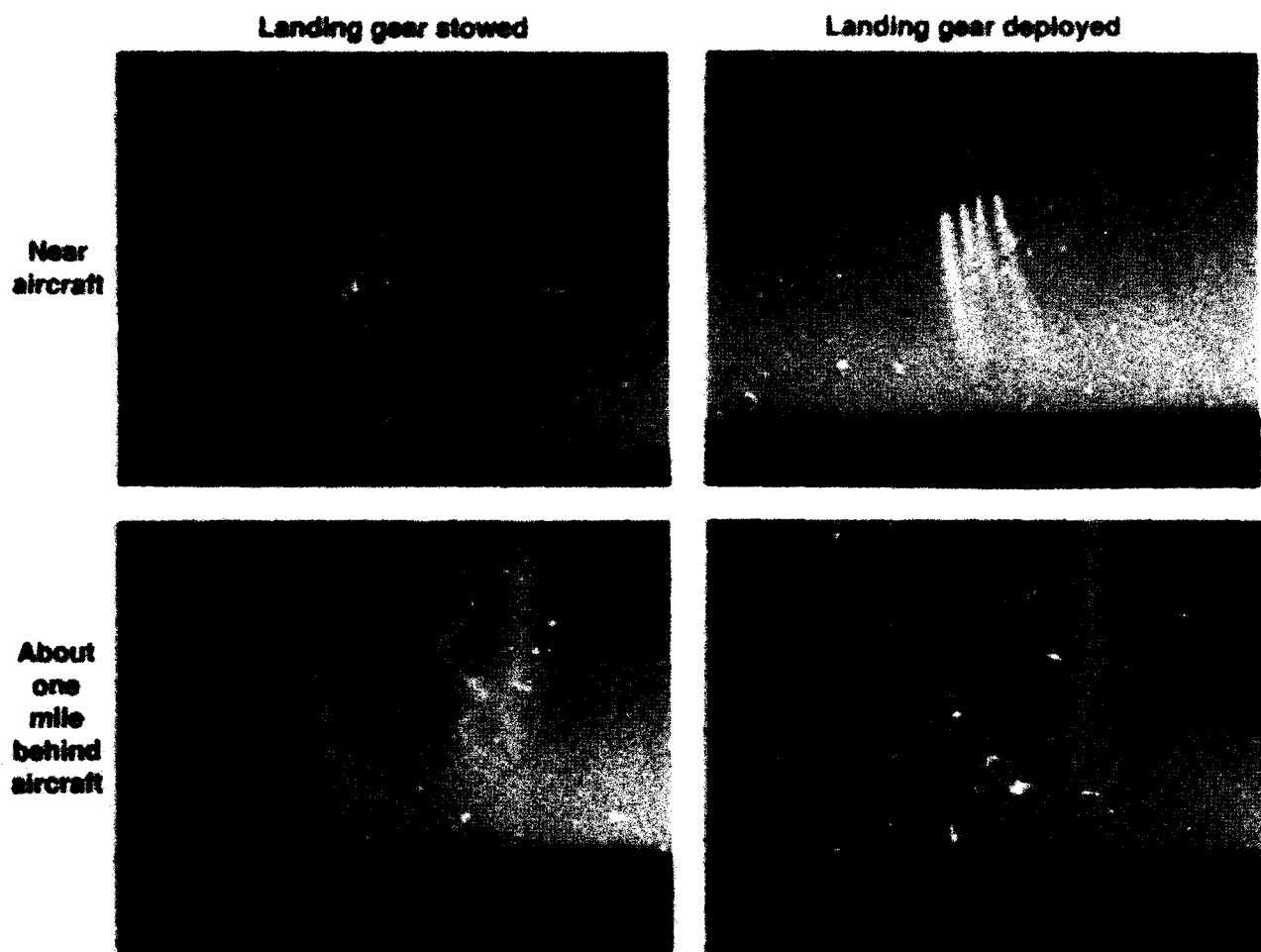
Figure 11. Photographs of wake configuration shed by B-747 with its inboard flaps fully deployed and with outboard flaps stowed[5,6].
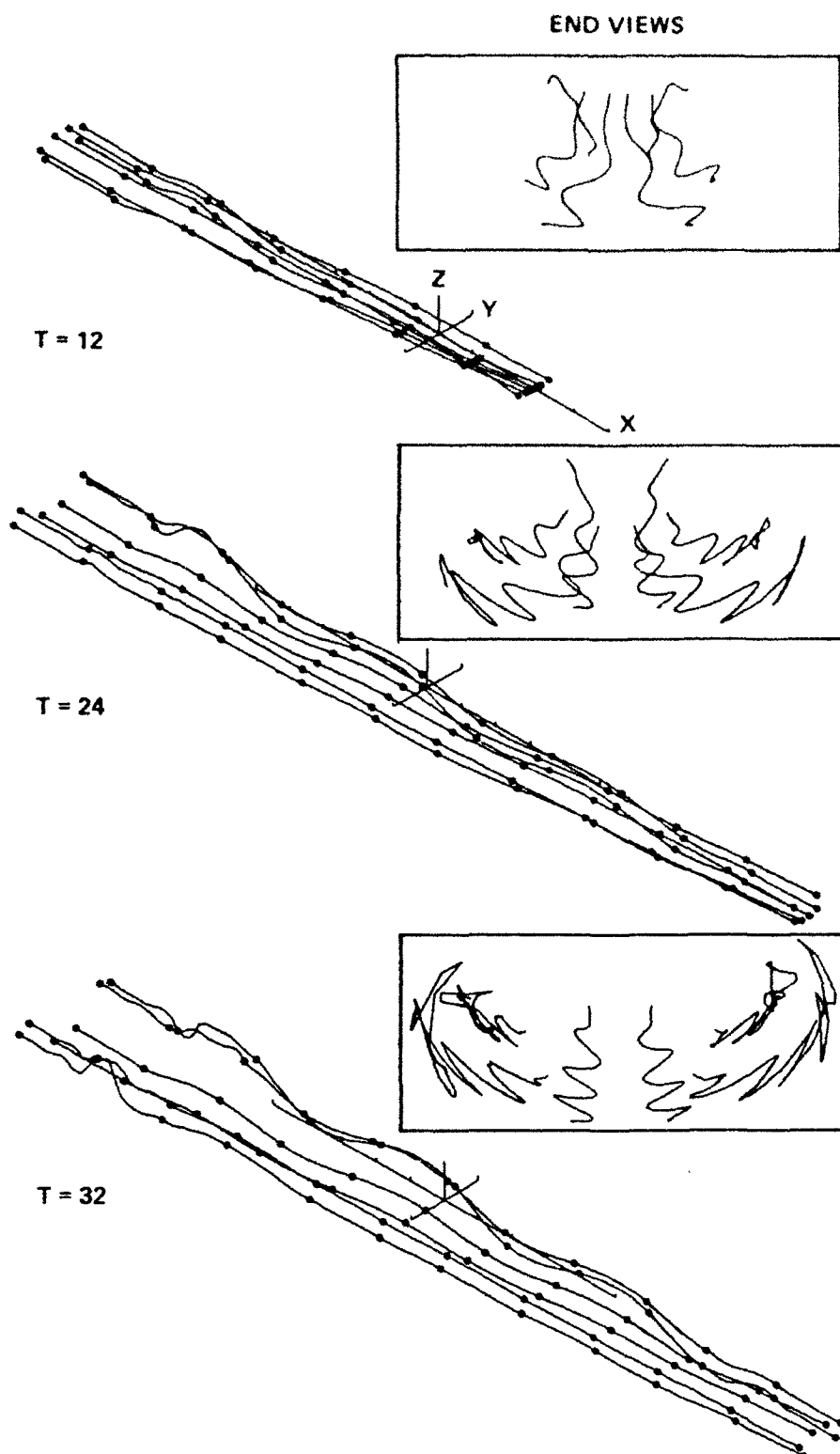
Figure12. Oblique and end views of time-dependent motion of
vortex-filament representation of vortex wake of B-747
in (30°/0°) configuration undergoing roll oscillations of
7° amplitude[40].

Vortex over sheet   **Vortex under sheet**
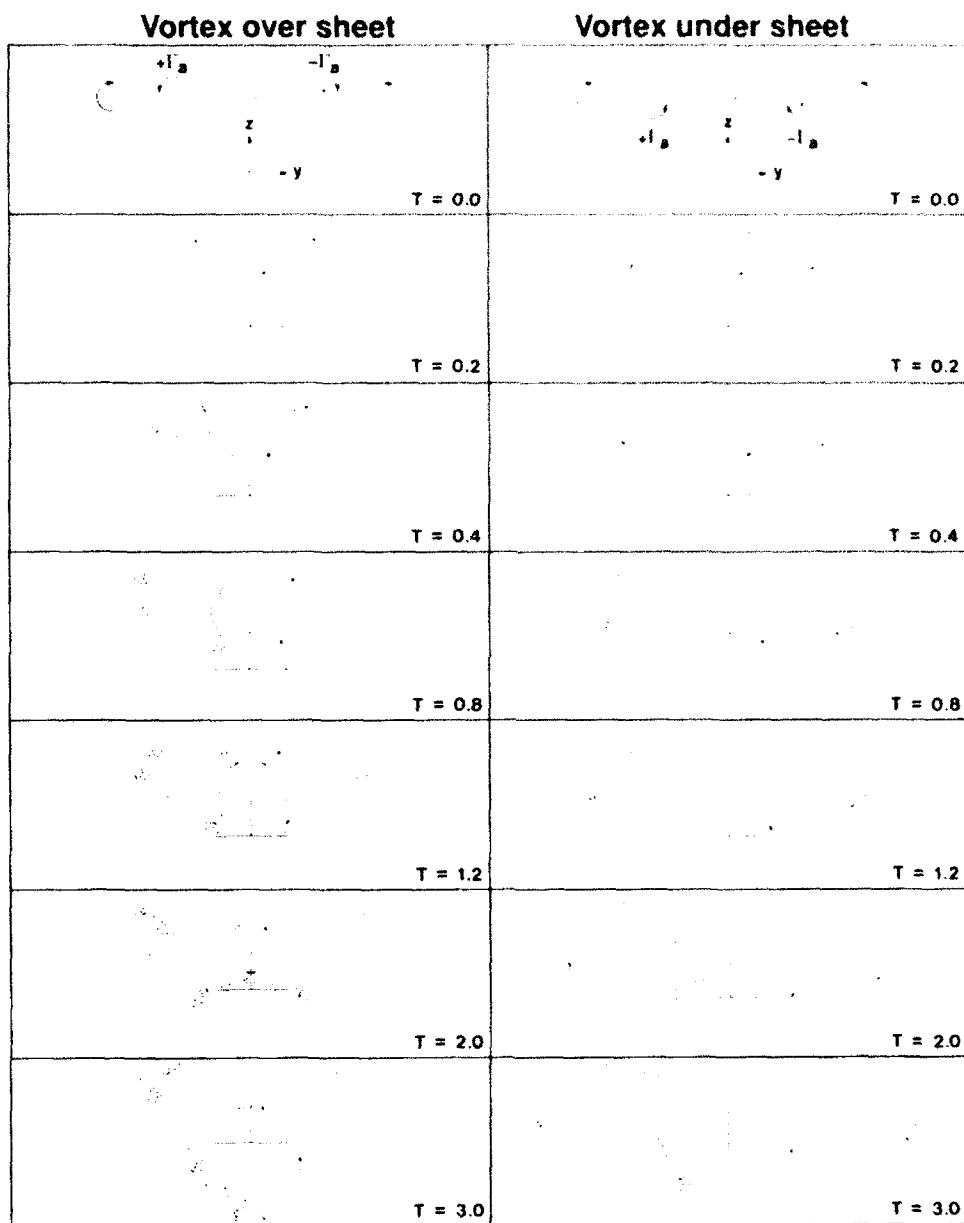
a. Negative vortex over vortex sheet.

b. Negative vortex under vortex sheet.

Figure 13. Point-vortex representation of the effect of vortex injection on lift-generated wakes shed by wing with triangular loading[41].
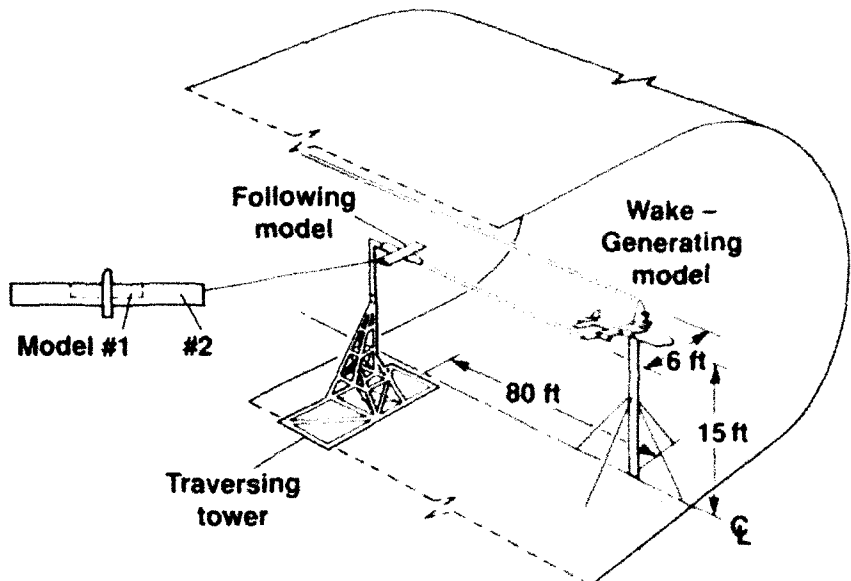
a. Diagram of setup in wind tunnel.
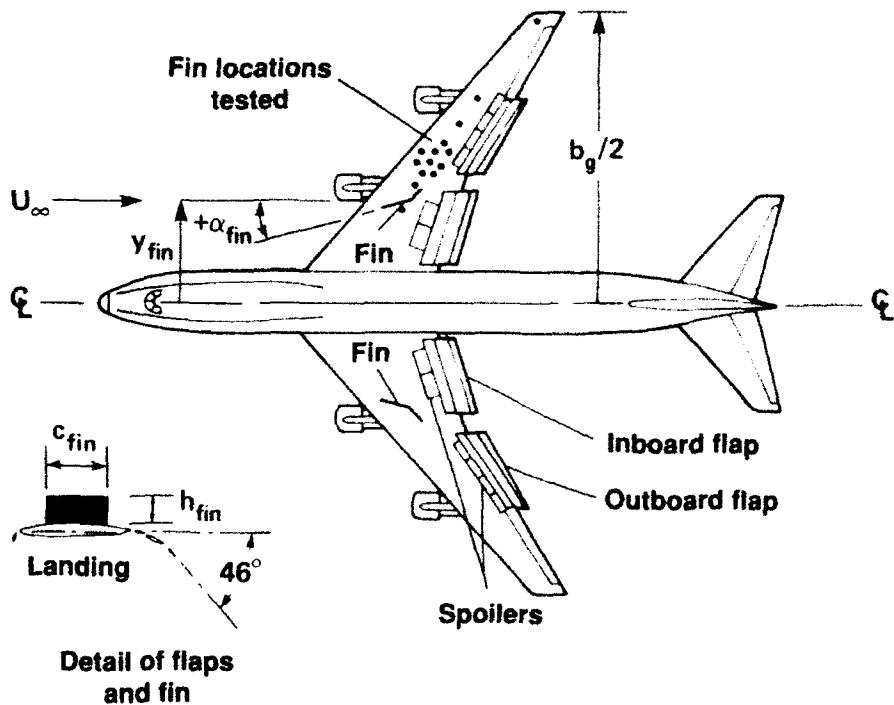
b. Plan view of wake-generating model; dots on starboard wing
indicate test locations of center of fin chords.

Figure 14. Experimental setup in the NASA Ames Research Center
40- x 80-foot wind tunnel that was used to obtain rolling-moment
measurements in the wakes of various aircraft configurations[42].

Variation of wake rolling moment with spanwise location of fin

$h_{fin}/b_g = 0.0567$; $c_{fin}/b_g = 0.085$; $\alpha_{fin} = +18°$

Comparison with other alleviation schemes
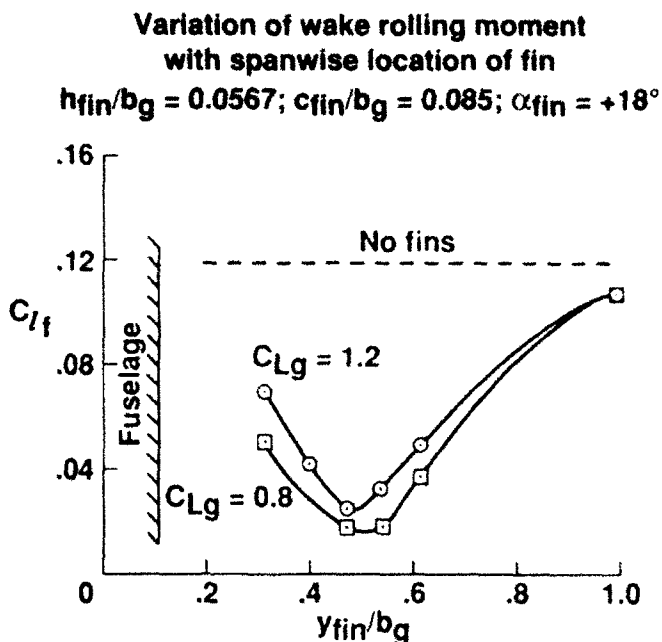
a. Rolling moment coefficient as a function of spanwise location of fin. $h_{fix}/b_g = 0.0567$; $c_{fin}/b_g = 0.085$; $a_g = +18°$.
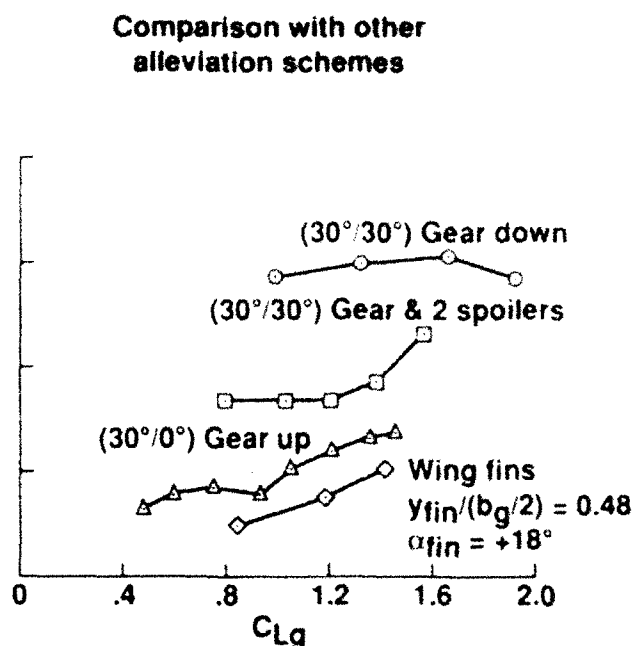
b. Comparison of rolling-moment coefficient obtained by use of other alleviation methods as a function of lift coefficient on wake-generating model.

Figure 15. Test results[42] for model of B-747 in NASA-ARC 40- x 80-foot wind tunnel at $x_{fin}/b_g = 13.6$ with a following model of a size that $b_{fin}/b_g = 0.19$.
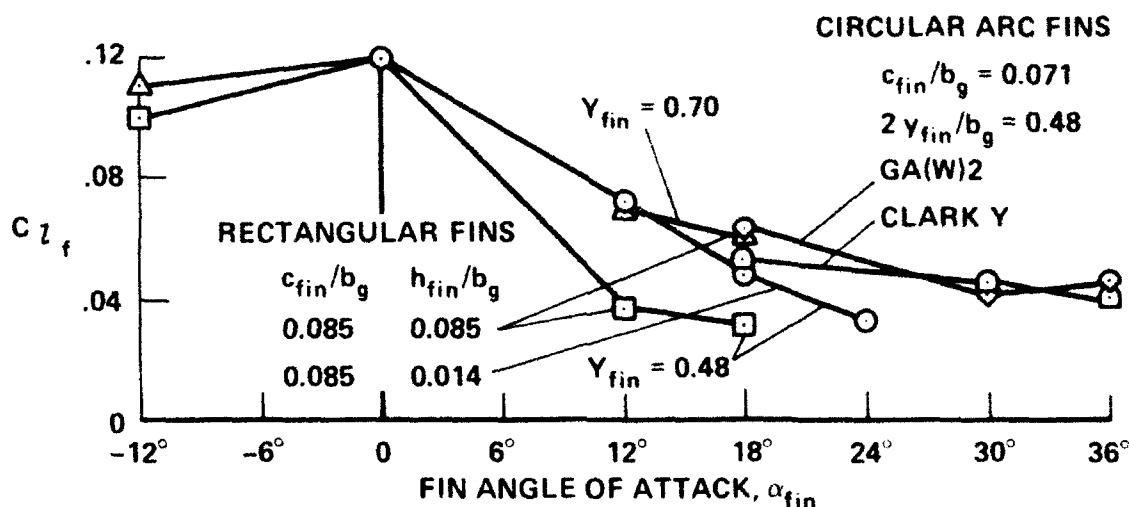
Figure 16. Variation of rolling moment induced on following wing ($b_{fin}/b_g = 0.19$) by vortex wake shed by starboard side of model of B-747 with angle of attack of rectangular and circular-arc fins; $a_g = 4°$, $b_{fin}/b_g = 13.6$.
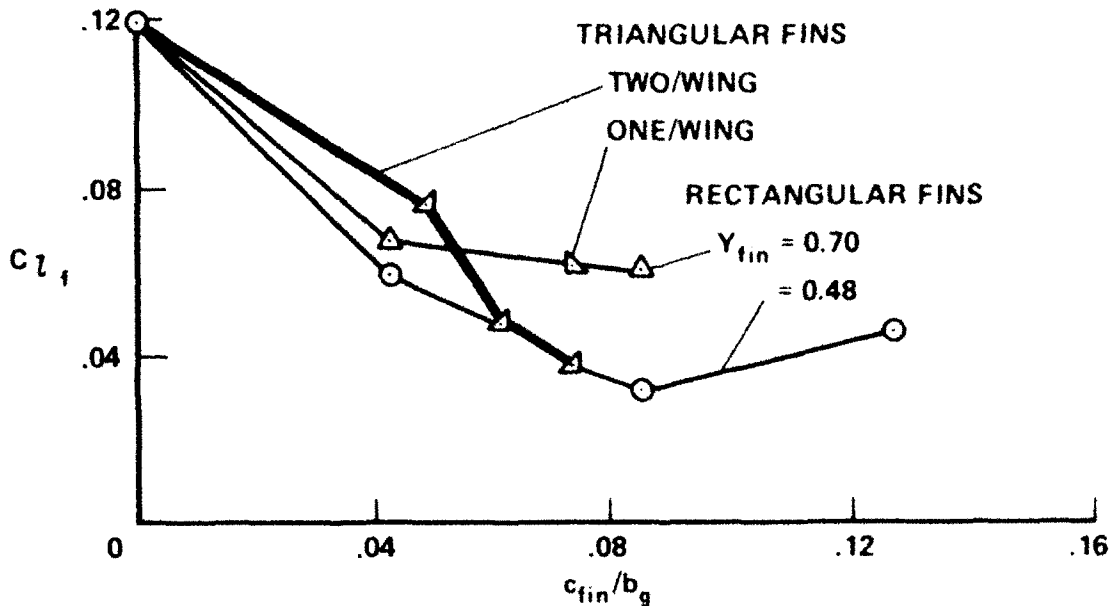
Figure 17. Variation of rolling moment induced on following wing ($b_{fin}/b_g = 0.19$) by vortex wake shed by starboard side of model of B-747 with chord of rectangular ($h_{fin}/b_g = 0.085$, $a_{fin} = 18°$) and triangular ($a_{fin} = 24°$) fins; $a_g = 4°$ ($C_{Lg} = 1.2$), $x_{fin}/b_g = 13.6$.
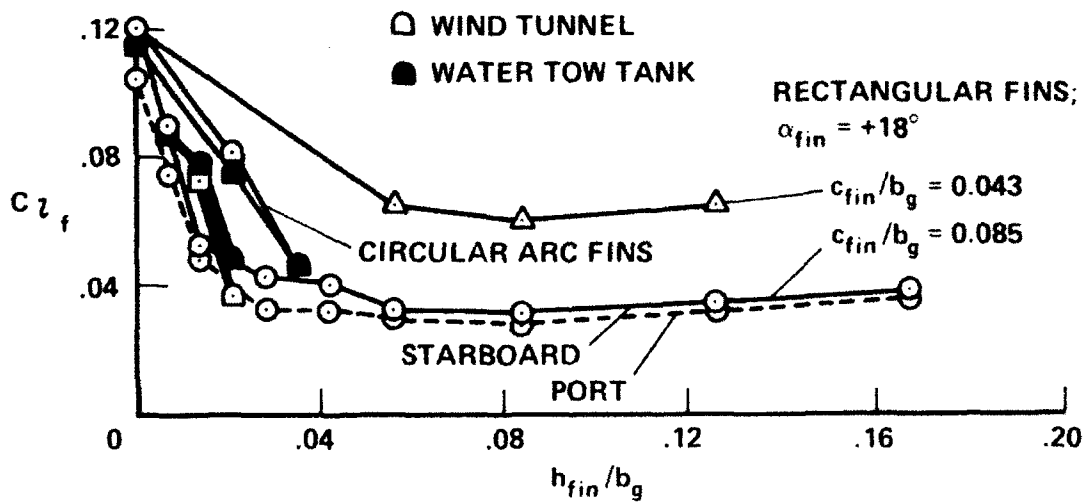
Figure 18. Variation of rolling moment induced on following wing ($b_{fin}/b_g = 0.19$) by vortex wake shed by starboard side of model of B-747 with fin height of rectangular or circular-arc fins[42] as measured in wind tunnel ($a_{fin} = 30°$), $x_{fin}/b_g = 13.6$, and in water tow tank ($a_{fin} = 24°$).
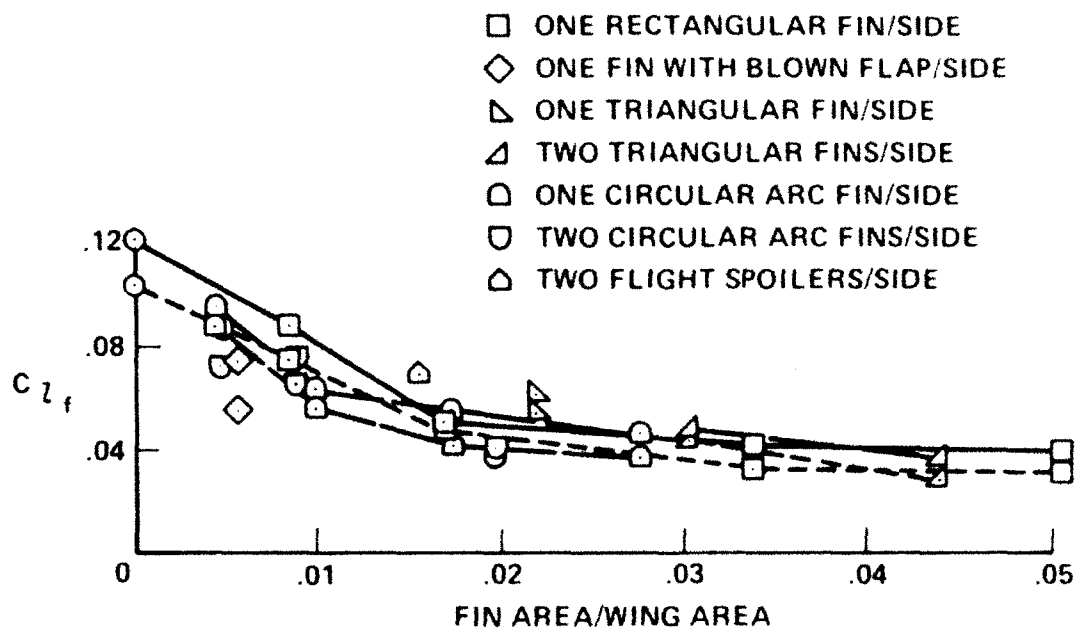
Figure 19. Variation of rolling moment induced on following wing ($b_{fin}/b_g = 0.19$) by vortex wake shed by starboard side of model of B-747 fin size for various fin planform shapes and configurations[42]; $x_{fin}/b_g = 13.6$, $b_{fin}/b_g = 0.19$, $a_g = 4°$.
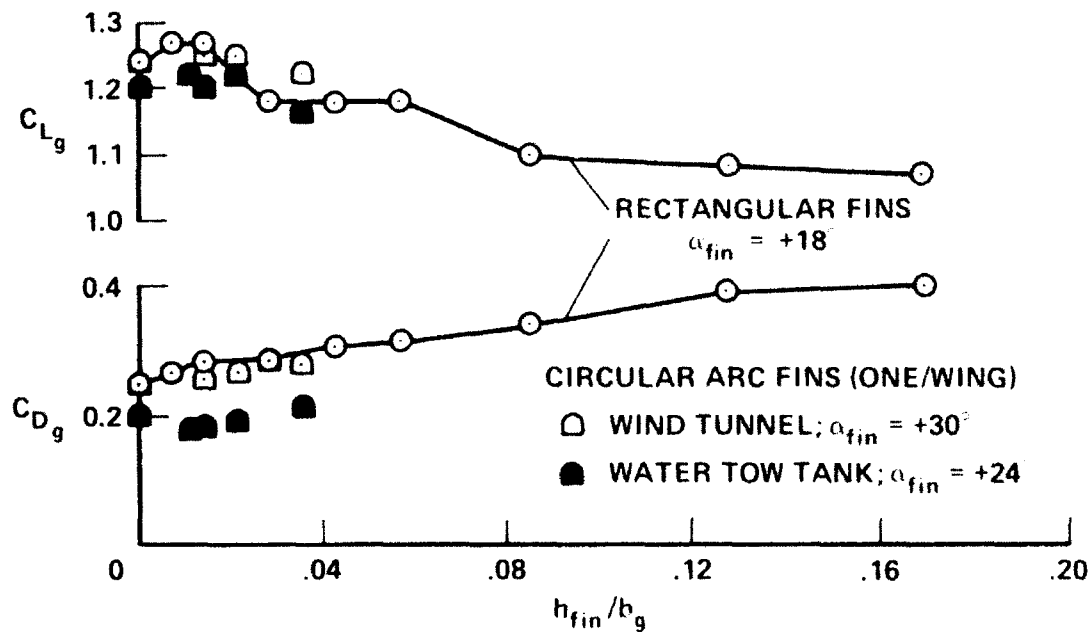
Figure 20. Variation of lift and drag on model of B-747 equipped with rectangular or circular-arc fins with height of fin[42]; $a_g = 4°$.
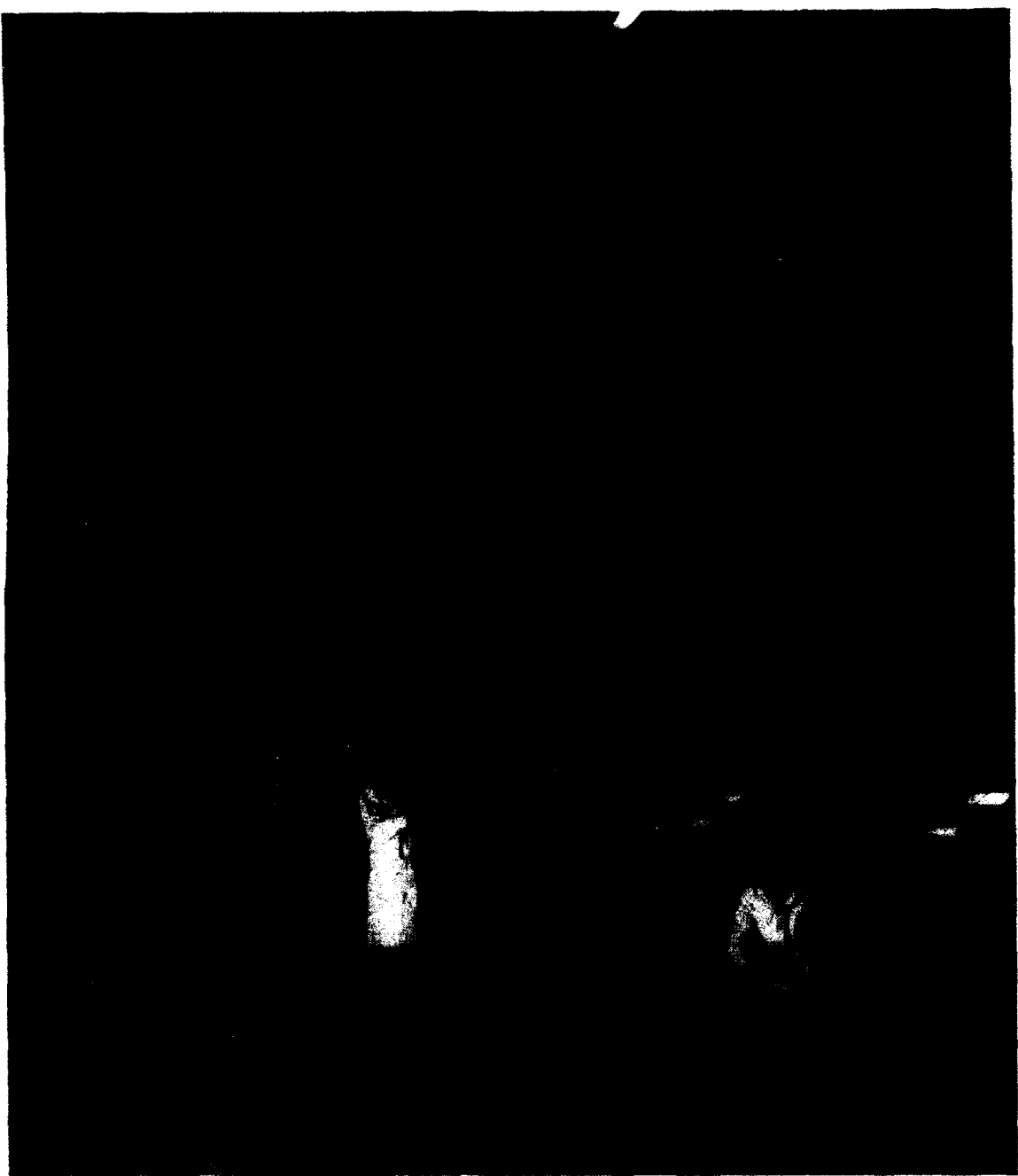
a. Overall view of setup.

Figure 21. Photographs of experimental setup in 40- x 80-foot wind tunnel to illustrate sizes of equipment and disposition[42].

b. Closeup view of model of B-747 mounted upside down
on support strut with two circular-arc fins mounted
midway out on each wing.

Figure 21. Photographs of experimental setup in 40- x 80-foot
wind tunnel to illustrate sizes of equipment and
disposition[42] (concluded).
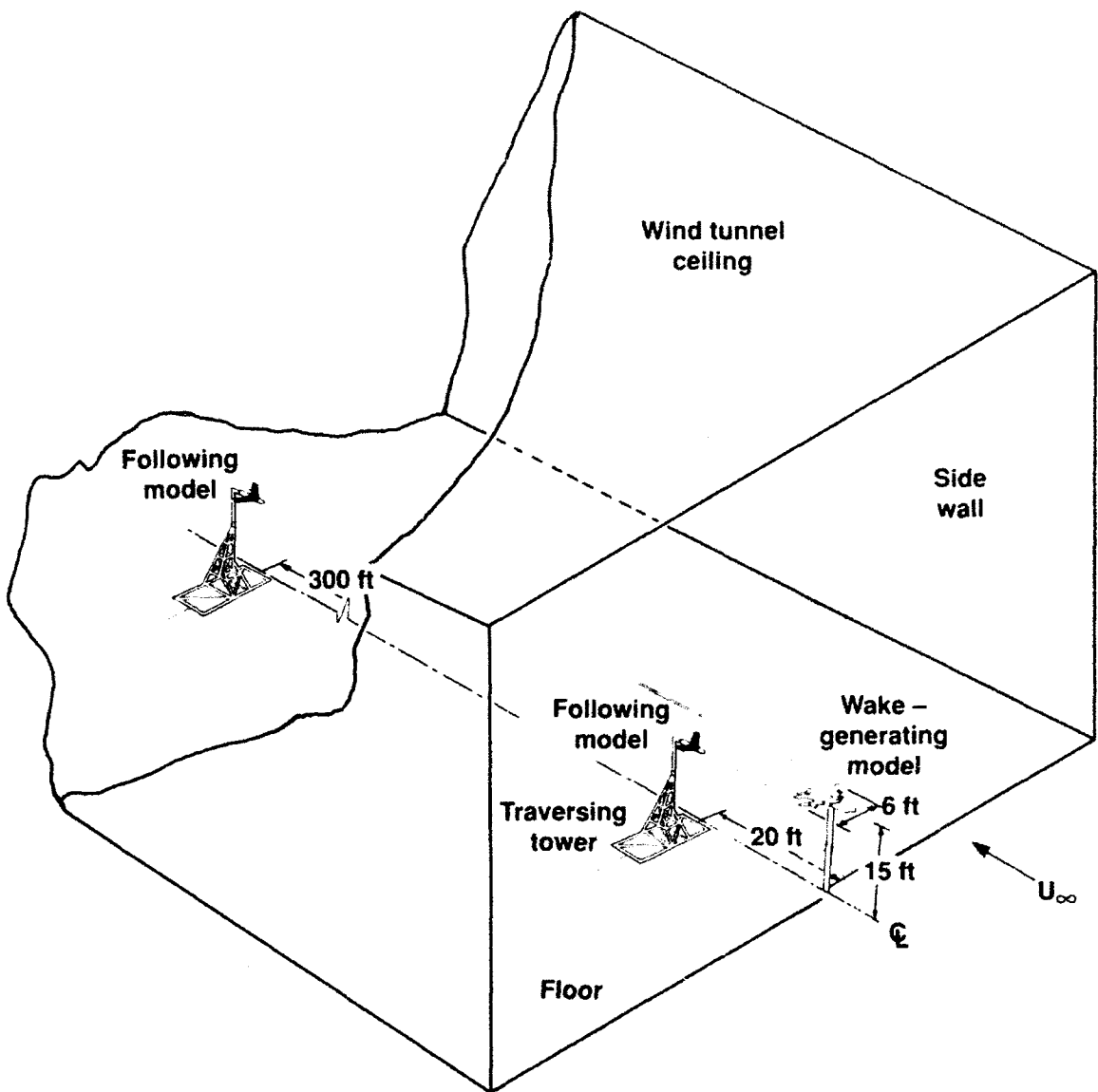
Figure 22. Overview of setup in 80- x 120-foot wind tunnel illustrating the relative sizes of the equipment and the two extreme locations of the following model that can be tested.

REFERENCES

1. Greene, G. C., Dunham, R. E., Burnham, D. C., Hallock, J. N., and Rossow, V. J., "Wake Vortex Research--Lessons Learned," FAA International Wake Vortex Symposium, Washington, D. C., October 29-31, 1991.

2. Burnham, D. C., "Wake Vortex Alleviation System Requirements," Report No. DOT-TSC-FA427-PM-84-19, U. S. Dept. of Transportation, May 1984.

3. Rossow, V. J., and Tinling, B. E., "Research on Aircraft/Vortex-Wake Interactions to Determine Acceptable Level of Wake Intensity," AIAA Journal of Aircraft, Vol. 25, No. 6, June 1988, pp. 481-492.

4. Corsiglia, V. R., and Dunham, R. E., "Aircraft Wake-Vortex Minimization by Use of Flaps," NASA Symposium on Wake Vortex Minimization, NASA SP-409, 1976, pp. 305-338.

5. Corsiglia, V. R., Rossow, V. J., and Ciffone, D. L., "Experimental Study of the Effect of Span Loading on Aircraft Wakes," AIAA Journal of Aircraft, Vol. 13, No. 12, Dec. 1976, pp. 968-973.

6. NASA Symposium on Wake Vortex Minimization, NASA SP-409, 1976.

7. Hallock, J. N., ed., Proceedings of the Aircraft Wake Vortices Conference, Report No. FAA-RD-77-68, U. S. Dept. of Transportation, March 15-17, 1977.

8. Lamb, H., Hydrodynamics, 6th ed., Dover, 1945, pp. 591-2.

9. Ciffone, D. L., "Correlation for Estimating Vortex Rotational Velocity Downstream Dependence," AIAA Journal of Aircraft, Vol. 11, No. 11, Nov. 1974, pp. 716-717.

10. Ciffone, D. L., and Orloff, K. L., "Far-Field Wake-Vortex Characteristics of Wings," AIAA Journal of Aircraft, Vol. 12, No. 5, May 1975, pp. 464-470.

11. Hallock, J., Burnham, D. C., Tombach, I. H., Brashears, M. R., Zalay, A. D., and Barber, M. R., "Ground-Based Measurements of the Wake Vortex Characteristics of a B-747 Aircraft in Various Configurations," AIAA 15th Aerospace Sciences Meeting, Los Angeles, CA, Jan. 1977, Paper 77-9.

12. Rossow, V. J., "On the Inviscid Rolled-Up Structure of Lift-Generated Vortices," AIAA Journal of Aircraft, Vol. 10, No. 11, Nov. 1973, pp. 647-650.

13. Donaldson, C. duP., Snedeker, R. S., and Sullivan, R. D., "Calculation of Aircraft Wake Velocity Profiles and Comparison with Experimental Measurements," AIAA Journal of Aircraft, Vol. 11, No. 9, Sept. 1974, pp. 547-555.

14. Rossow, V. J., Corsiglia, V. R., Schwind, R. G., Frick, J. K. D., Lemmer, O. J., "Velocity and Rolling-Moment Measurements in the Wake of a Swept-Wing Model in the 40- by 80-Foot Wind Tunnel," NASA TM X-62,414, April 1975.

15. Iversen, J. A., "Correlation of Turbulent Trailing Vortex Decay Data," AIAA Journal of Aircraft, Vol. 13, No. 5, May 1976, pp. 338-342.

16. Corsiglia, V. R., Jacobsen, R. A., and Chigier, N., "An Experimental Investigation of Trailing Vortices Behind a Wing with a Vortex Dissipator," Aircraft Wake Turbulence and its Detection, Olsen, J. H., Goldburg, A., and Rogers, M., eds., Plenum Press, 1971, pp. 229-242.

17. Patterson, J. C., Hastings, E. C., and Jordan, F. L., "Ground Development and Flight Correlation of the Vortex Attentuating Spline Device," NASA Symposium on Wake Vortex Minimization, NASA SP-409, 1976, pp. 271-303.

18. Croom, D. R., "The Development and use of Spoilers as Vortex Attenuators," NASA Symposium on Wake Vortex Minimization, NASA SP-409, 1976, pp. 339-368.

19. Corsiglia, V. R., and Rossow, V. J., "Wind-Tunnel Investigation of the Effect of Porous Spoilers on the Wake of a Subsonic Transport Model," NASA TM X-73,091, January 1976.

20. Croom, D. R., "Low-Speed Wind-Tunnel Parametric Investigation of Flight Spoilers as Trailing-Vortex-Alleviation Devices on a Transport Aircraft Model," NASA TP-1419, 1979.

21. Barber, M. R., and Tymczyszyn, J. J., "Wake Vortex Attenuation Flight Tests: A Status Report," NASA CP-2170, 1980, pp. 387-408.

22. Patterson, J. C., and Jordan, F. L., "Thrust-Augmented Vortex Attentuation," NASA Symposium on Wake Vortex Minimization, NASA SP-409, 1976, pp. 251-270.

23. Dunham, R. E., Jr., "Unsuccessful Concepts for Aircraft Wake Vortex Minimization," NASA Symposium on Wake Vortex Minimization, NASA SP-409, 1976, pp. 221-250.

24. Hallock, J. N., Wood, W. D., and Spitzer, E. A., "The Motion of Wake Vortices in the Terminal Environment," Proceedings of the Sixth Conference on Aerospace and Aernautical Meteorology, American Meteorology Society, 1974, pp. 393-398.

25. Hallock, J. N., Wood, W. D., and Spitzer, E. A., "Predictive Techniques for Wake Vortex Avoidance," Proceedings of 20th Symposium of Guidance and Control Panel, Plans and Developments for Air Traffic Systems, AGARD, 1975, 23-1 to 23-11.

26. Burnham, D. C., "B-747 Vortex Alleviation Flight Tests: Ground-Based Sensor Measurements," Report No. DOT-FAA-RD-81-99, U. S. Dept. of Transportation, Feb. 1982.

27. Wood, W. D., ed., FAA/NASA Proceedings Workshop on Wake Vortex Alleviation and Avoidance, Report No. FAA-RD-79-105, U. S. Dept. of Transportation, Nov. 28-29, 1978.

28. Lessen, M., Singh, P., and Paillet, F., "The Stability of a Trailing Line Vortex, Part I: Inviscid Theory," Journal of Fluid Mechanics, Vol. 63, Pt. 4, May 1974, pp 753-763.

29. Lessen, M., and Paillet, F., "The Stability of a Trailing Line Vortex, Part II: Viscous Theory," Journal of Fluid Mechanics, Vol. 65, Pt. 4, Oct. 1974, pp. 769-779.

30. Zalay, A. D., White, R. P. W., and Balcerak, J. C., "Investigation of Viscous Line Vortices with and without the Injection of Core Turbulence," RASA Rept. 74-01, Feb. 1974., Rochester Applied Science Associates, Rochester, NY.

31. Bilanin, A. J., and Teske, M. E., "Vortex Interactions and Decay in Aircraft Wakes," NASA CR-2870, 1977 (see also ARAP Rept. No. 271).

32. Scorer, R. S., Natural Aerodynamics, Pergamon Press, New York, 1958.

33. Crow, S. C., "Stability Theory for a Pair of Trailing Vortices," AIAA Journal, Vol. 8, No. 12, Dec. 1970, pp. 2172-9.

34. Aircraft Wake Turbulence and its Detection, Olsen, J. H., Goldburg, A., and Rogers, M., eds., Plenum Press, 1971.

35. Bilanin, A. J., and Widnall, S. E., "Aircraft Wake Dissipation by Sinusoidal Instability and Vortex Breakdown," AIAA Paper 73-107, 1973.

36. Rossow, V. J., "Prospects for Destructive Self-Induced Interactions in a Vortex Pair," AIAA Journal of Aircraft, Vol. 24, No. 7, July 1987, pp. 433-440.

37. Rossow, V. J., "Theoretical Study of Lift-Generated Vortex Wakes Designed to Avoid Rollup," AIAA Journal, Volume 13, No. 4, April 1975, pp. 476-484.

38. Smith, H. J., "A Flight Test Investigation of the Rolling Moments Induced on a T-37B Airplane in the Wake of a B-747 Airplane," NASA TM-56031, April 1975.

39. Barber, M. R., Hastings, E. C., Champine, R. A., and Tymczyszyn, J. J., "Vortex Attenuation Flight Experiments," NASA Symposium on Wake Vortex Minimization, NASA SP-409, 1976, pp. 369-403.

40. Rossow, V. J., "Wake Hazard Alleviation Associated with Roll Oscillations of Wake-Generating Aircraft," AIAA Journal of Aircraft, Vol. 23, No. 6, June 1986, pp. 484-491.

41. Rossow, V. J., "Effect of Wing Fins on Lift-Generated Wakes," AIAA Journal of Aircraft, Vol. 15, No. 3, March 1978, pp. 160-7.

42. Rossow, V. J., "Experimental Investigation of Wing Fin Configurations for Alleviation of Vortex Wakes of Aircraft," NASA TM 78520, Nov. 1978.

UNSTABLE WING VORTEX ROLLUP INDUCED BY
LIFT TAILORING IN THE WING-TIP REGION*

D.K. Lezius†
Lockheed Research & Development Division
Palo Alto, CA

ABSTRACT

The effects of modifying the circulation distributions near the tips of lifting wings on the stability of vortex rollup are investigated. Analytical considerations indicate that maintaining a positive spanwise lift gradient near and at the wing tips should result in unstable rollup of the vorticity originating in the region of increased wing-tip lift loading. The instability of the rollup is predicted by the Rayleigh stability criterion for rotating fluids and results from the attempted rollup of the wing vorticity in the tip region into a circular flow with radially decreasing circulation. Preliminary experiments with a rectangular wing with lift loading increasing toward the tip have demonstrated that rollup is prevented by turbulent rotating motions that are generated in the unstable arrangement of vorticity layers. The resulting turbulent vortex wake presents the appearance of one usually observed at large distances downstream of the wing.

INTRODUCTION

The core regions of aircraft trailing vortices generated by airfoils with spanwise lift distribution that decrease toward the wing-tip region are inherently stable flows. Such distributions of both, circulation and lift are typical of modern aircraft wings and of the lift loading near the wing tips of essentially most other wing plan forms. The stability of the swirling flow in the cores of wing-tip vortices forming behind lifting wings can be derived from two physical principles, the conservation laws governing inviscid vortex rollup due to Betz[1] and Rayleigh's[2] stability criterion regarding the stability of rotating flows. Betz's postulates predict that in the presence of a sufficiently strong gradient of circulation, or concentration of vorticity, at the wing tip, rollup of the vorticity into a wing vortex proceeds from the wing tip inward. Rayleigh's criterion for the stability of rotating fluid layers states that in the absence of viscosity, the flow is stable if the square of the circulation increases radially everywhere in the flow. Hence, if the lift distribution is such that the circulation increases monotonically from the wing tip toward the wing root, the circulation in the completely rolled-up vortex increases monotonically in the radial

direction, until the wing-root circulation is attained. Such a flow is hydrodynamically stable by Rayleigh's criterion and cannot maintain or amplify flow disturbances in the radial direction. Disturbances introduced into the flow as part of the rollup process are, in fact, strongly dampened, producing a highly stable tangential flow in the inner region of the vortex. This phenomenon accounts partly for the longevity of the vortex flows generated by large aircraft and for the hazard they pose to following air traffic, even at considerable distance.

Rayleigh's stability criterion also predicts hydrodynamically unstable conditions for the rollup flow into a vortex in which the circulation would decrease in the radial direction, i.e., if this rollup could occur, one would find that in the vortex $d\Gamma/dr < 0$. If such a "super-potential vortex" resulted from a specifically tailored circulation the wing-tip region, the turbulent motions generated by the instability would prevent orderly rollup into a vortex with high velocities near the center, and would instead initiate rapid vortex decay. A simple analysis suggests that conditions for instability would prevail if in the wing-tip region the circulation increased in the spanwise direction and could be maintained at the tip. The ensuring rollup would be disturbed by intense turbulent mixing and lead to rapid decay of the tangential velocities. So far, the evidence seems to suggest that lift-induced instabilities might be exploited beneficially in the wing-vortex hazard alleviation effort. The attractiveness of this approach lies in the possibility of achieving the desired lift distributions by purely aerodynamic means, i.e., by the deployment of leading-edge or wing tip extensions, flaps, or other high-lift devices, some of which are now common to modern wing designs.

This paper explores analytically the relationship between the circulation in the wing-tip region and the properties of the wake, assuming that stable and inviscid rollup could occur. The specific case of linearly increased circulation in the tip region is considered, and preliminary experimental evidence for the occurrence of unstable rollup is presented. Effects of the modified distributions of circulation and lift on induced drag will be briefly discussed, and on turbulence generation which has a direct effect on the rate of vortex decay.

ANALYTICAL CONSIDERATIONS

For the benefit of the following analysis, Betz's theory governing the stable rollup of vortex sheets from lifting wings can be summarized as follows: During rollup of a region of a free vortex sheet into a vortex, the circulation, centroid of vorticity and moment of inertia of vorticity associated with that portion of the vortex sheet remain constant. Although the conservation laws are usually applied to the fluid motion in the Trefftz plane at a distance far downstream and after completely rolled-up, the present analysis is applied at the wing trailing edge in order to establish that unstable conditions for the rollup exist. The conservation statements can be formally arranged[3-5] into expressions for the circulation within a vortex containing a partially rolled-up vorticity sheet,

$$\Gamma_v(r) = \Gamma_w(y) \tag{1}$$

and,

$$r = \frac{1}{\Gamma_w(y)} \int_y^{b/2} \Gamma_w(y') \, dy' \qquad (2)$$

where Γ_w and Γ_v are the circulation on the wing and in the rolled-up portion of the vortex, y and r the corresponding coordinates, respectively, and b is the wing span. Eq. (1) expresses the well known result that the circulation associated with lift over the rectangular wing with spanwise constant circulation $\Gamma_w(y) = \Gamma_0$ rolls up into a potential vortex in which

$$\Gamma_v(r) = \Gamma_0 \qquad (3a)$$

so that with $\Gamma_v(r) > 0$,

$$\frac{d\Gamma_v}{dr} = 0 \qquad (3b)$$

Eq. (3b) satisfies the Rayleigh condition for marginal stability, i.e., radial disturbances of the rotating flow will not be amplified. In the actual vortex core, the effects of viscosity establish solid-body rotation, so that the viscous rollup results in a highly stable core flow.

Consider a basically rectangular wing, in which the spanwise circulation increases from some point y^*, say past the middle of the half span, toward the wing tip where it can be maintained. The large gradient of circulation thus established at the tip by virtue of the step decrease of circulation to zero outside the tip guarantees the existence of a strong centroid of vorticity which becomes the center for the rollup process and the center of the wing vortex. Thus, rollup proceeds from the wing tip inward, attempting to wrap layers of decreasing circulation around the center, and thereby providing the condition for instability of the flow. By the use of Eq. (1), the differential rollup can be expressed as,

$$\frac{d\Gamma_v}{dr} = \frac{d\Gamma_w}{dy} \frac{dy}{dr} \qquad (4)$$

With $d\Gamma_w/dy > 0$, and for the inward directed rollup $dy/dr < 0$, there results,

$$\frac{d\Gamma_v}{dr} < 0 \tag{5}$$

which establishes the condition for instability in the flows. Hence, a spanwise region of positive circulation gradient toward the wing tip induces unstable rollup of the vorticity in that region. The physical realization of this process is that turbulent fluid exchange induced by the initially unstable distribution of vorticity in the wing-tip region prevents rollup into a vortex from actually occurring, as will be seen in the experimental results.

Most conventional wings, including those of large jet transport, carry lift distributions that either approximate the elliptical distribution over the span, or as in the landing configuration, have approximately elliptical distribution toward the tip. For these cases, rollup into a wing vortex with stable flow is guaranteed by the increasing circulation distribution as seen from the tip inward. An analysis of inviscid rollup from elliptically loaded wings[6] shows that to second order in r, the circulation in the fully rolled-up vortex can be expressed as,

$$\Gamma_v(r) = \Gamma_0 \sin\sqrt{6\left[\frac{r}{b} + \frac{1}{5}\left(\frac{r}{b}\right)^2 + O(r^3)\right]} \tag{6}$$

For the general distribution of circulation, the rollup from a wing area given by $y < b/2$ into a vortex region of radius r can be written as,

$$r = F(y) \tag{7}$$

or,

$$y = F^{-1}(r) \tag{8}$$

which gives for the vortex circulation,

$$\Gamma_v(r) = \Gamma_w\left[F^{-1}(r)\right] \tag{9}$$

Solution of Eq. (9) involves finding the inverse of Eq. (2) and cannot be formulated for the general distribution of $\Gamma_w(y)$.

The rollup analysis for a modified wing with positive circulation gradient near the tip is more conveniently carried out in non-dimensional coordinates where $y = 2y/b$, $y^* = 2y^*/b$ and $r = 2r/b$. For the case of spanwise constant lift loading followed by linear increase to the tip, Eq. (9) can be solved explicitly, to yield,

$$\Gamma_v(r) = \Gamma_0(\sqrt{9/4 + r^2} - r) \tag{10}$$

Hence Γ_v decreases in the radial direction from is maximum value at the center of the vortex, $\Gamma_v(0) = 3/2\Gamma_0 = \Gamma_1$. The excess wing circulation imposed in the region $y > y^*$ is recovered in the vortex area given by the radius,

$$r^* = 1 - (1 + \gamma)\, y^* + \frac{\gamma}{2}\, (1 + y^{*2}) \tag{11}$$

where,

$$\gamma = \frac{\Gamma_1/\Gamma_0 - 1}{1 - y^*} \tag{12}$$

is the non-dimensional circulation gradient. Substitution of r^* into Eq. (10) verifies that $\Gamma_v(r)$ decreases to the value of the rectangular wing section,

$$\Gamma_v(r^*) = \Gamma_0 \tag{13}$$

This section, where $\Gamma_w = \Gamma_0$, rolls up into the additional vortex region

$$r - r^* = y^* - y \tag{14}$$

The lateral separation of the vortices is obtained by combining the regions of rolled-up circulation given in Eqs. (11) and (14) and by setting $y = 0$. Thus results for the centers of the rotating motions in dimensional form, Contrary to the usual experience that the vortices roll up

$$b = 2r(0) = \frac{9}{8}\, b \tag{15}$$

inside the wing span, the centers of circulation in this case separate to a distance larger than the span. This occurs in order to accommodate vorticity that is opposite in sign from that represented by the centroids of vorticity generated at the tips, and follows from Eq. (11) in that the incremental radius δr^* required to roll up the region of increasing circulation is directly proportional to $\delta\gamma$, i.e., negative vorticity shed. This effect was observed in the experiments at approximately the predicted magnitude, as will be discussed below.

Since the argument of unstable vortex rollup applies to the entire region of spanwise increased circulation, one would expect this region, in particular, to participate in the observed initial rapid turbulent mixing behind the wing tip. In addition, radial inertia of the mixing motions may transport turbulent eddies outside the unstable region, and contribute there as well to more rapid dissipation of the vortex velocities. Previous work[7] on the effects of turbulence on the evolution of vortex motions indicates that temporally increasing levels of turbulence, e.g., as expressed by a time dependent turbulent eddy viscosity, augment the rate of vortex dissipation.

EXPERIMENTAL RESULTS

The possibility of unstable vortex roll up was tested with a rectangular wing of the symmetrical type NACA-0015, half span of 7 cm, and aspect ratio of 3.3. A test of this wing in water at chord Reynolds number $Re = 14,600$ and $6°$ angle of attack is shown in Figure 1. The view of the under side of the wing includes a dye port around which the vortex core turns in the rollup, but otherwise, the rollup proceeds as would be expected for a rectangular wing. The core remains relatively intact over the distance displayed in the figure, which covers approximately two span lengths.

A series of tests was subsequently conducted with the wing modified by adding a linear forward extension of the leading edge to achieve an increase of the cord length by 50% at the tip. It was assumed that the extension, starting at the arbitrarily selected position $y^* = b/4$, would raise the wing circulation to $\Gamma_1/\Gamma_0 = 1.5$ at the tip. In addition, the wing tip was terminated by an end plate with the purpose to maintain the increased lift in the tip region. Figure 2 shows the modified wing mounted on a hollow stem to provide for dye flow to the taps visible on the surface.

Tests of the vortex rollup were performed with the modified wing at $Re = 4.3 \times 10^4$ and at a range of angles of attack. Photographs of the dye-marked vortex wakes are shown in Figure 3. Due to the translucent nature of the material forming the leading edge extension, the modification is not as clearly visible as the original rectangular wing on which it is mounted. The effect of the increased lift in the tip region on the rollup process is demonstrated by the absence of a vortex core. Instead of the usual rollup, intensely turbulent motions were observed in the flow immediately upon leaving the wing region. The associated radial transport of angular momentum resulted in a greatly reduced tangential velocity, although in the side view, it was difficult to clearly identify the centers of the remaining vortex motions. At only several chord lengths behind the wing, the vortex flow had the appearance of an aged wake, that would normally be found at distances of many span lengths downstream. The additional observation that the apparent centers of the vortical motions moved outward beyond the wing span was seen as confirmation of the theoretical prediction that during the unstable rollup, the vortex centers

separate to a distance outside the wing tips, which indicates that the effective wingspan is larger than b. Measurements made directly on the photographic images seem to agree with the calculated vortex separation of $\bar{b} = 9/8b$.

The absence of detailed experimental measurements of the tangential velocities after unstable rollup and of the actual aerodynamic parameters from which the spanwise distribution of circulation could be determined, leave the degree of instability induced somewhat uncertain, and the effects of the modified circulation on the induced drag and other aerodynamic properties have not been analyzed. Although presumably, the circulation represented by the centroids of vorticity generated at the tips produces strong downwash and induced drag in the tip region, the additional lift temporarily produced by such modifications in flight conditions could result in small reductions in speed or angle of attack.

CONCLUSIONS

Analytical considerations and initial experimental results have indicated the possibility of inducing unstable wing vortex rollup by imposing spanwise positive circulation gradients in the area of the wing tip. The instability of the rollup results from the fundamentally unstable nature of a rotating flow with radially decreasing circulation. Further analysis should elucidate the unstable rollup process in additional detail with respect to rates of turbulence production and vortex decay, as well as changes in lift and drag in relation to modifying the tip region of wing circulation. Experimentation with larger wing models or full-scale flight test would yield further data to answer the question whether unstable rollup holds potential as a practical method for utilizing this phenomenon in reducing the intensity of trailing wing vortices. The practical implementation of tailoring lift loading on large aircraft so as to achieve unstable rollup during flight operations in the proximity of other aircraft might utilize appropriate camber- or chord-changing apparatus, such as slats, or other forms of variable-lift devices.

Figure 2. NACA-0015 airfoil with modified wingtip and end plate.

Figure 1. Vortex core from NACA-0015 airfoil at Re=14,600; α=6°.
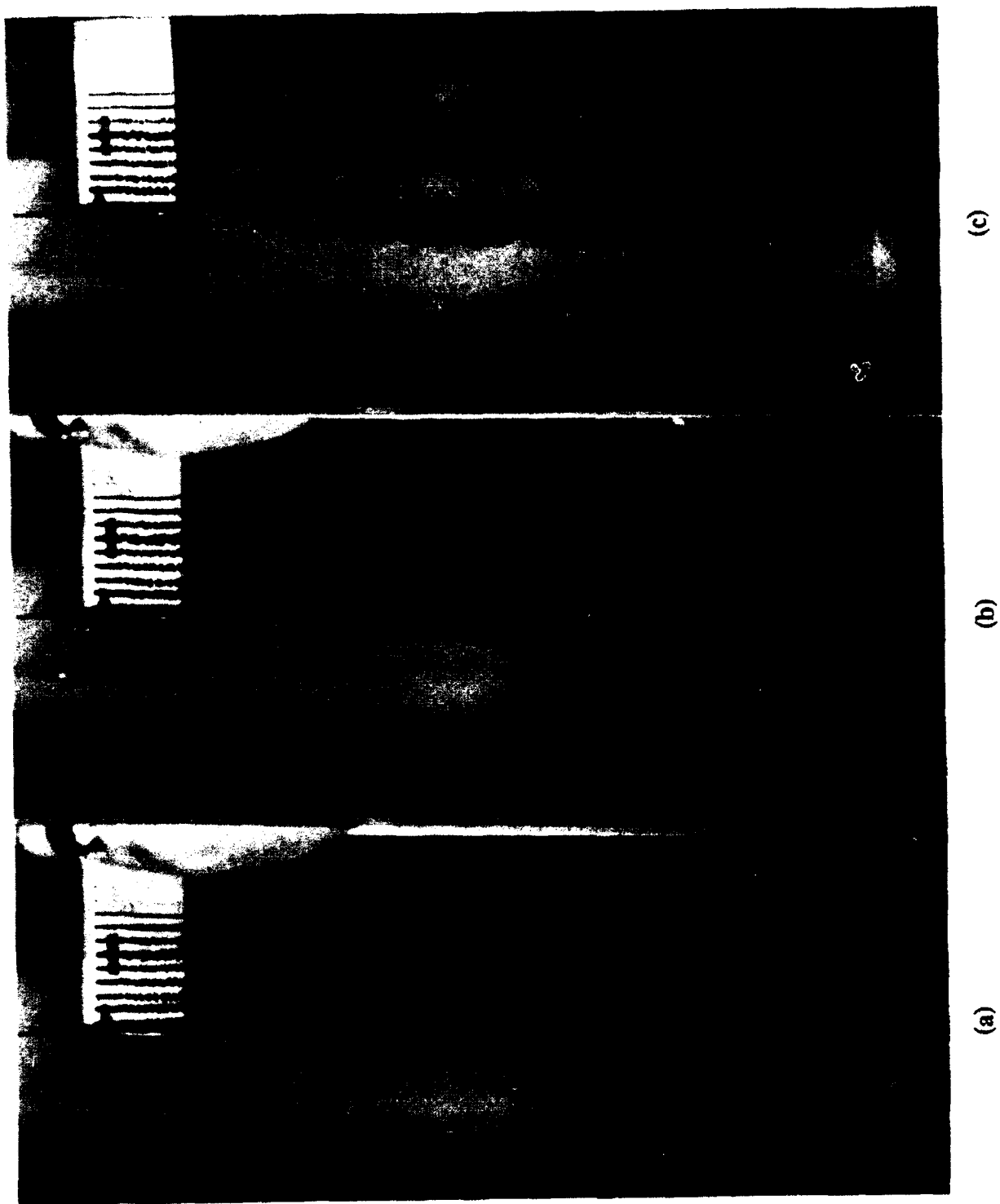
Figure 3. Unstable vortex rollup from modified wingtip at Re=43,000; (a) $\alpha=0°$; (b) $\alpha=8°$; (c) $\alpha=12°$.

REFERENCES

[1]Betz, A., "Behavior of Vortex Systems," NACA TM 713; translated from *Zeitschrift für Angewandte Mathematik und Mechanik*, Vol. 12, 1932, pp. 164-174.

[2]Rayleigh, Lord, "On the Dynamics of Revolving Fluids," Proc. Roy. Soc., A, Vol. 93, 1917, p. 148.

[3]Donaldson, Coleman duP., "A Brief Review of the Aircraft Trailing Vortex Problem," AFOSR-TR-1910, 1971.

[4]Donaldson, Coleman duP., Snedeker, R.S., and Sullivan, R.D., "A Method of Calculating Aircraft Wake Velocity Profiles and Comparison with Full-Scale Experimental Measurements," AIAA Paper No. 74-39, 1974.

[5]Rossov, V.J., "On the Inviscid Rolled-Up Structure of Lift-Generated Vortices," NASA TM X-62,224, 1973.

[6]Lezius, D.K., "Analytical Solution for Inviscid Vortex Rollup from Elliptically Loaded Wings," Journal of Aircraft, Vol. 12, No. 11, Nov. 1975, pp. 911-914.

[7]Lezius, D.K., "Water Tank Study of the Decay of Trailing Vortices," AIAA J., Vol. 12, No. 8, August 1974, pp. 1065-1071.

ROLE OF FAA/NWS TERMINAL WEATHER SENSORS AND TERMINAL AIR TRAFFIC AUTOMATION IN PROVIDING A VORTEX ADVISORY SERVICE[1]

James E. Evans
Jerry D. Welch
M.I.T. Lincoln Laboratory
P.O. Box 73
Lexington, MA 02173

INTRODUCTION

Existing and planned FAA/NWS terminal weather sensors and weather information systems are expected to provide an adequate sensory basis for a useful wake vortex advisory service (WVAS). These meteorological sensors, which provide broad terminal area coverage, should make it possible to reliably estimate and forecast when wake vortex advection characteristics make it possible to reduce the spacings between aircraft on final approach.

Effective operational use of such a weather adaptive WVAS would be very difficult without computerized scheduling and spacing aids for terminal air traffic controllers. The developmental Terminal Air Traffic Control Automation (TATCA) program will provide precisely the planning and spacing tools necessary to help controllers take advantage of wake vortex (WV) advisories and forecasts to improve terminal throughput and efficiency.

Wake Vortex Separation Standards

Current separation standards are larger than the required runway occupancy time for runways dedicated to landings. Depending on the weight class of the leading and trailing aircraft (AC), separation standards call for 3-, 4-, 5-, or 6-nm spacings. If there were no concern for the effects of wake vortices, spacings of less than 2.5 nm could be used safely at many airports under normal runway surface conditions.

Currently, there are three main reasons for conservative safety margins on separation:

- Uncertainty in predicting WV strength, movement, and decay rate - (meteorological uncertainty),

- Inherent imprecision in spacing aircraft on final approach, and

- A need for operational simplicity which argues against the use of complex or variable separation rules (operational difficulties).

The Benefits of Reduced Wake Vortex Separations

Credeur [1] has analyzed the capacity improvement that could be achieved by means of a WVAS for a single runway in Instrument Flight Rules (IFR) with 20% heavy aircraft and 80% large aircraft landing in order. If all the aircraft are landed with 10-s standard deviation in inter-arrival spacing, the maximum theoretical landing rate (i.e., the capacity) with current separation standards is about

$$C = 32 \ AC/hr$$

The most immediate and realizable goal of a wake vortex advisory system is to identify conditions when it is safe to reduce all inter-arrival spacings to 3 nm. Eliminating all spacings greater than 3 nm would increase the capacity to about

$$C_3 = 35 \ AC/hr$$

This 10% increase seems modest, but a 10% increase in capacity can significantly reduce average delay when the system is operating near its capacity limit. A more ambitious reduction in spacing to 2.5 nm between all aircraft would give an approximate capacity of

$$C_{2.5} = 42 \ AC/hr$$

This is a 31% increase in capacity. Although the feasibility of using a wake vortex advisory system to permit 2.5 nm separations between all aircraft types has not been established, it is a worthy goal. A capacity gain of this magnitude would result in a significant reduction in delay during busy periods.

A WVAS has another significant potential benefit in that it would tend to improve airport acceptance rates by a larger factor in IFR than in Visual Flight Rules (VFR). At many airports a WVAS could thereby reduce the severity of the capacity reduction that currently disrupts activity when visibility changes result in IFR conditions.

THE USE OF EXISTING AND PLANNED FAA/NWS TERMINAL WEATHER SENSORS AND WEATHER INFORMATION SYSTEMS IN PROVIDING A WAKE VORTEX ADVISORY AND PREDICTION SERVICE

Basic Approach

Past research [2] has shown that the wake vortex separation can be safely reduced when the vortices are being advected out of the arrival path of following aircraft or if atmospheric conditions are causing the vortices to dissipate prior to encounter. Wind advection can be easily analyzed to first order and has been shown experimentally to be capable of indicating when conditions are safe for reduced spacing [3]. By contrast, the research on the relationship of vortex breakup to atmospheric stability and to readily measured atmospheric parameters is in a much less conclusive stage. Hence, we recommend focusing on advection as the principal mechanism for an initial WVAS.

Additionally, we recommend focusing on WVAS service under IFR conditions. IFR conditions are a principal cause of delays at major airports (see Table 1) and the scheduled capacity of the airport in many cases is strongly weighted in the direction of the IFR capacity. During VFR conditions, many airports have excess capacity, and the aircraft may be able to fly profiles that reduce the impact of the wake vortex separations on capacity of individual runways.

Prediction Concept

The concept we recommend for an initial wind prediction product uses time-series analysis of the enhanced Low Level Wind Shear Alert System (LLWAS)[2] anemometers located near the approach zone in connection with areal estimates of the winds and overall environment using a volume scanning pencil-beam pulse Doppler radar such as the Terminal Doppler Weather Radar (TDWR)[3] [4]. These sensors are used to predict when the winds will be outside a "safety ellipse" for wake vortex advection, such as was identified in the 1970's.[4] Additional verification of the wind conditions in the approach zone would be obtained using in situ measurements of the winds by aircraft on approach using the Aircraft Communications Addressing and Reporting System (ACARS) [6] to downlink data to the ground. The combining of information from these various sensors will be accomplished by the Integrated Terminal Weather System (ITWS) [7]. In this section, we discuss the considerations leading to the above recommendation and present some very preliminary experimental results using the TDWR and LLWAS anemometers.

---

[2] The enhanced LLWAS differs from the previous LLWAS by providing a much greater density of anemometers in the final three miles of the approach, sensor siting to reduce sheltering, and improved data processing algorithms.

[3] If a scanning Doppler laser is also available (e.g., as a part of the overall wake vortex advisory and monitoring system), data from it would be used as well in the same manner as the data from the TDWR.

[4] The "safety ellipse," defined in [5], had a cross-runway semi-minor axis of 6 knots and an along-runway semi-major axis corresponding to 12 knots of headwind.

Previous efforts at wind prediction in the wake vortex context used the short-term (e.g., 8 minutes) past history of the wind at an anemometer near the approach zone to predict that the winds would continue to advect the wake vortices away from following aircraft in the near future.[3] Although this approach could be reasonably successful in a highly stationary weather situation, it will not be satisfactory in convective weather and certain low-visibility weather situations where strong wind changes can occur fairly rapidly without warning.

One example of this type of rapid change is shown in Figure 1 which shows the time trace of a Low Level Wind Shear System (LLWAS) anemometer at the Orlando International Airport on a day when delays were occurring due to thunderstorms in the terminal area. The wind was approximately 8 kts from the south for nearly an hour before suddenly changing to strong westerly flow at 19:00 GMT. The likelihood of this sudden change that occurs at approximately 19:00 GMT could not be anticipated from the anemometer data alone up to 18:55.

From the TDWR testbed radar data obtained at the same time, the wind stationarity is apparent, as is the cause of a sharp change in the wind at 19:00. First, however, it is appropriate to make a few remarks about the application of Doppler weather radar to characterizing the wake vortex advection environment. Numerous scientific and operationally oriented experiments over the past 30 years have shown that winds near the surface can be measured with sensitive narrow-beamwidth pencil-beam Doppler radars out to a range of 40-50 km under the weather conditions identified in table 1, which also correspond to conditions of serious delays. It is important to note, however, that this wind measurement capability generally can be achieved in clear air conditions[4] associated with adverse weather as well as in conditions where there is precipitation. Furthermore, even though the high-quality measurements needed for automatic data processing must often be accomplished in the presence of strong ground clutter, this clutter challenge has been largely surmounted in the case of the TDWR by the use of narrow beams (0.5 deg) and a variety of other clutter-suppression techniques [4].

Figure 2 shows the TDWR radar reflectivity and radial velocity fields during the period of the time in which the anemometer winds were fairly stationary. The reflectivity values associated with the region near the anemometer are typical of those associated with clear air return in summer in central Florida, and the radial velocity field is largely homogeneous at about 8 kts within a radius of several miles about the anemometer. Under such homogeneous areal wind environment conditions, one expects that the anemometer winds will remain stationary for some minutes.

Figure 3 shows the reflectivity and radial velocity fields some 15 minutes before the sharp wind change occurs at the anemometer. It is shown that a region of heavy rain is approaching the anemometer from the west. A sharp radial wind change is associated with the leading edge of the storm outflow (i.e., gust front). Under such conditions, a sharp change in the anemometer wind is expected in the next few minutes.

---

[3] Specifically, if the vector wind had been outside the "safety ellipse" for the previous eight minutes, it was considered safe to operate at a reduced wake vortex spacing for aircraft commencing final approach. [2]

[4] Due to scattering from refractive index inhomogeneities, insects, and/or particles blown by the wind. [9]

Abrupt changes in the winds at a given location can arise from a variety of causes. Table 2 summarizes some principal causes of wind changes and the weather system observables which can be used to detect these changes. A few comments are in order regarding each of the phenomena:

Microburst Outflows

Microburst outflows can be very common in areas with substantial convective activity. For example, recent studies have concluded that near an airport, one can expect two to eight microbursts (and approximately two gust fronts) each day with thunderstorms. Microbursts are detected automatically by the TDWR and enhanced LLWAS, and it is expected that the detection probability of microbursts will be near unity for the airports where the warnings from these two systems are integrated.

The expected presence of a convective cell above a runway in the immediate future can be readily anticipated from the TDWR storm track algorithm applied to data from either the TDWR or the ASR-9 weather channel. The TDWR can determine, to some degree, when a microburst is imminent by noting the descent of reflectivity and the presence of velocity features aloft. However, the warning time is typically about 5 minutes, whereas at least 10-minutes warning is desirable for the WVAS. Thus, if the atmospheric conditions are such that microbursts may occur, the prudent course of action would be to suspend any reduced wake vortex separation operations until the cells were no longer at a location where a downdraft would occur in the area of concern.

Gust Fronts

The TDWR seeks to detect gust fronts at least 20 minutes prior to their arrival at the airport. Tracking algorithms operating on the gust front detections permit the prediction of the time of arrival of a gust front at an airport location to an accuracy of typically several minutes [4]. The winds behind the gust front are estimated by a least squares fit of a uniform wind field to the observed radial velocity field behind the gust front. Typical accuracies using Doppler radar data alone are currently 6 kts and 30 deg in angle behind a gust front.[7] Table 3 summarizes the detection performance of the initial TDWR gust front/wind shift estimation algorithms (an improved algorithm is under development which should provide improved accuracy).

Frontal Bands

The wind shifts associated with frontal snow and rain bands in areas of widespread precipitation can be detected by techniques similar to those used for gust fronts.

---

[7] We recommend using anemometer data to improve on the accuracy of estimation for winds behind a gust front and to account for surface friction effects.

Thermal Instabilities

Thermal instabilities can cause strong localized changes in surface winds on days with substantial solar heating of the ground. These instabilities are typically manifested by a high degree of variation in the surface radial velocity fields over small spatial scales (e.g., a square km) and an increased spectrum width.[8] By contrast, laminar flow associated with relatively stable winds has a low spatial variation over areas of several square km and a low spectral width. The temperature lapse rate can be determined by the ITWS using ACARS derived temperature profiles together with surface temperatures from the Automated Surface Observing System (ASOS) and the Automatic Weather Observing System (AWOS).

In view of the importance of the TDWR gust front/wind shift detection algorithm to the predictive capability needed for a WVAS, a few remarks are in order on the algorithm status. Until recently, gust front detection and wind shift estimation had received much less emphasis in the TDWR program than microburst detection. However, recent TDWR operational tests at Denver, Kansas City, and Orlando have shown that the wind shift prediction functions are very enthusiastically received by air traffic control personnel as a planning aid for minimizing the delay associated with runway shifts. As a consequence, an aggressive program is underway to improve the performance of the algorithm.

It also should be noted that the current TDWR algorithm was designed to detect very sharp wind changes that could lead to hazardous shear for aircraft. Performance scoring has not, in general, considered all the wind shifts that might be of concern for a WVAS. Consequently, there needs to be some focused research on developing and evaluating algorithms to explicitly accomplish the following:

1. Determine that the wind field is likely to be stationary over periods (e.g., > 10-15 minutes) which are consistent with the operational considerations discussed below, and

2. Identify periods in which the wind field cannot be estimated reliably or may change adversely at least 10 minutes in advance.

The "fusion" of TDWR and anemometer data required to produce the desired wind field predictions would be accomplished by the ITWS. ITWS (see Figure 4) has access to a variety of data from the FAA and NWS terminal sensors [7] as well as access to NWS high-resolution numerical weather prediction results. It is expected that the initial ITWS system will be deployed in 1996, with enhancements occurring through the year 2000.

---

[8] The TDWR estimates both the mean radial velocity ant the standard deviation of the radial velocity field in the radar resolution volume (typically about 120 m x 120 m x 120 m). Increased standard deviations (the "spectrum width") correspond to cases with a high degree of turbulence or velocity dispersion within the resolution volume. [9]

THE OPERATIONAL PROBLEM

Although the necessary sensors and weather information processing system are becoming available to support a WVAS, present-day terminal radar control equipment and procedures would limit the ability of controllers to use either static or dynamic information from such a WVAS effectively.

Operational Barriers to the Use of Variable Wake Vortex Separations

The resolution limitations of the current Automated Radar Terminal System (ARTS) displays, limited control precision in spacing aircraft on final, and the need to minimize controller workload have led to separation standards that place aircraft at easily remembered, easily visualized, and conservative integer-mile spacings based on a small number of weight classifications.

Control precision in spacing aircraft on final has been consistently shown to have a standard deviation of about 20 seconds from the desired inter-arrival spacing value. For jet aircraft, 20 seconds translates into about a one-mile standard deviation on minimum spacing. Thus, if a safe wake vortex separation is determined for a given condition, the controller must aim for at least one more mile of separation to avoid violating the desired spacing. Taken together, the effect of these constraints is that it would be very difficult for controllers to make use of tighter and more complex separation standards in today's manual control environment.

The Role of the TATCA Final Approach Spacing Tool

As separation standards are reduced, the safety margins associated with spacing imprecision (whether arising consciously or not) become increasingly significant limitations on throughput. Hence, increased spacing precision will be important in realizing the benefits of reduced wake vortex spacings. Computerized aides for final approach controllers, provided by the FAA's developmental Terminal Air Traffic Control Automation (TATCA) system will make it easier for controllers to achieve the precise separations suggested by wake vortex advisories. TATCA's Final Approach Spacing Tool (FAST) [10] is being designed to assist controllers in meeting any desired minimum separation standard with increased precision.

Studies [11, 12] have shown that final approach spacing aids can improve control precision by roughly a factor of two, to a standard deviation of 0.5 nm in minimum spacing between arrivals. If necessary, FAST could be extended to handle more numerous and complex WV aircraft categories. The exact recommended separation for each aircraft pair could be provided directly by giving the final vector controller easily visualized, time-based, turn-to-final advisories. Human memory and low-resolution radar images would no longer limit aircraft delivery precision.

TATCA/FAST Implementation

The TATCA program is placing priority upon delivering an early developmental FAST capability to the field. Prototyping in developmental laboratories is currently refining the automation logic and its associated human-system interfaces. A field installation for developmental purposes is planned for the DFW Terminal Radar Approach Control (TRACON) Facility in FY 1993.

Commercially available auxiliary workstations will be installed at DFW to perform the major software functions. A special hardware interface — the TATCA Interface Unit (or TIU) — will acquire data from existing communications and radar processors. At ARTS IIIA sites, the existing displays will be replaced with Full Digital ARTS Displays (FDADs). FAST advisories will be passed to the FDADs directly by the TIU. A limited national deployment of FAST is planned to begin in FY 1996.

Operational Barriers to the Automatic Execution of Wake Vortex Advisories

There is, however, another operational consideration posed by the dynamics of air traffic management. An automatic WVAS coupled to terminal ATC automation tools could conceivably be designed to initiate, plan, coordinate, and execute significant capacity fluctuations in terminal airspace without requiring conscious intervention on the part of the controller team. In this sense, the capacity changes initiated by the automatic wake vortex advisor would be fundamentally different from capacity changes caused today by runway configuration changes, visibility changes, and even emergencies and other unpredictable events. Currently, no such change can be introduced without the active planning and volition of the controller team. Even though an urgent need for such a change in capacity can come without warning, the controller team can delay or prolong the change in order to assure safety and satisfy other constraints on the air traffic management process.

There are two approaches to this problem. One is to require controller intervention or approval before a change of any significant magnitude is allowed to be executed by the automatic system. The other approach is to force the wake vortex advisor to continually look ahead and provide the traffic management system with reliable forecasts o. changes in wake vortex separations. Both approaches would allow the controllers time to evaluate the proposed change and intervene if the anticipated result were not to their liking. The latter approach would not only provide a foundation for an eventual full automation of the advisory system, but it would also satisfy other important operational requirements for efficient and safe air traffic management. Let us now examine these operational requirements.

Forecasting Reductions in Runway Capacity

As an aircraft approaches the final approach path, its controllability (the ability to delay or expedite it relative to its current planned arrival time) steadily decreases. It would be difficult for the final vector control position in the TRACON to react to a suddenly mandated increase in minimum separation once he has several aircraft established on final. If aircraft are landing

at a rate approaching the theoretical capacity of the runway and if the TRACON and final approach path are fully loaded with aircraft, an abrupt and unforeseen reduction in separation standards could easily result in a string of missed approaches. Thus, it seems essential to have the ability to forecast significant reductions in runway capacity.

Forecasting Increases in Runway Capacity

Sudden increases in runway capacity are welcomed by controllers and do not on first inspection seem to pose operational problems. However, a reliable forecast of a future increase in runway capacity would allow the TRACON traffic manager, the en route metering system, and other upstream components of the air traffic management system a little more time to "fill the pipelines" with arrivals or departures. This would let controllers take greater advantage of the newly available airspace and concrete, thereby reducing congestion and delay.

Illustration of TRACON Controllability

Vandevenne, et al. [1] treat the available controllability for aircraft approaching the Boston, Denver, and Atlanta airports. For direct approaches to certain runways (like the Providence approach to runway 4 at Boston), the principal means for expediting an arrival is to delay the mandatory speed reductions to make them occur as late as possible. This provides only about one minute of speed-up capability. On the other hand, it is possible to delay arrivals to most runways by over 6 minutes with the use of path stretching vectors.

Warning Time Needed to Accommodate a Reduction in Capacity

Consider an example of a sudden capacity reduction. Assume the traffic pipeline in the TRACON is full and all aircraft are landing with 2.5 mile separations at 90% of capacity, or a rate of 38 AC/hr. If the standards were now to suddenly revert to 3-, 4-, 5-, and 6-nm separations, it would be difficult to accommodate the aircraft already inside the TRACON without at least one missed approach. If aircraft numbers two and three in the landing stream are both set up for 2.5-nm spacing, number two will have to go around. If the first plane in the landing stream is a "heavy," at least two following aircraft will have to go around.

The problem of a sudden capacity reduction is not as severe at the edge of the TRACON. If the flight length of a typical TRACON approach path is 60 miles and the average groundspeed on the paths in the TRACON is 180 kt, each aircraft will spend 20 minutes traversing the TRACON before landing, and there will be at least 12 aircraft airborne in the TRACON at any time. If the landing rate suddenly drops to 29 AC/hr (which is 90% of 32 AC/hr), the next aircraft to enter the TRACON will not be allowed to land for about 25 minutes. That extra 5 minutes could be absorbed in the TRACON by early speed reductions and path stretching. However, that 5-minute delay might well be increased if one or more aircraft on final are required to execute missed approaches.

In order to avoid these difficulties, a certain minimum warning time for the increase in aircraft separation is essential. Fortunately, the required delay for each aircraft becomes smaller along with the decrease in the available controllability for that aircraft as it approaches the final approach zone. For the reduction in landing rate from 38 AC/hr to 29 AC/hr considered above, a calculation based on a simple but reasonable model of available delay in a typical TRACON airspace indicates that an advanced warning time of about 10 minutes for increased aircraft separation would permit the traffic to be smoothly rescheduled so that no aircraft pairs violate the new larger separations after those new separations go into effect. Although a more detailed analysis based on actual TRACON arrival paths should be performed to verify this result, the resulting warning time seems consistent with the predictive capabilities of the wake vortex advisory system proposed above.

Warning Time Needed to Accommodate an Increase in Capacity

Let us now address the question of how far in advance the advisory system should forecast an increase in capacity. Consider a case in which the initial landing rate is 29 AC/hr and the wake vortex monitor (without advanced warning) indicates that the landing rate can immediately increase to 38 AC/hr. At the time of the landing rate change, there are 10 aircraft in the TRACON. Rather than landing in 20 minutes as originally scheduled, the 10th aircraft would now have to land in 16 minutes to keep up with the new, increased landing rate. However, since it is impossible to expedite an aircraft by more than about one minute in the TRACON, pockets of excess spacing will appear in the landing sequence.

The discrepancy between adding delay versus increasing throughput is also large in en route airspace. When the terminal capacity increases, aircraft farther upstream need to catch up by more than those downstream in order to keep the pipeline full. If it is desired to take full advantage of the increased capacity when wake vortex separation reductions are anticipated, the forecast should be made as early as possible. Unless there is considerable excess traffic in the pipeline, at some point far upstream of the terminal, gaps are unavoidable. Gaps in the stream waste runway capacity. But, unlike the case of a capacity reduction, advanced warning is never essential to maintain safe separation when a capacity increase is anticipated.

In the special case in which there are holding stacks in en route airspace available to respond to the excess capacity in the TRACON, then it is possible to calculate exactly how much warning is needed to maintain an uninterrupted, efficient flow. The limiting case is easily understood. If the forecast is made a full 20 minutes in advance of the actual capacity increase, all of the planes currently in the TRACON can land at the old rate, and the next one to enter can be brought out of a holding stack just in time to smoothly transition to the new landing rate. If the TRACON is then continuously fed at the new rate, there will be no need for any expediting action inside the TRACON. Thus, the minimum forecast time that will maintain gap-free flow is clearly always less than the TRACON transit time when a supply of aircraft is available outside the TRACON. The actual minimum forecast time that achieves uninterrupted flow can be calculated by using the following reasoning.

Gaps can be avoided in the TRACON arrival stream if the forecast time is chosen far enough in advance so that after the forecast is delivered, the first aircraft to enter the TRACON - if fully

expedited - is just able to catch up with the preceding aircraft and land with the new reduced separation. For the example in which the capacity jumps from 29 to 38 AC/hr and there is one minute of expediting available in the TRACON, the minimum forecast time that achieves uninterrupted flow is calculated to be about 14 minutes. This warning time is also consistent with the capabilities of the proposed wake vortex advisory system.

The Role of the TATCA Traffic Management Advisor

It is unlikely that introducing a look-ahead capability into today's manual terminal air traffic management system would have immediate benefits because of the difficulty of assimilating such information into a manual planning operation. Fortunately, another TATCA automation tool is being developed specifically to address and mitigate the problem of planning in the terminal environment. It is the Traffic Management Advisor (TMA).

The TMA is the scheduling and planning component of the TATCA system. The TMA will use aircraft performance characteristics along with current flight plan data, surveillance data, wind information, runway configuration information, and airport acceptance rate goals to begin preliminary planning for arrivals before the top-of-descent point in en route airspace, typically 150 nm (roughly 30 minutes) from the airport.

The TRACON component of the TMA will replan the arrivals within the TRACON and will allow arrival schedules to be adjusted dynamically as late as 5 minutes before landing. The resulting range of TMA planning times is expected to allow runways to be reassigned, aircraft to be re-sequenced, and traffic to be delayed or expedited in a more coordinated and efficient manner than is possible today.

Another function that the TMA can easily perform is to make its own estimate of the current and near-future landing rate based on its current arrival schedule and the degree of conformance of the current arrivals with that schedule. It can continually and automatically pass that information upstream to the en route metering system to assist in providing a well-matched and steady flow of traffic into the terminal.

Thus, the TMA has all of the capabilities necessary to handle complex replanning and scheduling actions and to disseminate dynamically generated plans to the controller team. These are precisely the operational capabilities that are essential if the terminal air traffic control system is to smoothly and efficiently react to the forecasts that will flow from a well-designed wake vortex advisory system.

SUMMARY AND RECOMMENDATION

The combination of improved weather sensing and automation and planning assistance would enable the ATC system to achieve more organized and efficient runway utilization in two ways. Peak runway throughput could be increased by improved knowledge of current wake vortex behavior. Congestion, disorder, and delay could be reduced by an improved ability to predict and utilize variable wake vortex separations.

Safe and effective operational use of an automatic wake vortex advisory system relies on an ability to forecast short-term (10- to 15-minute) changes in wake vortex advection characteristics. A wide area wind field assessment using Doppler radar together with the dense anemometer arrays of the enhanced LLWAS system can likely provide the necessary predictions of changes in wake vortex advection characteristics with forecast times that are reasonably well matched to the traffic management needs of terminal radar control. Continuous analysis of forecast accuracy will allow a quantitative confidence level to be associated with each value of forecast time. If the current conditions only instill high confidence that detrimental wind shifts will not occur within less than, say 10 minutes, the advisory system can be designed to recommend current wake vortex spacings that assure the ability to gracefully recover in the future to safer spacings in less than 10 minutes.

Operational difficulties as well as meteorological uncertainties must be addressed to achieve significant increases in landing capacity. Without computer aides for controllers, the need for simple, invariant, and conservative rules for controllers to use in spacing aircraft on final could limit the benefits of wake vortex monitoring and prediction technology.

As separation standards are reduced, the safety margins associated with spacing imprecision become relatively more significant limitations on throughput. Hence, increased spacing precision will be important in realizing the benefits of reduced wake vortex spacings.

The key elements of the necessary controller assistance system are now being developed as part of the Traffic Management Advisor and Final Approach Spacing Tool of the TATCA program. These aides will make it possible to integrate the information derived from a wake vortex monitor directly into the final approach spacing information presented to controllers on current and planned displays.

Figure 5 summarizes the overall system recommended for increasing runway capacity in the absence of a collateral safety monitor. If a safety monitor such as suggested in [4] were to be implemented, the information it obtained on wake vortex transport would be provided to the WVAS to produce improved estimates of the expected vortex behavior.

A major advantage of the recommended system is that most of the sensors and information processing systems required are in the process of development to meet other needs. Hence, a relatively modest investment to extend the planned capability to meet the needs for a wake vortex advisory service could provide the significant improvements in capacity that were discussed in Section 1. The specific areas requiring focused R & D include the following:

1.   Refinement of the operational interface and procedures between a WVAS, terminal automation, en route traffic management and centralized traffic planning,

2.   Assessment of the cost/benefit at specific airports for a WVAS using only wind advection monitoring and prediction,

3.   Quantification of wind prediction performance in the WVAS context using the extensive existing data sets obtained by the TDWR program, and

4.   Assessment of the capability for wake vortex dissipation prediction using parameters other than the wind speed and direction.

ACKNOWLEDGEMENTS

Table 1. Weather Causes of Serious Delays at Major US Airports*

AIRPORT	DAILY OPS.	CLIMATOLOGY (Days per Year)			DELAYS > 5 MIN. Annual Delay Min X 1000			
		T-Storm	Hvy Fog	Lo Vis.	Th	Hvy Fog	Lo Vis.	Wx
Chicago	2175	38	16	109	412	94	185	87%
Atlanta	2156	50	30	136	538	174	229	90%
Los Angeles	1589	3	44	121	24	188	150	83%
Dallas	1578	45	11	86	354	47	106	87%
Denver	1438	41	10	57	294	39	64	85%
San Fran.	1255	2	17	101	13	57	99	74%
St. Louis	1178	45	11	156	265	35	143	89%
Boston	1162	19	23	125	110	72	113	84%
Phoenix	1142	23	2	5	131	6	4	72%
Detroit	1137	33	22	121	187	67	107	87%

*The delay estimates are based on climatology of the various airports and the results of detailed studies of delay at O'Hare airport. [14] This study suggests that at these airports, adverse weather accounts for 90% of the serious delays (i.e., delays > 15 min.).

**Table 2. Principal Causes of Rapid Surface Wind Changes in the Approach
Zone and Predictive Clues that would be Utilized
by an Integrated Terminal Weather System**

Meteorological Phenomena	Frequency	Predictive Clues
Microburst Outflows	Common on thunderstorm days. Can occur in semi-arid environments (e.g., high plains east of Rocky Mts.) without thunder.	Convective cells developing and/or moving toward approach zone. Precursors aloft in storm. [5] Movement of a microburst outflow toward approach zone.
Gust fronts	Common on thunderstorm days.	Sharp propagating changes in Doppler velocity fields. Propagating lines of enhanced reflectivity.
Frontal bands	Common in snow storms and frontal rain storms.	Propagating surface radial velocity changes in bands. Propagating bands of precipitation.
Thermal instabilities	Common in summer.	Spatial variations in surface velocity field. Enhanced Doppler spectrum widths. Temperature lapse rate in lowest 1000 ft.

Table 3. Baseline TDWR Gust Front/Wind Shift Planning Product Performance

	Ff	10 Min. Forecast		20 Min. Forecast		Wind Shift Estimate	
		Pcf	Pff	Pcf	Pff	Ve(M/s)	Ae(°)
Denver 1988	.45	.97	.11	.83	.18	3	30
Kansas City	.50	.97	.18	.94	.21	3	30
Orlando	.56	.95	.13	.75	.30	2	15

Ff: fraction forecasted; Pcf: probability of correct forecast; Pff: probability of false forecast;
Ve: mean absolute velocity error (m/s); Ae: mean absolute direction error (deg)
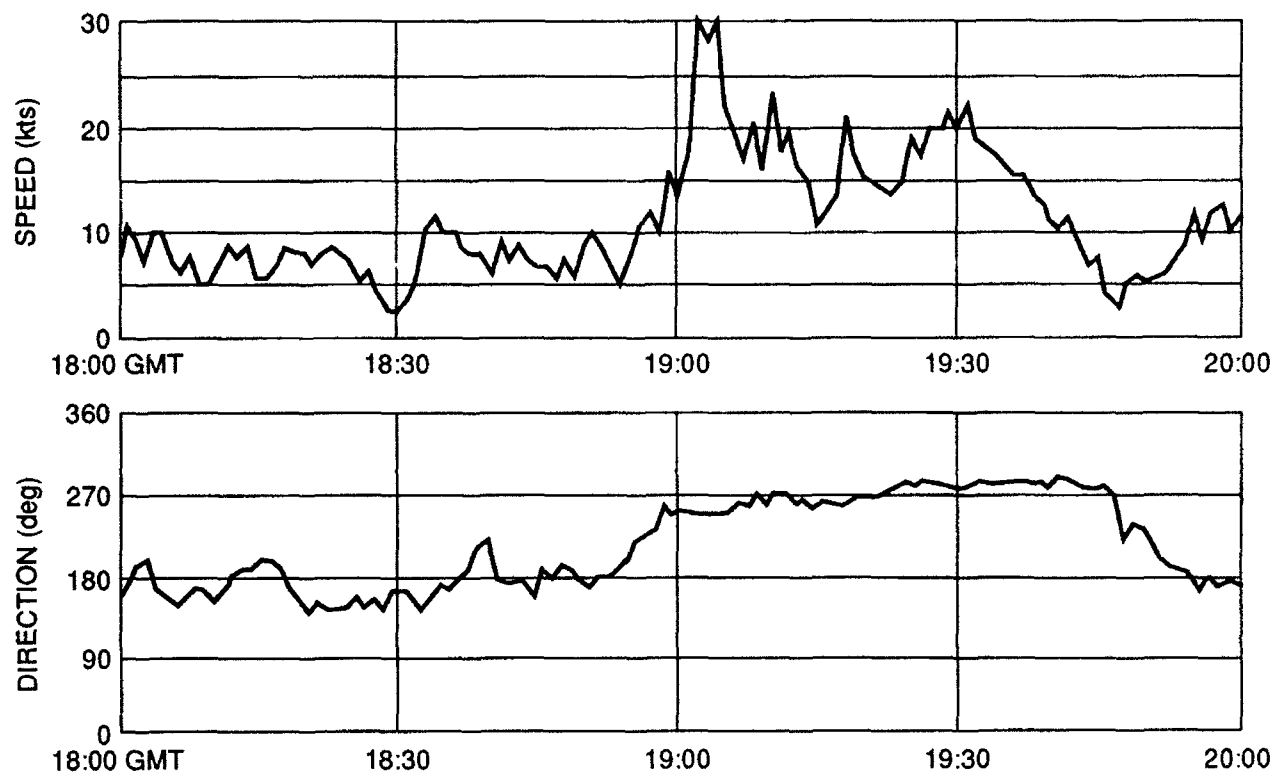
Figure 1. LLWAS sensor winds observed on sensor 4 at Orlando International
Airport on 13 July 1991.

RADIAL VELOCITY

REFLECTIVITY

Figure 2. TDWR prototype radar reflectivity and radial velocity fields near Orlando International Airport at 18:15 GMT on 13 July 1991. The range rings are in km. The airport runways are the three vertical lines approximately 10 km (5 nmi) north of the radar. The LLWAS anemometer indicated by the number 4 to the south of the runways. The radial winds indicate a constant wind from the south at approximately 8-12 knots with a patch of velocities closer to 4 knots to the south of the anemometer.

REFLECTIVITY

RADIAL VELOCITY

Figure 3. TDWR prototype radar reflectivity and radial velocity fields near Orlando International Airport at 18:45 GMT on 13 July 1991. A line of thunderstorms is approximately 6 km (3 nmi) to the west of the anemometer with a microburst approximately 7 km directly west of the radar. A gust front generated by outflows from the thunderstorm is forming approximately 4 km to the west of the anemometer.
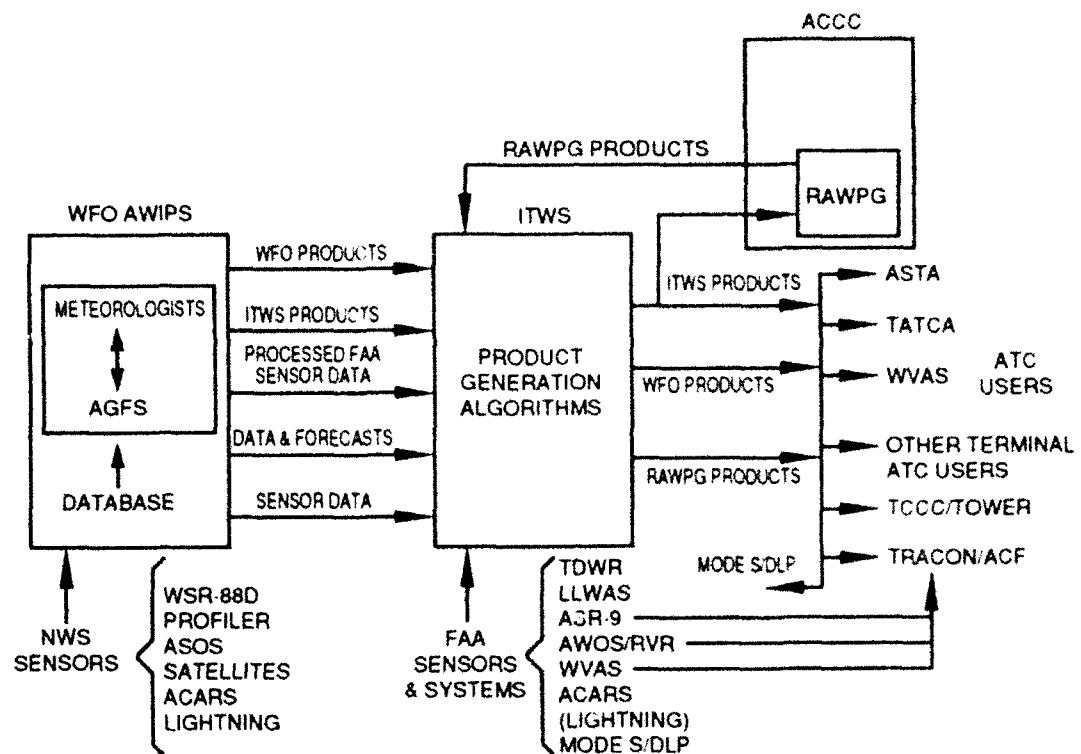
Figure 4. Integrated Terminal Weather System (ITWS) information sources and recipients. There is a high degree of connectivity to the National Weather Service Weather Forecast Office (WFO) Aviation Gridded Forecast System (AGFS) and to the NWS sensors in the terminal weather. Additionally, aviation weather products generated by the meteorologists at he enroute Area Control Computer Complex (ACCC) are provided by the Regional Aviation Weather Products Generator (AWPG).
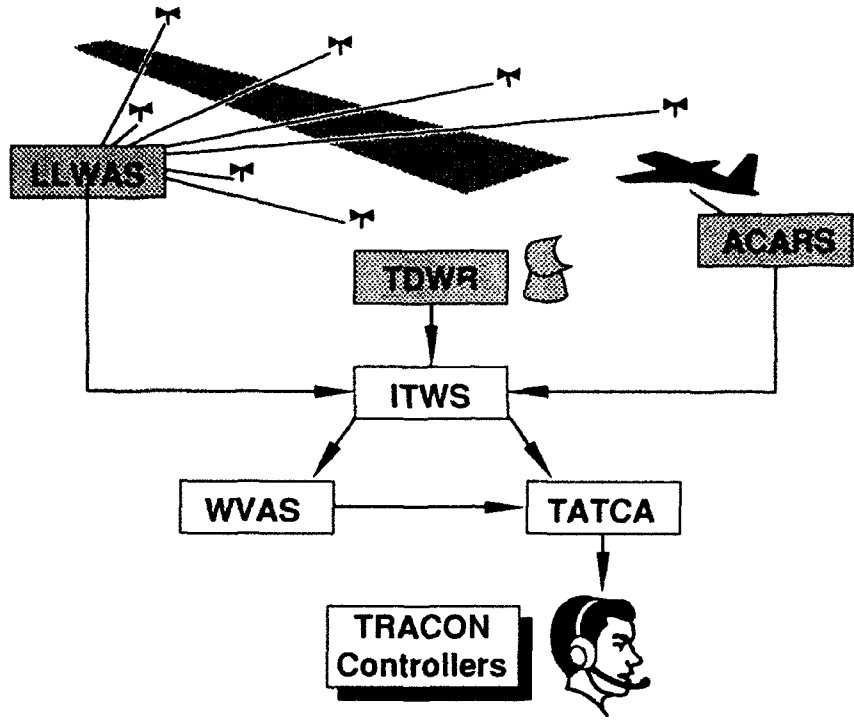
Figure 5. Block diagram of major components of the recommended system for weather adaptive aircraft aircraft wake vortex spacings.

REFERENCES

1.   Credeur, L., "Basic Analysis of Terminal Operation Benefits Resulting from Reduced Vortex Separation Minima," NASA Technical Memorandum 78624, NASA Langley Research Center, Hampton, VA 23665, October 1977.

2.   Hallock, J. N. and W. R. Eberle, editors, "Aircraft Wake Vortices: A State-of-the-Art Review of the United States R&D Program," FAA-RD-77-23, DOT Transportation Systems Center, Cambridge, MA, February 1977.

3.   St. John, O. B., "Collection of Operational Data on Wake Vortex Incidents in the U.K.," FAA-RD-77-68, Proc. of the Aircraft Wake Vortices Conference, Transportation Systems Center, Cambridge, MA, March 1977.

4.   Evans, J. and D. Turnbull, "Development of an Automated Windshear Detection System Using Doppler Weather Radar," IEEE Proceedings, vol. 77, no. 11, pp. 1661-1673, November 1989.

5.   Spitzer, E. A., J. N. Hallock, and W. D. Wood, "Status of the Vortex Advisory System," FAA-RD-77-68, Proc. of the Aircraft Wake Vortices Conference, Transportation Systems Center, Cambridge, MA, March 1977.

6.   Taylor, D. L., R. D. Londot and G. T. Ligler, "The Meteorological Data Collection and Reporting System: Status and Future Directions," 4th Intl. Conf. on Aviation Weather Systems, Paris, France, Am. Meteor. Soc., Boston, MA, June 1991.

7.   J. Evans, "The Integrated Terminal Weather System," 4th Intl. Conf. on Aviation Weather Systems, Paris, France, Am. Meteor. Soc., Boston, MA, June 1991.

8.   Weber, M., M. Wolfson, D. Clark, S. Troxel, A. Madiwale and J. Andrews, "Weather Information Requirements for Terminal Air Traffic Automation," 4th Intl. Conf. on Aviation Weather Systems, Paris, France, Am. Meteor. Soc., Boston, MA, June 1991.

9.   Doviak, R., and D. Zrnic', *Doppler Radar and Weather Observations*, Academic Press, Orlando, FL, 1984.

10. Erzberger, H. and Nedell, W., "Design of Automated System for Management of Arrival Traffic," NASA Technical Memorandum 102201, NASA Ames Research Center, June 1989.

11. Credeur, L. and W. R. Capron, "Simulation Evaluation of TIMER, a Time-Based Terminal Air Traffic Control, Flow Management Concept," NASA Technical Paper 2870, Langley Research Center, February 1989.

12. LeBron, J. E., "Estimates of Potential Increases in Airport Capacity Through ATC System Improvements in the Airport and Terminal Areas," FAA-DL5-87-1, October 1987.

13. Vandevenne, H. F. et al., "Planning Horizon Requirements for Automated Terminal Scheduling," 35th Air Traffic Control Association Fall Conference Proceedings, p. 440, September 1990.

RE-CLASSIFICATION OF WAKE VORTEX WAKE GROUPS; A CONTROLLER'S VIEW.

Stephen R. Sherratt
Directorate of ATC Requirements
National Air Traffic Services
London, U.K.

INTRODUCTION

There are two main sections to this paper, a consideration of the human factors of implementing an enlarged classification system and a brief look at how enhanced vortex advisory systems and aircraft weight data may be integrated into ATC systems. One of the prime aims of the FAA vortex wake programme is the development of revised classifications, followed by the issuing of recommendations for new standards. Hopefully this will improve safety levels and increase capacity at crowded airports and we in the United Kingdom share these goals.

As an air traffic controller however, I make a plea for *usability*. When the groups have been redefined we are the people who have to execute the separations with real airplanes.

It seems likely that more than the present three ICAO groups will be defined in order to improve/maintain safety margins and minimise impacts on airport capacity. The past procedure for implementing the classification seems to have been a case of working out the inter and intra group separations first and worrying about how the controller should implement them later. I suggest that in any future classification scheme the usability of the system could (and should) be tackled first. This is because if controllers find the system difficult to remember or execute then safety could be compromised, or any theoretical capacity gains negated.

BACKGROUND

Historically ICAO and the USA have classified aircraft into 3 groups, by Maximum Take-Off Weight. In contrast, in Britain we use 4 groups with lengthened separation distances for some group pairings. Table 1 shows how the US and UK groups compare in weight terms, (Table 2 shows the UK separation values).

From UK experience with four groups the difficulty of implementing more variables, (for the controller), lies in remembering the table of separations and applying them reliably in a stressful environment.

When traffic is light Vortex Wake separations are not a factor, but when the airport becomes busy wake turbulence separations become an extra mental burden for controllers. (At the same time the spacings become the primary constraint on runway capacity.)

In addition to communicating with pilots and other control sectors the busy controller is attempting to separate and sequence aircraft and simultaneously cope with the changes, problems and queries that continually arise in an operational environment. This illustrates the continual need to make judgements and decisions in a very dynamic work situation. Add to this the need to recall and implement a variety of Wake Turbulence spacings and it can be seen that a large demand on judgement and memory is made at a time when the controller's mind is already fully exercised.

I believe there is a way to rearrange the groups so that capacity constraints and mental demand are minimised.

ANALYSIS

If we examine the UK 4 group classification (Table 2) we can see the factors which make it difficult to remember. There are 5 separation values 3, 4, 5, 6, and 8 nautical miles, and 16 possible leader/follower combinations.

If we derive "rules" to express the matrix of Table 2, e.g. "Heavy followed by Medium is 5 miles", there are 8 rules if all the separations greater than 3 nm are expressed individually and we state "otherwise 3 miles" as one "rule".

You will notice that the matrix is not random but there is no regular pattern in it.

RE-CLASSIFICATION

It seems likely that more than three groups will be defined in order to improve safety margins and minimise impacts on airport capacity. For instance the big twins might usefully form a group of their own. Boeing 767s and A300s are *probably* being over-separated against lighter following types and the B757 is *probably* under-separated against following B737s and DC9s. Consequently one can speculate that at the heavy end of the weight spectrum the revised groups *may* look something like Table 3.

PROPOSAL

If the number of groups does increase then we controllers need something simple to memorise and apply. In contrast to Table 2, Table 4 is regular, and a pattern is easily discernible.

These new groups are arranged methodically, so that separation within every group is 3 miles (or some other value n) and when following one group heavier the separation rises by a standard increment, say 1 mile (or some other value x) then we need only remember two "rules":

1.   When following aircraft from same (or lighter) group separation is n miles;

2.   When following an aircraft from a heavier group, add x miles for each incremental difference in weight group.

The groups are numbered in ascending order, rather than designated HEAVY etc., so that the subtraction of a follower group number from the leader group number gives the value by which to multiply x. (Negative numbers can be ignored, since they indicate that a lighter type is ahead and minimum separation applies.)

This format can be extended to a larger (or smaller) range of groups and I suggest the values of n and x can be arranged to meet safety objectives and maximise capacity.

Half a mile as the increment between groups might be a reasonable proposition. A note of caution however, controllers are only human, so separations achieved in the manual environment are rarely perfect. A tolerance of $\pm$ half a mile is the best we can expect, when defining manual separations allowance should be made for this.

REFERENCE DATUM

One of the work packages in the FAA programme is Wake Vortex characterisation, using the results from this work I suggest it may be possible to assign each Aircraft type a "wake turbulence index" reflecting the Wake Vortex characteristics of each type. Pilots could then factor this value by calculated landing weight. The resulting figure would then indicate the group to which that flight should be allocated to when flying the approach, and this would then be communicated to ATC before the approach began.

The proposed grouping scheme facilitates this idea, which could have capacity benefits. The practicality of this suggestion needs to be investigated to avoid any undesireable effects on operations.

SUMMARY

This proposal builds an adaptable framework of groups, into which the scientific community can allocate aircraft by any appropriate measure, be it weight and/or some other parameter.

It is designed with the accent on usability. (One example of a foreseen difficulty in the process of allocating aircraft to the proposed groups is the intra-group separation for the heaviest aircraft—will it be safe to sequence 2 B747s just 2.5 or 3 nautical miles apart?)

AUTOMATION

Reference weight

Another of the work packages in the FAA Wake Vortex Programme is "enhancement of Vortex advisory systems" and integration into the ATC system. The regrouping methodology outlined above may form a starting point to develop algorithms to cope with more groups.

Ideally, the separation between 2 specific aircraft would usefully relate directly to the actual weight difference between them. Maybe the weight reference datum we are using at present is inappropriate for the approach phase of flight? Currently the weight groups are related to MTOW (Maximum Take-Off Weight) which does not reflect the reality of an aircraft at the end of a 10-hour flight, having burned off many tons of fuel, making an approach at much reduced weight. If actual weight can be communicated by Mode 'S' or GPS data link, then at some point in the future, this data can be fed to an automatic system.

Vortex Advisory System (VAS) and ATC

The original Chicago VAS trial related separations to atmospheric conditions, in particular the wind vector. A mechanism has yet to be found to enable ATC to change the separation in a stepless manner as the weather changes. A sudden change of state from short to long separations is virtually imposible for the controller to deal with effectively.

In the UK we are developing a system called PACTAS which is rather similar in principle to the TIMER work at NASA Langley. It changes the controller's separation measure from distance to time. The system gives the controller advice in the form of seconds early or seconds late on a national timetable to achieve maximum runway utilization. The controller adjusts the timing error toward zero by speed control or vectoring in the normal way. Using this device the distance between aircraft becomes less relevant to the controller, since he is aiming to reduce the time displacement to as close to zero as possible, thereby achieving the variable separation.

It should be possible to input dynamic VAS data to the PACTAS processor, and thereby adjust the separations by a few seconds to account for atmosphereic conditions. The changes due to atmospheric variance can then be adjusted continuously rather than in the incremental way that I believe was judged undesirable in the Chicago VAS trials.

In the same way dynamic aircraft weight data can be input to the system so that Wake Turbulence separation is optimal in relation to both weight difference and Atmospheric conditions. In simulation trials errors as small as $\pm$ 5 seconds have been achieved. This represents $\pm$ 0.2 nautical miles at 150 Knots groundspeed, so there could be scope for defining separartions more finely in an automatic ATC environment.

CONCLUSION

This has been an exposition of ideas and principles that may merit further investigation and I hope to have stimulated further thinking on the subject. Certainly there needs to be some work on the manner in which any reclassification is implemented, in order to meet the safety and capacity objectives and at the same time meet the human factor needs.

Table 1. Comparison of US and UK Weight Groups

	USA/ICAO	UK	
	HEAVY	HEAVY	
136,000 Kg	- -		
		MEDIUM	
		- - - - - - - - - - - - - - - -	40,000 Kg
	LARGE		
		SMALL	
		- - - - - - - - - - - - - - - -	17,000 Kg
7,000Kg	- -		
	SMALL	LIGHT	

Table 2. Separations Used in UK Four Group Scheme

FOLLOWER	LEADER	HEAVY	MEDIUM	SMALL	LIGHT
	HEAVY	4	3	3	3
	MEDIUM	5	3	3	3
	SMALL	6	4	3	3
	LIGHT	8	6	4	3

Table 3. Illustrative Example of Regrouping--Speculative Only

Present Boundary	Type	Weight (Kg)	Speculative Boundary
	747	395,000	
	MD11	270,000	
	A340	246,000	
	TriStar	220,000	
HEAVY	A330..........206,000.............L Kg?		
	A300	171,700	
	767	181.400	
136.000 Kg	A310	157.000	
	757ER	113,400	
	757.............108,800...........M Kg?		
	B727	95,000	
	MD80	72,600	
LARGE (USA)	A320	72,000	
MEDIUM (UK)	737	68,000	
	DC9	54,400	
	Etc.		

Table 4. Proposed Regrouping Pattern

LEADER	#Group	#5 heaviest	#4	#3	#2	#1 lightest
FOLLOWER						
heaviest	#5	3	3	3	3	3
	#4	4	3	3	3	3
	#3	5	4	3	3	3
	#2	6	5	4	3	3
lightest	#1	7	6	5	4	3

OPERATIONAL AND CAPACITY INVESTIGATIONS FOR THE ALLEVIATION OF WAKE VORTEX SEPARATION PROBLEMS AT THE AIRPORT OF FRANKFORT

Johannes Reichmuth
Deutsche Forschungsanstalt für Luft- und Raumfahrt e.V.
Institut für Flugführung
W-3300 Braunschweig
Fed.Rep. of Germany

ABBREVIATIONS

A/C	aircraft
AKF	Arbeitskreis Frankfurt
AKW	Arbeitskreis Wirbelschleppen
ATMOS	Air Traffic Management and Operations Simulator
ADSIM	Airfield Delay Simulation Model
BFS	Bundesanstalt fur Flugsicherung
COMPAS	Computer Orientated Metering Planning and Advisory System
DLH	Deutsche Lufthansa AG
DLR	Deutsche Forschungsanstalt für Luft- und Raumfahrt e.V.
DWD	Deutscher Wetterdienst
FAG	Frankfurter Flughafen Aktiengesellschaft
HVY	heavy
IMK	Institut für Meteorologie und Klimatologie der Universitat Hannover
NM	nautical mile
SGL	single runway approach
SIMOD	Simulation Model
STG	staggered
SWAT	Subjective Workload Assessment Technique
TMA	Terminal Area

INTRODUCTION

Since 1989 a working group named "Capacity for Frankfurt Airport," AKF, exists with the goal to identify means by which an increase of capacity at Frankfurt airport would be possible. This working group consists of members of BFS, DLH, FAG, DWD, IMK and DLR. This group worked out a list of so called candidates, each of them containing provisions which could lead to more capacity. One candidate was a wake vortex warning system for the two parallel runways at Frankfurt, separated only 517 m (Figure 1). Since March 1991 the work done in this area is coordinated by a special working group, AKW, chaired by the DWD with members from the same institutions as the AKF. Up to now work related to a wake vortex warning system was done in three main areas.

Field Measurements were performed by IMK and DLR at Frankfurt airport in order to obtain the necessary knowledge about vortex propagation and structure in the boundary layer (these measurements are described in the Field Measurement section of this symposium). The feasibility of a prognostic system which predicts the behaviour of the wake vortices under different meteorological conditions was investigated. The outcome of these measurements is that a prediction about wake vortex free regions can be made up to 20 min. and that a situation where the two parallel runways at Frankfurt could be operated independent of wake vortices would be present 60% of time.

Fast Time Simulations with the programs SIMOD and ADSIM were used to model the airspace structure of Frankfurt (Figure 2) and the behaviour of aerodrome traffic from arrival to departure. At DLR these programs were adapted to a Frankfurt scenario and are now able not only to simulate the present situation but also the effects on capacity and delays due to changes induced by a wake vortex warning system operationally. These fast time simulations predict an increase of arrivals of 1 to 5 aircraft per hour. The variation in the capacity depends not only on boundary conditions like additional departures, ground movement restrictions, etc., but also on weather conditions. Because Frankfurt airport is near its capacity limits during inbound rushes, a big effect on delay reduction is predicted by the Fast Time Simulations if a wake-vortex-independent minimal separation of 3 NM could be reached.

Real Time Simulation performed at the Air Traffic Management and Operations Simulator ATMOS at DLR Braunschweig allowed a closer look on three different operational concepts under well defined conditions. Controllers and pilots were involved in the concept development phase early. This helps to find displays and operations acceptable for a realistic environment. The present paper concentrates on the real time simulations performed in June and July this year. The implementation in the ATMOS environment will be described together with the three different operational concepts under simulation. Then the measurements and results will be presented. Lastly, possible conclusions will be discussed.

REAL TIME SIMULATION ENVIRONMENT

Architecture

ATMOS is a Real Time ATC Simulator which represents two controller working positions as shown in Figure 3. The layout is oriented on the situation at Frankfurt [1]. In the present simulation the working positions were used for a pick-up controller on the left and a feeder controller on the right hand side. Both working positions are equipped with radar screens, with flightstrip holders and trackball. The voice communication with up to six pseudopilots is performed via microphone and earphone. Each pseudopilot can control up to 6 simulated aircraft simultaneously by using a dedicated keyboard and terminal display. At the right side of each radar screen the display and input device of the Computer Oriented Metering and Advisory System (COMPAS) [2] is located. The callsigns of approaching aircraft are depicted for the advised arrival times on gate. Above the COMPAS screen another screen is used to show the additional information needed for the different operational concepts concerning wake vortices and wind. The hardware configuration is shown in Figure 4. Three main components are connected via a LAN: The basic ATC Simulator, the COMPAS planning system with the same hardware and software components as in Frankfurt and a display development and generation unit based on a silicon graphics graphic-workstation. The COMPAS system had to be included because the traffic flow behaviour at Frankfurt has changed since its introduction there [3] and is actively used by the approach controllers to handle the incoming flow from the adjacent sectors.

Traffic Scenario

The inbound flow was simulated by using a real traffic sample for an inbound rush at Frankfurt as an orientation. Gaps in the inbound flow were filled up in order to reach saturation. The spatial distribution of traffic was 32% from the north, 50% from the south and 18% from the west (Figure 2, shaded directions). The mixture of weight classes was set to 27% heavy, 63% medium and 10% light A/C. The portion of light A/C has been increased compared to reality at Frankfurt in order to generate enough combinations where the operational rules for a reduction of separation could apply. Two traffic examples were generated under these conditions. By changing the callsigns the same example could be presented to the controller several times, which allows a comparison of the different concepts with the same pair of controllers under the same boundary conditions. The traffic reaches the maximum after 12 min. and holds this flow over 90 min.

Wind Scenario

For two operational concepts the behaviour of the 1 min. average wind is the basic parameter for the wake vortex warning system. Therefore, two different wind scenarios were generated. One, called "variable wind", changed the crosswind component continuously from high to low and back to high values in order to see the effect of changes between different operational rules according to the wind. The other, called "stable wind", simulates only small variations around low crosswind components. This refers to a situation where the two runways of Frankfurt can

be regarded as wake vortex independent. In reality this is the case 60% of time. With this scenario the different concepts could be measured with respect to their maximal possible gain on capacity.

Simulation Runs

Figure 5 shows the simulation runs performed. The three concepts were compared with a reference simulation which was based on the operational procedures using the weight class dependent separation matrix (Figure 6). Concepts which depend on the wind situation were simulated with "stable wind" and "variable wind "scenarios. Each of the 6 simulation runs were performed repeatedly with 6 pairs of Frankfurt controllers. The sequence of simulation runs and also the pick-up and feeder positions were varied in order to make the measurements independent of sequence effects.

OPERATIONAL CONCEPTS

Three different concepts were developed together with controllers from BFS and pilots from DLH. The results of the field measurements performed by Tetzlaff [4] and Koepp [5] were taken into account here.

"Wind Prognosis" Concept

For the "wind prognosis" concept it is assumed that a prognosis system exists which can give information to the controller if there is a migration of wake vortices to the neighbouring runway or not. In addition it also gives information on how long such a situation will be present. If there is no risk of vortex migration between the runways, the display (Figure 7) shows green arrows not reaching the runway symbols. The number in between indicates the minimal time in minutes this situation is guaranteed to be stable. This number can decrease only in steps of 1 minute.

If the uncoupled situation is present the controller is allowed to stagger the A/C on the glidepaths independent of weight classes with 3 NM minimum separation in sequence. If the crosswind becomes stronger so that the vortices could reach the other runway the display changes to red arrows (Figure 8) which reach the runway symbols. The prognosis time now gives the guarantee that after a time indicated in minutes the "green" situation will return and remain stable for at least 6 minutes. This enables the controller to inform the COMPAS system in advance, which plans the arrivals after this time on the basis of constant 3 NM separation. If no prognosis time can be given, the display shows red arrows without prognosis time. In case of risk of wake vortex coupling the controller has to apply the weight class dependent separation rules (Figure 6).

"Actual Wind" Concept

The "actual wind" concept extends the possibility to apply weight-independent separations for all crosswind values. This is achieved by choosing the adequate strategy of runway utilization as a function of the actual wind. The display given to the controller shows therefore the 1 minute average value of the wind as an arrow in a coordinate system with the crosswind component on the vertical axis and the downwind component on its horizontal axis (Figure 9). The advised runway utilization strategies are depicted as underlying regions. If the wind vector points to a region the whole region is coloured. Every strategy has its own colour. The history of the last ten minutes for the wind is indicated by connected circles. The idea was to give the controller support to estimate trends in the development of wind over time. A blue region (Figure 9) stands for low crosswind components. The runways are uncoupled and the advice is therefore to use staggered mode, also indicated with STG for "staggered".

If the crosswind component is strong enough to guarantee that the vortices are blown away from the runway used by the preflying heavier aircraft within the time corresponding to 3 NM separation, it is allowed to land all aircraft on a single runway in a sequence with 3 NM separation. This can be applied for the left or the right runway. Therefore the whole region of strong wind is coloured green and the abbreviation character SGL for single appear on both side of Figure 10.

If a 3 NM minimal separation would be applied overall, these two strategies would span the whole crosswind space and they would even have an overlapping region. But if one takes into account all possible separations between 3 NM and 6 NM with their possible hazards for light aircraft, then the situation becomes a little bit more complicated. For medium crosswind values a vortex generated at a glidepath has no time to leave the runway within a time corresponding 3 NM separation. Within a time interval corresponding to 6 NM separation it would be possible under the same wind conditions that a vortex travels to the neighbours runway. For those crosswind values depicted as red regions in Figure 11 a more restrictive but also more general procedure has to be applied. The rule is here to stagger in such a way that a heavier preflying A/C utilizes the downwind runway. This is indicated on the display in addition to the colour with HVY (for "heavy"). The procedure can also be applied in the case of strong crosswind conditions (Figure 10) and therefore the HVY abbreviation on the downwind side is also shown there. In order to avoid the frequent changes between the procedures, if the wind is stabilized near the border of a procedure region, the HVY region is blown up if it is reached by the wind arrow and is shrinked again if the wind value leaves this extended region ("hysteresis").

"Displaced Threshold" Concept

The "displaced threshold" concept is a solution which does not need wind information. The glidepath of the following (lighter) aircraft is displaced in so far that the hazard region of the preflying heavier aircraft is avoided. If one take into account a 3 degree glidepath at Frankfurt and a vertical height of the hazard region of 50 m (above 50 m it is assumed that the vortices always sink within a time corresponding to 3 NM separation), a displacement of 1000 m is needed. The length of the touchdown region of 1000 m again has to be added, which gives a

displacement of 2000 m. This would shorten the 4000 m runway of Frankfurt to half. If the longitudinal displacement of the two runways itself of 225 m is utilized, one ends with an usable runway length of 2225 m for the left runway (Figure 12). This is enough for medium and light aircraft but not for all heavy aircraft. The operational rule is therefore to land the heavier preflying aircraft on the right and the following lighter aircraft on the left runway. Heavy aircraft will have to use the right runway always. This has the disadvantage that one has to apply wake vortex separation if there are two or more heavy aircraft immediately in sequence.

COLLECTED DATA

Traffic data, operational data and interrogated data were collected for every simulation run. For all A/C the times over metering fix and gate together with the time over threshold were stored. The spatial behaviour could be analysed by inspecting the plots of tracks. Also the runway chosen was extracted. The voice communication was stored on magnetic tape so that the contents could be analysed. The voice communication load was obtained by measurement of the push-button actuations of the controller microphones. All inputs in the COMPAS System were also measured.

During each run the subjective workload of the controllers was measured by means of the SWAT method [6]. Every 4 minutes the controllers were asked to give their estimates on workload in terms of time load, mental effort load and psychological stress load. The interrogation times were shifted between pick-up and feeder so that every 2 minutes an estimate was taken.

After each run a questionnaire was applied to collect the comments on the different operational concepts. A catalogue of 28 statements had been developed for the questionnaire: 4 statements about the simulation in general, 6 statements about operational rules and displays, 13 statements about operational utilization and 5 about the acceptance of the concepts in general.

RESULTS

Figure 13 shows the results reached for the different runs in terms of capacity. All three concepts show an increase of capacity of about 2.5 A/C per hour compared to the reference runs if the "variable wind" scenario was used. The runs performed with the "stable wind" scenario show a further increase to about 4 up to 5 A/C per hour. This shows that under optimal conditions the expected capacity gain could be realized. The differences between the concepts are not significant. The standard deviations for different controller teams in the order of 1.5 A/C per hour are shown in brackets. This result has been obtained respecting the minimum separation of 3 NM. Only for the reference simulation runs a value of 2.76 was found as shown in the lower part of Figure 13. This can be explained by a "routine" behaviour of the controllers who sometimes used a separation of 2.5 NM between medium type A/C, which is practised in reality.

The voice communication effort shows no significant difference between concepts and reference. Between 20% to 24% of total simulation time were needed by the controller to transmit their commands.

The COMPAS inputs affecting the traffic flow were in agreement with the "wind prognosis" concept requirements. Other inputs used were negligibly rare.

The workload, as measured by means of the SWAT method, also showed no significant differences between the reference and concept runs. 90-100% of assessments ranged below 50 on the 0-100 SWAT scale. This mean that the estimated workload was generally low in all simulation runs.

The questionnaire results show that for the controller the wind information itself was easily detectable. The monitoring of changes however requires more effort. The use of an additional display was disapproved. The operational rules for the "wind prognosis" concept and "displaced threshold" concept were estimated as clear and understandable. The rules for the "actual wind" concept were estimated as more complicated. While an early allocation of runway was mentioned as easy for the "wind prognosis" concept, for the "actual wind" concept this was only the case for "staggered" mode. No unique statement could be given for this concept in the case of "single" mode. For the "HVY" mode even an increase of workload was mentioned. An increase of workload was also quoted for the runway allocation using the "displaced threshold" concept. It is possible that these difficulties in runway allocation have their origin in the application of a runway utilization strategy which requires for the first time an allocation of a runway as a function of fixed rules.

For the "wind prognosis" concept the solution used a modified COMPAS display which shows on the same scale A/C planned with constant 3 NM and A/C planned with wake vortex separations was found to be not optimal.

For the "actual wind" concept the change to more restrictive modes ("HVY" mode) was difficult to predict. A solution of this problem was seen in a prognosis component. The "displaced threshold" concept was estimated to be too restrictive and too inflexible. Therefore a potential of a more efficient runway use at Frankfurt was denied.

The vote for the maximal estimated potential for efficient runway use was given to the "actual wind" concept.

CONCLUSIONS

Keeping in mind the idealized condition of the realtime simulations performed, a capacity increase seems possible with no detrimental effects on minimum separations and controller workload.

The "displaced threshold" concept is disapproved.

Therefore, the future concept refinements have to be based on a combination of the two concepts "wind prognosis" (i.e., reliable forecasts) and "actual wind" (i.e., optimal runway utilization strategy).

THANKS

The simulations described would have been impossible without the teamwork of many people; some of them are listed in Figure 14.

Especially I would like to thank also the controller teams of Frankfurt which gave us their experience and opinions in a highly motivated and competent way during this time.
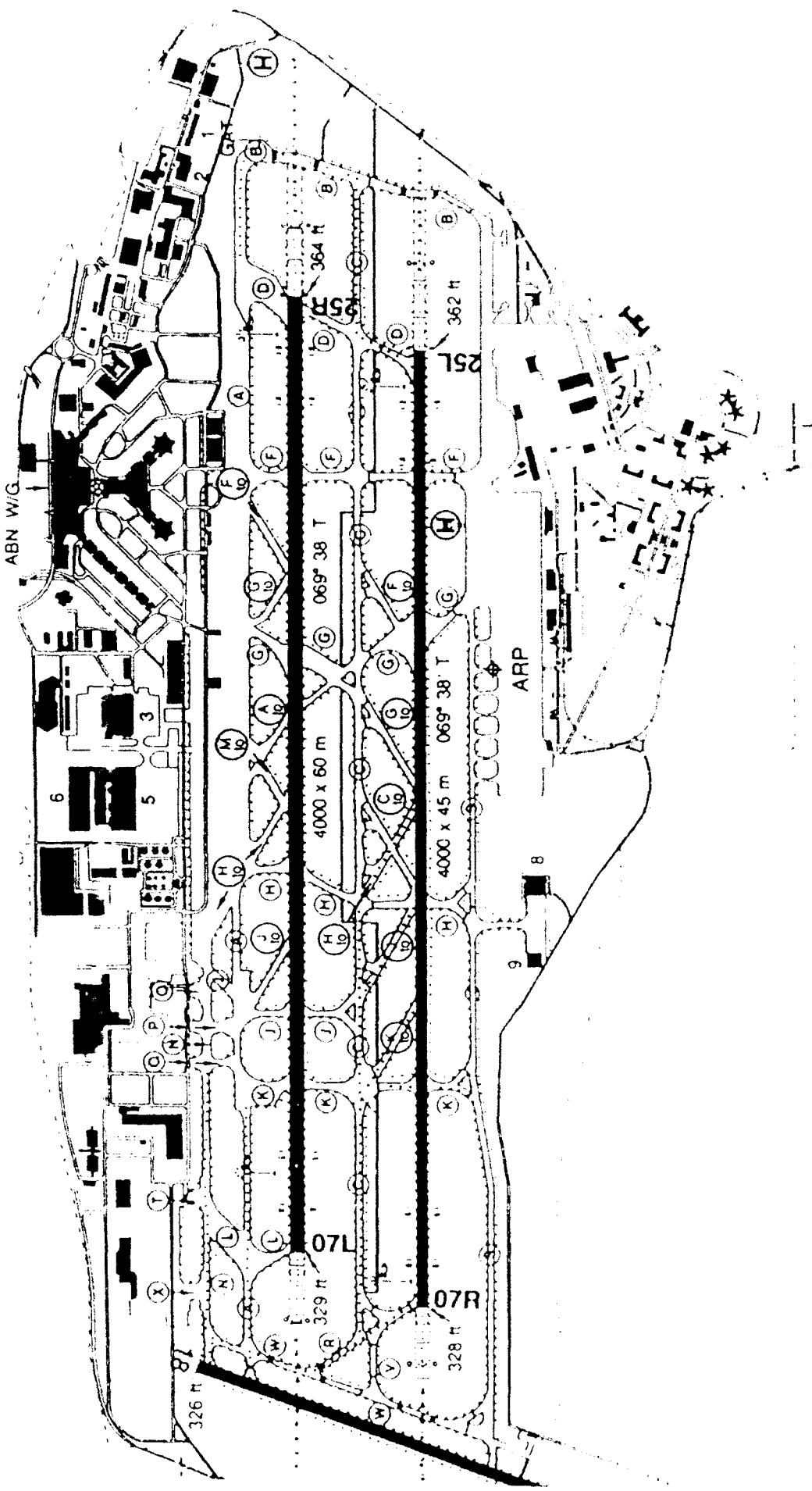
Figure 1. Parallel runway system at Frankfurt Airport.

Figure 2. Airspace structure of Frankfurt approach area.
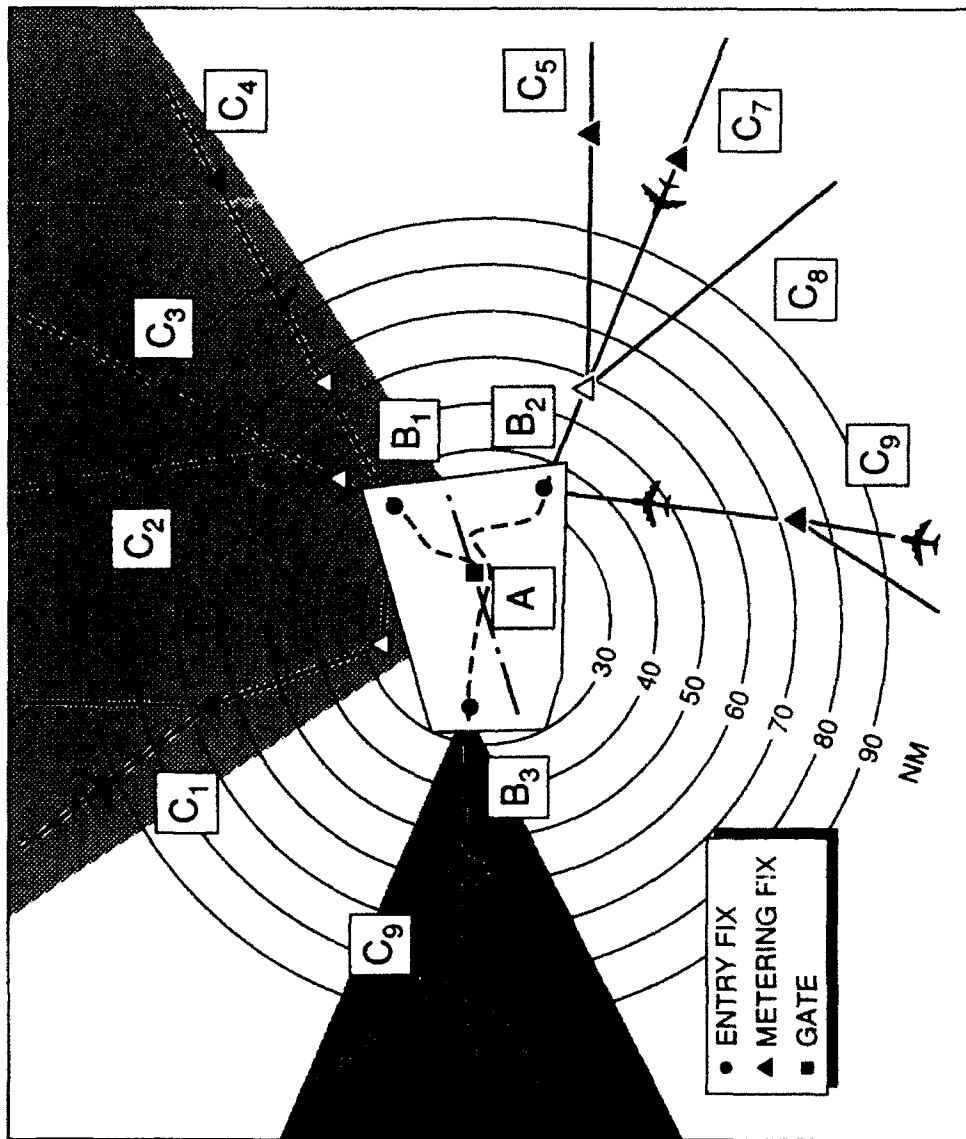
Figure 3. DLR Air Traffic Management and Operations Simulator (ATMOS).
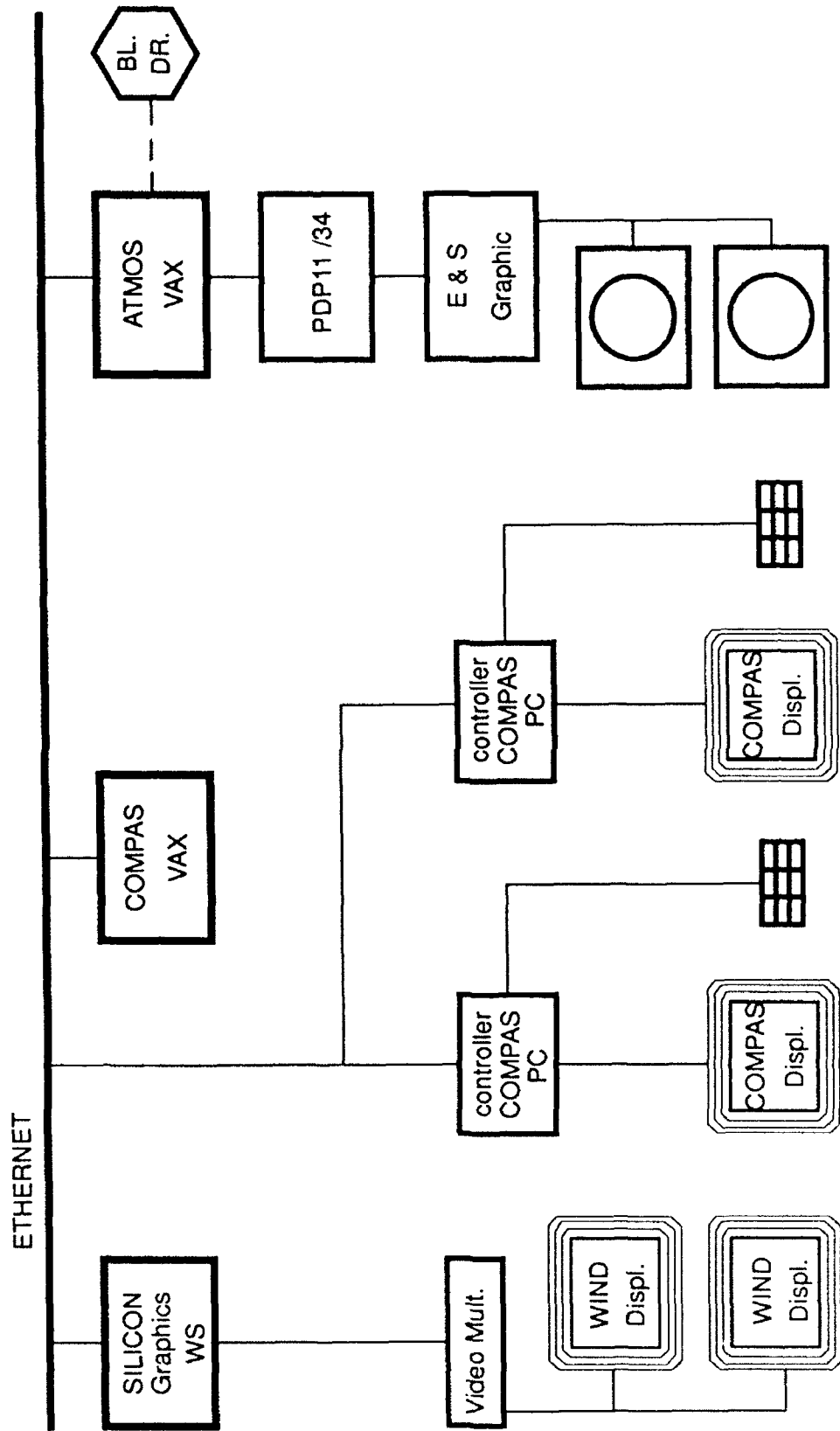
Figure 4. Hardware configuration.

windscenario "variable wind"			
reference	wind prognosis	actual wind	displaced threshold

windscenario "stable wind"	
wind prognosis	actual wind

traffic characteristics
spatial : 32% north, 50%south, 18% west
weight classes : 27% heavy, 63% medium; 10% light
pure inbound rush : 80 A/C within 90 minutes

Figure 5. Simulated scenarios and traffic characteristics.
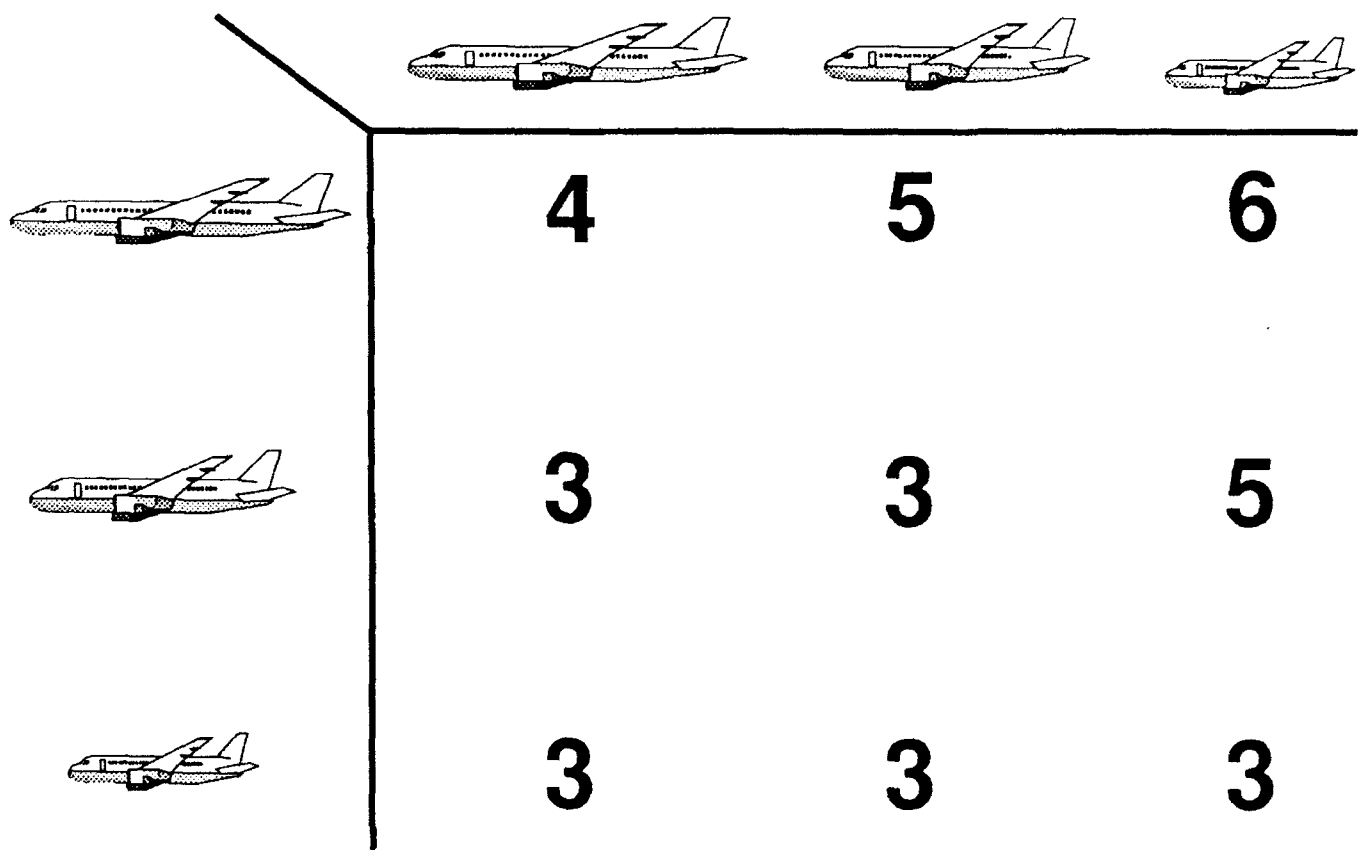
Figure 6. Wake vortex separation matrix.

190 25

max
12
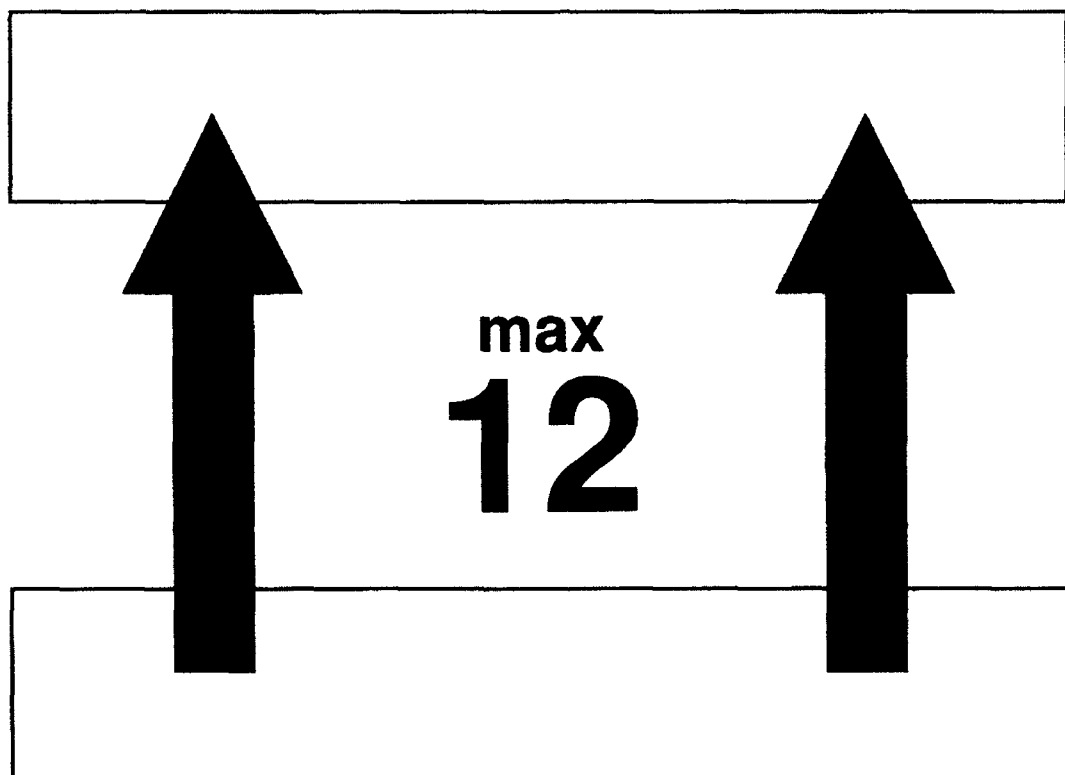
Figure 7. Display "wind prognosis", runways coupled.

250   9

min
20
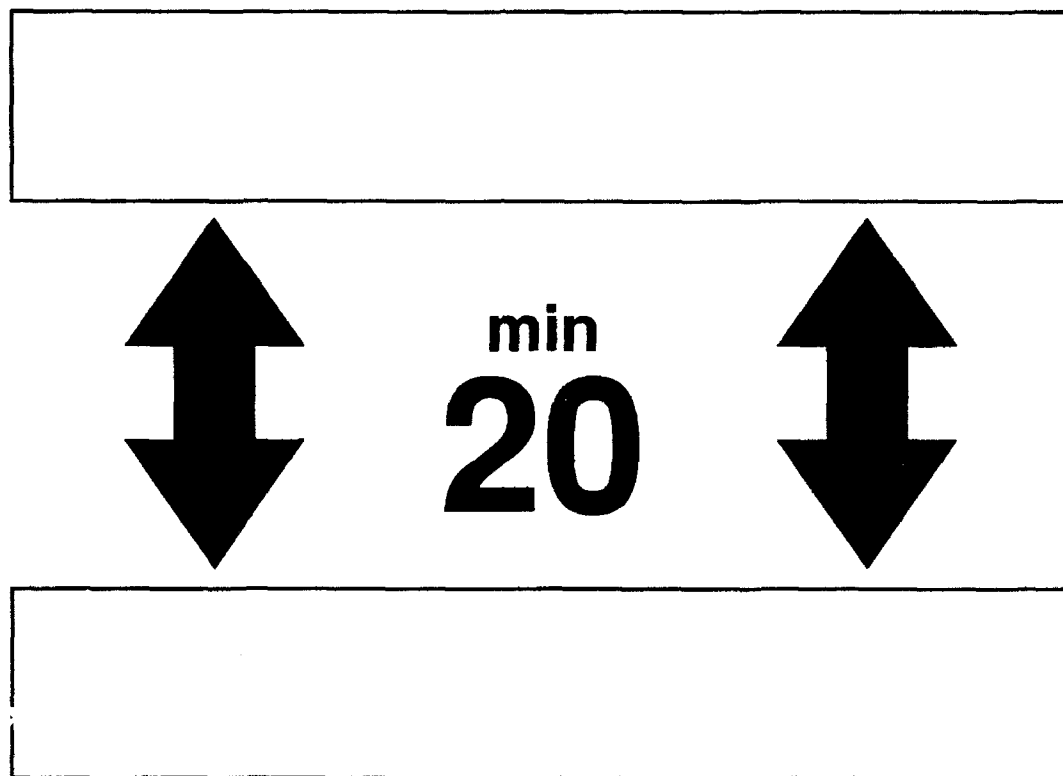
Figure 8. Display "wind prognosis", runways independent.
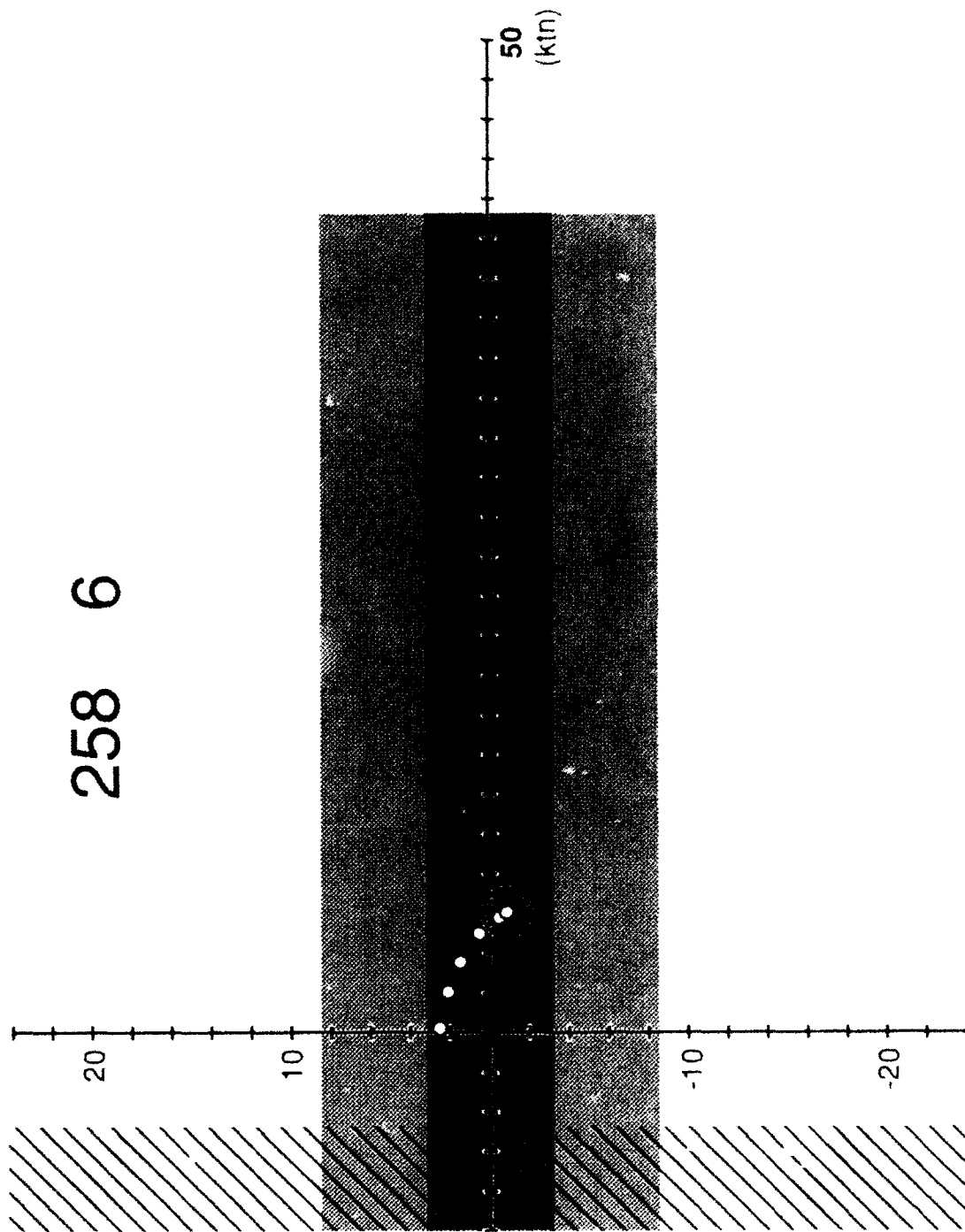
Figure 9. Display "actual wind", staggered mode.

Figure 10. Display "actual wind", single mode.
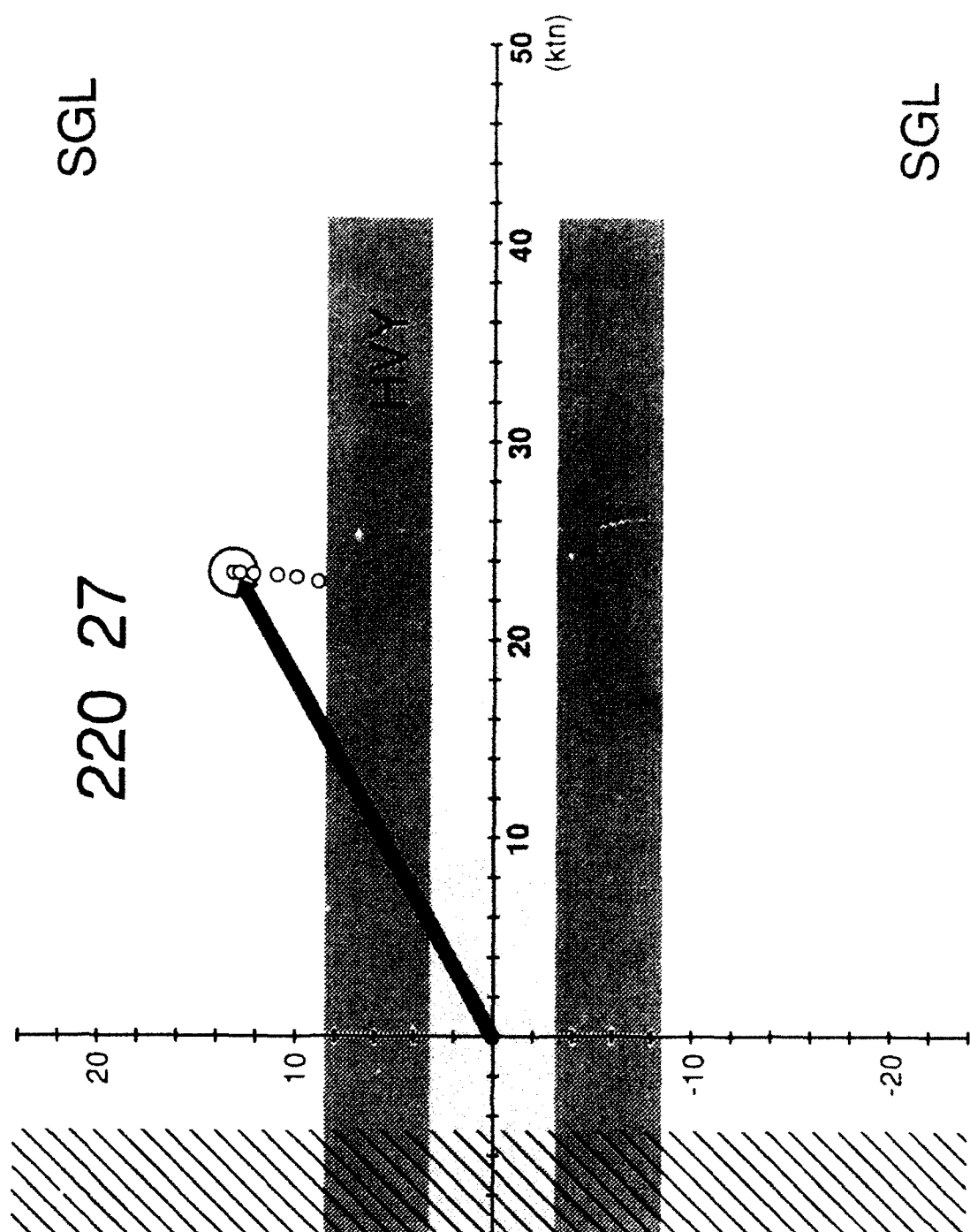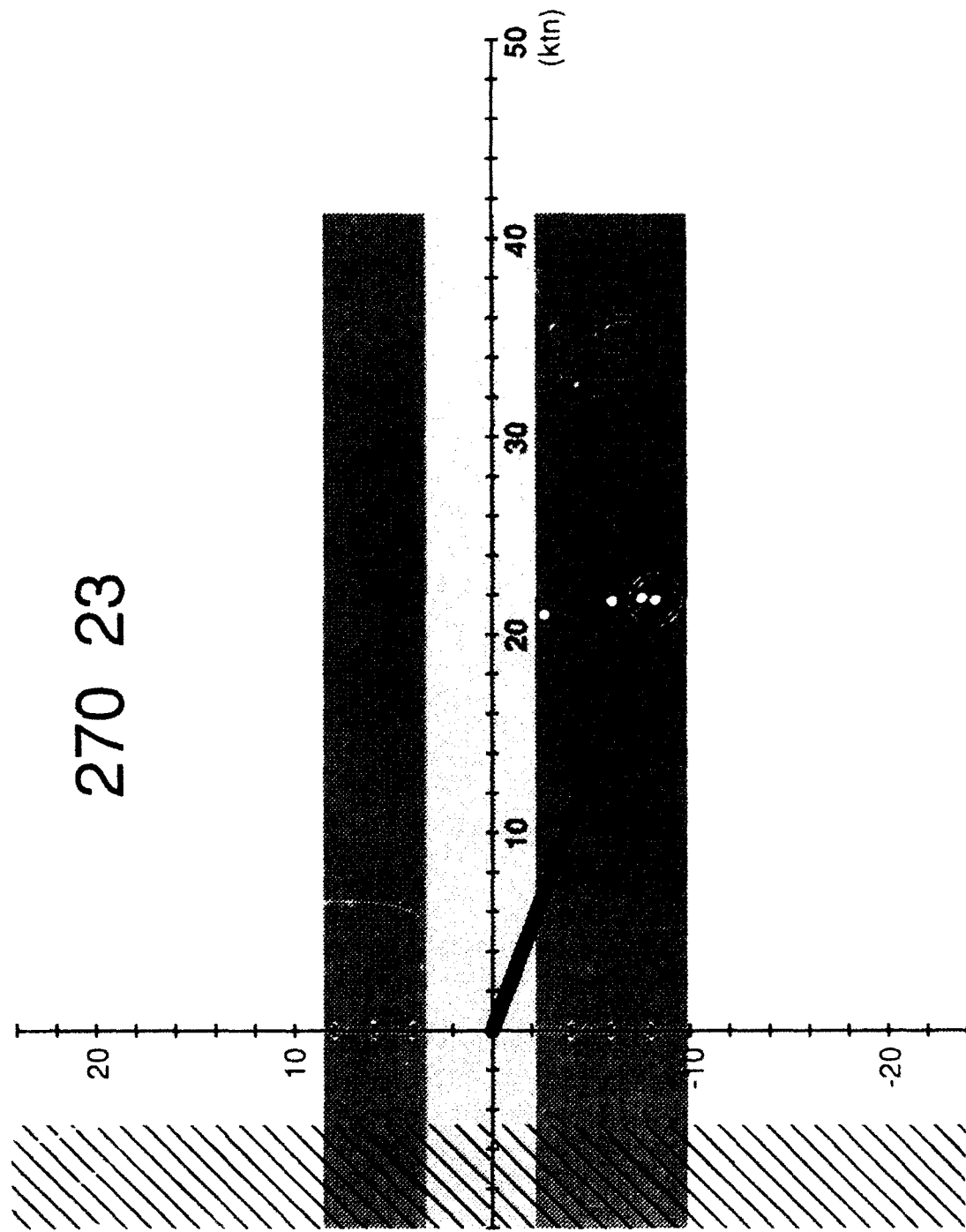
Figure 11. Display "actual wind", HVY mode.

runway direction 25

touch down region
1000m

4000m x 60m 25R

1000m
displacement

threshold right

2225m x 45m 25L

threshold left

runway direction 07

threshold left

07L   2225m x 60m

displacement
1000m

07R   4000m x 45m

1000m
touch down region
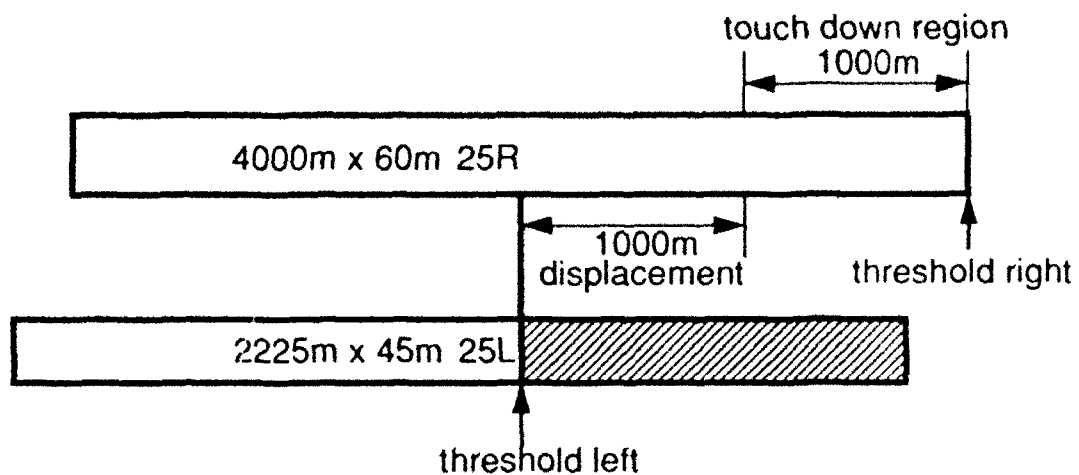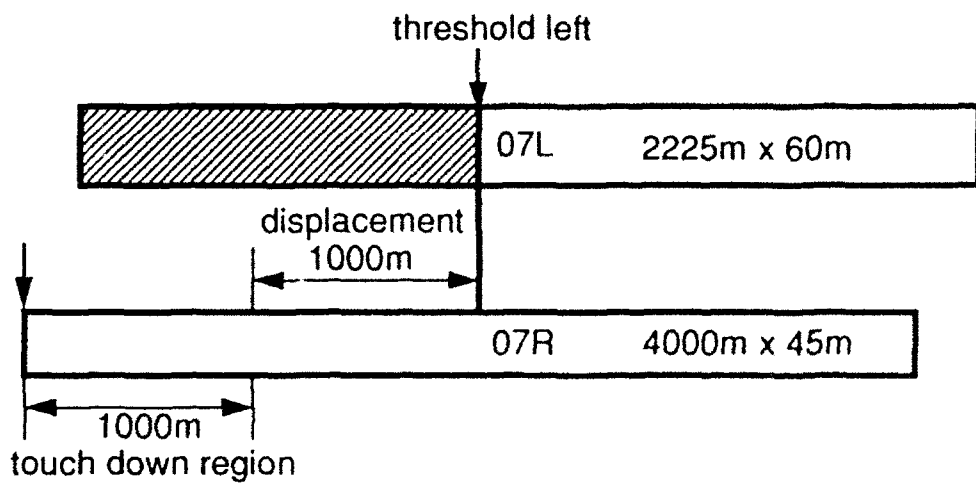
Figure 12. Glide path configuration "displaced threshold" concept.

- **capacity effect**
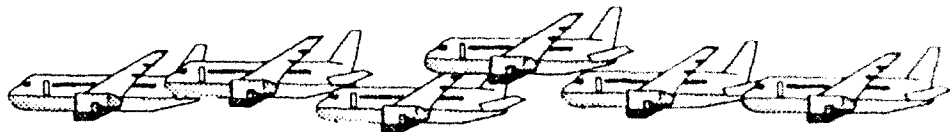
concept	A/C per hour	
	variable wind	stable wind
reference	39.0 (1.1)	
wind prognosis	41.9 (1.5)	43.7 (1.4)
actual wind	41.8 (1.2)	44.0 (1.7)
displaced threshold	41.5 (1.1)	

- **separation**
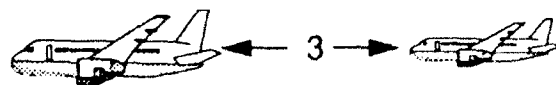
concept	distance 3 NM allowed
reference	2.76 (0.2)
all other	2.97 - 3.07 (0.15)

Figure 13. Results.

- **controller view**   Dahl   BFS
                                 Gebauer
                                 Müller (Hartmut)
                                 Müller (Horst)
                                 Schmidt

- **pilot view**   Jelkmann   DLH
                                 Wagner

- **metereological aspects**   Franke   IMK
                                 Tetzlaff

- **wake vortex propagation**   Jahn   DLR

- **concept development**   Klostermann   DLR

- **assessment concept**   Mittendorf   DLR
  and evaluation   Schick
                                 Steinke

- **displays**   Wiesner   DLR

- **simulation software**   Keck   DLR
                                 Schwarz

- **COMPAS**   Schenk   DLR
                                 Schubert

and many other more

Figure 14. Simulation team.

REFERENCES

1.   Beyer, R., the upgrading of ATMOS ATC-Simulation Seminar of EUROCONTROL. Luxembourg, June 11-13.

2.   Schick, F.V., M. Schubert, U. Völkers, Simulatorerprobung des Planungssystems COMPAS. DFVLR IB 112-86/25, Braunschweig, Dezember 1986.

3.   Schenk, H.D., COMPAS OP Ein Planungssystem für den Flughafen Frankfurt DLR-Nachrichen. Heft 62, Februar 1991.

4.   Tetzlaff, G., J. Franke, Wake Vortex Propagation in the Atmospheric Boundary Layer. FAA International Wake Vortex Symposium, Washington, D.C., Oct. 29-31, 1991.

5.   Koepp, F., Experimental Investigation of Wake Vortex Structure and Propagation Using the DLR Laser Doppler Anemometer. FAA International Wake Vortex Symposium, Washington, D.C., Oct. 29-31, 1991.

6.   Schick, F.V., U. Teegen, R. Uckermann, R.L. Hann, Validation of the Subjective Workload Assessment Technique in a Simulated Flight Task. DFVLR FB 89-01. Braunschweig, December 1988.

7.   Reichmuth, J., Wirbelschleppenwarnsystem Vertiefte Prüfung des operationellen Konzepts Teil 1: Projektdurchführung. DLR IB 112-91/36. Braunschweig, August 1991.

8.   Schick, F.V., M. Mittendorf, Wirbelschleppenwarnsystem Vertiefte Prüfung des operationellen Konzepts Teil 2: Bewertungsverfahren und Ergebnisse. DLR IB 112-91/37. Braunschweig, September 1991.

EFFECT OF REDUCED INTRAIL SEPARATIONS ON CAPACITY

Douglas Baart
Robert B. Rovinsky
Helen Monk
Mary Schweiker

ABSTRACT

Alleviating the congestion of our airports has been a major concern of the FAA and the airlines. Conservative separation standards, now in effect, increase arrival and departure delay and reduce airport capacity. Several products of the FAA'S Wake Vortex Program, if implemented, will permit reduced separation standards in terminal areas, in addition to improving safety.

Using the Runway Delay Simulation (RDSIM) Model, which emulates runway operations based on historical data, we examined these theoretical separation standards on capacity and delay at John F. Kennedy (JFK), Boston (BOS), and St. Louis (STL) airports. Generic runway configurations were also explored as a means of grouping many airports with similar runway configurations.

We also used SIMMOD, which provides considerable detail on the airfield and airspace of an airport, to analyze the benefits possible at Dallas Fort Worth (DFW) and Chicago O'Hare (ORD) from developing and installing future wake vortex detection/monitoring systems as well as changing future separations standards.

This paper presents the results of the above analyses, which indicate that the reduced separation standards can produce significant benefits to the aviation industry and economy. However, these benefits can only be realized by safely coordinating operational changes with air traffic procedures.

INTRODUCTION

Background

Wake Vortices are pairs of "horizontal tornadoes" that are produced by and behind aircraft in flight. They have the potential to be hazardous to following aircraft, especially during landing or takeoff. Wake Vortex hazards are one of the primary reasons FAA mandates up to six miles spacing between aircraft during approach and landing. Large spacings between aircraft,

however, reduce the capacity of the National Airspace system and increase delays. A Wake Vortex Research Program was recently begun by the FAA, with the goals of improving air safety while simultaneously increasing capacity and reducing delays.

The Federal Aviation Administration (FAA) Research and Development Service requested the FAA Technical Center to perform a capacity and delay study that would involve new wake vortex separation standards which could be realized by the implementation of wake vortex products. These products include a Vortex Advisory System (VAS), a Wake Vortex Avoidance System (WVAS), a Wake Vortex Detection/ Monitoring System, and an Advanced Wake Vortex Detection/Monitoring System. Theoretical wake vortex separation standards which could be achieved from each of these products are described in appendix A.

Also, the Operations Research Service (AOR) was tasked to conduct a benefits analysis of potential wake-vortex detection/monitoring systems which could be products of a wake-vortex research program, as well as the benefits of intermediate wake-vortex products such as new classification standards, allowing independent operations on closely spaced parallel runways, etc.

Theoretical instrument flight rules (IFR) separation standards for several wake vortex products were provided by Dr. James Hallock, Transportation Systems Center (TSC). Additional separation standards that were evolved from theory and used in the analysis are defined in FAA Report Number FAA-EM-78-8A, "Parameters of Future ATC Systems Relating to Airport Capacity/Delay," dated June 1978.

Purpose

The purpose of this study was to report the benefits achieved, in terms of reduced delay and increased capacity of specific and generic airports, as a result of reducing wake vortex separation standards. These separation standards would be a result of the specific wake vortex products that are mentioned above. This report provides both guidance and support to the Wake Vortex Program.

Method

The impact of the proposed wake vortex separation standards which could be achieved from several wake vortex products was evaluated by five methods:
- Arrival capacity analysis of generic runway configurations.
- Capacity and delay analyses of John F. Kennedy (JFK) International airport.
- Recent wake vortex delay analyses of Boston-Logan International (BOS) and Lambert-St. Louis (STL) International Airports.

- Recent wake vortex delay analyses of Chicago O'Hare International (ORD) and Dallas Fort Worth (DFW) using SIMMOD.
- Summary of prior wake vortex delay studies.

27-2

Appendix A defines the minimum intrail arrival aircraft separations referenced in this report. Appendix B describes the runway delay simulation model, RDSIM, which was used in the analyses. Appendix C describes the SIMMOD model used in the ORD and DFW studies.

ARRIVAL CAPACITY ANALYSIS OF GENERIC RUNWAY CONFIGURATIONS

Method

An IFR arrival capacity study was performed using the runway delay simulation model, the standard separations, and two theoretical separation standards. These new separation standards included a reduced heavy-to-heavy scenario and the reduced separations resulting from the implementation of a detection/ monitoring system.

Four categories of generic runway configurations were examined for the purpose of determining improvements in capacity. The configurations were single runway, independent parallel runways, closely spaced dependent parallel runways, and intersecting runways.

The runway configurations were analyzed for the following: (1) 100 percent arrivals, (2) IFR weather, and (3) different percentages of heavy aircraft in the fleet mix (5, 10, 20, and 40 percent). The percentages of heavy and large aircraft varied so that their combined total represented 80 percent of the fleet mix. The remainder of the fleet mix, 20 percent, was small aircraft.

Model Results

Figure 1 represents the arrival capacity change for a single runway under IFR weather as a function of heavy arrivals for the reduced separation standards of wake vortex products. The table indicates that the capacity, as determined from each scenario, will decrease with the increase of heavy arrivals. However, when comparing a detection/monitoring system scenario and a reduced heavy-to-heavy scenario to the current standard separation, an increase in capacity results. With as little as 5 percent heavies, the magnitude of this increase is substantial when reduced wake vortex separation standards are implemented as a result of a detection/monitoring system.

Since independent parallel runways are independent of one another, the gain in capacity realized by the reduced separation standards is double that which is observed in the single runway case. In addition, when operating under IFR, arrivals to closely spaced parallel runways and intersecting runways are treated as if they are landing on a single runway. Thus, the arrival capacity of closely spaced parallel and intersecting runways is that of a single arrival runway.

CAPACITY ANALYSES AT JFK

In addition to using generic airports, the impact of three products of the Wake Vortex Program on capacity and delay at JFK was studied. This airport was selected because of its large percentage of heavy aircraft operations.

The three products which reduce minimum intrail arrival separations are (1) reduced heavy-to-heavy separations, (2) Wake Vortex Detection/Monitoring System, and (3) Advanced Wake Vortex Detection/Monitoring System. These separation rules are described in Appendix A.

Method

The JFK capacity study employed an analytical technique to determine the saturation capacity of a single arrival runway. The intent of this exercise was to determine the increase in capacity that could be realized if wake vortex separation standards were reduced by the reduced heavy-to-heavy separations, the detection/monitoring system, and the advanced detection/ monitoring system. The resulting separation standards for each of these products are described in Appendix A.

The analysis was based on arrival priority in which a single runway was used to serve aircraft with a constant demand of traffic while operating at runway saturation. Runway saturation describes the event in which one aircraft lands immediately after another exits the runway. Instrument flight rules were used in the analysis since they provided the greatest gain in capacity when reducing separation standards. The percentage of heavy operations was altered to examine its effect on capacity.

Inter-arrival spacing was determined by the same fleet mix (47 percent heavy, 42 percent large, and 11 percent small) that was observed at JFK. In addition, an error term was introduced into the analysis to reflect the added time-buffer generally used by the controller to account for the uncertainty of the precision delivery.

Model Results

Figure 2 summarizes the model's results on a single runway at JFK under IFR weather for several wake vortex products. Each scenario reflects the changes in the number of operations a single runway at JFK could handle for changing percentages of heavy arrivals. The capacity produced by the current standard separation rules tends to steadily decrease with the increase of heavy arrivals. The reduced heavy-to-heavy scenario shows a slight initial decrease in capacity (up to 30 percent heavy arrivals), then a constant increase in capacity from 30 to 100 percent heavy operations. A capacity increase over the current set of separation rules was noted for all percentages of heavy operations for the detection/monitoring system. The capacity of the advanced detection/monitoring system increased substantially, although it was not affected by the percentage of heavies.

DELAY ANALYSIS AT JFK

Method

Four IFR runway configurations used during IFR weather at JFK were analyzed in the delay study. Each configuration consisted of an "arrival only" runway and a "departure only" runway. The analysis used RDSIM inputs and a 1990 demand forecast from the 1985 JFK Task Force Study. Dollar savings were based on the direct operating costs of the JFK fleet mix for the 1990 demand schedule, $2,088 per hour. Costs were obtained from Avmark, December 31, 1989.

Model Results

The delay savings for runway configurations which are typically used at JFK under IFR weather conditions are illustrated in table 1. These savings are a result of reducing wake vortex separation standards. Estimates of daily delay savings for the four IFR configurations with the 1990 JFK demand are listed below:

> $155 to $173 thousand with reduced heavy-to-heavy separations.
> $530 to $572 thousand with detection/monitoring system.
> $1.2 million with advanced detection/monitoring system.

RECENT WAKE VORTEX DELAY ANALYSES AT BOS AND STL

Method

A recent task force studied the benefits of reduced wake vortex separations at BOS and STL. They used the simulation model RDSIM and separation standards as described in appendix A for the Vortex Advisory System (VAS) and Wake Vortex Avoidance System (WVAS).

Model Results

Figure 3 shows the annual delay savings (in thousands of hours) which could be obtained with a VAS at BOS, for both VFR and IFR weather. This system can save approximately $16 million (12,800 hours) each year at the lowest demand and $30 million (24,200 hours) at the highest demand. Similarly, figure 4 shows the annual delay savings of a WVAS at BOS. Savings of $22 million (17,700 hours) each year at the lowest demand and $51 million (41,100 hours) at the highest demand were projected.

The curves show the relationship between annual delay savings and projected demand levels. The data may be generalized to determine the delay savings from any new separation standard that falls in the neighborhood of the original VAS and WVAS separations. These savings are based on the direct operating costs of the BOS fleet mix--$1,248 per hour in 1987 dollars.

Figure 5 shows the STL annual delay savings (in thousands of hours) that can be achieved by eliminating the wake vortex runway dependency between closely spaced parallels in VFR weather conditions. This accounts for a savings of approximately $12 million (8,000 hours) each year at the lowest demand and $127 million (86,000 hours) at the highest demand. The dollar savings are based on the direct operating costs of the STL fleet mix--$1,479 per hour in 1987 dollars.

In all cases, the potential delay savings are substantial.

WAKE VORTEX BENEFITS ANALYSIS OF ORD AND DFW

To provide maximum realism, Operations Research Service (AOR) staff decided to perform the study using SIMMOD, which is a simulation model providing detail on both the airfield and airspace of a particular airport. The FAA and its contractors had developed and tested SIMMOD over the last 10 years and SIMMOD studies have been performed for a number of major airports/airspaces in the United States and abroad. The output of SIMMOD provides extensive information on delays of the modeled system. Wake vortex program products, such as reduced separation standards or new classifications, could be readily input into the SIMMOD base cases.

AOR procured two contracts with companies that had already successfully completed SIMMOD studies for major airports. ATAC of Mountain View, Ca. was tasked to analyze wake vortex benefits at DFW and American Airlines Decision Technologies (AADT) of Dallas, Tx. was tasked to analyze ORD. Maximum discretion was given to the contractors to ensure realism and allow for differences in technique. The estimates of wake-vortex separation rules possible under a new program were obtained from the Transportation Systems Center (TSC) in Cambridge, Ma., and were modified by the contractors, through discussions with FAA and TSC, to make them realistic and workable for the airports. Later these separation rules were rechecked and confirmed with Air Traffic Personnel at each facility, to verify the reasonableness of the separation reduction assumptions. Ground and Airspace Delays and associated costs were obtained for three scenarios:

Matrix A, representing the base (existing) case;

Matrix B, representing the maximum possible benefits at the airport through wake vortex detection/monitoring systems, given little or no other change in airport configuration; and

Matrix C, representing the benefits to be gained by simply changing the separation rules for Heavy behind Heavy from four to three miles.

The assumptions used by the contractors are documented in their reports and in internal FAA memoranda (Available upon request). Matrices A, B, and C for DFW and ORD are given in Figure 6. Dr. Jim Hallock of TSC, Dr. Robert Machol, Chief Scientist, FAA, and Mr. Richard Page, Wake Vortex Program Manager, gave generously of their time and experience, to assist in the development of these assumptions and data. Mr. Roy Harmon, chief of Air Traffic at

ORD for American Airlines and Mr. Sam Smith, Deputy Manag ~f O'Hare Tower, provided confirmation of the numbers for ORD, and Mr. Ralph Barnett, of the Southwest Region, provided confirmation of the data for DFW. We acknowledge and appreciate all this help; however, the responsibility for the assumptions and final results remains with AOR.

The benefits of a Wake Vortex Program may include many factors, such as safety improvements and advances in aviation science or technology, which cannot be easily predicted or measured. What can be measured is the impact that reductions in separation standards resulting from wake vortex products will have on the capacity of airfields and on delay times. Due to a lack of scientific research, we could make no estimates on how the current departure separation standards could be expected to change. However, we were able to obtain scientific estimates of how arrival separation standards could change under wake vortex detection systems. Thus to measure benefits, SIMMOD runs were made using three sets of data on arrival separation standards. (These are given above in Matrices A, B, and C.) Matrix A is the airport's current IMC arrival separation rules. Matrix B is defined as the closest possible separation standards which could be achieved in the future without significantly changing the airport or airspace configuration. Matrix B was created by first obtaining theoretical data from TSC scientists and then modifying them through discussions with the modelers and their air traffic controllers. Changes were allowed in terms of adding high speed taxipaths and in changing the geometry of where the outer marker was in terms of airspeed control, but only one airport required a high speed taxiway and the modelers did not need the latter. The modelers chose separation standards for Matrix B heuristically so that the number of missed approaches did not change over those achieved for Matrix A. AOR staff checked the data with air traffic controllers at DFW and ORD. Finally, Matrix C is identical to Matrix A except for the change in separation standards for Heavy behind Heavy to three miles.

All other data for the SIMMOD runs were identical to data from earlier studies run by the modelers. The data were fairly recent. No changes were made in aircraft sequencing, air traffic control procedures, or airspace configurations.

For each scenario, corresponding to Matrix A, B, and C, five runs of the SIMMOD model were made and the results averaged to obtain statistical results. In the case of DFW, no changes in the base case (Matrix A) were necessary to run the model with Matrix B and C separation rules. In the case of ORD, runway occupancy times had to be decreased to 40 seconds (from 45 seconds) in order to prevent missed approaches when the reduced intrail separations of Matrix B were in use. AADT assumed that high speed runway exits could be designed to allow such a decrease in runway occupancy times at ORD.

The modelers further assumed that all operations were "normal," i.e., that there were no additional factors operating except those inherent to the schedule, separation rules and the runway configurations in use.

Each set of model runs produced data on "delay time," which is defined as the time spent waiting to depart plus the airspace delay. These values in SIMMOD have been shown to be consistent with the conventional measures; however, it is important to note that we are not measuring "reportable delays." For each minute of "delay" recorded by SIMMOD, a delay cost was computed. Each modeler computed these differently. AADT concentrated on airspace

however, reduce the capacity of the National Airspace system and increase delays. A Wake Vortex Research Program was recently begun by the FAA, with the goals of improving air safety while simultaneously increasing capacity and reducing delays.

The Federal Aviation Administration (FAA) Research and Development Service requested the FAA Technical Center to perform a capacity and delay study that would involve new wake vortex separation standards which could be realized by the implementation of wake vortex products. These products include a Vortex Advisory System (VAS), a Wake Vortex Avoidance System (WVAS), a Wake Vortex Detection/ Monitoring System, and an Advanced Wake Vortex Detection/Monitoring System. Theoretical wake vortex separation standards which could be achieved from each of these products are described in appendix A.

Also, the Operations Research Service (AOR) was tasked to conduct a benefits analysis of potential wake-vortex detection/monitoring systems which could be products of a wake-vortex research program, as well as the benefits of intermediate wake-vortex products such as new classification standards, allowing independent operations on closely spaced parallel runways, etc.

Theoretical instrument flight rules (IFR) separation standards for several wake vortex products were provided by Dr. James Hallock, Transportation Systems Center (TSC). Additional separation standards that were evolved from theory and used in the analysis are defined in FAA Report Number FAA-EM-78-8A, "Parameters of Future ATC Systems Relating to Airport Capacity/Delay," dated June 1978.

Purpose

The purpose of this study was to report the benefits achieved, in terms of reduced delay and increased capacity of specific and generic airports, as a result of reducing wake vortex separation standards. These separation standards would be a result of the specific wake vortex products that are mentioned above. This report provides both guidance and support to the Wake Vortex Program.

Method

The impact of the proposed wake vortex separation standards which could be achieved from several wake vortex products was evaluated by five methods:

- Arrival capacity analysis of generic runway configurations.
- Capacity and delay analyses of John F. Kennedy (JFK) International airport.
- Recent wake vortex delay analyses of Boston-Logan International (BOS) and Lambert-St. Louis (STL) International Airports.

- Recent wake vortex delay analyses of Chicago O'Hare International (ORD) and Dallas Fort Worth (DFW) using SIMMOD.
- Summary of prior wake vortex delay studies.

Appendix A defines the minimum intrail arrival aircraft separations referenced in this report. Appendix B describes the runway delay simulation model, RDSIM, which was used in the analyses. Appendix C describes the SIMMOD model used in the ORD and DFW studies.

ARRIVAL CAPACITY ANALYSIS OF GENERIC RUNWAY CONFIGURATIONS

Method

An IFR arrival capacity study was performed using the runway delay simulation model, the standard separations, and two theoretical separation standards. These new separation standards included a reduced heavy-to-heavy scenario and the reduced separations resulting from the implementation of a detection/ monitoring system.

Four categories of generic runway configurations were examined for the purpose of determining improvements in capacity. The configurations were single runway, independent parallel runways, closely spaced dependent parallel runways, and intersecting runways.

The runway configurations were analyzed for the following: (1) 100 percent arrivals, (2) IFR weather, and (3) different percentages of heavy aircraft in the fleet mix (5, 10, 20, and 40 percent). The percentages of heavy and large aircraft varied so that their combined total represented 80 percent of the fleet mix. The remainder of the fleet mix, 20 percent, was small aircraft.

Model Results

Figure 1 represents the arrival capacity change for a single runway under IFR weather as a function of heavy arrivals for the reduced separation standards of wake vortex products. The table indicates that the capacity, as determined from each scenario, will decrease with the increase of heavy arrivals. However, when comparing a detection/monitoring system scenario and a reduced heavy-to-heavy scenario to the current standard separation, an increase in capacity results. With as little as 5 percent heavies, the magnitude of this increase is substantial when reduced wake vortex separation standards are implemented as a result of a detection/monitoring system.

Since independent parallel runways are independent of one another, the gain in capacity realized by the reduced separation standards is double that which is observed in the single runway case. In addition, when operating under IFR, arrivals to closely spaced parallel runways and intersecting runways are treated as if they are landing on a single runway. Thus, the arrival capacity of closely spaced parallel and intersecting runways is that of a single arrival runway.

CAPACITY ANALYSES AT JFK

In addition to using generic airports, the impact of three products of the Wake Vortex Program on capacity and delay at JFK was studied. This airport was selected because of its large percentage of heavy aircraft operations.

The three products which reduce minimum intrail arrival separations are (1) reduced heavy-to-heavy separations, (2) Wake Vortex Detection/Monitoring System, and (3) Advanced Wake Vortex Detection/Monitoring System. These separation rules are described in Appendix A.

Method

The JFK capacity study employed an analytical technique to determine the saturation capacity of a single arrival runway. The intent of this exercise was to determine the increase in capacity that could be realized if wake vortex separation standards were reduced by the reduced heavy-to-heavy separations, the detection/monitoring system, and the advanced detection/ monitoring system. The resulting separation standards for each of these products are described in Appendix A.

The analysis was based on arrival priority in which a single runway was used to serve aircraft with a constant demand of traffic while operating at runway saturation. Runway saturation describes the event in which one aircraft lands immediately after another exits the runway. Instrument flight rules were used in the analysis since they provided the greatest gain in capacity when reducing separation standards. The percentage of heavy operations was altered to examine its effect on capacity.

Inter-arrival spacing was determined by the same fleet mix (47 percent heavy, 42 percent large, and 11 percent small) that was observed at JFK. In addition, an error term was introduced into the analysis to reflect the added time-buffer generally used by the controller to account for the uncertainty of the precision delivery.

Model Results

Figure 2 summarizes the model's results on a single runway at JFK under IFR weather for several wake vortex products. Each scenario reflects the changes in the number of operations a single runway at JFK could handle for changing percentages of heavy arrivals. The capacity produced by the current standard separation rules tends to steadily decrease with the increase of heavy arrivals. The reduced heavy-to-heavy scenario shows a slight initial decrease in capacity (up to 20 percent heavy arrivals), then a constant increase in capacity from 30 to 100 percent heavy operations. A capacity increase over the current set of separation rules was noted for all percentages of heavy operations for the detection/monitoring system. The capacity of the advanced detection/monitoring system increased substantially, although it was not affected by the percentage of heavies.

DELAY ANALYSIS AT JFK

Method

Four IFR runway configurations used during IFR weather at JFK were analyzed in the delay study. Each configuration consisted of an "arrival only" runway and a "departure only" runway. The analysis used RDSIM inputs and a 1990 demand forecast from the 1985 JFK Task Force Study. Dollar savings were based on the direct operating costs of the JFK fleet mix for the 1990 demand schedule, $2,088 per hour. Costs were obtained from Avmark, December 31, 1989.

Model Results

The delay savings for runway configurations which are typically used at JFK under IFR weather conditions are illustrated in table 1. These savings are a result of reducing wake vortex separation standards. Estimates of daily delay savings for the four IFR configurations with the 1990 JFK demand are listed below:

> $155 to $173 thousand with reduced heavy-to-heavy separations.
> $530 to $572 thousand with detection/monitoring system.
> $1.2 million with advanced detection/monitoring system.

RECENT WAKE VORTEX DELAY ANALYSES AT BOS AND STL

Method

A recent task force studied the benefits of reduced wake vortex separations at BOS and STL. They used the simulation model RDSIM and separation standards as described in appendix A for the Vortex Advisory System (VAS) and Wake Vortex Avoidance System (WVAS).

Model Results

Figure 3 shows the annual delay savings (in thousands of hours) which could be obtained with a VAS at BOS, for both VFR and IFR weather. This system can save approximately $16 million (12,800 hours) each year at the lowest demand and $30 million (24,200 hours) at the highest demand. Similarly, figure 4 shows the annual delay savings of a WVAS at BOS. Savings of $22 million (17,700 hours) each year at the lowest demand and $51 million (41,100 hours) at the highest demand were projected.

The curves show the relationship between annual delay savings and projected demand levels. The data may be generalized to determine the delay savings from any new separation standard that falls in the neighborhood of the original VAS and WVAS separations. These savings are based on the direct operating costs of the BOS fleet mix--$1,248 per hour in 1987 dollars.

Figure 5 shows the STL annual delay savings (in thousands of hours) that can be achieved by eliminating the wake vortex runway dependency between closely spaced parallels in VFR weather conditions. This accounts for a savings of approximately $12 million (8,000 hours) each year at the lowest demand and $127 million (86,000 hours) at the highest demand. The dollar savings are based on the direct operating costs of the STL fleet mix--$1,479 per hour in 1987 dollars.

In all cases, the potential delay savings are substantial.

WAKE VORTEX BENEFITS ANALYSIS OF ORD AND DFW

To provide maximum realism, Operations Research Service (AOR) staff decided to perform the study using SIMMOD, which is a simulation model providing detail on both the airfield and airspace of a particular airport. The FAA and its contractors had developed and tested SIMMOD over the last 10 years and SIMMOD studies have been performed for a number of major airports/airspaces in the United States and abroad. The output of SIMMOD provides extensive information on delays of the modeled system. Wake vortex program products, such as reduced separation standards or new classifications, could be readily input into the SIMMOD base cases.

AOR procured two contracts with companies that had already successfully completed SIMMOD studies for major airports. ATAC of Mountain View, Ca. was tasked to analyze wake vortex benefits at DFW and American Airlines Decision Technologies (AADT) of Dallas, Tx. was tasked to analyze ORD. Maximum discretion was given to the contractors to ensure realism and allow for differences in technique. The estimates of wake-vortex separation rules possible under a new program were obtained from the Transportation Systems Center (TSC) in Cambridge, Ma., and were modified by the contractors, through discussions with FAA and TSC, to make them realistic and workable for the airports. Later these separation rules were rechecked and confirmed with Air Traffic Personnel at each facility, to verify the reasonableness of the separation reduction assumptions. Ground and Airspace Delays and associated costs were obtained for three scenarios:

Matrix A, representing the base (existing) case;

Matrix B, representing the maximum possible benefits at the airport through wake vortex detection/monitoring systems, given little or no other change in airport configuration; and

Matrix C, representing the benefits to be gained by simply changing the separation rules for Heavy behind Heavy from four to three miles.

The assumptions used by the contractors are documented in their reports and in internal FAA memoranda (Available upon request). Matrices A, B, and C for DFW and ORD are given in Figure 6. Dr. Jim Hallock of TSC, Dr. Robert Machol, Chief Scientist, FAA, and Mr. Richard Page, Wake Vortex Program Manager, gave generously of their time and experience, to assist in the development of these assumptions and data. Mr. Roy Harmon, chief of Air Traffic at

27-6

delay, using a weighted factor of $23 per minute for ORD; ATAC used a flat figure of $1600/hour for all delay at DFW. The differences, while significant, were based on different assumptions and data history; they were accounted for in the comparison between the studies. The delay costs are based only on estimated cost of operation. Opportunity costs of the time of individual travelers are not considered, nor are the benefits and costs of increased capacity considered as part of this analysis.

The results showed that there is a potential for both significant reductions in delays and increases in airport capacity through reduced separation standards made possible by wake vortex detection and monitoring. There is also a considerably smaller potential for savings from one of the products of a wake vortex program, namely a reduction in separation for heavy aircraft following heavies. Considering that both airports have a relatively small percentage (10% for DFW, 12% for ORD) of heavies, these savings should increase rapidly at airports with a higher percentage of heavy aircraft, such as JFK or MSP, and over time at DFW.

DFW, which has few heavies and flies almost 80% of their traffic under VFR conditions, showed an estimated reduction in average daily delay of 5.3 hours. Using figures obtained from the MITRE Corporation which estimated delay costs at $1600 per hour, ATAC estimated that delay costs would be reduced by $3.1 million/year, of which $200,000 was accountable to the reduction in separation of heavy behind heavy. ORD, which runs exclusively under IFR, showed an estimated reduction in average daily delay ranging from 48 to 79 hours; this represents almost a 40% reduction in delays under a wake vortex detection/monitoring system. Using their estimates of delay costs of $23/minute ($1380/hour) AADT estimated a $30 million/year reduction in delay costs, of which approximately $1.6 million/year was accountable to the reduction in separation of heavy behind heavy.

The DFW and ORD cost figures are not as incommensurate as they appear at first. ORD flies 100% of their flights under IFR conditions and thus all of their flights were affected by the change from Matrix A to B. DFW flies 81% of their flights under pure VFR conditions and 13% under VFR with instrument approaches; only 6% of their flights are IFR. Thus for only 19% of their flights were there differences in separation standards and more than two thirds of these were impacted at a much less dramatic fashion. ORD also has more flights than DFW, and a higher proportion of Heavies. On the other hand, the cost figures used by ATAC for DFW were higher than ORD.

In spite of the similarity of the data, there is clearly enough airport specificity to the models and input data to prevent a straightforward extrapolation of the results to determine systemwide benefits.

The cost of these two studies were each under $10,000, and each took less than one month to complete. This relatively low cost and time were possible because the contractors had already completed SIMMOD studies for these airports and surrounding airspace.

As more information becomes available on future classification standards, a SIMMOD study could incorporate proposed changes and their effects. Also, airfields with parallel runways which require dependent operations could be modeled to see what effect wake vortex detection equipment would have on their capability for independent operations. Other airports with higher

ORD for American Airlines and Mr. Sam Smith, Deputy Manager of O'Hare Tower, provided confirmation of the numbers for ORD, and Mr. Ralph Barnett, of the Southwest Region, provided confirmation of the data for DFW. We acknowledge and appreciate all this help; however, the responsibility for the assumptions and final results remains with AOR.

The benefits of a Wake Vortex Program may include many factors, such as safety improvements and advances in aviation science or technology, which cannot be easily predicted or measured. What can be measured is the impact that reductions in separation standards resulting from wake vortex products will have on the capacity of airfields and on delay times. Due to a lack of scientific research, we could make no estimates on how the current departure separation standards could be expected to change. However, we were able to obtain scientific estimates of how arrival separation standards could change under wake vortex detection systems. Thus to measure benefits, SIMMOD runs were made using three sets of data on arrival separation standards. (These are given above in Matrices A, B, and C.) Matrix A is the airport's current IMC arrival separation rules. Matrix B is defined as the closest possible separation standards which could be achieved in the future without significantly changing the airport or airspace configuration. Matrix B was created by first obtaining theoretical data from TSC scientists and then modifying them through discussions with the modelers and their air traffic controllers. Changes were allowed in terms of adding high speed taxipaths and in changing the geometry of where the outer marker was in terms of airspeed control, but only one airport required a high speed taxiway and the modelers did not need the latter. The modelers chose separation standards for Matrix B heuristically so that the number of missed approaches did not change over those achieved for Matrix A. AOR staff checked the data with air traffic controllers at DFW and ORD. Finally, Matrix C is identical to Matrix A except for the change in separation standards for Heavy behind Heavy to three miles.

All other data for the SIMMOD runs were identical to data from earlier studies run by the modelers. The data were fairly recent. No changes were made in aircraft sequencing, air traffic control procedures, or airspace configurations.

For each scenario, corresponding to Matrix A, B, and C, five runs of the SIMMOD model were made and the results averaged to obtain statistical results. In the case of DFW, no changes in the base case (Matrix A) were necessary to run the model with Matrix B and C separation rules. In the case of ORD, runway occupancy times had to be decreased to 40 seconds (from 45 seconds) in order to prevent missed approaches when the reduced intrail separations of Matrix B were in use. AADT assumed that high speed runway exits could be designed to allow such a decrease in runway occupancy times at ORD.

The modelers further assumed that all operations were "normal," i.e., that there were no additional factors operating except those inherent to the schedule, separation rules and the runway configurations in use.

Each set of model runs produced data on "delay time," which is defined as the time spent waiting to depart plus the airspace delay. These values in SIMMOD have been shown to be consistent with the conventional measures; however, it is important to note that we are not measuring "reportable delays." For each minute of "delay" recorded by SIMMOD, a delay cost was computed. Each modeler computed these differently. AADT concentrated on airspace

concentrations of heavies could be used to better test the impacts of the Heavy-behind-Heavy standards change.

SUMMARY OF PRIOR WAKE VORTEX DELAY STUDIES

Figure 7 summarizes the impact of reduced wake vortex separations for six airports: Atlanta (ATL), Los Angeles (LAX), John F. Kennedy (JFK), LaGuardia (LGA), Miami (MIA), and Houston (IAH) using past task force studies and prior descriptions of products of the Wake Vortex Program, VAS and WVAS. These studies were completed between 1980 and 1985 using the simulation model RDSIM.

The curve, derived from the tabular data, shows the relationship between annual delay savings (in thousands of hours) and projected demand levels. The data may be generalized to determine the savings from any new separation standard that falls in the neighborhood of the original VAS and WVAS separations.

One can estimate the annual delay savings for the reduced separations for a given timeframe in the following way: multiply the number of hours of annual delay savings by the average fleet mix cost for these airports during that timeframe. Using this method, the dollar savings can be adjusted to reflect the impact of inflation on the actual dollar savings.

VAS Annual Savings (1982-1985)

The 1982-1985 annual savings of 84,100 hours are based on the use of a Vortex Advisory System. With an average fleet mix cost of $2,000 per hour, the VAS could have saved the airlines $168 million per year.

WVAS Annual Savings (1987-1990)

The 1987-1990 annual savings of 517,000 hours are based on the use of a Wake Vortex Avoidance System. With an average fleet mix cost of $2,000 per hour, the WVAS could have saved the airlines over $1 billion per year.

CONCLUSIONS

1. The analyses show that the products of the Wake Vortex Program can substantially increase airport capacity while significantly reducing delay.

2. The site specific and generic airports analyzed in this report had significant reductions in delay time as a result of reducing wake vortex separation standards (saving millions of dollars).

3. Increases in revenue, which can be attributable to the increase in capacity at these airports, can also show a marketable cause for justifying wake vortex products.

4. As airports serve a higher volume of traffic, the wake vortex products provide even greater annual delay savings.

5. This study concludes that the products developed by the Wake Vortex Program, which will result in reduced intrail arrival separations, can produce considerable benefits to the aviation industry and the economy. However, these benefits can only be realized by safely coordinating operational changes with air traffic procedures.

Table 1. Wake Vortex Daily Delay Savings at JFK—IFR
(in hours and thousands of 1989 dollars)

CONFIGURATIONS		REDUCED HEAVY-TO-HEAVY		VORTEX WARNING SYSTEM		ADVANCED VORTEX WARNING SYSTEM	
ARR	DEP	HOURS	DOLLARS	HOURS	DOLLARS	HOURS	DOLLARS
4R	4L	74	$155	265	$553	562	$1,173
22L	22R	83	$173	274	$572	574	$1,199
31R	31L	77	$161	269	$562	556	$1,161
4R	31L	74	$155	254	$530	570	$1,190
		$155 to $173		$530 to $572		$1,161 to $1,199	
ALL CONFIGURATIONS		8 to 9 % SAVINGS		29 to 30 % SAVINGS		61 to 64 % SAVINGS	

NOTES: IFR daily delay savings are presented in both hours and thousands of dollars for the JFK 1990 demand. The dollar savings were based on the direct operating costs of the JFK fleet mix for the 1990 demand schedule--$2,088 per hour. Costs were obtained from Avmark, December 31, 1989.

	Standard Separation	Detection/Monitor System		Reduce Heavy-to-Heavy	
% Heavy	Arrivals/ Hour	Arrivals/ Hour	% Increase	Arrivals /Hour	% Increase
5	28	29.5	5.4 %	28	0 %
10	27.6	29.4	6.5 %	27.6	0 %
20	26.6	29.1	9.4 %	26.7	.3 %
40	25.2	28.6	13.4 %	26	3.2 %

Figure 1. Arrival capacity - single runway - IFR.
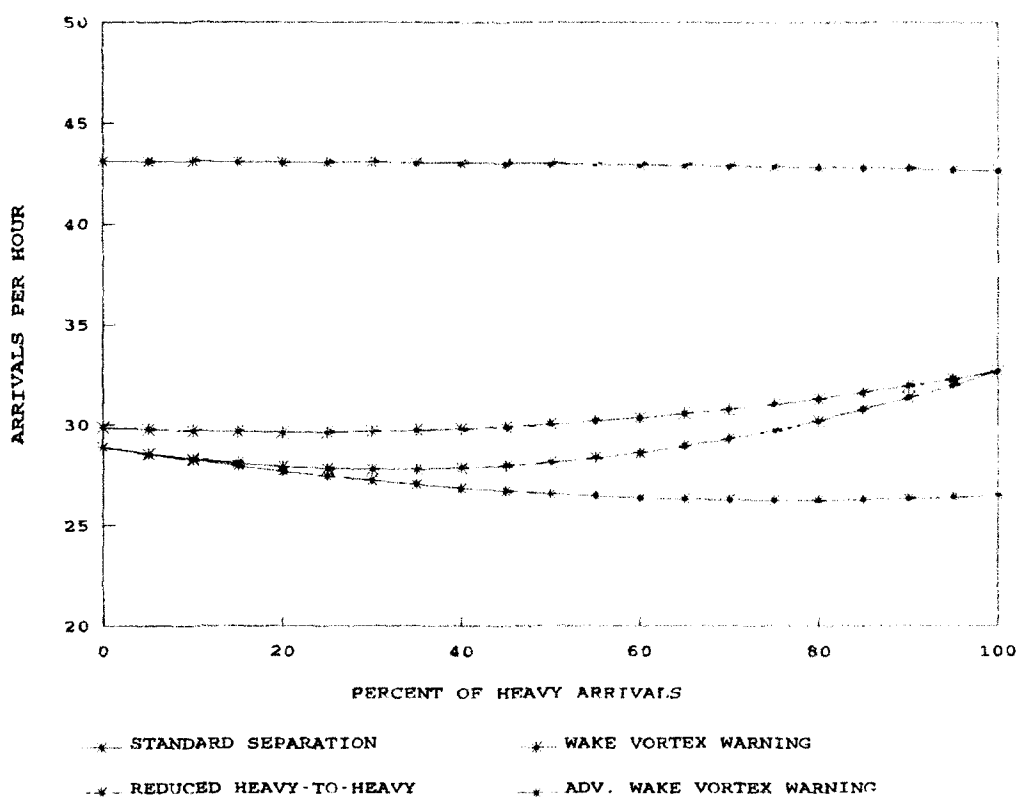
Figure 2 .JFK arrival capacity - single runway - IFR.
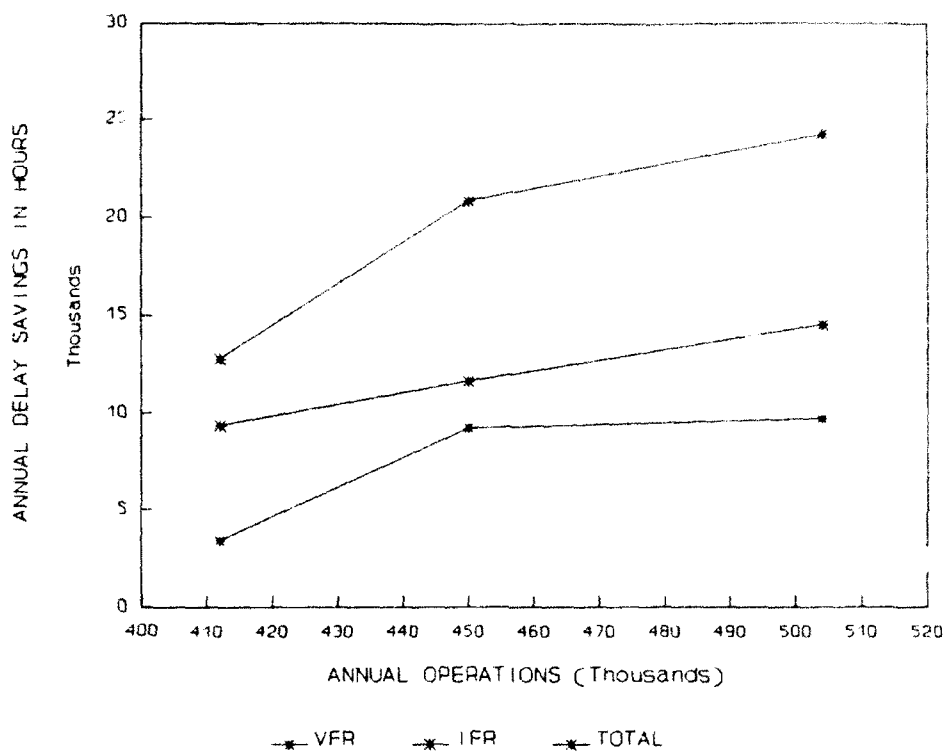
Figure 3. VAS annual delay savings at BOS.
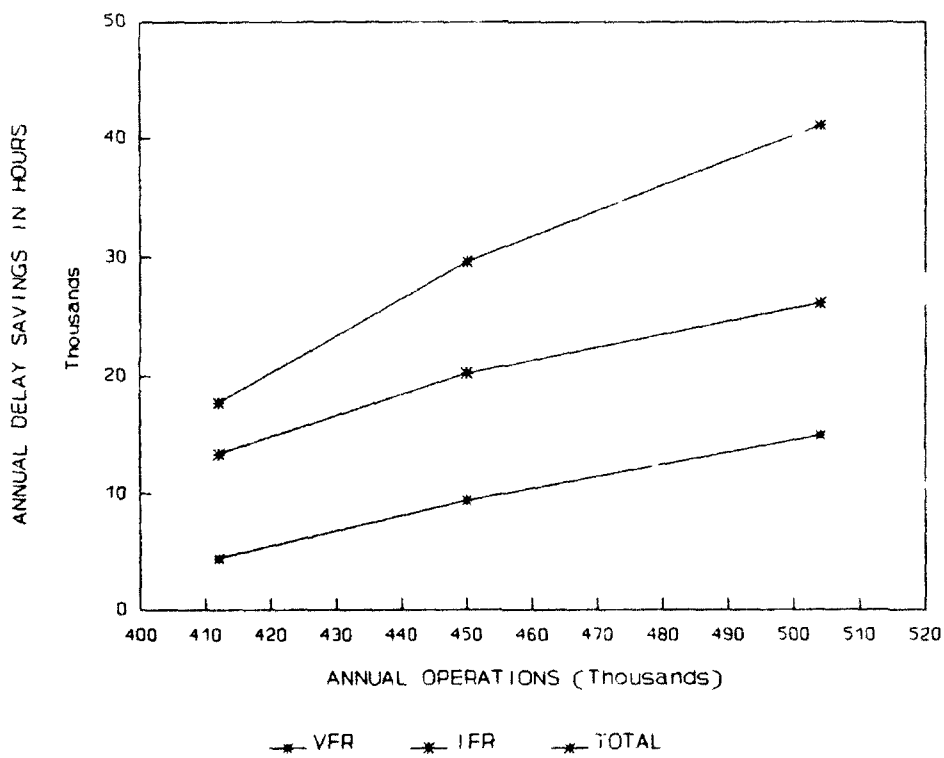
Figure 4. WVAS annual delay savings at BOS.
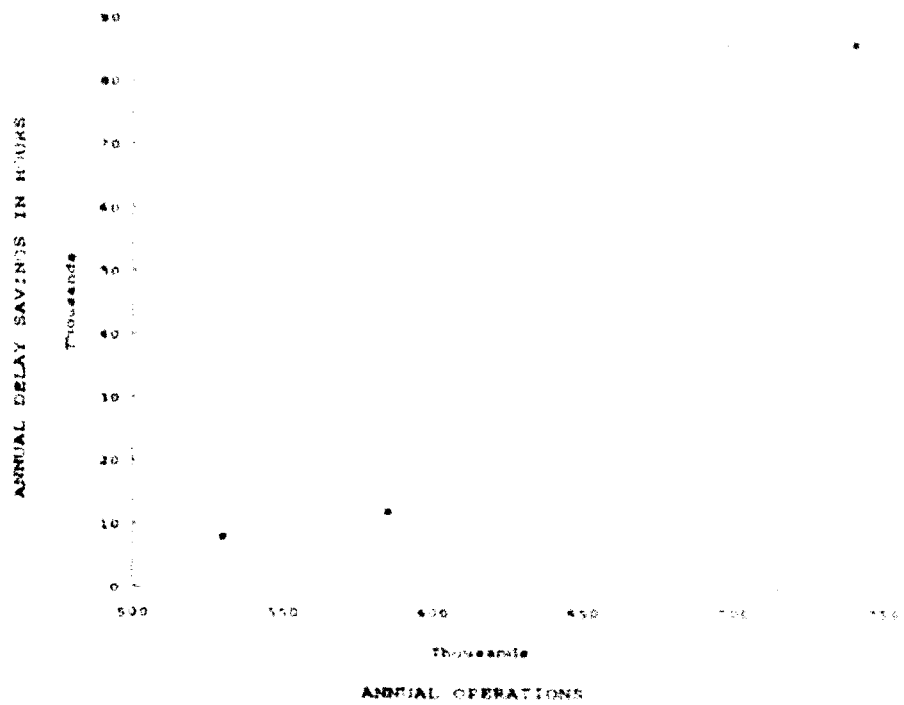
Figure 5. Wake vortex annual delay savings at STL - VFR.

Matrix A (DFW)

Miles Intrail

Lead Aircraft Category: Heavy   Large   Small

Following Aircraft

	Heavy	Large	Small
Heavy	4	2.5	2.5
Large	5	2.5	2.5
Small	6	4	2.5

[Caveat: The 2.5 above and similar coefficients below in the large leader category are to be used with the caveat that B-757 is treated as a heavy]

Matrix B. The Separation Rules possible under Advanced Wake Vortex Detection/Monitoring Systems for DFW.

Miles Intrail

Lead Aircraft Category: Heavy   Large   Small

Following Aircraft

	Heavy	Large	Small
Heavy	2.4	2.0	2.0
Large	3	2.0	1.9
Small	5	3	1.9

Matrix C for DFW.

Miles Intrail

Lead Aircraft Category: Heavy   Large   Small

Following Aircraft

	Heavy	Large	Small
Heavy	3	2.5	2.5
Large	5	2.5	2.5
Small	6	4	2.5

Figure 6. Wake vortex separation rules and assumptions used in the wake vortex benefits analysis.

Matrix A (ORD)

Miles Intrail

Lead Aircraft Category:	Heavy	Large	Small
Following Aircraft			
Heavy	4	2.5	3
Large	5	2.5	3
Small	6	4	2.5

[Caveat: The 2.5 above and similar coefficients below in the large leader category are to be used with the caveat that B-757 is treated as a heavy]

(2)   Matrix B. The Separation Rules possible under Advanced Wake Vortex Detection/Monitoring Systems for ORD.

Miles Intrail

Lead Aircraft Category:	Heavy	Large	Small
Following Aircraft			
Heavy	2	2	2
Large	3	2	2
Small	5	3	2

Matrix C for ORD.

Miles Intrail

Lead Aircraft Category:	Heavy	Large	Small
Following Aircraft			
Heavy	3	2.5	3
Large	5	2.5	3
Small	6	4	2.5

Figure 6. Continued.
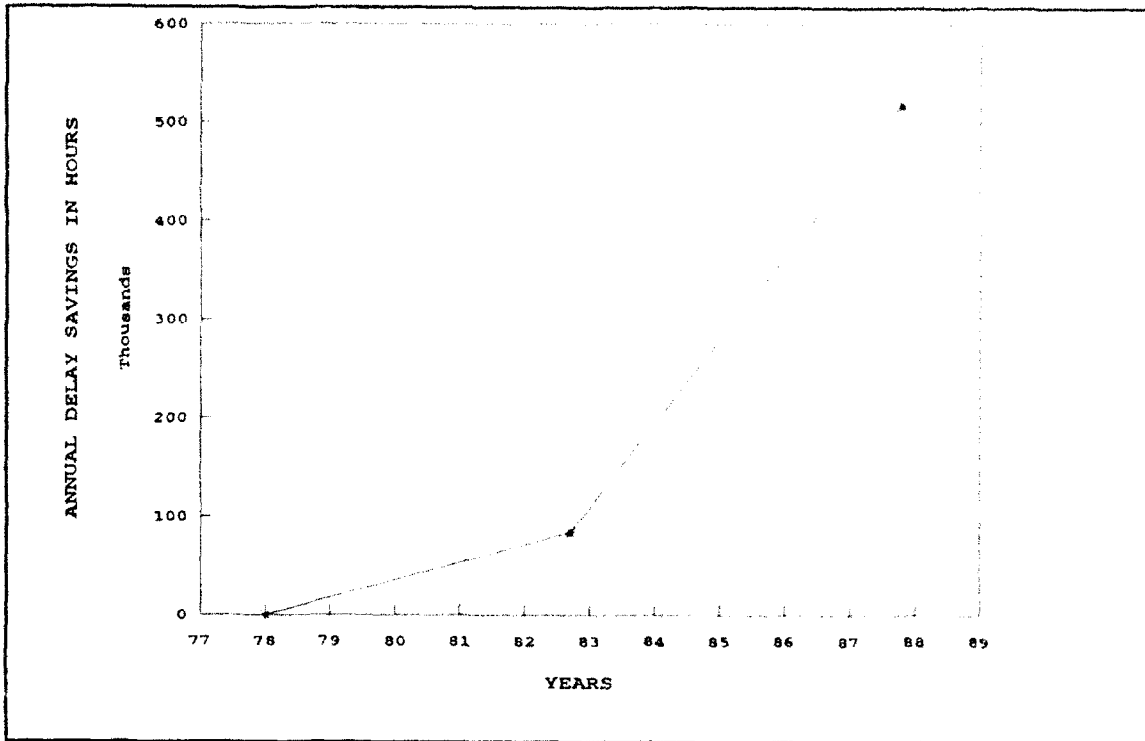
VAS ANNUAL SAVINGS (1982-1985)

Airport	Study Year	Forecast Year	Annual Operations	Savings in Hours
ATL	1980	1982	633,000	14,800
LAX	1981	1982	518,000	3,100
JFK	1981	1982	326,000	36,200
LGA	1981	1982	327,000	5,900
MIA	1981	1983	380,000	7,100
IAH	1983	1985	373,000	17,000
Total				84,100

WVAS ANNUAL SAVINGS (1987-1990)

Airport	Study Year	Forecast Year	Annual Operations	Savings in Hours
ATL	1980	1987	753,000	152,000
LAX		NOT STUDIED		
JFK	1981	1987	331,000	145,000
LGA	1981	1987	338,000	49,000
MIA	1981	1988	422,000	36,000
IAH	1983	1990	481,000	135,000
Total				517,000

Figure 7. Summary of VAS & WVAS annual delay savings.

APPENDIX A

Theoretical Minimum Intrail Arrival Separations

Current Separation Standards - IFR

Miles Intrail

Lead Aircraft Category:	Heavy	Large	Small
Following Aircraft			
Heavy	4	3	3
Large	5	3	3
Small	6	4	3

Current Separation Standards - VFR

Miles Intrail

Lead Aircraft Category:	Heavy	Large	Small
Following Aircraft			
Heavy	2.7	1.9	1.9
Large	3.6	1.9	1.9
Small	4.5	2.7	1.9

Proposed Separation Standards - Vortex Advisory System (VAS) - IFR

Miles Intrail

Lead Aircraft Category:	Heavy	Large	Small
Following Aircraft			
Heavy	3	3	3
Large	3	3	3
Small	4	3	3

Proposed Separation Standards - Wake Vortex Advisory System (VAS) - VFR

Miles Intrail

Lead Aircraft Category: Heavy   Large   Small

Following Aircraft

	Heavy	Large	Small
Heavy	2.7	1.9	1.9
Large	3	1.9	1.9
Small	4	2.7	1.9

Proposed Separation Standards - Wake Vortex Avoidance System (WVAS) - IFR

Miles Intrail

Lead Aircraft Category: Heavy   Large   Small

Following Aircraft

	Heavy	Large	Small
Heavy	2.5	2.5	2.5
Large	3	2.5	2.5
Small	3.5	3	2.5

Proposed Separation Standards - Wake Vortex Avoidance System (WVAS) - VFR

Miles Intrail

Lead Aircraft Category: Heavy   Large   Small

Following Aircraft

	Heavy	Large	Small
Heavy	2.5	1.9	1.9
Large	3	1.9	1.9
Small	3.5	2.7	1.9

The VAS and WVAS were two of the earlier products of the Wake Vortex Program. These separations were defined in the FAA's Report Number FAA-EM-78-8A, Parameters of Future ATC Systems Relating to Airport Capacity/Delay, Dated June 1978.

Proposed Separation Standards - Reduced Heavy-To-Heavy Scenario

Miles Intrail

Lead Aircraft Category: Heavy   Large   Small

Following Aircraft

	Heavy	Large	Small
Heavy	3	3	3
Large	5	3	3
Small	6	3	3

Proposed Separation Standards - Wake Vortex Detection/Monitoring System

Miles Intrail

Lead Aircraft Category: Heavy   Large   Small

Following Aircraft

	Heavy	Large	Small
Heavy	3	3	3
Large	3	3	3
Small	5	4	3

Proposed Separation Standards - Advanced Wake Vortex Detection/Monitoring System

Miles Intrail

Lead Aircraft Category: Heavy   Large   Small

Following Aircraft

	Heavy	Large	Small
Heavy	2	1	1
Large	3	2	1
Small	5	3	1

APPENDIX B

Computer Model and Methodology

RDSIM is the short form of ADSIM, the Airfield Delay Simulation Model. ADSIM is a fast-time, discrete event model that employs stochastic processes and Monte Carlo sampling techniques. It describes significant movements by aircraft on the airport and the effect of delay in the immediate airspace. ADSIM was validated in 1978 at Chicago's O'Hare International Airport against actual flow rates and delay data.

RDSIM simulates demand only for the runways and does not consider the taxiway network or the terminal complexes. It provides both capacity and delay information.

Delay Analysis

The experiments were repeated 40 times using Monte Carlo sampling techniques to introduce system variability into each run. The results were then averaged to produce the capacity/delay outputs for a given demand level. Using the same aircraft mix, computer specialists simulated different demand levels for each improvement to generate demand versus delay relationships.

Capacity Analysis

The arrival capacity for the generic runway was calculated using RDSIM. The maximum throughput capacities were based on unlimited arrival and departure queues.

APPENDIX C

The SIMMOD Model

SIMMOD is a comprehensive airport and airspace simulation model developed by the FAA (via contractor assistance). It is designed to be applicable to the study of airfield systems, single or multiple airports, terminal areas, and enroute airspace. SIMMOD simulates and tracks the movements of all individual aircraft from the time they push back from a gate and taxi to the runway, to landing and arrival at the gate of destination. Randomness in departures, arrivals, flight times, and other factors can be introduced to vary the output of successive runs.

The FAA designed SIMMOD to integrate the modeling of airport and airspace operations, and thus to be effective in analyzing the effects of airspace changes on ground operations and vice versa. The model can be used to evaluate proposed changes in aircraft scheduling, runway or taxiway improvement or impairment, facilities or navaid location, airspace design change, air traffic control procedural change, or a change in management. The modeler can set SIMMOD to produce statistical output giving travel times and delays, system capacity, and economic and environmental impacts.

Since its development, SIMMOD studies have been performed for a number of domestic and foreign airports/airspaces. Several consulting companies, airports and airport authorities, aircraft companies, and foreign governments as well as agencies of the FAA, have obtained and are using the model. A total of 88 copies of the model have been distributed at $250 each (plus a yearly charge of $250) and an active users group has developed.

SIMMOD is a complex model to set up, calibrate, and operate. It requires that a detailed description of the airport and airspace system be created in the form of SIMMOD input files. As a result, a considerable effort must be invested upfront before the model can be used for effective policy analysis at a new airport or airspace. The model is built and tested using actual data from "typical days" and hence policy analysis that is intended to study aberrant situations must be approached with caution. Once the work to perform a SIMMOD study is done, however, the input data can be easily modified and the model rerun to simulate "what if" scenarios at relatively low cost. Several airport and airport/airspace combinations have already been modeled.

EFFECT OF WAKE VORTEX INTERACTION ON DELAYS AT LAGUARDIA AIRPORT

William J. Dunlay, Jr.
KPMG Peat Marwick

James P. Muldoon
The Port Authority of New York and New Jersey

BACKGROUND

One of the primary runway use configurations at LaGuardia Airport (LGA) involves arrivals on Runway 22 and departures on Runway 31. The FAA requires a standard two-minute wake turbulence separation between a heavy jet departure on Runway 31 and an arrival on Runway 22. (See Figure 1.)

This wake-vortex interaction manifests itself mainly as large arrival delays, because controllers in the LGA Tower must ask the New York TRACON to create and maintain a 6 to 7 nautical mile gap between arrivals for each heavy jet departure.

This interaction is one of the major causes of delays at LGA and is expected to worsen in the future with an expected increasing percentage of heavy jet aircraft in the mix. (In 1986, this percentage was forecast to increase from 10% in 1985 to 20% by 1995. This forecast increase has not yet materialized; in 1990, only 6% of aircraft were heavy jets. However, this percentage is still expected to increase substantially in the future.)

Because of this wake-vortex interaction, the runway use with arrivals on Runway 22 and departures on Runway 31 involves much higher arrival delays than the other two major runway uses at LaGuardia: (1) arrive Runway 22 and depart Runway 13, and (2) arrive Runway 4 and depart Runway 13. These other two runway uses do not require wake-vortex separations between intersecting runway operations. It is judged that, if there were no wake vortex interaction between departures on Runway 31 and arrivals on Runway 22, all three runway uses would have similar aircraft delay levels.

Average daily arrival delays for the three main runway uses at LaGuardia Airport are shown in Figure 2.

PURPOSE

The purpose of this paper is to summarize the results of an airfield simulation analysis of the effects of the expected increase in the number of heavy jet aircraft at LaGuardia Airport on aircraft delays for the runway use involving arrivals on Runway 22 and departures on Runway 31.

INPUT DATA AND ASSUMPTIONS

As mentioned above, for the runway use involving arrivals on Runway 22, a special gap must be created in the arrival stream for each heavy jet departure in order to provide the required 2-minute wake turbulence separation at the intersection. FAA Tower controllers at LaGuardia Airport estimate that about one out of every four interarrival gaps so created is lost (i.e., the gap becomes too small to be used) or missed. Actual field measurements showed that more than 25% of the interarrival gaps created for heavy jet departures were lost or missed because the gap would shrink by as much as 30% to 40% below the required gap and would therefore be unusable.

The FAA Airfield Delay Simulation Model (ADSIM) was used for the analysis. A special feature was programmed into the ADSIM model to reflect the effects of missed interarrival gaps described above.

Wake turbulence rules would imply that a departure-arrival separation of 160 seconds should be used in the ADSIM model to reflect this interaction. The field observations also showed that the wake-vortex, departure-arrival separations actually imposed behind heavy jet departures averaged less than 160 seconds. Nevertheless, the 160 second separation was used in the analyses described in this paper, except where otherwise noted.

A demand level of 1,058 daily aircraft operations was assumed for 1985 with about 10% heavy jets; a daily demand level of 1,100 aircraft operations was assumed for 1995 with about 20% heavy jets.

RESULTS OF SIMULATION ANALYSIS

The main technical results of the LaGuardia Airport airfield simulation analysis of the runway use involving arrivals on Runway 22 and departures on Runway 31 are summarized in the following paragraphs.

Baseline VFR Arrival Delays

The average daily arrival delays in VFR conditions were estimated assuming both the standard departure-arrival separation and the actual measured departure-arrival separations.

The average daily arrival delays estimated assuming the standard separations were about 34 minutes and 93 minutes for 1985 and 1995, respectively. The average daily arrival delay

28-2

estimates assuming the actual separations were about 22 and 73 minutes for 1985 and 1995, respectively. These delay estimates are summarized in Table 1.

Thus, under VFR conditions, which occur about 90% of the time at the Airport, very high arrival delays would occur because of the wake turbulence interaction between heavy jet departures on Runway 31 and arrivals on Runway 22 and the expected increase in the percentage of heavy jet aircraft in the mix (20% by 1995). The following actions were identified as possible ways of alleviating these very high delays:

o   Reduce general aviation and commuter traffic at the Airport.

o   Encourage general aviation and commuter aircraft to land as much as feasible on Runway 31 instead of Runway 22.

o   Combination of both the above changes in general aviation and commuter operations.

o   For the purposes of this specific case, reclassify A-300/310 and B-767 aircraft as "large" aircraft rather than "heavy," or designate "heavy" departures on the basis of the actual takeoff weight of the aircraft rather than on maximum takeoff weight capability.

o   Limit the growth of heavy jet operations at the Airport and accept a corresponding increase in overall aircraft operations to provide equivalent seating capacity. Before considering this change, it would be critical to estimate its effects on aircraft delays for the other major runway uses and weather conditions at the Airport.

Reduction in General Aviation and Commuter Traffic

The effects of a 50% reduction in general aviation and commuter traffic on the arrival delays were analyzed for 1995. As shown in Table 2, the assumed reduction in general aviation and commuter traffic would reduce the arrival delays to about the level estimated for 1985 (about 35 minutes per operation).

General Aviation and Commuter Landings on Runway 31

An analysis was performed of the effects on arrival delays of having about 50% of the general aviation and commuter traffic land on the main departure runway, Runway 31, instead of on the main arrival runway, Runway 22. As shown in Table 3, the resulting arrival delay estimate was about 29 minutes per operation.

Combination of Changes in General Aviation and Commuter Operations

The combined effects on arrival delays of (1) reducing general aviation and commuter traffic, *and* (2) landing half the general aviation and commuter traffic on Runway 31 were also analyzed. As shown in Table 3, the arrival delay estimate for this combined case was only about 11 minutes per operation, which is roughly the level of the 1985 VFR arrival delays estimated for the other two runway uses.

Reclassification of B-767, A-300/310

An additional test case was run to analyze the effects of an assumed reclassification of B-767 and A-300/310 aircraft from heavy to large for purposes of this wake-vortex interaction. As shown in Table 4, a significant reduction in average arrival delay (from 93 minutes per operation to 49 minutes per operation) could be expected from such a reclassification.

No Future Increase in the Use of Heavy Aircraft

Significantly lower arrival delays were estimated for 1995 by assuming: (1) no increase in the number of heavy aircraft operations in 1995 over the 1985 level, and (2) an increase in narrowbody aircraft operations to provide the same aircraft seating capacity equivalent to the baseline 1995 demand level. Specifically, in this test case, total daily operations were assumed to be 1,166 with 10% heavy aircraft in the mix, or 66 more daily operations than with the 20% heavy aircraft assumed in the baseline 1995 demand schedule of 1,100 daily operations.

As shown in Table 5, the estimated average daily arrival delay for this test case was about 54 minutes per operation, or about 39 minutes per operation lower than the baseline delay estimate of 93 minutes per operation.

Figure 3 presents a graphical summary of the arrival delay estimates under VFR conditions for the baseline conditions and for conditions with the potential improvements described above.

Why Such Large Arrival Delays?

The wake-turbulence interaction between heavy jet departures on Runway 31 and arrivals on Runway 22 manifests itself mainly as large arrival delays, rather than large departure delays, because controllers in the TRACON must create and maintain a special gap in the arrival stream in which to release a heavy jet departure; a non-heavy departure can be released in a "normal" gap between arrivals without delaying an arrival. Thus, this interaction is unusual in that (1) arrivals must be delayed to release only one weight class of departures, and (2) heavy jet departures are usually given priority over arrivals.

Nevertheless, under existing wake-vortex rules such a procedure is necessary so that heavy jet departures, and other aircraft behind them, are not unduly penalized.

Interpreting the Large Arrival Delays

The large arrival delays presented in this paper were estimated using the FAA's ADSIM model and conservative assumptions about current ATC separation rules and procedures. In addition, these arrival delay estimates represent "total" arrival delay without regard to whether the delays would be incurred (1) in holding at the Airport or in the enroute airspace, or (2) at the "upline" airport in the form of a flow-control delay.

The delay estimates presented in this paper are best interpreted as indexes of operating efficiency that are intended for use in comparing alternatives. The absolute values of the delay estimates are only approximate, and actual delays would depend on precisely how the ATC rules would be interpreted and executed by the controllers in the LGA Tower and the New York TRACON. For example, as mentioned earlier, field measurements have shown that the wake-vortex departure-arrival separations actually imposed behind heavy jets on Runway 31 were, on the average, less than a strict interpretation of the wake-vortex rules would imply. Furthermore, when the actual measured separations were used in the ADSIM model, the resulting delay estimates were about 21% to 35% lower than those estimated using the standard separations.

Therefore, the arrival delay estimates presented in this paper are conservative, worst-case values and should be interpreted with caution. Nevertheless, they indicate that delays will become much worse with increased heavy jets and actions will be necessary to reduce those delays to reasonable levels.

SUMMARY AND CONCLUSIONS

Assuming the forecast doubling of heavy-jet operations by 1995, it was estimated that the average arrival delays for the runway use involving arrivals on Runway 22 and departures on Runway 31 would triple, compared with 1985 arrival delays, because of the required wake turbulence separations. Potential ways to reduce these delays were considered, including:

o   Reclassifying (for this "right angle" wake-vortex interaction) the A-300/310 and B-767 aircraft as "large" aircraft rather than "heavy" aircraft; or, equivalently, designating "heavy" jet departures on the basis of actual takeoff weight at LGA rather than maximum takeoff weight capability. A significant reduction in average arrival delay (of about 47%) was estimated for such a reclassification.

o   Limiting the number of heavy jet operations to 1985 levels and assuming a corresponding increase in overall aircraft operations that provides the same seating capacity as in the 1995 forecast. The corresponding average arrival delay was estimated to be 42% less than the delay estimated for the forecast 1995 number of heavy jet operations.

o   Other "demand-management" options, including limiting commuter and general aviation operations.

Since this analysis was completed in 1986, a number of follow-on investigations have been completed by Lockheed Missiles and Space Company under contract to the Port Authority of New York and New Jersey. These investigations will be discussed in a related conference paper by William R. Eberle, et al.

Table 1. Average Daily Arrival Delay Estimates

| Year | Average daily arrival delay (minutes per operation) | |
	Standard separations	Actual measured separations
1985 (10% heavy jets)	34	22
1995 (20% heavy jets)	93	73

Table 2. Arrival Delay Reduction Due to Reduced 1995 General Aviation and Commuter Demand

Assumed 1995 general aviation and commuter demand	Total 1995 daily operations	Average 1995 daily arrival delay (minutes per operation)
Full forecast	1,100	93
50% reduction	951	35

Table 3. Arrival Delays Using Runways 22 and 31

Assumed general aviation and commuter landings	1995 average daily arrival delay (minutes per operation)
All on Runway 22	93
50% on Runway 31	29
Combined: 50% reduction and 50% landing on Runway 31	11

Table 4. Effect of Reclassification of B-767, A-300/310 on Arrival Delays

Classification of A-300/310 and B-767	1995 average daily arrival delay (minutes per operation)
Heavy	93
Large	49

Table 5. Estimated 1995 Arrival Delays of Baseline and Reduced Heavy Aircraft Levels

1995 total daily operations	Percent heavy aircraft	Average daily arrival delay (minutes per operation)
1,100	20%	93
1,166	10%	54
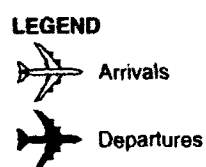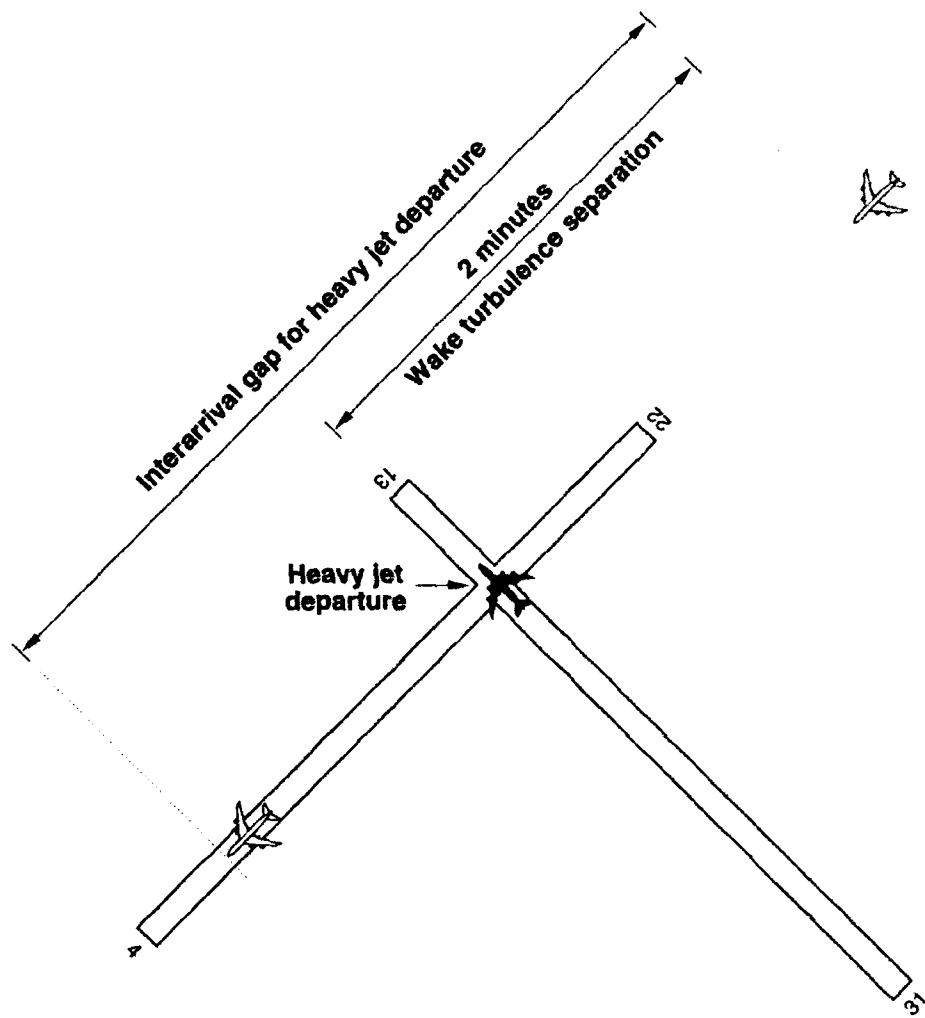
Figure 1. Wake turbulence separation behind heavy jet departures on runway 31.
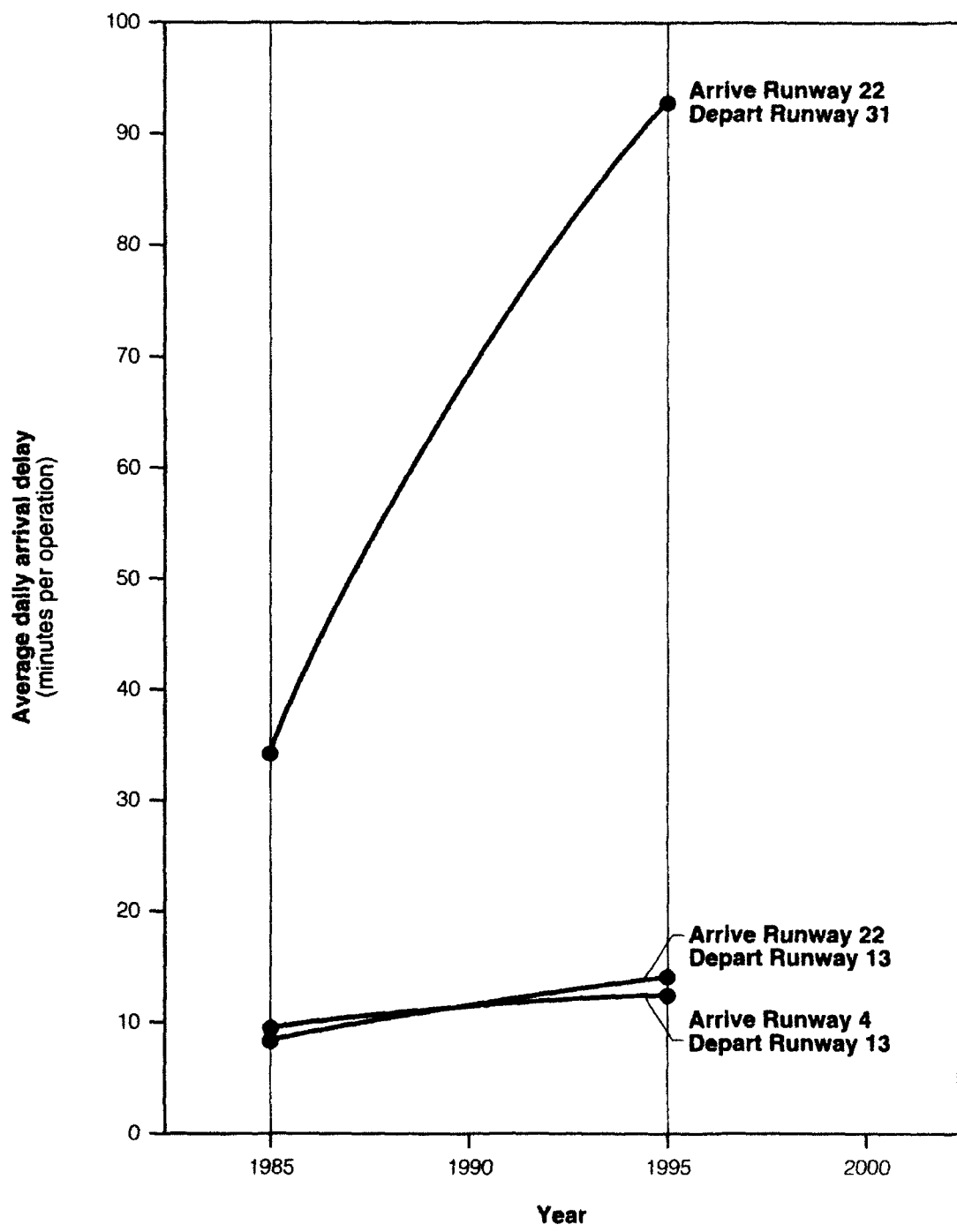
Figure 2. Average daily arrival delay: VFR conditions.
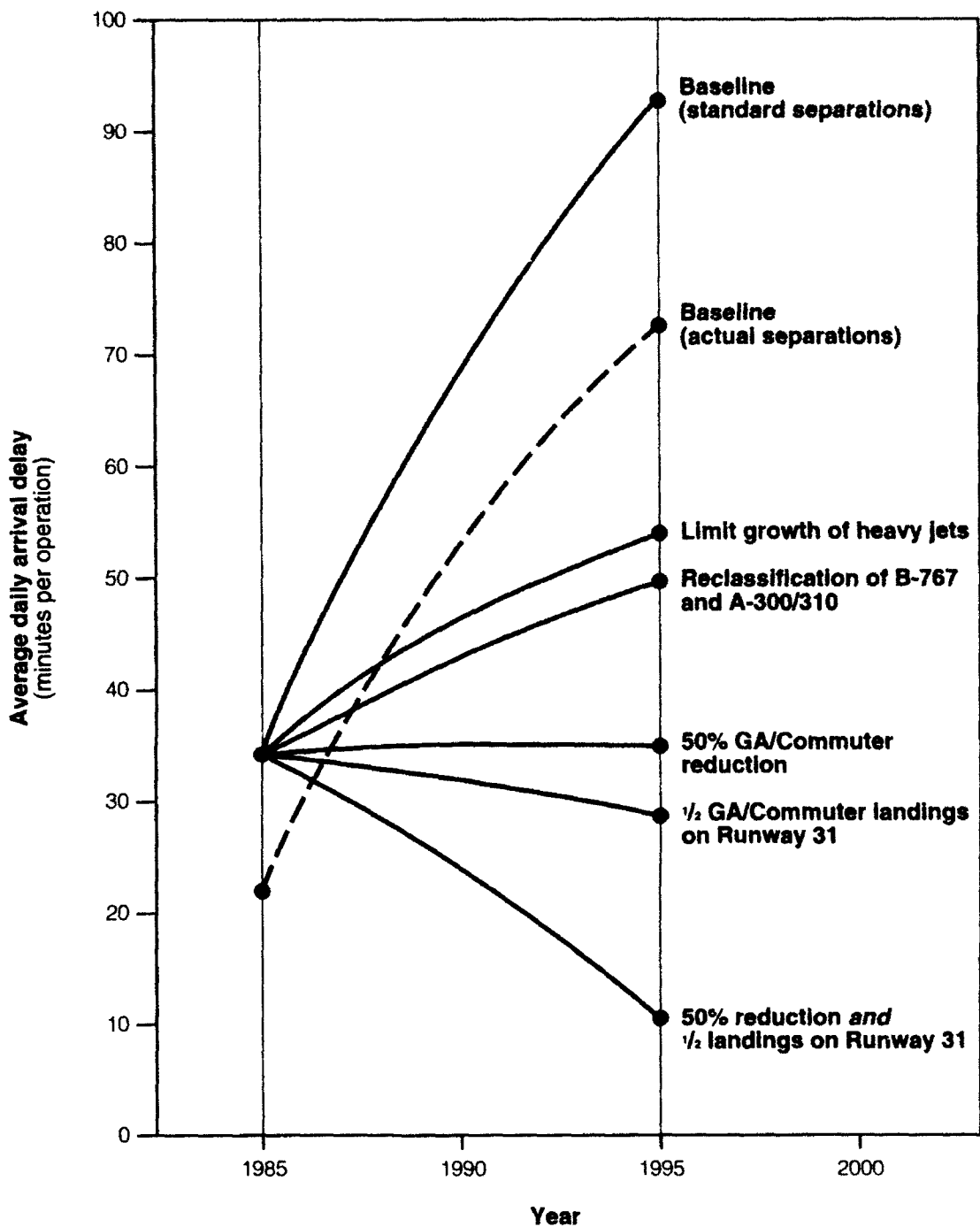
Figure 3. Average daily arrival delay: VFR conditions,
arrivals on runway 22 and departures on runway 31.

THE BENEFITS OF REDUCED SEPARATION STANDARDS
AT CHICAGO O'HARE INTERNATIONAL AIRPORT

Mary Rose Loney
First Deputy Commissioner
City of Chicago Department of Aviation

Douglas F. Goldberg
Landrum & Brown, Inc.
Cincinnati, Ohio

ABSTRACT

In its recently published study, the Chicago Delay Task Force, a tripartite FAA/City/Airline group organized to examine ways to reduce delays in the Chicago airport airspace system, recommended further examination of reduced wake vortex separation standards. The extent of the operational improvement afforded by reduced wake-vortex separation standards depends on a number of factors unique to an individual airport, including aircraft fleet mix, distribution of aircraft demand, runway geometry, and runway utilization. Therefore, an accurate assessment of the benefits of reduced separation standards must be very site specific.

In this paper, data collected for the Chicago Delay Task Force Study serve as the basis for an assessment of the operational benefits of reduced wake-vortex separation at Chicago O'Hare International Airport, using AIRSIM, an FAA approved airspace/airfield simulation model. Existing wake-vortex separation standards are simulated as the baseline scenario, while the aircraft separation research goals defined in the FAA Wake Vortex Research Program Plan are simulated as the test-case scenario. The operational benefits of reduced wake-vortex separation standards are defined as the difference in aircraft operational delays incurred under the test-case scenario relative to the performance of the baseline scenario. In addition, the effect on delay of changes in operating factors, such as fleet mix and meteorological conditions, is examined with respect to reduced separation standards.

This assessment demonstrates the ability to reduce annual delays at O'Hare by more than 10,000 hours with reduced wake-vortex separation standards, reflecting a direct airline operating cost savings of $20 million per year. In addition, the analysis suggests that the expected delay reduction increases: 1) as the percentage of "Heavy" (i.e., 300,000 pounds or greater) aircraft increases; 2) as the level of ATC coordination decreases; and 3) as the level of demand approaches airport capacity.

STUDY ASSUMPTIONS AND METHODOLOGY

Introduction

In response to a recommendation of the 1991 Chicago Delay Task Force, a simulation analysis was conducted to define the operational benefits expected to result at Chicago O'Hare International Airport upon implementation of the target separation standards defined in the FAA's Wake Vortex Research Program Plan. This paper summarizes the assumptions, methodology and findings of that analysis.

The operational impact of reduced wake vortex arrival separation standards at O'Hare was defined using AIRSIM, an airspace/airfield computer simulation model reviewed and accepted by the FAA. This analysis involved the evaluation of airfield operating performance with existing separation standards for comparison with the performance expected to occur with revised separation standards. The database developed for the Chicago Delay Task Force Study served as the "existing condition" Baseline which reflects the 1988 Chicago airfield/airspace operating environment, including August 1988 aircraft demand characteristics and existing aircraft separation standards. Simulation experiments were conducted using this database to define Baseline aircraft operational delays.

The Baseline 1988 O'Hare data was subsequently modified to reflect the target wake vortex separation standards defined in the FAA Wake Vortex Research Program Plan. Simulation experiments were conducted with the modified database to define the level of operational delays expected to occur at O'Hare with the use of reduced arrival separation standards. In addition, a set of simulation experiments was conducted to define the effect of changing the aircraft fleet mix on operational delays with both the existing and targeted aircraft separation standards. As shown in Figure 1, four simulation scenarios were examined, each of which includes five primary O'Hare runway operating use plans.

Elements of the Chicago airspace/airfield operating environment which influence the impact of reduced wake vortex separation standards include: 1) Runway Operating Plans, 2) Aircraft Separation Standards, and 3) Aircraft/Demand/Characteristics.

The sections which follow elaborate on each of these elements as they pertain to the simulation analysis.

Runway Operating Plans

The five primary runway operating plans illustrated in Figure 2 were simulated in this analysis. Three of the five plans are used during Visual Meteorological Conditions (VMC), in which the ceiling is at least 1,000 feet above ground level and the visibility is at least three statute miles and visual flight rules (VFR) are in use. The remaining two plans are used during Instrument Meteorological Conditions (IMC), in which the ceiling is less than 1,000 feet or the visibility is less than three statute miles and instrument flight rules (IFR) are in use. The annual percent utilization associated with each of the five runway operating plans is also shown, based on historical weather data, O'Hare ATC records and controller preferences. These percentages were

29-2

used to calculate average VFR, IFR and all-weather delay per operation. Actual FAA Air Traffic Control (ATC) operating practices vary among each of the runway use plans and were reflected in the simulations. Under VFR conditions, the dynamic use of a third arrival or departure runway at O'Hare to accommodate peak period demand is critical to the efficient operation of the Airport. Other ATC procedures applicable at O'Hare were reflected in the simulations, including use of "land and hold short" procedures, intersection takeoffs, and additional separation requirements.

Aircraft Separation Standards

Existing and targeted separation standards for successive aircraft arrivals are shown in Figure 3. The proposed standards include modifications to existing aircraft classifications, in terms of gross weight ranges, as well as the introduction of a "medium" aircraft classification. Current separation requirements are equivalent for all aircraft types with a maximum gross takeoff weight between 12,500 pounds and 300,000 pounds (i.e., large aircraft). The proposed revisions achieve a reduction in average separation by subdividing the "large" aircraft category into smaller categories commensurate with each aircraft's wake vortex characteristics. The most significant revision to existing separation standards occurs in the "medium" aircraft category. The effect of the proposed classification system at O'Hare is discussed in Section 3 "Aircraft Demand Characteristics". Existing standards are defined in FAA Order 7110.65f, Air Traffic Control, while the proposed standards are identified as research goals in the Wake Vortex Research Program Plan.

Aircraft Demand Characteristics

An aircraft flight schedule reflecting August 1988 peak month average weekday (PMAWD) aircraft activity was used in this analysis. This schedule, which contains 2,350 aircraft operations, was developed for the Chicago Delay Task Force based on information contained in the August 1988 edition of the Official Airline Guide and FAA O'Hare Tower Records. The August 1988 total aircraft operations fleet mix is summarized in Figure 4 for the existing and proposed classifications.

In order to identify the sensitivity of performance to aircraft fleet mix, the Baseline August 1988 flight schedule was modified to contain 25 percent "heavy" aircraft. The total number of operations and the hourly distribution remained identical to the Baseline schedule. The resulting total aircraft operations fleet mix is summarized in Figure 5.

The airfield/airspace operating environment unique to O'Hare, as described in this section, significantly influences operational performance with both existing and future wake vortex separation standards. The following section describes the delay impact of implementing reduced arrival separation standards at O'Hare.

SIMULATION RESULTS

The average all-weather delay per operation is summarized on Figure 6 for each scenario. As shown, use of reduced arrival separation standards is expected to reduce delay at O'Hare by 10.2 percent with the August 1988 flight schedule, and by 9.5 percent with the heavy fleet mix flight schedule. The level of ATC coordination necessary between arrivals and departures varies among runway operating plans at O'Hare due to intersecting and mixed runway operations. As a result, operational delays also vary among each of the runway operating plans as shown on Figure 7, which compares average delay per operation under the August 1988 flight schedule. The variability in operational performance by runway use plan affects the impact of reduced wake vortex arrival separation standards, as follows: The delay reduction is greater under runway operating plans with relatively low interactions between aircraft arrivals and departures.

The delay reduction is greater during IFR conditions than during VFR conditions. The reduced separation standards produced a greater savings in delay with the heavy fleet mix flight schedule than with the August 1988 flight schedule.

To facilitate review of the simulation results, this section is organized as follows: 1) Impact of Arrival/Departure Interactions, 2) Impact of VFR/IFR Weather Conditions, 3) Impact of Heavy Fleet Mix, and 4) Delay Cost Impact.

The following paragraphs elaborate upon the delay reduction benefit associated with the implementation of reduced arrival separation standards at O'Hare.

Impact of Arrival/Departure Interactions

The simulation analysis demonstrated that arrival/departure coordination significantly affects the impact of reduced wake vortex arrival separations. As would be expected, a reduction in arrival separation increases arrival throughput and subsequently decreases arrival delay. However, the increased arrival throughput often results in additional departure delays, particularly under runway operating plans that require high levels of departure coordination. The relationship between average arrival delay and average departure delay is illustrated on Figure 8. In each case, the reduction in arrival delay is greater than the increase in departure delay, thereby producing a net reduction in average delay per aircraft operation.

Runway Operating Plans VFR-1 and IFR-1 both require high levels of ATC coordination between aircraft arrivals and departures, primarily due to the use of intersecting and mixed operations runways. Under VFR-1, Runway 32R departures must be coordinated with Runway 27R arrivals, Runway 27L departures must be coordinated with Runway 32L arrivals, and Runway 32L departures must be coordinated with Runway 32L arrivals. Under IFR-1, departures from Runways 9L and 9R must be coordinated with arrivals on Runways 14L and 14R, respectively. The coordination between arrivals and departures under these configurations limits the ability to apply reduced arrival separation standards. As a result, the full delay reduction benefit of reduced arrival separation cannot be achieved.

The simulations demonstrated that the level of delay reduction expected to result from reduced separation standards increases as the level of arrival/departure coordination decreases. Reduced arrival separation is expected to produce greater delay reduction benefits under runway operating plans in which arrival runways are relatively independent from departure runways, such as VFR-2, VFR-3 and IFR-2 at O'Hare.

Impact of VFR/IFR Conditions

The simulation analysis demonstrated that the delay reduction benefits of reduced separation standards are greater under IFR conditions than under VFR conditions, as shown in Figure 9.

The percent delay reduction attributable to reduced separation is over 4.6 times greater under IFR conditions than under VFR conditions. Under VFR conditions, pilots are able to see the preceding aircraft, and thus, can often adjust the aircraft's flight path to avoid the leading aircraft's wake vortices. ATC may issue wake vortex advisories but is not responsible for maintaining separation under visual conditions. Rather, pilots are required to "see and avoid" other aircraft under VFR conditions. Under IFR conditions, ATC is responsible for assuring minimum in-trail separation between successive aircraft arrivals. As a result, average VFR separations are often less than average IFR separations. Under IFR conditions, therefore, a greater opportunity exists to reduce delay by reducing separation standards.

Moreover, capacity at O'Hare is substantially more constrained under IFR conditions than under VFR conditions. Under VFR conditions, controllers have greater flexibility in selecting runways to minimize the impact of wake vortex separation requirements. Land and hold short procedures and triple runway configurations, for example, are used under VFR conditions to enhance operational efficiency.

Such techniques are currently not applicable under IFR conditions, and thus, existing wake vortex separation requirements result in a greater impact on delay under IFR conditions than under VFR conditions. Consequently, a greater opportunity exists to reduce IFR delays than VFR delays by reducing separation standards. This relationship also suggests that reduced separation standards will have a greater delay reduction impact under conditions in which the level of demand approaches operational capacity.

Impact of Heavy Fleet Mix

As would be expected, average delays are consistently higher with the heavy fleet mix schedule, which contains 25.0 percent heavy aircraft, than with the August 1988 flight schedule, which contains 14.5 percent heavy aircraft. Figure 10 compares average VFR, IFR and all-weather delay for each scenario. On an all-weather basis, average delay per operation is approximately 20 percent higher with the heavy fleet mix flight schedule than with the August 1988 flight schedule. This is due to the additional separation required to protect trailing aircraft from the wake vortices created by leading heavy aircraft.

Similar to the August 1988 flight schedule scenario, reduced arrival separation results in a decrease in arrival delay and an increase in departure delay. However, the percent increase in departure delay is typically less with the heavy fleet mix flight schedule than with the August 1988 flight schedule. This relationship suggests that the reclassification of aircraft types in conjunction with heavy aircraft separation requirements facilitates the release of departures on dependent runways when the schedule contains a greater percentage of heavy aircraft.

Delay Cost Impact

Average aircraft operating costs were developed for the August 1988 flight schedule and the heavy fleet mix flight schedule to define the economic impact of reduced arrival separation standards. The cost of delay is estimated to be $30.41 per minute with the August 1988 flight schedule and $31.75 per minute with the heavy fleet mix flight schedule. The calculation of the direct economic benefit of reduced arrival separation standards is shown on Figure 11 based on the expected reduction in average delay per operation.

As shown, the direct economic impact of reduced separation standards is significant, even with the August 1988 fleet mix. A greater economic benefit can be expected as the percentage of heavy aircraft in the flight schedule increases due to a greater savings in delay per operation as well as a higher average operating cost associated with heavier aircraft. Historically, the average number of seats per departure has increased at O'Hare over the years, which indicates growth in the percentage of heavy aircraft.

Assuming this trend continues, the economic impact of reduced separation standards is expected to increase in future years. Figure 12 summarizes the delay reduction benefits of reduced arrival separation standards at O'Hare.

Based on the August 1988 flight schedule, reduced arrival separation at O'Hare is estimated to reduce delays by 10,850 hours annually, reflecting a savings of $19.8 million in direct aircraft operating costs. With the heavy fleet mix flight schedule, the annual delay hour savings would be 11 percent higher: a reduction of 12,060 annual delay hours reflecting $23.0 million savings in direct aircraft operating costs.

This analysis demonstrates that significant reductions in delay costs would result at O'Hare given the opportunity to safely reduce wake vortex arrival separation standards. Delay savings of this magnitude warrant continuation of the Wake Vortex Research Program Plan not only for operational benefits at O'Hare but at airports throughout the nation.

Scenario	1 (baseline)	2	3	4
Separation Standards	Existing	Future	Existing	Future
Percent Heavy Operations	14.5%	14.5%	25.0%	25.0%
Design Day Aircraft Operations	2,350	2,350	2,350	2,350
Number of Runway Operating Plans — VFR	3	3	3	3
Number of Runway Operating Plans — IFR	2	2	2	2

Prepared by Landrum & Brown, March 19, 1991.

Figure 1. Experimental design.
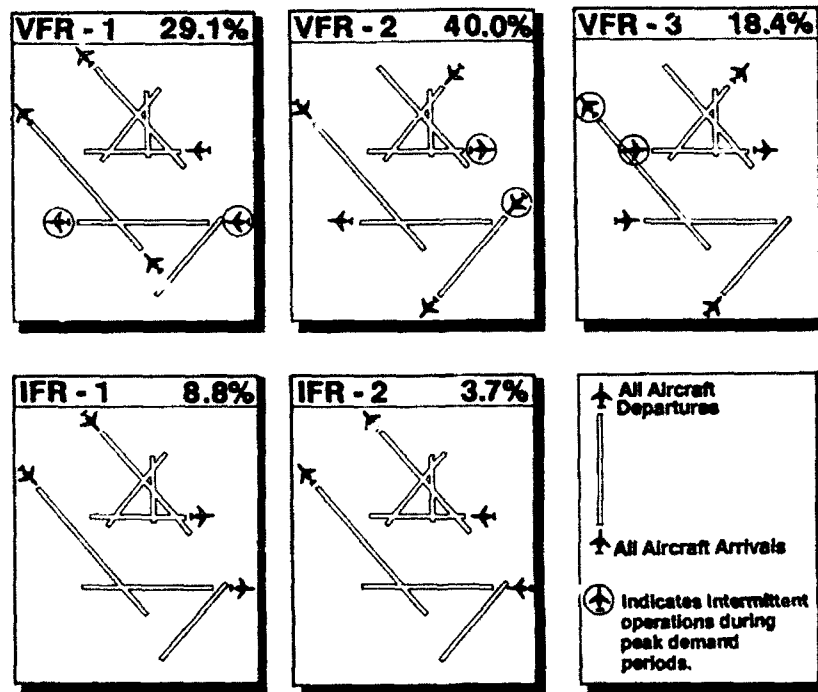
Figure 2. Simulated runway operating plans.

Existing Aircraft Separation Standards

Following Aircraft Classification	Maximum Certified Gross Takeoff Weight (Pounds)	Lead Aircraft (Wake Generating)		
		Small	Large	Heavy
Heavy	Weight(W) > 300,000	3.0	3.0	4.0
Large	12,500 < (W) < 300,000	3.0	3.0	5.0
Small	(W) < 12,500	3.0	4.0	6.0

Proposed Standards for Aircraft Separation

Following Aircraft Classification	Maximum Certified Gross Takeoff Weight (Pounds)	Lead Aircraft (Wake Generating)			
		Small	Medium	Large	Heavy
Heavy	(W) > 300,000	3.0	3.0	2.5	3.0
Large	90,000 < (W) < 300,000	3.0	3.0	2.5	4.0
Medium	19,000 < (W) < 90,000	2.5	2.5	3.0	5.0
Small	Weight(W) < 19,000	2.5	2.5	4.0	6.0

Prepared by Landrum & Brown, February 13, 1991.

Figure 3. Arrival separation standards (nautical miles).

29-8
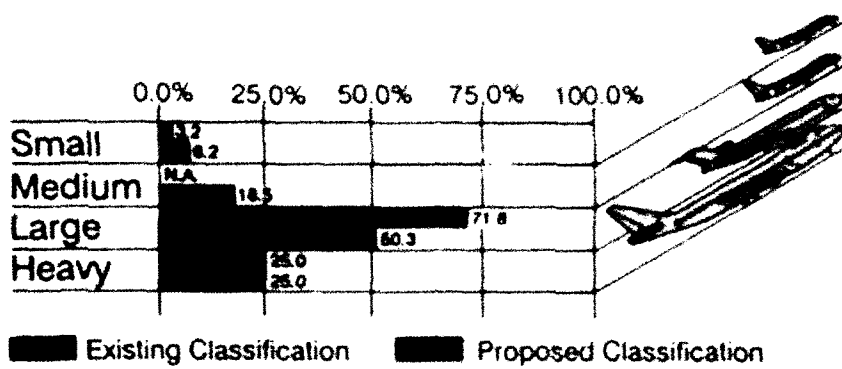
Figure 4. August 1988 flight schedule fleet mix distribution.
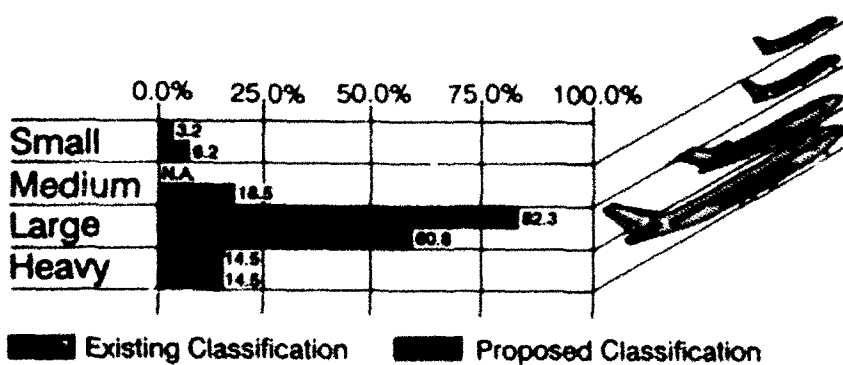
Figure 5. "Heavy fleet mix" flight schedule fleet mix distribution.

| Fleet Mix	Separation Standards		Delay Reduction	
	Existing	Future	Minutes	%
14.5% Heavy	8.8 Min.	7.9 Min.	0.9 Min.	10.2%
25.0% Heavy	10.5 Min.	9.5 Min.	1.0 Min.	9.5%
Delay Increase	1.7Min.	1.6 Min.		
% Change	19.3%	20.3%		

Figure 6. Average all-weather delay per operation.
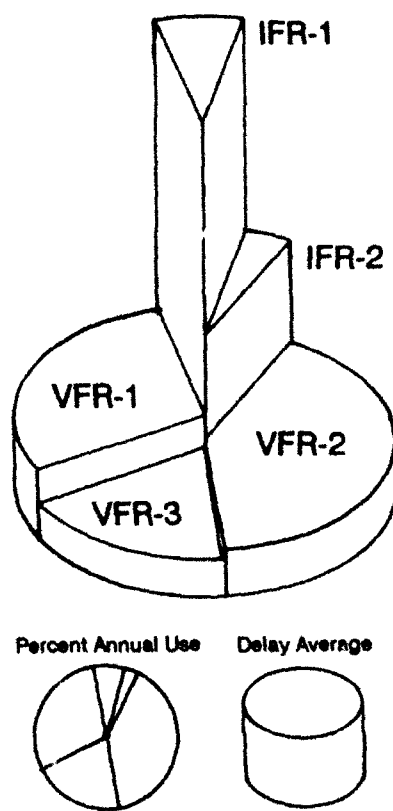
Figure 7. August 1988 average delay by runway use plan.
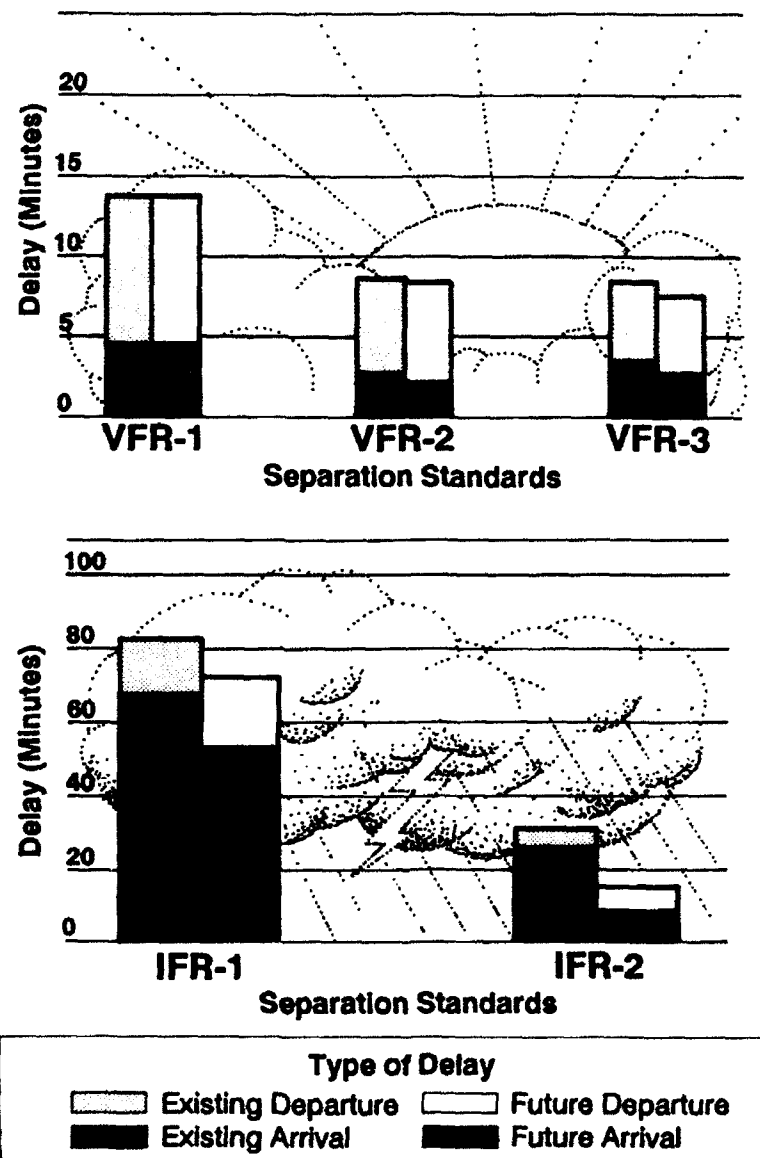
Figure 8. Average arrival/departure delay per aircraft,
August 1988 flight schedule.

Runway Use Plan		Delay Decrease	Percent Decrease
VFR Average		0.2	3.8%
IFR Average		5.9	17.5%
All-Weather Average		0.9	10.2%

□ Existing Separations ■ Future Separations
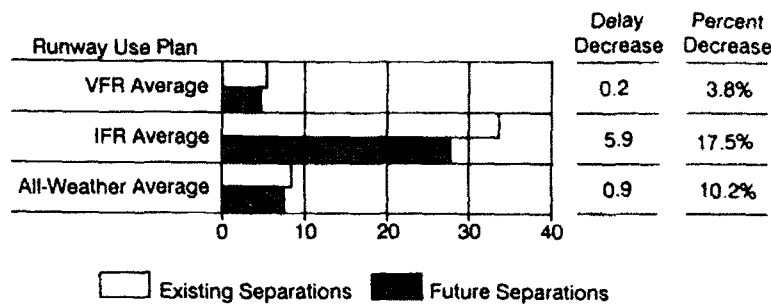
Figure 9. August 1988 average delay by weather condition.

Separation Standards

Schedule
▨ Baseline August 1988   □ Heavy Fleet Mix
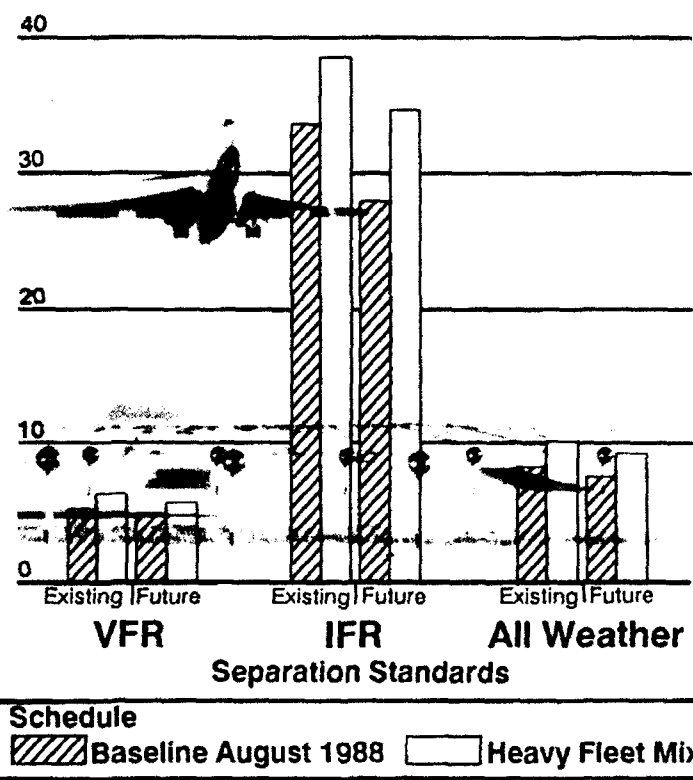
Figure 10. Average all-weather VFR and IFR delay per operation.

	August 1988 Flight Schedule	Heavy Fleet Mix Flight Schedule
Delay Savings Per Operation	0.9	1.0
Delay Cost Per Minute	$30.41	$31.75
Peak Month Average Weekday Operations	2,350	2,350
Daily Delay Cost Savings	$64,300	$74,600

Figure 11. Calculation of economic benefits.

	August 1988 Flight Schedule	Heavy Fleet Mix Flight Schedule
Delay Savings Per Operation	0.9	1.0
Peak Month Average Weekday Delay Savings	35.3 Hours	39.2 Hours
Peak Month Average Weekday Cost Savings	$64,300	$74,600
1988 Annual Operations	804,000	804,000
Annual Delay Savings 1/	10,850 Hours	12,060 Hours
Annual Cost Savings Operations	$19.8 Million	$23.0 Million
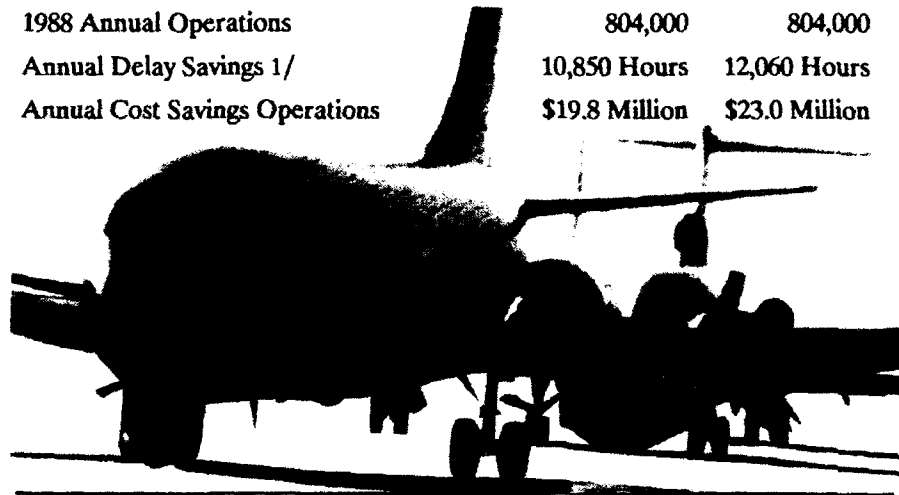
1/ Annual average delay per operation is assumed to be 90 percent at peak month average weekday delay per operation, based on historical demand / delay relationships

Figure 12. Summary of operational impacts.